Methods to Access Highly Functionalized Amidines, Novel Ring-fused Quinazolinones, and Guanidines via Quinazolinone Rearrangement

By

Victor A. Jaffett

A dissertation submitted in partial fulfillment of

the requirements for the degree of

Doctor of Philosophy

(Chemistry)

at the

UNIVERSITY OF WISCONSIN-MADISON

2019

Date of final oral examination: 04/30/2019

The dissertation is approved by the following members of the Final Oral Committee:

Jennifer E. Golden, Assistant Professor, Pharmaceutical Sciences and Chemistry
Steven D. Burke, Professor, Chemistry
Samuel H. Gellman, Professor, Chemistry
Weiping Tang, Professor, Pharmaceutical Sciences and Chemistry

Dedication

To Veronica, Maxwell, and Zoe. You are my inspiration and my joy. I love you.

Acknowledgements

To Professor Golden, I can never thank you enough for everything that you did for me. You put me on a path to success from the moment I joined the group and your faith in me was unwavering the entire way. You always held me to a high standard and pushed me to achieve more than I thought I was capable of. Thank you.

To Professor Burke, it was an honor to work with you. The experience and skills that I gained as a member of your lab were instrumental in my success.

To my lab mates, Muhammad Khalifa, Jhewelle Fitz-Henley, Gang Yan, Bereket Zekarias, Soren Rozema, Dr. Alok Nerukar, Dr. Xufeng Cao, and Dr. Satish Philkhana, thank you for welcoming me with open arms. I could not have asked for a better team to work with. You not only enhanced my work through our many conversations when we bounced ideas off one another, but you made coming to work fun. Please keep in touch. You will always have a place to stay with the Jaffetts.

To my parents, Carlos and Wilda Jaffett, thank you for your love and encouragement in all my endeavors. Even when I deviated from the conventional path, you were always my greatest supporters. All that I have been able to achieve in my life is a direct result of the lessons you taught me when I was young. Thank you and I love you.

To Maxwell and Zoe, you keep me young. Your passion and love for life makes me want to be the best I can be. I love you both and I look forward to seeing all that you will accomplish as you continue your journey.

To my wife Veronica, are my rock. Whether in my Army career or my education, I never picked the easy route and you have been there to support me without fail. This degree is as much yours as it is mine. I cannot wait to see where our adventures take us from here. I love you.

Abstract

The Golden research group discovered a regiospecific intramolecular rearrangement of a quinazolinone core that afforded bioactive (*E*)-amidobenzamidines. In our efforts to access C3-modifications on the chemotype, we developed a telescoped, four-step, six transformation protocol to generate C3-substituted (*E*)-arylamidines. The methodology used a multicomponent Ugi-Mumm in conjunction with a subsequent intramolecular aza-Wittig strategy to access highly diversified quinazolinones which undergo a regiospecific rearrangement to form novel, C3-substituted (*E*)-arylamidines. Additionally, this method led to the formation of C5-substituted ring-fused quinazolines proposed to be generated via an intramolecular ring closing acyl transfer of an elusive (*Z*)-amidobenzamidine intermediate. We also discovered an unprecedented intramolecular rearrangement of the quinazolinone core that generated a cyclic guanidine. These cyclic guanidines, can also be generated to undergo a similar intramolecular ring closure to afford ring-fused acylguanidines.

Table of Contents

Chapter 1: Formation of (*E*)-amidobenzamidines via an intramolecular rearrangement of quinazolinones

The quinazolin-4-one core (**Fig. 1**, blue highlight) is a privileged scaffold represented in a diverse array of natural products and therapeutics.[1] Quinazolinones are known to have an extensive scope of pharmacological activities including antimicrobial,[2] anti-inflammatory,[3] anticancer,[4] and antiviral[5] properties. Quinazolinone formation and reactivity has been a focus of research in the Golden group since this scaffold was discovered and investigated as part of an antiviral-centric medicinal chemistry program.[6a-c]

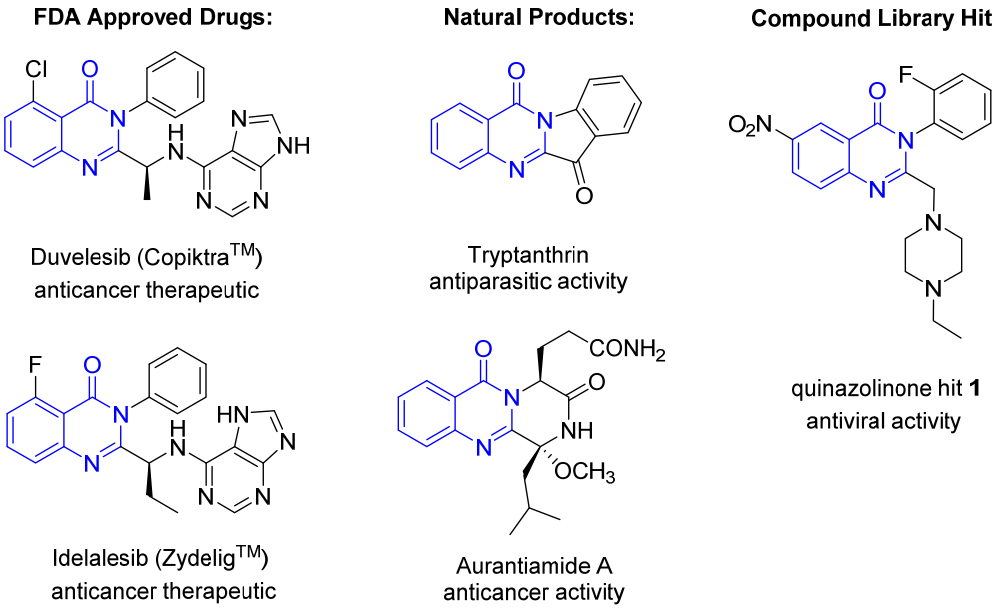

Figure 1. Quinazolinone-based drugs, natural products and a screening hit

In 2014, a high throughput screen of over 348,000 compounds from the NIH Molecular Libraries Small Molecule Repository, identified a quinazolinone compound **1** as a hit against Venezuelan equine encephalitis virus (VEEV).[6a] VEEV is a member of the *Togaviridae* family of alphaviruses, which also includes Eastern and Western equine encephalitis viruses (EEEV and

WEEV, respectively).[7] These mosquito-borne pathogens cause flu-like symptoms characterized by fever, severe headache and, in rare cases, can progress to fatal encephalitis.[8] There are currently no FDA approved vaccines or small molecule treatments for humans available for any alphavirus infection. VEEV can be easily cultured in high concentrations in common cell lines, is indefinitely stable when freeze-dried, and causes acute infection in an aerosolized form.[7] Therefore, VEEV is classified by the CDC and NIAID as a category B biological agent.[9]

In our efforts to explore the structure-activity relationships (SAR) of the quinazolinone chemotype,[6b] 2-(chloromethyl)-6-nitro-3-phenylquinazolin-4(3H)-one (**2**) was treated with *tert*-butyl methyl(2-(methylamino)ethyl)carbamate to engender the mono-*N*-Boc protected ethylenediamine chain appended quinazolinone (**3**) (**Scheme 1, panel A**). However, Boc-deprotection with TFA, followed by neutralization with saturated aqueous K_2CO_3 to liberate the free amine, revealed a novel transformation and non-quinazolinone product, (*E*)-amidobenzamidine (**4**). Running this reaction with N^1,N^2-dimethylethane-1,2-diamine, instead of the Boc-protected diamine, resulted in the direct formation of the (*E*)-amidobenzamidine product and eliminated the need for the protection/deprotection efforts.

Use of the mono-Boc protected diamine to isolate quinazolinone **3** was informative with respect to the mechanism for this reaction. In this case, the nucleophilic amine displaced the chlorine atom, affording an intermediate that was incapable of undergoing any further transformation. While diamines separated by a two-carbon linker productively converted to amidines, reactions conducted with three-carbon linked *tert*-butyl methyl(3-(methylamino)propyl)carbamate stalled (**Scheme 1, panel B**). In this case, deprotection of *tert*-butyl methyl(3-(methylamino)propyl)carbamate substituted quinazolinone (**6**) and subsequent basification of the reaction mixture resulted in the formation of deprotected quinazolinone (**7**),

without subsequent formation of the corresponding amidine (8). Given these results, it was rationalized that amidine formation likely occurred with the two-carbon linker as a result of an intramolecular nucleophilic attack on the quinazolinone core to form a six-membered, spirocyclic intermediate (**5, panel A**), followed by C-N bond cleavage and regiospecific formation of (*E*)-amidobenzamidine (**4**). Nucleophilic attack by the free secondary amine of the N^1,N^3-dimethylpropane-1,3-diamine appended quinazolinone would result in a seven-membered, spirocyclic intermediate **(9, panel B**), the formation of which we assume to be energetically less favored. As such, a series of (*E*)-amidobenzamidines were generated featuring a six-membered

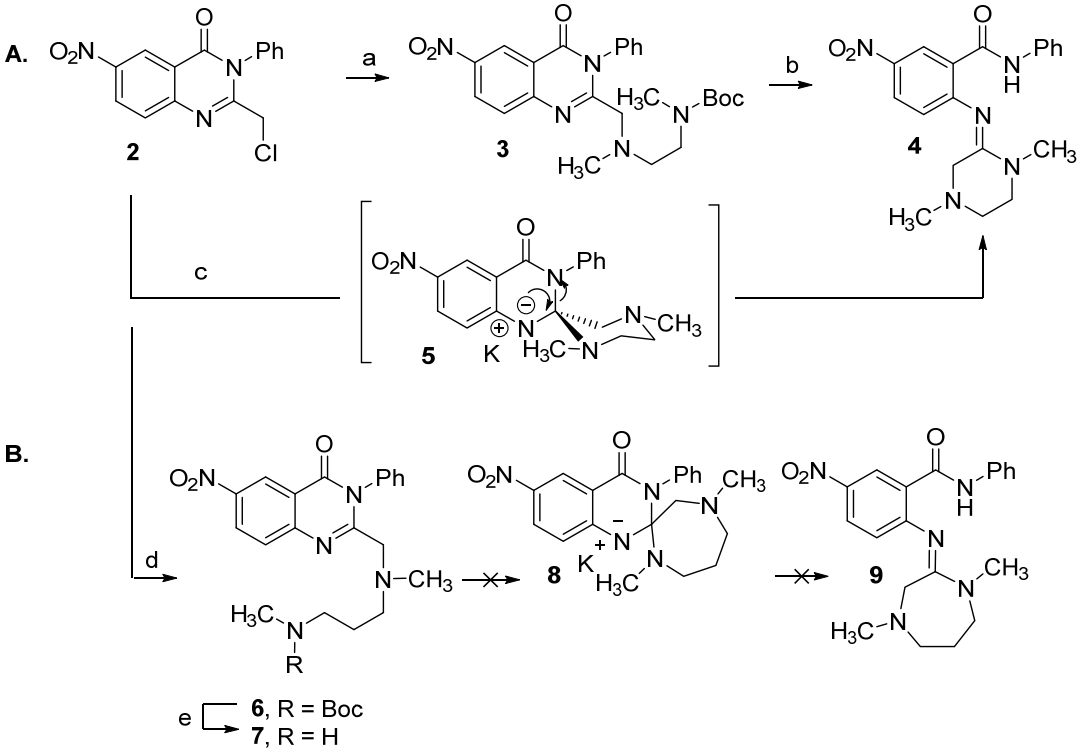

Reaction Conditions: (a) *tert*-Butyl methyl(2-(methylamino)ethyl)carbamate, KI, K_2CO_3, CH_3CN, MWI, 80°C, 10 min, 35%; (b) TFA, CH_2Cl_2, rt, 45 min, then aq $NaHCO_3$, 50%; (c) N^1,N^2-dimethylethane-1,2-diamine, K_2CO_3, CH_3CN, 50 °C, 2 h, 69%; (d) *tert*-butyl methyl(3-(methylamino) propyl)carbamate, KI, K_2CO_3, CH_3CN, MWI, 80°C, 10 min, 31%; (e) TFA, CH_2Cl_2, rt, 45 min, then aq $NaHCO_3$, 7%.

Scheme 1. Panel A: Synthesis of six-membered ring (*E*)-amidobenzamidines and, **Panel B:** inaccessibility of a 7-membered ring amidobenzamidine

amidine ring as part of the scaffold. To our knowledge, this was the first intramolecular quinazolinone rearrangement leading to amidine formation.

The (*E*)-amidobenzamidine possesses an *N′,N,N*-trisubstituted amidine motif (**Fig 2.**, blue highlight), which is prevalent within pharmaceutically active compounds known for a broad array of therapeutic applications including antiarrhythmia,[10] anthelmintic,[11] antiparasitic,[12] antidepressant,[13] and antipsychotic[14] activity. Our (*E*)-amidobenzenamidines turned out to also harbor bioactivity. We were excited to discover that the (*E*)-amidobenzamidine chemotype was a potent antiviral in our alphavirus program.

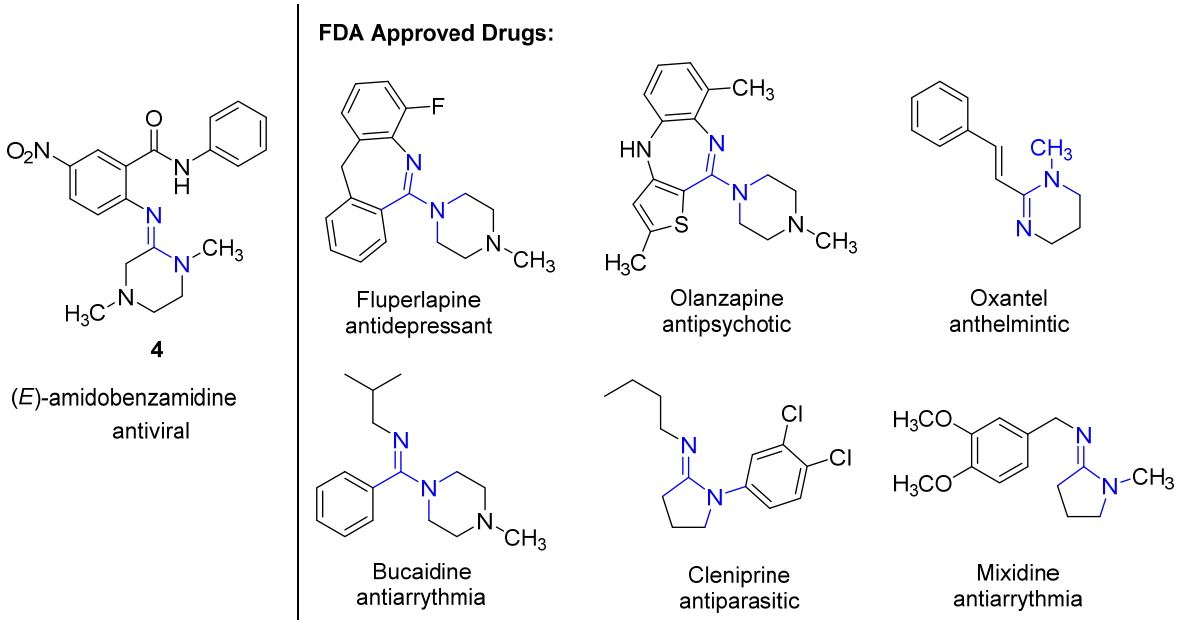

Figure 2. *N′,N,N*-trisubstituted amidine motif (blue highlight) in FDA approved drugs and the new (*E*)-amidobenzamidine chemotype

Further examination of the chemotype explored alteration of the piperazine ring and found limitations in generating five- or six-membered ring amidine analogues in which the methylamine was replaced by a methylene or oxygen linkage (**Scheme 2**).[6c] It was hypothesized that reaction of 2-(3-chloropropyl)-6-nitro-3-phenylquinazolin-4(3H)-one (**8a**) with *n*-butylamine would yield

five-membered ring (*E*)-2-((1-methylpyrrolidin-2-ylidene)amino)-*N*-phenylbenzamide (**9a**). This was attractive from a late-stage diversification perspective, as amines would not be incorporated until needed in the last rearrangement step. However, the reaction failed to produce the desired product and instead generated 2-cyclopropyl-6-nitro-3-phenylquinazolin-4(3H)-one (**12a**) in 65% yield. This transformation can be explained by deprotonation of the α-imine carbon on the quinazolinone by the basic amine, followed by the intramolecular nucleophilic substitution to form the cyclopropane ring. Reactions conducted using 2-(4-chlorobutyl)-6-nitro-3-phenylquinazolin-4(3H)-one (**10b**) produced the desired (*E*)-2-((1-butylpiperidin-2-ylidene)amino)-5-nitro-*N*-phenylbenzamide (**11b**) in moderate yield without formation of cyclobutyl-substituted quinazolinone (**12b**).

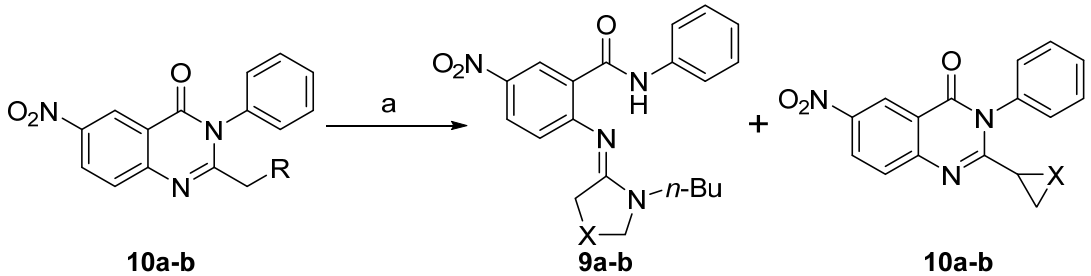

10a-b
10a, R= $(CH_2)_2Cl$
10b, R= $(CH_2)_3Cl$

9a-b
11a, X= CH_2, 0%
11b, X= $(CH_2)_2$, 62%

10a-b
12a, X= CH_2, 65%
12b, X= $(CH_2)_2$, 0%

Reaction Conditions: (a) *n*-butylamine, DMF, 70 °C, 15 h.

Scheme 2. Attempted diversification from chloroalkyl quinazolinones 8a-b

The failure of this method to produce **11a** meant that an alternate protocol had to be developed to generate five- and six-membered rings containing replacements for the methylamine group in the (*E*)-amidobenzamidines (**Scheme 3**). In 1980, Rabilloud and Sillon disclosed the formation of quinazolinones[15] through the reaction of equimolar equivalents of anthranilic acid and a carboxylic acid in the presence of triphenylphosphite and pyridine at 100 °C for 4 h. This

process formed a 2-substituted 4H-1,3-benzoxazine-4-one intermediate that was intercepted by an equivalent of aniline which, after heating at 100 °C for an additional 3 h, produced a quinazolinone. This method was modified by our group in that two equivalents of the carboxylic acid and three equivalents of triphenylphosphite relative to the anthranilic acid were added in pyridine and heated to 100 °C by microwave to reduce the reaction time to 3 min. Next, four equivalents of aniline were added, and the reaction mixture was heated to 100 °C by microwave for an additional minute.[6c] These modifications were important to (a) permitting a telescoped process that involved five discreet transformations and only one final purification, (b) a process that could be executed in one day, start-to-finish, and (c) permitted access to unprecedented 5-membered benzamidines, 6-membered, ether-containing benzamidines, and carbocylic benzamidines that had not been accessible prior to this methodology. For instance, this protocol expediently afforded quinazolinone (**14**) via reaction between 4-((*tert*-butoxycarbonyl)(methyl)amino)butanoic acid (**13**) and 2-amino-5-nitrobenzoic acid (**Scheme 3**). Upon Boc-deprotection and basification, the desired (*E*)-2-((1-methylpyrrolidin-2-ylidene)amino)-*N*-phenylbenzamide (**15**) was formed in 80% yield, revealing an efficient telescoped method to generate these analogues. These compounds were also potent antivirals that advanced our understanding of critical pharmacophoric elements.

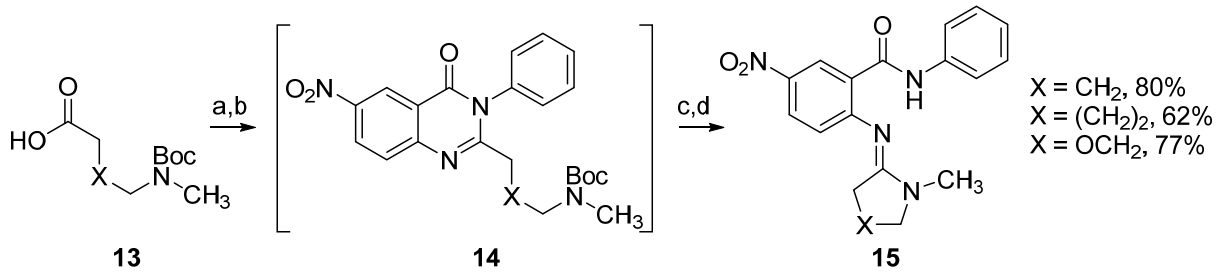

13 **14** **15**

Reaction Conditions: (a) 2-amino-5-nitrobenzoic acid, $P(OPh)_3$, pyridine, MWI, 100 °C, 3 min; (b) aniline, MWI, 100 °C, 1 min; (c) pyridine removal, TFA, CH_3CN, 1-2 h; (d) sat. $NaHCO_3$ (aq), 40 °C, 1-1.5 h.

Scheme 3. Five-membered ring (*E*)-amidobenzamidine synthesis

With these solutions in hand and with promising bioactivity to pursue, the Golden group sought to further explore the chemical space around the amidine moiety. As part of that effort, group members attempted to diversify the α-amidine C3 position, but this proved to be a significant challenge (**Scheme 4**). Attempts to react 2-(chloroethyl)-3-phenylquinazolin-4(3H)-one intermediate (**16**) with N^1,N^2-dimethylethane-1,2-diamine resulted in only trace amounts (3.5%) of the C3 substituted (*E*)-amidobenzamidine (**17**).[16] Additionally, efforts to assemble the requisite quinazolinone intermediate (**19**) using the developed triphenylphosphite conditions[6c] and N-(2-((tert-butoxycarbonyl)(methyl)amino)ethyl)-N-methylalanine (**18**) were unproductive.[16]

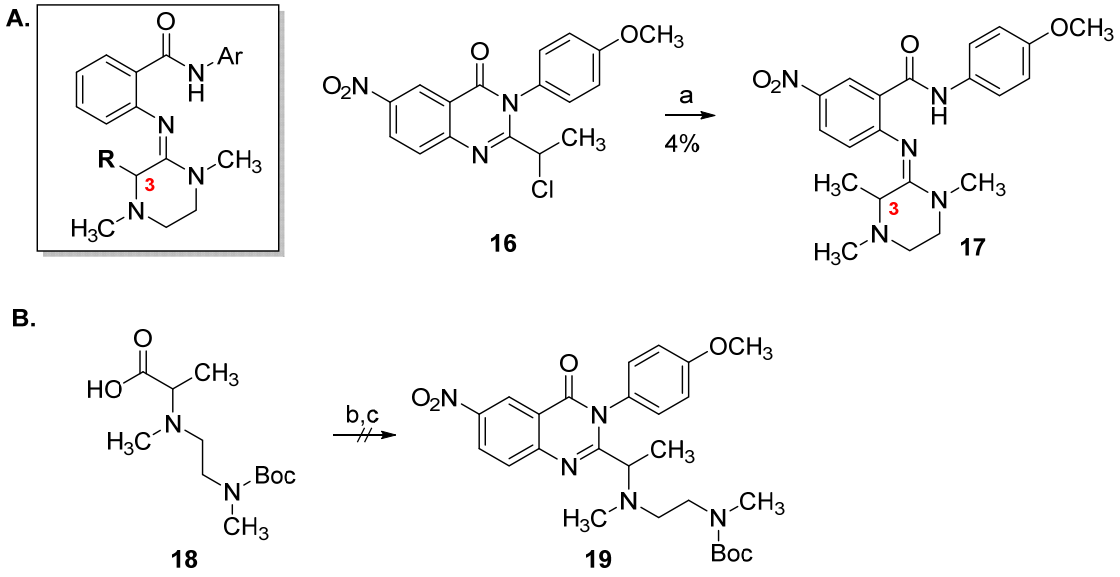

Reaction Conditions: (a) N^1,N^2-dimethylethane-1,2-diamine, K_2CO_3, CH_3CN, 50 °C, 2 h, 0-3.5%; (b) 2-amino-5-nitrobenzoic acid, $P(OPh)_3$, pyridine, MWI, 100 °C, 3 min; (b) 4-methoxyaniline, MWI, 100 °C, 1 min, 0%.

Scheme 4. Attempted routes to access C3-methyl substituted (*E*)-amidobenzamidine

Considering these challenges, another approach was devised, starting from *N*-Fmoc-*N*-methyl-alanine (**20**).[17] The amino acid reacted using the first two steps of the telescoped method to successfully create the (9H-fluoren-9-yl)methyl (1-(3-(4-methoxyphenyl)-6-nitro-4-oxo-3,4-

dihydroquinazolin-2-yl)ethyl)(methyl)carbamate (**21**) in 43% yield. The amine was then deprotected under basic conditions to form quinazolinone (**22**) which underwent a reductive amination with *tert*-butyl methyl(2-oxoethyl)carbamate to assemble the desired Boc-protected diamine appended quinazolinone (**19**). The ensuing deprotection and basification resulted in the desired C3-methyl substituted (*E*)-amidobenzamidine (**17**) in 10% overall yield over the six steps. Though this approach generated the desired analogue in modest yield, an alternative protocol was sought that would permit a more feasible and improved yield of C3-modified (*E*)-amidobenzamidines.

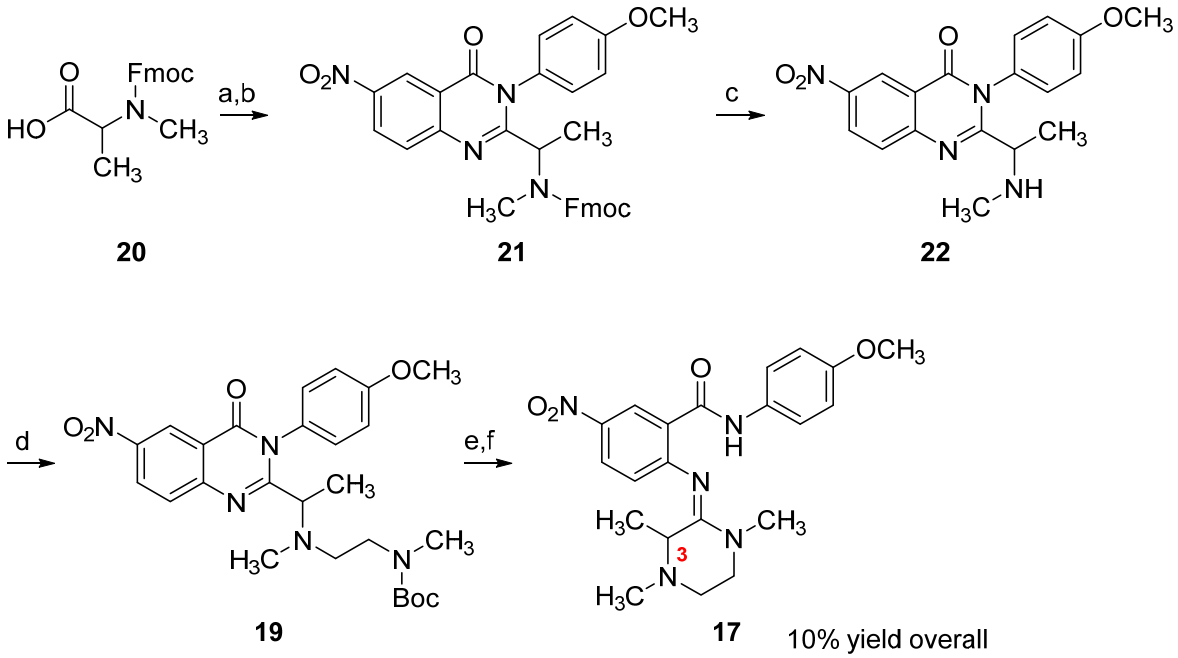

20 **21** **22** **19** **17**

Reaction Conditions: (a) 2-amino-5-nitrobenzoic acid, $P(OPh)_3$, pyridine, MWI, 100 °C, 40 min; (b) 4-methoxyaniline, MWI, 100 °C, 1 min, 43%; (c) piperidine, CH_2Cl_2, 2 h, 68%; (d) *tert*-butyl methyl(2-oxoethyl)carbamate , AcOH, CH_3OH, $NaBH_3CN$, 16 h, 75%; (e) TFA, CH_3CN, 3 h; (f) sat. $NaHCO_3$ (aq), 3 h, 46%.

Scheme 5. Modified C3-methyl substituted (*E*)-amidobenzamidine synthesis

References:

1. (a) Welsch, M.E.; Snyder, S.A.; Stockwell, B.R. Privileged scaffolds for library design and drug discovery. *Curr Opin Chem Biol.* **2010**, *14*, 347–361.; (b) Jafari, E.; Khajouei, M.R.; Hassanzadeh, F.; Hakimelahi, G.H.; Khodarahmi, G.A. *Res Pharm Sci.* **2016**, 11, 1–14.

2. (a) Dave, R.S.; Odedara, R.J.; Kalaria, R.I.; Upadhyay, J.J. Synthesis, characterization and antimicrobial activity of new quinazolin- 4(3H)-one schiff base derivatives. *J Chem Pharm Res*. **2012**, *4*, 4864-4869; (b) Rajasekaran A.; Rajamanickam, V.; Darlinquine, S. *Eur Rev Med Pharmacol Sci*. **2013**, *17*, 95-104.

3. (a) Chao, Q; Deng, L.; Shih, H.; Leoni, L.M.; Genini, D.; Carson, D.A.; Cottam, H.B. *J Med Chem.* **1999**, *42*, 3860-3873; (b) Dash, B.; Dash, S.; Laloo, D.; Medhi, C. Design, Synthesis and Preliminary Pharmacological Screening (antimicrobial, analgesic and anti-inflammatory activity) of Some Novel Quinazoline Derivatives. *J Appl Pharm Sci.* **2017**, *7*, 83-96.

4. (a) Abbas, S.Y.; El-Bayouki, K.A.M.; Basyouni, W.M.; Mostafa, E.M. New series of 4(3H)-quinazolinone derivatives: syntheses and evaluation of antitumor and antiviral activities. *Med Chem Res*. **2018**, *27*, 571-582; (b) El-Hashash, M.A.EA.M.; Salem, M.S.; Al-Mabrook, S.A.M. Synthesis and anticancer activity of novel quinazolinone and benzamide derivatives. *Res Chem Intermed*. **2018**, *44*, 2545-2559; (c) Dohle, W.; Jourdan, F.L.; Menchon, G.; Prota,A.E.; Foster, P.A.; Mannion, P.; Hamel, E.; Thomas, M.P.; Kasprzyk, P.G.; Ferrandis, E.; Steinmetz, M.O.; Leese, M.P.; Potter, B.V.L. Quinazolinone-Based Anticancer Agents: Synthesis, Antiproliferative SAR, Antitubulin Activity, and Tubulin Co-crystal Structure. *J Med Chem.* **2018**, *61*, 1031-1044.

5. (a) Gao, X.; Cai, X.; Yan, K.; Song, B.; Gao, L.; Chen, Z. Synthesis and antiviral bioactivities of 2-aryl- or 2-methyl-3-(substituted- benzalamino)-4(3H)-quinazolinone derivatives. *Molecules*. **2007**, *12*, 2621-2642; (b) Wang, Z.; Wang, M.; Yao, X.; Li, Y.; Tan, J.; Wang, L.; Qiao, W.; Geng, Y.; Liu, Y.; Wang, Q. Design, synthesis and antiviral activity of novel quinazolinones. *Eur. J. Med. Chem*. **2012**, 53, 275-282.

6. (a) Chung D-H; Jonsson, C.B.; Tower, N.A.; Chu, Y-K; Sahin, E.; Golden, J.E.; Noah, J.W., Schroeder, C.E.; Sotsky, J.B.; Sosa, M.I.; Cramer, D.E.; McKellip, S.N.; Rasmussen, L.; White, E.L.; Schmaljohn, C.S.; Julander, J.G.; Smith, J.M.; Filone, C.M.; Connor, J.H.; Sakurai, Y.; Daveyet, R.A. Discovery of a Novel Compound with Anti-Venezuelan Equine Encephalitis Virus Activity That Targets the Nonstructural Protein 2. *PLoS Pathog*. **2014**, 10, e1004213; (b) Schroeder, C.E.; Yao, T.; Sotsky, J.; Smith, R.A.; Roy, S.; Chu, Y-K.; Guo, H.; Tower, N.A.; Noah, J.W.; McKellip, S.; Sosa, M.; Rasmussen, L.; Smith, L.H.; White, E.L.; Aubé, J.; Jonsson, C.B.; Chung, D.; Golden, J.E. Development of (E)-2-((1,4-Dimethylpiperazin-2-ylidene)amino)-5-nitro-N-phenylbenzamide, ML336: Novel 2-Amidinophenylbenzamides as Potent Inhibitors of Venezuelan Equine Encephalitis Virus. *J. Med. Chem*. **2014**, 57, 8608−862; (c) Schroeder, C.E.; Neuenswander, S.A.; Yao, T.; Aubé, J.; Golden, J.E. One-pot, regiospecific assembly of (E)-benzamidines from δ- and γ-amino acids via an intramolecular aminoquinazolinone rearrangement. *Org. Biomol. Chem*. **2016**, 14, 3950–3955.

7. Atasheva, S.; Kim, D.Y.; Akhrymuk, M.; Morgan, D.G.; Frolova, E.I.; Frolov, I. *Journal of Virology*, **2013**, 87, 2023–2035.

8. Schmaljohn, A.L,; McClain, D. Alphaviruses (Togaviridae) and Flaviviruses (Flaviviridae) In: *Medical Microbiology. 4th edition*. Baron S., Ed. University of Texas Medical Branch at Galveston; Galveston, TX, **1996**. Chapter 54.

9. NIAID Emerging Infectious Diseases/Pathogens. *National Institute of Allergy and Infectious Diseases*, U.S. Department of Health and Human Services, 8 Apr. 2019, www.niaid.nih.gov/research/emerging-infectious-diseases-pathogens.

10. (a) Grebow, P.; Feeney, W.; Johnston, M.; Lettieri, J.; Li, H.; Magnien, E.; O'Brien, P.; Swillo, R.; Weinryb, I.; Wolf ; P.; Marsiglia, J. C. The pharmacodynamics of bucainide (RHC G233): pharmacokinetic parameters and relationship between plasma levels and the effect on the electrocardiogram in the dog. *Res. Commun. Chem. Pathol. Pharmacol.* **1981**, 32, 407-421; (b) Takeda, K.; Akera, T.; Brody, T. M. Cardiovascular actions of mixidine fumarate. *Eur. J. Pharmacol*., **1980**, 68, 129-137; (c) Pruss, T. P.; Hageman, W. E.; Jacoby, H. I. Cardiovascular profile of mixidine fumarate, a compound which attenuates myocardial chronotropic responses..*J. Pharmacol. Exp. Ther*. **1980**, *212*, 514-518.

11. (a) Sinniah, B.; Sinniah D. The anthelmintic effects of pyrantel pamoate, oxantel-pyrantel pamoate, levamisole and mebendazole in the treatment of intestinal nematodes. *Ann. Trop. Med. Parasitol.*, **1981**, 75, 315-321; (b) McFarland, J. W.; Howes, H. L. Novel anthelmintic agents. 6. Pyrantel analogs with activity against whipworm. *J. Med. Chem.* **1972**, 15, 365-368; (c) Howes, H. L.; Lynch, J. E. Anthelmintic Studies with Pyrantel. I. Therapeutic and Prophylactic Efficacy against the Enteral Stages of Various Helminths in Mice and Dogs. *J. Parasitol.* **1967**, 53, 1085-1091.

12. (a) Andrews P.; Stendel, W. Mechanism of action of clenpyrin on the cattle tick Boophilus microplus. *Pestic. Sci.*, **1975**, 6, 129-143; (b) Rawlins, S. C.; Mansingh, A. Susceptibility of engorged adults of the cattle tick, Boophilus microplus (Canestrini), to acaricides. *Insect Sci. Its Appl.*, **1981**, 1, 377-378.

13. (a) S. Levine, J. Int. Med. Res., 1979, 7, 1; (b) M. E. J. Lean and L. J. Borthwick, Eur. J. Clin. Pharmacol., 1983, 25, 41; (c) J. Coupet, S. K. Fisher, C. E. Rauh, L. Fong and B. Beer, Eur. J. Pharmacol., 1985, 112, 231; (d) R. B. Lydiard and A. J. Gelenberg, Pharmacotherapy, 1981, 1, 163; (e) C. Rüdeberg, S. Urwyler, C. Schulthess and P. L. Herrling, Naunyn-Schmiedeberg's Arch. Pharmacol., 1986, 332, 357.

14. (a) Jann, M. W. Clozapine. *Pharmacotherapy*, **1991**, 11, 179-195; (b) Woggon, B.; Angst, J.; Bartels, M.; Heinrich, K.; Hippius, H.; Koukkou, M.; Krebs, E.; Küfferle, B.; Müller-Oerlinghausen, B.; Pöldinger, W.; Rüther E.; Schied, H. W. Antipsychotic Efficacy of Fluperlapine; An Open Multicenter Trial. *Neuropsychobiology*, **1984**, 11, 116-120; (c) Mann, K.; Bartels, M.; Gartner, H. J.; Schied, H. W.; Wagner W.; H. Heimann, Differential effects of a new dibenzo-epine neuroleptic compared with haloperidol. Results of an open and crossover

study. *Pharmacopsychiatry*. **1987**, 20, 155-159; (d) Prinssen, E. P.; Ellenbroek, B. A.; Cools, A. R. Combined antagonism of adrenoceptors and dopamine and 5-HT receptors underlies the atypical profile of clozapine. *Eur. J. Pharmacol.* **1994**, 262, 167-170; (e) Xue, X.; Song, Y.; Yu, X.; Fan, Q.; Tang J.; Chen, X. Olanzapine and haloperidol for the treatment of acute symptoms of mental disorders induced by amphetamine-type stimulants: A randomized controlled trial. *Medicine*, **2018**, 97, e9786-9790; (f) Komossa, K.; Rummel-Kluge, C.; Hunger, H.; Schmid, F.; Schwarz, S.; Duggan, L.; Kissling, W. ;Leucht, S. Olanzapine versus other atypical antipsychotics for schizophrenia. *Cochrane Database Syst. Rev.*, 2010, 3, CD006654.

15. Rabilloud, G.; Sillion, B. Synthesis of 4H-3,1-benzoxazin-4-ones and 4-(3H)quinazolinones from anthranilic acids and their derivatives by the use of triphenyl phosphite and pyridine. *J. Heterocylic Chem.* **1980** 17, 1065-1068.

16. Cao, X. Unpublished work.

17. Jonsson, C.; Colleen B.; Cao, X.; Lee, J.; Gabbard, J.D.; Chu, Y-K.; Fitzpatrick, E.A.; Julander, J.; Chung, D-H., Stabenow, J.; Golden, J.E. Efficacy of a ML336 derivative against Venezuelan and eastern equine encephalitis viruses. *Antiviral Res.* **2019**,167, 25-34.

Chapter 2. Telescoped synthesis of C3-functionalized (*E*)-arylamidines using Ugi-Mumm and regioselective quinazolinone rearrangements

As summarized in the preceding chapter, the synthetic methods in hand were inadequate to address the need for exploring C3-amidine substitution. It was uncertain if the methods themselves were contributing to poor yields of C3-modified (*E*)-benzamidines or if C3-substitution was unfavorable due to steric interactions or some other complication. To study this further, we took note of a 2011 paper by the Tron lab.[1] In this work, a convergent route to ispinesib, a mitotic spindle kinesin inhibitor was established through a methodology study of quinazolinone preparation. In the methodology component of their study, Tron and co-workers generated thirteen 2,3-disubstituted-4-(3H)-quinazolinones (**28**). These quinazolinones were structurally similar to aminoalkylquinazolinones that we had prepared with our technologies; however, Tron's quinazolinones were unique in three important ways. First, these quinazolinones contained a substituent off of the alkyl amine (**Scheme 6**, R^3 in **28**) while ours did not. Secondly, the amide-like nitrogen could bear an aryl or alkyl substituent (**Scheme 6**, R^4 in **28**), while our chemistry had generated *N*-*alkyl*amidoquinazolinones in modest yield. Third, the Tron quinazolinones were limited to those with only short, 2-alkylamine substituents, or in the case of ispinesib (**29**) a 3-carbon linked diamine substituent, neither of which would be expected to rearrange to an amidine due to inadequate linkage length. Interestingly, these compounds had been prepared using a Ugi four-component reaction, followed by an intramolecular Staudinger/aza-Wittig reaction (**Scheme 6**).

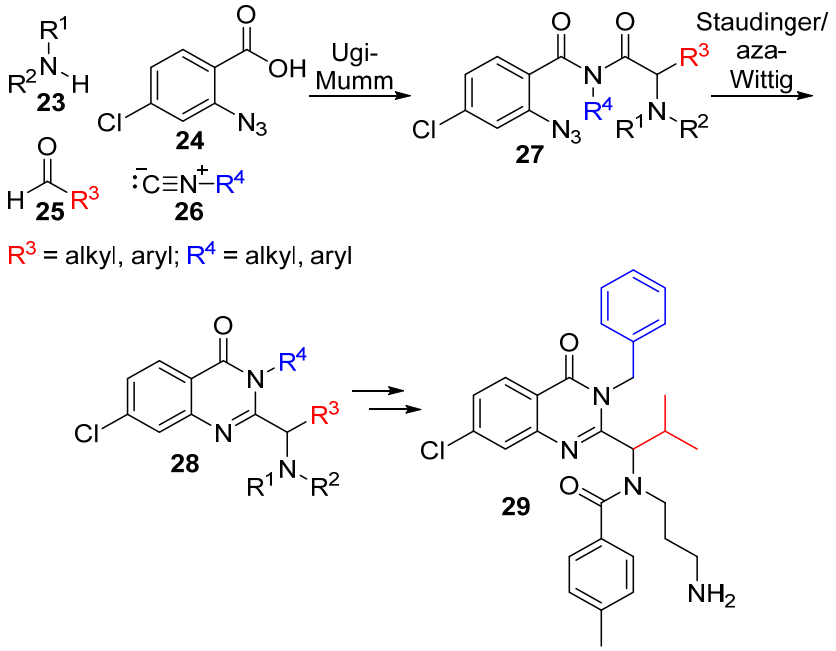

Scheme 6. Tron's convergent strategy to form quinazolinones en route to ispenisib[1]

The approach was attractively convergent, and formation of the uniquely substituted quinazolinone intermediate was interesting since a suitably functionalized quinazolinone (**32**) might rearrange to form a C3-substituted amidine (**Scheme 7, 33**). Furthermore, Tron's researchers were able to streamline their strategy into a one-pot method, increasing efficiency and reducing waste. Consequently, this approach to synthesizing quinazolinones offered potential diversification of the amidine scaffold (R^3 and R^4, **33**) which would assist in better understanding of structure activity relationships in our antiviral program and offer potential orthogonal activity we could explore.

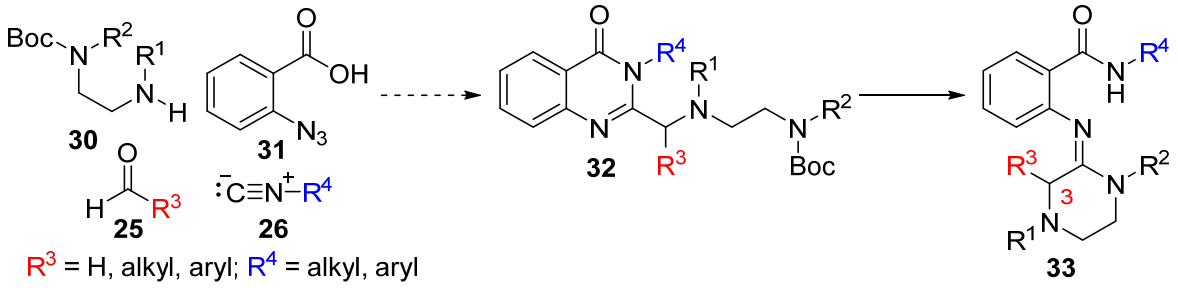

Scheme 7. Theoretical application of Ugi-Staudinger/aza-Wittig to the formation of C3-modified-(*E*)-amidobenzamidines

In order to pursue this idea, we also took note of limitations. Tron's method described only a limited number of examples, and overall yields varied from 45-81%. This raised questions as to how robust the method was and if it would provide us the scope of components we sought. Additionally, the method required a range of reaction times to generate the imides, thus reducing efficiency depending on reaction component. Most of the imide-forming reactions were done within a day; however, Tron's researchers observed that aryl aldehydes were significantly slower to react under their conditions, taking up to three days to complete imide formation. Notably, formaldehyde was not a competent reagent in this chemistry, meaning that unsubstituted 2-alkylaminoquinazolinones were inaccessible. These intermediates were important, too, as they would be expected to deliver C3-unsubstituted-*N*-alkyl-amidobenzamidines which were beneficial to our medicinal chemistry program. Therefore, we required a general set of conditions which would provide rapid access to diversification of the quinazolinone intermediate irrespective of the components. Given these considerations, we examined this approach for making complex and diverse quinazolinones incorporating a wide range of Ugi components, such as formaldehyde, aryl aldehydes, and heterocyclic azido acids, which could subsequently be transformed into novel, C3-substituted (*E*)-arylamidines.

To generate the 2-alkylamino-2,3-disubstituted-4-(3H)-quinazolinones (**35**), the Tron group utilized a variation of the Ugi four-component reaction to generate *o*-azidophenyl imide intermediates (**34**), which they then converted to the desired quinazolinones using an aza-Wittig ring closure (**Scheme 8**). To describe this, a review of the classical Ugi reaction is appropriate. The Ugi four-component reaction was discovered in 1959 by Dr. Ivar Ugi[2] and is lauded as one of the most efficient, widely used multicomponent reactions, particularly since the advent of combinatorial chemistry circa 1995.[3a-d] Multicomponent reactions, such as the Ugi four-component reaction are unique in their efficiency and economy because they incorporate all or most of the atoms from three or more starting materials to form the desired product in one pot.[3a] Notably, the reagents are added concomitantly at the beginning, then react in a sequential manner until an irreversible step traps the final product.[3b] Tron's method required the use of a secondary amine in order to generate their imide intermediate (**34**).[1] This is owing to a fundamental difference in the mechanism of the reaction when this substitution is made from a secondary to a primary amine.

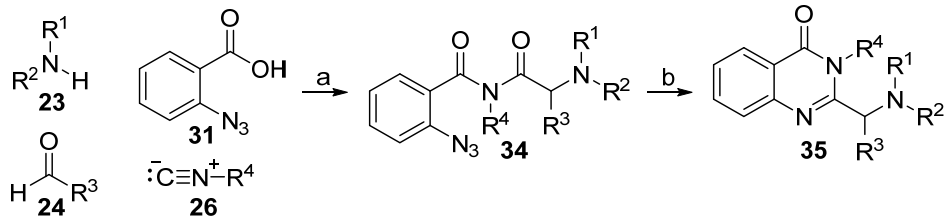

Reaction Conditions: (a) CH_2Cl_2, 4 Å molecular sieves, rt; (b) PPh_3, toluene, reflux.

Scheme 8. Synthesis of 2-alkylamino-2,3-disubstituted-4(3H)-quinazolinone via Ugi four-component reaction and tandem Staudinger/aza-Wittig strategy

In 1961, Dr. Ugi demonstrated that secondary amines react with aldehydes, carboxylic acids, and isocyanides to produce imides.[4] The proposed mechanism for this transformation

(**Scheme 9**) began with a condensation reaction between the secondary amine and the aldehyde (**36**) to form iminium ion (**39**). Next, nucleophilic attack on iminium ion by the isocyanide produced nitrilium ion (**40**). Consequently, nucleophilic attack on the carbon atom of the nitrilium ion (**40**) by the carboxylate formed imidate intermediate (**41**). However, **t**he tertiary amine substituent, formed from the incorporation of the secondary amine, was incapable of participating in the O-N acyl migration. Instead, imidate intermediate (**41**) underwent a Mumm rearrangement[5] between the imine nitrogen and the carbonyl to irreversibly form the imide product (**42**). Imides bearing an *o*-azidophenyl substituent at the R^5 position were demonstrated by Takeuchi, et al. to be competent reagents to undergo an intramolecular ring closure, via a tandem Staudinger/aza-Wittig reaction, to generate substituted quinazolinones.[6]

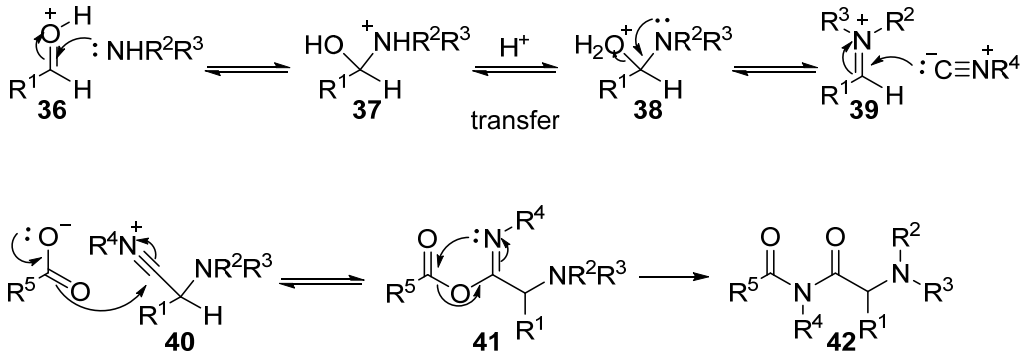

Scheme 9. Ugi four-component reaction mechanism using secondary amines to form imides

The initial discovery of the Ugi four-component reaction combined an aldehyde, primary amine, isocyanide and carboxylic acid.[2] This reaction resulted in the formation of an α-aminoacyl amide. The reaction mechanism proposed by Dr. Ugi[7a-d] (**Scheme 10**) began with a condensation reaction between the primary amine and the aldehyde (**36**) to form an imine which then reacted with a Brønsted-Lowry acid to form iminium ion (**45**). Then, nucleophilic attack by the isocyanide

on iminium ion (**45**) formed nitrilium ion (**46**). Next, nucleophilic attack on the carbon atom of the nitrilium ion (**46**) by the carboxylate generated imidate intermediate (**47**), which quickly and irreversibly underwent an O-N acyl migration[5] between the secondary amine substituent and the carbonyl which trapped bisamide product (**48**). These bisamides are not amenable to follow-on transformations to generate quinazolinones and therefore, not suitable for this method.

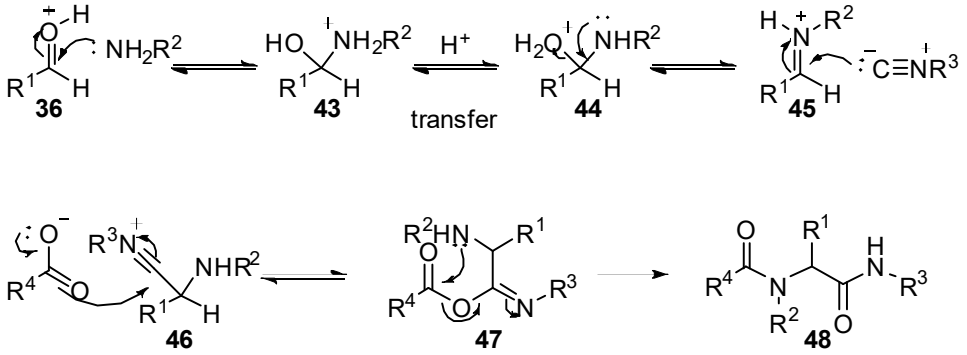

Scheme 10. Ugi four-component reaction mechanism using primary amines to form bisamides

In their initial investigations into their proposed method (**Scheme 11**), the Tron group were pleased to discover that they were indeed able to engender the desired imide intermediate (**52**) in 80% yield upon reacting equimolar amounts of *N*-methyl benzylamine (**49**), heptanal (**50**), 2-azidobenzoic acid (**31**), and 1-pentyl isocyanide (**51**). Additionally, as predicted, this substrate underwent an intramolecular ring closure with Staudinger/aza-Wittig conditions, forming quinazolinone (**53**) in 80% yield, 64% overall.

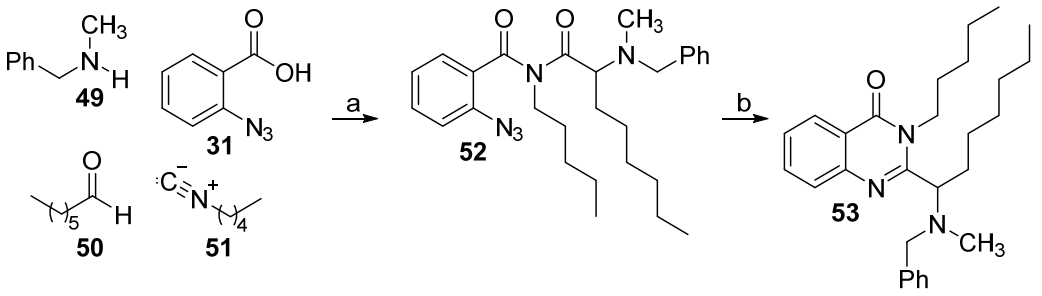

Reaction Conditions: (a) CH_2Cl_2, 4 Å molecular sieves, rt, 80%; (b) PPh_3, toluene, reflux 80%.

Scheme 11. Generation of quinazolinone **53** via Ugi four-component reaction/intra-molecular aza-Wittig strategy

In their examination of scope, Tron's researchers encountered an issue with the use of bulky isocyanides, specifically when they attempted the reaction with *tert*-butyl isocyanide (**55**). They observed no generation of the desired imide (**56**), but instead they isolated α-acyloxycarboxamide (**57**), the result of a Passerini three-component reaction (**Scheme 12**). They hypothesized that the steric bulk of the *tert*-butyl substituent inhibited the irreversible Mumm rearrangement, allowing the intermediates to revert back to the starting materials and access an alternate Passerini reaction pathway.

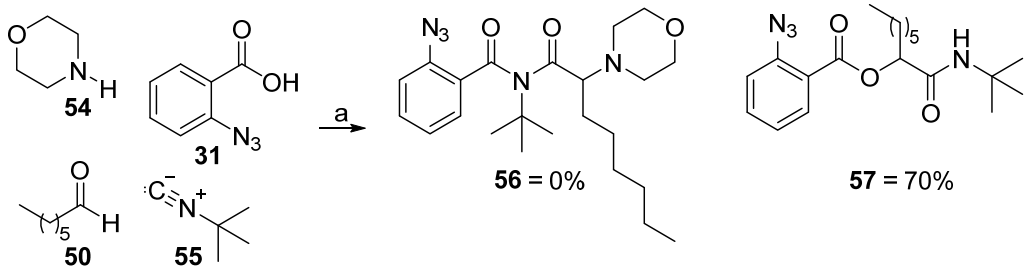

Reaction Conditions: (a) CH_2Cl_2, 4 Å molecular sieves, rt, 70%

Scheme 12. Reaction with *tert*-butyl isocyanide forming α-acyloxycarboxamides

To better understand this competing pathway, it is helpful to examine the Passerini three-component reaction (**Scheme 13**). The Passerini three-component reaction precedes the Ugi in its

discovery in 1921,[8] and is the first isocyanide based multicomponent reaction. The Passerini three-component reaction incorporated an aldehyde, isocyanide and carboxylic acid. The reaction mechanism[9] began with the nucleophilic attack on the activated aldehyde (**58**) by the isocyanide to yield nitrilium ion (**59**). Subsequently, a nucleophilic attack by the carboxylate on the nitrilium ion carbon formed imidate intermediate (**60**). This intermediate then quickly and irreversibly underwent a Mumm rearrangement to generate α-acyloxycarboxamide (**61**). Given that this mechanism integrates three out of the four components of the Ugi reaction, the possibility of Passerini side reactions was possible, and in fact has been documented in other reactions employing the Ugi reaction.[10] With these considerations in mind, we set out to examine if Tron's multicomponent approach could be applied to assemble diverse and complex quinazolinones which could successfully rearrange into novel C3-substituted, (*E*)-amidoarylamidines to enhance our efforts to explore new biological space.

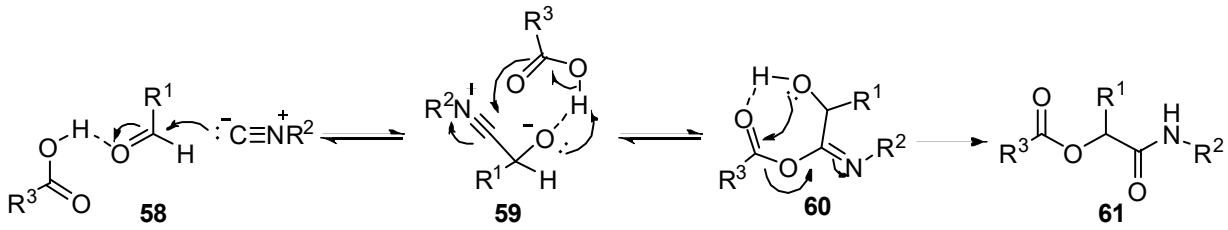

Scheme 13. Passerini three-component reaction mechanism generating α-acyloxycarboxamides

We began our work by examining Tron's published reaction conditions and applying them to a small sampling of Ugi four component reaction partners: *tert*-butyl methyl(2-(methylamino)ethyl)carbamate (**62**), which forms the diamine chain of appropriate length to facilitate the rearrangement based on our previously reported chemistry; aldehydes of varying steric bulk: isobutyraldehyde, isovaleraldehyde, or formaldehyde; 2-azidobenzoic acid; and an alkyl or aryl isocyanide: cyclohexyl- or 4-methoxyphenyl isocyanide (**Scheme 14**). The resulting

quinazolinones were subjected to trifluoroacetic acid Boc-deprotection conditions and then basified to pH 10 with sat. K_2CO_3 (aq) in acetonitrile, to assess the efficiency of the rearrangement to generate amidines bearing bulky C3-substituents. The intermediates were isolated with the aim of evaluating the efficiency of each reaction in the sequence. The reactions incorporating cyclohexyl isocyanide formed imides **63-b** in 83% and 55% yield respectively and though, some stating material remained after 12 hours, there was no observed Passerini side product **64a-b**. Consistent with Tron's findings, the reaction incorporating formaldehyde, generated 30% of the Passerini side product and no production of the desired imide. Furthermore, the reactions incorporating 4-methoxyphenyl isocyanide yielded the desired imides **63d-e** in 58% and 61% respectively, with no generation of the Passerini side product **64d-e**. The isolated imides were then subjected to the Staudinger/aza-Wittig cyclization conditions and produced the quinazolinone intermediates **65a-b** and **65d-e** in moderate to good yields ranging from 60-88%. The resulting quinazolinones were then subjected to the Boc-deprotection and subsequent basification conditions and generated the novel C3-substituted amidines **66a-b** and **66d-e** in 30-51% yield. Amidine **66a**, incorporating isobutyraldehyde and cyclohexyl isocyanide, had the highest overall yield with 32% for the six transformations over four steps, the other analogues yielded about 15% overall. Encouraged by these initial results, we started optimization with the goals of 1) improving imide yield, while continuing to suppress Passerini α-acyloxycarboxamide generation, 2) increasing the overall amidine yields, 3) streamlining the process, and 4) generating diverse C3-modified (*E*)-amidobenzamidines.

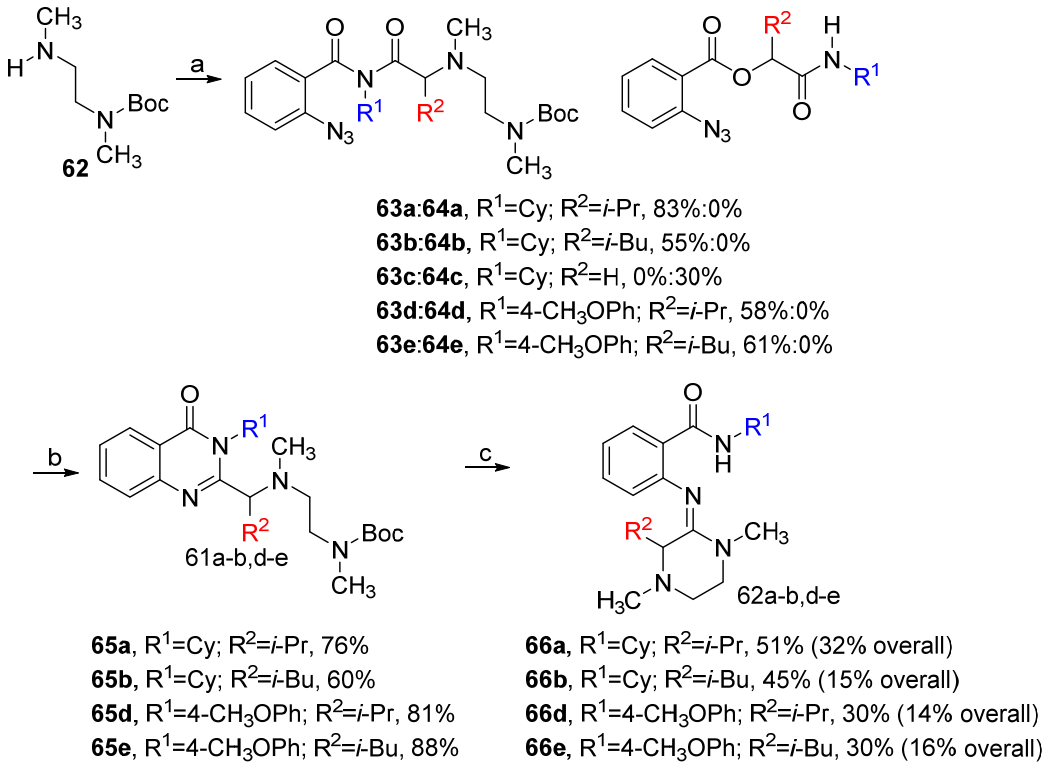

Reaction conditions: (a) 2-Azidobenzoic acid, R^1NC, R^2CHO (1 eq. each), 4 Å MS, CH_2Cl_2, rt, 12 h; (b) PPh_3, toluene, reflux, 12 h; (c) TFA, CH_2Cl_2, 0 °C–rt, 12 h; (d) aq. K_2CO_3, CH_3CN, μW, 150 °C, 1 h. Yields are based on isolated and purified products.

Scheme 14. Pilot chemistry to N-alkyl/C3 modified amidines.

We selected imide **63d** which incorporated *tert*-butyl methyl(2-(methylamino)ethyl)carbamate, isobutyraldehyde, 2-azidobenzoic acid, and 4-methoxyphenyl isocyanide to begin our imide generation optimization (**Table 1**), since it was one of the lowest yielding imides and resulted in the lowest overall yield for the reaction sequence. We observed that the 2-azidobenzoic acid was not completely soluble in CH_2Cl_2. Therefore, we added the reagent as a 1 M solution in 3:1 CH_2Cl_2:CH_3OH. In addition to aiding in the dissolution of the starting material, methanol been shown through DFT calculations to assist in the Ugi four-component reaction by stabilizing the nitrilium intermediate.[7a] We immediately observed a 10% increase in imide yield and no observed Passerini side product (**Entry 2**). In considering the

mechanism, we sought to increase the concentration of the reactive iminium ion intermediate to facilitate complete consumption of the azido acid. Consequently, we increased the equivalence of both the amine and the aldehyde to 1.5 equivalents but found only marginal improvement, also, we began to observe generation of a Passerini side product (**Entry 3**). Next, the equivalence of the isocyanide was also increased to 1.5 equivalents. We rationalized that increasing the isocyanide concentration would accelerate the interception of the iminium ion and formation of the nitrilium ion and thereby completely consume the azido acid starting material. We were pleased to observe an increased isolated imide yield of 85%, however, in addition to the increased yield of the desired imide, we also observed an increase in the observed Passerini side product (**Entry 4**). In our attempts to circumvent the side product formation, we examined the effect of reaction concentration and found that increasing the reaction concentration from 0.1 M to 0.2 M did not affect the overall yield significantly but suppressed the competing Passerini formation (**Entry 5**). Though, pre-reacting the amine and the aldehyde for nine minutes to allow time to pre-form the iminium ion with the reaction concentration at 0.2 M resulted in 91% isolated yield and complete consumption of the 2-azidobenzoic acid (**Entry 6**).

In order to validate the reaction conditions, they were applied to form imide **63b**, which was generated from *tert*-butyl methyl(2-(methylamino)ethyl)carbamate, isovaleraldehyde, 2-azidobenzoic acid, and cyclohexyl isocyanide and exhibited the lowest yield, 55%, in the pilot Ugi four-component reaction. The revised conditions only resulted in a marginal 5% improvement in the yield compared to that of the pilot reaction. We therefore continued to increase the equivalents of the reagents relative to the 2-azidobenzoic acid, under the premise that generating higher concentrations of the desired intermediates might facilitate complete conversion to product. We found that four equivalents of the aldehyde and isocyanide and two equivalents of the amine

relative to the azidobenzoic acid yielded the desired imide at an impressive 98% (**Entry 11**). This reflected a 43% increase in imide yield without any trace of a Passerini side product.

These optimized conditions were then applied to substrate **63d**, which reached 91% yield after the initial round of optimization (**Entry 6**), and still resulted in a good isolated imide yield of 85% (**Entry 7**). We were also pleased to observe the application of these conditions to imide **63e**, which incorporated isovaleraldehyde and 4-methoxyphenyl isocyanide, increased the yield from 61% (**Entry 12**) to 78% (**Entry 15**). Likewise, imide **63a**, comprised of isobutyraldehyde and cyclohexyl isocyanide increased from 83% (**Entry 16**) to 89% (**Entry 17**). Satisfied with these results we turned our attention to the other reactions in the sequence.

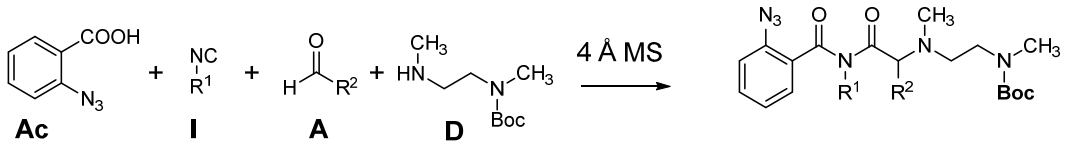

Entry	stoichiometry (D:A:Ac:I)	Conditions of premixing D and A or not before addition of Ac and I	Final Reaction Conc	Solvent	Isocyanide (I)	Aldehyde (A)	Imide Yield	Acid SM Consumed	Passerini
					R^1	R^2			
1	(1:1:1:1)	no premix	0.1 M	CH_2Cl_2	4-MeO-phenyl	i-Pr	58%	N	N
2	(1:1:1:1)	no premix	0.1 M	CH_2Cl_2:CH_3OH	4-MeO-phenyl	i-Pr	68%	N	N
3	(1.5:1.5:1:1)	no premix	0.1 M	CH_2Cl_2:CH_3OH	4-MeO-phenyl	i-Pr	73%	N	2% (LCMS)
4	(1.5:1.5:1:1.5)	no premix	0.1 M	CH_2Cl_2:CH_3OH	4-MeO-phenyl	i-Pr	85%	N	7% (LCMS)
5	(1.5:1.5:1:1.5)	no premix	0.2 M	CH_2Cl_2:CH_3OH	4-MeO-phenyl	i-Pr	82%	N	N
6	(1.5:1.5:1:1.5)	premix 9 min	0.2 M	CH_2Cl_2:CH_3OH	4-MeO-phenyl	i-Pr	91%	N	N
7	(2:4:1:4)	no premix	0.2 M	CH_2Cl_2:CH_3OH	4-MeO-phenyl	i-Pr	85%	Y	N
8	(1:1:1:1)	no premix	0.1 M	CH_2Cl_2	cyclohexyl	i-Bu	55%	N	N
9	(2:2:1:2)	premix 8 min	0.2 M	CH_2Cl_2:CH_3OH	cyclohexyl	i-Bu	60%	N	N
10	(2:3:1:3)	premix 6 min	0.2 M	CH_2Cl_2:CH_3OH	cyclohexyl	i-Bu	80%	N	N
11	(2:4:1:4)	premix 6 min	0.2 M	CH_2Cl_2:CH_3OH	cyclohexyl	i-Bu	98%	Y	N
12	(1:1:1:1)	no premix	0.1 M	CH_2Cl_2	4-MeO-phenyl	i-Bu	61%	N	
13	(2:2:1:2)	premix 10 min	0.2 M	CH_2Cl_2:CH_3OH	4-MeO-phenyl	i-Bu	62%	Y	N
14	(2:3:1:3)	premix 17 min	0.2 M	CH_2Cl_2:CH_3OH	4-MeO-phenyl	i-Bu	65%	Y	N
15	(2:4:1:4)	premix 12 min	0.2 M	CH_2Cl_2:CH_3OH	4-MeO-phenyl	i-Bu	78%	Y	N
16	(1:1:1:1)	no premix	0.1 M	CH_2Cl_2	cyclohexyl	i-Pr	83%	N	N
17	(2:4:1:4)	premix 10 min	0.2 M	CH_2Cl_2:CH_3OH	cyclohexyl	i-Pr	89%	Y	N

D = diamine; A = aldehyde; Ac = Acid; I = isocyanide; SM = starting material

Table 1. Ugi imide (**63**) optimization

The Staudinger/aza-Wittig conditions implemented in the pilot sequence provided reasonable yields. Therefore, our efforts focused on the quinazolinone *N*-Boc deprotection/ rearrangement protocol. In our pilot reactions, the *N*-Boc deprotection was performed with trifluoroacetic acid, and subsequent basification of the TFA salt with Na_2CO_3 promoted the quinazolinone rearrangement. However, we observed that when the 2-alkylamino quinazolinone substrates were subjected to these conditions, side products were generated, which complicated the final isolation of the amidine and consequently diminished the isolated yield. Therefore, we attempted the deprotection in CH_2Cl_2 using 4 N HCl in dioxane for 12 hours and we were gratified to see the reaction proceeded far cleaner than the previous TFA deprotection. The resulting HCl salt was concentrated *in vacuo*, and then basified in methanol with triethylamine under microwave conditions (100 °C) for 30 min. These modified conditions resulted in the isolation of amidine **66a** (**Table 2**) in 66% yield from quinazolinone **65a**, bringing the overall yield for the analogue to 45% (82% average yield per step) over the four-step sequence, an improvement of 13% overall compared to the original pilot sequence. With conditions in-hand, we continued our feasibility assessment to determine the effects of substituent modifications on the reaction sequence.

We were pleased to observe that the overall reaction yields for the pilot analogues all increased, though **66d** only exhibited a modest 2% increase in overall yield owing to a low yield for the deprotection and rearrangement steps. However, **66b** and **66e** increased by 5% and 11% overall yield, respectively. Importantly, when the optimized conditions were applied in an attempt form imide **63c**, which incorporated formaldehyde and failed to form the imide in the pilot reaction, we were able to isolate 45% of the imide and subsequently formed the desired C3-unsubstituted-*N*-cyclohexyl-(*E*)-amidobenzamidine **66c** in 23% overall yield (69% average yield per step). Additionally, we employed our method to an analogue combining *tert*-butyl methyl(2-

(methylamino)ethyl)carbamate, benzaldehyde, 2-azidobenzoic acid, and cyclohexyl isocyanide. Tron's existing work reported sluggish reactivity when incorporating aryl aldehydes as a Ugi four-component reaction partner, taking up to three days for complete conversion to the imide. Under our conditions, we observed complete conversion in 12 hours and 97% isolated yield of imide **63g**. This substrate was also competent in the follow-on reactions, generating quinazolinone **65g** in 82% yield and finally forming amidine **66g** in 68% (54% overall yield). Interestingly, the quinazolinone rearrangement to (*E*)-amidobenzamidines demonstrated robustness in its ability to rearrange despite significant steric bulk in the ensuing amidine C3-position.

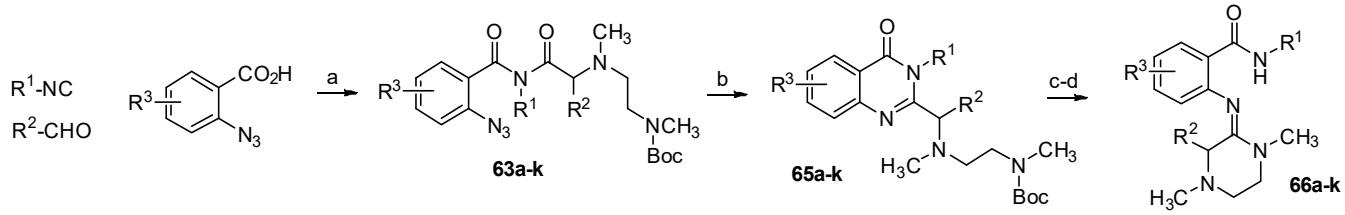

Entry	Isocyanide	Aldehyde	Acid	Imide **59a-k**		Quinazolinone **61a-k**		Benzamidine **62a-k**		Overall yield **62a-k** (%)
	R^1	R^2	R^3	cmpd	yield (%)	cmpd	yield (%)	cmpd	yield (%)	
1	cyclohexyl	isopropyl	H	**63a**	89	**65a**	76	**66a**	66	45
2	cyclohexyl	isobutyl	H	**63b**	98	**65b**	60	**66b**	34	20
3	cyclohexyl	H	H	**63c**	45	**65c**	89	**66c**	58	23
4	4-CH_3O-phenyl	isopropyl	H	**63d**	85	**65d**	88	**66d**	23[c]	17
5	4-CH_3O-phenyl	isobutyl	H	**63e**	78	**65e**	88	**66e**	39[c]	27
6	cyclohexyl	cyclopropyl	H	**63f**	89	**65f**	70	**66f**	65	40
7	cyclohexyl	phenyl	H	**63g**	97	**65g**	82	**66g**	68	54
8	isopropyl	isopropyl	H	**63h**	88	**65h**	71	**66h**	52	32
9	cyclohexyl	isopropyl	5-CH_3	**63i**	78	**65i**	69	**66i**	64	34
10	cyclohexyl	isopropyl	5-F	**63j**	ND	**65j**	84	**66j**	40	34
11	cyclohexyl	isopropyl	4-CH_3	**63k**	67	**65k**	70	**66k**	61	29

[a]Conditions: (a) **62**, R^2CHO, 6-12 min, then 2-azidobenzoic acid in 3:1 CH_2Cl_2/CH_3OH, R^1NC, (2:4:1:4), 4 Å MS, CH_2Cl_2, rt, 12 h; (b) PPh_3, toluene, rt, 30 min, then 110°C, 12h; (c) 4N HCl, dioxane, 0°C – rt, 12h; (d) Et_3N, CH_3OH, MWI 100°C, 30 min. [b]Isolated yields: avg of n≥2 expts. [c]1 h reaction time; ND = not determined, crude material advanced.

Table 2. Feasibility assessment and yields for optimized stepwise sequence leading to novel quinazolinones and benzamidines[a,b]

We hypothesized that the overall yield for the four-step, six-transformation process could be improved by removing intermediate isolation and telescoping the entire procedure.[11] Tron's

researchers were able to convert the Ugi four-component reaction and Staudinger/aza-Wittig strategy into a one-pot reaction, requiring an exchange of solvent and a single purification to isolate their desired quinazolinones.[1] Also, the Golden lab's previous work demonstrated that our quinazolinone formation and subsequent rearrangement chemistry to form C3-unsubstituted benzamidines was amenable to a one-pot process.[12] However, we could not assume that our method would likewise be amenable to streamlining by removing the intermediate isolation. Tron's existing work employed equimolar equivalents of the Ugi components as compared to our method which used in some cases four-fold excess reagents relative to the 2-azidobenzoic acid. There was no guarantee that these excess reagents would not generate side products that could interfere in the quinazolinone cyclization or ensuing quinazolinone rearrangement under our reaction conditions.

To investigate a more streamlined approach, we looked for opportunity to further refine and improve the sequence. In our examination of the reaction conditions, we observed that the isolation following the Staudinger/aza-Wittig cyclization was complicated by the presence of the triphenylphosphine oxide by-product. We therefore decided to employ resin-bound triphenylphosphine. This alteration allowed us to filter off the resin after the Staudinger/aza-Wittig quinazolinone cyclization step and in the process remove the triphenylphosphine oxide.[13] We were pleased to find that this simplified the purification of the quinazolinone intermediate. Hence, we implemented this modification into the telescoped process in order to reduce the presence of by-products in the late stage reactions and consequently simplify the benzamidine isolation.

Our initial attempt to telescope the four-step, six-transformation protocol, sought to generate (E)-amidobenzamidine **66a**, a scaffold generated via the stepwise method that incorporated *tert*-butyl methyl(2-(methylamino)ethyl)carbamate, isobutyraldehyde, 2-

azidobenzoic acid, and cyclohexyl isocyanide (**Scheme 15**). We were excited to see that our modifications to the aza-Wittig procedure, as well as telescoping the reaction sequence, resulted in a 61% overall yield (88% average yield per step), an increase of 16% overall from the stepwise procedure. Additionally, the telescoped protocol resulted in 64% overall yield for this analogue when run at 1.0 mmol scale. Considering those positive outcomes, we attempted to generate the remainder of the analogues previously prepared by the stepwise sequence via the telescoped approach, and every analogue was isolated in significantly higher yield, the lowest improvement was 11% for amidine **66i**. Amidine **66b** exhibited the largest improvement in overall yield, 40%, as a result of the implementation of the telescoped sequence being isolated in 60% overall yield. Notably, benzamidine **66d**, which produced only 17% overall yield in the stepwise procedure was generated in 40% yield (79% average yield per step) when incorporating the streamlined approach. Also, (*E*)-amidobenzamidine **66f**, which incorporated cyclopropane carboxaldehyde and cyclohexyl isocyanide, produced the highest overall yield in this series at 70% (91% average yield per step). This was an improvement of 30% compared to the initial stepwise result for that analogue.

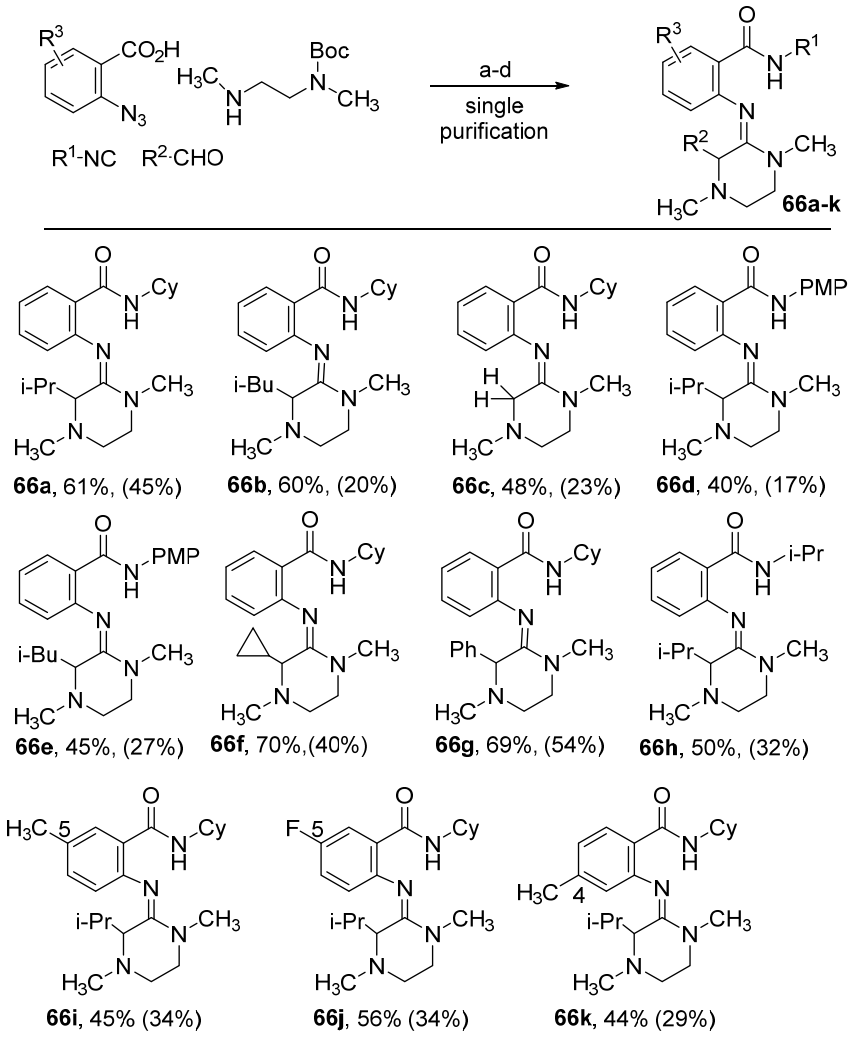

Conditions: (a) Amine, R_2CHO, 6–12 min, then 2-azidobenzoic acid in 3 : 1 CH_2Cl_2/CH_3OH, R_1NC, (2 : 4 : 1 : 4), 4 Å MS, CH_2Cl_2, rt, 12 h; (b) PS-PPh_3, tol, rt, 30 min, then 110 °C, 12 h; (c) 4 N HCl, dioxane, 0 °C–rt, 12 h; (d) Et_3N, CH_3OH, MWI 100 °C, 30 min. Yields: avg of n ≥ 2 expts. Parenthetical yields: stepwise protocol. PMP = p-methoxyphenyl, Cy = cyclohexyl.

Scheme 15. Amidines resulting from a telescoped Ugi–Mumm–Staudinger/aza-Wittig-quinazolinone rearrangement sequence

Encouraged by these results we sought to broaden the diversification of the benzamidine scaffold (**Scheme 16**). We were interested in the effects of increasing steric bulk in the vicinity of the C3-substuent on the benzamidine and examining its effect on the quinazolinone rearrangement. Specifically, would the introduction of steric bulk in benzene ring directed at the C3-substitutent

hinder the rearrangement or otherwise affect the scaffold. In our previous work, we attributed the exclusive isolation of (*E*)-amidobenzamidine to the steric interaction that would result between the planar *N*-substitutent of the amidine and the benzene core. The C3-amidine substituent could potentially force the piperazine-like ring to modify its conformation in order to accommodate the additional steric bulk. Therefore, we sought to generate benzamidine **66m**, which incorporated 3-methyl-2-azidobenzoic acid as a Ugi component, and **66n**, which incorporated 3-fluoro-2-azidobenzoic acid as a Ugi component, both in conjunction with isobutyraldehyde which form a C3-isopropyl-benzamidine. Surprisingly, both analogues were competent in the four-step protocol, generating the desired (*E*)-C3-isopropyl-amidobenzamide in 35% and 42% respectively. Interestingly, 6-methyl- and 6-fluoro-2-azidobenzoic acid were not compatible with the method as they formed exclusively Passerini α-acyloxycarboxamide side product under our multicomponent reaction conditions. We assume that the steric interaction of the 6-substituent on the benzene core hindered the Mumm rearrangement and thereby favored the alternate Passerini three component reaction pathway.

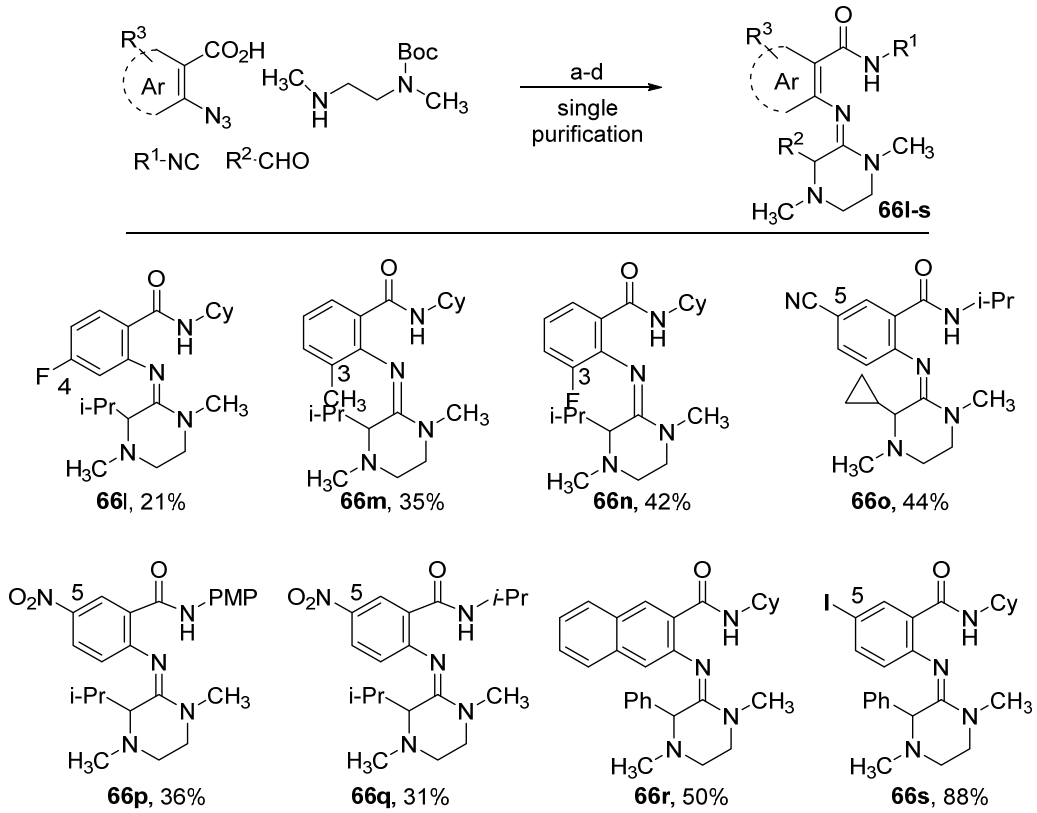

Conditions: (a) Amine, R_2CHO, 6–12 min, then 2-azidobenzoic acid in 3 : 1 CH_2Cl_2/CH_3OH, R_1NC, (2 : 4 : 1 : 4), 4 Å MS, CH_2Cl_2, rt, 12 h; (b) PS-PPh_3, tol, rt, 30 min, then 110 °C, 12 h; (c) 4 N HCl, dioxane, 0 °C–rt, 12 h; (d) Et_3N, CH_3OH, MWI 100 °C, 30 min. Yields: avg of n ≥ 2 expts. PMP = p-methoxyphenyl, Cy = cyclohexyl.

Scheme 16. Amidines resulting from a telescoped Ugi–Mumm–Staudinger/aza-Wittig-quinazolinone rearrangement sequence

In order to understand how the scaffold was able to accommodate the steric bulk of the substituents at the C3-position, we attempted to recrystallize numerous substrates in hopes of elucidating more information through x-ray crystallography. Fortunately, amidine **66s**, which was assembled using 5-iodo-2-azidobenzoic acid and benzaldehyde, was successfully recrystallized from acetonitrile and formed crystals that provided further insight (**Fig. 4)**. The crystal structure revealed that significant puckering of the piperazine-like ring enabled the steric bulk of the C3-amidine substituent to be accommodated. This is consistent with our previous hypothesis explaining exclusive (*E*)-amidobenzamidine formation, since the planarity of the *N*-alkyl

substituent would preclude such an accommodation in the (*Z*)-configuration. Additionally, the amidine is also forced to rotate the *N*-aryl bond placing the amidine N-C double bond out of plane with the phenyl ring. We assume the cost of losing orbital overlap that allows for electron delocalization into the aryl π-system is lower than the steric interaction that would result from keeping the amidine N-C double bond in the plane of the phenyl ring.

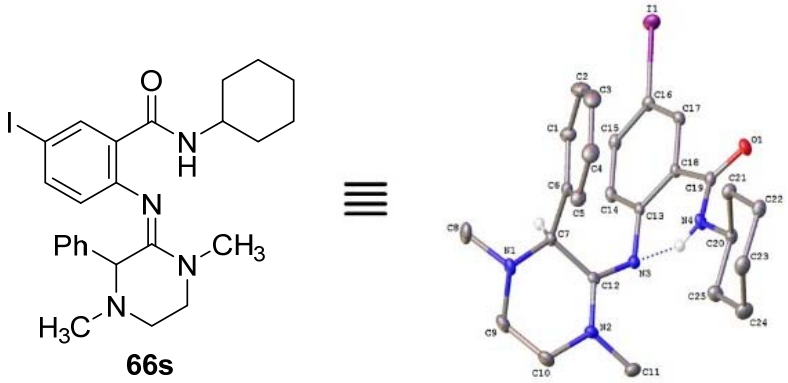

Figure 4. Molecular drawing of **66s** shown with 50% probability ellipsoids.

Importantly, the telescoped method allowed for significant modifications to the original (*E*)-amidobenzamidine scaffold. Amidine **66u**, incorporated a cyclic asymmetric diamine, which demonstrates the potential to incorporate chirality into the scaffold. Moreover, amidine **66t** demonstrated the efficient incorporation of 5-thiazole carboxaldehyde in order to install an aryl heterocyclic C3-substituent with an overall yield of 60%. Additionally, 3-azido-2-furanoic acid and 3-azido-thiophene-2-carboxylic acid were both competent in producing novel heterocyclic quinazolinones which could undergo the rearrangement and form amidines **66v-x**. Notably, **66x** illustrates the possible complexity and diversification that can be introduced into the (*E*)-arylamidine scaffold incorporating thiophene into the core, as well as integrating 2-morpholinoethyl isocyanide and an asymmetric diamine.

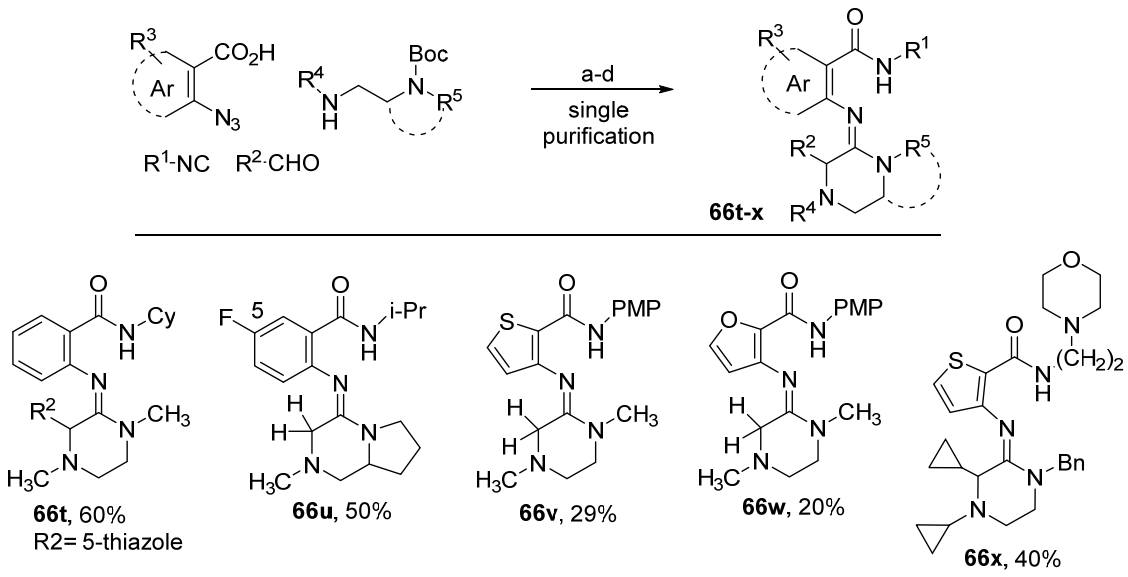

Conditions: (a) Amine, R_2CHO, 6–12 min, then 2-azidobenzoic acid in 3 : 1 CH_2Cl_2/CH_3OH, R_1NC, (2 : 4 : 1 : 4), 4 Å MS, CH_2Cl_2, rt, 12 h; (b) PS-PPh3, tol, rt, 30 min, then 110 °C, 12 h; (c) 4 N HCl, dioxane, 0 °C–rt, 12 h; (d) Et_3N, CH_3OH, MWI 100 °C, 30 min. Yields: avg of n ≥ 2 expts. PMP = p-methoxyphenyl, Cy = cyclohexyl.

Scheme 17. (E)-arylamidines resulting from a telescoped Ugi–Mumm–Staudinger/aza-Wittig-quinazolinone rearrangement sequence

However, we found some limitations with respect to the quinazolinone rearrangement while trying to incorporate certain components into the scaffold. In our efforts to incorporate heterocycles into the core, we discovered that both 3-azido-2-benzofuranoic acid and the analogous 3-azido-benzo[*b*]thiophene-2-carboxylic acid when used in conjunction with cyclopropane carboxaldehyde and 5-thiazolecarboxaldehyde, respectively, did not rearrange to form (*E*)-arylamidines. We were only able to isolate the free-based 2-alkylquinazolinones **67 and 68** (**Fig. 5**), even after trying to force the rearrangement by heating the reaction mixture to 170 °C. We speculate that this is due to a steric effect of the fused heterocyclic core.

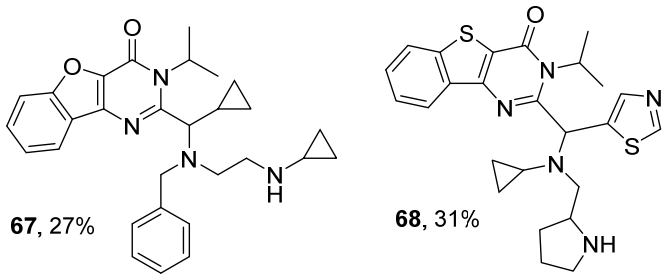

Figure 5. Isolated 2-alkylquinazolinones **67** and **68**

The (*E*)-amidobenzamidine chemotype discovered by the Golden lab is a noteworthy addition to the *N′,N,N*-trisubstituted amidine scaffold, which features a broad range of diverse pharmacologically relevant molecules. It was incumbent upon us to find a method to efficiently diversify the (*E*)-arylamidine in order to effectively assess the structure activity relationships of the chemotype as it applied to the antiviral program, and potentially other pathogens. In those efforts we sought to incorporate substitution in the C3-position of the amidine, but we also required a method that would give us access to broader diversification. By incorporating a Ugi-Mumm-Stuadinger/aza-Wittig strategy, we were able to build a modular approach, which gives access to complex 2-alkylamino substituted 2,3-disubstituted-4(3H)-quinazolinones that can effectively form diversely substituted novel C3-substituted-(*E*)-arylamidines. This method allowed for the efficient generation of *N*-alkyl and *N*-aryl amides, but also permitted the incorporation of formaldehyde to produce C3-unsubstituted analogues, allowed for the expeditious incorporation of aryl aldehydes into key intermediates and allowed for the incorporation of heterocycles into the core. Moreover, we were able to telescope the method thereby reducing waste and saving time, but importantly providing access to the novel C3-modified-(*E*)-arylamidines in good yields after the four-step, six-transformation procedure.[15]

References:

1. Mossetti, R.; Pirali, T.; Saggiorato, D.; Tron, G.C. Imides: forgotten players in the Ugi reaction. One-pot multicomponent synthesis of quinazolinones. *Chem. Commun.*, **2011**, **47**, 6966-6968.

2. Ugi, I.; Meyr, R.; Fetzer, U.; Steinbrückner, C. Versuche mit Isonitrikn. *Angew. Chem.* **1959**, 71, 386.

3. (a) Dömling A.; Ugi, I. Multicomponent Reactions with Isocyanides. *Angew. Chem. Int. Ed.* **2000**, 39, 3168-3210; (b) Dömling A. Recent Developments in Isocyanide Based Multicomponent Reactions in Applied Chemistry. *Chem. Rev*. **2006**, 106, 17-89; (c) Akritopoulou-Zanze, I. Isocyanide-based multicomponent reactions in drug discovery. *Curr Opin Chem Biol*. **2008**, 12, 324–331;(d) Bienaymé, H.; Hulme, C.; Oddon, G.; Schmitt, P. Maximizing Synthetic Efficiency: Multi-Component Transformations Lead the Way. *Chem. Eur. J.* **2000**, 6, 3321−3329.

4. Ugi, I.; Meyr, R. Isonitriles. V. Extended scope of the Passerini reaction.*Chem. Ber.* **1961**, 94, 2229−2233.

5. Mumm, O. Umsetzung von Säureimidchloriden mit Salzen organischer Säuren und mit Cyankalium. *Ber. Dtsch. Chem. Ges*. **1910**, 43, 886-893.

6. Takeuchi, H.; Hagiwara, S.; Eguchi, S. A new efficient synthesis of imidazolinones and quinazolinone by intramolecular aza-Wittig reaction**.** *Tetrahedron*, **1989**, 45, 6375-6386.

7. (a) Chéron, N.; Ramozzi, R.; El Kaïm, L.; Grimaud, L.; Fleurat-Lessard, P. Challenging 50 Years of Established Views on Ugi Reaction: A Theoretical Approach. *J. Org. Chem*. **2012**, 77, 1361−1366; (b) Iacobucci, C.; Reale, S.; Gal, J-F.; De Angelis, F. Insight into the Mechanisms of the Multicomponent Ugi and Ugi–Smiles Reactions by ESI-MS(/MS). *Eur. J. Org. Chem.* **2014**, 7087–7090. (c) Iacobucci, C.; Reale, S.; De Angelis, F. Elusive Reaction Intermediates in Solution Explored by ESI-MS: Reverse Periscope for Mechanistic Investigations. *Angew. Chem. Int. Ed*. **2016**, 55, 2980–2993; (d) Ugi, I.; Offermann, K. Asymmetric 1,3-Induction during the α-Addition of Immonium Ions and Carboxylate Anions onto Isonitriles. *Angew. Chem. Int. Ed. Engl.* **1963,** *2*, 624.

8. Passerini M.; Simone, L. *Gazz. Chim. Ital.*, 1921, **51**, 126.

9. Ramozzi R.; Morokuma, K. Revisiting the Passerini Reaction Mechanism: Existence of the Nitrilium, Organocatalysis of Its Formation, and Solvent Effect. *J. Org. Chem.*, **2015**, 80, 5652-5657.

10. (a) Zhang, J.; Yu, P.; Li, S-Y.; Sun, H.; Xiang, S-H.; Wang, J.; Houk, K.N.; Tan B. Asymmetric phosphoric acid–catalyzed four-component Ugi reaction. *Science.* **2018**, 361, eaas8707; (b) Wehlan, H.; Oehme, J.; Schäfer, A.; Rossen, K. Development of Scalable Conditions for the

Ugi Reaction—Application to the Synthesis of (*R*)-Lacosamide. *Org. Process Res. Dev.* **2015**, 19, 1980−1986.

11. Hayashi, Y. Pot economy and one-pot synthesis. *Chem. Sci.* **2016**, 7, 866-880.

12. Schroeder, C.E.; Neuenswander, S.A.; Yao, T.; Aubé, J.; Golden, J.E. One-pot, regiospecific assembly of (E)-benzamidines from δ- and γ-amino acids via an intramolecular aminoquinazolinone rearrangement. *Org. Biomol. Chem*. **2016**, 14, 3950–3955.

13. Ley, S.V.; Baxendale, I.R.; Bream, R.N.; Jackson, P.S.; Leach, A.G.; Longbottom, D.A.; Nesi, M.; Scott, J.S.; Storer, R.I.; Taylor, S.J. Multi-step organic synthesis using solid-supported reagents and scavengers: a new paradigm in chemical library generation. *J. Chem. Soc., Perkin Trans. 1*, **2000**, 3815-4195.

14. Schroeder, C.E.; Yao, T.; Sotsky, J.; Smith, R.A.; Roy, S.; Chu, Y-K.; Guo, H.; Tower, N.A.; Noah, J.W.; McKellip, S.; Sosa, M.; Rasmussen, L.; Smith, L.H.; White, E.L.; Aubé, J.; Jonsson, C.B.; Chung, D.; Golden, J.E. Development of (E)-2-((1,4-Dimethylpiperazin-2-ylidene)amino)-5-nitro-N-phenylbenzamide, ML336: Novel 2-Amidinophenylbenzamides as Potent Inhibitors of Venezuelan Equine Encephalitis Virus. *J. Med. Chem*. **2014**, 57, 8608−862.

15. Jaffett, V.A.; Nerukar, A.; Cao, X.; Guzei, I.; Golden, J.E. Telescoped synthesis of C3-functionalized (*E*)-arylamidines using Ugi–Mumm and regiospecific quinazolinone rearrangements. *Org. Biomol. Chem.* **2019**, 17, 3118-3128.

Chapter 3. Telescoped synthesis of C5-functionalized novel tetracyclic quinazolinones using Ugi-Mumm and regioselective quinazolinone rearrangements

Using an optimized, telescoped, Ugi four-component reaction and tandem Staudinger/aza-Wittig strategy, the Golden lab synthesized complex 2-alkylamino 2,3-disubstituted-4-(3H)-quinazolinones that were challenging to construct by other methods (**69, Scheme, 18**).[1] The quinazolinones were subsequently transformed into novel C3-modified-(*E*)-amidoarylamidines (**71**), a chemotype of interest for our group's antiviral program, via an intramolecular rearrangement that proceeded through spirocyclic intermediate (**70**).[2]

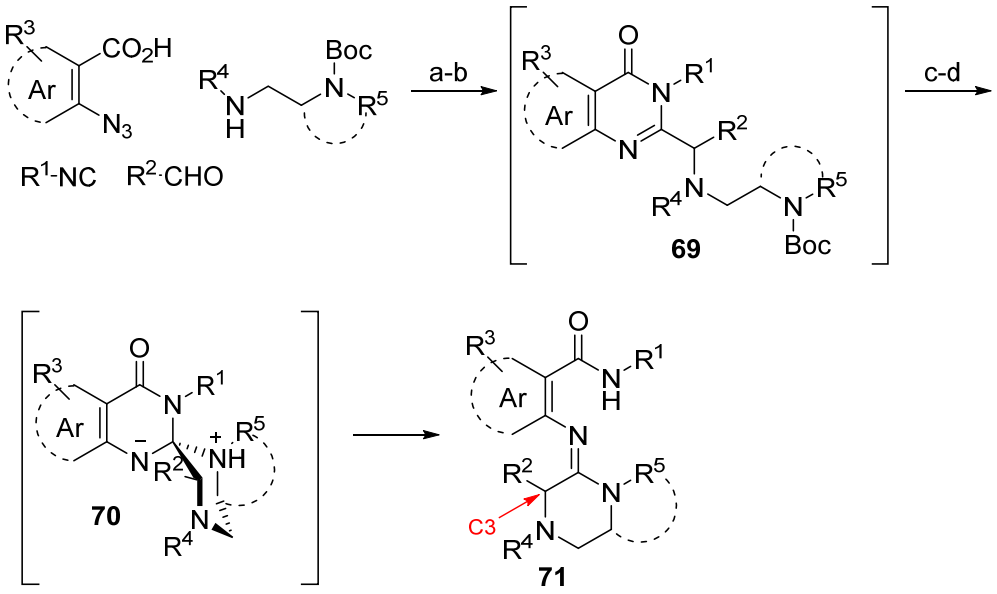

Conditions: (a) Amine, R_2CHO, 6–12 min, then 2-azidobenzoic acid in 3 : 1 CH_2Cl_2/CH_3OH, R_1NC, (2 : 4 : 1 : 4), 4 Å MS, CH_2Cl_2, rt, 12 h; (b) PS-PPh_3, tol, rt, 30 min, then 110 °C, 12 h; (c) 4 N HCl, dioxane, 0 °C–rt, 12 h; (d) Et_3N, CH_3OH, MWI 100 °C, 30 min.

Scheme 18. (*E*)-arylamidines resulting from a telescoped Ugi–Mumm–Staudinger/aza-Wittig-quinazolinone rearrangement sequence[1]

Hitherto, quinazolinone intermediates were generated containing terminal *N*-Boc protected secondary amines (**72**, **Scheme 19**), resulting in exclusive (*E*)-benzamidine formation (**73**). We

attributed this to the steric interaction that would result between the planar *N*-alkyl substituent of the resulting cyclic amidine and the phenyl ring in the formation of a (*Z*)-amidobenzamidine (**74**).

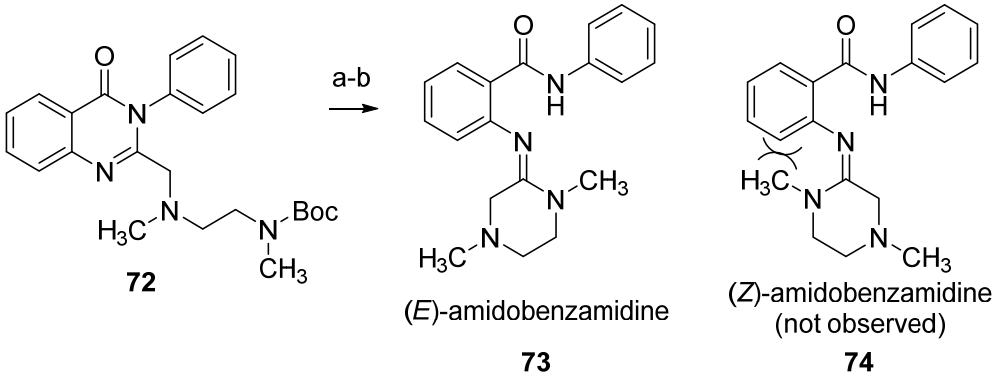

Conditions: (a) TFA, CH_3CN, 1-2 h; (b) sat. $NaHCO_3$ (aq), 40 °C, 1-1.5 h

Scheme 19. Rearrangment of 2-alkylamino quinazolinone **72** to yield (*E*)-amidobenzamidine **73** and proposed steric interaction preventing formation of (*Z*)-amidobenzamidine **74**

Consequently, the regiospecificity of the rearrangement was investigated by employing our telescoped multicomponent approach to access a quinazolinone intermediate containing a terminal *N*-Boc protected primary amine (**Scheme 20**). Using racemic *tert*-butyl *N*-(pyrrolidin-2-ylmethyl)carbamate (**75)**, formalin, 2-azido-5fluorobenzoic acid, an benzyl isocyanide in the Ugi four component reaction conditions followed by the Staudinger/aza-Wittig cyclization, formation of 2-alkylamino quinazolinone (**76**) bearing a terminal *N*-Boc protected primary amine was anticipated. Upon deprotection and subsequent basification under microwave conditions, the resulting amidine would no longer contain an *N*-alkyl substituent, but rather an *NH* group, thereby reducing steric repulsion with the phenyl ring of the core. It was uncertain if this would permit isolation of an elusive (*Z*)-benzamidine (**78**).

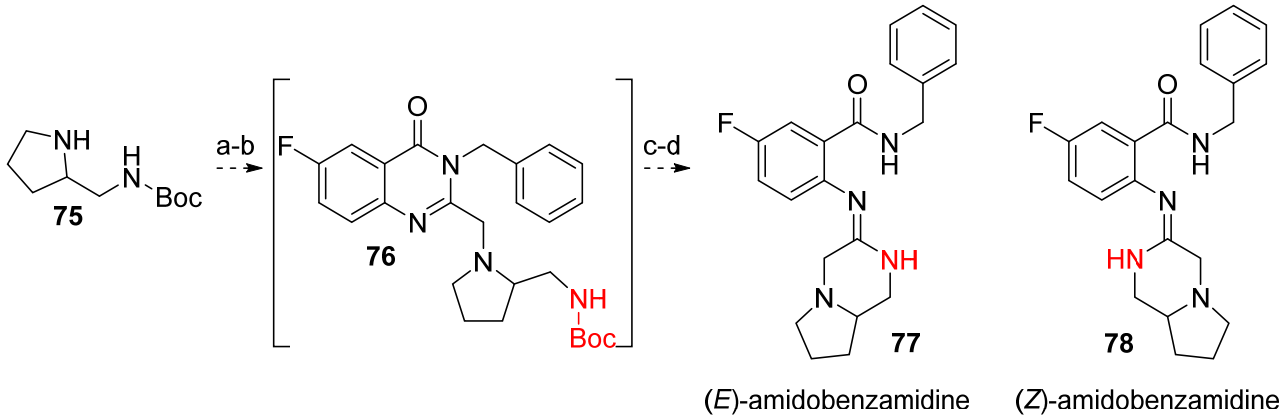

[a]Conditions: (a) **72**, formalin, 6-12 min, then 5-fluoro-2-azidobenzoic acid in 3:1 CH_2Cl_2/CH_3OH, benzyl isocyanide, (2:4:1:4), 4 Å MS, CH_2Cl_2, rt, 12 h; (b) PS-PPh_3, toluene, rt, 60 min, then 110 °C, 12h; (c) 4N HCl, dioxane, 0 °C – rt, 12h; (d) Et_3N, CH_3OH, MWI 100 °C, 30 min.

Scheme 20. Proposed reaction to generate amidobenzamidines **77** and **78**

We were surprised to find that the isolated product was neither the (*E*)- or (*Z*)-amidobenzamidine, but rather tetracyclic quinazolinone **79** in 40% yield (**Scheme 21**). The overall yield was comparable to other C3-unsubstituted amidines we generated using formaldehyde in our telescoped approach (see **Chapter 2**, **Scheme 14**), and likely was the result of low turnover in the initial imide forming step. However, this still reflected a 79% average yield per step, over the four-step telescoped procedure. Intrigued by this result, we sought a better understanding of this unexpected transformation.

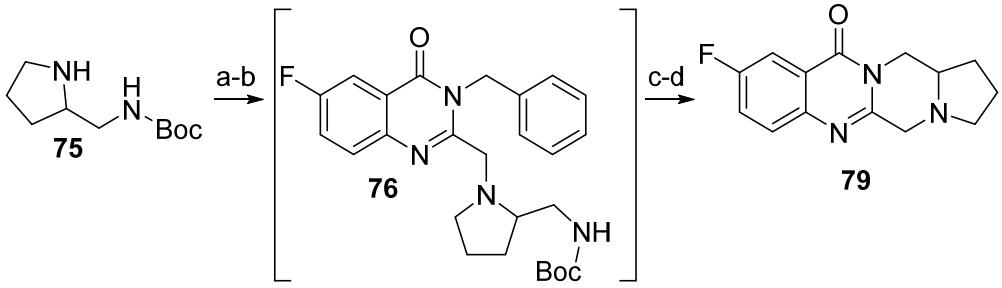

Conditions: same as shown in **Scheme 20**.

Scheme 21. Tetracyclic fused quinazolinone **79** resulting from a telescoped Ugi–Mumm–Staudinger/aza-Wittig-quinazolinone rearrangement sequence

In order to simplify the reaction and eliminate the possibility of the transformation being induced by the excess reagents present under the telescoped reaction conditions, we sought to synthesize 1,2,3,4-tetrahydro-2-methyl-6*H*-pyrazino[2,1-*b*]quinazolin-6-one using our original stepwise method to generate (*E*)-amidobenzamidines (**82**, **Scheme 22**). This procedure enabled us to arrest the reaction and isolate the terminal *N*-Boc protected 2-alkylamino-quinazolinone intermediate (**81**) in 84% yield. We were pleased to observe that upon *N*-Boc deprotection with trifluoroacetic acid, followed by basification to pH 10, we isolated quinazolinone **82** in 76% yield. With this result in hand we formulated a hypothesis for the mechanism of the novel quinazolinone rearrangement.

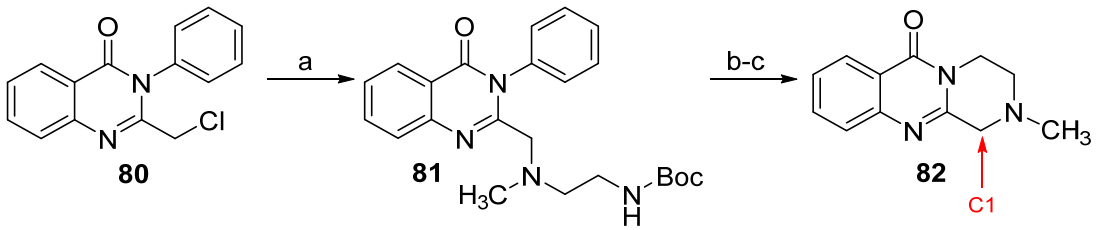

Conditions: (a) *tert*-butyl methyl(2-(methylamino)ethyl)carbamate, KI, K_2CO_3, CH_3CN, 80 °C, 70 min, 84%; (b) TFA, CH_2Cl_2, 1 h; (c) Na_2CO_3 (aq) pH 10, 76%.

Scheme 22. Stepwise procedure to form C1-unsubstituted tricyclic quinazolinone **95**.

We hypothesized that the transformation began with the deprotection and basification to liberate the terminal free amine of 2-alkylamino substituted quinazolinone (**83**, **Scheme 23**). Next, nucleophilic attack on the imine carbon of the quinazolinone intermediate by the terminal primary amine formed the spirocycle intermediate **84**. Following a proton transfer to form intermediate **85**, the spirocyclic quinazolinone then undergoes the irreversible quinazolinone opening to form either the (*E*)-amidobenzamidine (**77**) or the (*Z*)-amidobenzamidine (**78**). However, the resulting cyclic amidine bearing the *NH* instead of the *N*-alkyl substituent, such as the benzamidine formed in this step provided access to tautomers **87** and **88**.[3] We assumed that the tautomers can rotate about the

N-C bond (**86**) to access either isomer. Nevertheless, whether it directly forms the (*Z*)-amidine **78** or an equilibrium exists between the (*E*)- and (*Z*)-amidines, only (*Z*)-amidobenzamidine **78** is oriented to undergo a nucleophilic attack on the amide carbonyl initiating the intramolecular ring closure. The proposed nucleophilic attack by the amidine is similar to what is hypothesized to occur when using 1,8-diazabicyclo[5.4.0]undec-7-ene as a catalyst in N,N'-carbonyldiimidazole-mediated amidations.[4] This would result in intermediate **89**, which after proton transfer and subsequent elimination of benzylamine formed the observed tetracyclic quinazolinone (**79**).

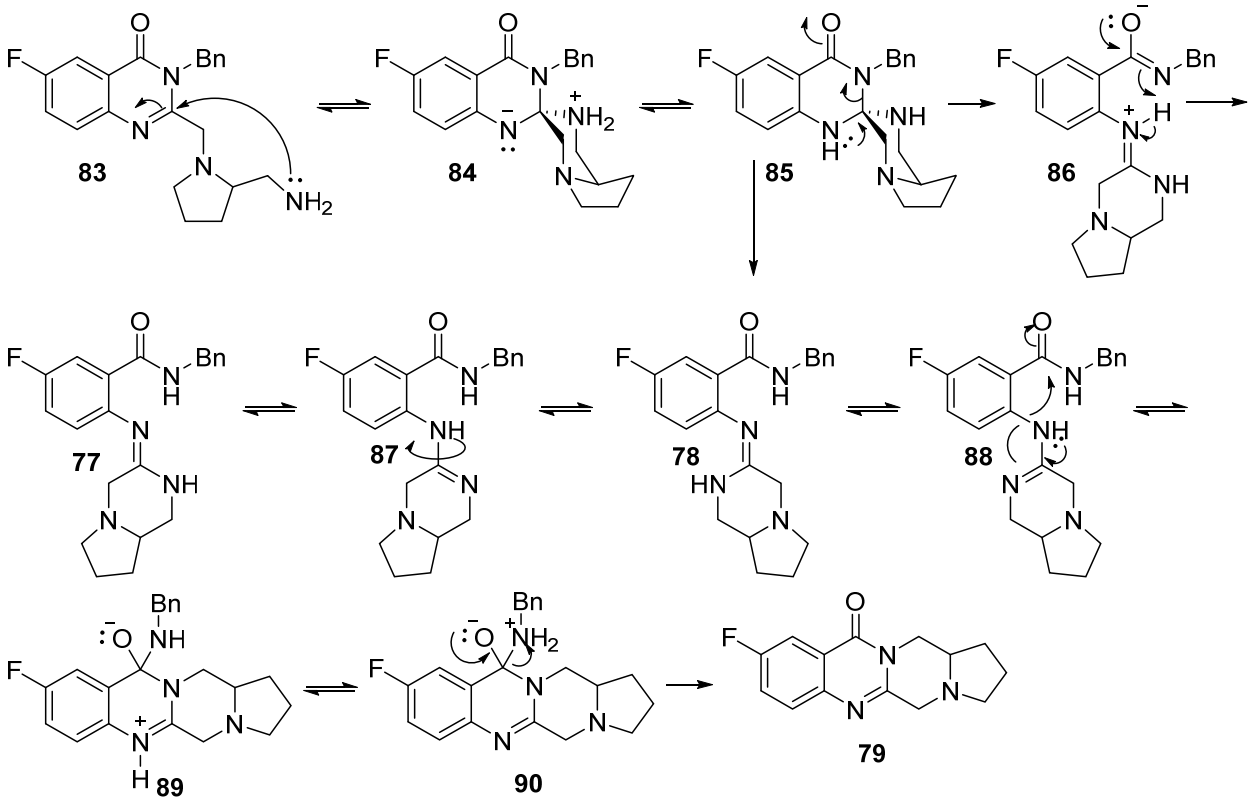

Scheme 23. Proposed mechanism for quinazolinone rearrangement to form quinazolinone **79**.

The quinazolinone core that resulted from this transformation was known. Representation of this framework was reported in a patent by Dr. Hardy, *et al.* in which a library of similar compounds are reported as positive allosteric modulators of metabotropic glutamate receptor 5

(mGluR5).[5] These compounds are protected as potential treatments for psychological conditions such as schizophrenia, psychosis, and conditions associated with reduced function of the *N*-Methyl-D-Aspartate (NDMA) receptor which is activated by mGluR5 (**Scheme 24**).[6,7] In their work, the quinazolinone core was formed starting from an amide coupling between chloroacetylchloride and 2-aminomethyl-*N*-Boc-pyrrolidine **91** to generate *tert*-butyl 2-((2-chloroacetamido)methyl) pyrrolidine-1-carboxylate **92**. The resulting amide was then reacted with 2-amino-4-bromobenzoic acid, to form pyrrolidine appended quinazolinone **93**, via $POCl_3$ induced condensation reaction and *in situ* *N*-Boc deprotection. Subsequently, quinazolinone **93** was refluxed in acetonitrile under basic conditions to enable the intramolecular nucleophilic displacement of the chlorine, by the pyrrolidine substituent, generating quinazolinone **94**. Their method for generating the quinazolinone intermediate was also streamlined as they carried forward crude material and only ran a column after the quinazolinone was formed.[5]

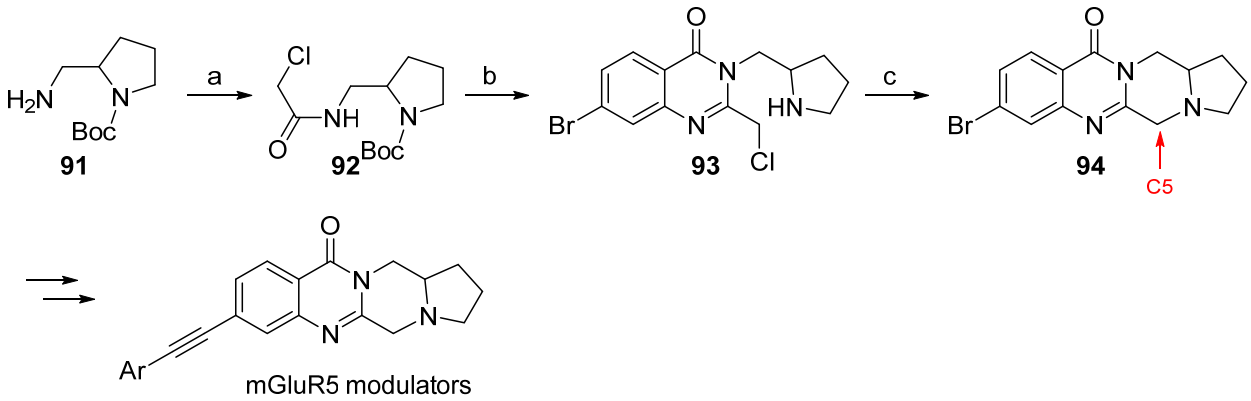

Scheme 24. Patent preparation of tetracyclic quinazolinone mGluR5 positive allosteric modulator[5]

Through this method, a broad range of modifications were implemented. Yet, the patent did not disclose any substrates with substitution in the C5-position (indicated by red arrow in **Scheme 24**). Their approach could potentially incorporate functionalization at this position using

α-substituted chloroacetylchloride derivatives. However, if it were necessary to generate a diastereomerically pure substrate, there is not a large variety of chiral α-substituted chloroacetylchloride starting materials commercially available. Furthermore, in many cases the enantiopure substrates tend to be very expensive. For example, (2S)-2-chloro-2-phenylacetyl chloride and its enantiomer are available from Chemspace™ for $325.30/g.[8] Moreover, the patent did not disclose yields for the transformations to form quinazolinone intermediate **94**, so it is difficult to ascertain the efficiency of their method. Notably, substitution at this position is exhibited in several biologically active natural products containing the 4-(3H)-quinazolinone moiety, two such examples are fumiquinazoline F and fiscaline B (**Fig. 5**).[9]

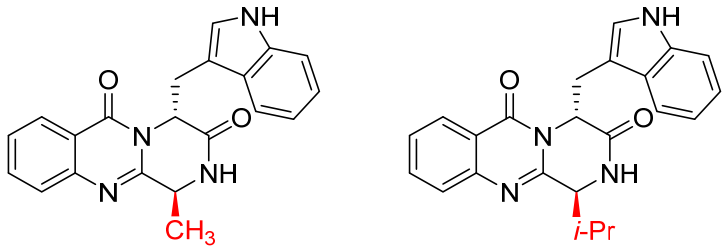

Fumiquinazoline F
anti-microbial and
tumor cell inhibition activity

Fiscaline B
Substance P inhibitor
to NK-1 receptor

Figure 5. Representative biologically active 4-(3H)-quinazolinone containing natural products containing α-imino substitution[10-12]

We envisioned that our telescoped method, which produced the tetracyclic quinazolinone, offered access to functionalizing the scaffold in the C5-position (**93**, **Scheme 25**). The inclusion of an aryl or alkyl aldehyde would functionalize 2-alkylamino-substitutent of quinazolinone intermediate **92**. This functionalization would produce the desired C5-functionalization in quinazolinone **93**. However, we were not sure if the addition of a substituent would impede the observed transformation. Additionally, we questioned the effect of the diamine stereocenter on the

formation of the new stereocenter and whether there would be any inherent diastereoselectivity in the transformation.

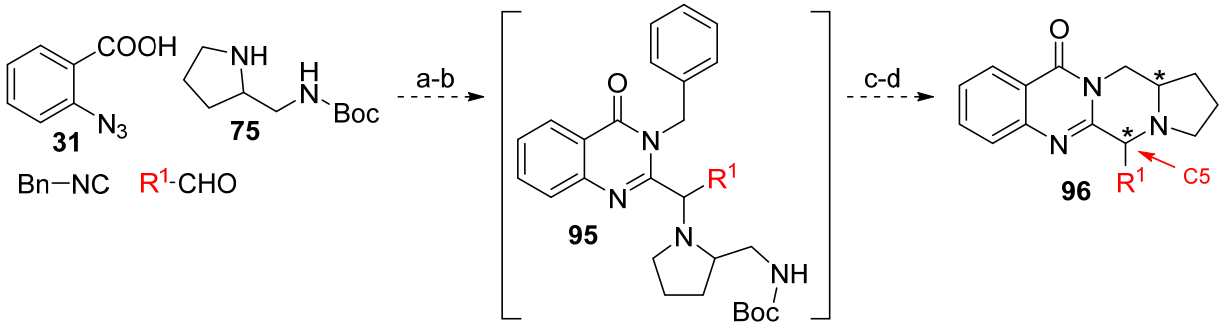

Scheme 25. Proposed telescoped method to generate C5-substituted quinazolinone **96**

In order to examine the feasibility of generating C5-susbtituted quinazolinone **96**, we piloted a reaction using benzaldehyde, in lieu of formaldehyde, in the telescoped multicomponent strategy used to generate the original unsubstituted tetracyclic quinazolinone. Benzaldehyde was selected for this initial experiment because the installation of a phenyl substituent would contribute significant steric bulk in the C5-position, giving some insight into steric effects on the novel quinazolinone rearrangement. Additionally, benzaldehyde demonstrated excellent reactivity in generating (*E*)-arylamidines in good overall yield (50-88%) via our previous telescoped method. This made it more likely that it would be a competent component in at least the first three steps of the telescoped reaction sequence (see **Chapter 2**, **Scheme 14** and **15**). The pilot reaction incorporated racemic *tert*-butyl *N*-(pyrrolidin-2-ylmethyl) carbamate (**75**), benzaldehyde, 2-azidobenzoic acid, and benzyl isocyanide (**Scheme 26**). Excitedly, the telescoped reaction formed the desired C5-phenyl-substututed quinazolinone **97a** in 68% overall yield and 84:16 d.r.

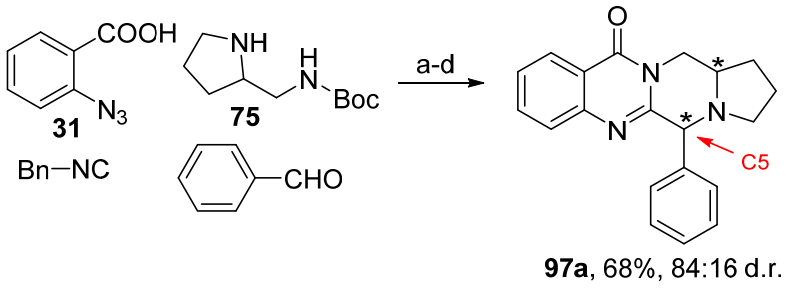

Conditions: (a) **75**, benzaldehyde, 10 min, then 2-azidobenzoic acid in 3:1 CH_2Cl_2/CH_3OH, benzyl isocyanide, (2:4:1:4), 4 Å MS, CH_2Cl_2, rt, 12 h; (b) PS PPh_3, toluene, rt, 60 min, then 110 °C, 12h; (c) 4N HCl, dioxane, 0 °C – rt, 12h; (d) Et_3N, CH_3OH, MWI 100 °C, 60 min.

Scheme 26. Pilot reaction generating C5-phenyl-susbtituted quinazolinone **97a**

Given the mechanism of the Ugi four-component reaction (see **Chapter 2**, **Scheme 9**), we rationalized that the step which determined the diastereoselectivity in the product is the nucleophilic attack on iminium ion **98** by the benzyl isocyanide to form the nitrilium ion intermediate **99** or **100**. NOE experiments validated that the major diastereomer was formed by the nucleophilic attack from the face opposite the *N*-Boc-ethylamino substituent on the pyrrolidine ring of the iminium ion intermediate **98**. In our substrate scope we generated quinazolinone **97h**, **Scheme 27** and subsequently recrystallized the minor diastereomer from acetonitrile. The crystal structure definitively demonstrates the resulting stereochemistry and validates our mechanistic hypothesis of the resulting diastereoselectivity.

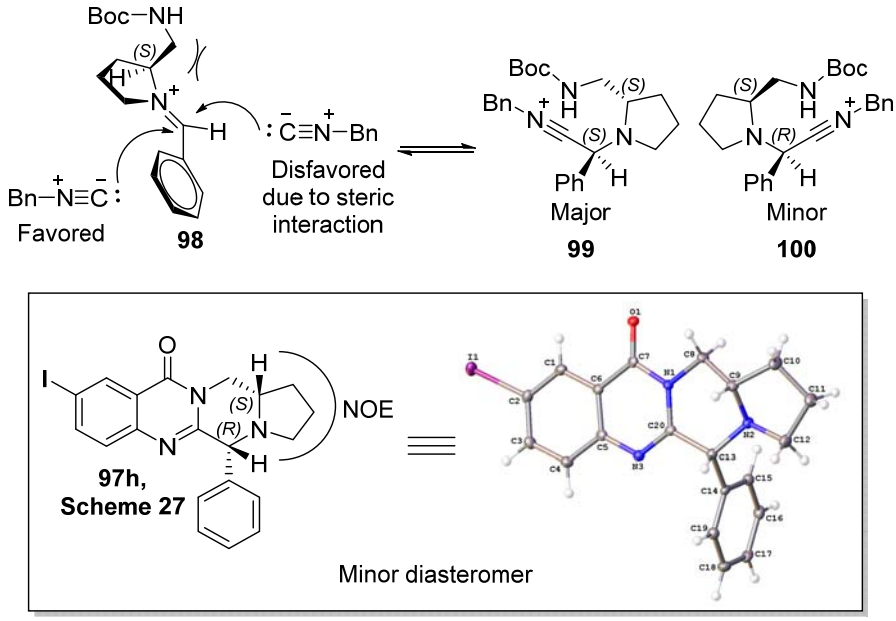

Figure 6. Mechanistic rationale for observed diasteromeric preference and depiction of observed NOE for minor diastereomer of **97h**, **Scheme 27** with crystal structure

Encouraged by this result, we examined if other isocyanides could be substituted in the reaction. Isopropyl and cyclohexyl isocyanide were included to see in order to improve atom efficiency, since the intermediate loses an equivalent of benzylamine in the quinazolinone formation (**Table 3**). We also tried chiral (S)-(-)α-methylbenzyl isocyanide to see if there was an effect on d.r. Isopropyl isocyanide generated the desired C5-phenyl-susbstituted quinazolinone **97a** in 59% overall yield, however the diastereoselectivity of the reaction was reduced to 64:36 d.r, (**Entry 2**). The reaction incorporating cyclohexyl isocyanide resulted in only 39% overall yield with a 77:23 d.r. (**Entry 3**). We rationalized that the deterioration of diastereoselectivity with the incorporation of alkyl isocyanides was the result of their higher nucleophilicity compared to that of benzyl isocyanides.[13] Historically, chiral isocyanides, have not been demonstrated to induce any stereocontrol in Ugi four component reactions.[14] Nevertheless, we attempted using (S)-(-)α-methylbenzyl isocyanide to form **97a** and isolated the desired quinazolinone in 64% overall yield,

and 83:17 d.r. (**Entry 4**). With these results in-hand we proceeded forward with benzyl isocyanide, since it produced the desired quinazolinone in the highest yield and diastereomeric ratio.

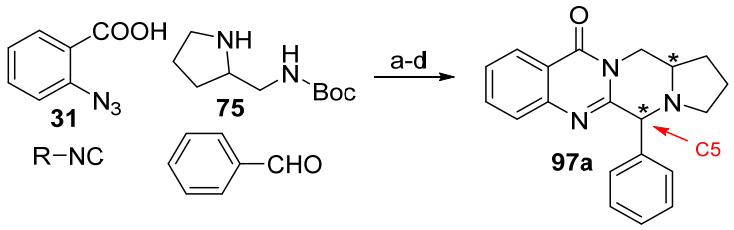

Entry	R	Overall yield	d.r.
1	benzyl	68%	84:16
2	isopropyl	59%	67:33
3	cyclohexyl	39%	77:23
4	(S)-(-)α-methylbenzyl isocyanide	64%	83:17

Conditions: (a) **75**, benzaldehyde, 10 min, then **31** in 3:1 CH_2Cl_2/CH_3OH, R-isocyanide, (2:4:1:4), 4 Å MS, CH_2Cl_2, rt, 12 h; (b) PS PPh_3, toluene, rt, 60 min, then 110 °C, 12h; (c) 4N HCl, dioxane, 0 °C – rt, 12h; (d) Et_3N, CH_3OH, MWI 100 °C, 60 min.

Table 3. Isocyanide Screen

Next, we began to examine the reaction scope. We generated several analogues and were pleased to see that the telescoped, four-step, seven-transformation procedure was tolerant of a variety of substituents on the ring (**Scheme 27**). Introduction of steric bulk with the installation of a 3-methyl substituent on the 2-azidobenzoic acid, generated the desired quinazolinone (**97e**) in 75% overall yield, and 83:17 d.r. The reaction was likewise tolerant of halogen substitution on the phenyl ring, generating **97f** and **97h** in 63% and 66% overall yield, respectively, and 83:17 d.r. The yield of **97g**, was markedly lower, owing to the poor solubility of the 2-azido-4-fluorobenzoic acid. Notably, we were please to find that electron donating substituents were competent in our method generating quinazolinones **97j** (81%, 83:17 d.r.) and **97k** (78%, 84:16 d.r.). In our previous work that disclosed the one-pot assembly of C3-unsubstituted (*E*)-amidobenzamidines, the

incorporation of a C5-methoxy substituent in the anthranilic region of the quinazolinone resulted in significantly diminished yield (0-16%) of the desired amidine.[2b] This was hypothesized to be the result of reduction in the electrophilicity of the quinazolinone imine, thereby hindering the intramolecular rearrangement. Not surprisingly, these substrates required additional heating under microwave conditions, 120 ºC for 1 hour in order to produce the rearrangement. In our previous method, 3-azido-2-benzofuranoic acid was not competent in producing the rearranged (E)-arylamine and instead produced the unrearranged diamine appended quinazolinone (see **Chapter 2**, **Fig. 5**).[1] Given the proposed mechanism for the observed formation of the tetracyclic quinazolinone and passage through a (*Z*)-amidobenzamidine intermediate, we attempted to incorporate 3-azido-2-benzofuranoic acid into the novel scaffold. However, it was likewise not able to rearrange to form the desired quinazolinone and only produced the unrearranged quinazolinone intermediate. This further demonstrates a steric hindrance of the benzofuran incorporation into the quinazolinone core which preclude its utility in our quinazolinone rearrangement methodology. Still, we successfully incorporated a 3-thiophene substituent into quinazolinone **97l** in 57% overall yield, though there was a reduction in the d.r. to 63:17.

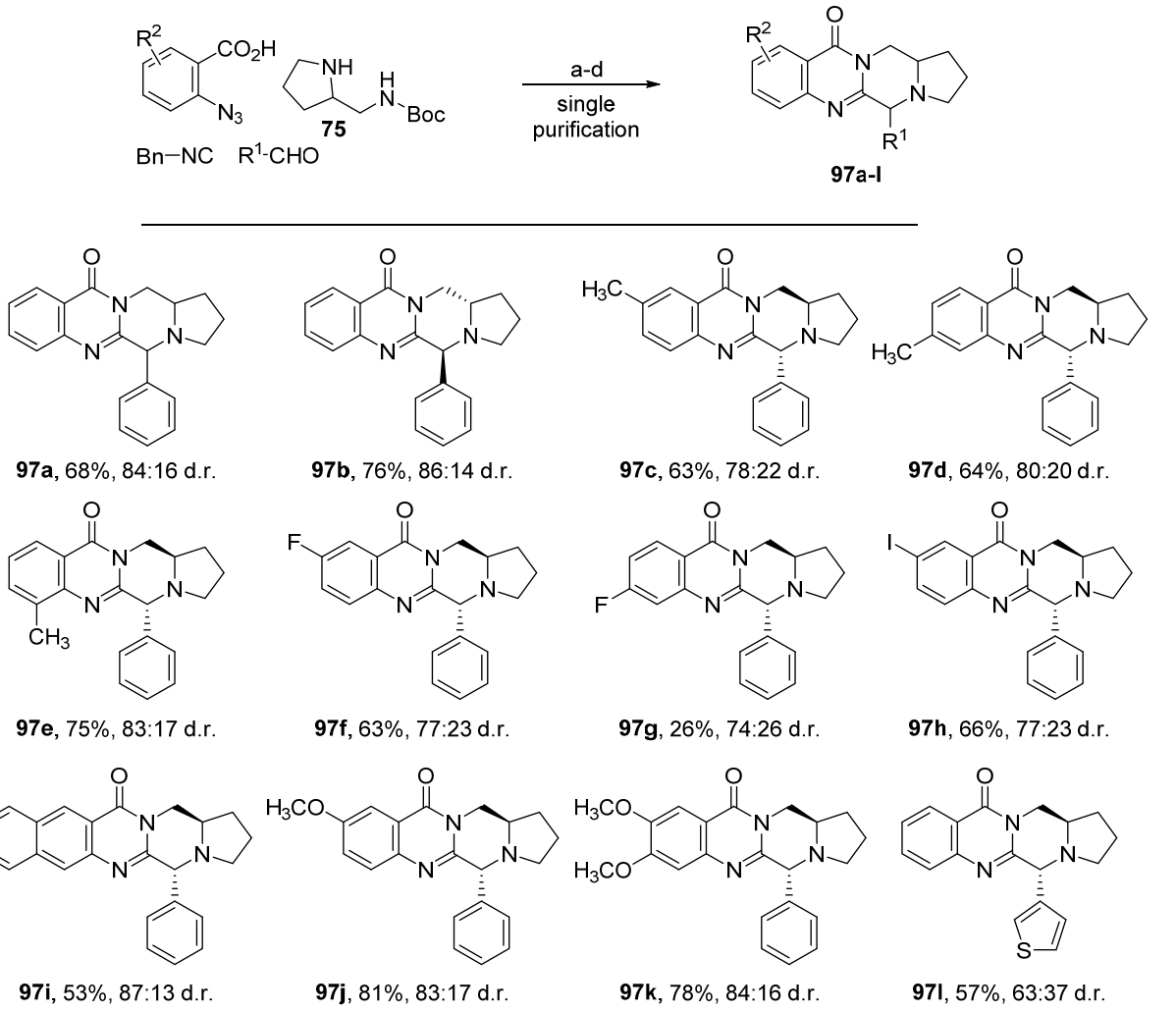

Conditions: (a) **75**, benzaldehyde, 10 min, then 2-azidobenzoic acid in 3:1 CH_2Cl_2/CH_3OH, benzyl isocyanide, (2:4:1:4), 4 Å MS, CH_2Cl_2, rt, 12 h; (b) PS-PPh_3, toluene, rt, 60 min, then 110 °C, 12h; (c) 4N HCl, dioxane, 0 °C – rt, 12h; (d) Et_3N, CH_3OH, MWI 100 °C, 60 min.

Scheme 27. Quinazolinones resulting from telescoped Ugi-Mumm-Staudinger/aza-Wittig quinazolinone rearrangement procedure

Next, we attempted to improve the diastereoselectivity of the reaction. Examples of diastereoselective Ugi four-component reactions have been reported in the literature, incorporating chiral starting materials or chiral auxiliaries to induce diastereoselectivity. However, to date asymmetric versions of the Ugi four component reactions remain a challenge.[15] A noteworthy contribution was conducted by the Orru lab in 2010 where they built on the Ugi-Joullié reaction

that incorporated a chiral cyclic imine into a Ugi three-component reaction to generate bisamide products (**Fig. 6**, **Panel A**).[16] Dr. Orru and researchers developed a sterically demanding cyclic imine (**87**) which was able to generate their desired bisamide product (**88**) in 83% yield with greater than 99:1 d.r.[17] However, this cyclic imine was the preformed intermediate resulting from a primary amine and an aldehyde, and our method requires the use of secondary amines generating highly reactive iminium ions. Nevertheless, these methods inform us as to the level of steric bulk which might be required to impart a higher diastereoselectivity. Recently the Tan lab, published an article describing the use of a chiral phosphoric acid to activate the imine intermediate and generate chiral bisamides in up to 96% yield and 99% ee (**Panel B**).[18] This example again relies on the use of a primary amine, since the activation by the chiral phosphoric acid requires the lone pair donation by the imine intermediate, which is not feasible with our iminium ion intermediate.

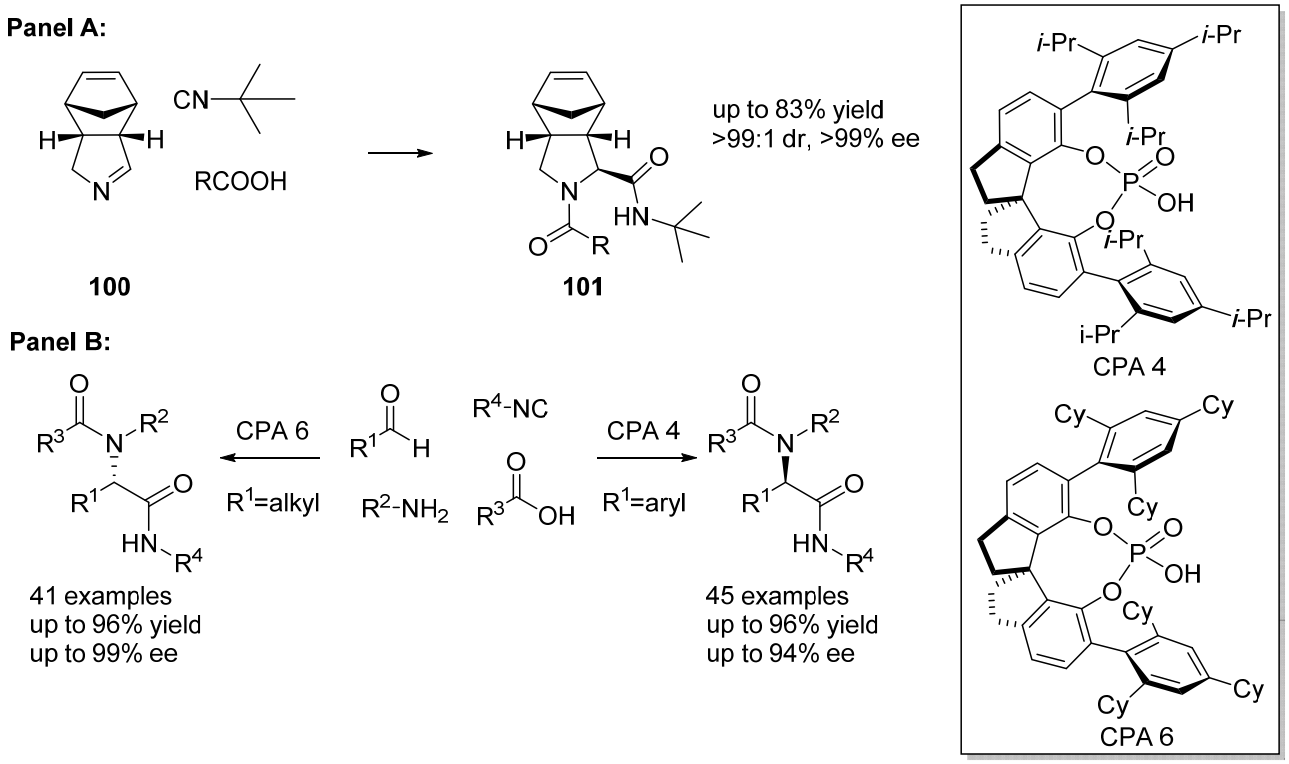

Figure 6. **Panel A**: Orru lab incorporation of 3-azabicyclo[3.3.0]oct-2-ene **100** in diastereoselective Ugi-Joullié reaction. **Panel B:** Tan lab asymmetric Ugi reaction with primary amine and chiral phosphoric acid catalyst.

Considering these examples and our scaffold, we assessed whether we could make a modification to improve the diastereoselectivity of the reaction. Observing the relative position of the steric bulk to the imine carbon in Orru's example, we tested whether increasing the steric bulk of the aldehyde would improve diastereoselectivity. In order to test this, we incorporated pivaldehyde into our telescoped procedure (**Scheme 28**). We observed that the final step in the reaction required heating to 150 ºC in order to observe any rearrangement. Also, we were only able to isolate 24% of quinazolinone **97m**; however, we found only a single diastereomer. Therefore, we investigated the imide forming step of the reaction to investigate the cause of the low yield.

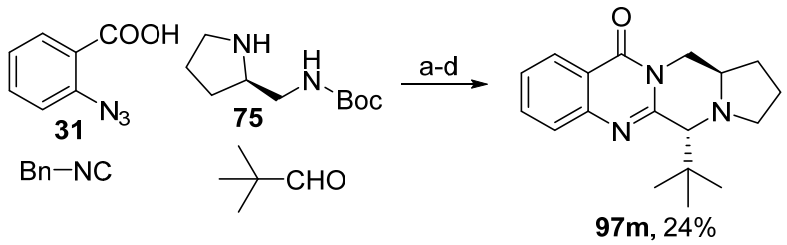

Conditions: (a) **75**, pivaldehyde, 10 min, then **31** in 3:1 CH_2Cl_2/CH_3OH, benzyl isocyanide, (2:4:1:4), 4 Å MS, CH_2Cl_2, rt, 12 h; (b) PS-PPh_3, toluene, rt, 60 min, then 110 °C, 12h; (c) 4N HCl, dioxane, 0 °C – rt, 12h; (d) Et_3N, CH_3OH, MWI 150 °C, 60 min, 24%, single diastereomer.

Scheme 28. Reaction with pivaldehyde to form C5-*tert*-butly-susbtituted quinazolinone **97m**

We found that under our normal reaction conditions (2.0 equiv. of the diamine, 4.0 equiv. of the aldehyde and benzyl isocyanide, and 1.0 equiv. of 2-azidobenzoic acid) we generated only 49% of the desired imide, but also isolated 40% of the Passerini α-acyloxycarboxamide byproduct (**Entry 1**, **Table 4**). We attributed this result to the steric effect of the bulky substitutent, slowing the rate of the nucleophilic attack on the iminium intermediate. This would also explain, why we observed no minor diastereomer in the reaction, as the steric bulk would slow the rate of attack to both faces of the iminium ion further slowing the rate of production of the minor diastereomer. To

improve the overall yield of the telescoped sequence, we attempted to optimize this substrate for imide production. We rationalized that using an equimolar equivalent of the amine to the aldehyde should increase the concentration of the iminium intermediate and thereby favor the desired Ugi pathway, versus the competing Passerini reaction. We therefore tried equimolar amounts of all the reagents and modified the pre-reaction time to see if allowing additional time to form the iminium intermediate would increase the yield and shut down the Passerini side reaction. We found that increasing the equivalence of the diamine to 4.0 equivalents, equimolar to the aldehyde and isocyanide, improved the yield to 82% with no need for an extended pre-reaction time (**Entry 6**). This result in hand, we proceeded to investigate the follow-on reactions with this intermediate.

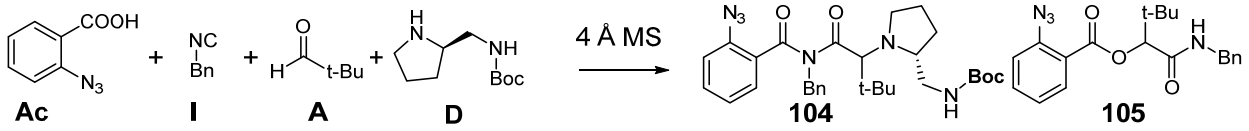

Ac **I** **A** **D** **104** **105**

Entry	Stoichiometry (D:A:Ac:I)	Premix Time	**104** isolated yield	**105** isolated yield
1	(2:4:1:4)	8 min	49%	40%
2	(2:4:1:4)	1 h	31%	61%
3	(1:1:1:1)	9 min	12%	31%
4	(1:1:1:1)	1 h	6%	41%
5	(4:4:1:4)	1 h	82%	4%
6	(4:4:1:4)	6 min	82%	0%

Table 4. Optimization of Ugi Imide **104**

Subjecting imide intermediate **104** to the Staudinger/aza-Wittig conditions yielded intermediate quinazolinone **106** in 53% yield (**Scheme 29**). The subsequent deprotection was facile, but rearrangement required heating to 150 ºC for 1 hour, before any turnover was observed by LCMS. Upon completion, as monitored by LCMS, the product quinazolinone was isolated in 46%, an overall yield of 20% over the four steps. Consequently, we attempted to generate

quinazolinone **97m** using the modified Ugi four-component reaction conditions in the telescoped process. We found that we again were only able to isolate the desired quinazolinone **97m**, in 24%. This is in line with what we observed in the stepwise protocol. The steric bulk appears to impede the rearrangement to form quinazolinone **106**, as well as the requisite quinazolinone rearrangement required to access the intermediate amidine.

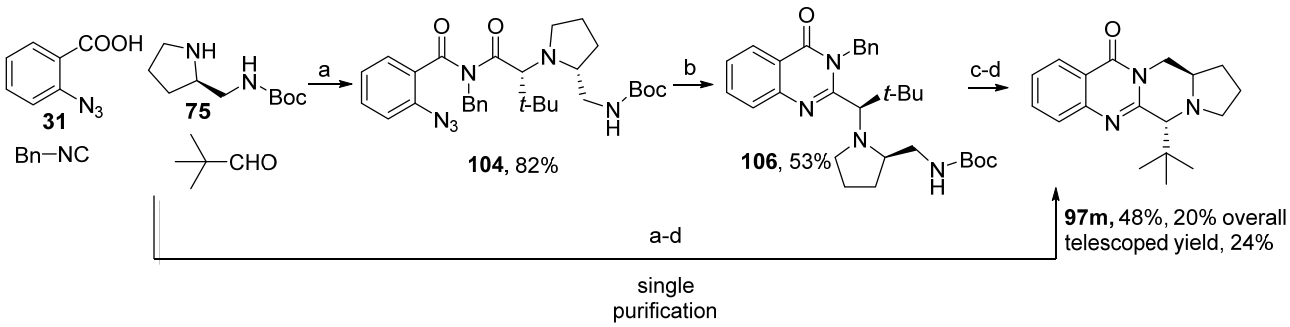

Conditions: (a) **75**, pivaldehyde, 10 min, then 2-azidobenzoic acid in 3:1 CH_2Cl_2/CH_3OH, benzyl isocyanide, (4:4:1:4), 4 Å MS, CH_2Cl_2, rt, 12 h, 82%; (b) PS PPh_3, toluene, rt, 60 min, then 110°C, 12h, 53%; (c) 4N HCl, dioxane, 0 °C – rt, 12h; (d) Et_3N, CH_3OH, MWI 150°C, 60 min, 48%, single diastereomer, 20% overall. Telescoped yield, 24% single diasteromer.

Scheme 29. Stepwise and telescoped reactions with pivaldehyde to form C5-*tert*-butly-susbtituted quinazolinone **97m**

We then tried to use a bulky aryl aldehyde to observe its effect on diastereoselectivity. We incorporated 2,6-dimethylbenzaldehyde as the aldehyde component of the telescoped multicomponent procedure (**Scheme 30**). We were able to isolate 83% of quinazolinone **97n**. However, we observed an almost complete loss of diastereoselectivity at 55:45 d.r. It is likely that the steric bulk affects both faces of the aldehyde and essentially negates the preference gained by the 2-ethylemino substituent of the pyrrolidine.

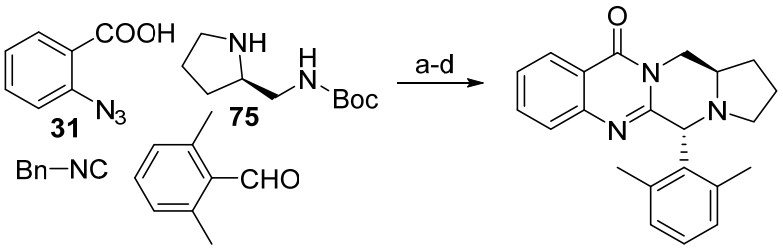

97n, 83%, 55:45

Conditions: (a) **75**, pivaldehyde, 10 min, then 2-azidobenzoic acid in 3:1 CH_2Cl_2/CH_3OH, benzyl isocyanide, (2:4:1:4), 4 Å MS, CH_2Cl_2, rt, 12 h; (b) PS-PPh_3, toluene, rt, 60 min, then 110 °C, 12h; (c) 4N HCl, dioxane, 0 °C – rt, 12h; (d) Et_3N, CH_3OH, MWI 150 °C, 60 min, 24%, single diastereomer.

Scheme 30. Reaction with pivaldehyde to form C5-*tert*-butly-susbtituted quinazolinone **97m**

Subsequently we tried to add more steric bulk to the diamine to increase the already existing diastereoselectivity. We synthesized *N*-[(2S)-3-methyl-2-(methylamino)butyl]-1,1-dimethylethyl ester carbamic acid (**107**) in accordance with existing literature.[19,20] This acyclic diamine placed an isopropyl substituent α to the nitrogen of the iminium intermediate (**110, Scheme 31**). However, after 24 hours, there was no desired imide intermediate (**108**) by LCMS. Upon isolation, we observed 45% Passerini side product (**109**). When incorporating pyrrolidine substituted diamine **75**, the ring prevented rotation of the bond. In the case of the acyclic reaction, the rotatable bond likely resulted in steric hinderance on both faces of the iminium intermediate. This possibly caused the preference for the competing Passerini reaction.

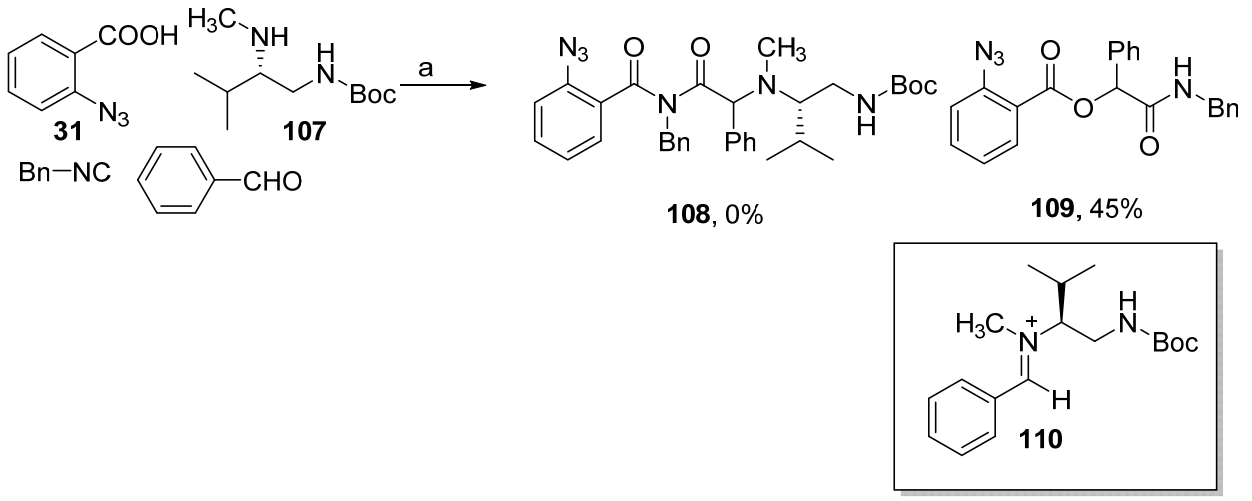

Conditions: (a) **75**, benzaldehyde, 10 min, then **31** in 3:1 CH_2Cl_2/CH_3OH, benzyl isocyanide, (2:4:1:4), 4 Å MS, CH_2Cl_2, rt, 12 h, **108**, 0%, **109**, 45%.

Scheme 31. Reaction with chiral acyclic diamine **107**

As we move forward in the examination of the reaction's scope and optimization, we will look at a couple of key aspects regarding the novel scaffold. First, what other modifications are tolerated in the rearrangement to form tetracyclic quinazolinones? And most importantly, can we find a method to improve the diastereoselectivity of the reaction.

The observed quinazolinone rearrangement to form C5-substituted quinazolinones has a few remaining regions to be explored with respect to reaction scope (**Fig. 7**). First, we must expand the scope to explore the effect of an alkyl substituent at in the C5-position. Tertiary aldehydes have worked in the reaction, though with significant reduction in overall yield. How will the inclusion of a primary and secondary alkyl substituted aldehyde effect the outcome of the reaction and will we see a notable change in d.r.? Additionally, the five membered ring is well tolerated under these conditions, but we should examine whether a six-membered ring is to undergo the observed transformation.

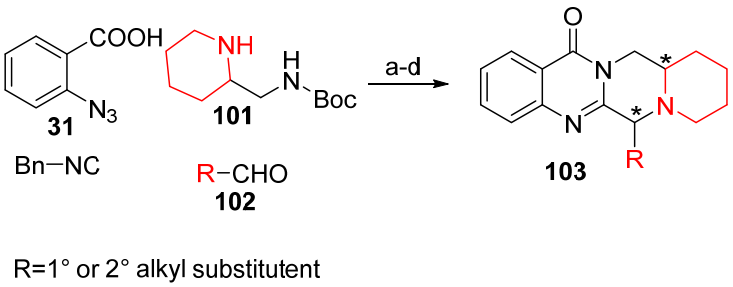

Figure 6. Proposed sites for further exploration of reaction scope

The greatest impact with respect to progress in the project remains controlling diastereoselectivity in the Ugi four-component reaction forming the imide intermediate. The incorporation of *tert*-butyl *N*-(pyrrolidin-2-ylmethyl) carbamate (**75**) as a Ugi component has exhibited good diastereoselectivity in our products, in some cases reaching up to 87:13 d.r. Yet, considering the results under current conditions, we can make some modifications that potentially offer improvements in diastereoselectivity. We have already observed that incorporating a bulky acyclic diamine is not tolerated for this reaction (see **Scheme 31**). However, increasing the steric bulk of the *N*-Boc-ethylamino substituent of the pyrrolidine will theoretically further hinder formation of the minor diastereomer and improve reaction selectivity (**Fig. 7**). We propose the incorporation of a diastereomerically pure α-methyl-2-pyrrolidinemethanamine (**104**) in order to test this hypothesis. These diamines can be synthesized, though it would result in the generation of all four diastereomers. We propose separating the enantiomeric pairs and piloting the reaction. If successful, we will evaluate chiral resolution of the enantiomers to generate enantiopure products.

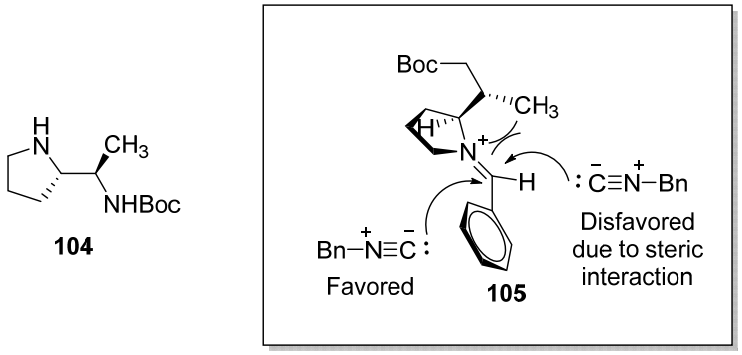

Figure 7. α-methyl-2-pyrrolidinemethanamine **104** and proposed more sterically demanding iminium intermediate **105**

The serendipitous discovery of a novel intramolecular quinazolinone rearrangement generating tetracyclic quinazolinones offered access to regiospecific modifications to an underrepresented pharmacologically relevant chemotype. Through the incorporation of our telescoped Ugi-Mumm-Staudinger/aza-Wittig strategy, we generated several 2-alkylamino substituted 2,3-disubstituted-4(3H)-quinazolinones which can effectively undergo two subsequent intramolecular rearrangements to produce novel C5-substituted tetracyclic quinazolinones. Notably, the mechanism is hypothesized to proceed through a (*Z*)-amidobenzamidine intermediate, which until now has not been exemplified in any of our previous work. *Additionally, our telescoped methodology allowed for efficient access to these unique C5-substituted quinazolinones in excellent yield and good d.r. following the four step, seven transformation process.* We intend to continue to broaden our evaluation of the reaction scope, specifically with respect to tolerance of alkyl-substituted aldehydes and the incorporation of 2-ethylamino piperidine. Also, we will continue to assess whether we can impart better control over the formation of the stereocenter through the incorporation of additional steric bulk to the diamine building block.

References:

1. Jaffett, V.A.; Nerukar, A.; Cao, X.; Guzei, I.; Golden, J.E. Telescoped synthesis of C3-functionalized (*E*)-arylamidines using Ugi–Mumm and regiospecific quinazolinone rearrangements. *Org. Biomol. Chem.* **2019**, 17, 3118-3128.

2. (a) Schroeder, C.E.; Yao, T.; Sotsky, J.; Smith, R.A.; Roy, S.; Chu, Y-K.; Guo, H.; Tower, N.A.; Noah, J.W.; McKellip, S.; Sosa, M.; Rasmussen, L.; Smith, L.H.; White, E.L.; Aubé, J.; Jonsson, C.B.; Chung, D.; Golden, J.E. Development of (E)-2-((1,4-Dimethylpiperazin-2-ylidene)amino)-5-nitro-N-phenylbenzamide, ML336: Novel 2-Amidinophenylbenzamides as Potent Inhibitors of Venezuelan Equine Encephalitis Virus. *J. Med. Chem*. **2014**, 57, 8608−862; (b) Schroeder, C.E.; Neuenswander, S.A.; Yao, T.; Aubé, J.; Golden, J.E. (*E*)-benzamidines from δ- and γ-amino acids via an intramolecular aminoquinazolinone rearrangement. *Org. Biomol. Chem*. **2016**, 14, 3950–3955.

3. Shriner, R.L.; Neumann, F.W. The Chemistry of the Amidines. *Chem. Rev.*, **1944**, 35, 351–425

4. Larrivée-Aboussafy, C.; Jones, B.P.; Price, K.E.; Hardink, M.A.; McLaughlin, R.W.; Lillie, B.M.; Hawkins, J.M.; VaidyanathanR. DBU Catalysis of N,N′-Carbonyldiimidazole-Mediated Amidations. *Org. Lett.*, **2010**, 12, 324-327.

5. Hardy, L.W.; Heffernan, M.L.; Frank, X.; Spear, K.L.; Saraswat, L.D. Compounds for Treating Disorders Mediated by Metabotropic Glutamate Receptor 5, and Methods Thereof. WO2011075699A2, 23 June 2011.

6. Stahl, S.M. The Genetics of Schizophrenia Converge Upon the NMDA Glutamate Receptor. *CNS Spectrum*, **2007**, 12, 583-588.

7. Lecourtier, L.; Homayoun, H.; Tamagnan, G; Moghaddam, B. Positive Allosteric Modulation of Metabotropic Glutamate 5 (mGlu5) Receptors Reverses N-Methyl-D-Aspartate Antagonist-Induced Alteration of Neuronal Firing in Prefrontal Cortex. *Biological Psychiatry*. **2007**, 62, 739-746; Uslaner, J.M. et al. Dose-dependent effect of CDPPB, the mGluR5 positive allosteric modulator, on recognition memory is associated with GluR1 and CREB phosphorylation in the prefrontal cortex and hippocampus. *Neuropharmacology.* **2009**, 57, 531-538.

8. Chem-space. *(2S)-2-chloro-2-phenylacetyl chloride*., 8, April. 2019, https://chem-space.com/search/5cab9ee1-43b214-18b7495c-d3fb3ad/CSC010983190?currency=usd&uom=g

9. Resende, D.I.S.P.; Boonpothong, P.; Sousa, E.; Kijjoa, A.; Pinto, M.M.M. Chemistry of the fumiquinazolines and structurally related alkaloids. *Nat.Prod.Rep.* **2019**, 36, 7–34.

10. Wang, H.; Ganesan, A. Total Synthesis of the Fumiquinazoline Alkaloids: Solution-Phase Studies. *J. Org. Chem.* **2000**, 65, 1022-1030.

11. Silva, M.G.; Furtado, N.A.; Pupo, M.T.; Fonseca, M.J.; Said, S.; Da Silva Filho, A.A.; Bastos, J. K. Antibacterial activity from Penicillium corylophilum Dierckx. *Microbiol. Res.* **2004**, 159, 317–322.

12. Nepali, K.; Ojha, R.; Singh, A.; Budhiraja, A.; Bedi, P.M.S.; Dhar, K.L. Design, Synthesis and Evaluation of Arylidene Pyrrolo and Pyrido Fused Quinazolones as Antimicrobial Agents. *Lett Drug Des Discov* , **2013**, 10, 522-528.

13. Mironov, M.M. General Aspects of Isocyanide Reactivity. In: *Isocyanide Chemistry: Applications in Synthesis and Material Science.* Nenajdenko, V.A., Ed. Wiley, Weinheim, Germany. **2012**, Chapter 2.

14. Caputo, S.; Basso, A.; Moni, L.; Riva, R.;Rocca, V.; Banfi, L. Diastereoselective Ugi reaction of chiral 1,3-aminoalcohols derived from an organocatalytic Mannich reaction. *Beilstein J. Org. Chem.* **2016,** *12,* 139–143.

15. van Berkel, S. S.; Bögels, B. G.; Wijdeven, M. A.; Westermann, B.;Rutjes, F. P. Recent Advances in Asymmetric Isocyanide-Based Multicomponent Reactions *Eur. J. Org. Chem.* **2012**, 3543–3559.

16. Bowers, M.M.; Carroll, P.; Joullié, M.M. Model studies directed toward the total synthesis of 14-membered cyclopeptide alkaloids: synthesis of prolyl peptides via a four-component condensation. *J. Chem. Soc. Perkin Trans. 1.* **1989**, 857–865.

17. Znabet, A.; Ruijter, E.; de Kanter, F.; Köhler, V.; Helliwell, M.; Turner, N.; Orru, R. Highly Stereoselective Synthesis of Substituted Prolyl Peptides Using a Combination of Biocatalytic Desymmetrization and Multicomponent Reactions. *Angew. Chem.* **2010**, *122*, 5417-5420.

18. Zhang, J.; Yu, P.; Li, S-Y.; Sun, H.; Xiang, S-H.; Wang, J.; Houk, K.N.; Tan B. Asymmetric phosphoric acid–catalyzed four-component Ugi reaction. *Science*. **2018**, 361, eaas8707

19. Blaney, E.L.; Martin, B.P.; Nowak, T.; Watson, M.J. Therapeutic Compounds as Inhibitors of the Orexin-1 Receptor. PCT Int. Appl., 2016034882, 10 Mar 2016.

20. Drabina, P.; Sedlák, M.; Růžička, A.; Malkov, A.V.; Kočovský, P. Synthesis of (R)- and (S)-2-N-methylamino-2,3-dimethylbutanamides and (R)- and (S)-(5-isopropyl-1,5-dimethyl-4,5-dihydro-1H-imidazol-4-on-2-yl)pyridines. *Tetrahedron: Assym.* **2008**,19, 384-390.

Chapter 4. Discovery and application of twisted aryl guanidine chemotype via novel quinazolinone rearrangement

Structural modification of chemotypes developed in the Golden lab has been driven by medicinal chemistry needs and has precipitated new methodology development. In our analysis of the (*E*)-amidobenzamidine structure activity relationship in our antiviral program, we sought to generate an analogue bearing a C3-gem-difluoro substitution on an (*E*)-amidobenzamidine (**108**, **Scheme 32**). This was a challenging analog for which several synthetic approaches were considered. Even then, it was unclear that the product would be stable; however, this would facilitate our understanding of essential structure-activity relationships if successful. One of the first synthetic attempts leveraged a method previously reported by the Golden lab,[1] involving an amide coupling between 2-amino-5-nitrobenzoic acid (**105**) and chlorodifluoroacetyl chloride to form 2-[(2-chlorodifluoroacetyl)amino]-5-nitro-benzoic acid (**106**). This intermediate would subsequently form 2-chlorodifluoro-substituted quinazolinone **107** upon $POCl_3$ mediated cyclization and dehydrative amidation. Finally, exposure to N^1,N^2-dimethylethane-1,2-diamine was envisioned to generate the desired C3-gem-difluoro-(*E*)-amidobenzamidine (**108**).

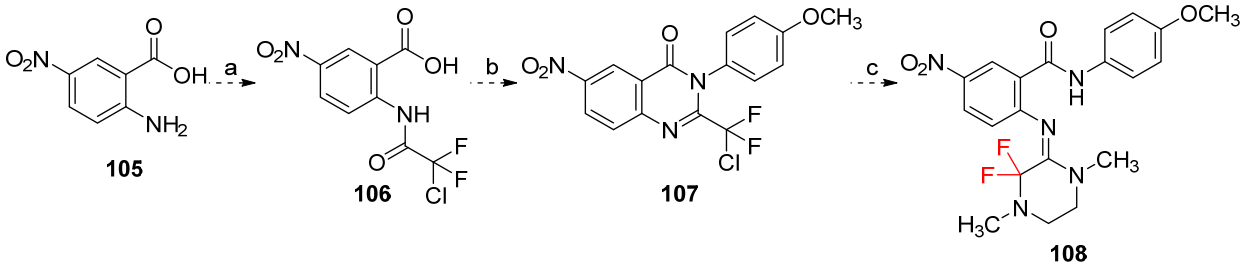

Conditions: (a) Chlorodifluoroacetyl chloride, triethylamine, CH_2Cl_2, 0 °C–rt, 16 h; (b) $POCl_3$, 4-methoxyaniline, CH_3CN, MWI 150 °C, 60 min (c) N^1,N^2-dimethylethane-1,2-diamine, K_2CO_3, DMF, rt, 2 h.

Scheme 32. Proposed synthetic route to C3-gem-difluoro (*E*)-amidobenzamidine **108**[1]

Notably, generation of product would require nucleophilic substitution by an amine on difluorochloroalkylquinazolinone **107**. It was recognized that this intermediate was significantly different from the chloroalkylquinazolinones typically employed, as the trihalogenated carbon would polarize the bond between itself and the imine-like carbon of the core, and this would be exacerbated by the presence of a C6 nitro group. However, if the reaction was even partially productive in generating the desired difluroramidine, critical data could be obtained.

The quinazolinone-forming reactions along the synthetic route proceeded in moderate yield; however, the final step was sluggish to generate any product after two hours at room temperature (**Scheme 33**). The reaction was encouraged by adding KI and heating the reaction mixture to 50 °C. After an additional two hours, very little consumption of the quinazolinone intermediate (**107**) was observed. After another three hours at 50 °C, there appeared to be some turnover to a new product, but the starting material was still the major spot by TLC. Therefore, the reaction was left for an additional 12 h stirring at 50 °C. Following the extended reaction time, there still appeared to be significant starting material by TLC, and the reaction was stopped. We were surprised to find that the reaction did not form C3-gem-difluoro (*E*)-amidobenzamidine (**108**, **Scheme 32**), but instead, produced cyclic guanidine (**109**) in 30% yield. Intrigued by this result, we took a closer look at this transformation.

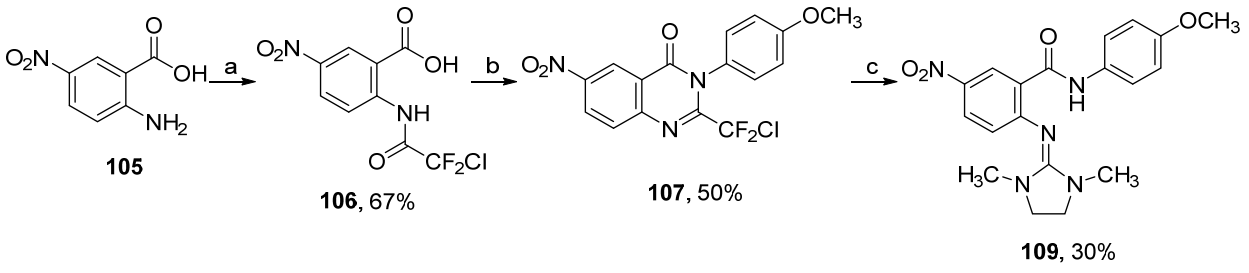

Conditions: (a) Chlorodifluoroacetyl chloride, Et_3N, CH_2Cl_2, 0 °C–rt, 16 h, 67%; (b) $POCl_3$, 4-methoxyaniline, CH_3CN, MWI 150 °C, 60 min, 50%; (c) N^1,N^2-dimethylethane-1,2-diamine, KI, K_2CO_3, DMF, 50 °C, 18 h.

Scheme 33. Reaction resulting in the discovery of novel guanidine chemotype.

Mechanistically, the guanidine might have resulted from nucleophilic attack on the imine carbon of quinazolinone **107** by N^1,N^2-dimethylethane-1,2-diamine to form intermediate **110** (**Scheme 34**). This is reasonable given the electron withdrawing effects of 2-chlorodifluoromethyl substituent (and C6 nitro group) on quinazolinone **107**. Next, reformation of the imine carbon under basic conditions would eliminate the stable by-product, chlorodifluoromethane[2a-b] while also generating quinazolinone intermediate (**111**). Consequently, intramolecular attack of the terminal secondary amine on the imine carbon would form spirocycle (**112**), which then could undergo irreversible ring opening, thereby forming guanidine (**109**).

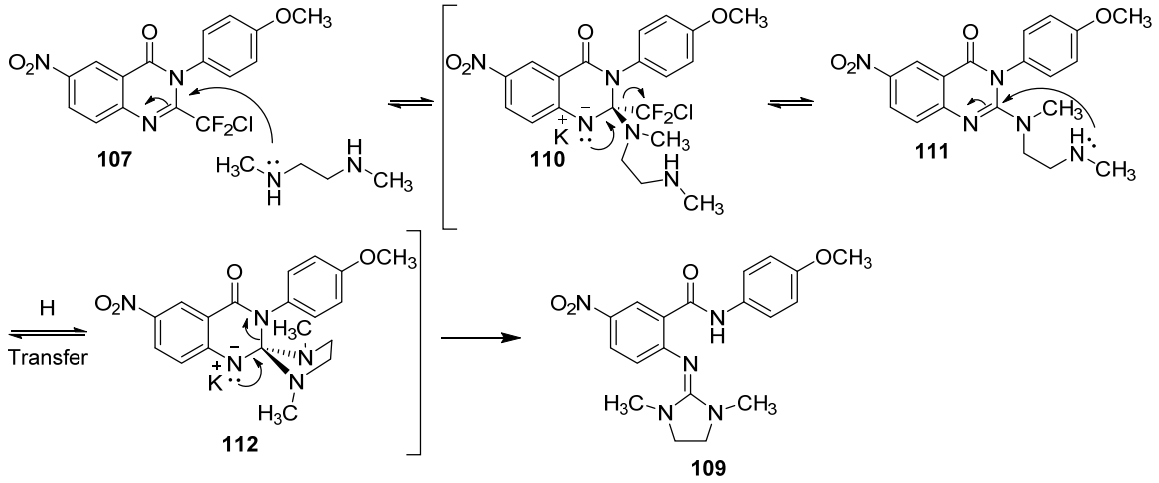

Scheme 34. Proposed mechanism beginning with nucleophilic attack on imine carbon of quinazolinone **107** generating guanidine **109**.

We also considered other mechanisms resulting from nucleophilic substitution in which the amine attacked the chlorodifluoromethyl carbon to liberate chloride ion and form spirocycle **113 (Scheme 35)**. However, upon reformation of the quinazolinone imine, spirocycle **113** would need to extrude difluorocarbene to form quinazolinone **111**. From this point the mechanism would proceed down the same path as the previously proposed mechanism.

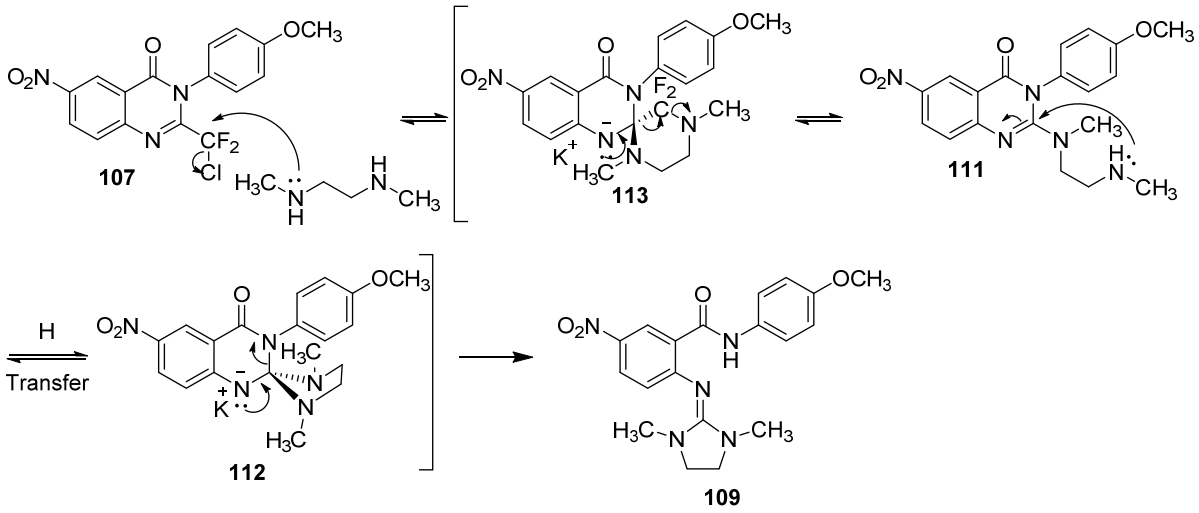

Scheme 35. Proposed mechanism beginning with nucleophilic attack on chlorodifluoromethyl substitutent of quinazolinone **107** generating guanidine **109**.

At this point, fellow graduate student, Ms. Bereket Zekarias, took over the project as I moved on with the telescoped synthesis of C3-funtionalized (*E*)-arylamidines in Chapter 2. However, it is worth noting some key findings that have evolved from my discovery of the guanidine-forming reaction.

A. ***New Synthetic Approach to Cyclic Guanidines:*** Based on a few studies Bereket performed that reinforced the nucleophilic addition to the quinazolinone imine mechanism pathway (**Scheme 34**), she greatly simplified the synthetic approach using a chloroquinazolone **114** that underwent facile rearrangement to either 5- or 6-membered guanidines in high yield. (**Scheme 36**)

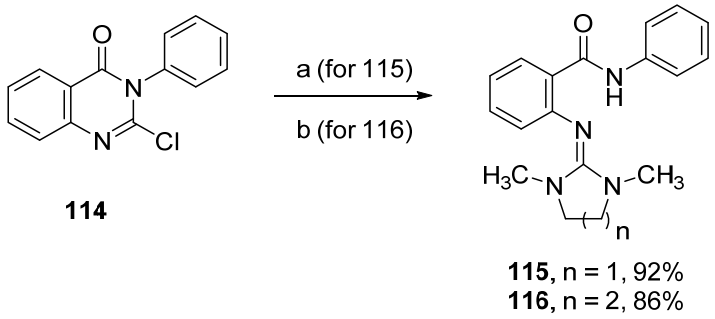

Conditions: (a) N^1,N^2-dimethylethane-1,2-diamine , Et_3N (3.0eq), CH_3CN, 150 °C MWI 2h, (b) N^1,N^3-dimethylpropane-1,3-diamine , Et_3N (3.0eq), CH_3CN, 150 °C MWI 2h.

Scheme 36. Optimized reaction conditions for the generation of cyclic guanidines

B. ***Adaptation to Ring-fused Acylguanidines:*** I recommended that Bereket incorporate *N*-(*tert*-butoxycarbonyl)-*N*-methylethylenediamine with her optimized guanidine-forming conditions, as the reaction should undergo a subsequent rearrangement akin to the *NH*-amidine rearrangement (see **Scheme 22** in **Chapter 3**) and form 2,3-dihydro-1-methyl-imidazo [2,1-*b*]quinazolin-5(1*H*)-one, a tricyclic acylguanidine, (**119**, **Scheme 37**). She isolated quinazolinone (**117**) in 69% yield, and tricyclic acylguanidine **119** was isolated in 79% yield. For the observed transformation, we invoked a similar mechanism to that proposed for the formation of quinazolinones via a (*Z*)-amidobenzamidine intermediate (see **Scheme 23**, **Chapter 3**). We propose that the nucleophilic attack by the (*E*)-guanidine (**118**) is akin to that of 1,4,6,-tirazabicyclo[3.3.0]oct-4-ene when used as an acyl transfer catalyst in the amidation of esters.[3]

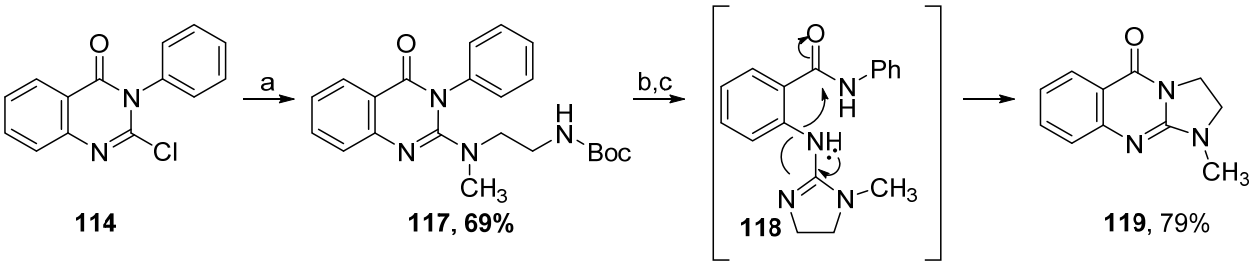

Conditions: (a) *N*-(*tert*-butoxycarbonyl)-*N*-methylethylenediamine, Et_3N (3.0eq), CH_3CN, 150 °C MWI 2h; (b) 4M HCl/Dioxane, CH_2Cl_2, rt, 2h; (c) Et_3N, MeOH, 100 °C MWI 1h.

Scheme 37. Generation of tricyclic acylguanidine **119** via guanidine rearrangement **118**

C. ***Examination of Reaction Scope and Scaffold Diversification:*** With optimized procedures in hand, fellow graduate student, Mr. Gang Yan made tremendous strides with elucidating reaction scope. To date, he synthesized over 30 analogues of the cyclic guanidines in up to 96% yield from the 2-chloro-quinazolinone. Additionally, he generated 18 ring-fused acylguanidines. [4]

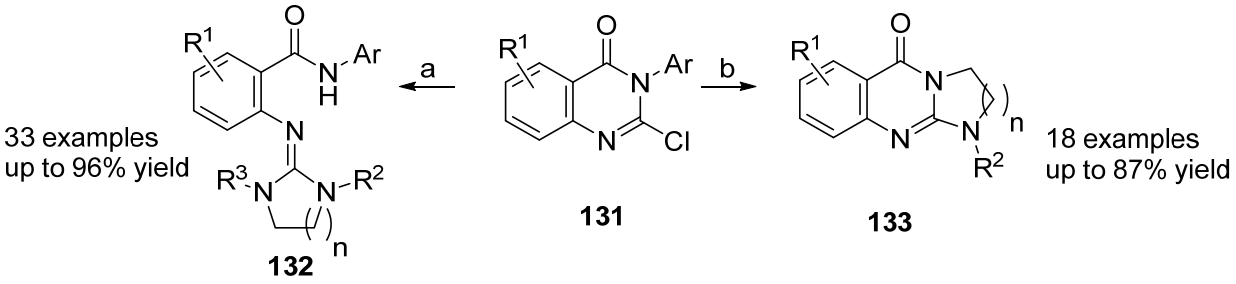

Conditions: (a) $R^2NH(CH_2)_nCH_2NHR^3$, Et_3N (3.0eq), CH_3CN, 150 °C MWI 2h, n=1-2 (b) $R^2NH(CH_2)_nCH_2NH_2$, Et_3N (3.0eq), CH_3CN, 150 °C MWI 2h, n=1-2.

Scheme 37. General scope of new synthetic approach to cyclic guanidines **132** and ring-fused acylguanidines **133**

D. ***Investigation of Cyclic Guanidine Structure:*** An obtained crystal structure of a cyclic guanidine **115** has provided interesting insights into the structural complexity of the scaffold. We discovered that the cyclic guanidine is rotated out of the plane with the phenyl ring. This has led

Gang to begin exploring whether it will be possible to induce axial chirality into the structure through asymmetrization of the diamine component and steric modifications to the phenyl ring.

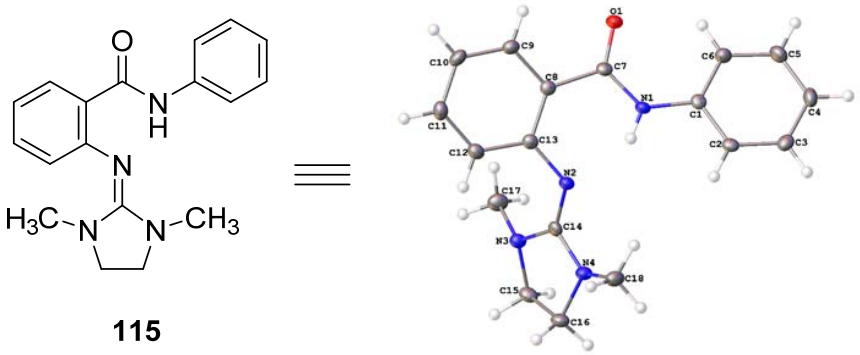

115

Figure 8. Crystal structure of **115**

The discovery of the novel cyclic guanidine structure and its subsequent ability to rearrange to form ring-fused acylguanidines offers an opportunity to explore a rich new chemical space. Additionally, preliminary data on the original discovered guanidine (**109**, **Scheme 33**) shows that the compound has a 2 μM EC_{50} against TC-83, an attenuated strain of VEEV. The methods developed by our lab enabled the generation of a diverse library of cyclic guanidines and ring-fused acylguanidines to enable us to better understand the activity of this new chemotype. Furthermore, the crystal structure of the cyclic guanidines suggest that we might be able to generate substrates with axial chirality.

References:

1. (a) Schroeder, C.E.; Yao, T.; Sotsky, J.; Smith, R.A.; Roy, S.; Chu, Y-K.; Guo, H.; Tower, N.A.; Noah, J.W.; McKellip, S.; Sosa, M.; Rasmussen, L.; Smith, L.H.; White, E.L.; Aubé, J.; Jonsson, C.B.; Chung, D.; Golden, J.E. Development of (E)-2-((1,4-Dimethylpiperazin-2-ylidene)amino)-5-nitro-N-phenylbenzamide, ML336: Novel 2-Amidinophenylbenzamides as Potent Inhibitors of Venezuelan Equine Encephalitis Virus. *J. Med. Chem.* **2014**, 57, 8608−862; (b) Schroeder, C.E.; Neuenswander, S.A.; Yao, T.; Aubé, J.; Golden, J.E. (E)-benzamidines from δ- and γ-amino acids via an intramolecular aminoquinazolinone rearrangement. *Org. Biomol. Chem.* **2016**, 14, 3950–3955.

2. (a) Bergman, J.; Bergman, S. Studies of rutaecarpine and related quinazolinocarboline alkaloids. *J. Org. Chem*. **1985**, 50, 1246–1255; (b) Wang B.; Mai Y-C.; Li Y.;. Hou, J-Q; Huang, S-L.; Ou, T-M.; Tan, J-H.; An L-K.; Li, D.; Gu L-Q.; Huang, Z-S. Synthesis and evaluation of novel rutaecarpine derivatives and related alkaloids derivatives as selective acetylcholinesterase inhibitors. *Eur. J. Med. Chem.* **2010**, 45, 1415–1423.

3. Kiesewetter, M.K.; Scholten, M.D.; Kirn, N.; Weber, R.L.; Hedrick, J.L.; Waymouth, R.M. Cyclic Guanidine Organic Catalysts: What Is Magic About Triazabicyclodecene? *J. Org. Chem.* **2009**, 74, 9490–9496.

4. Unpublished work. Yan, G. Li, X., Zekarias, B. Jaffett, V.A., Golden, J.E.

Selected Experimental Procedures

General Methods

Compounds not described below were purchased from commercial vendors. Purity of all final compounds was confirmed by HPLC/MS analysis and determined to be ≥ 95%.

Analytical TLC experiments were performed on aluminum-backed Silica Gel plates (TLC Silica gel 60 F_{254}) from EMD Millipore and analyzed with 254 nm UV light using diluted samples. All compounds were characterized with the following instrumentation: Varian Unity-Inova 400 MHz NMR spectrometer (operating at 400 and 101 MHz, respectively) or a Varian Unity-Inova 500 MHz NMR spectrometer (operating at 500 and 126 MHz, respectively) in $CDCl_3$ ($CDCl_3$: $^1H = \delta$ 7.26 ppm, $^{13}C = \delta$ 77.16 ppm). The chemical shifts (δ) reported are given in parts per million (ppm) and the coupling constants (J) are in Hertz (Hz). The spin multiplicities are reported as s = singlet, br s = broad singlet, d = doublet, t = triplet, q = quartet, p = pentuplet, dd = doublet of doublet, ddd = doublet of doublet of doublet, and m = multiplet. The LC-MS analysis was performed on an Agilent 1290 Infinity II HPLC system with 1290 Infinity II Diode Array Detector and an Agilent 6120 Quadrupole LC-MS system. The analytical chromatography method utilized the following parameters: Poroshell 120 EC-C18, 1.9 μm column, UV detection wavelength = 254 nm, Flow rate = 1.0 mL/min, Gradient = 5-100% LC-MS grade Methanol over 4 min; The organic mobile phase and aqueous mobile phase contained 0.1% LC-MS grade formic acid. The mass spectrometer utilized the following parameters: an Agilent multimode source that simultaneously acquires ESI+/APCI+; Final compounds were determined to be > 95% purity by UV-LCMS at 254 nm. Microwave irradiated (MWI) reactions were carried out using an Anton Paar Monowave 300 Microwave Synthesis Reactor. Flash chromatography separations were carried out using a Teledyne Isco CombiFlash Rf 200 purification system with silica gel columns (normal-phase). High resolution mass spectra (HRMS) were performed by Analytical Instrument Center at the School of Pharmacy on an Electron Spray Injection (ESI) mass spectrometer. Melting points were measured on OptiMelt MPA100 Automated Melting Point System.

1.1 General procedure A: Representative Procedure for the Synthesis of 2-azidobenzoic acid derivatives[1]

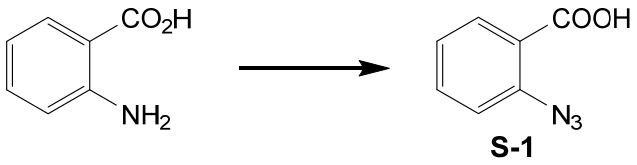

S-1

2-Azidobenzoic acid S-1. To a flame-dried, 250 mL round bottom flask under nitrogen was added anthranilic acid (1.4 g, 10.0 mmol, 1.0 equiv.) and dry acetonitrile (100 mL, 0.1 M). The solution was cooled to 0 °C in an ice bath. After 20 min *tert*-butyl nitrite (1.8 mL, 15.0 mmol, 1.5 equiv.) was added dropwise followed by azidotrimethylsilane (1.6 mL, 12.0 mmol, 1.2 equiv.). The reaction mixture was allowed to warm slowly to rt under nitrogen for 12 h. The reaction mixture was concentrated *in vacuo*, diluted with EtOAc (50 mL) and washed saturated brine solution (2x 50 mL). After separation, the organic layer was dried over $MgSO_4$, filtered and concentrated *in vacuo* to yield 2-azidobenzoic acid, **S-1** (1.47 g, 90%) as a light brown solid. Material carried forward without further purification. Characterization matched literature reference.[1]

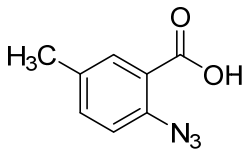

S-2

2-Azido-5-methylbenzoic acid S-2. Obtained using **general procedure A** as a light brown solid (467 mg, 82%). Material carried forward without further purification. Characterization matched literature reference.[2]

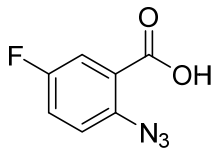

S-3

2-Azido-5-fluorobenzoic acid S-3 Obtained using **general procedure A** as an off-white solid (513 mg, 88%). Material carried forward without further purification. Characterization matched literature reference.[2]

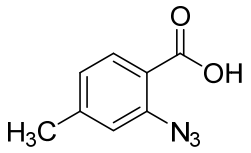

S-4

2-Azido-4-methylbenzoic acid S-4. Obtained using **general procedure A** as a light brown solid (201 mg, 86%). Material carried forward without further purification. ^{1}H NMR (400 MHz, Chloroform-*d*) δ 8.01 (d, *J* = 8.4 Hz, 1H), 7.05 (d, *J* = 6.5 Hz, 1H), 2.44 (s, 3H). ^{13}C NMR (101 MHz, $CDCl_3$) δ 168.3, 145.8, 140.0, 133.4, 126.0, 119.9, 118.0, 21.6.

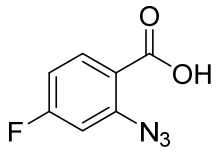

S-5

2-Azido-4-fluorobenzoic acid S-5. Obtained using **general procedure A** as a light brown solid (491 mg, 84%). Material carried forward without further purification. Characterization matched literature reference.[1]

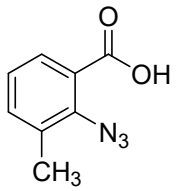

S-6

2-Azido-3-methylbenzoic acid S-6. Obtained using **general procedure A** as a light brown solid (283 mg, 97%). Material carried forward without further purification. Characterization matched literature reference.[3]

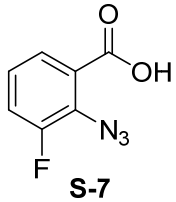

S-7

2-Azido-3-fluorobenzoic acid S-7. Obtained using **general procedure A** as a light brown solid (231 mg, 79%). Crude material carried forward. ^{1}H NMR (400 MHz, DMSO-d_6) δ 13.50 (s, 1H), 7.61 (dt, *J* = 7.8, 1.3 Hz, 1H), 7.53 (ddd, *J* = 11.4, 8.3, 1.5 Hz, 1H), 7.30 (td, *J* = 8.1, 5.1 Hz, 1H). ^{19}F NMR (376 MHz, DMSO) δ -123.87. ^{13}C NMR (101 MHz, DMSO) δ 166.2, 166.2, 157.7, 155.3, 127.3, 127.2, 127.2, 127.0, 127.0, 126.6, 126.5, 120.2, 119.9.

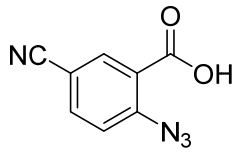

S-8

2-Azido-5-cyanobenzoic acid S-8. Obtained using **general procedure A**. The crude residue was purified by normal-phase chromatography (0.5% MeOH/CH_2Cl_2) to yield 2-azido-5-cyanobenzoic acid, **S-8** (171 mg, 45%) as orange solid. ^{1}H NMR (400 MHz, Chloroform-*d*) δ 8.37 (d, *J* = 2.1 Hz, 1H), 7.86 (dd, *J* = 8.5, 2.0 Hz, 1H), 7.39 (d, *J* = 8.5 Hz, 1H). ^{13}C NMR (101 MHz, $CDCl_3$) δ 166.7, 145.1, 137.2, 137.1, 121.6, 120.7, 117.2, 108.7.

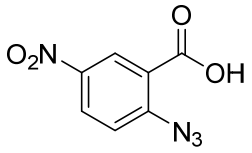

S-9

2-Azido-5-nitrobenzoic acid S-9. Obtained using **general procedure A** as an orange solid (476 mg, 71%). Material carried forward without further purification. Characterization matched literature reference.[4]

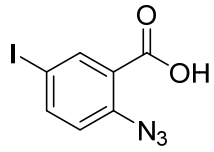

S-10

2-Azido-5-iodobenzoic acid S-10. Obtained using **general procedure A** as a light orange solid (859 mg, 92%). Crude material carried forward. Characterization matched literature reference.[1]

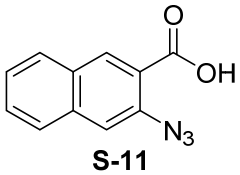

S-11

3-Azido-2-naphthanoic acid S-11. Obtained using **general procedure A** as a red solid (120 mg, 53%). Crude material carried forward. Characterization matched literature reference.[2]

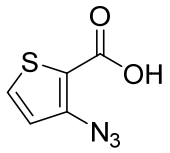

S-12

3-Azidothiophene-2-carboxylic acid S-12. Obtained using **general procedure A** as a brown solid (541 mg, 92%). Crude material carried forward. Characterization matched literature reference.[5]

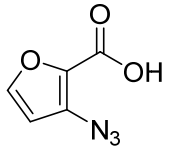

S-13

3-Azidofuran-2-carboxylic acid S-13. Obtained using literature procedure[5] as a brown solid (122 mg, 54%). Crude material carried forward. Characterization matched literature reference.[5]

1.2 Procedure for the Synthesis of *tert*-butyl benzyl(2-cyclopropylamino)ethyl) carbamate

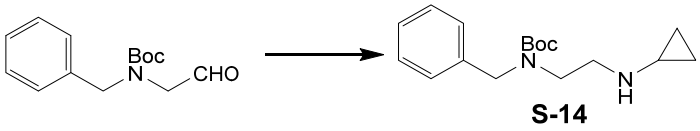

S-14

***tert*-Butyl benzyl(2-cyclopropylamino)ethyl) carbamate S-14.** To a flame-dried, 50 mL three-neck flask containing activated 3 Å molecular sieves under nitrogen was added aldehyde[6] (1.45 g, 5.8 mmol, 1.0 equiv.) in MeOH (23 mL, 0.25 M). Cyclopropylamine (0.42 mL, 6.1 mmol, 1.05 equiv.) was added neat dropwise while stirring at rt. The reaction mixture stirred at rt for 3 h and then cooled to 0 °C in ice bath for 20 min. $NaBH_4$ was slowly added, and the resulting reaction mixture was stirred at rt for 14 h under nitrogen. The reaction mixture was diluted with CH_2Cl_2 (15 mL) and then filtered through celite. The collected filtrate was concentrated *in vacuo*. Crude mixture was diluted with CH_2Cl_2 (20 mL), washed 2 X with saturated brine solution (20 mL). Organic layer was dried over $MgSO_4$ and concentrated in vacuo. Purified by normal phase chromatography (10-50% EtOAc/hexane) to yield diamine **S-14** as a clear oil (772 mg, 46%). ^{1}H NMR (400 MHz, Chloroform-*d*) δ 7.37 – 7.09 (m, 5H), 4.46 (s, 2H), 3.31 (d, *J* = 26.3 Hz, 2H), 2.80 (s, 2H), 2.10 (s, 1H), 1.56 – 1.34 (m, 9H), 0.40 (td, *J* = 6.5, 4.3 Hz, 2H), 0.30 – 0.22 (m, 2H). ^{13}C NMR (101 MHz, $CDCl_3$) δ 156.0, 138.5, 128.7, 128.5, 127.7, 127.1, 79.8, 47.5, 46.7, 30.1, 28.4, 6.4.

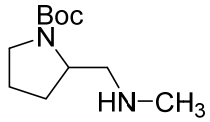

S-15

***tert*-Butyl 2-((methylamino)methyl)pyrrolidine-1-carboxylate S-15.** Obtained using literature procedure[7] as a clear oil (844 mg, 95%). Characterization matched literature reference.[8]

1.3 General procedure B: Representative Procedure for the Synthesis of Imides:

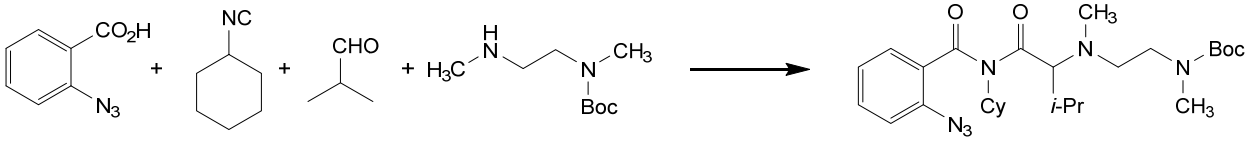

1 **2** **3** **4** **63a**

***tert*-Butyl (2-((1-(2-azido-*N*-cyclohexylbenzamido)-3-methyl-1-oxobutan-2-yl)(methyl)amino) ethyl)(methyl)carbamate 63a.** To a flame-dried, 25 mL three-necked round bottom flask under nitrogen was added activated, powdered, 4Å molecular sieves (50 mg) followed by amine, **4** (115 mg, 0.61 mmol, 2.0 equiv.) in dry CH_2Cl_2 (0.3 mL, 0.1 M). A solution of aldehyde, **3** (112 µL, 1.2 mmol, 4.0 equiv.) in dry CH_2Cl_2 (0.3 mL, 0.1M) was added with stirring followed by carboxylic acid, **1** (50 mg, 0.31 mmol, 1.0 equiv.) in 3:1 dry CH_2Cl_2/MeOH (0.4 mL, 0.1 M) and finally isocyanide, **2** (152 µL, 1.2 mmol, 4.0 equiv.) in dry CH_2Cl_2 (0.4 mL, 0.1 M). The reaction mixture was stirred at rt for 12 h after which the reaction was complete as judged by complete consumption of carboxylic acid on TLC (20% MeOH/CH_2Cl_2). The crude reaction mixture was filtered through a pad of celite and the filtrate was concentrated *in vacuo.* The crude residue was purified by normal-phase chromatography (0-20% EtOAc/hexanes) to yield the imide, **63a** (141 mg, 89%) as pale yellow oil. ^{1}H NMR (400 MHz, Chloroform-*d*) δ 7.56 – 7.48 (m, 1H), 7.38 (d, *J* = 7.6 Hz, 1H), 7.25 (d, *J* = 8.1 Hz, 1H), 7.22 – 7.16 (m, 1H), 3.95 (s, 1H), 3.28 – 3.12 (m, 3H), 2.83 (d, *J* = 8.8 Hz, 4H), 2.73 – 2.52 (m, 1H), 2.35 (d, *J* = 7.7 Hz, 3H), 2.31 – 2.20 (m, 1H), 2.06 (ddt, *J* = 13.3, 10.1, 6.7 Hz, 2H), 1.88 – 1.68 (m, 5H), 1.62 – 1.53 (m, 1H), 1.44 (s, 8H), 1.30 – 1.05 (m, 3H), 0.82 (d, *J* = 6.6 Hz, 3H), 0.68 (d, *J* = 6.6 Hz, 3H). ^{13}C NMR (101 MHz, $CDCl_3$) δ 175.4, 172.1, 155.7, 138.0, 132.3, 129.5, 125.0, 119.2, 79.2, 74.4, 60.3, 52.2, 52.0, 47.5, 47.0, 37.9, 37.1, 34.5, 32.3, 29.5, 28.4, 27.6, 26.6, 26.4, 25.2, 19.7, 19.5. HRMS (ESI): Calculated for $C_{27}H_{42}N_6O_4$ (M^++H): 515.33403; Found: 515.33594.

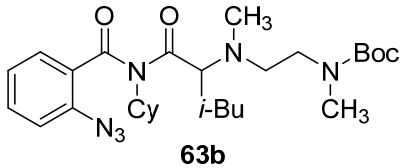

63b

***tert*-Butyl (2-((1-(2-azido-*N*-cyclohexylbenzamido)-4-methyl-1-oxopentan-2-yl)(methyl)amino) ethyl)(methyl)carbamate 63b.** Obtained using **general procedure B**. Purified by normal-phase chromatography (0-10% EtOAc/hexanes) to yield the imide, **63b** (158 mg, 98%) as a pale-yellow oil. ^{1}H NMR (400 MHz, Chloroform-*d*) δ 7.56 – 7.49 (m, 1H), 7.45 (d, *J* = 7.6 Hz, 1H), 7.25 (d, *J* = 8.3 Hz, 1H), 7.20 (td, *J* = 7.5, 1.0 Hz, 1H), 4.18 (s, 1H), 3.33 – 3.15 (m, 1H), 2.81 (s, 3H), 2.60 – 2.42 (m, 2H), 2.23 – 2.08 (m, 4H), 2.00 (q, *J* = 12.2 Hz, 1H), 1.80 (t, *J* = 8.5 Hz, 4H), 1.70 (d, *J* = 12.1 Hz, 1H), 1.64 – 1.49 (m, 2H), 1.43 (s, 9H), 1.36 (dt, *J* = 13.8, 6.5 Hz, 1H), 1.31 – 1.15 (m, 4H), 0.73 (d, *J* = 6.6 Hz, 3H), 0.66 (d, *J* = 6.6 Hz, 3H). ^{13}C NMR (101 MHz, $CDCl_3$) δ 176.6, 171.0, 155.6, 138.5, 132.6, 130.2, 129.0, 124.8, 119.4, 79.2, 66.4, 59.0, 50.8, 47.0, 46.5, 37.9, 35.0, 34.7, 34.5, 31.8, 29.5, 28.4, 26.5, 26.4, 25.3, 24.4, 22.7, 21.8. HRMS (ESI): Calculated for $C_{28}H_{44}N_6O_4$ (M^++H): 529.34968; Found: 529.35162.

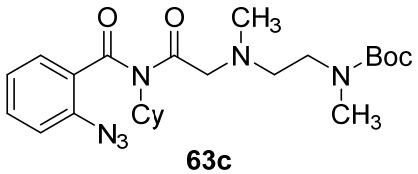

63c

***tert*-Butyl (2-((2-(2-azido-*N*-cyclohexylbenzamido)-2-oxoethyl)(methyl)amino)ethyl)(methyl) carbamate 63c.** Obtained using **general procedure B**. Purified by normal-phase chromatography (0-20% EtOAc/hexanes) to yield the imide, **63c** (65 mg, 45%) as a pale-yellow oil. ^{1}H NMR (400 MHz, Chloroform-*d*) δ 7.53 – 7.45 (m, 2H), 7.26 – 7.21 (m, 1H), 7.19 (td, *J* = 7.6, 1.1 Hz, 1H), 4.24 (s, 1H), 3.24 (d, *J* = 13.3 Hz, 2H), 3.03 (s, 2H), 2.81 (s, 3H), 2.41 – 2.31 (m, 2H), 2.06 (dd, *J* = 12.6, 4.0 Hz, 2H), 2.02 (s, 4H), 1.85 – 1.71 (m, 4H), 1.62 (dt, *J* = 13.5, 3.5 Hz, 1H), 1.43 (s, 9H), 1.36 – 1.09 (m, 3H). ^{13}C NMR (101 MHz, $CDCl_3$) δ 173.9, 170.2, 155.4, 138.7, 132.4, 130.4, 128.5, 124.5, 119.6, 79.5, 63.0, 58.2, 53.4, 52.8, 45.6, 45.5, 40.7, 34.6, 30.3, 28.4, 26.4, 25.3. HRMS (ESI): Calculated for $C_{24}H_{36}N_6O_4$ (M^++H): 473.28708; Found: 473.28737.

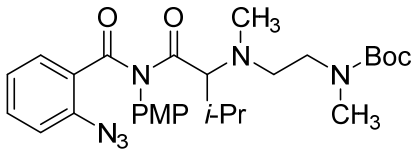

63d

***tert*-Butyl (2-((1-(2-azido-*N*-(4-methoxyphenyl)benzamido)-3-methyl-1-oxobutan-2-yl) (methyl)amino)ethyl)(methyl)carbamate 63d**. Obtained using **general procedure B** . Purified by normal-phase chromatography (0-15% EtOAc/hexanes) to yield the imide, **63d** (140 mg, 85%) as a pale-yellow oil. ^{1}H NMR (400 MHz, Chloroform-*d*) δ 7.38 – 7.28 (m, 2H), 7.14 – 7.03 (m, 4H), 6.84 (d, *J* = 8.5 Hz, 2H), 3.77 (s, 4H), 3.51 – 3.16 (m, 2H), 2.83 (d, *J* = 12.5 Hz, 4H), 2.42 (s, 3H), 2.15 (dp, *J* = 10.4, 6.6 Hz, 1H), 1.45 (s, 10H), 0.99 (d, *J* = 6.9 Hz, 3H), 0.94 (d, *J* = 6.6 Hz, 3H). ^{13}C NMR (101 MHz, $CDCl_3$) δ 175.0, 170.6, 159.4, 155.7, 136.4, 131.0, 130.8, 130.3, 129.4, 128.5, 124.6, 118.5, 114.3, 79.3, 72.36, 55.4, 52.0, 51.6, 47.5, 47.0, 38.2, 38.0, 34.6, 28.5, 28.2, 28.0, 20.1, 19.6. HRMS (ESI): Calculated for $C_{28}H_{38}N_6O_5$ (M^++H): 539.29765; Found: 539.29880.

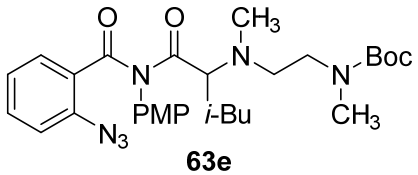

63e

***tert*-Butyl (2-((1-(2-azido-*N*-(4-methoxyphenyl)benzamido)-4-methyl-1-oxopentan-2-yl) (methyl)amino)ethyl)(methyl)carbamate 63e.** Obtained using **general procedure B**. Purified by normal-phase chromatography (0-15% EtOAc/hexanes) to yield the imide, **63e** (132 mg, 78%) as a pale-yellow oil . ^{1}H NMR (400 MHz, Chloroform-*d*) δ 7.36 (td, *J* = 7.8, 1.5 Hz, 2H), 7.21 – 7.04 (m, 4H), 6.94 – 6.76 (m, 2H), 4.05 – 3.85 (m, 1H), 3.77 (s, 3H), 3.44 – 3.09 (m, 2H), 2.81 (d, *J* = 5.4 Hz, 3H), 2.75 – 2.56 (m, 2H), 2.35 (s, 3H), 1.63 (dd, *J* = 14.0, 7.4 Hz, 2H), 1.44 (s, 9H), 0.89 (d, *J* = 5.7 Hz, 3H), 0.80 (d, *J* = 6.0 Hz, 3H). ^{13}C NMR (101 MHz, $CDCl_3$) δ 176.8, 170.5, 159.4, 155.6, 136.5, 131.2, 130.8, 130.0, 129.2, 128.7, 124.7, 118.4, 114.4, 79.2, 64.4, 55.4, 51.4, 47.5, 47.0, 38.1, 37.7, 36.1, 35.5, 34.6, 28.5, 24.5, 23.0, 21.8. HRMS (ESI): Calculated for $C_{29}H_{40}N_6O_5$ (M^++H): 553.31330; Found: 553.31416.

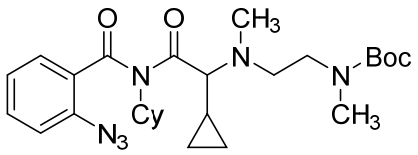

63f

***tert*-Butyl (2-((2-(2-azido-*N*-cyclohexylbenzamido)-1-cyclopropyl-2-oxoethyl)(methyl)amino) ethyl)(methyl)carbamate 63f.** Obtained using **general procedure B**. Purified by normal-phase chromatography (0-50% EtOAc/hexanes) to yield the imide, **63f** (140 mg, 89%) as a yellow oil. ^{1}H NMR (400 MHz, Chloroform-*d*) δ 7.50 (t, *J* = 7.8 Hz, 1H), 7.45 (d, *J* = 7.5 Hz, 1H), 7.23 (d, *J* = 8.1 Hz, 1H), 7.18 (t, *J* = 7.6 Hz, 1H), 4.24 – 4.05 (m, 1H), 3.38 – 3.09 (m, 1H), 2.83 (s, 3H), 2.71 – 2.52 (m, 2H), 2.45 (dd, *J* = 30.8, 8.5 Hz, 1H), 2.17 (s, 4H), 2.02 (d, *J* = 11.9 Hz, 1H), 1.90 – 1.66 (m, 5H), 1.68 – 1.54 (m, 1H), 1.44 (s, 9H), 1.31 – 1.11 (m, 3H), 1.00 (dddd, *J* = 13.1, 9.7, 8.1, 5.0 Hz, 1H), 0.56 (d, *J* = 8.1 Hz, 2H), 0.14 (d, *J* = 10.4 Hz, 1H). ^{13}C NMR

(101 MHz, $CDCl_3$) δ ^{13}C NMR (101 MHz, $CDCl_3$) δ 176.3, 176.0, 170.8, 155.6, 138.5, 132.5, 130.2, 128.7, 124.7, 119.3, 79.2, 73.6, 59.0, 51.2, 50.5, 46.9, 46.5, 38.7, 34.8, 34.6, 31.1, 29.7, 28.4, 26.5, 26.4, 25.3, 8.6, 8.1, 4.4, 2.7. HRMS (ESI): Calculated for $C_{27}H_{40}N_6O_4$ (M^++H): 513.31838; Found: 513.31920.

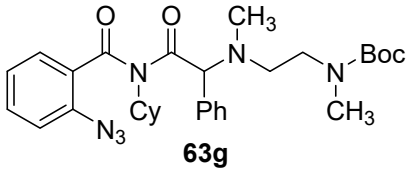

63g

***tert*-Butyl(2-((2-(2-azido-*N*-cyclohexylbenzamido)-2-oxo-1-phenylethyl)(methyl)amino) ethyl)(methyl)carbamate 63g.** Obtained using **general procedure B**. Purified by normal-phase chromatography (0-20% EtOAc/hexanes) to yield the imide, **63g** (163 mg, 97%) as a yellow oil. ^1H NMR (400 MHz, Chloroform-*d*) δ 7.41 (td, *J* = 7.8, 1.6 Hz, 1H), 7.37 – 7.27 (m, 1H), 7.26 – 7.18 (m, 5H), 7.12 – 7.04 (m, 2H), 4.49 (s, 1H), 3.86 (d, *J* = 13.3 Hz, 1H), 3.36 – 3.05 (m, 2H), 2.66 (s, 3H), 2.45 (t, *J* = 7.0 Hz, 2H), 2.16 (d, *J* = 7.0 Hz, 3H), 2.11 – 1.80 (m, 2H), 1.76 – 1.58 (m, 3H), 1.52 , 1.47 – 1.31 (m, 13H), 1.15 – 1.04 (m, 2H). ^{13}C NMR (101 MHz, $CDCl_3$) δ 175.8, 171.2, 155.6, 138.0, 135.5, 132.3, 129.7, 129.6, 129.5, 128.8, 128.1, 124.8, 119.0, 79.1, 74.4, 59.6, 51.3, 46.8, 46.2, 39.6, 39.4, 34.4, 30.6, 29.6, 28.4, 26.4, 26.3, 25.2. HRMS (ESI): Calculated for $C_{30}H_{40}N_6O_4$ (M^++H): 549.31838; Found: 549.31889.

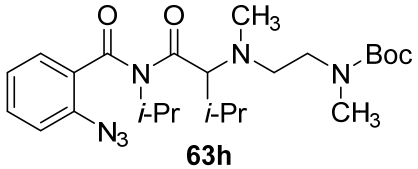

63h

***tert*-Butyl (2-((1-(2-azido-*N*-isopropylbenzamido)-3-methyl-1-oxobutan-2-yl)(methyl)amino) ethyl)(methyl)carbamate 63h.** Obtained using **general procedure B**. Purified by normal-phase chromatography (0-40% EtOAc/hexanes) to yield the imide, **63h** (128 mg, 88%) as a yellow oil. ^1H NMR (400 MHz, Chloroform-*d*) δ 7.57 – 7.47 (m, 1H), 7.38 (d, *J* = 7.6 Hz, 1H), 7.25 (d, *J* = 8.2 Hz, 1H), 7.21 (t, *J* = 7.6 Hz, 1H), 4.26 (d, *J* = 13.7 Hz, 1H), 3.39 (dd, *J* = 20.1, 10.1 Hz, 2H), 3.21 (ddd, *J* = 13.8, 7.6, 5.9 Hz, 1H), 2.84 (d, *J* = 8.8 Hz, 4H), 2.65 (dd, *J* = 35.8, 11.9 Hz, 1H), 2.38 (d, *J* = 5.5 Hz, 3H), 2.08 (dq, *J* = 10.1, 6.6 Hz, 1H), 1.45 (d, *J* = 5.3 Hz, 12H), 1.40 (d, *J* = 6.8 Hz, 3H), 0.85 (d, *J* = 6.6 Hz, 3H), 0.76 (d, *J* = 6.9 Hz, 3H). ^{13}C NMR (101 MHz, $CDCl_3$) δ 175.8, 171.9, 155.7, 137.8, 132.1, 129.2, 129.1, 125.0, 119.1, 79.2, 74.0, 52.1, 52.0, 47.6, 47.0, 37.8, 37.1, 34.5, 28.4, 27.6, 22.0, 19.9, 19.8, 19.6. HRMS (ESI): Calculated for $C_{24}H_{38}N_6O_4$ (M^++H): 475.30273; Found: 475.30264.

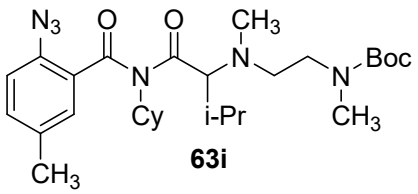

63i

***tert*-Butyl (2-((1-(2-azido-*N*-cyclohexyl-5-methylbenzamido)-3-methyl-1-oxobutan-2-yl) (methyl)amino)ethyl)(methyl)carbamate 63i.** Obtained using **general procedure B**. Purified by normal-phase chromatography (0-40% EtOAc/hexanes) to yield the imide, **63i** (175 mg, 78%) as yellow oil. ^{1}H NMR (400 MHz, Chloroform-*d*) δ 7.32 (dd, *J* = 8.2, 2.0 Hz, 1H), 7.20 – 7.04 (m, 2H), 4.04 (t, *J* = 11.7 Hz, 1H), 3.48 – 3.23 (m, 1H), 3.21 – 3.07 (m, 2H), 2.83 (d, *J* = 9.8 Hz, 4H), 2.74 – 2.47 (m, 1H), 2.34 (d, *J* = 8.9 Hz, 6H), 2.30 – 2.19 (m, 1H), 2.11 – 1.94 (m, 2H), 1.78 (dtd, *J* = 22.0, 12.5, 12.0, 3.6 Hz, 5H), 1.60 (dd, *J* = 7.1, 3.5 Hz, 1H), 1.44 (s, 9H), 1.32 – 1.10 (m, 3H), 0.79 (d, *J* = 6.6 Hz, 3H), 0.63 (d, *J* = 6.9 Hz, 3H).^{13}C NMR (101 MHz, $CDCl_3$) δ 175.2, 172.1, 155.6, 135.3, 135.0, 133.0, 130.2, 129.3, 119.1, 79.2, 74.7, 60.0, 52.0, 47.5, 46.9, 37.8, 36.9, 34.4, 32.4, 29.4, 28.4, 27.5, 26.6, 26.4, 25.2, 20.7, 19.6, 19.5. HRMS (ESI): Calculated for $C_{28}H_{44}N_6O_4$ (M^++H): 529.34968; Found: 529.35027.

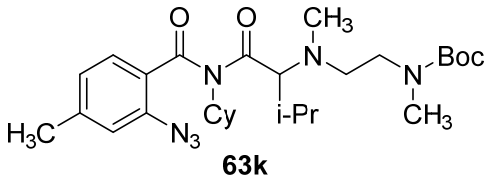

63k

***tert*-Butyl (2-((1-(2-azido-*N*-cyclohexyl-4-methylbenzamido)-3-methyl-1-oxobutan-2-yl) (methyl)amino)ethyl)(methyl)carbamate 63k.** Obtained using **general procedure B**. Purified by normal-phase chromatography (0-40% EtOAc/hexanes) to yield the imide, **63k** (143 mg, 67%) as a yellow oil. ^{1}H NMR (400 MHz, Chloroform-*d*) δ 7.25 (d, *J* = 6.5 Hz, 2H), 7.00 (s, 1H), 6.96 (d, *J* = 7.9 Hz, 1H), 3.98 (d, *J* = 12.4 Hz, 1H), 3.26 – 3.09 (m, 3H), 2.80 (d, *J* = 8.3 Hz, 4H), 2.39 (s, 3H), 2.31 (s, 3H), 2.21 (dt, *J* = 12.3, 5.9 Hz, 1H), 2.02 (ddd, *J* = 13.6, 10.3, 6.8 Hz, 2H), 1.82 – 1.67 (m, 4H), 1.41 (s, 9H), 1.27 – 1.08 (m, 4H), 0.78 (d, *J* = 6.6 Hz, 3H), 0.65 (d, *J* = 6.7 Hz, 3H). ^{13}C NMR (101 MHz, $CDCl_3$) δ 175.31, 172.41, 155.75, 143.64, 138.20, 129.94, 126.89, 125.87, 119.76, 79.32, 74.48, 60.19, 52.04, 47.56, 38.03, 34.53, 32.41, 29.59, 28.51, 27.64, 26.66, 26.51, 25.32, 21.61, 19.89, 19.65. HRMS (ESI): Calculated for $C_{28}H_{44}N_6O_4$ (M^++H): 529.34968; Found: 529.35153.

1.4 General procedure C: Representative Procedure for the Synthesis of Quinazolinones:

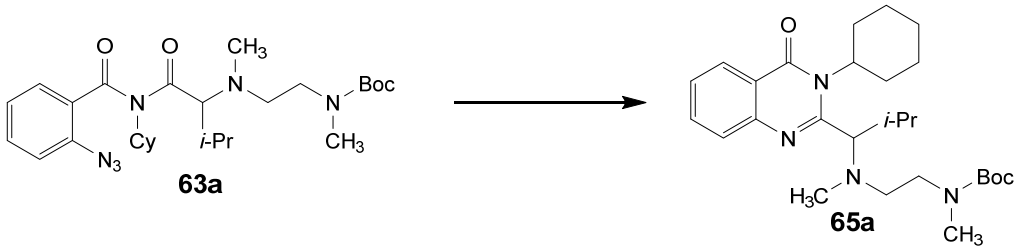

***tert*-Butyl (2-((1-(3-cyclohexyl-4-oxo-3,4-dihydroquinazolin-2-yl)-2-methylpropyl)(methyl) amino)ethyl)(methyl)carbamate 65a**. To a flame-dried, 25 mL, three-necked round bottom flask equipped with a reflux condenser, under nitrogen was added triphenylphospine (101 mg, 0.38 mmol, 1.5 equiv.) followed by dry toluene (1.0 mL). A solution of imide **63a** (132 mg, 0.26 mmol, 1.0 equiv.) in dry toluene (1.6 mL) was added and the reaction mixture was stirred at rt for 30 min. Next, the reaction mixture was heated to 110 °C and stirred at reflux for 12h, after which the reaction was complete as judged by complete consumption of imide **63a** on TLC (30% EtOAc/hexanes). The crude reaction mixture was filtered through a pad of celite and the filtrate was concentrated *in vacuo.* The crude residue was purified by normal-phase chromatography (0-50% EtOAc/hexanes) to yield the quinazolinone, **65a** (92 mg, 76%) as clear colorless oil. ^{1}H NMR (400 MHz, Chloroform-d) δ 8.21 (dd, J = 8.0, 1.4 Hz, 1H), 7.67 (t, J = 7.7 Hz, 1H), 7.58 (d, J = 8.1 Hz, 1H), 7.40 (t, J = 7.5 Hz, 1H), 4.19 (t, J = 12.1 Hz, 1H), 3.51 – 3.45 (m, 2H), 3.15 (d, J = 38.2 Hz, 2H), 2.90 (dd, J = 23.8, 11.6 Hz, 2H), 2.77 (s, 3H), 2.67 (s, 1H), 2.58 (d, J = 12.9 Hz, 3H), 1.94 (d, J = 9.5 Hz, 2H), 1.77 – 1.60 (m, 4H), 1.40 (s, 10H), 1.36 (s, 1H), 1.21 (t, J = 7.0 Hz, 1H), 1.12 (d, J = 6.7 Hz, 3H), 0.79 (d, J = 6.4 Hz, 3H). HRMS (ESI): Calculated for $C_{27}H_{42}N_4O_3$ (M^++H): 471.33297; Found: 471.33369.

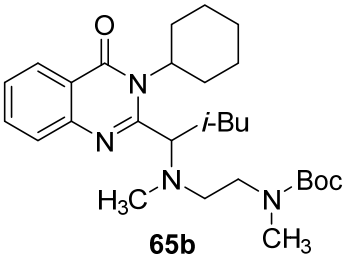

***tert*-Butyl (2-((1-(3-cyclohexyl-4-oxo-3,4-dihydroquinazolin-2-yl)-3-methylbutyl)(methyl) amino)ethyl)(methyl)carbamate 65b.** Obtained using **general procedure C**. Purified by normal-phase chromatography (0-20% EtOAc/hexanes) to yield the quinazolinone, **65b** (81 mg, 60%) as yellow oil. ^{1}H NMR (400 MHz, Chloroform-*d*) δ 8.20 (d, *J* = 7.9 Hz, 1H), 7.66 (t, *J* = 7.5 Hz, 1H), 7.61 (d, *J* = 8.1 Hz, 1H), 7.40 (t, *J* = 7.4 Hz, 1H), 4.35 (s, 1H), 3.77 – 3.69 (m, 1H), 3.65 (t, *J* = 7.1 Hz, 0H), 3.54 (s, 1H), 3.42 – 3.06 (m, 3H), 2.84 (d, *J* = 10.7 Hz, 3H), 2.76 – 2.60 (m,

5H), 2.52 – 2.31 (m, 5H), 2.26 (s, 1H), 1.91 (d, *J* = 11.0 Hz, 3H), 1.81 – 1.54 (m, 5H), 1.44 (s, 5H), 1.40 – 1.22 (m, 14H), 0.92 (d, *J* = 6.2 Hz, 3H), 0.87 (t, *J* = 7.1 Hz, 6H).^{13}C NMR (101 MHz, $CDCl_3$) δ 163.4, 155.5, 154.5, 146.2, 133.6, 127.3, 126.5, 126.2, 122.2, 79.2, 64.0, 58.9, 58.3, 56.2, 51.2, 49.5, 47.7, 47.1, 38.9, 35.3, 34.6, 29.7, 29.2, 28.5, 28.3, 27.0, 25.8, 25.3, 24.8, 24.8, 23.7, 22.9, 22.8, 21.8. HRMS (ESI): Calculated for $C_{28}H_{44}N_4O_3$ (M^++H): 485.34862; Found: 485.34931.

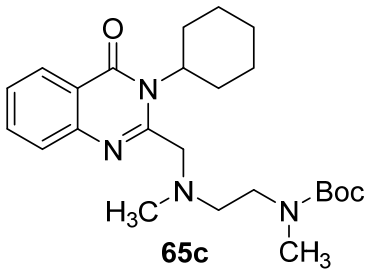

65c

***tert*-Butyl (2-(((3-cyclohexyl-4-oxo-3,4-dihydroquinazolin-2-yl)methyl)(methyl)amino)ethyl) (methyl)carbamate 65c** Obtained using **general procedure C**. Purified by normal-phase chromatography Purified by normal-phase chromatography (0-5% MeOH/CH_2Cl_2) to yield the quinazolinone, **65c** (29 mg, 89%) as a yellow oil.. ^{1}H NMR (400 MHz, Chloroform-*d*) δ 8.23 (d, *J* = 7.9 Hz, 1H), 7.70 (t, *J* = 7.6 Hz, 1H), 7.63 (d, *J* = 8.1 Hz, 1H), 7.44 (t, *J* = 7.5 Hz, 1H), 4.57 – 4.30 (m, 1H), 3.68 (s, 2H), 3.42 – 3.26 (m, 2H), 2.83 (d, *J* = 8.1 Hz, 3H), 2.76 (dd, *J* = 12.0, 3.6 Hz, 1H), 2.68 (d, *J* = 7.2 Hz, 3H), 2.38 (s, 3H), 1.98 – 1.87 (m, 2H), 1.82 – 1.62 (m, 3H), 1.39 (d, *J* = 29.0 Hz, 14H). ^{13}C NMR (101 MHz, $CDCl_3$) δ 162.8, 155.5, 153.9, 146.5, 133.8, 126.9, 126.8, 126.4, 122.5, 79.4, 77.4, 63.9, 60.4, 54.5, 46.8, 46.1, 42.0, 41.9, 34.8, 28.8, 28.4, 26.8, 25.2. HRMS (ESI): Calculated for $C_{24}H_{36}N_4O_3$ (M^++H): 429.28602; Found: 429.28666.

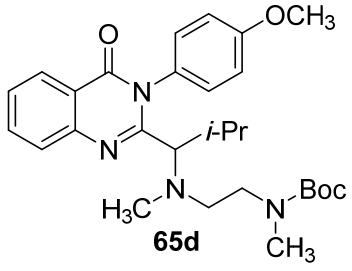

65d

***tert*-Butyl (2-((1-(3-(4-methoxyphenyl)-4-oxo-3,4-dihydroquinazolin-2-yl)-2-methylpropyl) (methyl)amino)ethyl)(methyl)carbamate 65d.** Obtained using **general procedure C**. Purified by normal-phase chromatography (0-15% EtOAc/hexanes) to yield the quinazolinone, **65d** (88mg, 81%) as an off-white foam. ^{1}H NMR (400 MHz, Chloroform-*d*) δ 8.28 (dd, *J* = 8.0, 1.4 Hz, 1H), 7.74 (t, *J* = 7.6 Hz, 1H), 7.69 (dd, *J* = 8.2, 1.3 Hz, 1H), 7.49 – 7.41 (m, 1H), 7.33 – 7.18 (m, 1H), 7.05 (d, *J* = 7.6 Hz, 3H), 3.88 (s, 3H), 3.20 (d, *J* = 75.7 Hz, 1H), 3.03 (d, *J* = 12.6 Hz, 3H), 2.66 (d, *J* = 69.6 Hz, 5H), 2.34 – 2.24 (m, 3H), 1.40 (s, 9H), 0.93 (d, *J* = 6.7 Hz, 3H), 0.84 (d, *J* = 7.3 Hz, 3H).^{13}C NMR (101 MHz, $CDCl_3$) δ 163.0, 159.8, 156.2, 155.7, 147.1, 134.2, 130.8, 129.9,

129.6, 127.5, 127.0, 126.5, 121.0, 114.6, 79.1, 70.9, 55.5, 50.0, 49.0, 47.6, 46.6, 39.8, 3.4, 29.6, 29.4, 28.4, 20.8, 20.3. HRMS (ESI): Calculated for $C_{28}H_{38}N_4O_4$ (M^++H): 495.29658; Found: 495.29764.

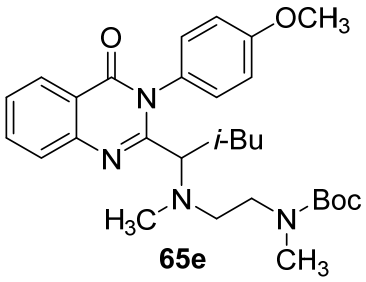

65e

***tert*-Butyl (2-((1-(3-(4-methoxyphenyl)-4-oxo-3,4-dihydroquinazolin-2-yl)-3-methylbutyl) (methyl)amino)ethyl)(methyl)carbamate 65e.** Obtained using **general procedure C**. Purified by normal-phase chromatography (0-15% EtOAc/hexanes) to yield quinazolinone **65e** (86mg, 88%) as off-white foam. ^{1}H NMR (400 MHz, Chloroform-d) δ 8.37 – 8.10 (m, 1H), 7.74 (qd, *J* = 8.2, 1.6 Hz, 2H), 7.46 (ddd, J = 8.2, 6.4, 1.8 Hz, 1H), 7.41 – 7.26 (m, 1H), 7.15 – 6.95 (m, 3H), 3.87 (s, 3H), 3.42 (s, 1H), 3.19 – 2.75 (m, 2H), 2.61 (d, *J* = 65.4 Hz, 3H), 2.40 – 2.21 (m, 1H), 2.13 (s, 3H), 2.05 (d, *J* = 6.9 Hz, 1H), 1.48 (s, 1H), 1.43 – 1.31 (m, 10H), 0.80 (d, *J* = 6.5 Hz, 3H), 0.77 (d, *J* = 6.2 Hz, 4H). ^{13}C NMR (101 MHz, CDCl3) δ 163.1, 159.8, 147.0, 134.2, 130.9, 129.5, 128.9, 127.7, 127.0, 126.7, 121.2, 114.5, 79.1, 62.4, 55.5, 38.6, 34.2, 34.1, 33.9, 33.2, 28.4, 25.1, 23.1, 22.2. HRMS (ESI): Calculated for $C_{27}H_{42}N_6O_4$ (M^++H): 509.31223; Found: 509.31305.

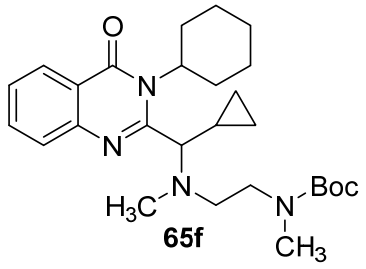

65f

***tert*-Butyl(2-(((3-cyclohexyl-4-oxo-3,4-dihydroquinazolin-2-yl)(cyclopropyl)methyl) (methyl)amino)ethyl)(methyl)carbamate 65f.** Obtained using **general procedure C**. Purified by normal-phase chromatography (0-30% EtOAc/hexanes) to yield the quinazolinone, **65f** (95mg, 70%) as a yellow oil. ^{1}H NMR (400 MHz, Chloroform-*d*) δ 8.21 (d, *J* = 7.7 Hz, 1H), 7.66 (d, *J* = 7.5 Hz, 1H), 7.59 (d, *J* = 8.1 Hz, 1H), 7.41 (t, *J* = 7.5 Hz, 1H), 3.28 (d, *J* = 26.4 Hz, 2H), 3.14 – 3.01 (m, 1H), 2.91 – 2.68 (m, 6H), 2.52 (s, 1H), 2.44 (s, 3H), 1.88 (t, *J* = 6.0 Hz, 2H), 1.74 – 1.59 (m, 3H), 1.48 – 1.21 (m, 16H), 0.86 (qd, *J* = 11.6, 11.2, 6.2 Hz, 2H), 0.49 (dq, *J* = 9.9, 5.8 Hz, 2H). ^{13}C NMR (101 MHz, $CDCl_3$) δ 161.1, 153.4, 144.4, 131.5, 124.9, 124.4, 124.2, 119.9, 77.2, 56.8, 49.5, 45.2, 44.3, 38.2, 32.5, 27.5, 26.9, 26.5, 26.2, 24.6, 23.2. HRMS (ESI): Calculated for $C_{27}H_{40}N_4O_3$ (M^++H): 469.31732; Found: 469.31814.

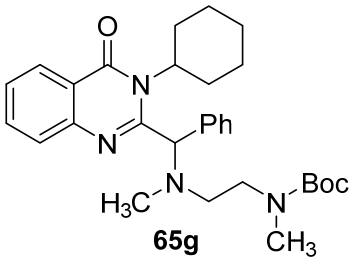

65g

***tert*-Butyl (2-(((3-cyclohexyl-4-oxo-3,4-dihydroquinazolin-2-yl)(phenyl)methyl)(methyl) amino) ethyl)(methyl)carbamate 65g.** Obtained using **general procedure C**. Purified by normal-phase chromatography (0-25% EtOAc/hexanes) to yield the quinazolinone, **65g** (99mg, 82%) as a colorless oil. ^{1}H NMR (400 MHz, Chloroform-*d*) δ 8.20 (d, *J* = 8.0 Hz, 1H), 7.73 – 7.69 (m, 2H), 7.46 – 7.41 (m, 1H), 7.38 – 7.27 (m, 5H), 5.06 (d, *J* = 32.8 Hz, 1H), 4.36 – 4.05 (m, 1H), 3.69 (s, 1H), 3.36 (d, *J* = 45.0 Hz, 3H), 3.12 – 2.95 (m, 1H), 2.87 (s, 1H), 2.72 (d, *J* = 6.1 Hz, 4H), 2.53 (s, 5H), 2.33 (s, 1H), 1.81 – 1.51 (m, 3H), 1.42 (d, *J* = 21.3 Hz, 13H), 1.20 – 1.11 (m, 2H). ^{13}C NMR (101 MHz, $CDCl_3$) δ 163.2, 155.8, 146.6, 137.4, 133.9, 129.2, 128.8, 128.72, 128.2, 127.5, 126.8, 126.5, 122.3, 79.3, 59.3, 51.8, 47.5, 46.9, 40.7, 34.8, 28.6, 28.3, 26.6, 26.5, 25.2. HRMS (ESI): Calculated for $C_{30}H_{40}N_4O_3$ (M^++H): 505.31732; Found: 505.31802.

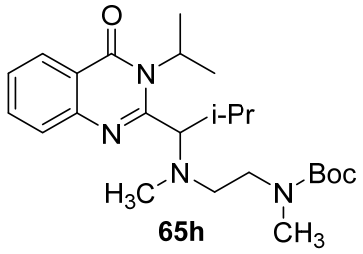

65h

***tert*-Butyl (2-((1-(3-isopropyl-4-oxo-3,4-dihydroquinazolin-2-yl)-2-methylpropyl)(methyl) amino)ethyl)(methyl)carbamate 65h.** Obtained using **general procedure C**. Purified by normal-phase chromatography (0-40% EtOAc/hexanes) to yield the quinazolinone, **65h** (75 mg, 71%) as a colorless oil. ^{1}H NMR (400 MHz, Chloroform-*d*) δ 8.22 (dd, *J* = 8.0, 1.4 Hz, 1H), 7.73 – 7.64 (m, 1H), 7.59 (dd, *J* = 8.2, 1.2 Hz, 1H), 7.47 – 7.36 (m, 1H), 4.68 (p, *J* = 6.7 Hz, 1H), 3.52 (d, *J* = 10.1 Hz, 1H), 3.24 (dt, *J* = 14.2, 7.2 Hz, 1H), 3.18 – 2.86 (m, 1H), 2.84 – 2.63 (m, 5H), 2.54 (d, *J* = 7.5 Hz, 3H), 1.71 (d, *J* = 6.7 Hz, 3H), 1.65 (d, *J* = 6.8 Hz, 3H), 1.42 (s, 9H), 1.11 (d, *J* = 6.7 Hz, 3H), 0.81 (d, *J* = 6.4 Hz, 3H). ^{13}C NMR (101 MHz, $CDCl_3$) δ 163.1, 156.1, 155.7, 146.6, 133.7, 127.2, 126.4, 126.3, 122.0, 79.3, 76.8, 71.5, 71.3, 50.7, 47.8, 47.2, 39.4, 39.1, 34.7, 30.0, 29.8, 28.5, 21.1, 20.6, 19.9. HRMS (ESI): Calculated for $C_{24}H_{38}N_4O_3$ (M^++H): 431.30167; Found: 431.30255.

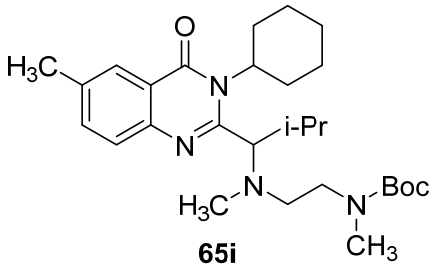

65i

***tert*-Butyl (2-((1-(3-cyclohexyl-6-methyl-4-oxo-3,4-dihydroquinazolin-2-yl)-2-methylpropyl) (methyl)amino)ethyl)(methyl)carbamate 65i.** Obtained using **general procedure C**. Purified by normal-phase chromatography (0-15% EtOAc/hexanes) to yield the quinazolinone, **65i** (114 mg, 69%) as a colorless oil. 1H NMR (400 MHz, Chloroform-d) δ 7.99 (s, 1H), 7.48 (d, J = 1.2 Hz, 2H), 4.17 (t, J = 12.1 Hz, 1H), 3.45 (d, J = 10.1 Hz, 1H), 3.14 (d, J = 45.9 Hz, 2H), 2.95 – 2.53 (m, 12H), 2.45 (s, 3H), 1.93 (d, J = 9.8 Hz, 2H), 1.73 – 1.61 (m, 4H), 1.40 (s, 9H), 1.33 (d, J = 8.6 Hz, 2H), 1.11 (d, J = 6.7 Hz, 3H), 0.78 (d, J = 6.4 Hz, 3H). ^{13}C NMR (101 MHz, CDCl3) δ 163.3, 155.8, 155.4, 144.6, 136.5, 135.2, 127.1, 125.8, 121.8, 79.4, 71.5, 59.5, 40.3, 34.6, 30.2, 29.3, 28.7, 28.6, 27.1, 26.9, 25.4, 21.5, 21.2, 20.7. HRMS (ESI): Calculated for $C_{28}H_{44}N_4O_3$ (M^++H): 485.34862; Found: 485.34952.

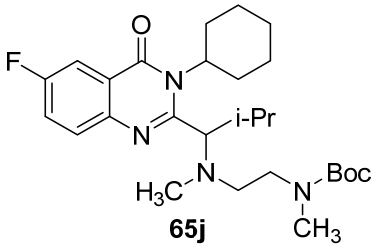

65j

tert-butyl (2-((1-(3-cyclohexyl-6-fluoro-4-oxo-3,4-dihydroquinazolin-2-yl)-2-methylpropyl) (methyl)amino)ethyl)(methyl)carbamate 65j. Obtained using crude material from **general procedure B** carried forward in **general procedure C.** Purified by normal-phase chromatography (0-15% EtOAc/hexanes) to yield the quinazolinone, **65j** (176 mg, 84% over both steps) as pale-yellow oil. ^{1}H NMR (400 MHz, Chloroform-*d*) δ 7.83 (dd, *J* = 8.7, 3.0 Hz, 1H), 7.59 (dd, *J* = 8.9, 4.9 Hz, 1H), 7.39 (td, *J* = 8.5, 3.0 Hz, 1H), 4.19 (t, *J* = 12.0 Hz, 1H), 3.46 (d, *J* = 10.0 Hz, 1H), 3.30 – 3.03 (m, 3H), 3.03 – 2.83 (m, 3H), 2.80 – 2.64 (m, 3H), 2.58 (d, *J* = 9.9 Hz, 3H), 1.94 (d, *J* = 9.8 Hz, 2H), 1.69 (q, *J* = 12.8, 8.9 Hz, 3H), 1.40 (s, 10H), 1.35 (d, *J* = 8.6 Hz, 3H), 1.12 (d, *J* = 6.7 Hz, 3H), 0.79 (d, *J* = 6.3 Hz, 3H). ^{19}F NMR (376 MHz, $CDCl_3$) δ -113.65. ^{13}C NMR (101 MHz, $CDCl_3$) δ 162.3, 161.9, 159.4, 155.6, 155.5, 143.05, 129.5, 129.4, 123.1, 123.0, 122.4, 122.1, 111.1, 110.9, 79.2, 71.5, 59.5, 40.1, 34.5, 30.0, 29.0, 28.4, 26.8, 26.7, 25.2, 21.0, 20.6. HRMS (ESI): Calculated for $C_{27}H_{41}FN_4O_3$ (M^++H): 489.32355; Found: 489.32439.

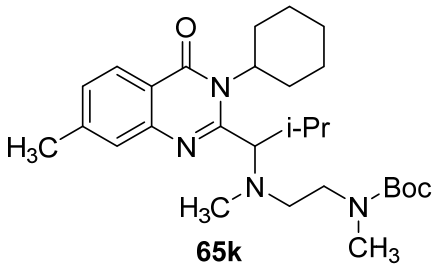

65k

tert-butyl (2-((1-(3-cyclohexyl-7-methyl-4-oxo-3,4-dihydroquinazolin-2-yl)-2-methylpropyl)(methyl)amino)ethyl)(methyl)carbamate 65k. Obtained using **general procedure C**. Purified by normal-phase chromatography (0-20% EtOAc/hexanes) to yield the quinazolinone, **65k** (84 mg, 70%) as a colorless oil, 70%. ^{1}H NMR (400 MHz, Chloroform-*d*) δ 8.08 (d, *J* = 8.1 Hz, 1H), 7.38 (s, 1H), 7.21 (dd, *J* = 8.2, 1.6 Hz, 1H), 4.15 (q, *J* = 8.2, 4.8 Hz, 1H), 3.46 (d, *J* = 10.0 Hz, 1H), 3.14 (d, *J* = 25.8 Hz, 2H), 3.00 – 2.81 (m, 3H), 2.80 – 2.64 (m, 5H), 2.55 (d, *J* = 13.0 Hz, 3H), 2.45 (s, 3H), 1.96 – 1.87 (m, 2H), 1.68 (dd, *J* = 18.0, 9.6 Hz, 4H), 1.40 (s, 9H), 1.33 (d, *J* = 8.1 Hz, 3H), 1.11 (d, *J* = 6.6 Hz, 3H), 0.77 (d, *J* = 6.4 Hz, 3H). ^{13}C NMR (101 MHz, $CDCl_3$) δ 163.2, 156.4, 155.8, 146.6, 144.6, 128.0, 126.9, 126.3, 119.7, 79.3, 71.6, 59.4, 49.8, 47.8, 40.2, 34.6, 30.1, 29.3, 28.8, 28.53, 27.0, 26.9, 25.3, 21.9, 21.1, 20.7. HRMS (ESI): Calculated for $C_{28}H_{44}N_4O_3$ (M^++H): 485.34862; Found: 485.34862.

1.5 General procedure D: General Procedure for the synthesis of Benzamidines:

Step 1. Representative Procedure for Boc-deprotection:

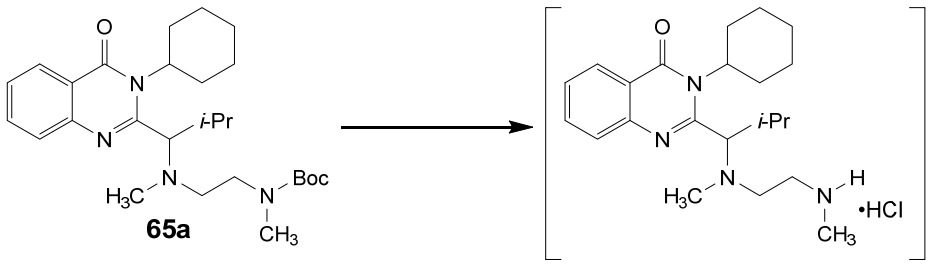

65a

To a flame-dried, 10 mL, one-necked round bottom flask under nitrogen was dissolved quinazolinone **65a** (84 mg, 0.18 mmol, 1.0 equiv.) in dry CH_2Cl_2 (1.0 mL) and the solution cooled to 0 °C in an ice-bath with stirring. HCl in dioxane (4M, 0.22 mL, 5.0 equiv.) was added dropwise. Following the addition the ice-bath was removed and the reaction mixture allowed to warm to rt. The reaction mixture was stirred at rt for 12h after which the reaction was complete as judged by complete consumption of quinazolinone on TLC (30% EtOAC/hexanes). The solvent was

removed *in vacuo* to yield the HCl salt of Boc-deprotected quinazolinone which was carried forward without purification (65 mg, 89%).

Step 2. Representative Procedure for the synthesis of Benzamidines:

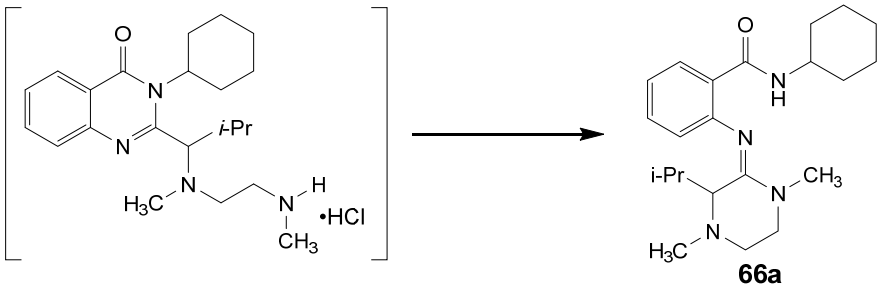

66a

(*E*)-*N*-cyclohexyl-2-((3-isopropyl-1,4-dimethylpiperazin-2-ylidene)amino)benzamide 66a. Triethylamine (100 µL, 0.7 mmol, 5 equiv.) was added to a solution of HCl salt of quinazolinone (55 mg, 0.14 mmol, 1.0 equiv.) in MeOH (1.4 mL, 0.1M) in a 4 mL microwave vial while stirring. The vial was capped and heated in a microwave reactor at 100 °C for 30 min. The reaction mixture was allowed to cool to rt and the solvent removed *in vacuo*. The crude residue was purified by normal-phase chromatography (0-5% MeOH/CH_2Cl_2) to yield the benzamidine, **66a** (37 mg, 66% over two steps) as a yellow oil. ^{1}H NMR (500 MHz, Chloroform-*d*) δ 8.93 (d, *J* = 8.0 Hz, 1H), 8.17 (dd, *J* = 7.9, 1.7 Hz, 1H), 7.28 – 7.24 (m, 1H), 7.05 – 7.01 (m, 1H), 6.59 (dd, *J* = 7.8, 1.2 Hz, 1H), 3.95 (tdt, *J* = 11.5, 7.9, 3.9 Hz, 1H), 3.47 – 3.39 (m, 2H), 3.36 (ddd, *J* = 12.3, 7.1, 4.6 Hz, 1H), 3.23 (ddd, *J* = 11.9, 7.0, 4.4 Hz, 1H), 3.11 (s, 3H), 2.63 (ddd, *J* = 12.0, 6.6, 4.7 Hz, 1H), 2.49 (s, 3H), 2.07 – 1.97 (m, 2H), 1.76 – 1.69 (m, 3H), 1.68 – 1.61 (m, 1H), 1.38 (ddt, *J* = 17.9, 12.8, 6.4 Hz, 2H), 1.21 – 1.10 (m, 3H), 0.79 (d, *J* = 6.7 Hz, 3H), 0.63 (d, *J* = 6.9 Hz, 3H). ^{13}C NMR (126 MHz, $CDCl_3$) δ 165.9, 160.5, 148.5, 131.2, 131.1, 125.8, 122.4, 122.0, 63.9, 48.7, 48.4, 47.8, 45.0, 37.4, 33.8, 33.7, 32.4, 25.9, 25.3, 20.1, 19.2. HRMS (ESI): Calculated for $C_{22}H_{34}N_4O$ (M^++H): 371.28054; Found: 371.28091.

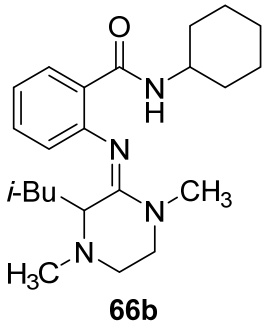

66b

[

(*E*)-*N*-cyclohexyl-2-((3-isobutyl-1,4-dimethylpiperazin-2-ylidene)amino)benzamide 66b. Obtained using **general procedure D**. Purified by normal-phase chromatography (0-10% MeOH/CH_2Cl_2) to yield the benzamidine, **66b** (20mg, 34%) as a pale-yellow gum. ^{1}H NMR (400 MHz, Chloroform-*d*) δ 8.56 (d, *J* = 8.1 Hz, 1H), 8.18 (dd, *J* = 7.9, 1.6 Hz, 1H), 7.30 – 7.25 (m, 2H), 7.05 (td, *J* = 7.6, 1.1 Hz, 1H), 6.61 (dd, *J* = 7.8, 1.1 Hz, 1H), 3.97 (dddd, *J* = 14.6, 10.6, 7.9, 3.9 Hz, 1H), 3.61 (td, *J* = 11.8, 5.3 Hz, 1H), 3.49 (dd, *J* = 10.6, 3.7 Hz, 1H), 3.41 (ddd, *J* = 14.0, 11.7, 5.2 Hz, 1H), 3.12 (ddd, *J* = 12.1, 5.3, 1.7 Hz, 1H), 3.08 (s, 3H), 2.73 – 2.66 (m, 1H), 2.50 (s, 3H), 2.02 – 1.94 (m, 2H), 1.71 (dq, *J* = 11.7, 4.0 Hz, 2H), 1.63 (dt, *J* = 12.6, 3.8 Hz, 1H), 1.54 (ddd, *J* = 14.1, 10.6, 3.9 Hz, 1H), 1.49 – 1.34 (m, 3H), 1.16 (dddd, *J* = 26.0, 15.5, 12.6, 5.6 Hz, 3H), 0.91 (ddd, *J* = 13.6, 9.7, 3.6 Hz, 1H), 0.66 (d, *J* = 6.6 Hz, 3H), 0.27 (d, *J* = 6.5 Hz, 3H). ^{13}C NMR (101 MHz, $CDCl_3$) δ 165.7, 161.8, 148.6, 131.4, 131.3, 125.6, 122.9, 122.4, 56.8, 48.2, 44.9, 43.8, 42.2, 40.1, 37.3, 33.8, 33.6, 25.9, 25.1, 25.1, 24.4, 23.4, 20.3. HRMS (ESI): Calculated for $C_{23}H_{36}N_4O$ (M^++H): 385.29619; Found: 385.29719.

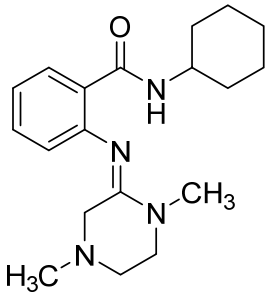

66c

(*E*)-*N*-cyclohexyl-2-((1,4-dimethylpiperazin-2-ylidene)amino)benzamide 66c. Obtained using **general procedure D**. Purified by normal-phase chromatography (0-10% MeOH/CH_2Cl_2) to yield the benzamidine, **66c** (12 mg, 58%) as an amber gum. ^{1}H NMR (500 MHz, Chloroform-*d*) δ 8.42 (d, *J* = 8.0 Hz, 1H), 8.12 (dd, *J* = 7.9, 1.7 Hz, 1H), 7.29 – 7.25 (m, 1H), 7.09 – 7.04 (m, 1H), 6.65 (d, *J* = 7.8 Hz, 1H), 3.94 (tdt, *J* = 11.0, 7.8, 3.8 Hz, 1H), 3.37 (t, *J* = 5.5 Hz, 2H), 3.12 (s, 3H), 2.95 (s, 2H), 2.61 (t, *J* = 5.6 Hz, 2H), 2.19 (s, 3H), 1.99 (dq, *J* = 12.4, 4.0 Hz, 2H), 1.71 (dp, *J* = 11.9, 3.9 Hz, 2H), 1.63 (dt, *J* = 12.2, 3.9 Hz, 1H), 1.40 (tdd, *J* = 15.5, 12.0, 3.6 Hz, 2H), 1.15 (td, *J* = 12.4, 9.1 Hz, 3H). ^{13}C NMR (126 MHz, $CDCl_3$) δ 166.0, 155.5, 148.3, 131.3, 131.2, 126.0, 123.2, 122.7, 55.1, 52.4, 49.7, 48.4, 45.5, 36.5, 33.6, 25.9, 25.1. HRMS (ESI): Calculated for $C_{19}H_{28}N_4O$ (M^++H): 329.23359; Found: 329.23434.

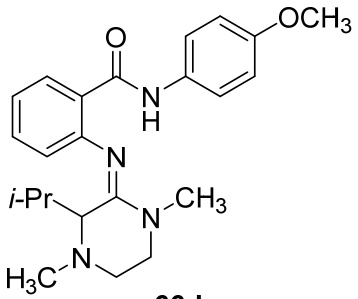

66d

(*E*)-2-((3-isopropyl-1,4-dimethylpiperazin-2-ylidene)amino)-*N*-(4-methoxyphenyl) benzamide 66d. Obtained using **general procedure D**. Purified by normal-phase chromatography (0-10% MeOH/CH_2Cl_2) to yield the benzamidine, **66d** (20mg, 23%) as a pale-yellow waxy solid. 1H NMR (400 MHz, Chloroform-d) δ 10.97 (s, 1H), 8.24 (dd, J = 8.0, 1.7 Hz, 1H), 7.53 (d, J = 8.5 Hz, 2H), 7.36 – 7.29 (m, 1H), 7.09 (t, J = 7.6 Hz, 1H), 6.88 (d, J = 8.7 Hz, 2H), 6.67 (d, J = 7.9 Hz, 1H), 3.79 (d, J = 1.3 Hz, 3H), 3.46 – 3.35 (m, 3H), 3.27 – 3.21 (m, 1H), 3.19 (s, 3H), 2.63 (dt, J = 11.9, 5.7 Hz, 1H), 2.52 (s, 3H), 1.75 (h, J = 6.8 Hz, 1H), 0.77 (d, J = 6.7 Hz, 3H), 0.65 (d, J = 6.8 Hz, 3H). ^{13}C NMR (101 MHz, CDCl3) δ 165.0, 161.0, 156.1, 148.6, 132.0, 131.7, 131.3, 125.9, 122.6, 122.3, 122.0, 114.3, 64.0, 55.6, 48.3, 47.7, 44.9, 37.6, 32.5, 20.0, 19.3. HRMS (ESI): Calculated for $C_{23}H_{30}N_4O_2$ (M^++H): 395.24415; Found: 395.24443.

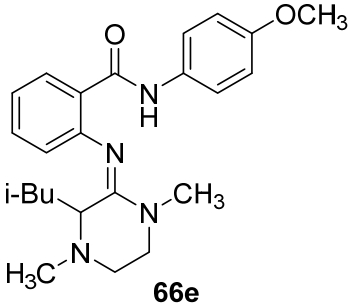

66e

(*E*)-2-((3-isobutyl-1,4-dimethylpiperazin-2-ylidene)amino)-*N*-(4-methoxyphenyl)benzamide 66e. Obtained using **general procedure D**. Purified by normal-phase chromatography (0-20% EtOAc/CH_2Cl_2) to yield the benzamidine, **66e** (26 mg, 39%) as a light-brown solid. m.p.: 109-111°C. ^{1}H NMR (400 MHz, Chloroform-d) δ 10.68 (s, 1H), 8.25 (dd, J = 8.0, 1.7 Hz, 1H), 7.62 – 7.50 (m, 2H), 7.34 (td, J = 7.6, 1.7 Hz, 1H), 7.19 – 7.06 (m, 1H), 6.94 – 6.85 (m, 2H), 6.76 – 6.64 (m, 1H), 3.80 (s, 3H), 3.61 (ddd, J = 12.4, 8.8, 4.4 Hz, 2H), 3.38 (ddd, J = 14.0, 11.6, 5.3 Hz, 1H), 3.18 (s, 3H), 3.11 (ddd, J = 12.1, 5.4, 1.7 Hz, 1H), 2.69 (dd, J = 14.3, 5.1 Hz, 1H), 2.50 (s, 3H), 1.56 (ddd, J = 14.0, 10.6, 3.7 Hz, 1H), 1.47 (dqd, J = 10.4, 6.6, 3.9 Hz, 0H), 0.92 (ddd, J = 13.5, 9.7, 3.5 Hz, 1H), 0.65 (d, J = 6.7 Hz, 3H), 0.28 (d, J = 6.5 Hz, 3H). ^{13}C NMR (101 MHz, $CDCl_3$) δ 164.6, 162.2, 155.9, 148.5, 132.1, 131.7, 131.3, 125.6, 123.0, 122.5, 121.6, 114.2, 77.4, 77.0,

76.7, 56.8, 55.5, 44.7, 43.4, 42.1, 39.9, 37.3, 24.4, 23.3, 20.2. HRMS (ESI): Calculated for $C_{24}H_{32}N_4O_2$ (M^++H): 409.25980; Found: 409.25931.

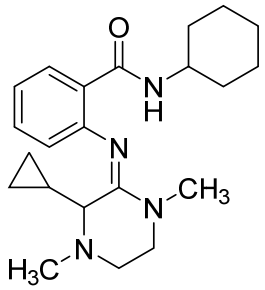

66f

(*E*)-*N*-cyclohexyl-2-((3-cyclopropyl-1,4-dimethylpiperazin-2-ylidene)amino)benzamide 66f. Obtained using **general procedure D**. Purified by normal-phase chromatography (0-5% MeOH/CH_2Cl_2) to yield amidine **66f** (17.5 mg, 65%) as a pale-yellow gum. ^{1}H NMR (400 MHz, Chloroform-*d*) δ 8.62 (d, *J* = 8.1 Hz, 1H), 8.18 (dt, *J* = 7.9, 1.5 Hz, 1H), 7.28 – 7.21 (m, 1H), 7.09 – 7.01 (m, 1H), 6.56 (d, *J* = 7.8 Hz, 1H), 3.96 (dtt, *J* = 11.2, 7.8, 4.1 Hz, 1H), 3.58 – 3.44 (m, 2H), 3.30 (dd, *J* = 10.3, 4.2 Hz, 1H), 3.09 (s, 3H), 2.92 (d, *J* = 8.6 Hz, 1H), 2.76 (dd, *J* = 11.8, 4.6 Hz, 1H), 2.46 (s, 3H), 1.98 (d, *J* = 12.9 Hz, 2H), 1.78 – 1.62 (m, 4H), 1.41 (qd, *J* = 12.5, 6.0 Hz, 3H), 1.23 – 1.06 (m, 3H), 0.90 (ddt, *J* = 13.8, 8.8, 4.3 Hz, 1H), 0.40 (td, *J* = 8.7, 4.5 Hz, 1H), 0.28 (tt, *J* = 8.6, 5.4 Hz, 1H). ^{13}C NMR (101 MHz, $CDCl_3$) δ 165.8, 160.4, 148.9, 131.3, 131.1, 126.4, 122.6, 122.3, 62.1, 48.3, 47.4, 45.5, 42.3, 37.3, 33.8, 33.7, 25.9, 25.2, 25.2, 11.6, 4.1, 3.7, 1.2. HRMS (ESI): Calculated for $C_{22}H_{32}N_4O$ (M^++H): 369.26489; Found: 369.26570.

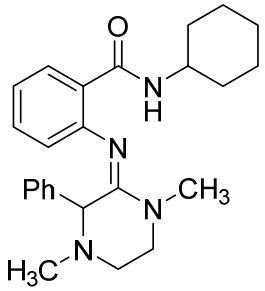

66g

(*E*)-*N*-cyclohexyl-2-((1,4-dimethyl-3-phenylpiperazin-2-ylidene)amino)benzamide 66g. Obtained using **general procedure D**. Purified by normal-phase chromatography (0-10% MeOH/CH_2Cl_2) to yield benzamidine, **66g** (38mg, 70%) as a pale-yellow gum. ^{1}H NMR (500 MHz, CDCl3) δ 8.36 (d, J = 7.7 Hz, 1H), 7.88 (dd, J = 7.9, 1.5 Hz, 1H), 7.18 (t, J = 7.4 Hz, 1H), 7.11 (t, J = 7.5 Hz, 2H), 7.08 – 7.03 (m, 1H), 6.93 – 6.89 (m, 1H), 6.85 (d, J = 7.2 Hz, 2H), 6.37 (d, J = 7.7 Hz, 1H), 4.41 (s, 1H), 3.86-3.83 (m, 1H), 3.57 – 3.51 (m, 2H), 3.24 (s, 3H), 3.03 – 2.95 (m, 1H), 2.62-2.58 (m, 1H), 2.16 (s, 3H), 2.05 – 1.94 (m, 2H), 1.80 – 1.69 (m, 2H), 1.68-1.584 (m, 1H), 1.46 – 1.34 (m, 2H), 1.23 – 1.11 (m, 3H). ^{13}C NMR (126 MHz, CDCl3) δ 165.3, 165.2, 157.6,

148.1, 135.7, 130.8, 130.6, 129.3, 128.0, 127.9, 125.5, 123.2, 122.1, 65.3, 49.1, 48.3, 46.6, 42.1, 37.4, 33.7, 33.7, 25.9, 25.2, 25.2. HRMS (ESI): Calculated for $C_{25}H_{32}N_4O$ (M^++H): 405.26489; Found: 405.26680.

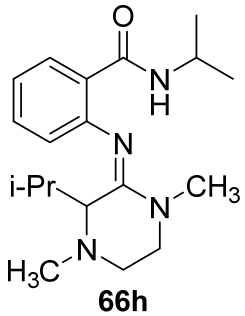

66h

(*E*)-*N*-isopropyl-2-((3-isopropyl-1,4-dimethylpiperazin-2-ylidene)amino)benzamide 66h. Obtained using **general procedure D**. Purified by normal-phase chromatography (0-5% MeOH/CH_2Cl_2) to yield the benzamidine, **66h** (11 mg, 52%) as a pale-yellow oil . ^{1}H NMR (500 MHz, Chloroform-*d*) δ 8.94 (d, *J* = 7.6 Hz, 1H), 8.18 (dd, *J* = 7.9, 1.6 Hz, 1H), 7.28 (dd, *J* = 7.5, 1.7 Hz, 1H), 7.06 – 7.02 (m, 1H), 6.60 (dd, *J* = 7.9, 1.2 Hz, 1H), 4.31 – 4.22 (m, 1H), 3.48 – 3.41 (m, 2H), 3.36 (ddd, *J* = 12.2, 7.0, 4.6 Hz, 1H), 3.24 (ddd, *J* = 11.8, 7.0, 4.4 Hz, 1H), 3.13 (s, 3H), 2.64 (ddd, *J* = 12.0, 6.7, 4.7 Hz, 1H), 2.50 (s, 3H), 1.72 (h, *J* = 6.7 Hz, 1H), 1.22 (d, *J* = 6.5 Hz, 6H), 0.80 (d, *J* = 6.7 Hz, 3H), 0.64 (d, *J* = 6.8 Hz, 3H). ^{13}C NMR (126 MHz, $CDCl_3$) δ 166.0, 160.5, 148.6, 131.3, 131.2, 125.8, 122.4, 122.1, 64.0, 48.8, 47.9, 45.1, 41.3, 37.3, 32.5, 23.3, 23.2, 20.2, 19.3. HRMS (ESI): Calculated for $C_{19}H_{30}N_4O$ (M^++H): 331.249238; Found: 331.24986.

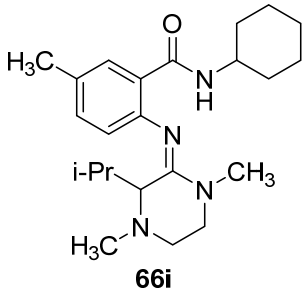

66i

(*E*)-*N*-cyclohexyl-2-((3-isopropyl-1,4-dimethylpiperazin-2-ylidene)amino)-5-methylbenzamide 66i. Obtained using **general procedure D**. Purified by normal-phase chromatography (0-5% MeOH/CH_2Cl_2) to yield the benzamidine, **66d** (41 mg, 64%) as a pale-yellow oil. ^{1}H NMR (400 MHz, Chloroform-*d*) δ 8.90 (d, *J* = 8.1 Hz, 1H), 7.96 (d, *J* = 2.2 Hz, 1H), 7.06 (dd, *J* = 8.0, 2.2 Hz, 1H), 6.49 (d, *J* = 8.0 Hz, 1H), 3.93 (tdt, *J* = 11.4, 7.8, 3.9 Hz, 1H), 3.48 – 3.36 (m, 2H), 3.34 (ddd, *J* = 12.0, 7.0, 4.6 Hz, 1H), 3.22 (ddd, *J* = 11.8, 7.0, 4.5 Hz, 1H), 3.09 (s, 3H), 2.62 (ddd, *J* = 11.9, 6.6, 4.7 Hz, 1H), 2.48 (s, 3H), 2.30 (s, 3H), 2.07 – 1.94 (m, 3H), 1.73 (ddt, *J* = 11.9, 8.0, 4.5 Hz, 2H), 1.71 – 1.58 (m, 1H), 1.38 (tdt, *J* = 16.5, 12.1, 3.8 Hz, 2H), 1.13 (qdt, *J* = 10.6, 6.7, 3.2 Hz, 3H), 0.79 (d, *J* = 6.7 Hz, 3H), 0.63 (d, *J* = 6.9 Hz, 3H). ^{13}C NMR (101 MHz, $CDCl_3$) δ 166.1, 160.6, 146.0, 131.9, 131.5, 125.5, 122.3, 64.0, 48.7, 48.5, 47.9, 45.0,

37.4, 33.8, 33.8, 32.5, 25.9, 25.3, 20.8, 20.1, 19.3. HRMS (ESI): Calculated for $C_{23}H_{36}N_4O$ (M^++H): 385.296188; Found: 385.29605.

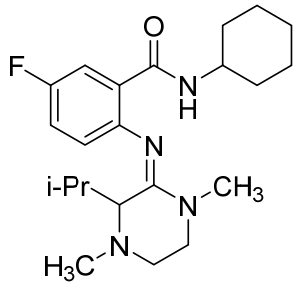

66j

(*E*)-*N*-cyclohexyl-5-fluoro-2-((3-isopropyl-1,4-dimethylpiperazin-2-ylidene)amino)benzamide 66j. Obtained using **general procedure D**. Purified by normal-phase chromatography (0-5% MeOH/CH_2Cl_2) to yield the benzamidine, **66j** (8 mg, 40%) as a pale-yellow gum . ^{1}H NMR (400 MHz, CDCl3) δ 8.99 (d, J = 7.4 Hz, 1H), 7.90 (dd, J = 10.1, 2.9 Hz, 1H), 6.99 (td, J = 8.4, 3.1 Hz, 1H), 6.56 (dd, J = 8.6, 4.9 Hz, 1H), 4.03 – 3.87 (m, 1H), 3.48-3.46 (m, 1H), 3.41 – 3.31 (m, 2H), 3.28-3.22 (m, 1H), 3.13 (s, 3H), 2.70 – 2.60 (m, 1H), 2.50 (s, 3H), 2.10 – 1.95 (m, 2H), 1.80 – 1.59 (m, 4H), 1.51 – 1.35 (m, 2H), 1.24-1.18 (m, 3H), 0.81 (d, J = 6.7 Hz, 3H), 0.65 (d, J = 6.8 Hz, 3H). ^{19}F NMR (376 MHz, CDCl3) δ -122.09. ^{13}C NMR (101 MHz, CDCl3) δ 164.6, 164.6, 160.9, 159.6, 157.2, 149.9, 127.1, 127.1, 123.5, 123.4, 118.1, 117.8, 117.3, 117.1, 63.9, 48.7, 48.6, 47.8, 45.1, 37.3, 33.7, 33.6, 32.5, 25.8, 25.2, 20.0, 19.1. HRMS (ESI): Calculated for $C_{22}H_{33}FN_4O$ (M^++H): 389.271116; Found: 389.27059.

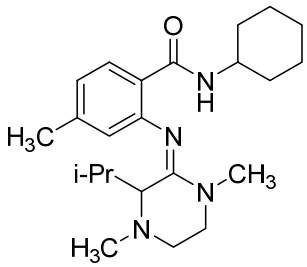

66k

(*E*)-*N*-cyclohexyl-2-((3-isopropyl-1,4-dimethylpiperazin-2-ylidene)amino)-4-methylbenzamide 66k. Obtained using **general procedure D**. Purified by normal-phase chromatography (0-5% MeOH/CH_2Cl_2) to yield the benzamidine, **66k** (30 mg, 61%) as a pale-yellow gum. ^{1}H NMR (400 MHz, Chloroform-*d*) δ 8.84 (d, *J* = 8.0 Hz, 1H), 8.06 (d, *J* = 8.0 Hz, 1H), 6.84 (d, *J* = 8.0 Hz, 1H), 6.39 (s, 1H), 3.94 (dtd, *J* = 11.3, 7.6, 4.1 Hz, 1H), 3.49 – 3.30 (m, 3H), 3.23 (ddd, *J* = 11.8, 6.9, 4.5 Hz, 1H), 3.10 (s, 3H), 2.63 (ddd, *J* = 12.0, 6.7, 4.7 Hz, 1H), 2.50 (s, 3H), 2.29 (s, 3H), 2.01 (tt, *J* = 8.4, 3.8 Hz, 2H), 1.78 – 1.59 (m, 4H), 1.46 – 1.31 (m, 2H), 1.21 – 1.06 (m, 3H), 0.80 (d, *J* = 6.7 Hz, 3H), 0.64 (d, *J* = 6.8 Hz, 3H). ^{13}C NMR (101 MHz, $CDCl_3$) δ

166.0, 160.5, 148.4, 141.3, 131.3, 123.3, 123.1, 123.0, 64.1, 48.8, 48.4, 47.9, 45.01, 37.4, 33.9, 33.8, 32.6, 25.9, 25.3, 21.4, 20.1, 19.4.

1.6 General procedure E: Representative Procedure for the Telescoped Synthesis of Benzamidines:

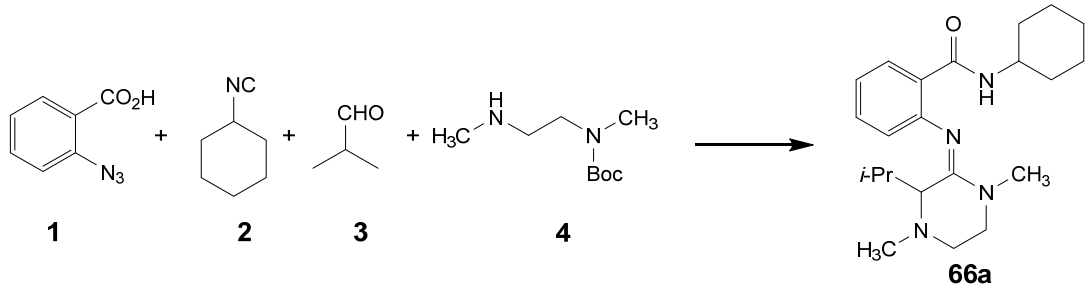

(*E*)-*N*-cyclohexyl-2-((3-isopropyl-1,4-dimethylpiperazin-2-ylidene)amino)benzamide 66a. An oven-dried, 10 mL round bottom flask under nitrogen was charged with activated, powdered, 4 Å molecular sieves (50 mg). The flask was placed under vacuum and flame-dried, then backfilled with nitrogen. Diamine **4** (115 mg, 0.61 mmol, 2.0 equiv.) was dissolved in dry CH_2Cl_2 (0.5 mL, 1.3 M) and added to the reaction vessel. Aldehyde **3** (112 µL, 1.2 mmol, 4.0 equiv.) was dissolved in dry CH_2Cl_2 (0.46 mL, 2.6 M) in a 1-dram glass vial and added dropwise over 1 min via syringe to the reaction vessel while stirring at rt. Upon completion of the addition, carboxylic acid **1** (50 mg, 0.31 mmol, 1.0 equiv.) was dissolved in a 3:1 mixture of dry CH_2Cl_2/MeOH (0.4 mL, .8 M), taken up into a syringe and the needle was placed into the septum of the reaction vessel. Isocyanide **2** (153 µL, 1.2 mmol, 4.0 equiv.) was dissolved in dry CH_2Cl_2 (0.3 mL, 3.6 M) in a 1-dram glass vial, taken up into a syringe and the needle was placed into the septum of the reaction vessel. Carboxylic acid **1** was added dropwise to the reaction vessel while stirring over 1 min followed immediately by isocyanide **2**. The reaction mixture was stirred at rt for 12 h after which the reaction was complete as judged by complete consumption of carboxylic acid **1** on TLC (10% MeOH/CH_2Cl_2). The crude reaction mixture was filtered through a 0.45 µM syringe filter and the filtrate was concentrated *in vacuo*. To a flame-dried, 10 mL round bottom flask under nitrogen was added triphenylphospine on resin (438 mg, 0.61 mmol, 1.4 meq/g, 2.0 equiv.) followed by dry toluene (1.0 mL). A solution of the crude reaction mixture in dry toluene (2.0 mL) was added dropwise and the reaction mixture was stirred at rt for 1 h. After 1 h at rt, the reaction mixture was heated to 110 °C and stirred for 12 h at reflux after which the reaction was complete as judged by complete consumption of the intermediate by TLC (30% EtOAc/hexanes). The crude reaction mixture was filtered through a pad of celite, rinsed with CH_2Cl_2 (10 mL x 5), and the filtrate was concentrated *in vacuo*. To a flame-dried, 10 mL round bottom flask under nitrogen was dissolved the crude reaction mixture in dry CH_2Cl_2 (3.0 mL, 0.1 M) and the solution cooled to 0 °C in an ice-bath while stirring for 20 min. HCl in dioxane (4.0 M, 0.8 mL, 10.0 equiv.) was added dropwise. The reaction mixture was allowed to slowly warm to rt. The reaction mixture was stirred at rt for 12h after which the reaction was complete as judged by complete consumption of

intermediate on TLC (30% EtOAC/hexanes). The reaction mixture was dried *in vacuo*. Triethylamine (0.4 mL, 3.1 mmol, 10.0 equiv.) was added to a solution of the crude reaction mixture in MeOH (3.1 mL, 0.1 M) in a 10 mL microwave vial and the reaction mixture was heated in a microwave reactor at 100 °C for 1 h. The reaction mixture was allowed to cool to rt and the solvent was removed *in vacuo*. The crude mixture was dissolved in CH_2Cl_2 (10 mL) and washed with water (10 mL), then saturated brine solution (10 mL), The organic layer was dried over $MgSO_4$, filtered and concentrated *in vacuo*. The crude residue was purified by normal-phase chromatography (0-60% EtOAc/Hex) to yield the benzamidine, **66a** (69 mg, 61%) as a pale-yellow oil.

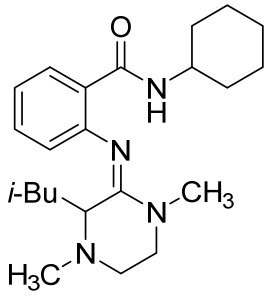

66b

(*E*)-*N*-cyclohexyl-2-((3-isobutyl-1,4-dimethylpiperazin-2-ylidene)amino)benzamide 66b. Obtained using **general procedure E**. Purified by normal-phase chromatography (0-50% EtOAc/hexane) to yield the benzamidine, **66b** (71 mg, 60%) as pale-yellow gum.

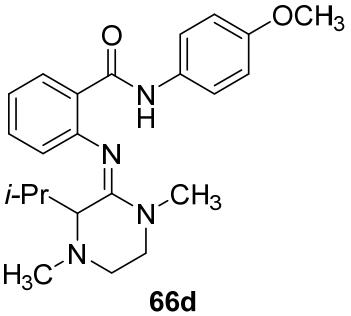

66d

(*E*)-2-((3-isopropyl-1,4-dimethylpiperazin-2-ylidene)amino)-*N*-(4-methoxyphenyl)benzamide 66d. Obtained using **general procedure E**. Purified by normal-phase chromatography (0-20% EtOAc/CH_2Cl_2) to yield the benzamidine, **66d** (120mg, 40%) as a pale-yellow waxy solid.

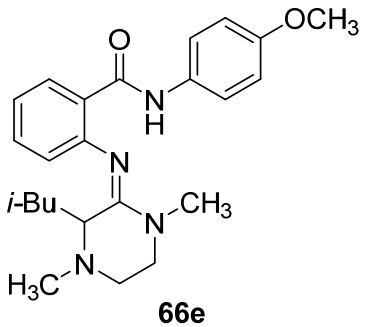

66e

(*E*)-2-((3-isobutyl-1,4-dimethylpiperazin-2-ylidene)amino)-*N*-(4-methoxyphenyl)benzamide 66e. Obtained using **general procedure E**. Purified by normal-phase chromatography (0-20% EtOAc/CH_2Cl_2) to yield the benzamidine, **66e** (56 mg, 45%) as a light-brown solid .

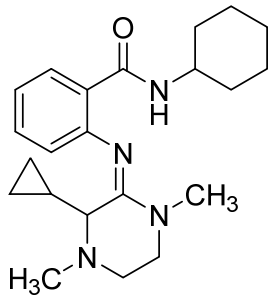

66f

(*E*)-*N*-cyclohexyl-2-((3-cyclopropyl-1,4-dimethylpiperazin-2-ylidene)amino)benzamide 66f. Obtained using **general procedure E**. Purified by normal-phase chromatography (1-5% MeOH/EtOAc) to yield the benzamidine, **66f** (80 mg, 70%) as pale-yellow gum.

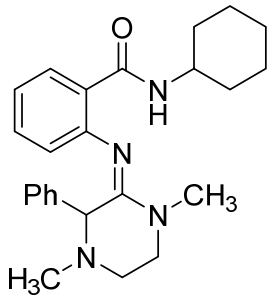

66g

(*E*)-*N*-cyclohexyl-2-((1,4-dimethyl-3-phenylpiperazin-2-ylidene)amino)benzamide 66g. Obtained using **general procedure E**. Purified by normal-phase chromatography (0-5% MeOH/EtOAc) to yield the benzamidine, **66g** (85 mg, 68%) as a pale-yellow oil.

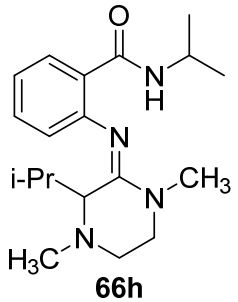

66h

(*E*)-*N*-isopropyl-2-((3-isopropyl-1,4-dimethylpiperazin-2-ylidene)amino)benzamide 66h. Obtained using **general procedure E**. Purified by normal-phase chromatography (0-20% EtOAc/CH_2Cl_2) to yield the benzamidine, **66h** (51 mg, 50%) as a pale-yellow oil.

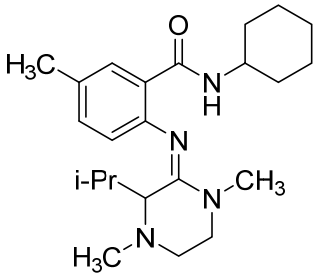

66i

(*E*)-*N*-cyclohexyl-2-((3-isopropyl-1,4-dimethylpiperazin-2-ylidene)amino)-5-methylbenzamide 66i. Obtained using **general procedure E**. Purified by normal-phase chromatography (0-40% EtOAc/hexane) to yield the benzamidine, **66i** (53 mg, 45%) as a pale-yellow gum.

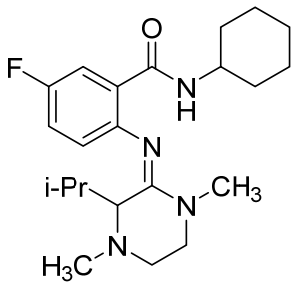

66j

***E*)-*N*-cyclohexyl-5-fluoro-2-((3-isopropyl-1,4-dimethylpiperazin-2-ylidene)amino) benzamide 66j.** Obtained using **general procedure E**. Purified by normal-phase chromatography (0-40% EtOAc/hexane) to yield the benzamidine, **66j** (67 mg, 56%) as a pale-yellow gum.

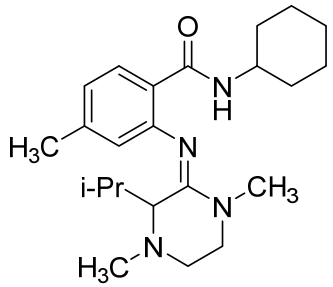

66k

(*E*)-*N*-cyclohexyl-2-((3-isopropyl-1,4-dimethylpiperazin-2-ylidene)amino)-4-methylbenzamide 66k. Obtained using **general procedure E**. Purified by normal-phase chromatography (0-50% EtOAc/hexane) to yield the benzamidine, **66k** (53 mg, 45%) as a pale-yellow gum.

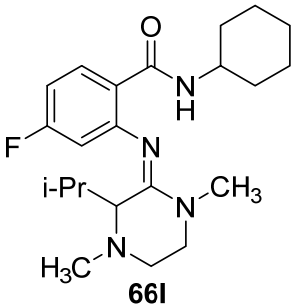

66l

(*E*)-*N*-cyclohexyl-4-fluoro-2-((3-isopropyl-1,4-dimethylpiperazin-2-ylidene)amino) benzamide 66l. Obtained using **general procedure E**. Purified by normal-phase chromatography (0-40% EtOAc/hexane) to yield the benzamidine, **66l** (25mg, 21%) as a pale-yellow gum. ^{1}H NMR (400 MHz, Chloroform-*d*) δ 8.81 (d, *J* = 8.0 Hz, 1H), 8.19 (dd, *J* = 8.8, 7.1 Hz, 1H), 6.73 (td, *J* = 8.4, 2.5 Hz, 1H), 6.30 (dd, *J* = 10.3, 2.5 Hz, 1H), 3.94 (tdt, *J* = 11.5, 7.9, 3.9 Hz, 1H), 3.52 – 3.42 (m, 2H), 3.37 (ddd, *J* = 12.3, 6.8, 4.7 Hz, 1H), 3.24 (ddd, *J* = 11.7, 6.8, 4.5 Hz, 1H), 3.13 (s, 3H), 2.65 (ddd, *J* = 12.0, 6.8, 4.7 Hz, 1H), 2.52 (s, 3H), 2.02 (dt, *J* = 11.8, 4.1 Hz, 2H), 1.70 (ddt, *J* = 29.4, 14.9, 5.2 Hz, 5H), 1.40 (qd, *J* = 12.5, 3.3 Hz, 2H), 1.22 – 1.06 (m, 3H), 0.82 (d, *J* = 6.7 Hz, 3H), 0.68 (d, *J* = 6.9 Hz, 3H). ^{19}F NMR (376 MHz, $CDCl_3$) δ -109.97. ^{13}C NMR (101 MHz, CDCl3) δ 165.2, 165.0, 162.7, 160.8, 150.5, 150.4, 133.5, 133.4, 122.2, 122.2, 108.9, 108.7, 108.6, 108.4, 63.8, 48.6, 48.4, 47.7, 45.1, 37.3, 33.8, 33.7, 32.5, 29.7, 25.8, 25.2, 20.1, 19.1. HRMS (ESI): Calculated for $C_{22}H_{33}FN_4O$ (M^++H): 389.27116; Found: 389.27155.

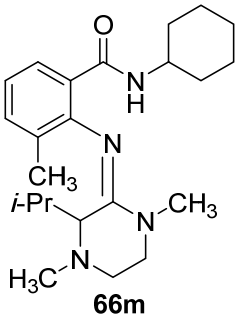

66m

(*E*)-*N*-cyclohexyl-2-((3-isopropyl-1,4-dimethylpiperazin-2-ylidene)amino)-3-methylbenzamide 66m. Obtained using **general procedure E**. Purified by normal phase chromatography (0-30% EtoAc/CH_2Cl_2) to yield the benzamidine, **66m** (41 mg, 35%) as a pale-yellow oil. ^{1}H NMR (400 MHz, Chloroform-*d*) δ 8.66 (d, *J* = 7.9 Hz, 1H), 8.04 (dd, *J* = 7.9, 1.6 Hz, 1H), 7.23 (dd, *J* = 7.4, 1.5 Hz, 1H), 6.97 (t, *J* = 7.6 Hz, 1H), 3.92 (dtt, *J* = 11.6, 8.0, 4.0 Hz, 1H), 3.60 (ddd, *J* = 12.6, 9.6, 3.2 Hz, 1H), 3.20 (s, 4H), 3.13 (s, 1H), 3.05 (ddd, *J* = 15.4, 8.6, 3.7 Hz, 1H), 2.94 (d, *J* = 3.0 Hz, 1H), 2.62 (ddd, *J* = 11.4, 9.6, 3.6 Hz, 1H), 2.38 (s, 3H), 2.11 (d, *J* = 3.8 Hz, 4H), 2.07 – 1.94 (m, 1H), 1.72 (tdd, *J* = 12.8, 8.1, 5.1 Hz, 1H), 1.63 (qd, *J* = 7.0, 3.0 Hz, 1H), 1.49 – 1.30 (m, 2H), 1.14 (tddd, *J* = 11.6, 8.7, 6.3, 3.8 Hz, 3H), 0.83 (d, *J* = 6.9 Hz, 3H), 0.67 (d, *J* = 6.9 Hz, 4H). ^{13}C NMR (101 MHz, $CDCl_3$) δ 166.1, 160.5, 147.5, 133.2, 129.1, 127.8, 126.0, 121.6, 65.8, 51.5, 49.0, 48.4, 47.4, 37.2, 33.8, 33.7, 32.8, 25.8, 25.3, 25.2, 21.2, 19.2, 17.6. HRMS (ESI): Calculated for $C_{22}H_{33}FN_4O$ (M^++H): 389.27112; Found: 389.27196.

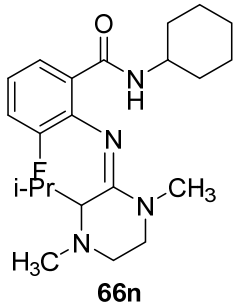

66n

(*E*)-*N*-cyclohexyl-3-fluoro-2-((3-isopropyl-1,4-dimethylpiperazin-2-ylidene)amino) benzamide 66n. Obtained using **general procedure E**. Purified by normal-phase chromatography (0-15% EtOAc/CH_2Cl_2) to yield the benzamidine, **66n** (65 mg, 42%) as a pale-yellow gum. Colorless oil, 42%. ^{1}H NMR (400 MHz, Chloroform-*d*) δ 9.00 (s, 1H), 7.99 (d, *J* = 7.9 Hz, 1H), 7.10 (ddd, *J* = 10.1, 8.0, 1.6 Hz, 1H), 6.94 (td, *J* = 8.0, 5.1 Hz, 1H), 3.94 (tdt, *J* = 11.4, 7.8, 3.8 Hz, 1H), 3.51 (ddd, *J* = 12.1, 8.0, 3.8 Hz, 1H), 3.33 (ddd, *J* = 12.6, 5.9, 4.1 Hz, 1H), 3.19 (s, 3H), 3.12 (t, *J* = 3.2 Hz, 2H), 2.66 (ddd, *J* = 12.1, 8.0, 4.1 Hz, 1H), 2.45 (s, 3H), 2.07 – 1.97 (m, 2H), 1.77 – 1.61 (m, 4H), 1.46 – 1.34 (m, 2H), 1.16 (dddd, *J* = 12.4, 8.6, 6.8, 2.7 Hz, 3H), 0.82 (d, *J* = 6.8 Hz, 3H), 0.70 (d, *J* = 6.9 Hz, 3H). ^{19}F NMR (376 MHz, $CDCl_3$) δ -127.01. ^{13}C NMR (101 MHz, $CDCl_3$) δ 165.1, 162.9, 153.8, 151.4, 137.2, 137.1, 127.9, 126.7, 121.4, 121.4, 118.0, 117.8, 66.0, 49.9,

48.6, 48.3, 46.0, 37.5, 33.8, 33.7, 33.6, 29.8, 25.9, 25.3, 20.6, 18.7. HRMS (ESI): Calculated for $C_{22}H_{33}FN_4O$ (M^++H): 389.27112; Found: 389.27196.

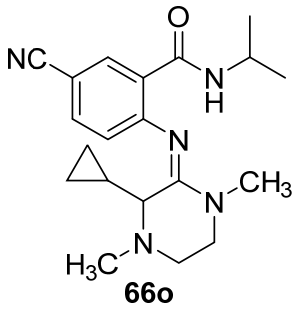

66o

(*E*)-5-cyano-2-((3-cyclopropyl-1,4-dimethylpiperazin-2-ylidene)amino)-*N*-isopropylbenzamide 66o. Obtained using **general procedure E**. Purified by normal-phase chromatography (0-15% MeOH/EtOAC) to yield the benzamidine, **66o** (48 mg, 44%) as a light-brown solid . m.p.: 147-148°C. ^{1}H NMR (400 MHz, Chloroform-*d*) δ 8.61 (d, *J* = 7.7 Hz, 1H), 8.52 (d, *J* = 2.1 Hz, 1H), 7.50 (dd, *J* = 8.2, 2.1 Hz, 1H), 6.62 (d, *J* = 8.2 Hz, 1H), 4.32 – 4.18 (m, 1H), 3.58 (td, *J* = 11.0, 5.5 Hz, 1H), 3.45 (ddd, *J* = 12.8, 10.4, 5.1 Hz, 1H), 3.35 (ddd, *J* = 11.7, 5.1, 2.4 Hz, 1H), 3.13 (s, 3H), 2.93 (d, *J* = 8.4 Hz, 1H), 2.79 (ddd, *J* = 13.2, 5.7, 2.3 Hz, 1H), 2.46 (s, 3H), 1.23 (d, J = 6.6 Hz, 3H), 1.20 (d, J = 6.5 Hz, 3H), 0.89 (dtd, *J* = 13.3, 8.3, 5.0 Hz, 1H), 0.51 – 0.40 (m, 1H), 0.36 – 0.25 (m, 1H), 0.14 (dq, *J* = 10.5, 5.2 Hz, 1H), -0.48 (dq, *J* = 10.3, 5.2 Hz, 1H). ^{13}C NMR (101 MHz, CDCl3) δ 163.8, 160.6, 153.0, 135.7, 134.2, 126.8, 123.3, 119.2, 105.0, 61.9, 47.2, 45.3, 42.3, 41.4, 37.2, 23.1, 23.0, 11.5, 3.9, 3.6. HRMS (ESI): Calculated for $C_{20}H_{27}N_5O$ (M^++H): 354.22884; Found: 354.22999.

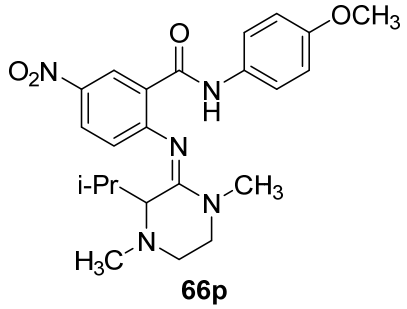

66p

(*E*)-2-((3-isopropyl-1,4-dimethylpiperazin-2-ylidene)amino)-*N*-(4-methoxyphenyl)-5-nitrobenzamide 66p. Obtained using **general procedure E**. Purified by normal-phase chromatography (0-3% EtOAc/CH_2Cl_2) to yield the benzamidine, **66p** (49 mg, 36%) as yellow solid. m.p.: 167-168°C. ^{1}H NMR (400 MHz, Chloroform-*d*) δ 10.93 (s, 1H), 9.17 (d, *J* = 2.8 Hz, 1H), 8.16 (dd, *J* = 8.8, 2.9 Hz, 1H), 7.59 – 7.46 (m, 2H), 6.97 – 6.84 (m, 2H), 6.71 (d, *J* = 8.8 Hz, 1H), 3.81 (s, 3H), 3.57 – 3.46 (m, 2H), 3.45 (d, *J* = 6.4 Hz, 1H), 3.27 (s, 4H), 2.76 – 2.65 (m, 1H), 2.55 (s, 3H), 1.76 (h, *J* = 6.7 Hz, 1H), 0.80 (d, *J* = 6.7 Hz, 3H), 0.70 (d, *J* = 6.8 Hz, 3H). ^{13}C NMR

(101 MHz, CDCl3) δ 162.5, 162.0, 156.3, 154.3, 142.3, 131.3, 127.8, 126.4, 125.7, 122.6, 121.8, 114.3, 64.3, 55.5, 48.0, 47.5, 44.9, 37.8, 32.8, 20.0, 19.1. Calculated for HRMS (ESI): $C_{23}H_{29}N_5O_4$ (M^++H): 440.22923; Found: 440.22903.

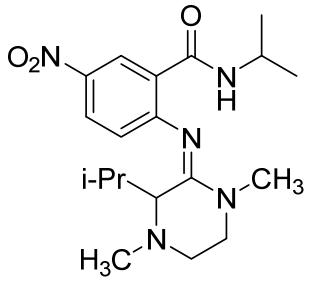

66q

(*E*)-*N*-isopropyl-2-((3-isopropyl-1,4-dimethylpiperazin-2-ylidene)amino)-5-nitrobenzamide 66q. Obtained using **general procedure E**. Purified by normal-phase chromatography (0-7% EtOAc/CH_2Cl_2) to yield the benzamidine, **66q** (36 mg, 31%) as a yellow-orange solid. m.p.: 140-141°C. ^{1}H NMR (400 MHz, Chloroform-*d*) δ 9.10 (d, *J* = 2.8 Hz, 1H), 8.93 (d, *J* = 7.6 Hz, 1H), 8.12 (dd, *J* = 8.8, 2.9 Hz, 1H), 6.65 (d, *J* = 8.8 Hz, 1H), 4.27 (dq, *J* = 13.2, 6.5 Hz, 1H), 3.53 (ddd, *J* = 11.9, 6.9, 4.5 Hz, 1H), 3.46 (dd, *J* = 6.7, 4.9 Hz, 1H), 3.42 (d, *J* = 6.0 Hz, 1H), 3.25 (ddd, *J* = 12.6, 6.6, 4.5 Hz, 1H), 3.19 (s, 3H), 2.71 (ddd, *J* = 12.1, 6.9, 4.8 Hz, 1H), 2.53 (s, 3H), 1.71 (h, *J* = 6.7 Hz, 1H), 1.23 (dd, *J* = 6.6, 1.4 Hz, 6H), 0.83 (d, *J* = 6.7 Hz, 3H), 0.69 (d, *J* = 6.8 Hz, 3H). ^{13}C NMR (101 MHz, $CDCl_3$) δ 163.7, 161.3, 154.4, 142.0, 127.68, 126.0, 125.6, 122.5, 77.4, 77.0, 76.7, 64.2, 48.5, 47.7, 45.1, 41.6, 37.4, 32.9, 23.02, 23.0, 20.1, 19.0. Calculated for HRMS (ESI): $C_{19}H_{29}N_5O_3$ (M^++H): 376.23432; Found: 376.23487.

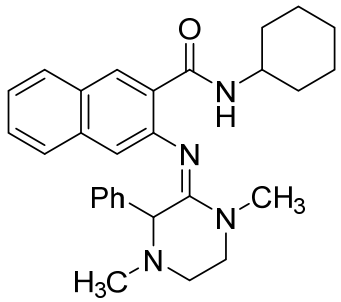

66r

(*E*)-*N*-cyclohexyl-3-((1,4-dimethyl-3-phenylpiperazin-2-ylidene)amino)-2-naphthamide 66r. Obtained using **general procedure E**. Purified by normal-phase chromatography (0-20% EtOAc/CH_2Cl_2) to yield the naphthamidine, **66r** (69 mg, 50%) as apale-yellow gum. ^{1}H NMR (400 MHz, Chloroform-d) δ 8.68 (d, J = 8.0 Hz, 1H), 8.47 (s, 1H), 7.79 (dd, J = 8.3, 1.2 Hz, 1H), 7.36 (d, J = 3.8 Hz, 2H), 7.29 (dd, J = 8.2, 3.9 Hz, 1H), 7.23 – 7.17 (m, 1H), 7.09 (t, J = 7.6 Hz, 2H), 6.81 (dd, J = 7.9, 1.4 Hz, 2H), 6.66 (s, 1H), 4.51 (s, 1H), 3.90 (tdt, J = 11.3, 7.8, 3.9 Hz, 1H), 3.63 – 3.51 (m, 2H), 3.29 (s, 3H), 3.02 (ddd, J = 12.5, 8.7, 5.0 Hz, 1H), 2.62 (dt, J = 12.5, 4.7 Hz, 1H), 2.14 (s, 3H), 2.10 – 1.98 (m, 2H), 1.84 – 1.57 (m, 2H), 1.53 – 1.35 (m, 2H), 1.28 – 1.13 (m, 4H). ^{13}C NMR (101 MHz, CDCl3) δ 164.9, 157.8, 145.04, 135.7, 134.7, 131.7, 129.3, 129.3,

128.9, 127.9, 127.8, 127.0, 126.1, 126.0, 124.0, 119.1, 64.9, 49.2, 48.4, 46.3, 42.0, 37.4, 33.6, 25.8, 25.2, 25.1. Calculated for HRMS (ESI): $C_{29}H_{34}N4O$ (M^++H): 455.28054; Found: 455.28019.

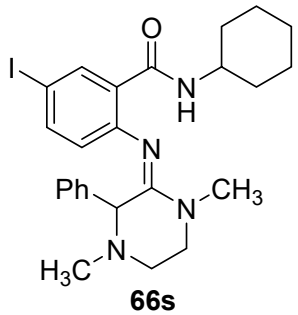

66s

(*E*)-*N*-cyclohexyl-2-((1,4-dimethyl-3-phenylpiperazin-2-ylidene)amino)-5-iodobenzamide 66s. Obtained using **general procedure E**. Purified by normal-phase chromatography (0-15% EtOAc/CH_2Cl_2) to yield benzamidine **66s** (144mg, 88%) as pale yellow oil. Recrystallized from acetonitrile to form clear colorless crystal (See Crystallographic Experimental Section). m.p.: 85-87°C. ^{1}H NMR (400 MHz, Chloroform-*d*) δ 8.27 (d, *J* = 7.9 Hz, 1H), 8.15 (d, *J* = 2.2 Hz, 1H), 7.32 (dd, *J* = 8.3, 2.3 Hz, 1H), 7.24 – 7.18 (m, 1H), 7.14 (d, *J* = 7.6 Hz, 2H), 7.13 (d, *J* = 8.6 Hz, 0H), 6.85 (d, *J* = 6.9 Hz, 1H), 6.12 (d, *J* = 8.3 Hz, 1H), 4.33 (s, 1H), 3.80 (dtd, *J* = 10.9, 7.3, 3.9 Hz, 1H), 3.64 – 3.42 (m, 2H), 3.22 (s, 3H), 2.98 (ddd, *J* = 12.7, 7.6, 5.2 Hz, 1H), 2.59 (dt, *J* = 12.5, 5.0 Hz, 1H), 2.15 (s, 3H), 2.04 – 1.88 (m, 2H), 1.80 – 1.61 (m, 2H), 1.48 – 1.32 (m, 2H), 1.15 (dtdd, *J* = 23.1, 11.8, 7.9, 3.5 Hz, 2H). ^{13}C NMR (101 MHz, CDCl3) δ 163.7, 157.7, 147.9, 139.3, 139.0, 135.4, 129.2, 128.0, 128.0, 127.4, 125.2, 84.9, 65.5, 49.2, 48.3, 46.8, 42.1, 37.3, 33.5, 33.5, 25.8, 25.1, 25.1. Calculated for HRMS (ESI): $C_{21}H_{35}IN4O$ (M^++H): 531.16154; Found: 531.16069.

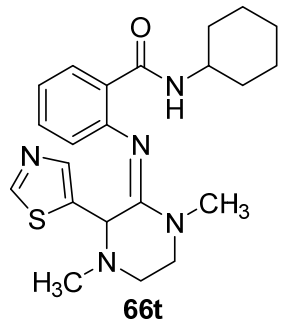

66t

(*E*)-*N*-cyclohexyl-2-((1,4-dimethyl-3-(thiazol-5-yl)piperazin-2-ylidene)amino)benzamide 66t. Obtained using **general procedure E**. Purified by normal-phase chromatography (0.5-3.5% MeOH/CH_2Cl_2) to yield the benzamidine, **66t** (76 mg, 60%) as an amber gum . ^{1}H NMR (400 MHz, Chloroform-d) δ 8.70 (s, 1H), 8.05 (d, J = 7.9 Hz, 1H), 7.99 (dd, J = 7.9, 1.7 Hz, 1H), 7.30 (s, 1H), 7.15 (td, J = 7.6, 1.7 Hz, 1H), 7.06 – 6.99 (m, 1H), 6.38 (d, J = 7.8 Hz, 1H), 4.86 (s, 1H), 3.87 (dtd, J = 10.9, 7.4, 4.0 Hz, 1H), 3.55 (td, J = 11.0, 5.1 Hz, 1H), 3.38 (ddd, J = 11.5, 4.6, 2.7 Hz, 1H), 3.18 (s, 3H), 2.97 (ddd, J = 12.6, 10.6, 4.6 Hz, 1H), 2.64 (ddd, J = 12.9, 5.3, 2.4 Hz, 1H), 2.17 (s, 3H), 2.03 – 1.94 (m, 2H), 1.79 – 1.61 (m, 5H), 1.46 – 1.32 (m, 1H), 1.16 (dq, J = 14.3, 11.5, 11.0 Hz, 3H). ^{13}C NMR (101 MHz, CDCl3) δ 165.1, 156.3, 153.5, 147.3, 143.9, 131.1, 131.0,

130.9, 125.8, 122.8, 122.6, 56.5, 49.2, 48.4, 45.8, 41.6, 37.3, 33.6, 25.8, 25.1. HRMS (ESI): Calculated for $C_{22}H_{29}N_5OS$ (M^++H): 412.21656; Found: 412.21798.

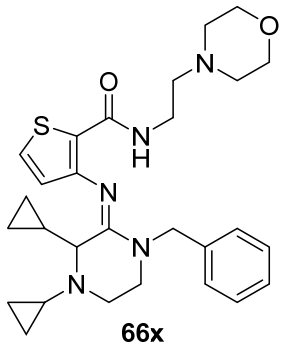

66x

(*E*)-3-((1-benzyl-3,4-dicyclopropylpiperazin-2-ylidene)amino)-*N*-(2-morpholinoethyl) thiophene-2-carboxamide 66x. Obtained using **general procedure E**. Purified by normal-phase chromatography (0-3% MeOH/CH_2Cl_2) to yield the thiophene carboxamidine, **66x** (54 mg, 40%) as a pale-yellow gum . (54 mg, 40%). ^{1}H NMR (400 MHz, Chloroform-*d*) δ 7.70 (t, *J* = 5.9 Hz, 1H), 7.43 – 7.24 (m, 7H), 6.49 (d, *J* = 5.2 Hz, 1H), 5.29 (d, *J* = 15.3 Hz, 1H), 4.40 (d, *J* = 15.3 Hz, 1H), 3.64 – 3.47 (m, 6H), 3.32 (ddd, *J* = 24.2, 11.5, 7.1 Hz, 3H), 3.19 (dq, *J* = 13.0, 6.4 Hz, 1H), 2.97 (q, *J* = 6.2, 5.1 Hz, 1H), 2.39 – 2.16 (m, 7H), 1.11 (dp, *J* = 12.5, 4.3, 3.7 Hz, 1H), 0.62 – 0.26 (m, 5H), 0.16 (dq, *J* = 10.0, 5.1 Hz, 1H), -0.30 (dq, *J* = 10.2, 5.1 Hz, 1H). ^{13}C NMR (101 MHz, $CDCl_3$) δ 163.3, 162.3, 149.1, 137.5, 129.0, 127.8, 127.5, 127.1, 124.0, 122.9, 66.9, 62.2, 58.0, 53.5, 51.6, 45.2, 43.6, 36.1, 34.2, 12.3, 7.9, 6.7, 3.9, 3.8. HRMS (ESI): Calculated for $C_{28}H_{37}N_5O_2$ (M^++H): 508.274073; Found: 508.27490.

1.7 General procedure F: Representative Procedure for the Telescoped Synthesis of α-Unsubstituted Benzamidines:

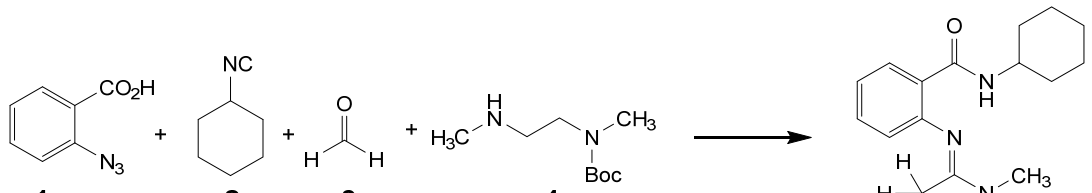

1 **2** **3** **4** **66c**

(*E*)-*N*-cyclohexyl-2-((1,4-dimethylpiperazin-2-ylidene)amino)benzamide 66c. An oven-dried, 10 mL round bottom flask under nitrogen was charged with activated, powdered 4 Å molecular sieves (150 mg). The flask was placed under vacuum and flame-dried, then backfilled with nitrogen. Diamine **4** (115 mg, 0.61 mmol, 2.0 equiv.) was dissolved in dry CH2Cl2 (0.9 ml, 0.7

M) and added to the reaction vessel. Formalin **3** (0.1 mL, 1.2 mmol, 4.0 equiv.) was measured with syringe added dropwise over a minute to the reaction vessel while stirring at rt. Upon completion of the addition, carboxylic acid **1** (50 mg, 0.31 mmol, 1.0 equiv.) was dissolved in a 3:1 mixture of dry CH_2Cl_2/HPLC grade MeOH. (0.4 mL, 0.8 M), taken up into a syringe and the needle was placed into the septum of the reaction vessel. Isocyanide **2** (153 µL, 1.2 mmol, 4.0 equiv.) was dissolved in dry CH_2Cl_2 (0.3 mL, 3.6 M) in a 1-dram glass vial, taken up into a syringe and the needle was placed into the septum of the reaction vessel. Carboxylic acid **1** was added dropwise to the reaction vessel while stirring over 1 min followed immediately by isocyanide **2**. The reaction mixture was stirred at rt for 12 h, after which the reaction was complete as judged by complete consumption of carboxylic acid **1** on TLC (10% MeOH/CH_2Cl_2). The crude reaction mixture was filtered through a 0.45 µm syringe filter and the filtrate was concentrated in vacuo. To a flame-dried, 10 mL round bottom flask under nitrogen was added triphenylphospine on resin (438 mg, 0.61 mmol, 1,4 meq/g, 2.0 equiv.) followed by dry toluene (1.0 mL). A solution of the crude reaction mixture in dry toluene (2.0 ml) was added dropwise and the reaction mixture was stirred at rt for 1 h. Next, the reaction mixture was heated to 110 °C and stirred at reflux for 12 h after which the reaction was complete as judged by complete consumption of the intermediate by TLC (30% EtOAc/hexanes). The crude reaction mixture was filtered through a pad of celite, rinsed with CH_2Cl_2 (10 mL) x 5, and the filtrate was concentrated *in vacuo*. To a flame-dried, 10 mL round bottom flask under nitrogen was dissolved the crude reaction mixture in dry CH_2Cl_2 (3.1 mL, 0.1 M) and the solution cooled to 0 °C in an ice bath while stirring. HCl in dioxane (4.0 M, 0.75 mL, 10.0 equiv.) was added dropwise. The reaction mixture was allowed to slowly warm to rt. The reaction mixture was stirred at rt for 12 h after which the reaction was complete as judged by complete consumption of intermediate on TLC (30% EtOAC/hexanes). The solvent was removed *in vacuo*. Triethylamine (0.4 mL, 3.1 mmol, 10.0 equiv.) was added to a solution of the crude reaction mixture in MeOH (3.1 mL, 0.1 M) in a 10 mL microwave vial and the reaction mixture was heated in a microwave reactor at 100 °C for 1 h. The reaction mixture was allowed to cool to rt and the solvent removed *in vacuo*. The crude mixture was dissolved in CH_2Cl_2 (10 mL) and washed with water (10 mL), then saturated brine solution (10 mL), dried over $MgSO_4$, filtered and concentrated *in vacuo*. The crude residue was purified by normal-phase chromatography (1-5% EtOAc:MeOH) to yield the benzamidine, **66c** (48 mg, 48%) as an amber gum.

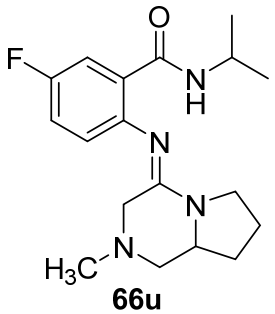

66u

(*E*)-5-fluoro-*N*-isopropyl-2-((2-methylhexahydropyrrolo[1,2-a]pyrazin-4(1H)-ylidene)amino) benzamide 66u. Obtained using **general procedure F**. Purified by normal-phase chromatography (0-3% EtOAc/CH_2Cl_2) to yield the benzamidine, **66u** (51 mg, 50%) as a pale-yellow gum. ^{1}H NMR (400 MHz, Chloroform-d) δ 8.62 (d, J = 7.7 Hz, 1H), 7.85 (dd, J = 10.0, 3.1 Hz, 1H), 7.07 – 6.94 (m, 1H), 6.69 (dd, J = 8.7, 5.0 Hz, 1H), 4.31 – 4.15 (m, 1H), 3.78 – 3.51 (m, 3H), 3.30 (d, J = 16.3 Hz, 1H), 3.08 (dd, J = 10.8, 3.8 Hz, 1H), 2.56 (d, J = 16.2 Hz, 1H), 2.24 (s, 3H), 2.09 (dq, J = 11.8, 6.2, 5.7 Hz, 2H), 1.95 (dd, J = 12.7, 8.7 Hz, 2H), 1.48 (qd, J = 11.7, 7.9 Hz, 1H), 1.19 (dd, J = 6.5, 1.6 Hz, 6H). ^{19}F NMR (376 MHz, CDCl3) δ -121.28. ^{13}C NMR (101 MHz, $CDCl_3$) δ 170.2, 164.7, 164.7, 159.9, 157.5, 154.5, 144.7, 144.7, 144.6, 127.2, 127.1, 124.7, 124.6, 118.3, 118.1, 117.2, 116.9, 57.9, 57.8, 54.2, 45.8, 45.2, 41.3, 30.4, 23.1, 23.0, 22.5. HRMS (ESI): Calculated for $C_{18}H_{25}FN_4O$ (M^++H): 333.20852; Found: 333.20814.

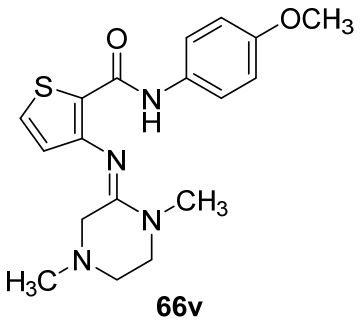

66v

(*E*)-3-((1,4-dimethylpiperazin-2-ylidene)amino)-*N*-(4-methoxyphenyl)thiophene-2-carboxamide 66v. Obtained using **general procedure F**. Purified by normal-phase chromatography (0-3% MeOH/EtOAc) to yield the thiophene carboxamidine, **66v** (32mg, 29%) as a light-brown solid. m.p.: 125-127°C. ^{1}H NMR (400 MHz, Chloroform-d) δ 10.21 (s, 1H), 7.55 – 7.46 (m, 2H), 7.35 (d, J = 5.2 Hz, 1H), 6.89 – 6.83 (m, 2H), 6.60 (d, J = 5.2 Hz, 1H), 3.80 (s, 3H), 3.43 (t, J = 5.6 Hz, 2H), 3.22 (s, 4H), 2.67 (t, J = 5.6 Hz, 2H), 2.30 (s, 3H). ^{13}C NMR (101 MHz, $CDCl_3$) δ 160.9, 157.1, 155.7, 147.9, 132.1, 128.1, 124.5, 123.8, 121.2, 114.2, 55.5, 55.4, 52.0, 49.7, 45.5, 36.7. HRMS (ESI): Calculated for $C_{18}H_{22}N_4O_2S$ (M^++H): 359.15362; Found: 359.15459.

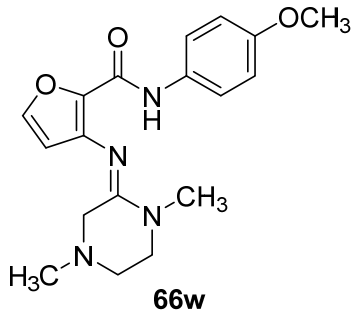

66w

(*E*)-3-((1,4-dimethylpiperazin-2-ylidene)amino)-*N*-(4-methoxyphenyl)furan-2-carboxamide 66w. Obtained using **general procedure F**. Purified by normal-phase chromatography (5-30% EtOAc/CH_2Cl_2) to yield furan carboxamidine, **66w** (21 mg, 20%) as a light-brown solid. m.p.: 150-151°C. ^{1}H NMR (400 MHz, Chloroform-*d*) δ 9.82 (s, 1H), 7.51 (d, *J* = 9.0 Hz, 2H), 7.44 (d, *J* = 1.9 Hz, 1H), 6.87 (d, *J* = 9.1 Hz, 2H), 6.17 (d, *J* = 1.9 Hz, 1H), 3.79 (s, 3H), 3.43 (t, *J* = 5.6 Hz, 2H), 3.31 (s, 2H), 3.20 (s, 3H), 2.69 (t, *J* = 5.6 Hz, 2H), 2.35 (s, 3H). ^{13}C NMR (101 MHz, CDCl3) δ 157.7, 157.5, 155.7, 143.8, 137.5, 136.7, 132.0, 121.2, 114.2, 108.9, 55.5, 55.4, 51.9, 49.7, 45.5, 36.9. HRMS (ESI): Calculated for $C_{18}H_{22}N_4O_3$ (M^++H): 343.17647; Found: 343.17700.

1.8 Procedure for the Synthesis of 9-fluoro-2,3,13,13a-tetrahydro-1H-pyrrolo[1',2':4,5] pyrazino[2,1-*b*]quinazolin-11(5H)-one 79.

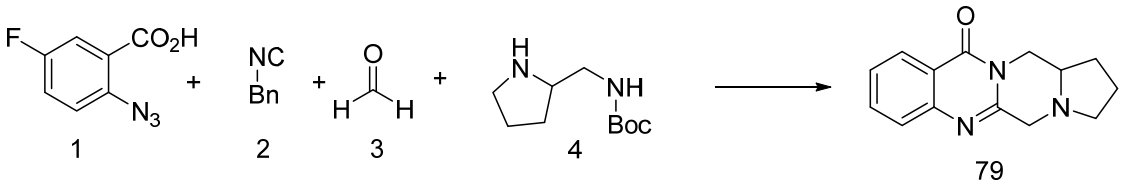

An oven-dried, 10 mL round bottom flask under nitrogen was charged with activated, powdered 4 Å molecular sieves (150 mg). The flask was placed under vacuum and flame-dried, then backfilled with nitrogen. *tert*-Butyl 2-(aminomethyl)pyrrolidine-1-carboxylate **4** (124 mg, 0.61 mmol, 2.0 equiv.) was dissolved in dry CH_2Cl_2 (0.9 ml, 0.7 M) and added to the reaction vessel. Formalin **3** (0.1 mL, 1.2 mmol, 4.0 equiv.) was measured with syringe added dropwise over a minute to the reaction vessel while stirring at rt. Upon completion of the addition, 2-azido-5-fluorobenzoic acid **1** (56 mg, 0.31 mmol, 1.0 equiv.) was dissolved in a 3:1 mixture of dry CH_2Cl_2/HPLC grade MeOH. (0.4 mL, 0.8 M), taken up into a syringe and the needle was placed into the septum of the reaction vessel. Benzyl isocyanide **2** (153 µL, 1.2 mmol, 4.0 equiv.) was dissolved in dry CH_2Cl_2 (0.3 mL, 3.6 M) in a 1-dram glass vial, taken up into a syringe and the needle was placed into the septum of the reaction vessel. Carboxylic acid **1** was added dropwise to the reaction vessel while stirring over 1 min followed immediately by benzyl isocyanide **2**. The reaction mixture was stirred at rt for 12 h, after which the reaction was complete as judged by complete consumption of carboxylic acid **1** on TLC (10% MeOH/CH_2Cl_2). The crude reaction mixture was filtered through a 0.45 µm syringe filter and the filtrate was concentrated in vacuo. To a flame-dried, 10 mL round bottom flask under nitrogen was added triphenylphospine on resin (438 mg, 0.61 mmol, 1,4 meq/g, 2.0 equiv.) followed by dry toluene (1.0 mL). A solution of the crude reaction mixture in dry toluene (2.0 ml) was added dropwise and the reaction mixture was stirred at rt for 1 h. Next, the reaction mixture was heated to 110 °C and stirred at reflux for 12 h after which the reaction was complete as judged by complete consumption of the intermediate by TLC (30% EtOAc/hexanes). The crude reaction mixture was filtered through a pad of celite, rinsed with CH_2Cl_2 (10 mL) x 5, and the filtrate was concentrated *in vacuo*. To a flame-dried, 10 mL round bottom flask under nitrogen was dissolved the crude reaction mixture in dry CH_2Cl_2 (3.1 mL, 0.1 M) and the solution

cooled to 0 °C in an ice bath while stirring. HCl in dioxane (4.0 M, 0.75 mL, 10.0 equiv.) was added dropwise. The reaction mixture was allowed to slowly warm to rt. The reaction mixture was stirred at rt for 12 h after which the reaction was complete as judged by complete consumption of intermediate on TLC (30% EtOAC/hexanes). The solvent was removed *in vacuo*. Triethylamine (0.4 mL, 3.1 mmol, 10.0 equiv.) was added to a solution of the crude reaction mixture in MeOH (3.1 mL, 0.1 M) in a 10 mL microwave vial and the reaction mixture was heated in a microwave reactor at 100 °C for 1 h. The reaction mixture was allowed to cool to rt and the solvent removed *in vacuo*. The crude mixture was dissolved in CH_2Cl_2 (10 mL) and washed with water (10 mL), then saturated brine solution (10 mL), dried over $MgSO_4$, filtered and concentrated *in vacuo*. The crude residue was purified by normal-phase chromatography (0-3% MeOH:CH_2Cl_2) to yield the quinazolinone, **79** (32 mg, 48%) as an light brown solid. ^{1}H NMR (400 MHz, Chloroform-*d*) δ 7.90 (dd, *J* = 8.5, 3.0 Hz, 1H), 7.62 (dd, *J* = 8.9, 4.8 Hz, 1H), 7.45 (td, *J* = 8.5, 3.0 Hz, 1H), 4.52 (dd, *J* = 13.4, 3.9 Hz, 1H), 4.23 (d, *J* = 16.3 Hz, 1H), 3.57 – 3.48 (m, 2H), 3.23 (td, *J* = 8.4, 3.3 Hz, 1H), 2.59 (dtd, *J* = 14.1, 10.2, 8.5, 4.1 Hz, 1H), 2.37 (q, *J* = 8.6 Hz, 1H), 2.16 (dddd, *J* = 12.6, 9.4, 6.8, 4.1 Hz, 1H), 2.03 – 1.84 (m, 2H), 1.73 – 1.62 (m, 1H). ^{19}F NMR (376 MHz, $CDCl_3$) δ -113.32. ^{13}C NMR (101 MHz, $CDCl_3$) δ 161.8, 161.4, 161.4, 159.4, 151.0, 144.0, 144.0, 129.1, 129.0, 123.1, 122.9, 121.6, 121.5, 111.5, 111.3, 59.3, 56.6, 54.3, 47.8, 29.7, 28.8, 22.2. HRMS (ESI): Calculated for $C_{14}H_{14}FN_3O$ (M^++H): 260.11937; Found: 260.11849.

1.9 Procedure for the Synthesis of *tert*-butyl (2-(methyl((4-oxo-3-phenyl-3,4-dihydroquinazolin-2-yl)methyl)amino)ethyl)carbamate

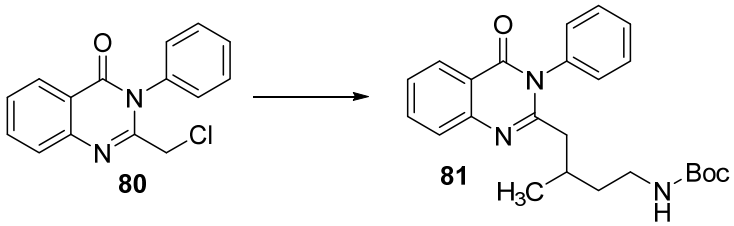

An oven dried 4 mL microwave vial was charged with 2-(chloromethyl)-3-phenylquinazolin-4(3H)-one **80** (83 mg, 0.31 mmol, 1.0 equiv.), potassium carbonate (85 mg, 0.62 mmol, 2.0 equiv.), and potassium iodide (20 mg, 0.12 mmol, 0.4 equiv.). *tert*-Butyl (2-(methylamino)ethyl)carbamate (75 mg, 0.43 mmol, 1.4 equiv.) added to reaction vessel as a solution in dry CH_3CN (1.3 mL, 0.3 M). Reaction mixture heated to 80 °C for 10 min. Reaction mixture appeared complete by TLC (60% EtOAc:Hex). Diluted reaction mixture in CH_2Cl_2 (2.0 ml), filtered, and concentrated *in vacuo*. Purified by normal phase chromatography (0-30% EtOAc:Hex) to yield quinazolinone **81** (105 mg, 84% yield) ^{1}H NMR (400 MHz, Chloroform-*d*) δ 8.29 (dd, *J* = 8.0, 1.5 Hz, 1H), 8.02 (d, *J* = 8.2 Hz, 1H), 7.78 (t, *J* = 7.7 Hz, 1H), 7.62 – 7.47 (m, 4H), 7.26 (d, *J* = 7.0 Hz, 1H), 6.17 (s, 1H), 3.32 (s, 2H), 3.15 (s, 2H), 2.49 (t, *J* = 5.6 Hz, 2H), 2.24 (s, 3H), 1.54 (d, *J* = 14.6 Hz, 9H).

1.10 Procedure for the Synthesis of 2-methyl-1,2,3,4-tetrahydro-6H-pyrazino[2,1-*b*]quinazolin-6-one

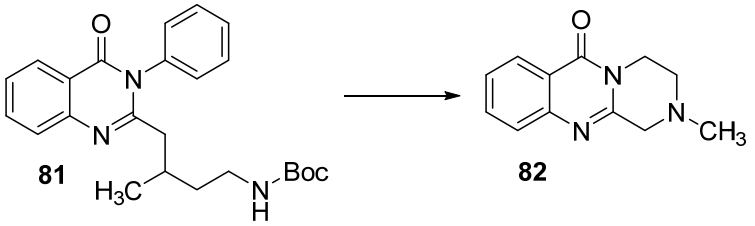

An oven dried 25 mL round bottom flask under nitrogen was charged with quinazolinone **81** (105 mg, 0.26 mmol, 1.0 equiv.) in 3.6 mL dry CH_2Cl_2 (3.6 mL, 0.07 M). Trifluoroacetic acid (1.7 mL, 22.0 mmol, 85.5 equiv.) added dropwise to the reaction vessel and the reaction mixture stirred at rt for 2 h. Next, saturated aqueous sodium carbonate (10.5 mL) was slowly added to the reaction mixture after which the reaction mixture was at pH 10. The reaction mixture was extracted with CH_2Cl_2 (2 X 10 mL). Combined organic layers were dried over $MgSO_4$, filtered and concentrated *in vacuo*. The crude residue was purified by normal-phase chromatography (0-2.5% MeOH:CH_2Cl_2) to yield the benzamidine, **82** (42 mg, 76%) as an white solid. ^{1}H NMR (400 MHz, Chloroform-*d*) δ 8.27 (dd, *J* = 8.1, 1.5 Hz, 1H), 7.73 (ddd, *J* = 8.5, 7.1, 1.6 Hz, 1H), 7.60 (d, *J* = 8.2 Hz, 1H), 7.44 (ddd, *J* = 8.2, 7.1, 1.2 Hz, 1H), 4.09 (t, *J* = 5.8 Hz, 2H), 3.70 (s, 2H), 2.86 (t, *J* = 5.8 Hz, 2H), 2.48 (s, 3H). ^{13}C NMR (101 MHz, $CDCl_3$) δ 161.9, 151.4, 147.4, 134.4, 126.6, 126.6, 126.4, 120.5, 59.0, 51.7, 45.3, 42.7. HRMS (ESI): Calculated for $C_{12}H_{13}N_3O$ (M^++H): 216.11314; Found: 216.11276.

1.11 General procedure G: Representative Procedure for the Telescoped Synthesis of C5 substituted Tetracyclic Quinazolinones:

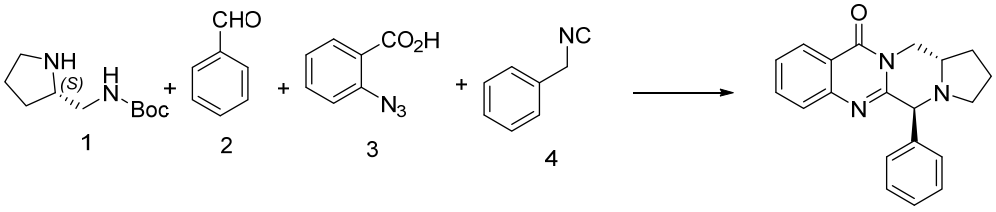

(5*S*,13a*S*)-5-phenyl-2,3,13,13a-tetrahydro-1H-pyrrolo[1',2':4,5]pyrazino[2,1-*b*]quinazolin-11(5H)-one 97b. An oven-dried, 10 mL round bottom flask under nitrogen was charged with activated, powdered, 4 Å molecular sieves (50 mg). The flask was placed under vacuum and flame-dried, then backfilled with nitrogen. *tert*-Butyl (S)-(pyrrolidin-2-ylmethyl)carbamate **1** (124 mg, 0.61 mmol, 2.0 equiv.) was dissolved in dry CH_2Cl_2 (0.5 mL, 1.3 M) and added to the reaction vessel. Benzaldehyde **2** (125 μL, 1.2 mmol, 4.0 equiv.) was dissolved in dry CH_2Cl_2 (0.46 mL, 2.6 M) in a 1-dram glass vial and added dropwise over 1 min via syringe to the reaction vessel while stirring at rt. Upon completion of the addition, 2-azidobenzoic acid **3** (50 mg, 0.31 mmol, 1.0 equiv.) was dissolved in a 3:1 mixture of dry CH_2Cl_2/MeOH (0.4 mL, .8 M), taken up into a syringe

and the needle was placed into the septum of the reaction vessel. Benzylisocyanide **4** (151 µL, 1.2 mmol, 4.0 equiv.) was dissolved in dry CH_2Cl_2 (0.3 mL, 3.6 M) in a 1-dram glass vial, taken up into a syringe and the needle was placed into the septum of the reaction vessel. Carboxylic acid **3** was added dropwise to the reaction vessel while stirring over 1 min followed immediately by isocyanide **4**. The reaction mixture was stirred at rt for 12 h after which the reaction was complete as judged by complete consumption of carboxylic acid **3** on TLC (10% MeOH/CH_2Cl_2). The crude reaction mixture was filtered through a 0.45 µm syringe filter and the filtrate was concentrated *in vacuo*. To a flame-dried, 10 mL round bottom flask under nitrogen was added triphenylphospine on resin (438 mg, 0.61 mmol, 1.4 meq/g, 2.0 equiv.) followed by dry toluene (1.0 mL). A solution of the crude reaction mixture in dry toluene (2.0 mL) was added dropwise and the reaction mixture was stirred at rt for 1 h. After 1 h at rt, the reaction mixture was heated to 110 °C and stirred for 12 h at reflux after which the reaction was complete as judged by complete consumption of the intermediate by TLC (30% EtOAc/hexanes). The crude reaction mixture was filtered through a pad of celite, rinsed with CH_2Cl_2 (10 mL) x 5, and the filtrate was concentrated *in vacuo*. To a flame-dried, 10 mL round bottom flask under nitrogen was dissolved the crude reaction mixture in dry CH_2Cl_2 (3.0 mL, 0.1 M) and the solution cooled to 0 °C in an ice-bath while stirring for 20 min. HCl in dioxane (4.0 M, 0.8 mL, 10.0 equiv.) was added dropwise. The reaction mixture was allowed to slowly warm to rt. The reaction mixture was stirred at rt for 12h after which the reaction was complete as judged by complete consumption of intermediate on TLC (30% EtOAC/hexanes). The reaction mixture was dried *in vacuo*. Triethylamine (0.4 mL, 3.1 mmol, 10.0 equiv.) was added to a solution of the crude reaction mixture in MeOH (3.1 mL, 0.1 M) in a 10 mL microwave vial and the reaction mixture was heated in a microwave reactor at 100 °C for 1 h. The reaction mixture was allowed to cool to rt and the solvent was removed *in vacuo*. The crude mixture was dissolved in CH_2Cl_2 (10 mL) and washed with water (10 mL), then saturated brine solution (10 mL), The organic layer was dried over $MgSO_4$, filtered and concentrated *in vacuo*. The crude residue was purified by normal-phase chromatography (0-60% EtOAc/Hex) to yield the fused quinazolinone, **97b**, (63 mg, 65%) as a white solid. ^{1}H NMR (400 MHz, Chloroform-*d*) δ 8.31 (dd, *J* = 8.0, 1.4 Hz, 1H), 7.76 (dd, *J* = 6.8, 1.5 Hz, 1H), 7.73 (dd, *J* = 8.2, 1.5 Hz, 1H), 7.51 – 7.48 (m, 1H), 7.48 – 7.42 (m, 2H), 7.37 – 7.24 (m, 4H), 5.15 (s, 1H), 4.45 (dd, *J* = 14.0, 3.1 Hz, 1H), 3.74 (dtt, *J* = 9.5, 6.8, 3.1 Hz, 1H), 3.32 (dd, *J* = 14.0, 5.3 Hz, 1H), 3.13 (ddd, *J* = 9.0, 5.0, 3.3 Hz, 1H), 2.74 (td, *J* = 8.9, 7.1 Hz, 1H), 2.14 – 2.01 (m, 1H), 1.86 – 1.73 (m, 2H), 1.50 – 1.36 (m, 1H). ^{13}C NMR (101 MHz, $CDCl_3$) δ 161.8, 155.0, 147.0, 137.2, 134.3, 128.6, 127.7, 127.3, 126.9, 126.9, 126.6, 120.8, 66.1, 54.7, 53.9, 41.1, 30.7, 24.4. HRMS (ESI): Calculated for $C_{20}H_{19}N_3O$ (M^++H): 318.16009; Found: 318.15894.

(5*R*,13a*S*)-5-phenyl-2,3,13,13a-tetrahydro-1H-pyrrolo[1',2':4,5]pyrazino[2,1-*b*]quinazolin-11(5H)-one 97b´, (11 mg, 11%) isolated as pale yellow solid. ^{1}H NMR (400 MHz, Chloroform-*d*) δ 8.25 (dd, *J* = 8.1, 1.5 Hz, 1H), 7.61 (ddd, *J* = 8.5, 7.1, 1.6 Hz, 1H), 7.47 – 7.30 (m, 7H), 4.71 (dd, *J* = 13.2, 3.4 Hz, 1H), 4.45 (s, 1H), 3.59 (dd, *J* = 13.1, 11.0 Hz, 1H), 2.90 (ddd, *J* = 9.9, 7.9, 2.8 Hz, 1H), 2.81 – 2.59 (m, 1H), 2.18 (dq, *J* = 9.8, 7.6, 6.5 Hz, 2H), 1.96 – 1.71 (m, 3H). ^{13}C NMR (101 MHz, $CDCl_3$) δ 162.3, 154.2, 147.4, 140.7, 134.0, 129.3, 128.3, 127.8, 127.3, 126.4,

126.3, 119.9, 72.4, 58.7, 53.7, 48.6, 28.7, 21.6. HRMS (ESI): Calculated for $C_{20}H_{19}N_3O$ (M^++H): 318.16009; Found: 318.15903.

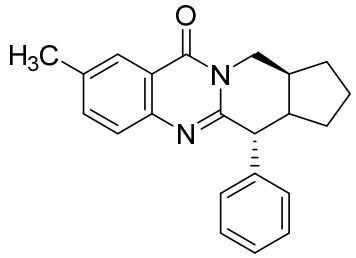

97c

(5*R*,13a*R*)-9-methyl-5-phenyl-2,3,13,13a-tetrahydro-1H-pyrrolo[1',2':4,5]pyrazino[2,1-*b*]quinazolin-11(5H)-one 97c, obtained using 2-azido-5-methylbenzoic acid and *tert*-Butyl (R)-(pyrrolidin-2-ylmethyl)carbamate following **General Procedure G.** Purified by normal phase chromatography (0-15% EtOAc:Hex) to yield quinazolinone **97c**, (49 mg, 50%) as a yellow waxy solid. ^{1}H NMR (400 MHz, Chloroform-*d*) δ 8.14 – 8.06 (m, 1H), 7.63 (d, *J* = 8.3 Hz, 1H), 7.58 (dd, *J* = 8.4, 2.0 Hz, 1H), 7.44 (dt, *J* = 8.2, 1.2 Hz, 2H), 7.36 – 7.30 (m, 2H), 7.30 – 7.26 (m, 1H), 5.12 (s, 1H), 4.45 (dd, *J* = 14.0, 3.1 Hz, 1H), 3.72 (tq, *J* = 9.5, 3.1 Hz, 1H), 3.31 (dd, *J* = 14.0, 5.3 Hz, 1H), 3.19 – 3.02 (m, 1H), 2.73 (td, *J* = 8.9, 7.1 Hz, 1H), 2.50 (s, 3H), 2.07 (dtd, *J* = 12.6, 6.7, 4.1 Hz, 1H), 1.84 – 1.64 (m, 2H), 1.47 – 1.36 (m, 1H). ^{13}C NMR (101 MHz, $CDCl_3$) δ 161.80, 154.14, 145.03, 137.40, 136.81, 135.79, 128.57, 127.66, 127.08, 126.97, 126.25, 120.52, 77.40, 77.08, 76.76, 66.09, 54.68, 53.91, 41.11, 30.74, 24.46, 21.33. HRMS (ESI): Calculated for $C_{21}H_{21}N_3O$ (M^++H): 332.117574; Found: 332.17552.

(5*S*,13a*R*)-9-methyl-5-phenyl-2,3,13,13a-tetrahydro-1H-pyrrolo[1',2':4,5]pyrazino[2,1-*b*]quinazolin-11(5H)-one 97c´, (14 mg, 14%) as a yellow oil. ^{1}H NMR (400 MHz, Chloroform-*d*) δ 8.04 (d, *J* = 1.7 Hz, 1H), 7.47 – 7.28 (m, 8H), 4.71 (dd, *J* = 13.0, 3.3 Hz, 1H), 4.44 (s, 1H), 3.59 (t, *J* = 12.1 Hz, 1H), 2.89 (d, *J* = 8.9 Hz, 1H), 2.72 (s, 1H), 2.44 (s, 3H), 2.27 – 2.09 (m, 2H), 1.83 (dt, *J* = 31.1, 10.9 Hz, 3H). ^{13}C NMR (101 MHz, $CDCl_3$) δ 162.3, 145.4, 135.5, 129.3, 128.2, 127.7, 127.2, 125.7, 123.1, 119.6, 72.3, 53.7, 28.7, 21.6, 21.3. HRMS (ESI): Calculated for $C_{21}H_{21}N_3O$ (M^++H): 332.117574; Found: 332.17502.

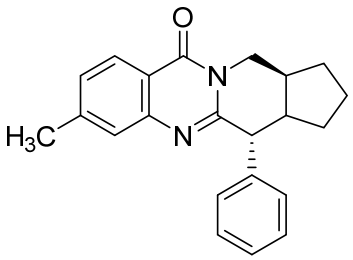

97d

(5*R*,13a*R*)-8-methyl-5-phenyl-2,3,13,13a-tetrahydro-1H-pyrrolo[1',2':4,5]pyrazino[2,1-*b*]quinazolin-11(5H)-one 97d, obtained using 2-azido-4-methylbenzoic acid and *tert*-Butyl (R)-(pyrrolidin-2-ylmethyl)carbamate following **General Procedure G.** Purified by normal phase chromatography (0-15% EtOAc:Hex) to yield quinazolinone **97d**, (51 mg, 51%) as a yellow waxy solid. ^{1}H NMR (400 MHz, Chloroform-*d*) δ 8.19 (d, *J* = 8.1 Hz, 1H), 7.55 – 7.50 (m, 1H), 7.44 (dq, *J* = 6.5, 1.2 Hz, 2H), 7.38 – 7.27 (m, 4H), 5.12 (s, 1H), 4.43 (dd, *J* = 14.0, 3.1 Hz, 1H), 3.72 (dtt, *J* = 9.5, 6.8, 3.1 Hz, 1H), 3.31 (dd, *J* = 14.0, 5.3 Hz, 1H), 3.19 – 3.05 (m, 1H), 2.73 (td, *J* = 8.8, 7.2 Hz, 1H), 2.51 (s, 3H), 2.15 – 1.99 (m, 1H), 1.88 – 1.71 (m, 2H), 1.42 (dtd, *J* = 12.5, 10.5, 9.8, 8.0 Hz, 1H). ^{13}C NMR (101 MHz, $CDCl_3$) δ 161.7, 155.1, 147.1, 145.3, 137.4, 128.6, 128.2, 127.7, 127.0, 127.0, 126.7, 118.4, 66.2, 54.7, 53.9, 41.0, 30.7, 24.5, 21.9. HRMS (ESI): Calculated for $C_{21}H_{21}N_3O$ (M^++H): 332.117574; Found: 332.17495.

(5*S*,13a*R*)-8-methyl-5-phenyl-2,3,13,13a-tetrahydro-1H-pyrrolo[1',2':4,5]pyrazino[2,1-*b*]quinazolin-11(5H)-one 97d´, (13 mg, 13%) as a yellow waxy solid. ^{1}H NMR (400 MHz, Chloroform-*d*) δ 8.13 (d, *J* = 8.1 Hz, 1H), 7.43 – 7.39 (m, 2H), 7.34 (qd, *J* = 7.6, 7.0, 3.5 Hz, 3H), 7.25 (d, *J* = 6.0 Hz, 1H), 7.21 (d, *J* = 8.1 Hz, 1H), 4.70 (dd, *J* = 13.2, 3.3 Hz, 1H), 4.43 (s, 1H), 3.57 (dd, *J* = 13.1, 11.0 Hz, 1H), 2.93 – 2.85 (m, 1H), 2.79 – 2.64 (m, 1H), 2.38 (s, 3H), 2.18 (q, *J* = 9.0 Hz, 2H), 1.92 – 1.73 (m, 3H). ^{13}C NMR (101 MHz, $CDCl_3$) δ 162.25, 154.20, 147.49, 144.91, 140.85, 129.23, 128.89, 128.24, 128.03, 127.73, 127.03, 126.56, 126.18, 117.50, 77.35, 77.23, 77.03, 76.71, 72.39, 58.75, 53.67, 48.44, 48.35, 28.70, 21.74, 21.56, 0.01. HRMS (ESI): Calculated for $C_{21}H_{21}N_3O$ (M^++H): 332.117574; Found: 332.17512.

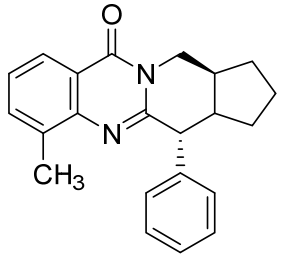

97e

(5*R*,13a*R*)-7-methyl-5-phenyl-2,3,13,13a-tetrahydro-1H-pyrrolo[1',2':4,5]pyrazino[2,1-*b*]quinazolin-11(5H)-one 97e, obtained using 2-azido-3-methylbenzoic acid and *tert*-Butyl (R)-(pyrrolidin-2-ylmethyl)carbamate following **General Procedure G.** Purified by normal phase chromatography (0-10% EtOAc:Hex) to yield quinazolinone **97e**, (63 mg, 62%) as a light brown waxy solid. ^{1}H NMR (400 MHz, Chloroform-*d*) δ 8.14 (dd, *J* = 8.1, 1.5 Hz, 1H), 7.60 (d, *J* = 7.3 Hz, 1H), 7.47 (d, *J* = 7.5 Hz, 2H), 7.42 – 7.23 (m, 4H), 5.12 (s, 1H), 4.41 (dd, *J* = 14.0, 3.4 Hz, 1H), 3.76 (s, 1H), 3.40 (d, *J* = 13.8 Hz, 1H), 3.17 (d, *J* = 8.4 Hz, 1H), 2.73 (q, *J* = 8.4 Hz, 1H), 2.59 (s, 3H), 2.09 (d, *J* = 9.3 Hz, 1H), 1.80 (td, *J* = 7.9, 4.5 Hz, 2H), 1.44 (p, *J* = 12.6, 11.2 Hz, 1H). ^{13}C NMR (101 MHz, $CDCl_3$) δ 162.1, 145.7, 136.0, 134.8, 128.5, 127.6, 127.1, 126.1, 124.5,

120.7, 66.3, 55.1, 54.2, 40.9, 30.8, 24.6, 17.4. HRMS (ESI): Calculated for $C_{21}H_{21}N_3O$ (M^++H): 332.117574; Found: 332.17543.

(5*S*,13a*R*)-7-methyl-5-phenyl-2,3,13,13a-tetrahydro-1H-pyrrolo[1',2':4,5]pyrazino[2,1-*b*]quinazolin-11(5H)-one 97e´, (13 mg, 13%) as a yellow waxy solid. ^{1}H NMR (400 MHz, Chloroform-*d*) δ 8.08 (dd, *J* = 8.1, 1.5 Hz, 1H), 7.52 – 7.43 (m, 3H), 7.40 – 7.22 (m, 4H), 4.70 (dd, *J* = 13.2, 3.4 Hz, 1H), 4.48 (s, 1H), 3.57 (dd, *J* = 13.1, 11.0 Hz, 1H), 3.02 (td, *J* = 8.6, 2.5 Hz, 1H), 2.80 – 2.62 (m, 1H), 2.27 (s, 3H), 2.22 – 2.13 (m, 2H), 2.00 – 1.72 (m, 3H). ^{13}C NMR (101 MHz, $CDCl_3$) δ 162.7, 152.6, 145.9, 140.7, 135.8, 134.4, 129.2, 127.9, 127.6, 125.9, 124.0, 119.7, 72.12, 58.9, 53.7, 48.3, 28.7, 21.6, 16.8. HRMS (ESI): Calculated for $C_{21}H_{21}N_3O$ (M^++H): 332.117574; Found: 332.17550.

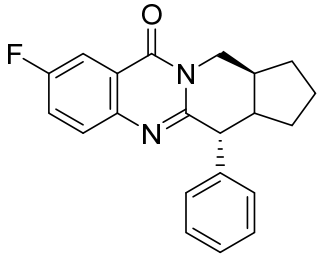

97f

(5*R*,13a*R*)-9-fluoro-5-phenyl-2,3,13,13a-tetrahydro-1H-pyrrolo[1',2':4,5]pyrazino[2,1-*b*]quinazolin-11(5H)-one 97f, obtained using 2-azido-5-fluorobenzoic acid and *tert*-Butyl (R)-(pyrrolidin-2-ylmethyl)carbamate following **General Procedure G.** Purified by normal phase chromatography (0-10% EtOAc:Hex) to yield quinazolinone **97f**, (50 mg, 48%) as an orange waxy solid. ^{1}H NMR (400 MHz, Chloroform-*d*) δ 7.93 (dd, *J* = 8.5, 3.0 Hz, 1H), 7.72 (dd, *J* = 9.0, 4.9 Hz, 1H), 7.48 (td, *J* = 8.6, 3.0 Hz, 1H), 7.43 (dt, *J* = 8.3, 1.2 Hz, 2H), 7.37 – 7.28 (m, 3H), 5.13 (s, 1H), 4.40 (dd, *J* = 14.0, 3.4 Hz, 1H), 3.82 – 3.62 (m, 1H), 3.38 (dd, *J* = 14.0, 5.3 Hz, 1H), 3.12 (ddd, *J* = 9.1, 5.7, 4.1 Hz, 1H), 2.73 (q, *J* = 8.4 Hz, 1H), 2.18 – 1.96 (m, 1H), 1.84 – 1.69 (m, 2H), 1.49 – 1.36 (m, 1H). ^{19}F NMR (376 MHz, $CDCl_3$) δ -112.89. ^{13}C NMR (101 MHz, $CDCl_3$) δ 162.0, 161.2, 161.1, 159.5, 154.3, 154.3, 143.7, 143.7, 137.1, 129.7, 129.7, 128.6, 127.8, 127.0, 123.0, 122.8, 122.0, 121.9, 111.8, 111.5, 66.0, 54.5, 53.8, 41.4, 30.7, 24.4. HRMS (ESI): Calculated for $C_{20}H_{18}FN_3O$ (M^++H): 336.15067; Found: 336.15045.

(5*S*,13a*R*)-9-fluoro-5-phenyl-2,3,13,13a-tetrahydro-1H-pyrrolo[1',2':4,5]pyrazino[2,1-*b*]quinazolin-11(5H)-one 97f´, (15 mg, 14%) as a yellow waxy solid. ^{1}H NMR (400 MHz, Chloroform-*d*) δ 7.87 (dd, *J* = 8.5, 3.0 Hz, 1H), 7.44 – 7.28 (m, 7H), 4.69 (dd, *J* = 13.2, 3.4 Hz, 1H), 4.43 (s, 1H), 3.59 (dd, *J* = 13.2, 11.0 Hz, 1H), 2.90 (ddd, *J* = 9.9, 7.9, 2.7 Hz, 1H), 2.81 – 2.59 (m, 1H), 2.18 (q, *J* = 9.3, 8.9 Hz, 2H), 2.02 – 1.68 (m, 3H). ^{19}F NMR (376 MHz, $CDCl_3$) δ -113.44. ^{13}C NMR (101 MHz, $CDCl_3$) δ 161.9, 161.7, 161.6, 159.4, 153.5, 153.5, 144.1, 140.6,

129.8, 129.8, 129.2, 128.3, 127.8, 122.8, 122.5, 121.0, 121.0, 111.1, 110.9, 72.3, 58.7, 53.6, 48.7, 28.7, 21.5. HRMS (ESI): Calculated for $C_{20}H_{18}FN_3O$ (M^++H): 336.15067; Found: 336.14997.

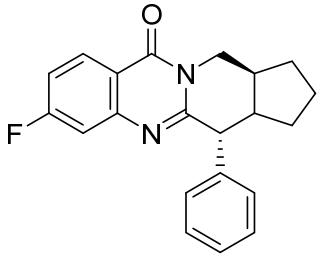

97g

(5*R*,13a*R*)-8-fluoro-5-phenyl-2,3,13,13a-tetrahydro-1H-pyrrolo[1',2':4,5]pyrazino[2,1-*b*]quinazolin-11(5H)-one 97g, obtained using 2-azido-4-fluorobenzoic acid and *tert*-Butyl (R)-(pyrrolidin-2-ylmethyl)carbamate following **General Procedure G.** Purified by normal phase chromatography (0-10% EtOAc:Hex) to yield quinazolinone **97g**, (20 mg, 19%) as an orange waxy solid. ^{1}H NMR (400 MHz, Chloroform-*d*) δ 8.31 (t, *J* = 7.5 Hz, 1H), 7.43 (d, *J* = 7.6 Hz, 2H), 7.37 – 7.26 (m, 3H), 7.20 (t, *J* = 8.8 Hz, 1H), 5.13 (s, 1H), 4.40 (dd, *J* = 14.0, 3.2 Hz, 1H), 3.72 (q, *J* = 6.7, 5.1 Hz, 1H), 3.36 (dd, *J* = 14.1, 5.2 Hz, 1H), 3.12 (dt, *J* = 9.0, 4.6 Hz, 1H), 2.74 (q, *J* = 8.3 Hz, 1H), 2.15 – 1.99 (m, 2H), 1.80 (dq, *J* = 9.1, 4.7 Hz, 2H), 1.42 (p, *J* = 9.7 Hz, 1H). ^{19}F NMR (376 MHz, $CDCl_3$) δ -103.35. ^{13}C NMR (101 MHz, $CDCl_3$) δ 167.7, 165.2, 161.0, 156.4, 149.2, 149.1, 136.9, 129.6, 129.5, 128.6, 127.8, 1270, 117.5, 117.5, 115.5, 115.3, 112.6, 112.4, 66.1, 60.4, 54.5, 53.8, 41.2, 30.7, 24.3. HRMS (ESI): Calculated for $C_{20}H_{18}FN_3O$ (M^++H): 336.15067; Found: 336.15018.

(5*S*,13a*R*)-8-fluoro-5-phenyl-2,3,13,13a-tetrahydro-1H-pyrrolo[1',2':4,5]pyrazino[2,1-*b*]quinazolin-11(5H)-one 97g´, (7 mg, 7%) as a yellow waxy solid. ^{1}H NMR (400 MHz, Chloroform-*d*) δ 8.25 (t, *J* = 7.6 Hz, 1H), 7.36 (dt, *J* = 24.3, 8.2 Hz, 5H), 7.15 – 6.93 (m, 2H), 4.69 (dd, *J* = 13.2, 3.3 Hz, 1H), 4.44 (s, 1H), 3.58 (t, *J* = 12.5 Hz, 1H), 2.91 (t, *J* = 8.7 Hz, 1H), 2.72 (tt, *J* = 10.6, 5.4 Hz, 1H), 2.18 (q, *J* = 10.3, 9.0 Hz, 2H), 1.95 – 1.61 (m, 3H). ^{19}F NMR (376 MHz, $CDCl_3$) δ -104.08. ^{13}C NMR (101 MHz, $CDCl_3$) δ 167.58, 165.05, 161.60, 155.56, 149.58, 149.45, 140.45, 129.20, 129.13, 129.02, 128.30, 127.88, 116.64, 116.62, 115.40, 115.17, 112.55, 112.34, 77.35, 77.03, 76.71, 72.31, 58.64, 53.62, 48.53, 28.69, 21.56. HRMS (ESI): Calculated for $C_{20}H_{18}FN_3O$ (M^++H): 336.15067; Found: 336.15030.

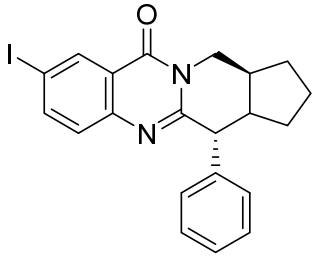

97h

(5*R*,13a*R*)-9-iodo-5-phenyl-2,3,13,13a-tetrahydro-1H-pyrrolo[1',2':4,5]pyrazino[2,1-*b*]quinazolin-11(5H)-one 97h, obtained using 2-azido-5-iodoobenzoic acid and *tert*-Butyl (R)-(pyrrolidin-2-ylmethyl)carbamate following **General Procedure G.** Purified by normal phase chromatography (0-15% EtOAc:Hex) to yield quinazolinone **97h**, (56 mg, 41%) as a pale yellow foam. ^{1}H NMR (400 MHz, Chloroform-*d*) δ 8.64 (d, *J* = 2.1 Hz, 1H), 8.02 (dd, *J* = 8.6, 2.1 Hz, 1H), 7.45 (d, *J* = 8.6 Hz, 1H), 7.42 (dt, *J* = 8.1, 1.3 Hz, 2H), 7.37 – 7.32 (m, 2H), 7.32 – 7.28 (m, 1H), 5.12 (s, 1H), 4.39 (dd, *J* = 14.0, 3.4 Hz, 1H), 3.71 (td, *J* = 6.4, 5.8, 2.8 Hz, 1H), 3.36 (dd, *J* = 14.0, 5.3 Hz, 1H), 3.11 (dt, *J* = 9.1, 4.6 Hz, 1H), 2.72 (q, *J* = 8.3 Hz, 1H), 2.15 – 2.02 (m, 1H), 1.80 (ddd, *J* = 9.3, 5.1, 2.7 Hz, 2H), 1.40 (dq, *J* = 12.6, 9.4 Hz, 1H). ^{13}C NMR (101 MHz, $CDCl_3$) δ 160.4, 155.8, 146.3, 143.1, 137.0, 135.7, 129.2, 128.6, 127.8, 127.0, 122.4, 90.9, 66.2, 54.5, 53.8, 41.5, 30.7, 24.4. HRMS (ESI): Calculated for $C_{20}H_{18}IN_3O$ (M^++H): 444.05674; Found: 444.05555.

(5*S*,13a*R*)-9-fluoro-5-phenyl-2,3,13,13a-tetrahydro-1H-pyrrolo[1',2':4,5]pyrazino[2,1-*b*]quinazolin-11(5H)-one 97h´, (19 mg, 14%) as a yellow foam. ^{1}H NMR (400 MHz, Chloroform-*d*) δ 8.58 (d, *J* = 2.0 Hz, 1H), 7.86 (dd, *J* = 8.6, 2.1 Hz, 1H), 7.41 – 7.36 (m, 3H), 7.35 – 7.31 (m, 2H), 7.17 (d, *J* = 8.6 Hz, 1H), 4.68 (dd, *J* = 13.2, 3.4 Hz, 1H), 4.41 (s, 1H), 3.58 (dd, *J* = 13.2, 10.9 Hz, 1H), 2.90 (ddd, *J* = 9.3, 7.8, 2.8 Hz, 1H), 2.71 (ddt, *J* = 16.0, 6.7, 3.4 Hz, 1H), 2.28 – 2.11 (m, 2H), 1.94 – 1.68 (m, 3H). ^{13}C NMR (101 MHz, $CDCl_3$) δ 160.9, 154.9, 146.7, 142.7, 140.4, 135.2, 129.3, 129.2, 128.3, 127.9, 121.6, 90.6, 72.4, 58.6, 53.6, 48.7, 28.7, 21.6.HRMS (ESI): Calculated for $C_{20}H_{18}IN_3O$ (M^++H): 444.05674; Found: 444.05575.

(5*S*,13a*S*)-9-iodo-5-phenyl-2,3,13,13a-tetrahydro-1H-pyrrolo[1',2':4,5]pyrazino[2,1-*b*]quinazolin-11(5H)-one *ent*-97h, obtained using 2-azido-5-iodoobenzoic acid and *tert*-Butyl (*S*)-(pyrrolidin-2-ylmethyl)carbamate following **General Procedure G.** Purified by normal phase chromatography (0-15% EtOAc:Hex) to yield quinazolinone **ent-97h**, (81 mg, 59%) as a pale yellow foam.

(5*R*,13a*S*)-9-fluoro-5-phenyl-2,3,13,13a-tetrahydro-1H-pyrrolo[1',2':4,5]pyrazino[2,1-*b*]quinazolin-11(5H)-one *ent*-97h´, (22 mg, 16%) as a yellow foam.

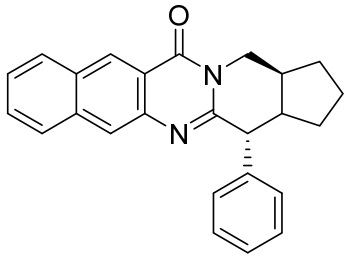

97i

(5*R*,15a*R*)-5-phenyl-2,3,15,15a-tetrahydro-1H-benzo[*g*]pyrrolo[1',2':4,5]pyrazino[2,1-*b*]quinazolin-13(5H)-one 97i, obtained using 3-azido-2-naphthanoic acid and *tert*-Butyl (R)-(pyrrolidin-2-ylmethyl)carbamate following **General Procedure G.** Purified by normal phase chromatography (0-15% EtOAc:Hex) to yield quinazolinone **97i**, (52 mg, 46%) as a light orange solid. ^{1}H NMR (400 MHz, Chloroform-*d*) δ 8.92 (s, 1H), 8.23 (s, 1H), 8.07 (dd, *J* = 8.4, 1.2 Hz, 1H), 8.00 – 7.94 (m, 1H), 7.61 (ddd, *J* = 8.3, 6.7, 1.3 Hz, 1H), 7.57 – 7.48 (m, 3H), 7.39 – 7.32 (m, 2H), 7.30 (d, *J* = 7.1 Hz, 1H), 5.16 (s, 1H), 4.49 (dd, *J* = 14.0, 3.0 Hz, 1H), 3.77 (q, *J* = 8.4 Hz, 1H), 3.35 (dd, *J* = 13.9, 5.3 Hz, 1H), 3.18 (q, *J* = 7.5, 5.9 Hz, 1H), 2.79 (td, *J* = 8.9, 7.1 Hz, 1H), 1.82 (qd, *J* = 9.6, 8.3, 5.4 Hz, 2H), 1.48 (dt, *J* = 12.1, 9.2 Hz, 1H). ^{13}C NMR (101 MHz, $CDCl_3$) δ 162.3, 154.0, 142.4, 136.7, 131.5, 129.3, 128.6, 128.4, 128.4, 128.0, 127.7, 126.9, 126.3, 125.0, 119.8, 8, 66.3, 54.8, 54.0, 40.9, 30.8, 24.6. HRMS (ESI): Calculated for $C_{24}H_{21}N_3O$ (M^++H): 368.17574; Found: 368.17533.

(5*S*,15a*R*)-5-phenyl-2,3,15,15a-tetrahydro-1H-benzo[*g*]pyrrolo[1',2':4,5]pyrazino[2,1-*b*]quinazolin-13(5H)-one 97i´, (8 mg, 7%) as an amber waxy solid. ^{1}H NMR (400 MHz, Chloroform-*d*) δ 8.87 (s, 1H), 8.01 (d, *J* = 8.2 Hz, 1H), 7.94 (s, 1H), 7.84 (d, *J* = 8.3 Hz, 1H), 7.55 – 7.43 (m, 5H), 7.40 – 7.30 (m, 3H), 4.75 (dd, *J* = 12.9, 3.4 Hz, 1H), 4.48 (s, 1H), 3.62 (dd, *J* = 12.9, 11.0 Hz, 1H), 3.01 – 2.84 (m, 1H), 2.75 (q, *J* = 10.6 Hz, 1H), 2.30 – 2.12 (m, 2H), 1.95 – 1.70 (m, 2H). ^{13}C NMR (101 MHz, $CDCl_3$) δ 162.92, 153.14, 142.64, 140.91, 136.62, 131.43, 129.30, 129.28, 128.28, 128.15, 127.86, 127.75, 125.98, 124.98, 119.10, 77.34, 77.02, 76.70, 72.57, 58.85, 53.78, 48.50, 28.75, 21.57. HRMS (ESI): Calculated for $C_{24}H_{21}N_3O$ (M^++H): 368.17574; Found: 368.17518.

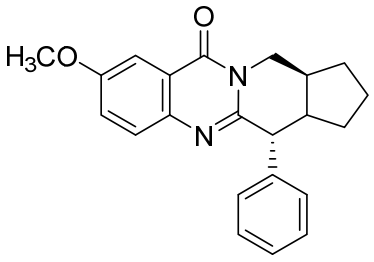

97j

(5*R*,13a*R*)-9-methoxy-5-phenyl-2,3,13,13a-tetrahydro-1H-pyrrolo[1',2':4,5]pyrazino[2,1-*b*]quinazolin-11(5H)-one 97j, obtained using 2-azido-5-methoxybenzoic acid and *tert*-Butyl (R)-(pyrrolidin-2-ylmethyl)carbamate following **General Procedure G** and microwaved for 1 h at 120 °C**.** Purified by normal phase (0-60% (15% EtOAc:DCM):Hex) to yield quinazolinone **97j**, (72 mg, 68%) as pale yellow waxy solid. ^{1}H NMR (400 MHz, Chloroform-*d*) δ 7.70 – 7.61 (m, 2H), 7.44 (d, *J* = 7.5 Hz, 2H), 7.42 – 7.27 (m, 4H), 5.12 (s, 1H), 4.45 (dd, *J* = 14.0, 3.2 Hz, 1H), 3.93 (s, 3H), 3.73 (d, *J* = 8.4 Hz, 1H), 3.39 – 3.25 (m, 1H), 3.18 – 3.07 (m, 1H), 2.73 (q, *J* = 8.4 Hz, 1H), 2.13 – 2.02 (m, 1H), 1.79 (dq, *J* = 8.4, 4.4 Hz, 2H), 1.41 (ddd, *J* = 14.0, 7.9, 4.8 Hz, 1H). ^{13}C NMR (101 MHz, $CDCl_3$) δ 161.7, 158.3, 141.7 128.9, 128.6, 127.7, 127.0, 124.7, 121.5, 106.1,

66.0, 55.9, 54.7, 53.9, 41.3, 30.7, 29.7, 24.4. HRMS (ESI): Calculated for $C_{21}H_{21}N_3O_2$ (M^++H): 348.17065; Found: 348.17019.

(5*S*,13a*R*)-9-methoxy-5-phenyl-2,3,13,13a-tetrahydro-1H-pyrrolo[1',2':4,5]pyrazino[2,1-*b*]quinazolin-11(5H)-one 97j´, (14 mg, 13%) as pale yellow waxy solid. ^{1}H NMR (400 MHz, Chloroform-*d*) δ 7.61 (d, *J* = 2.6 Hz, 1H), 7.44 – 7.29 (m, 6H), 7.22 (dd, *J* = 9.1, 2.8 Hz, 1H), 4.71 (dd, *J* = 13.2, 3.3 Hz, 1H), 4.44 (s, 1H), 3.89 (d, *J* = 1.9 Hz, 3H), 3.60 (t, *J* = 12.0 Hz, 1H), 2.90 (t, *J* = 8.4 Hz, 1H), 2.72 (d, *J* = 9.2 Hz, 1H), 2.19 (q, *J* = 9.0 Hz, 2H), 1.99 – 1.66 (m, 3H). ^{13}C NMR (101 MHz, $CDCl_3$) δ 162.2, 158.1, 151.9, 142.2, 140.9, 129.2, 129.0, 128.2, 127.7, 124.5, 120.6, 105.4, 72.3, 58.8, 55.8, 53.7, 48.6, 29.7, 28.7, 22.7, 21.6, 14.1. HRMS (ESI): Calculated for $C_{21}H_{21}N_3O_2$ (M^++H): 348.17065; Found: 348.17024.

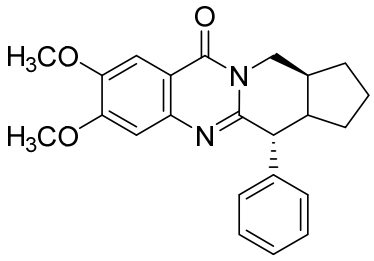

97k

(5*R*,13a*R*)-8,9-dimethoxy-5-phenyl-2,3,13,13a-tetrahydro-1H-pyrrolo[1',2':4,5]pyrazino [2,1-*b*]quinazolin-11(5H)-one 97k, obtained using 2-azido-4,5-dimethoxybenzoic acid and *tert*-Butyl (R)-(pyrrolidin-2-ylmethyl)carbamate following **General Procedure G** and microwaved for 1 h at 120 °C**.** Purified by normal phase (0-60% (15% EtOAc:DCM):Hex) to yield quinazolinone **97k**, (76 mg, 66%) as orange waxy solid. ^{1}H NMR (400 MHz, Chloroform-*d*) δ 7.62 (s, 1H), 7.43 (dt, *J* = 8.0, 1.2 Hz, 2H), 7.37 – 7.32 (m, 2H), 7.32 – 7.28 (m, 1H), 7.14 (s, 1H), 5.11 (s, 1H), 4.41 (dd, *J* = 14.0, 3.5 Hz, 1H), 4.01 (d, *J* = 1.6 Hz, 6H), 3.77 – 3.60 (m, 1H), 3.39 (dd, *J* = 14.0, 5.3 Hz, 1H), 3.09 (dt, *J* = 9.2, 4.6 Hz, 1H), 2.73 (q, *J* = 8.2 Hz, 1H), 2.12 – 1.99 (m, 1H), 1.80 (dp, *J* = 7.5, 5.1, 4.3 Hz, 2H), 1.43 (dq, *J* = 12.6, 9.3 Hz, 1H). ^{13}C NMR (101 MHz, $CDCl_3$) δ 161.2, 155.0, 153.8, 149.0, 143.3, 137.4, 128.6, 127.7, 127.1, 114.0, 107.7, 105.8, 66.1, 56.4, 56.3, 54.6, 53.8, 41.4, 30.7, 24.4. HRMS (ESI): Calculated for $C_{22}H_{23}N_3O_3$ (M^++H): 378.18122; Found: 378.18063.

(5S,13aR)-8,9-dimethoxy-5-phenyl-2,3,13,13a-tetrahydro-1H-pyrrolo[1',2':4,5]pyrazino [2,1-*b*]quinazolin-11(5H)-one 97k´, (15mg, 12%) as an orange waxy solid. ^{1}H NMR (400 MHz, Chloroform-*d*) δ 7.56 (s, 1H), 7.50 – 7.30 (m, 5H), 6.83 (s, 1H), 4.71 (dd, *J* = 13.2, 3.4 Hz, 1H), 4.42 (s, 1H), 3.96 (s, 3H), 3.88 (s, 3H), 3.67 – 3.55 (m, 1H), 3.03 – 2.80 (m, 1H), 2.70 (dd, *J* = 13.4, 6.1 Hz, 1H), 2.18 (dq, *J* = 16.7, 6.4, 4.8 Hz, 2H), 2.01 – 1.70 (m, 3H). ^{13}C NMR (101 MHz, $CDCl_3$) δ 161.6, 154.8, 152.9, 148.9, 143.8, 141.0, 131.7, 129.3, 128.7, 128.3, 127.7, 113.2, 107.7, 105.1, 58.8, 56.3, 56.2, 53.7, 48.5, 28.7, 21.5. HRMS (ESI): Calculated for $C_{22}H_{23}N_3O_3$ (M^++H): 378.18122; Found: 378.18093.

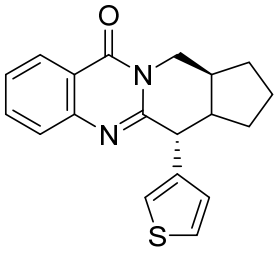

97l

(5*R*,13a*R*)-5-(thiophen-3-yl)-2,3,13,13a-tetrahydro-1H-pyrrolo[1',2':4,5]pyrazino[2,1-*b*]quinazolin-11(5H)-one 97l, obtained using 3-thiophenecarboxaldehyde and *tert*-Butyl (R)-(pyrrolidin-2-ylmethyl)carbamate following **General Procedure G.** Purified by normal phase chromatography (0-15% EtOAc:Hex) to yield quinazolinone **97l**, (36 mg, 36%) as amber gum. ^{1}H NMR (400 MHz, Chloroform-*d*) δ 8.30 (dd, *J* = 8.0, 1.5 Hz, 1H), 7.77 (ddd, *J* = 8.4, 7.0, 1.5 Hz, 1H), 7.71 (dd, *J* = 8.3, 1.3 Hz, 1H), 7.49 (ddd, *J* = 8.2, 7.0, 1.4 Hz, 1H), 7.29 (dd, *J* = 5.0, 3.0 Hz, 1H), 7.23 (dd, *J* = 2.9, 1.5 Hz, 1H), 7.05 (dd, *J* = 5.0, 1.3 Hz, 1H), 5.13 (d, *J* = 1.2 Hz, 1H), 4.39 (dd, *J* = 13.9, 3.7 Hz, 1H), 3.77 – 3.60 (m, 1H), 3.50 (dd, *J* = 13.9, 5.3 Hz, 1H), 3.10 (dt, *J* = 9.4, 4.8 Hz, 1H), 2.73 (q, *J* = 8.2 Hz, 1H), 2.17 – 2.04 (m, 1H), 1.80 (pd, *J* = 6.1, 2.2 Hz, 2H), 1.46 (dt, *J* = 12.3, 9.1 Hz, 1H). ^{13}C NMR (101 MHz, $CDCl_3$) δ 161.8, 154.7, 147.1, 134.4, 127.2, 126.9, 126.9, 126. 7, 126.1, 122.4, 122.4, 120.8, 63.1, 54.5, 53.6, 41.5, 30.7, 29.7, 24.2. HRMS (ESI): Calculated for $C_{18}H_{17}N_3OS$ (M^++H): 324.11165; Found: 324.11497.

(5*S*,13a*R*)-5-(thiophen-3-yl)-2,3,13,13a-tetrahydro-1H-pyrrolo[1',2':4,5]pyrazino[2,1-*b*]quinazolin-11(5H)-one 97l´, (21 mg, 21%) as amber gum. ^{1}H NMR (400 MHz, Chloroform-*d*) δ 8.26 (dd, *J* = 8.0, 1.5 Hz, 1H), 7.65 (ddd, *J* = 8.5, 7.1, 1.6 Hz, 1H), 7.50 (d, *J* = 8.3 Hz, 1H), 7.43 – 7.36 (m, 2H), 7.29 – 7.26 (m, 1H), 7.09 (dd, *J* = 5.0, 1.2 Hz, 1H), 4.67 (dd, *J* = 13.2, 3.4 Hz, 1H), 4.61 (s, 1H), 3.56 (dd, *J* = 13.2, 10.9 Hz, 1H), 3.02 (ddd, *J* = 9.6, 8.2, 2.7 Hz, 1H), 2.78 – 2.61 (m, 1H), 2.25 – 2.12 (m, 2H), 1.99 – 1.69 (m, 3H). ^{13}C NMR (101 MHz, $CDCl_3$) δ 162.3, 153.4, 147.4, 140.9, 134.0, 127.7, 127.3, 126.5, 126.4, 125.4, 124.0, 120.0, 67.3, 58.8, 53.9, 48.4, 28.8, 21.5. HRMS (ESI): Calculated for $C_{18}H_{17}N_3OS$ (M^++H): 324.11165; Found: 324.11511.

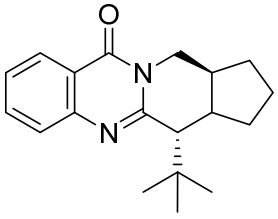

97m

(5*R*,13a*R*)-5-(tert-butyl)-2,3,13,13a-tetrahydro-1H-pyrrolo[1',2':4,5]pyrazino[2,1-*b*]quinazolin-11(5H)-one 97m, obtained using pivaldehyde and *tert*-Butyl (R)-(pyrrolidin-2-ylmethyl)carbamate following **General Procedure G** and microwaved for 2 h at 150 °C. Purified by normal phase chromatography (0-30% EtOAc:Hex) to yield quinazolinone **97m**, (22 mg, 24%) as amber gum. ^{1}H NMR (400 MHz, Chloroform-*d*) δ 8.28 (dd, *J* = 7.9, 1.5 Hz, 1H), 7.74 (ddd, *J* = 8.5, 7.0, 1.6 Hz, 1H), 7.65 (d, *J* = 8.1 Hz, 1H), 7.45 (t, *J* = 7.8 Hz, 1H), 4.52 (dd, *J* = 14.6, 3.5 Hz, 1H), 3.86 (dd, *J* = 14.6, 5.2 Hz, 1H), 3.74 (q, *J* = 6.3, 5.7 Hz, 1H), 3.48 (s, 1H), 3.22 – 3.09 (m, 1H), 2.78 (dt, *J* = 10.3, 7.1 Hz, 1H), 1.90 (dt, *J* = 12.9, 6.5 Hz, 1H), 1.75 (ddt, *J* = 13.5, 9.4, 6.1 Hz, 2H), 1.32 (dq, *J* = 12.4, 8.2 Hz, 1H), 1.08 (s, 9H). ^{13}C NMR (101 MHz, $CDCl_3$) δ 162.1, 154.6, 146.9, 134.2, 127.1, 126.7, 126.4, 120.3, 72.83, 57.8, 55.2, 41.1, 38.7, 30.0, 28.4, 23.6. HRMS (ESI): Calculated for $C_{18}H_{23}N_3O$ (M^++H): 298.19139; Found: 298.19127.

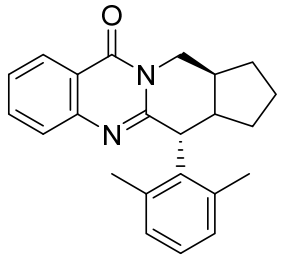

97n

(5*R*,13a*R*)-5-(2,6-dimethylphenyl)-2,3,13,13a-tetrahydro-1H-pyrrolo[1',2':4,5]pyrazino[2,1-*b*]quinazolin-11(5H)-one 97n, obtained using 2,6-dimethylbenzaldehyde and *tert*-Butyl (R)-(pyrrolidin-2-ylmethyl)carbamate following **General Procedure G.** Purified by normal phase chromatography (0-15% EtOAc:Hex) to yield quinazolinone **97n**, (49 mg, 46%) as pale white solid. ^{1}H NMR (400 MHz, Chloroform-*d*) δ 8.26 (dd, *J* = 8.0, 1.5 Hz, 1H), 7.60 (ddd, *J* = 8.5, 7.1, 1.6 Hz, 1H), 7.43 (dd, *J* = 8.3, 1.1 Hz, 1H), 7.38 (ddd, *J* = 8.1, 7.1, 1.2 Hz, 1H), 7.13 – 7.04 (m, 2H), 6.98 – 6.92 (m, 1H), 4.99 (s, 1H), 4.75 (dd, *J* = 13.2, 3.4 Hz, 1H), 3.58 (dd, *J* = 13.2, 10.9 Hz, 1H), 2.79 (ddd, *J* = 9.6, 7.1, 2.9 Hz, 1H), 2.71 – 2.60 (m, 1H), 2.55 (s, 3H), 2.23 – 2.13 (m, 2H), 2.10 (s, 3H), 1.88 – 1.67 (m, 3H). ^{13}C NMR (101 MHz, $CDCl_3$) δ 162.3, 154.3, 147.8, 137.5, 137.4, 137.1, 133.9, 129.6, 127.9, 127.5, 127.3, 126.3, 126.2, 119.9, 66.3, 59.2, 52.8, 48.1, 28.6, 21.6, 21.6, 20.6. HRMS (ESI): Calculated for $C_{18}H_{17}N_3OS$ (M^++H): 346.19139; Found: 346.19012.

(5*S*,13a*R*)-5-(2,6-dimethylphenyl)-2,3,13,13a-tetrahydro-1H-pyrrolo[1',2':4,5]pyrazino[2,1-*b*]quinazolin-11(5H)-one 97n´, (39 mg, 37%) as pale yellow waxy solid. ^{1}H NMR (400 MHz, Chloroform-*d*) δ 8.28 (dd, *J* = 8.0, 1.5 Hz, 1H), 7.63 (ddd, *J* = 8.4, 7.2, 1.5 Hz, 1H), 7.48 (d, *J* = 8.2 Hz, 1H), 7.47 – 7.38 (m, 1H), 7.16 (dd, *J* = 8.1, 6.8 Hz, 1H), 7.06 (d, *J* = 7.5 Hz, 2H), 5.22 (s, 1H), 5.13 (dd, *J* = 13.4, 3.2 Hz, 1H), 3.64 – 3.49 (m, 1H), 3.46 – 3.34 (m, 1H), 2.92 (s, 1H), 2.61 (q, *J* = 8.6 Hz, 1H), 2.30 (s, 6H), 1.94 – 1.47 (m, 2H). ^{13}C NMR (101 MHz, $CDCl_3$) δ 161.4, 147.6, 133.9, 128.7, 128.0, 127.1, 126.5, 126.4, 120.1, 62.3, 56.4, 53.6, 43.3, 29.5, 24.7, 21.1, 14.1. HRMS (ESI): Calculated for $C_{18}H_{17}N_3OS$ (M^++H): 346.19139; Found: 346.18999.

1.12 Procedure for the Synthesis of 2-(2-chloro-2,2-difluoroacetamido)-5-nitrobenzoic acid

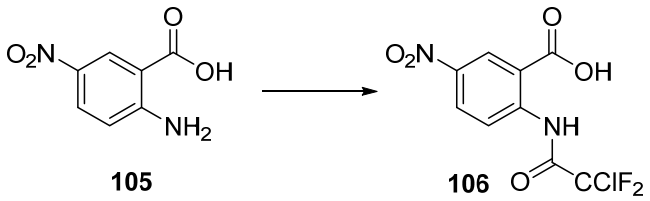

To an oven dried 100 mL round bottom flask under nitrogen was added 2-amino-5-nitrobenzoic acid (910 mg, 5.0 mmol, 1.0 equiv.) and CH_2Cl_2 (14 mL, 0.4 M). The suspension stirred at rt and trimethylamine (0.8 mL, 5.8 mmol, 1.2 equiv.) was added dropwise to the reaction vessel. The suspension dissolved into a clear yellow solution. The reaction mixture was cooled to 0 °C in an ice bath while stirring inder nitrogen for 25 min. Next, chlorodifluoroacetyl chloride was added dropwise to the reaction mixture (0.7 mL, 7.5 mmol, 1.5 equiv.) as a solution in CH_2Cl_2 (4 mL, 1.9 M). The reaction mixture ice bath was remocved and the reaction mixture was allowed to warm to rt. After 18 hours, the reaction mixture was concentrated *in vacuo* and the crude material was purified by normal phase chromatography (0-20% MeOH: CH_2Cl_2) to yield **106**, (823 mg**,** 56%), as a yellow solid. ^{1}H NMR (400 MHz, Chloroform-*d*) δ 12.26 (s, 1H), 9.08 (d, *J* = 2.7 Hz, 1H), 8.92 (d, *J* = 9.3 Hz, 1H), 8.54 (dd, *J* = 9.3, 2.7 Hz, 1H). ^{19}F NMR (376 MHz, $CDCl_3$) δ -64.74.

1.13 Procedure for the Synthesis of 2-(chlorodifluoromethyl)-3-(4-methoxyphenyl)-6-nitroquinazolin-4(3H)-one

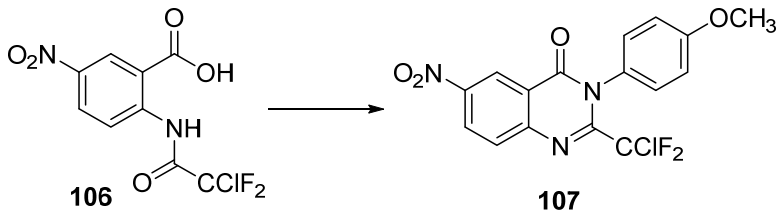

To a 30 mL microwave vial was added 106, (823 mg, 2.8 mmol, 1.0 equiv.) and CH_3CN (7.0 mL, 0.4 M). The solid was sonicated into solution. Then $POCl_3$ (0.6 mL, 6.0 mmol, 2.1 equiv.) was added dropwise. Next, 4-methoxyaniline (464 mg, 3.8 mmol, 1.4 equiv.) was added as a solution in CH_3CN (2.3 mL, 1.7 M). A solid immediately precipitated out. Reaction mixture was heated in microwave at 150 °C for 1 h. Crude mixture was concentrated in vacuo and purified by regular

phase chromatography (0-15%, EtOAc:Hex) to yield quinazolinone **107**, (530 mg, 50%), as yellow solid. ^{1}H NMR (400 MHz, Chloroform-*d*) δ 9.14 (d, *J* = 2.6 Hz, 1H), 8.65 (dd, *J* = 8.9, 2.7 Hz, 1H), 8.03 (d, *J* = 9.0 Hz, 1H), 7.40 – 7.16 (m, 3H), 7.05 (d, *J* = 9.0 Hz, 2H), 3.89 (s, 3H). ^{19}F NMR (376 MHz, $CDCl_3$) δ -52.72.

1.14 Procedure for the Synthesis of 2-((1,3-dimethylimidazolidin-2-ylidene)amino)-N-(4-methoxyphenyl)-5-nitrobenzamide

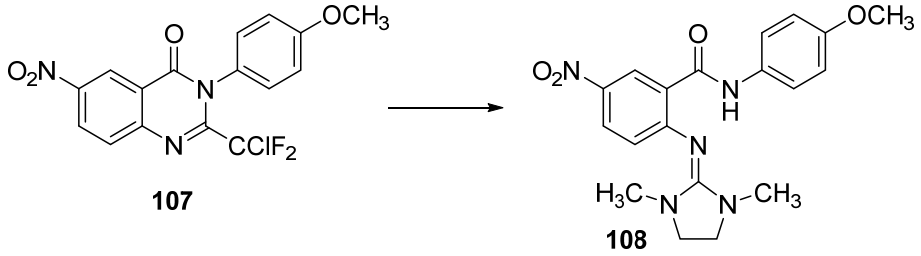

To a 10 mL round bottom under nitrogen was added **107** (200 mg, 0.5 mmol, 1.0 equiv.), potassium carbonate (145 mg, 1.0 mmol, 2.0 equiv.), potassium iodide (9.0 mg, 0.05 mmol, 0.1 equiv.), then dry DMF (5.0 mL, 1.0 M). The reaction stirred at rt and *N*,*N*′-dimethyl-1,2-ethanediamine was added dropwise. Reaction mixture stirred for 6 h and little conversion observed by TLC. Reaction vessel heated to 50 °C and stirred for 18 h under nitrogen. Reaction still appeared incomplete by TLC. Reaction mixture cooled to rt and concentrated *in vacuo*. Crude mixture was diluted in EtOAc (10 ml) and washed with water (5 X 10 mL). Organic layer ried over $MgSO_4$, filtered and concentrated *in vacuo*. Purified by normal phase chromatography (50-100%, EtOAc:Hex) to yield guanidine **108**, (61 mg, 30%) as a yellow solid. ^{1}H NMR (400 MHz, Chloroform-*d*) δ 12.11 (s, 1H), 9.20 (d, *J* = 2.8 Hz, 1H), 8.09 (ddd, *J* = 8.9, 3.0, 1.1 Hz, 1H), 7.62 (d, *J* = 8.6 Hz, 2H), 7.06 – 6.83 (m, 2H), 6.74 (d, *J* = 8.9 Hz, 1H), 3.81 (d, *J* = 1.1 Hz, 3H), 3.59 (s, 5H), 2.84 (d, *J* = 1.1 Hz, 6H). ^{13}C NMR (101 MHz, $CDCl_3$) δ 162.9, 159.1, 156.0, 154.3, 140.0, 132.2, 128.1, 126.1, 121.4, 121.4, 114.2, 55.5, 48.2, 34.9. HRMS (ESI): Calculated for $C_{19}H_{21}N_5O_4$: (M^++H): 384.16663, Found: 384.16731.

References:

1. K. Barral, A. D. Moorhouse and J. E. Moses, *Org. Lett.*, 2007, **9**, 1809.
2. A.-C. Bédard, J. Santandrea and S. K. Collins, *J. Flow Chem.*, 2015, **5**, 142.
3. M. S. Yusubov, R. Y. Yusubova, V. N. Nemykin, and V. V. Zhdankin, *J. Org. Chem.,* 2013, **78**, 3767.
4. T. Nishikubo and T. Takaoka, *Nippon Kagaku Kaishi*, 1975, **2**, 327.

S. Gronowitz, C. Westerlund, and A. B. Hörnfeldt, *Acta. Chem. Scand.*, 1975, **B29**, 224.

Appendix A. Selected H^1, F^{19}, and C^{13} NMR Spectra for Compounds

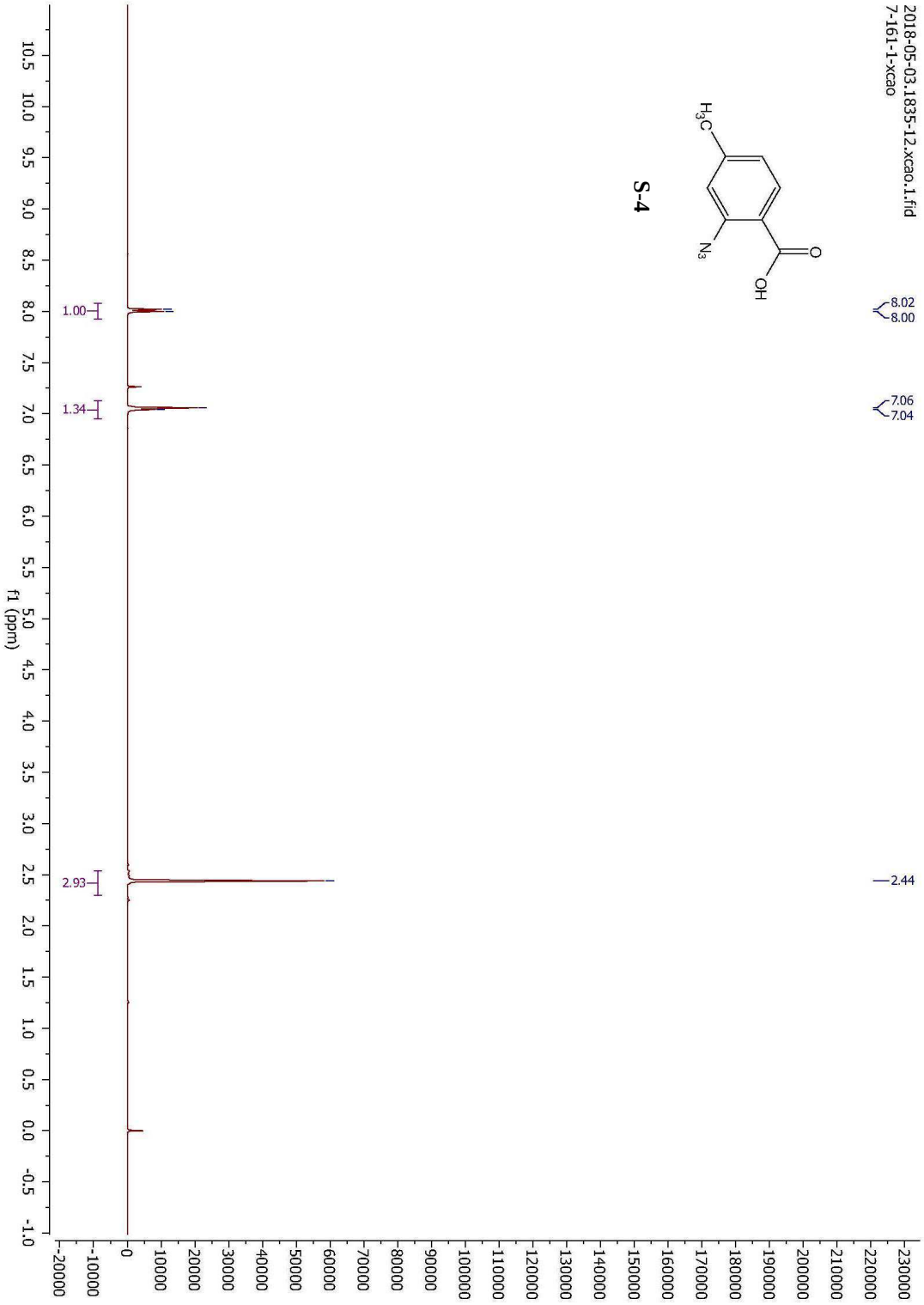

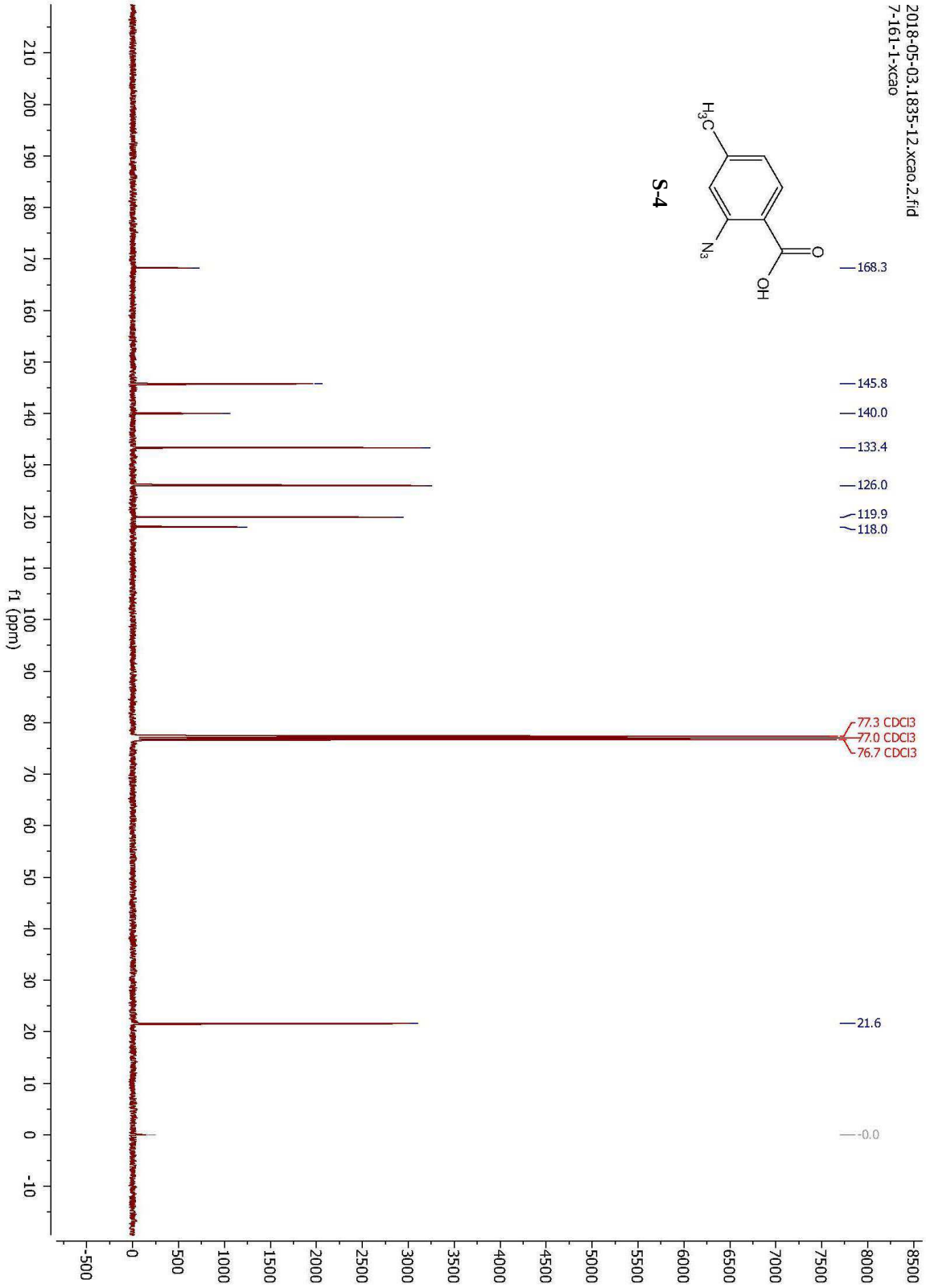
2018-05-03.1835-12.xcao.2.fid
7-161-1-xcao
S-4
H3C
N3
O
OH
168.3
145.8
140.0
133.4
126.0
119.9
118.0
77.3 CDCl3
77.0 CDCl3
76.7 CDCl3
21.6
-0.0
f1 (ppm)

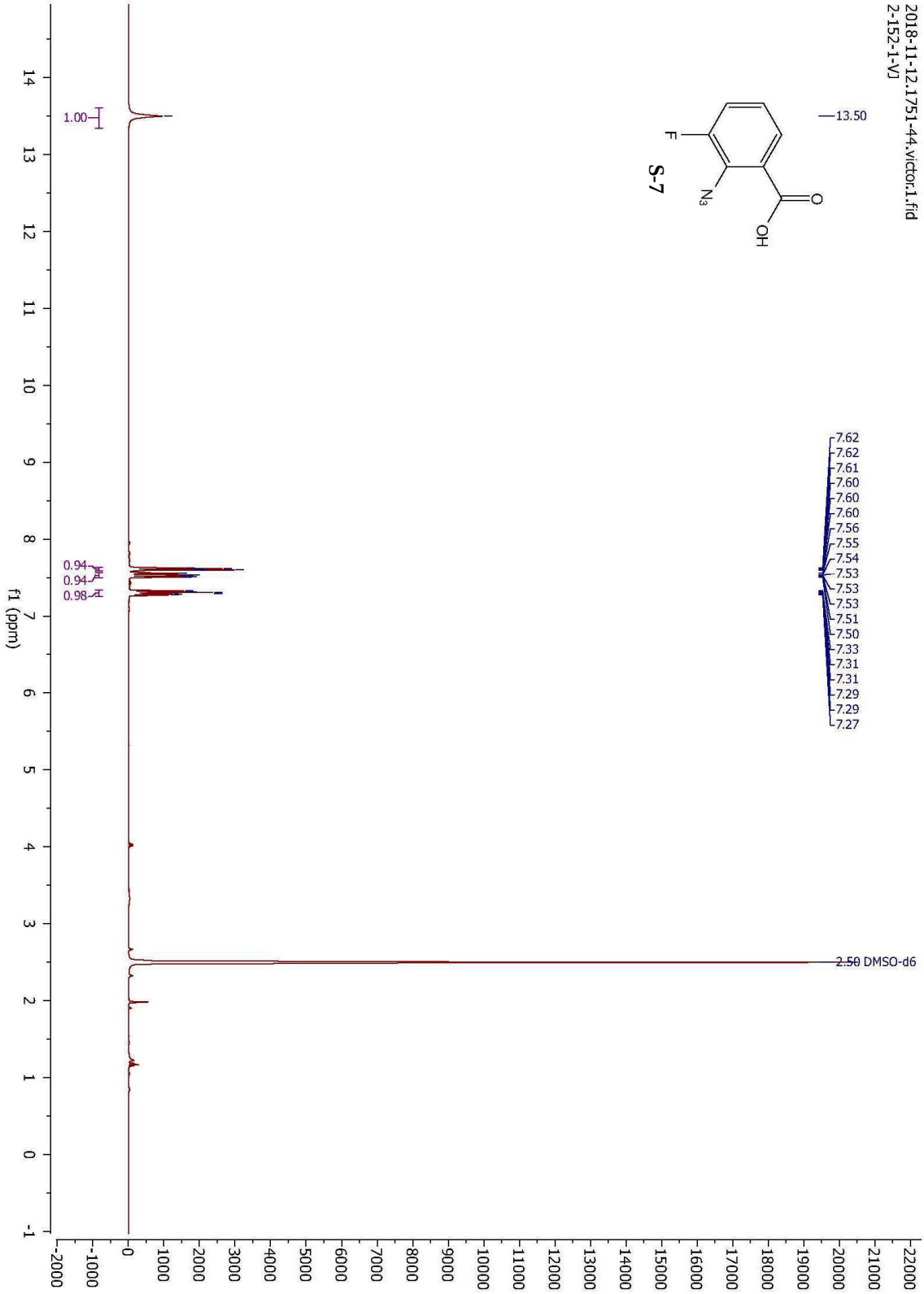
2018-11-12.1751-44.victor.1.fid
2-152-1-VJ
S-7
F
N3
O
OH
13.50
1.00
0.94
0.94
0.98
7.62
7.62
7.61
7.60
7.60
7.60
7.56
7.55
7.54
7.53
7.53
7.53
7.51
7.50
7.33
7.31
7.31
7.29
7.29
7.27
2.50 DMSO-d6
f1 (ppm)

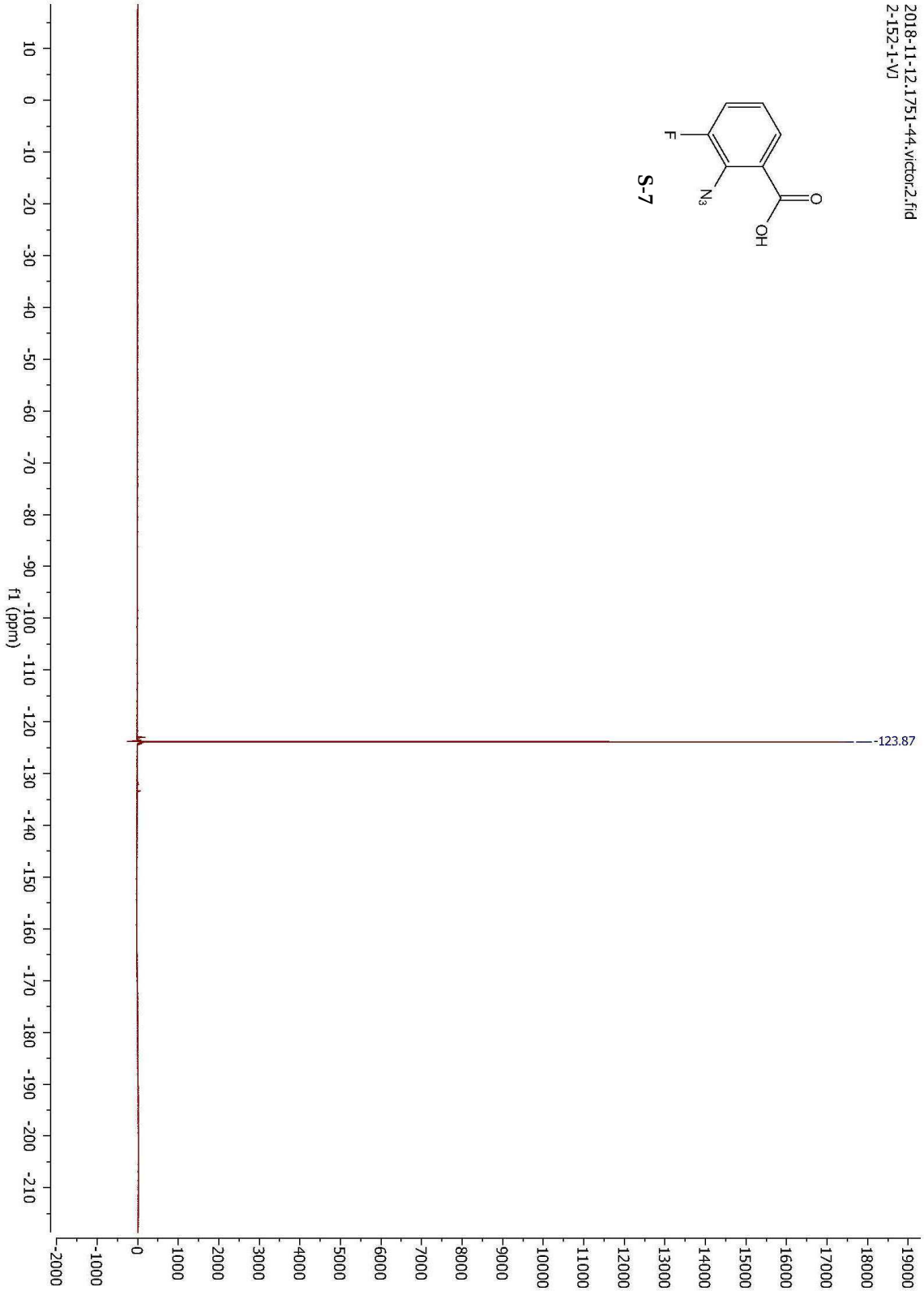
2018-11-12.1751-44.victor.2.fid
2-152-1-VJ
S-7
F
N3
O
OH
-123.87
f1 (ppm)

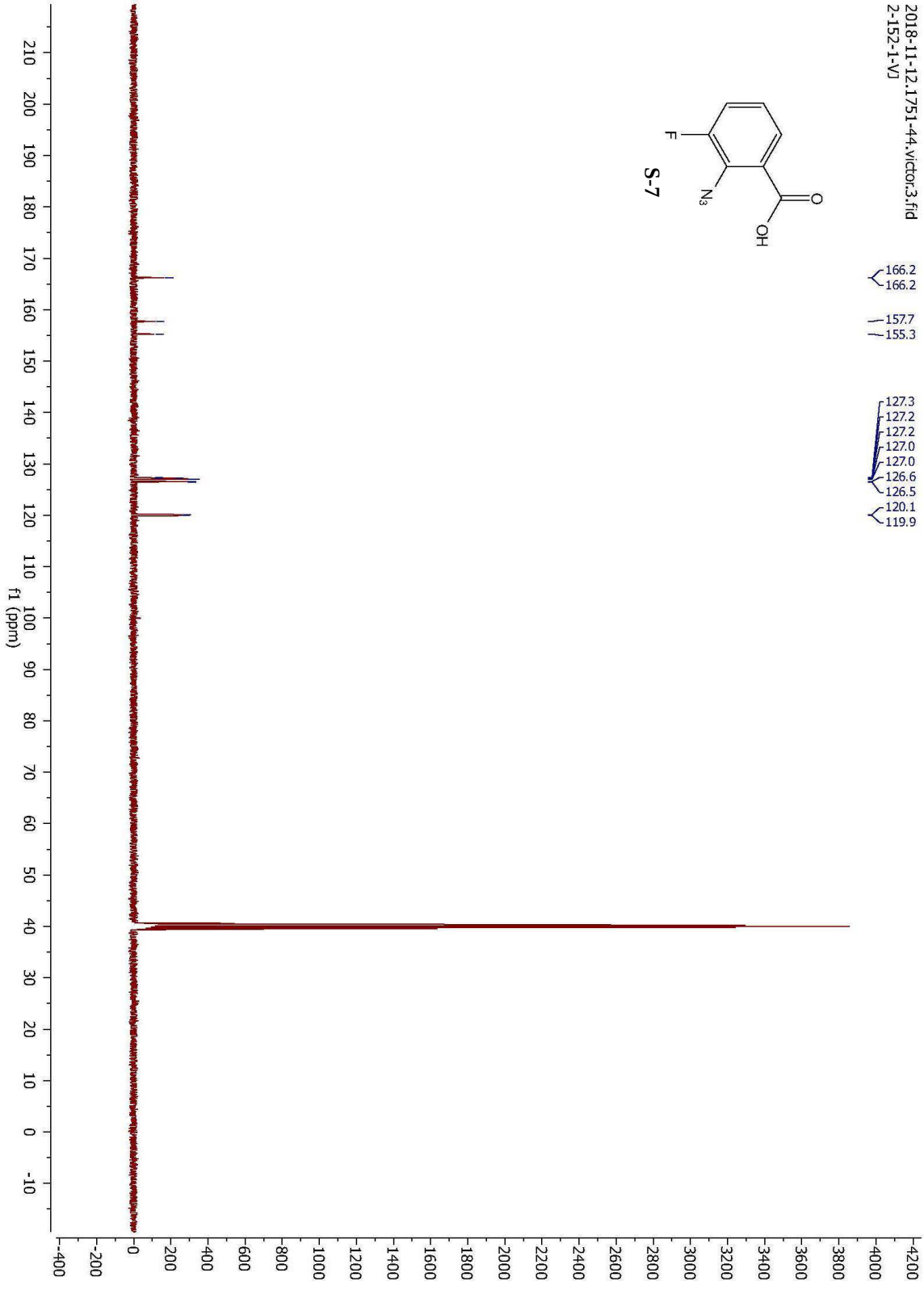
2018-11-12.1751-44.victor.3.fid
2-152-1-VJ
S-7
F
N3
O
OH
166.2
166.2
157.7
155.3
127.3
127.2
127.2
127.0
127.0
126.6
126.5
120.1
119.9
f1 (ppm)

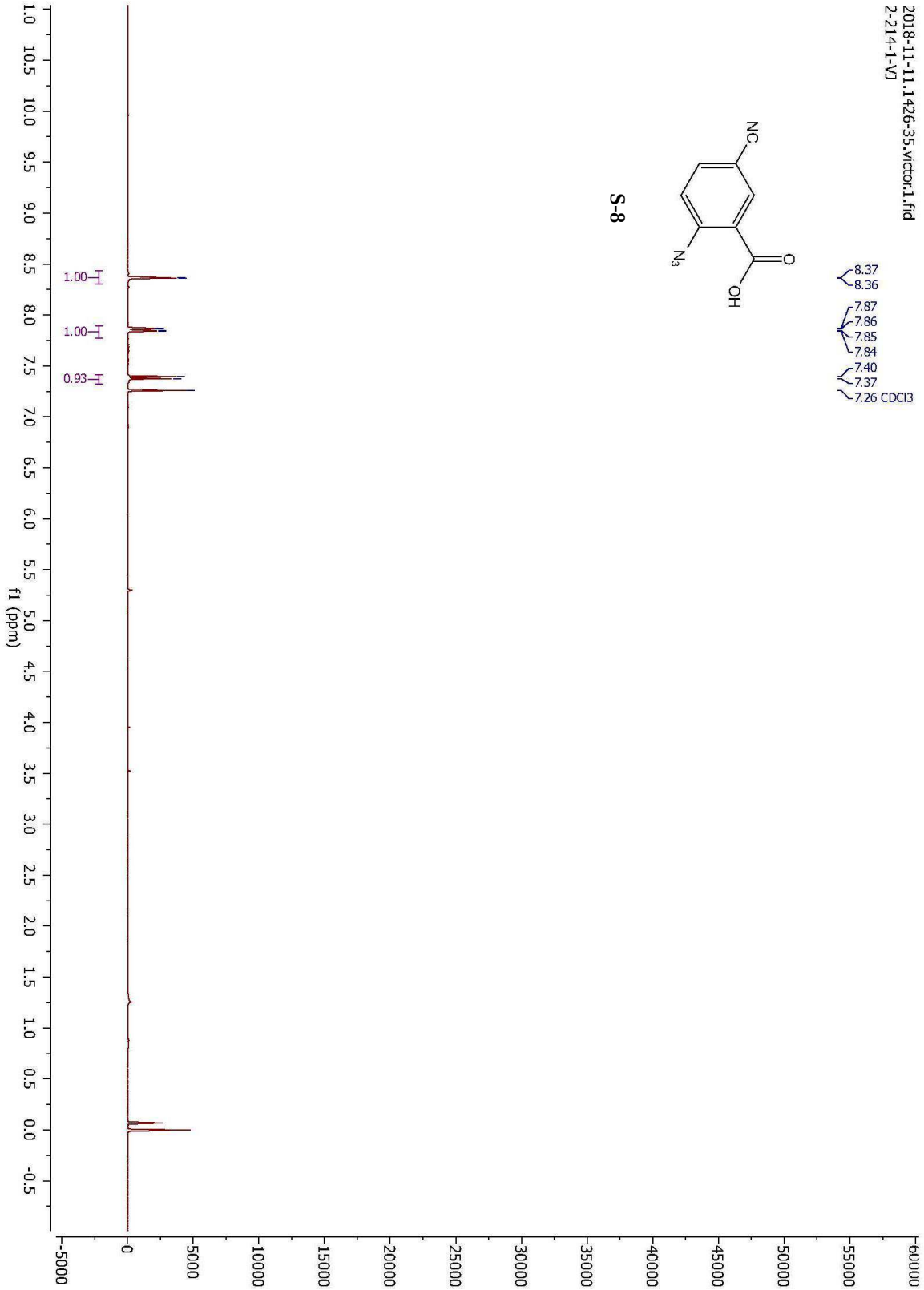
2018-11-11.1426-35.victor.1.fid
2-214-1-VJ
S-8
NC
N3
O
OH
8.37
8.36
7.87
7.86
7.85
7.84
7.40
7.37
7.26 CDCl3
1.00
1.00
0.93
f1 (ppm)

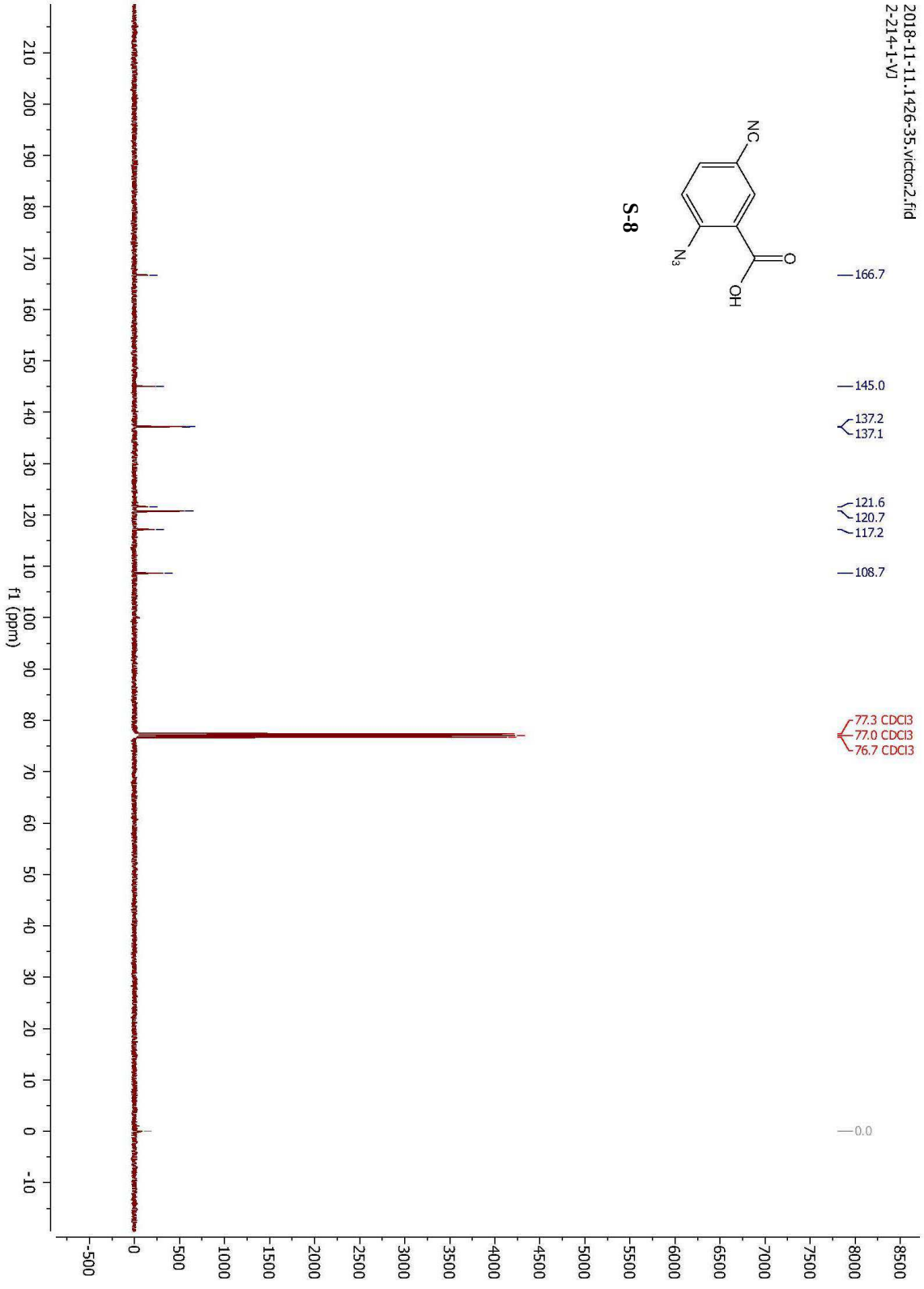
2018-11-11.1426-35.victor.2.fid
2-214-1-VJ
S-8
NC
N3
O
OH
166.7
145.0
137.2
137.1
121.6
120.7
117.2
108.7
77.3 CDCl3
77.0 CDCl3
76.7 CDCl3
0.0
f1 (ppm)

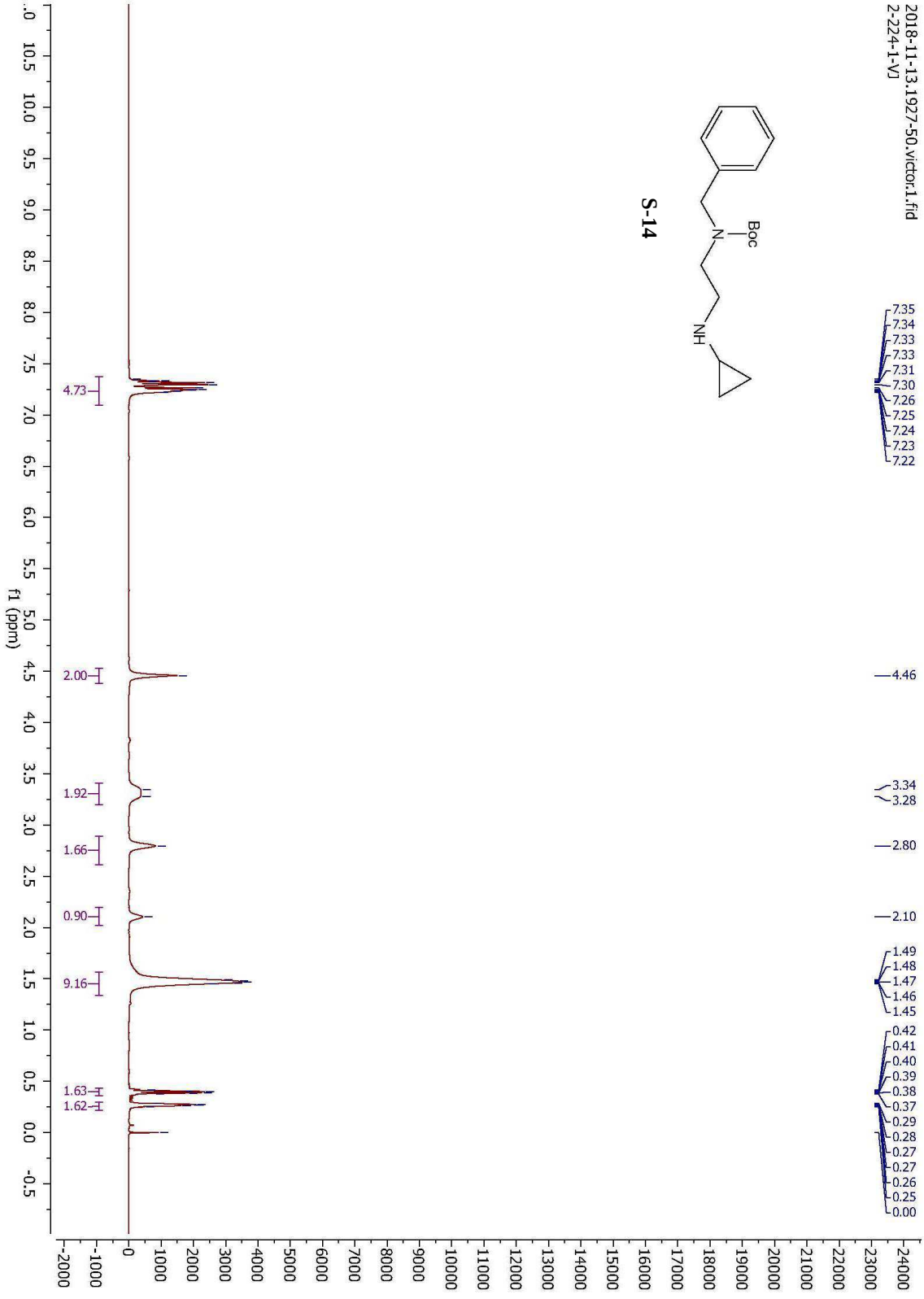
2018-11-13.1927-50.victor.1.fid
2-224-1-VJ
S-14
Boc
N
NH
7.35
7.34
7.33
7.33
7.31
7.30
7.26
7.25
7.24
7.23
7.22
4.46
3.34
3.28
2.80
2.10
1.49
1.48
1.47
1.46
1.45
0.42
0.41
0.40
0.39
0.38
0.37
0.29
0.28
0.27
0.27
0.26
0.25
0.00
4.73
2.00
1.92
1.66
0.90
9.16
1.63
1.62
f1 (ppm)

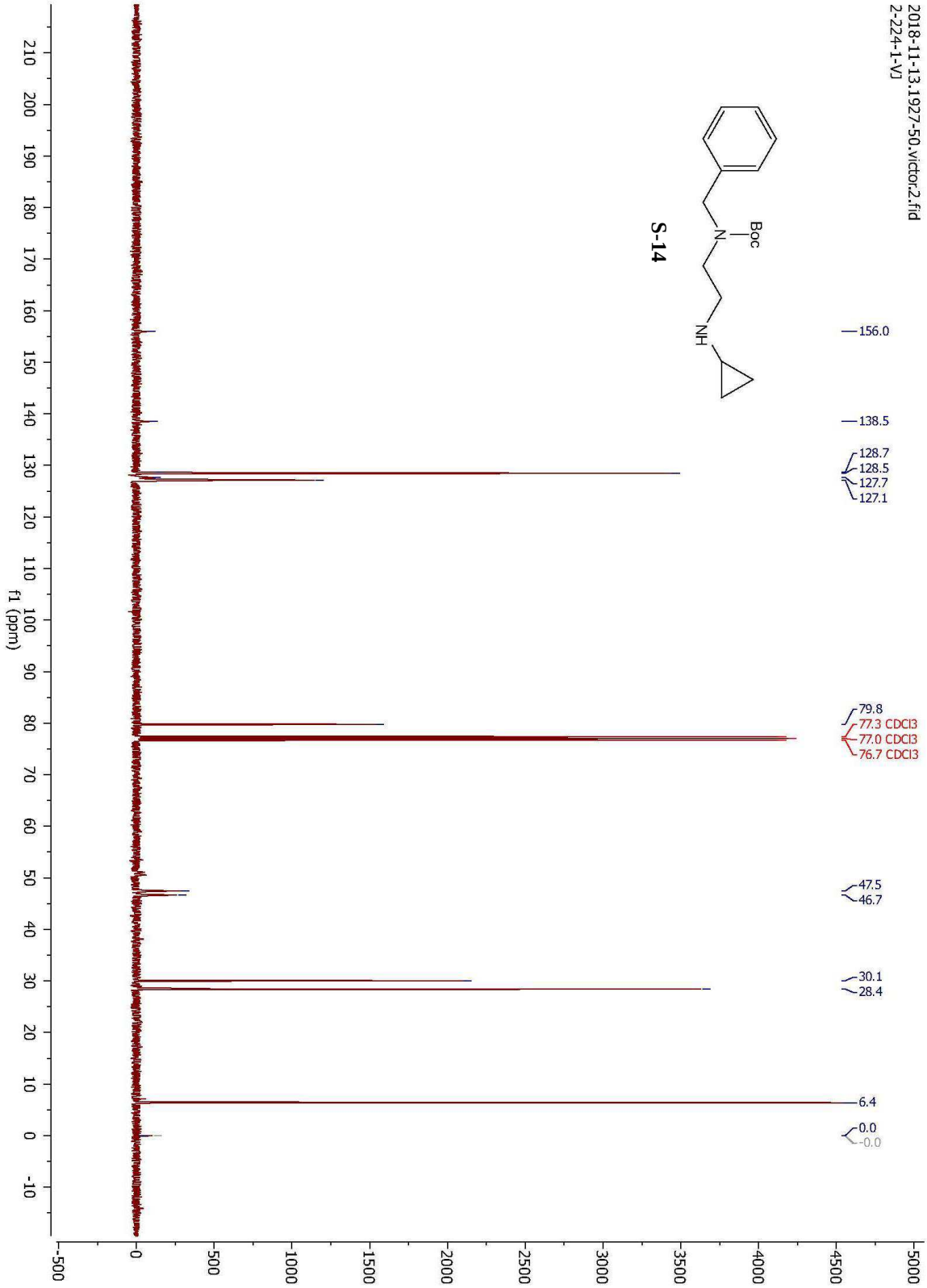
2018-11-13.1927-50.victor.2.fid
2-224-1-VJ
S-14
Boc
N
NH
156.0
138.5
128.7
128.5
127.7
127.1
79.8
77.3 CDCl3
77.0 CDCl3
76.7 CDCl3
47.5
46.7
30.1
28.4
6.4
0.0
-0.0
f1 (ppm)

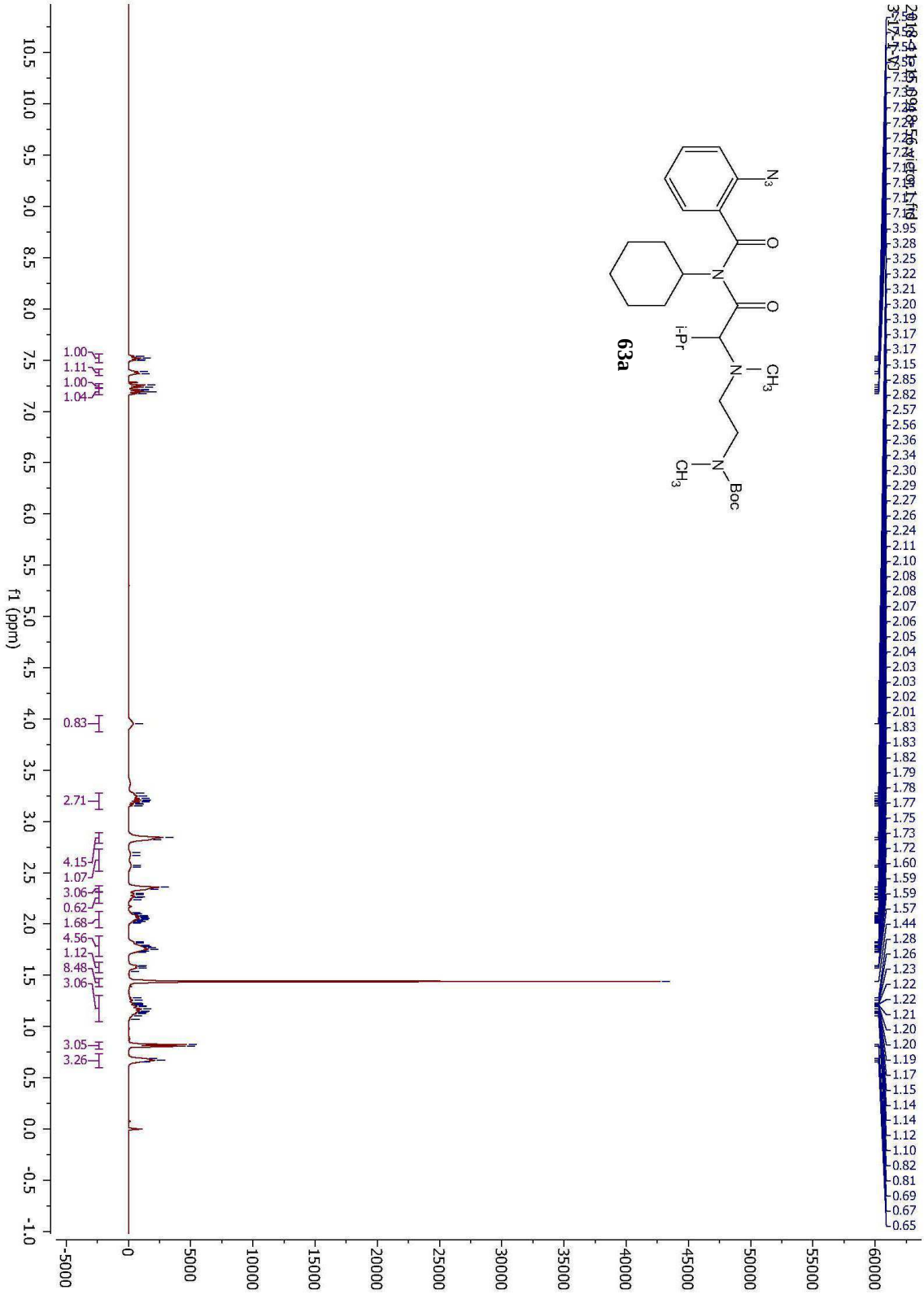
63a
f1 (ppm)
1.00
1.11
1.00
1.04
0.83
2.71
4.15
1.07
3.06
0.62
1.68
4.56
1.12
8.48
3.06
3.05
3.26

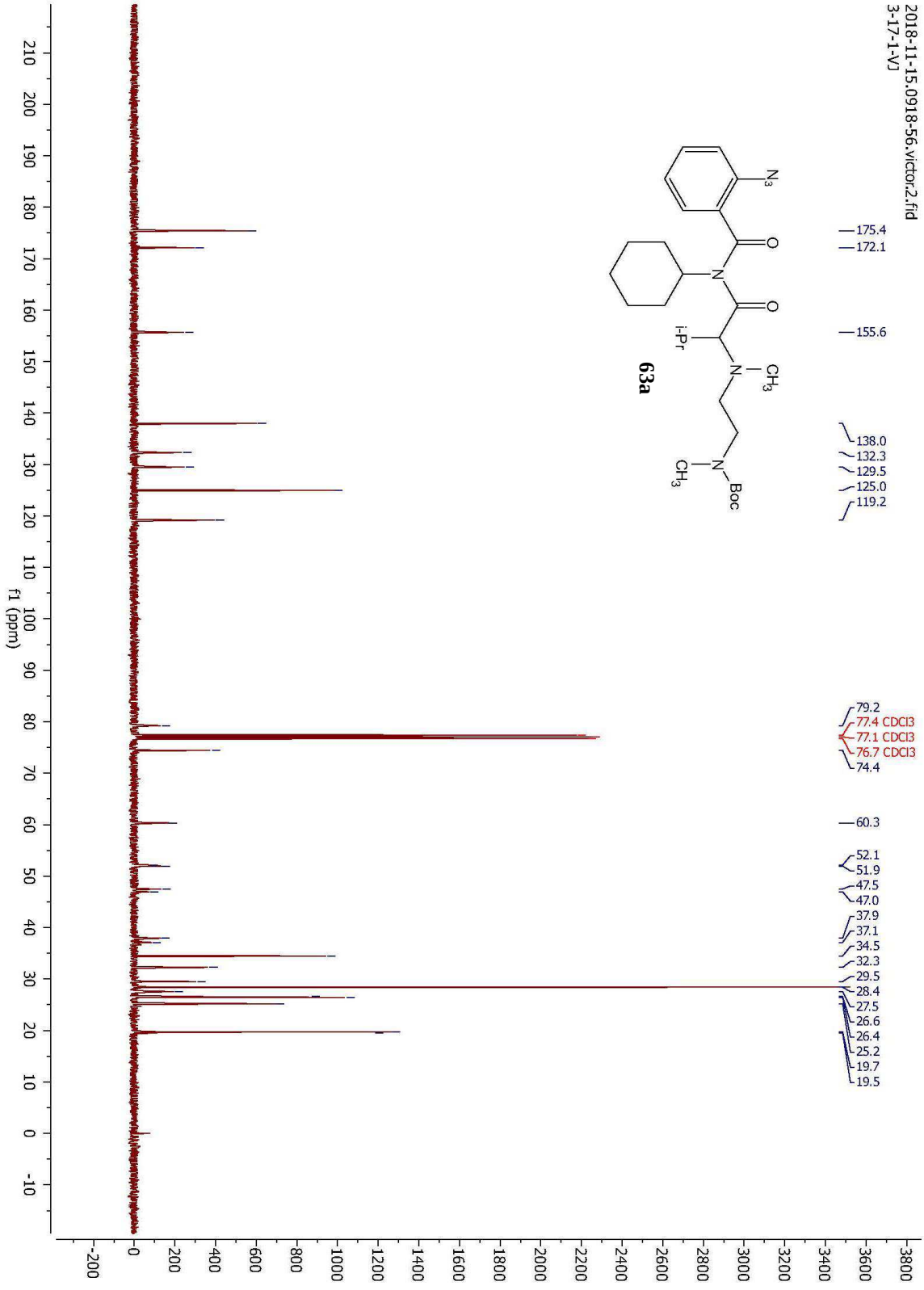
2018-11-15.0918-56.victor2.fid
3-17-1-VJ
63a
175.4
172.1
155.6
138.0
132.3
129.5
125.0
119.2
79.2
77.4 CDCl3
77.1 CDCl3
76.7 CDCl3
74.4
60.3
52.1
51.9
47.5
47.0
37.9
37.1
34.5
32.3
29.5
28.4
27.5
26.6
26.4
25.2
19.7
19.5
f1 (ppm)

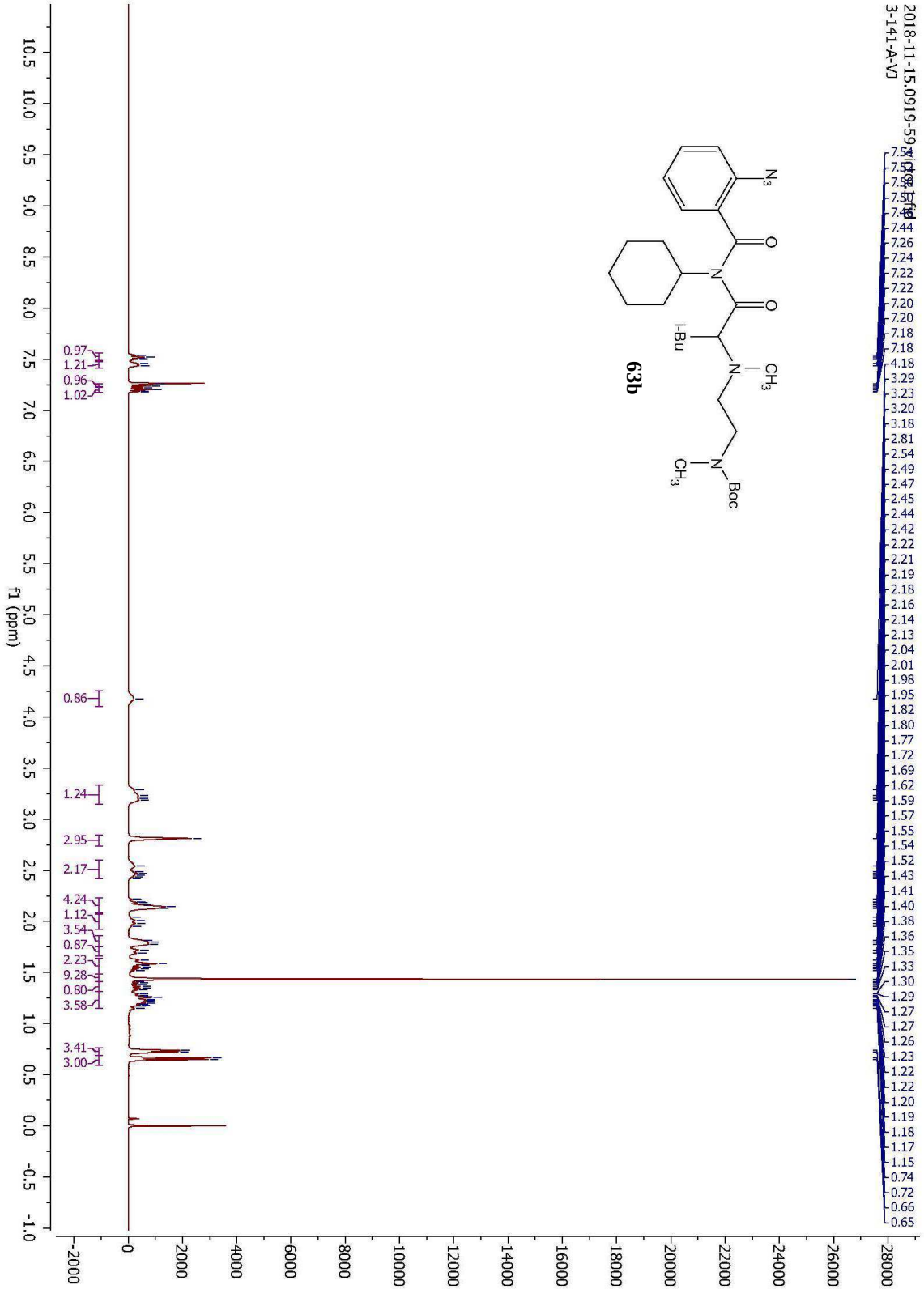
2018-11-15.0919-59-1H-3-141-A-VJ
63b
f1 (ppm)
0.97
1.21
0.96
1.02
0.86
1.24
2.95
2.17
4.24
1.12
3.54
0.87
2.23
9.28
0.80
3.58
3.41
3.00

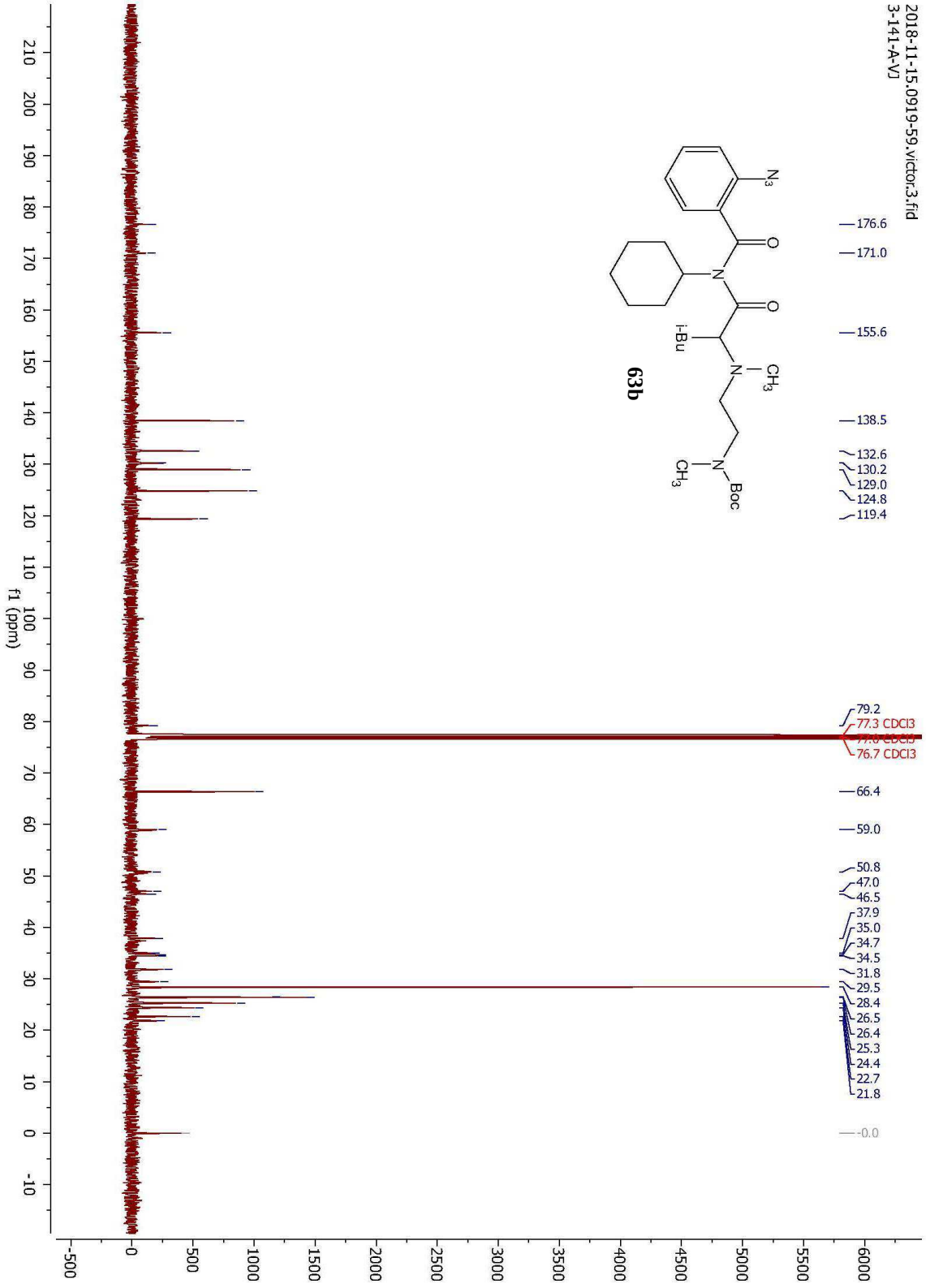
2018-11-15.0919-59.victor.3.fid
3-141-A-VJ
63b
f1 (ppm)
176.6
171.0
155.6
138.5
132.6
130.2
129.0
124.8
119.4
79.2
77.3 CDCl3
76.7 CDCl3
66.4
59.0
50.8
47.0
46.5
37.9
35.0
34.7
34.5
31.8
29.5
28.4
26.5
26.4
25.3
24.4
22.7
21.8
0.0

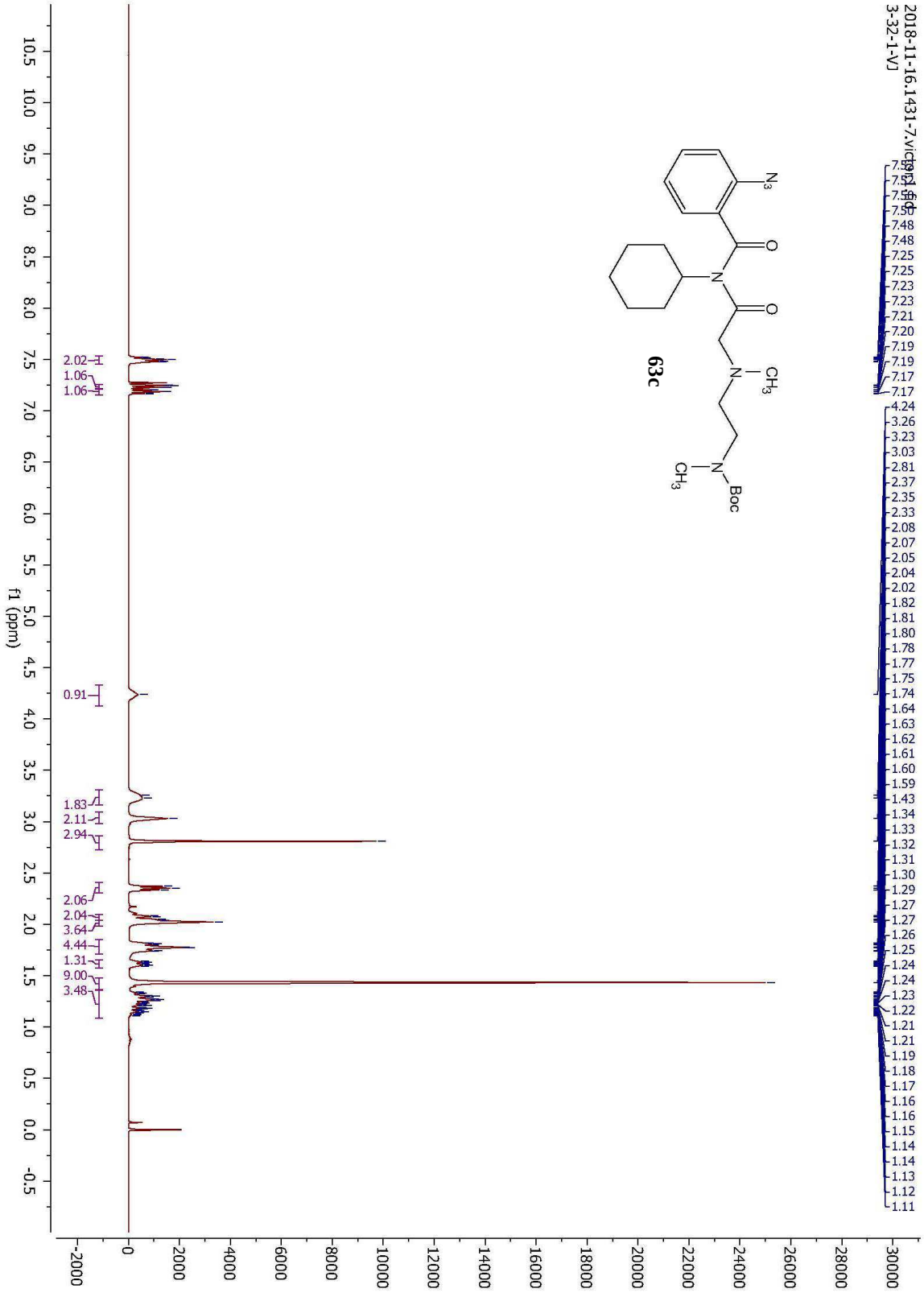
2018-11-16.1431-7.victoria 6cd
3-32-1-VJ
63c
f1 (ppm)

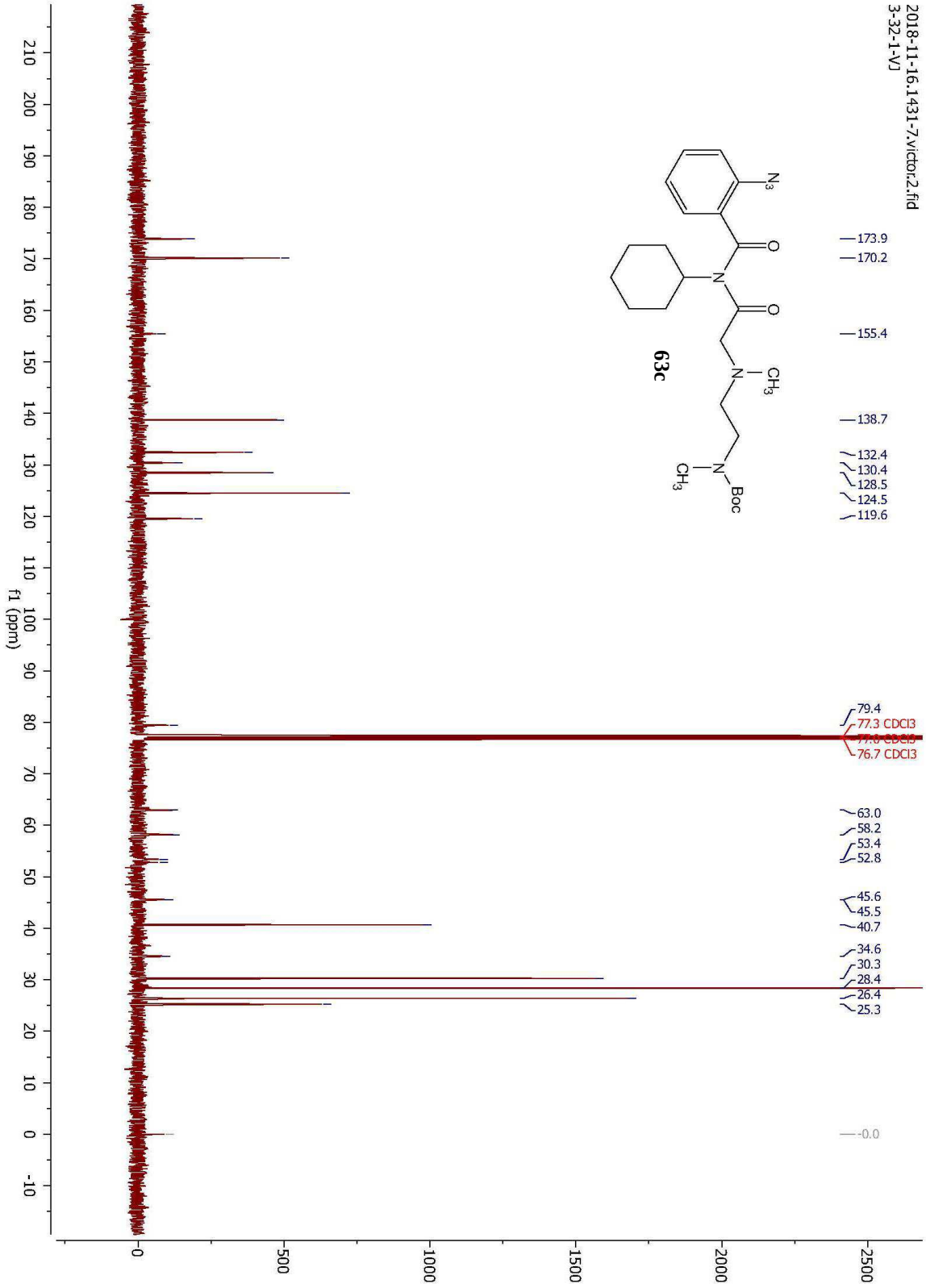
2018-11-16.1431-7.victor.2.fid
3-32-1-VJ
63c
173.9
170.2
155.4
138.7
132.4
130.4
128.5
124.5
119.6
79.4
77.3 CDCl3
77.0 CDCl3
76.7 CDCl3
63.0
58.2
53.4
52.8
45.6
45.5
40.7
34.6
30.3
28.4
26.4
25.3
-0.0
f1 (ppm)

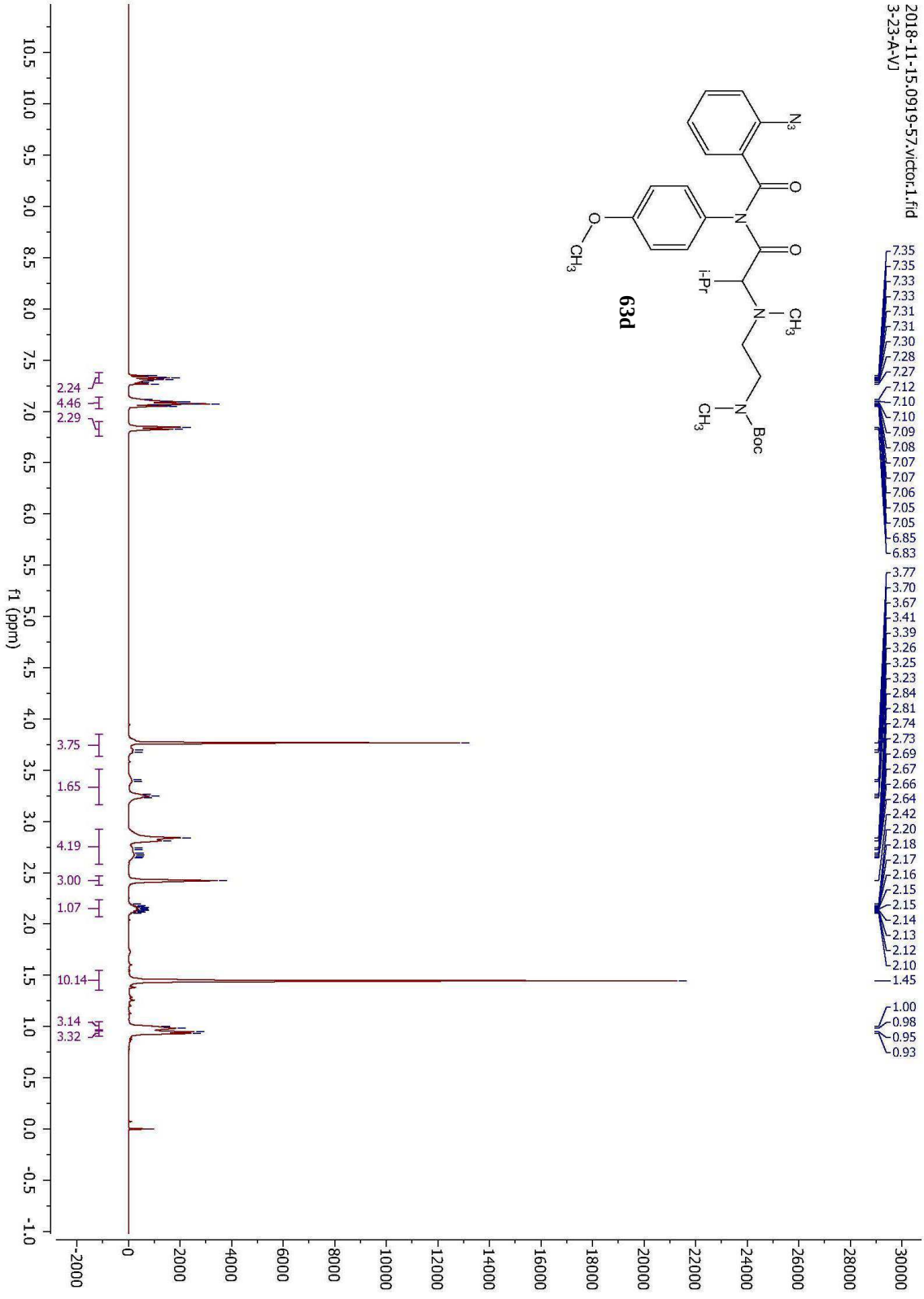
2018-11-15.0919-57.victor.1.fid
3-23-A-VJ
63d
f1 (ppm)

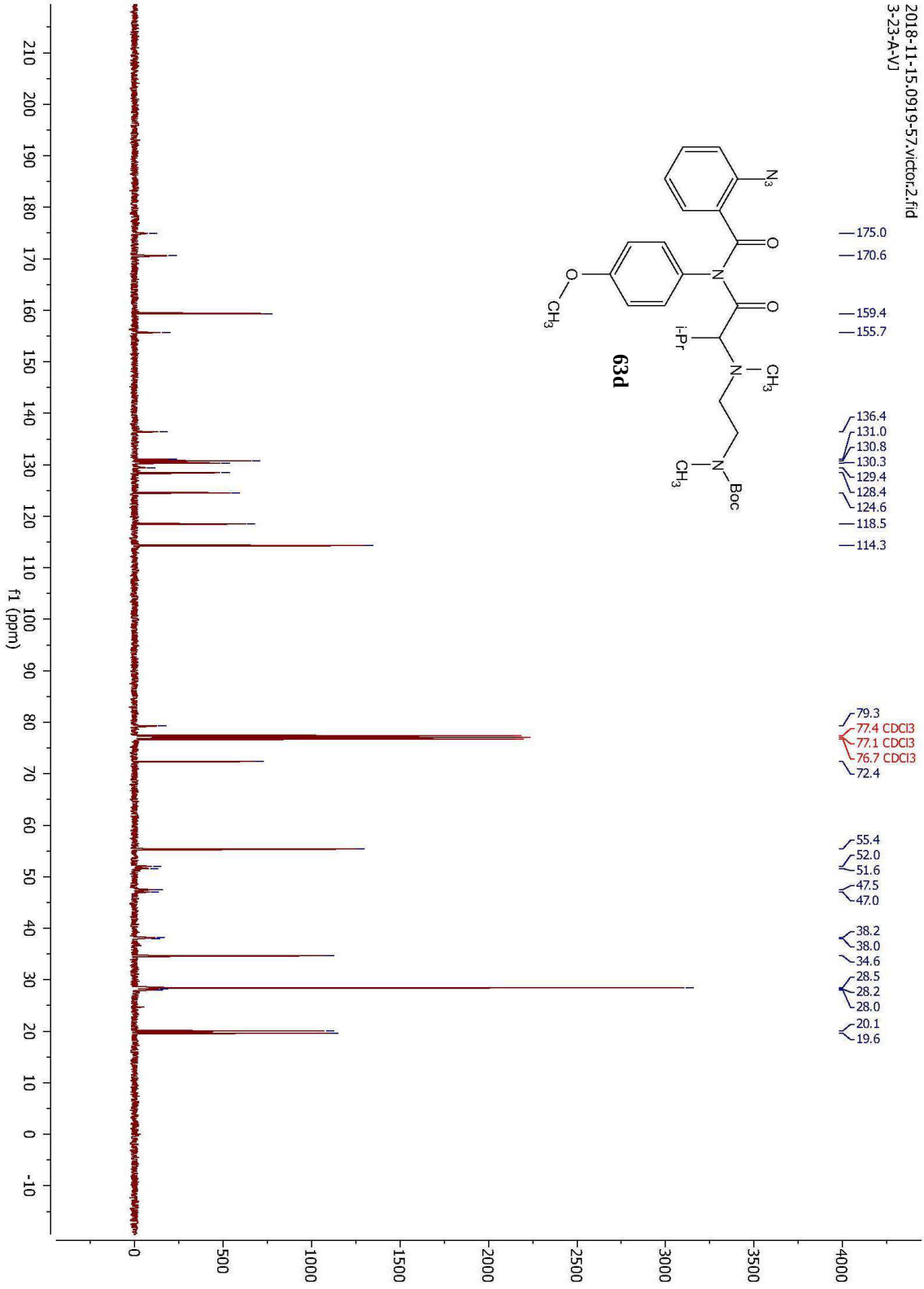
2018-11-15.0919-57.victor.2.fid
3-23-A-VJ
63d
175.0
170.6
159.4
155.7
136.4
131.0
130.8
130.3
129.4
128.4
124.6
118.5
114.3
79.3
77.4 CDCl3
77.1 CDCl3
76.7 CDCl3
72.4
55.4
52.0
51.6
47.5
47.0
38.2
38.0
34.6
28.5
28.2
28.0
20.1
19.6
f1 (ppm)

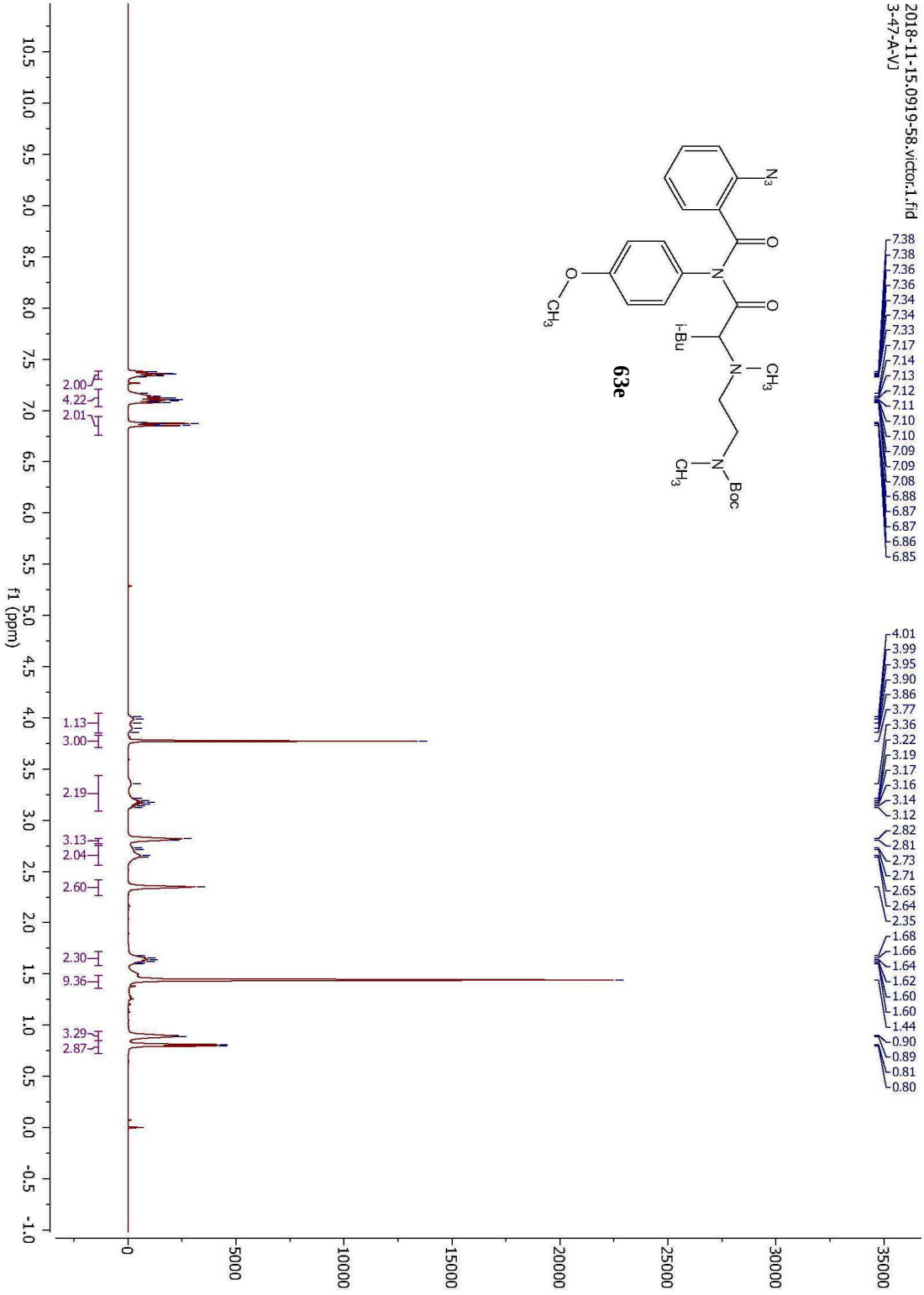
2018-11-15.0919-58.victor.1.fid
3-47-A-VJ
63e
f1 (ppm)

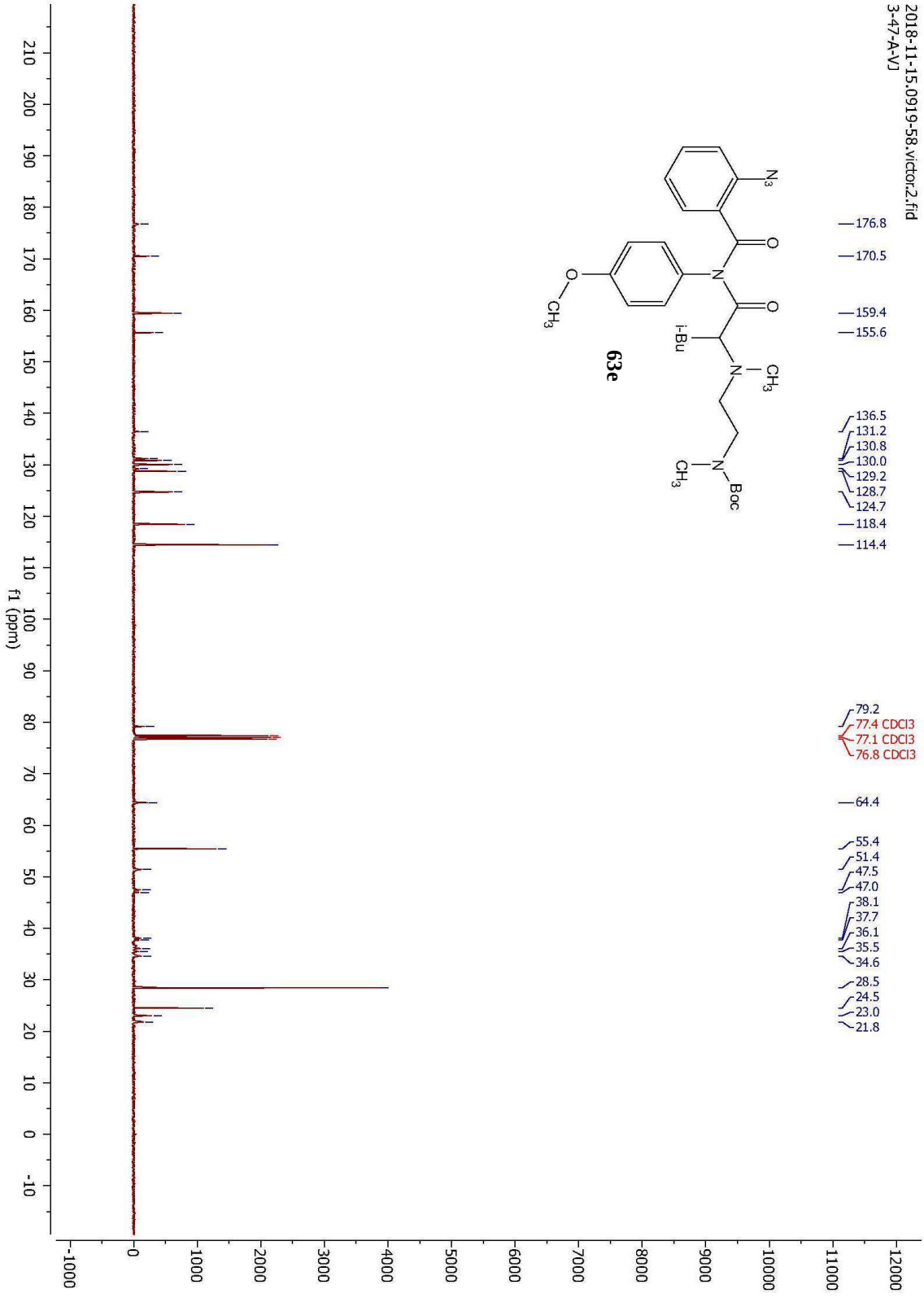
2018-11-15.0919-58.victor.2.fid
3-47-A-VJ
63e
176.8
170.5
159.4
155.6
136.5
131.2
130.8
130.0
129.2
128.7
124.7
118.4
114.4
79.2
77.4 CDCl3
77.1 CDCl3
76.8 CDCl3
64.4
55.4
51.4
47.5
47.0
38.1
37.7
36.1
35.5
34.6
28.5
24.5
23.0
21.8
f1 (ppm)

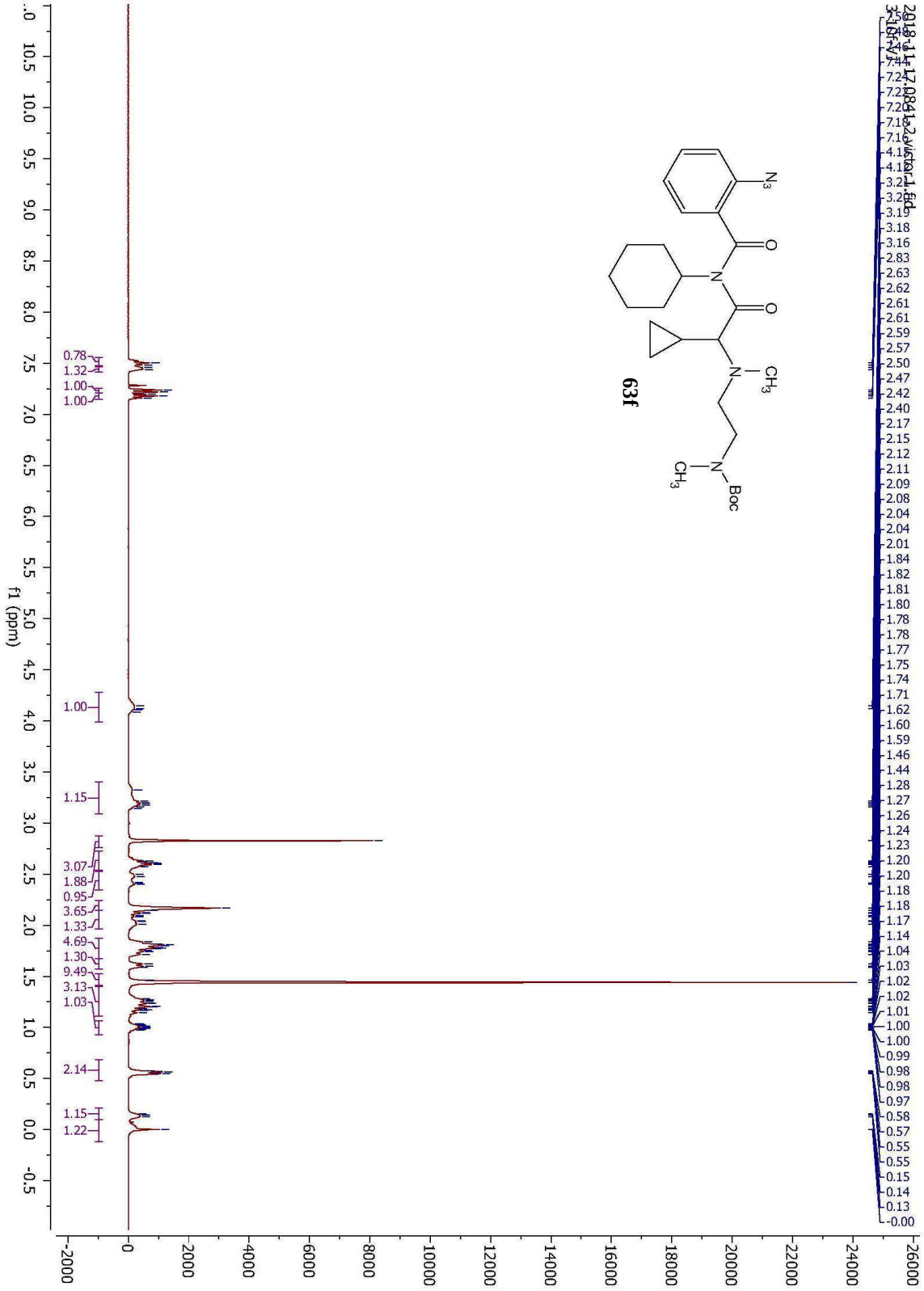
63f
f1 (ppm)

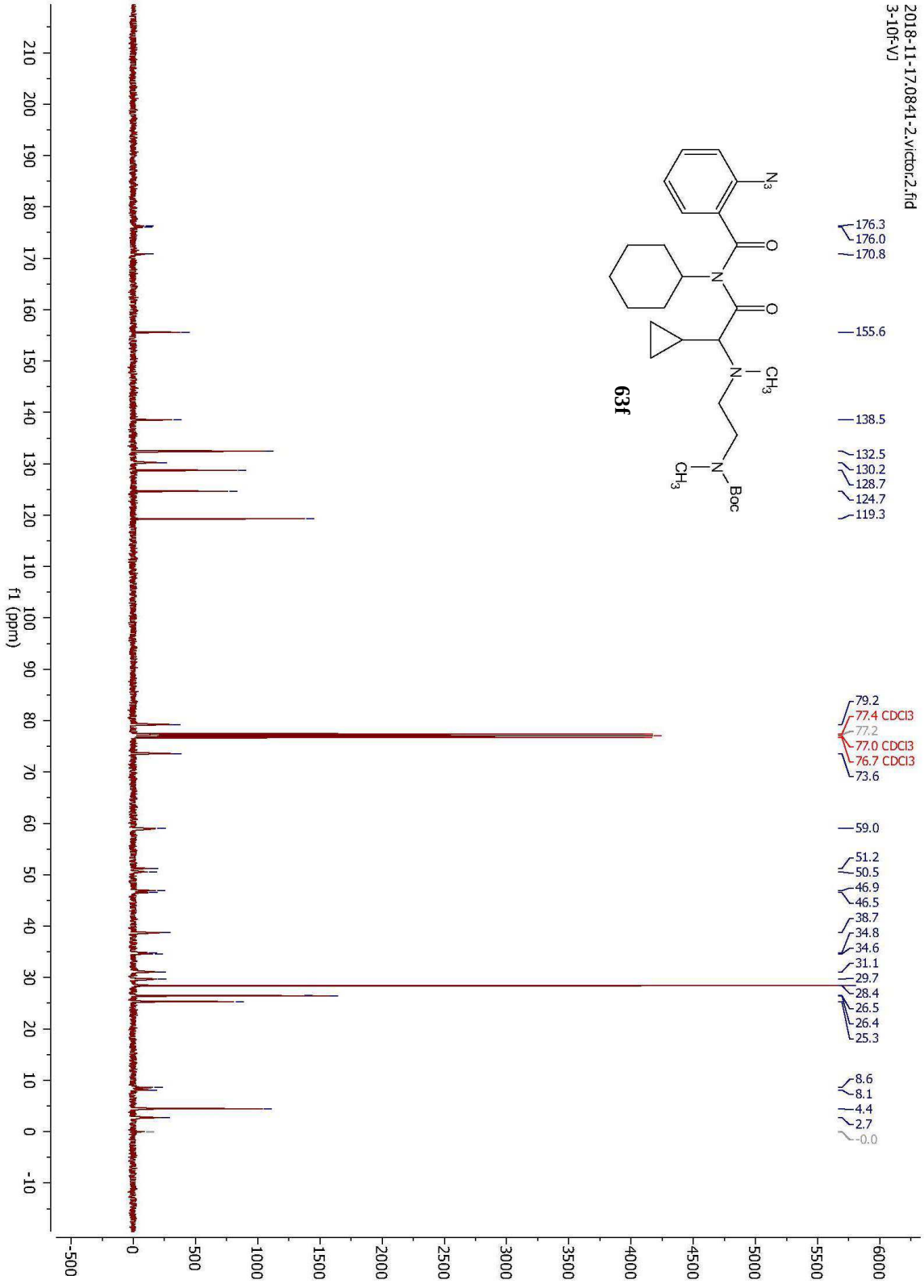
2018-11-17.0841-2.victor.2.fid
3-10f-VJ
63f
176.3
176.0
170.8
155.6
138.5
132.5
130.2
128.7
124.7
119.3
79.2
77.4 CDCl3
77.2
77.0 CDCl3
76.7 CDCl3
73.6
59.0
51.2
50.5
46.9
46.5
38.7
34.8
34.6
31.1
29.7
28.4
26.5
26.4
25.3
8.6
8.1
4.4
2.7
-0.0
f1 (ppm)

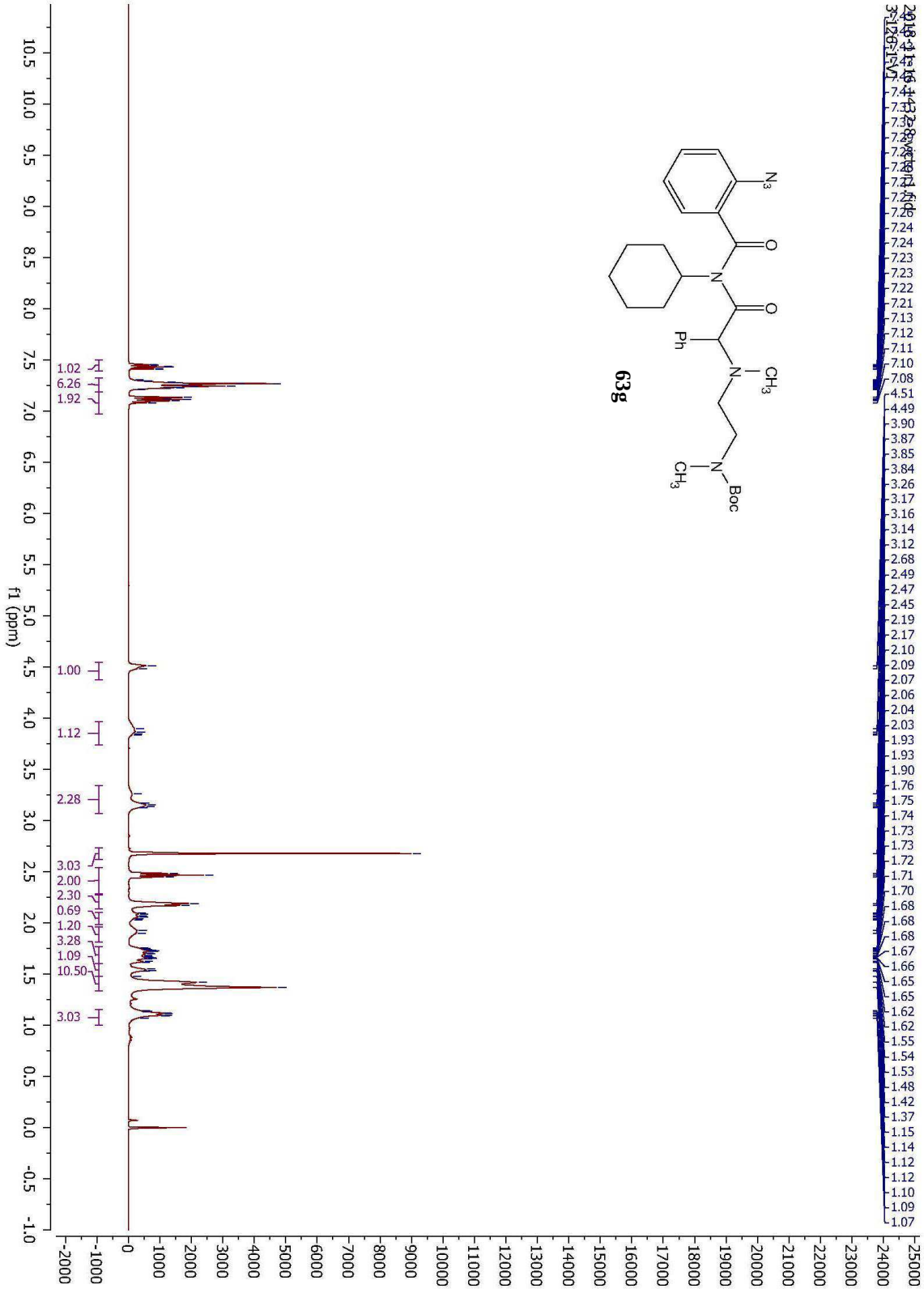
63g
f1 (ppm)
1.02
6.26
1.92
1.00
1.12
2.28
3.03
2.00
2.30
0.69
1.20
3.28
1.09
10.50
3.03

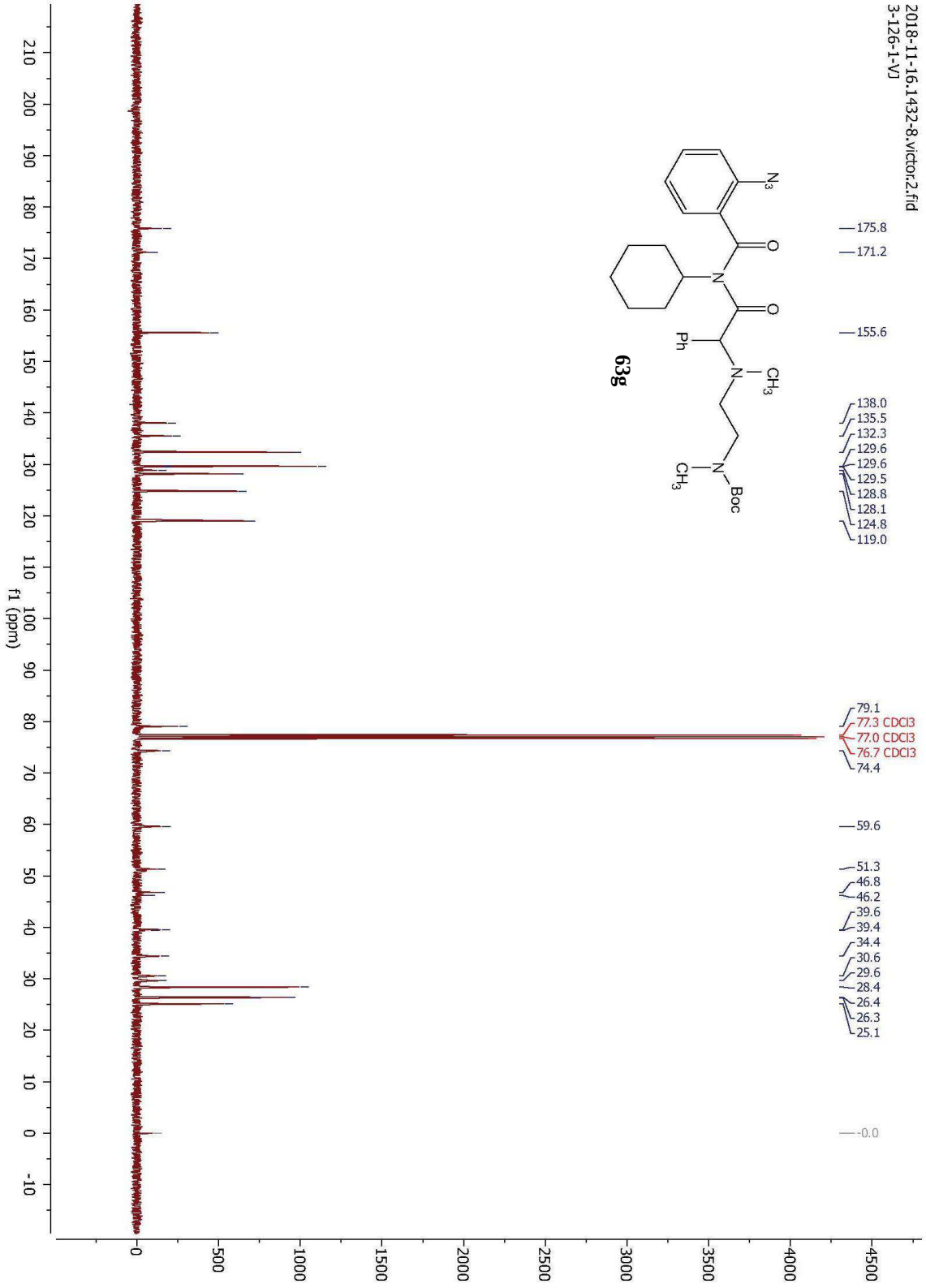
2018-11-16.1432-8.victor.2.fid
3-126-1-VJ
63g
175.8
171.2
155.6
138.0
135.5
132.3
129.6
129.6
129.5
128.8
128.1
124.8
119.0
79.1
77.3 CDCl3
77.0 CDCl3
76.7 CDCl3
74.4
59.6
51.3
46.8
46.2
39.6
39.4
34.4
30.6
29.6
28.4
26.4
26.3
25.1
-0.0
f1 (ppm)

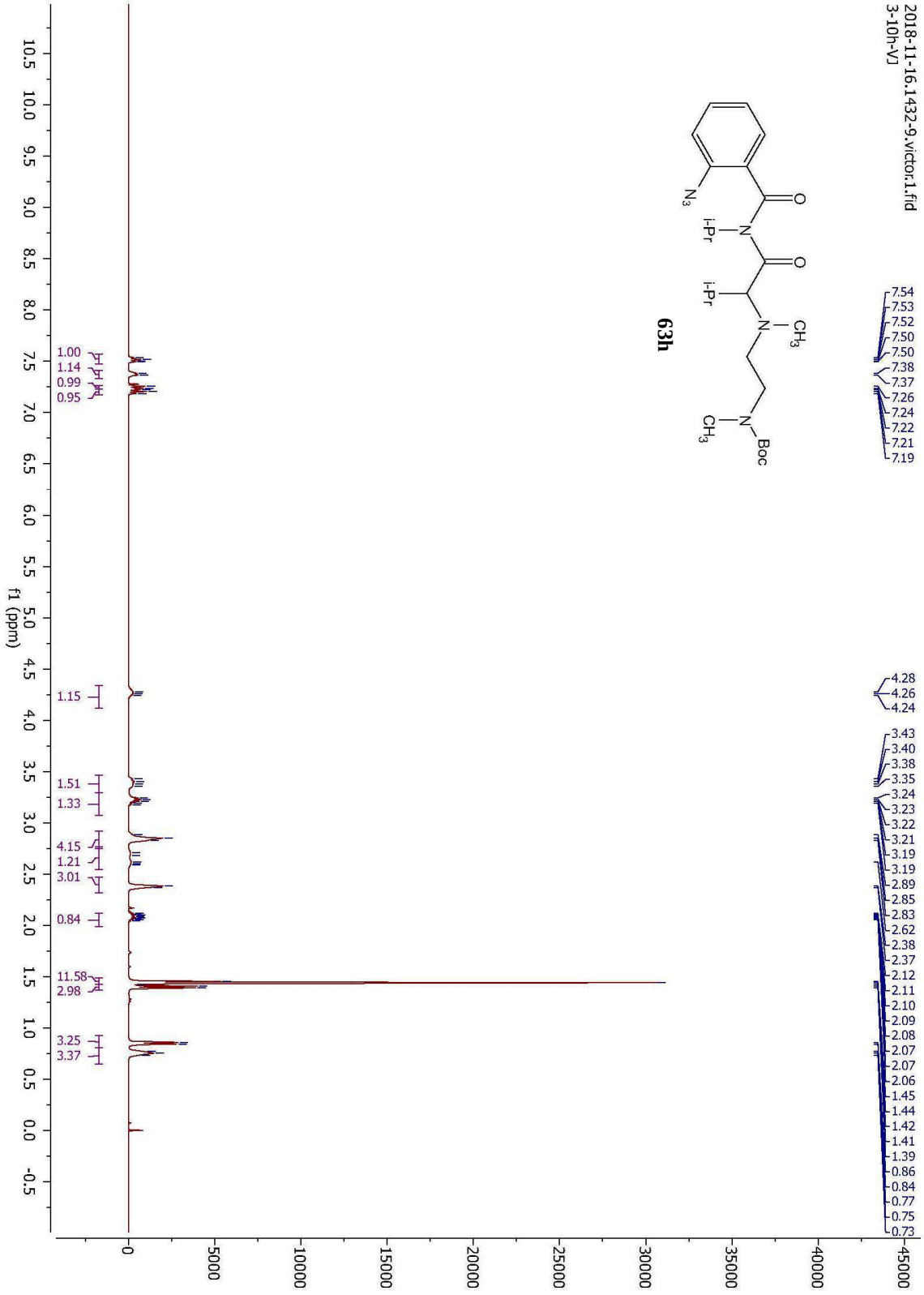
2018-11-16.1432-9.victor.1.fid
3-10h-VJ
63h
f1 (ppm)

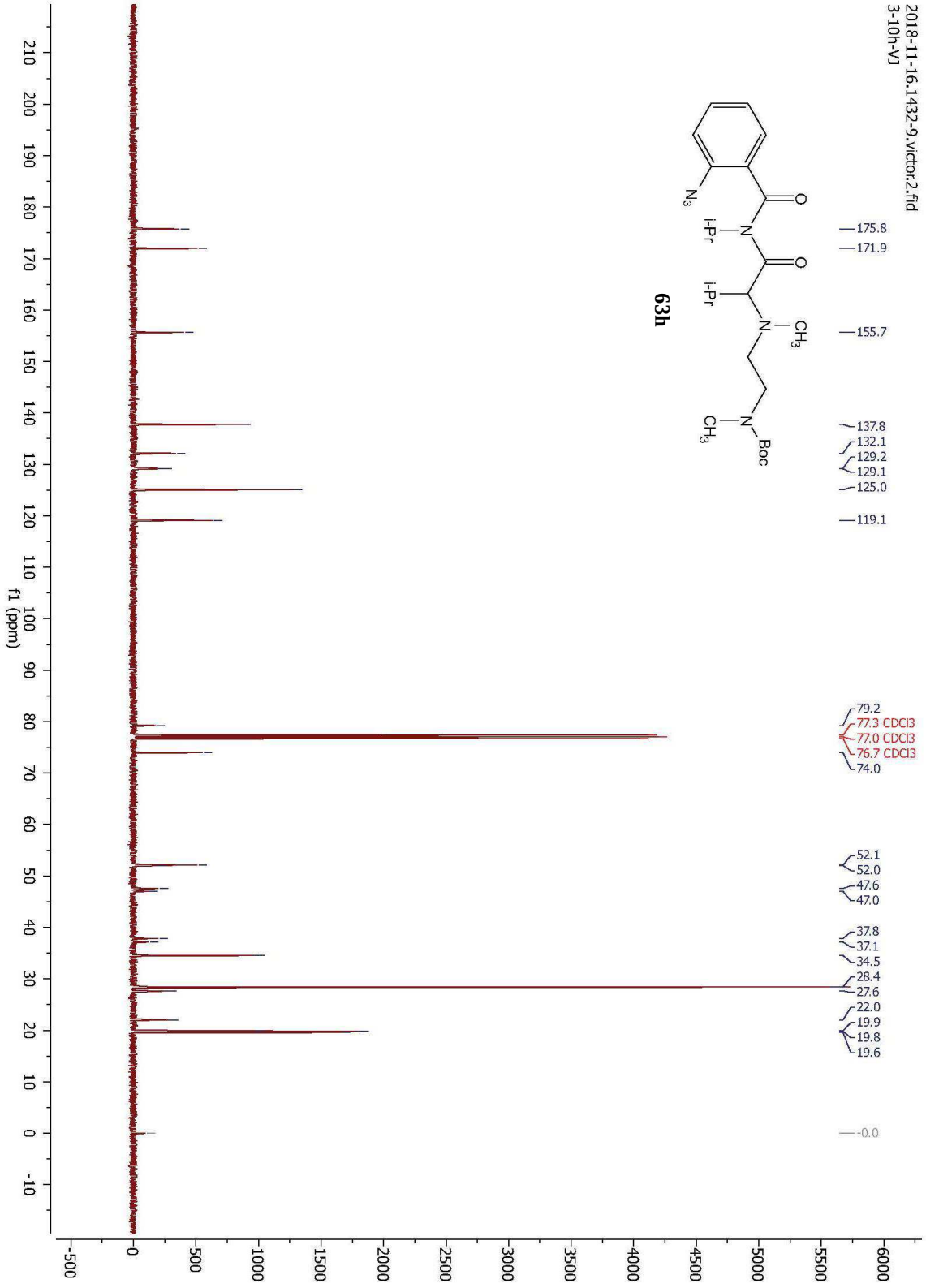
2018-11-16.1432-9.victor.2.fid
3-10h-VJ
63h
175.8
171.9
155.7
137.8
132.1
129.2
129.1
125.0
119.1
79.2
77.3 CDCl3
77.0 CDCl3
76.7 CDCl3
74.0
52.1
52.0
47.6
47.0
37.8
37.1
34.5
28.4
27.6
22.0
19.9
19.8
19.6
-0.0
f1 (ppm)

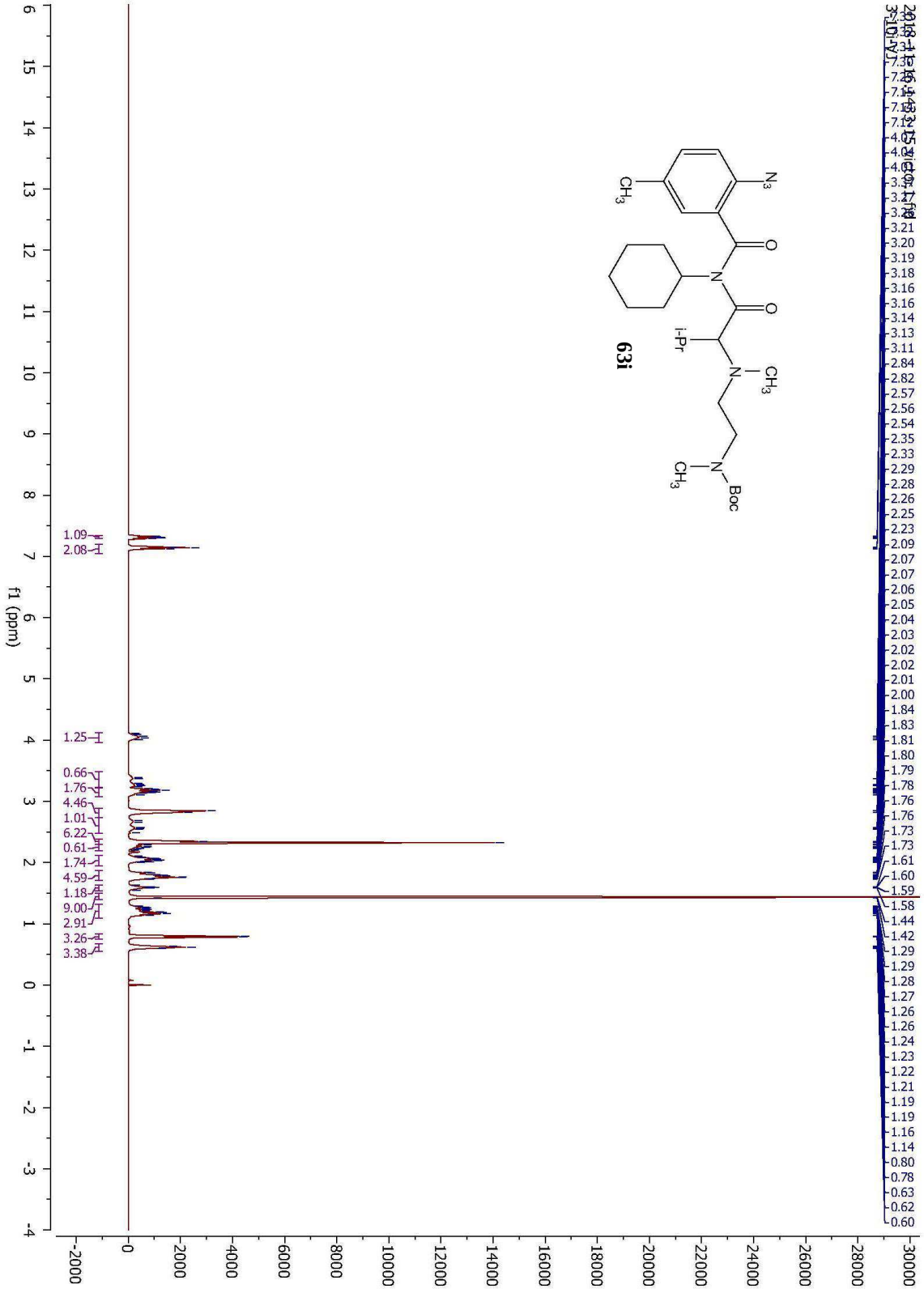
63i
f1 (ppm)
1.09
2.08
1.25
0.66
1.76
4.46
1.01
6.22
0.61
1.74
4.59
1.18
9.00
2.91
3.26
3.38

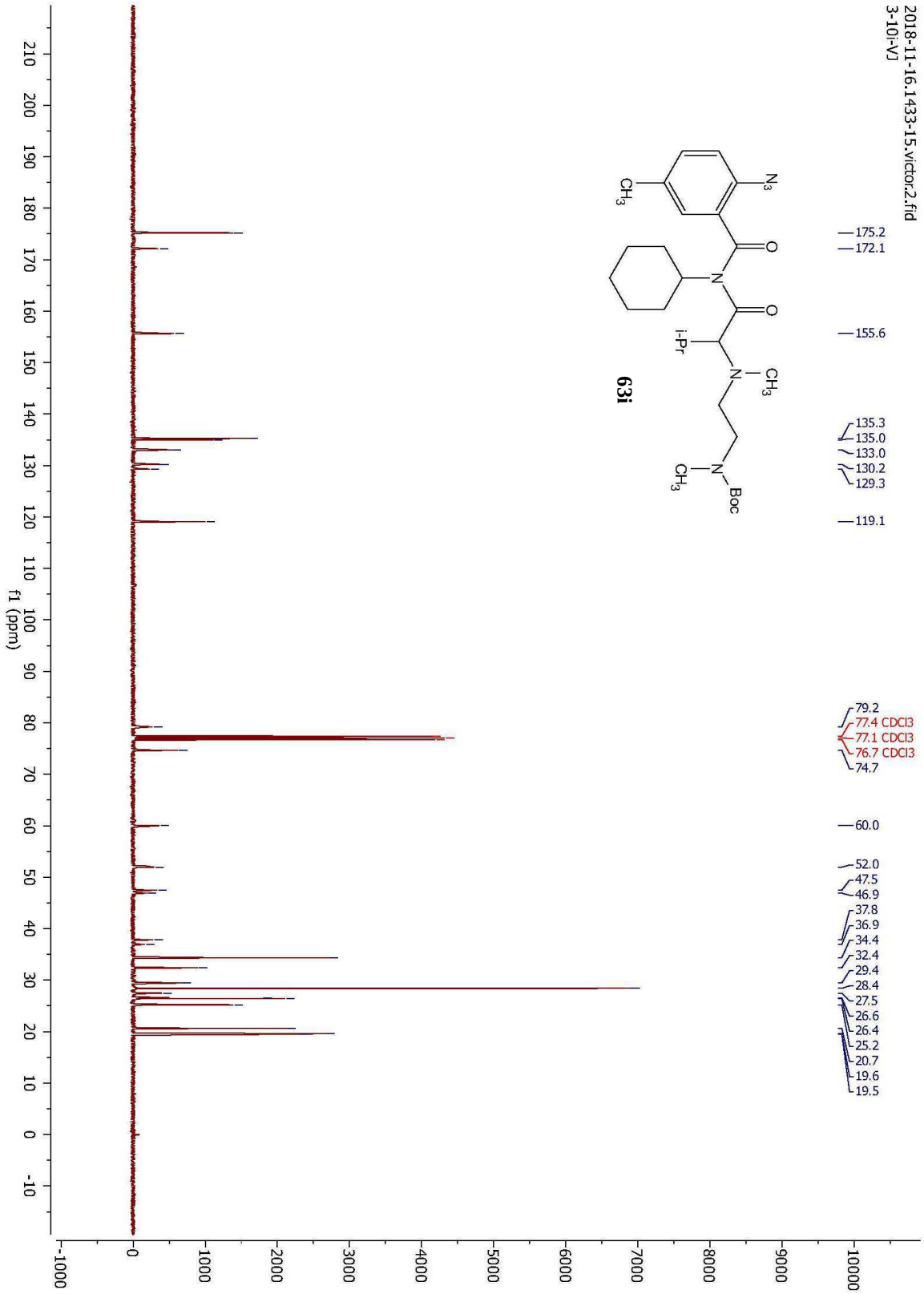
2018-11-16.1433-15.victor2.fid
3-10i-VJ
63i
175.2
172.1
155.6
135.3
135.0
133.0
130.2
129.3
119.1
79.2
77.4 CDCl3
77.1 CDCl3
76.7 CDCl3
74.7
60.0
52.0
47.5
46.9
37.8
36.9
34.4
32.4
29.4
28.4
27.5
26.6
26.4
25.2
20.7
19.6
19.5
f1 (ppm)

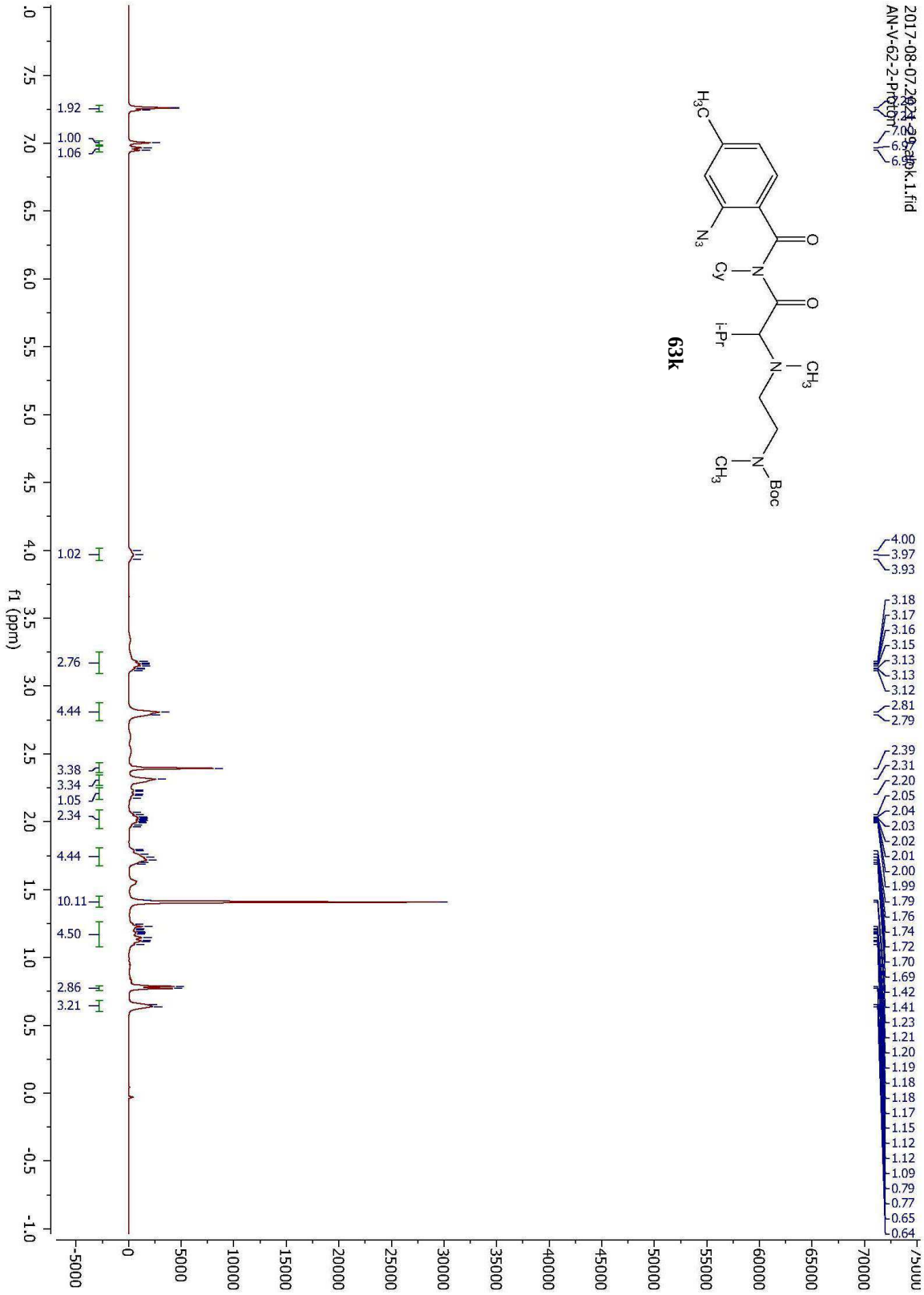
63k
f1 (ppm)

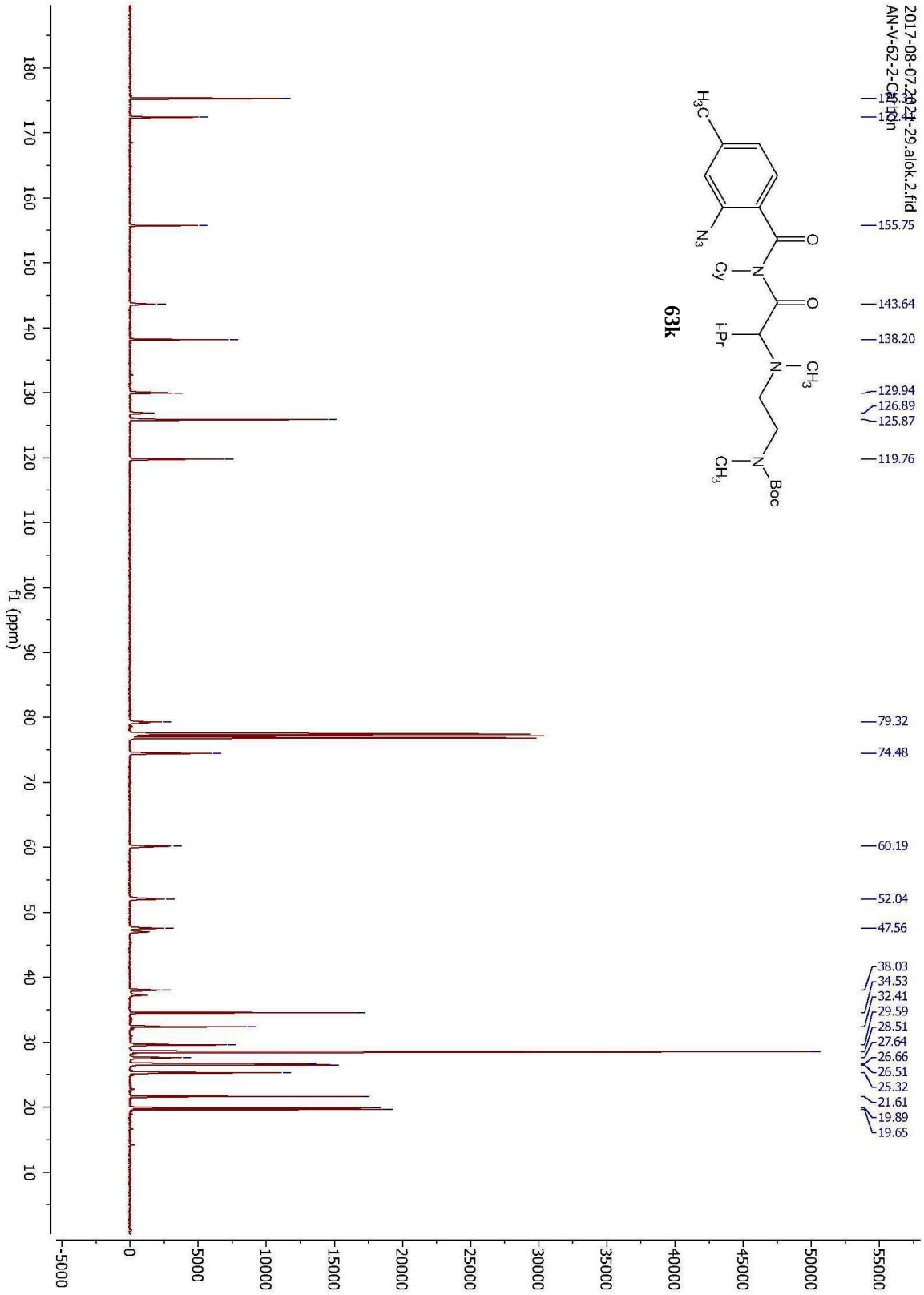
2017-08-07-2017-29.alok.2.fid
AN-V-62-2-C-13.10n
155.75
143.64
138.20
129.94
126.89
125.87
119.76
79.32
74.48
60.19
52.04
47.56
38.03
34.53
32.41
29.59
28.51
27.64
26.66
26.51
25.32
21.61
19.89
19.65
63k
f1 (ppm)

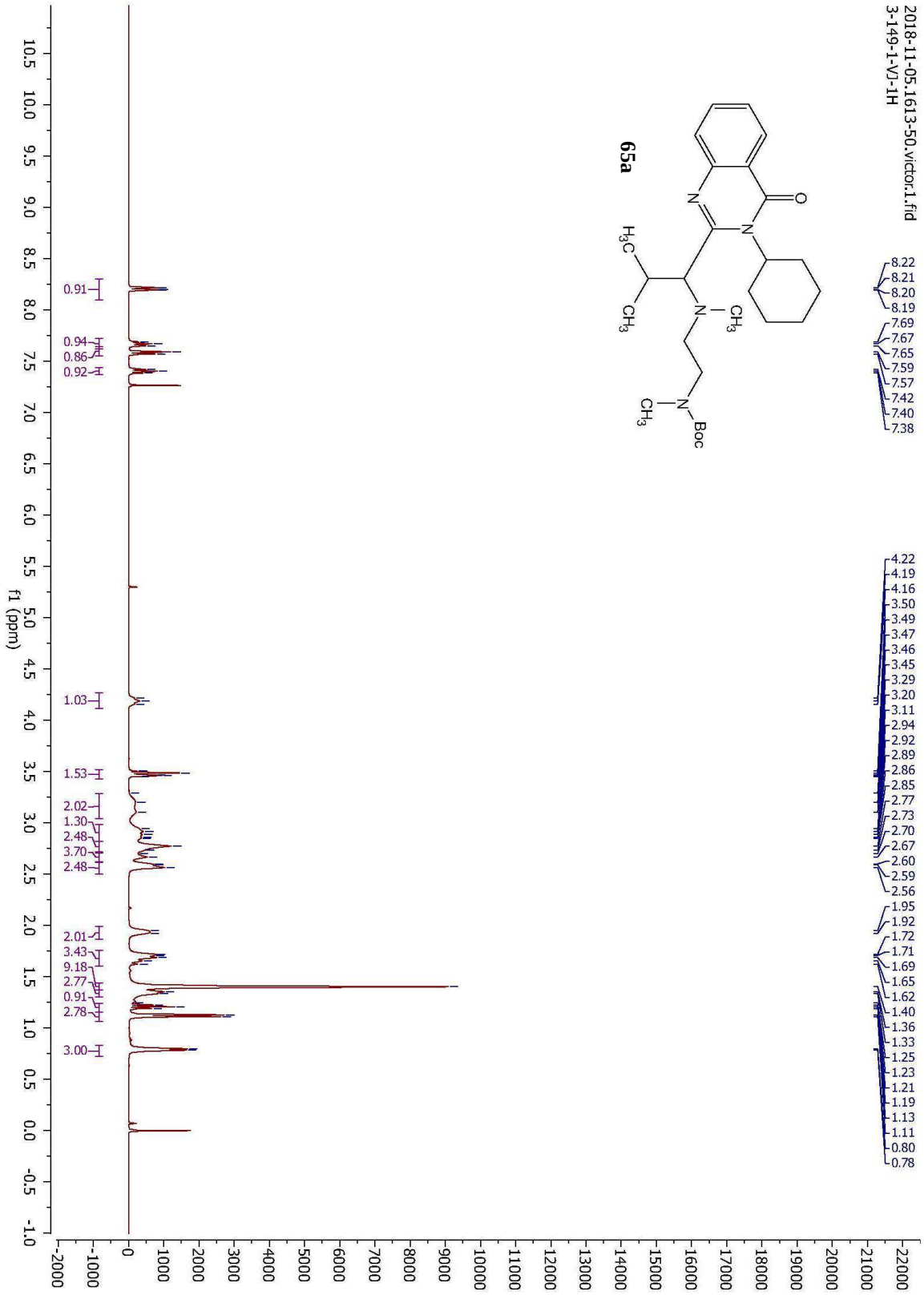
2018-11-05.1613-50.victor.1.fid
3-149-1-VJ-1H
65a
f1 (ppm)

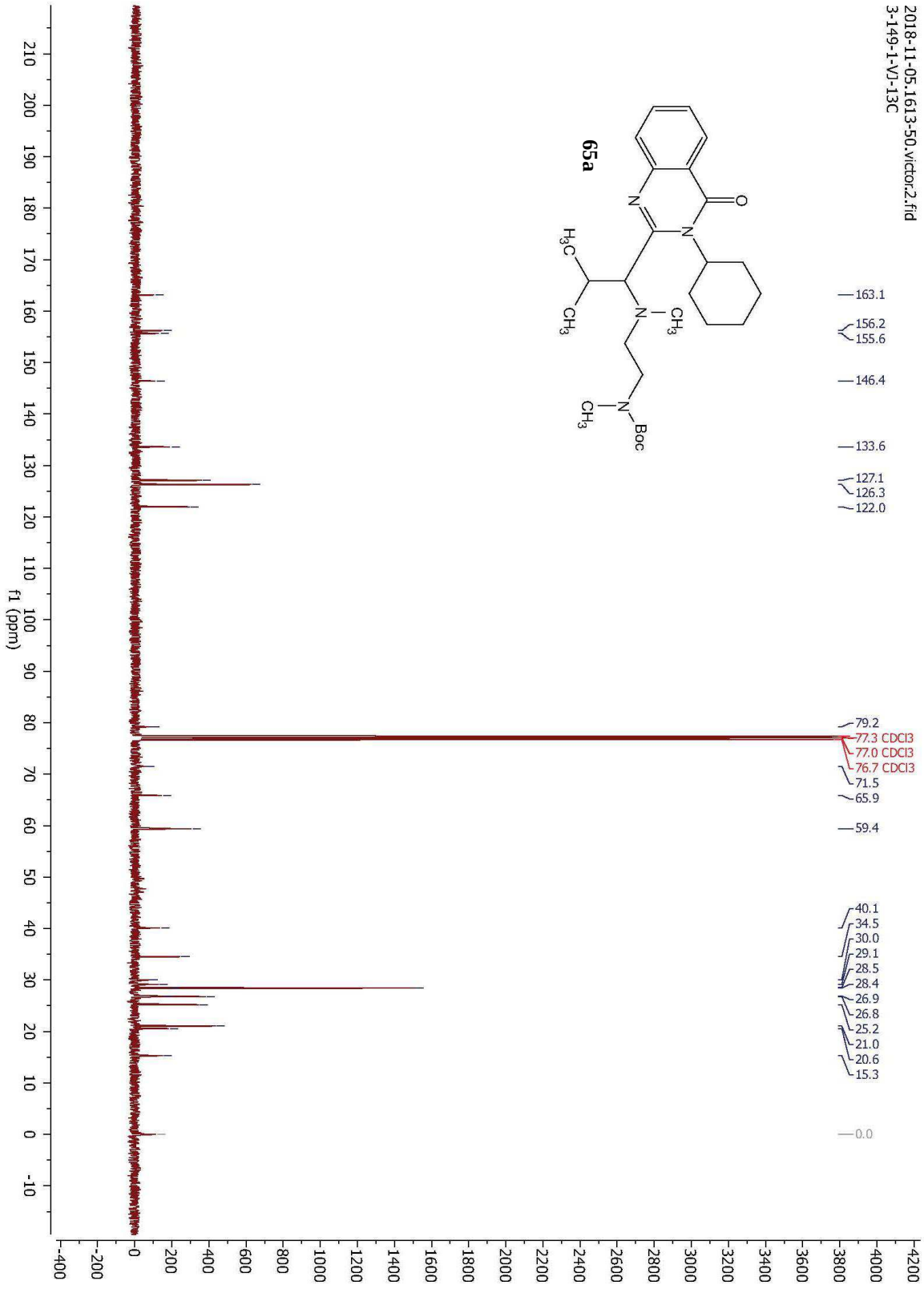
2018-11-05.1613-50.victor2.fid
3-149-1-VJ-13C
65a
163.1
156.2
155.6
146.4
133.6
127.1
126.3
122.0
79.2
77.3 CDCl3
77.0 CDCl3
76.7 CDCl3
71.5
65.9
59.4
40.1
34.5
30.0
29.1
28.5
28.4
26.9
26.8
25.2
21.0
20.6
15.3
0.0
f1 (ppm)

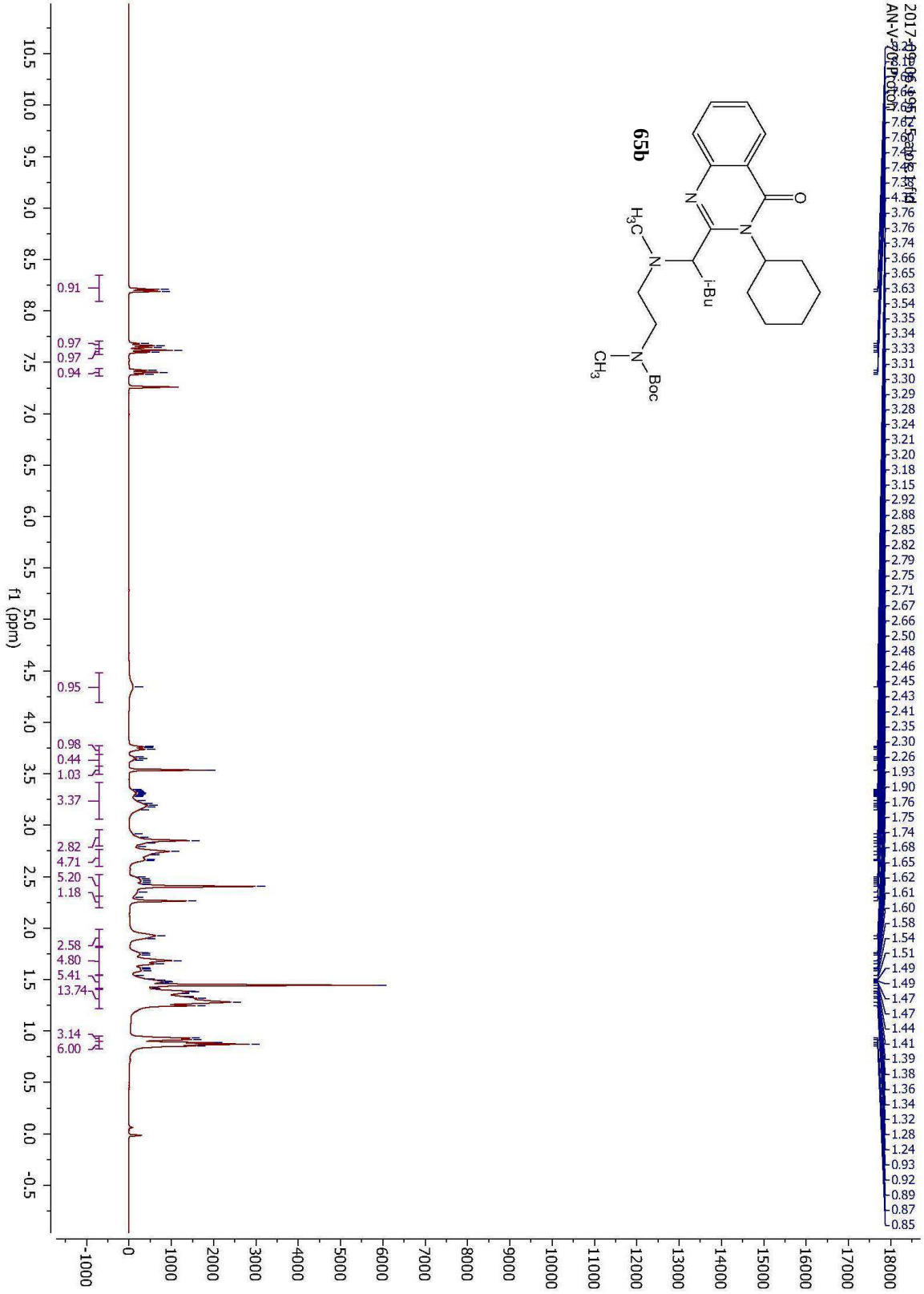
65b
f1 (ppm)
0.91
0.97
0.97
0.94
0.95
0.98
0.44
1.03
3.37
2.82
4.71
5.20
1.18
2.58
4.80
5.41
13.74
3.14
6.00

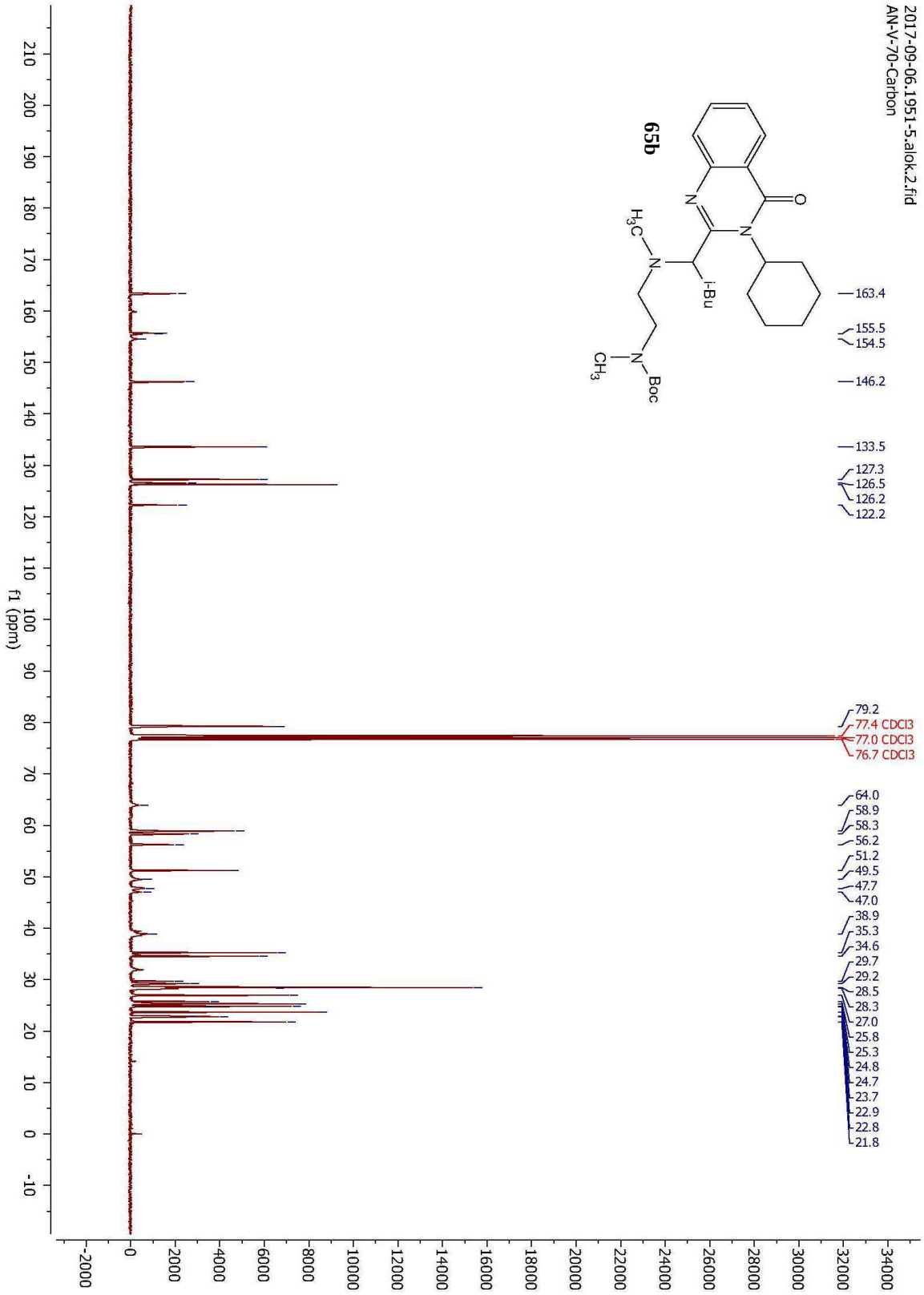
2017-09-06.1951-5.alok.2.fid
AN-V-70-Carbon
65b
f1 (ppm)
163.4
155.5
154.5
146.2
133.5
127.3
126.5
126.2
122.2
79.2
77.4 CDCl3
77.0 CDCl3
76.7 CDCl3
64.0
58.9
58.3
56.2
51.2
49.5
47.7
47.0
38.9
35.3
34.6
29.7
29.2
28.5
28.3
27.0
25.8
25.3
24.8
24.7
23.7
22.9
22.8
21.8

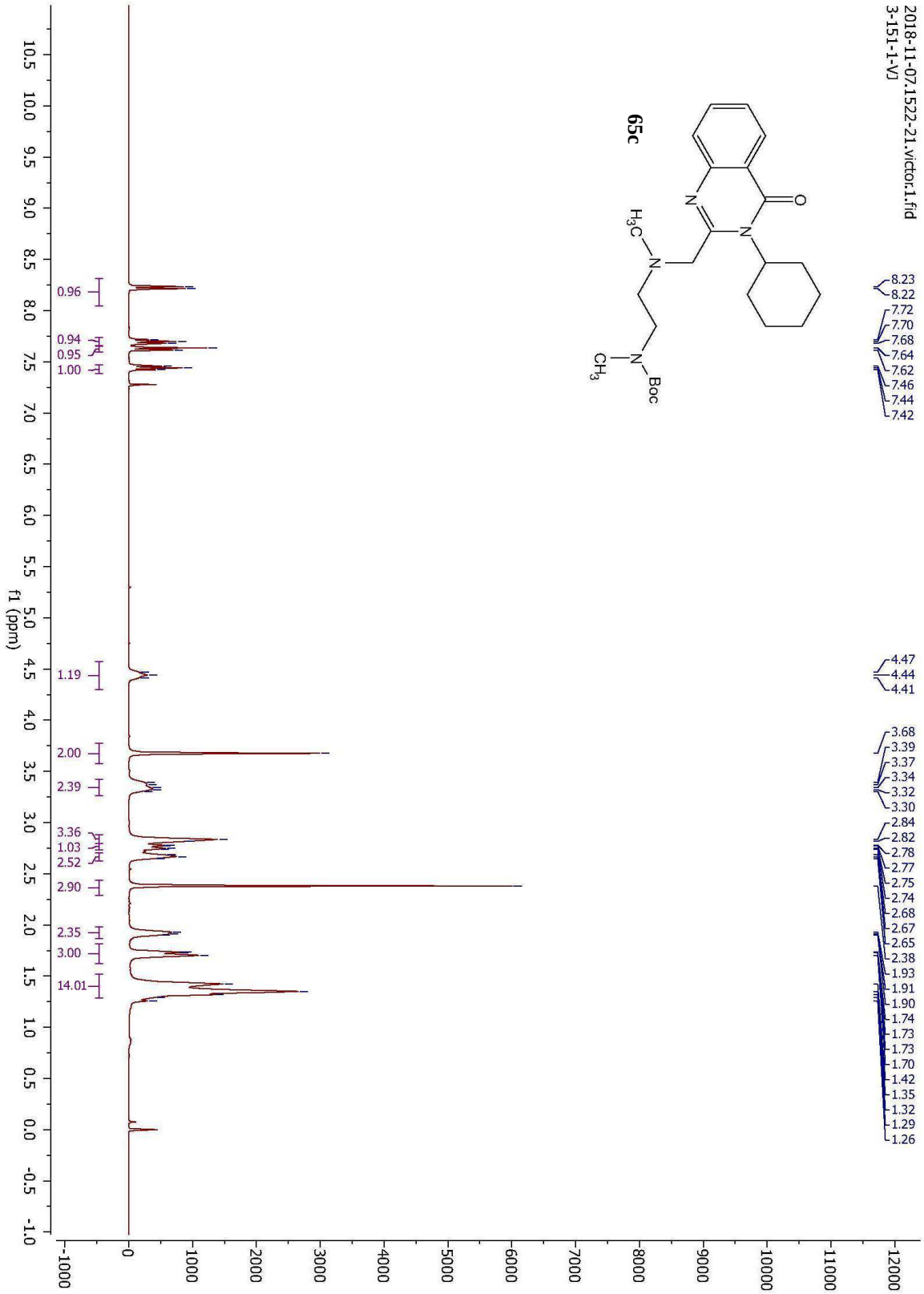
2018-11-07.1522-21.victor.1.fid
3-151-1-VJ
65c
f1 (ppm)
0.96
0.94
0.95
1.00
1.19
2.00
2.39
3.36
1.03
2.52
2.90
2.35
3.00
14.01
8.23
8.22
7.72
7.70
7.68
7.64
7.62
7.46
7.44
7.42
4.47
4.44
4.41
3.68
3.39
3.37
3.34
3.32
3.30
2.84
2.82
2.78
2.77
2.75
2.74
2.68
2.67
2.65
2.38
1.93
1.91
1.90
1.74
1.73
1.73
1.70
1.42
1.35
1.32
1.29
1.26

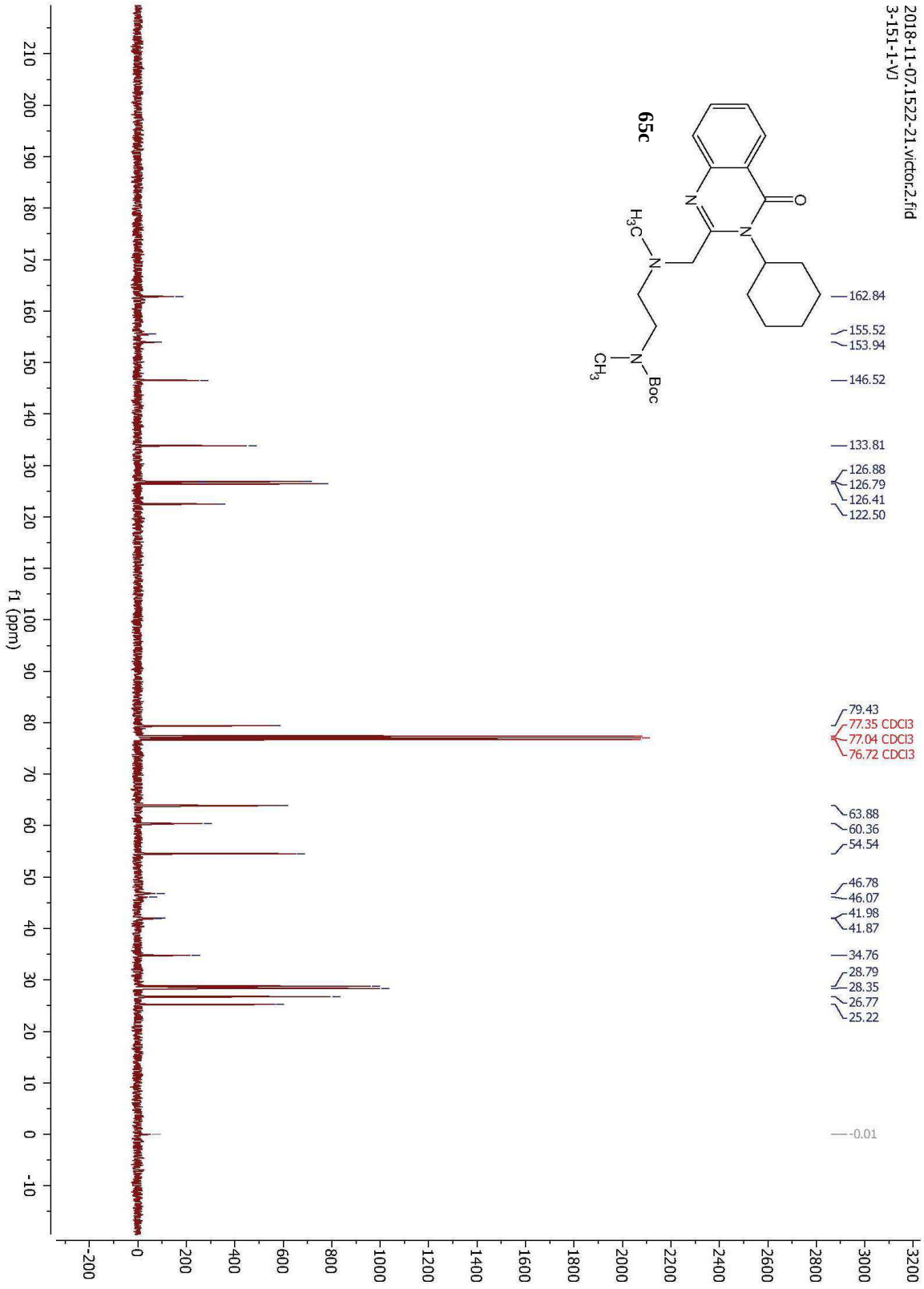
2018-11-07.1522-21.victor2.fid
3-151-1-VJ
65c
162.84
155.52
153.94
146.52
133.81
126.88
126.79
126.41
122.50
79.43
77.35 CDCl3
77.04 CDCl3
76.72 CDCl3
63.88
60.36
54.54
46.78
46.07
41.98
41.87
34.76
28.79
28.35
26.77
25.22
-0.01
f1 (ppm)

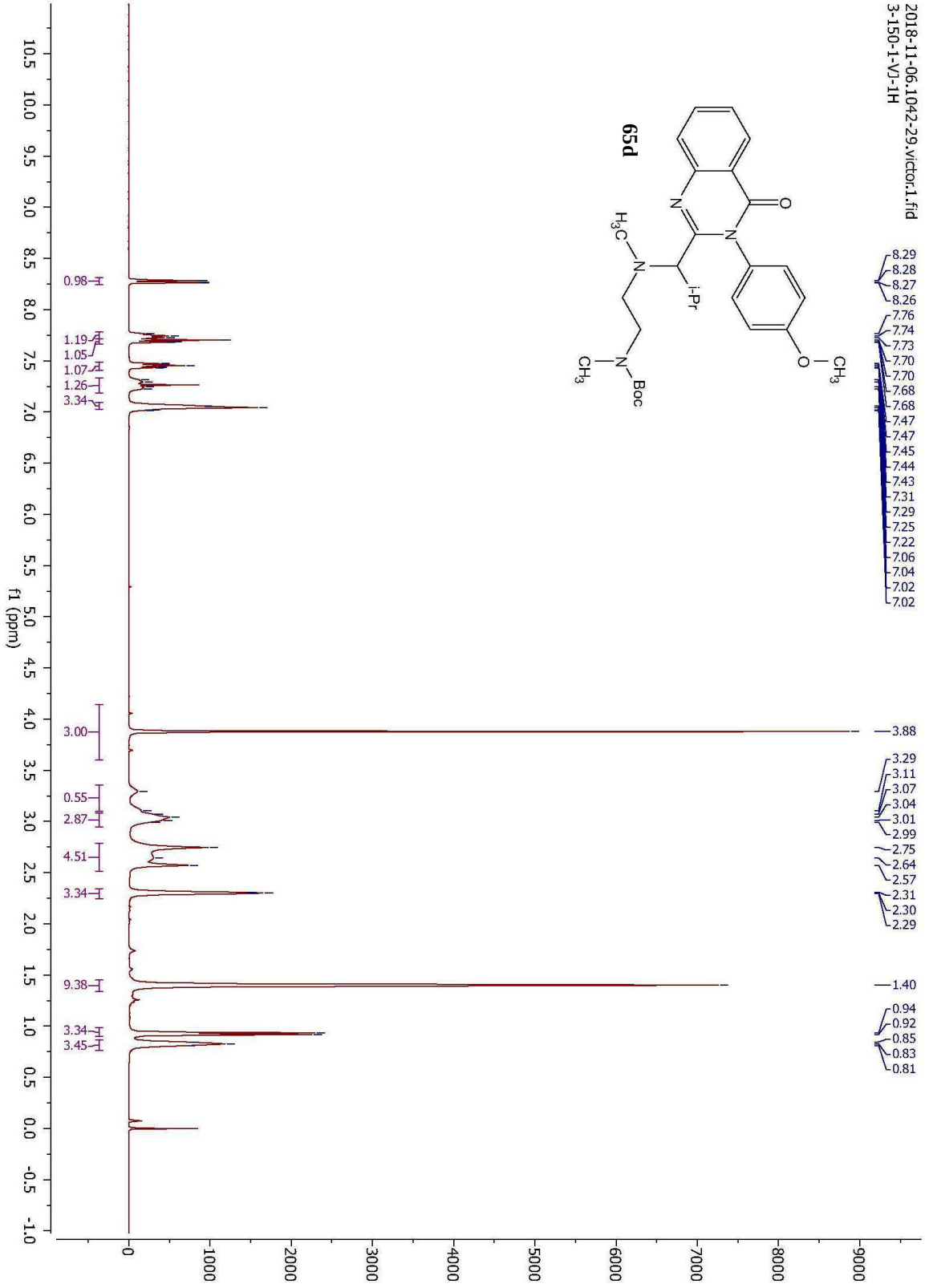
2018-11-06.1042-29.victor.1.fid
3-150-1-VJ-1H
65d
f1 (ppm)
0.98
1.19
1.05
1.07
1.26
3.34
3.00
0.55
2.87
4.51
3.34
9.38
3.34
3.45
8.29
8.28
8.27
8.26
7.76
7.74
7.73
7.70
7.70
7.68
7.68
7.47
7.47
7.45
7.44
7.43
7.31
7.29
7.25
7.22
7.06
7.04
7.02
7.02
3.88
3.29
3.11
3.07
3.04
3.01
2.99
2.75
2.64
2.57
2.31
2.30
2.29
1.40
0.94
0.92
0.85
0.83
0.81

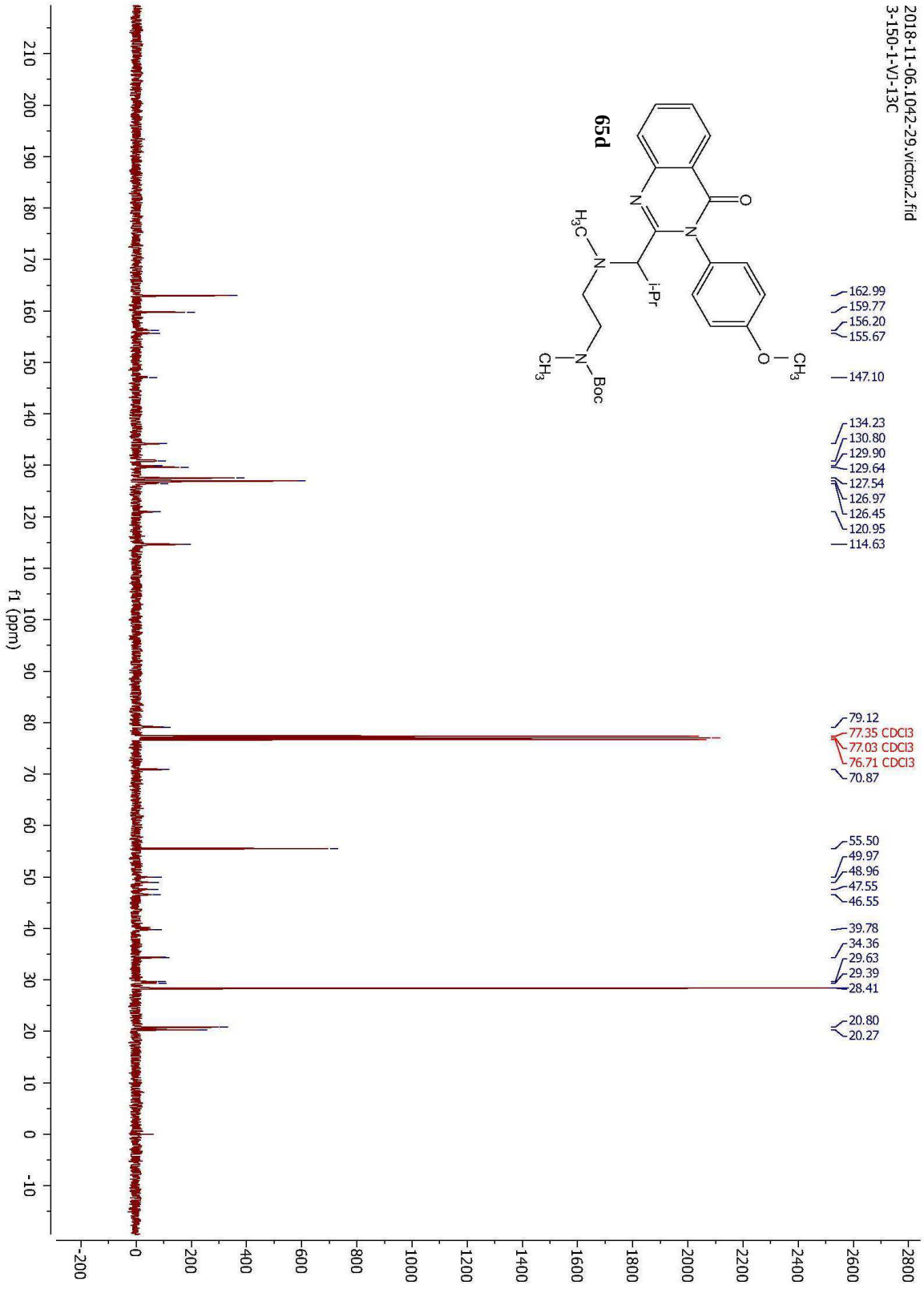
2018-11-06.1042-29.victor2.fid
3-150-1-VJ-13C
65d
i-Pr
Boc
162.99
159.77
156.20
155.67
147.10
134.23
130.80
129.90
129.64
127.54
126.97
126.45
120.95
114.63
79.12
77.35 CDCl3
77.03 CDCl3
76.71 CDCl3
70.87
55.50
49.97
48.96
47.55
46.55
39.78
34.36
29.63
29.39
28.41
20.80
20.27
f1 (ppm)

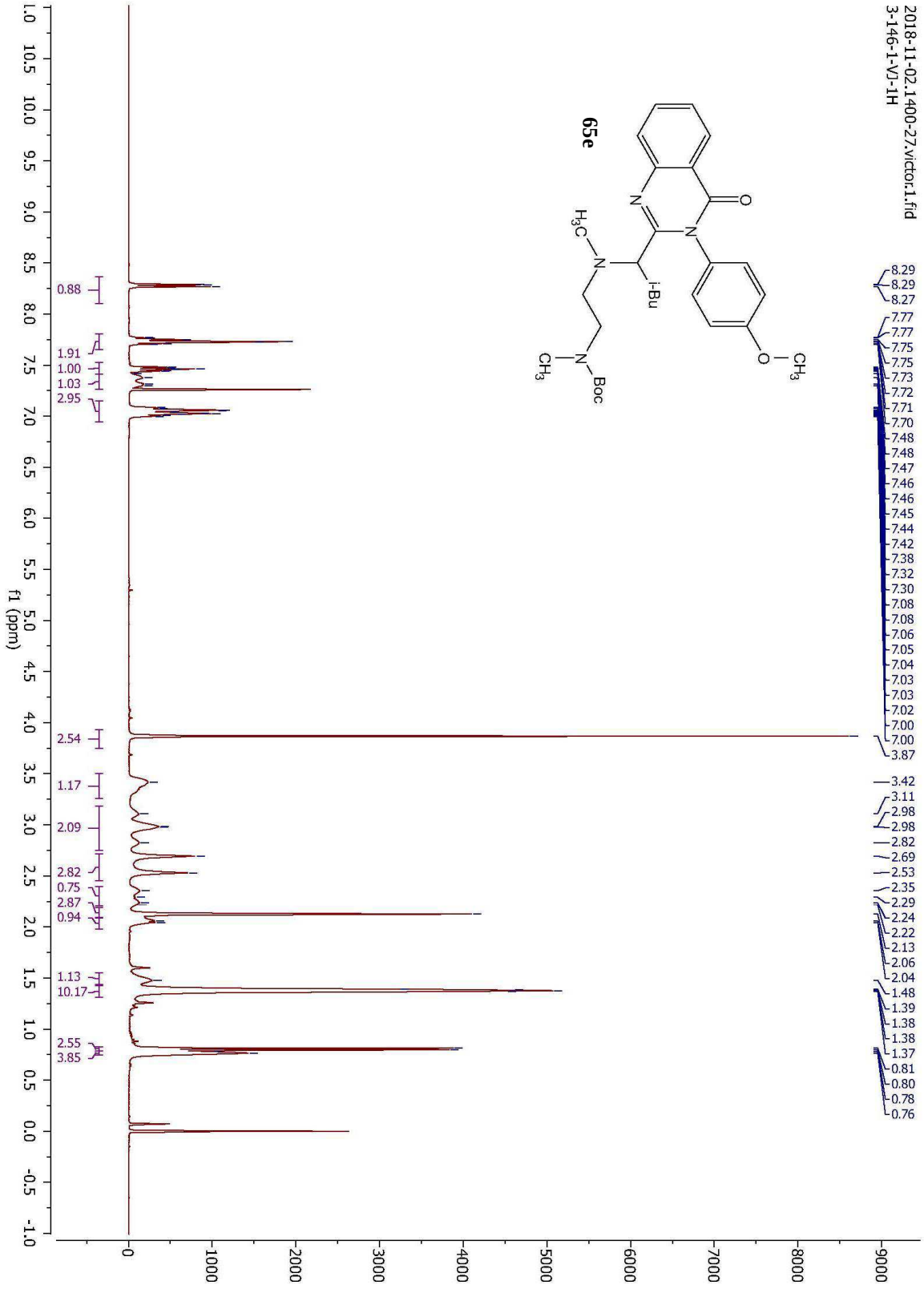
2018-11-02.1400-27.victor.1.fid
3-146-1-VJ-1H
65e
f1 (ppm)

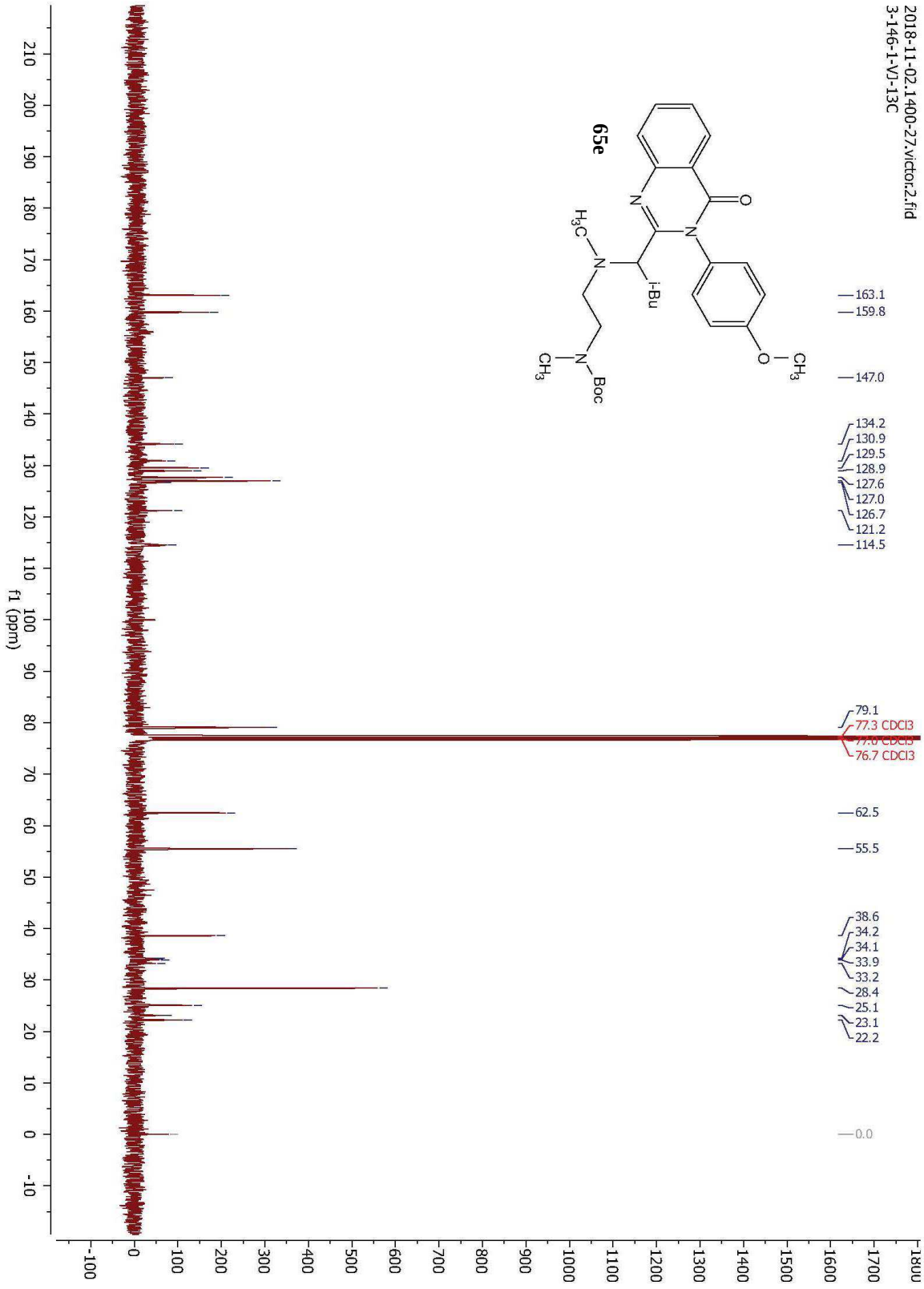
2018-11-02.1400-27.victor2.fid
3-146-1-VJ-13C
65e
i-Bu
Boc
163.1
159.8
147.0
134.2
130.9
129.5
128.9
127.6
127.0
126.7
121.2
114.5
79.1
77.3 CDCl3
76.7 CDCl3
62.5
55.5
38.6
34.2
34.1
33.9
33.2
28.4
25.1
23.1
22.2
0.0
f1 (ppm)

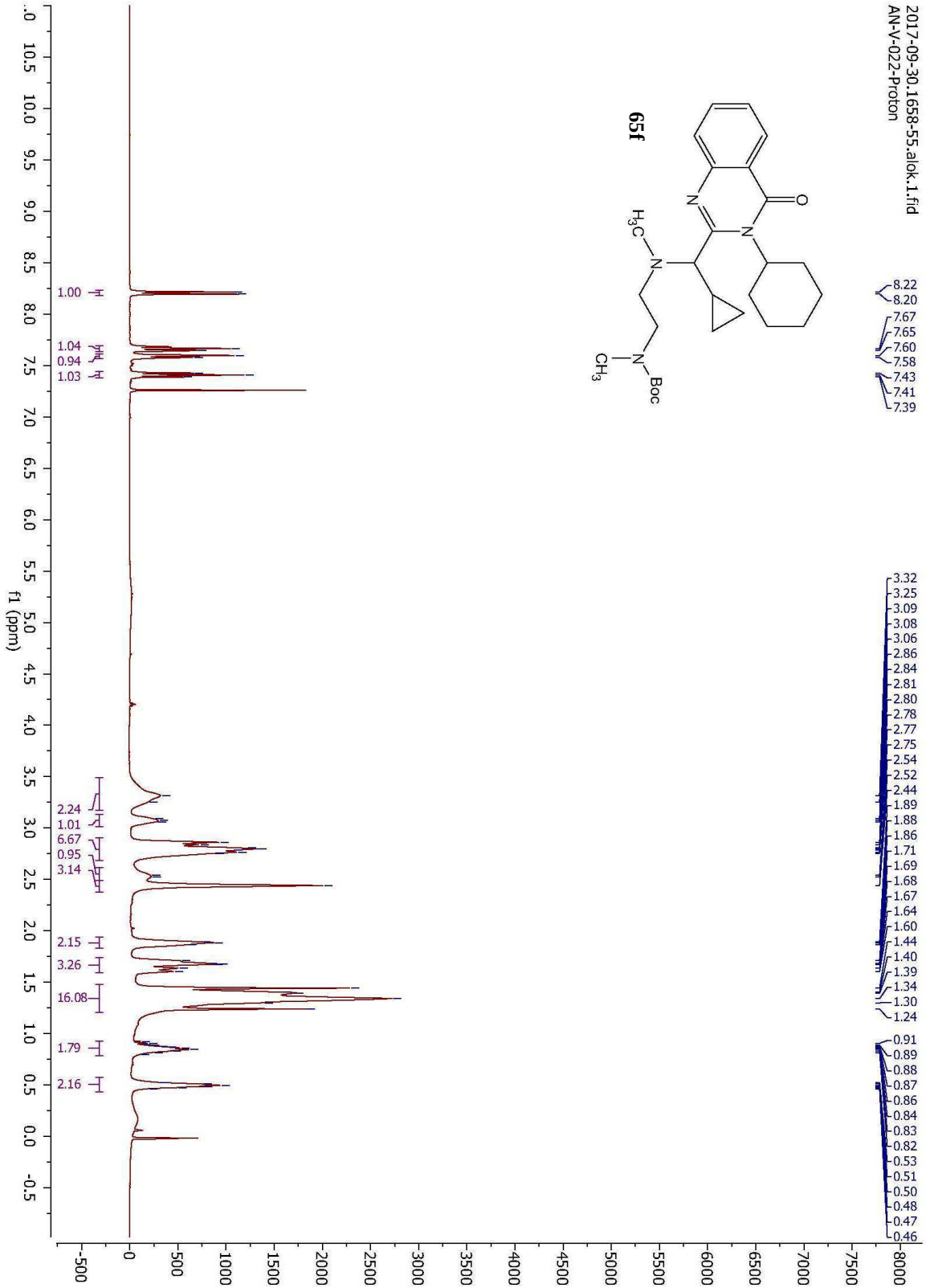
2017-09-30.1658-55.alok.1.fid
AN-V-022-Proton
65f
f1 (ppm)

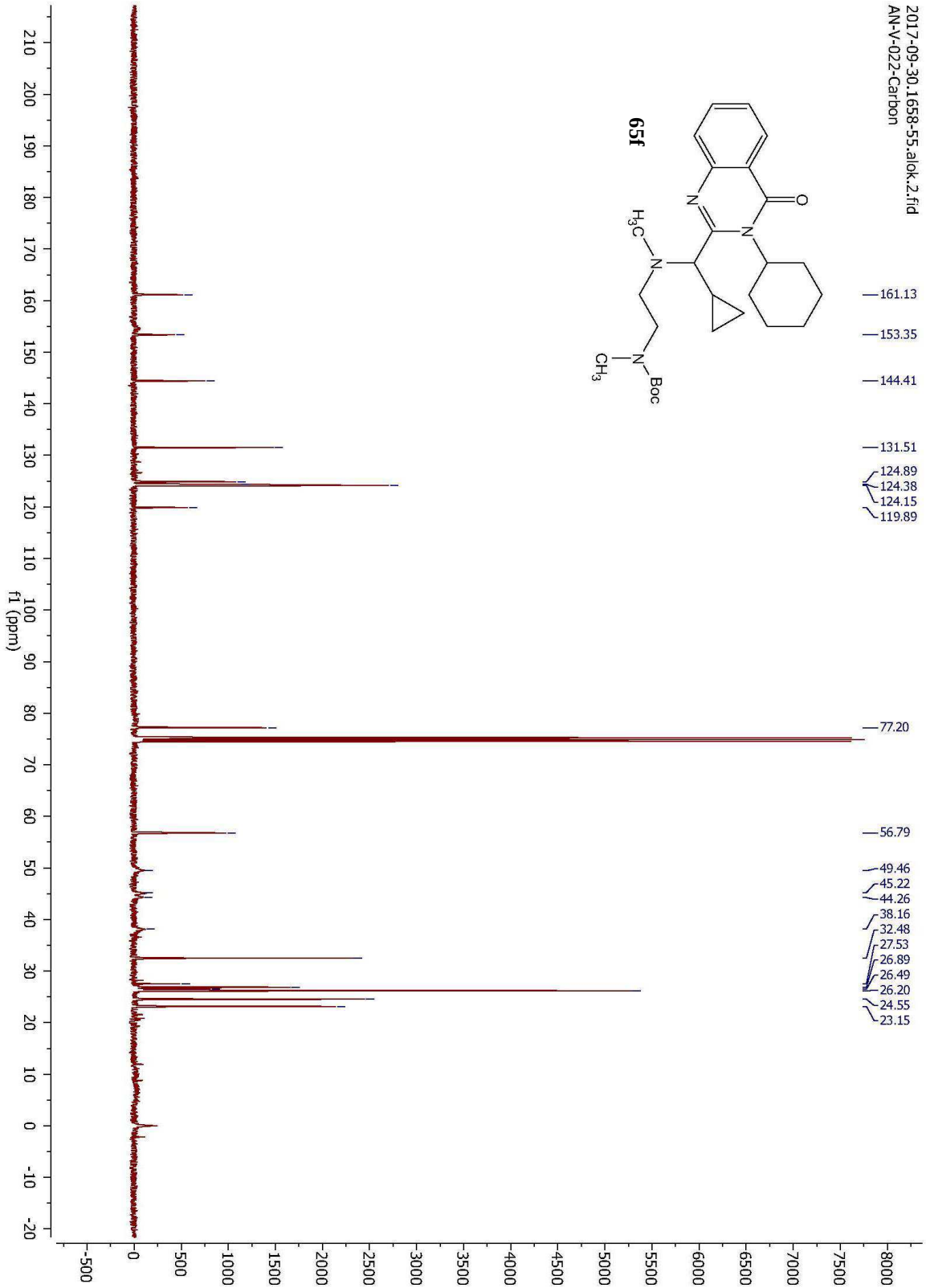
2017-09-30.1658-55.alok.2.fid
AN-V-022-Carbon
65f
161.13
153.35
144.41
131.51
124.89
124.38
124.15
119.89
77.20
56.79
49.46
45.22
44.26
38.16
32.48
27.53
26.89
26.49
26.20
24.55
23.15
f1 (ppm)

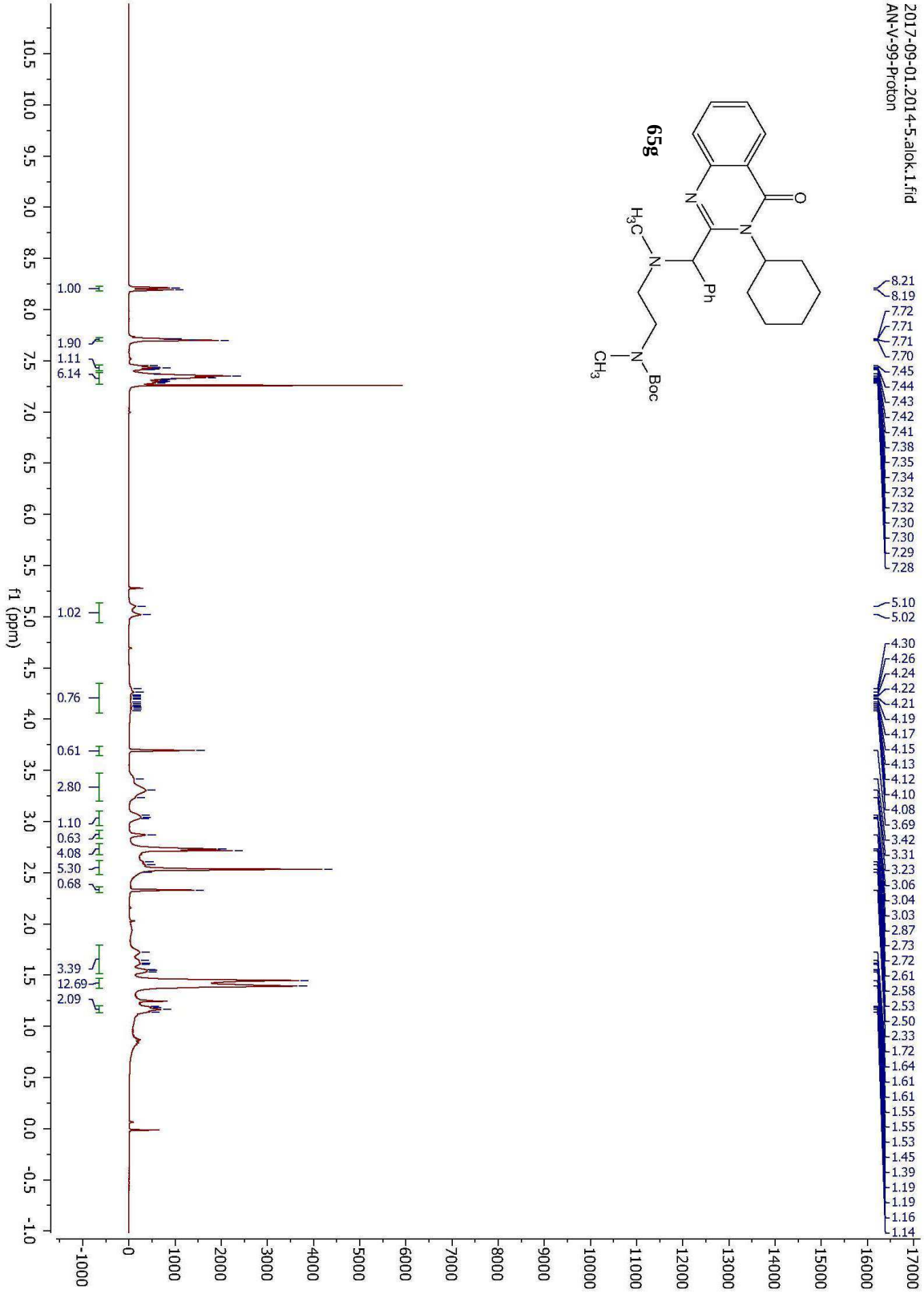
2017-09-01.2014-5.alok.1.fid
AN-V-99-Proton
65g
f1 (ppm)
1.00
1.90
1.11
6.14
1.02
0.76
0.61
2.80
1.10
0.63
4.08
5.30
0.68
3.39
12.69
2.09
8.21
8.19
7.72
7.71
7.71
7.70
7.45
7.44
7.43
7.42
7.41
7.38
7.35
7.34
7.32
7.32
7.30
7.30
7.29
7.28
5.10
5.02
4.30
4.26
4.24
4.22
4.21
4.19
4.17
4.15
4.13
4.12
4.10
4.08
3.69
3.42
3.31
3.23
3.06
3.04
3.03
2.87
2.73
2.72
2.61
2.58
2.53
2.50
2.33
1.72
1.64
1.61
1.61
1.55
1.55
1.53
1.45
1.39
1.19
1.19
1.16
1.14

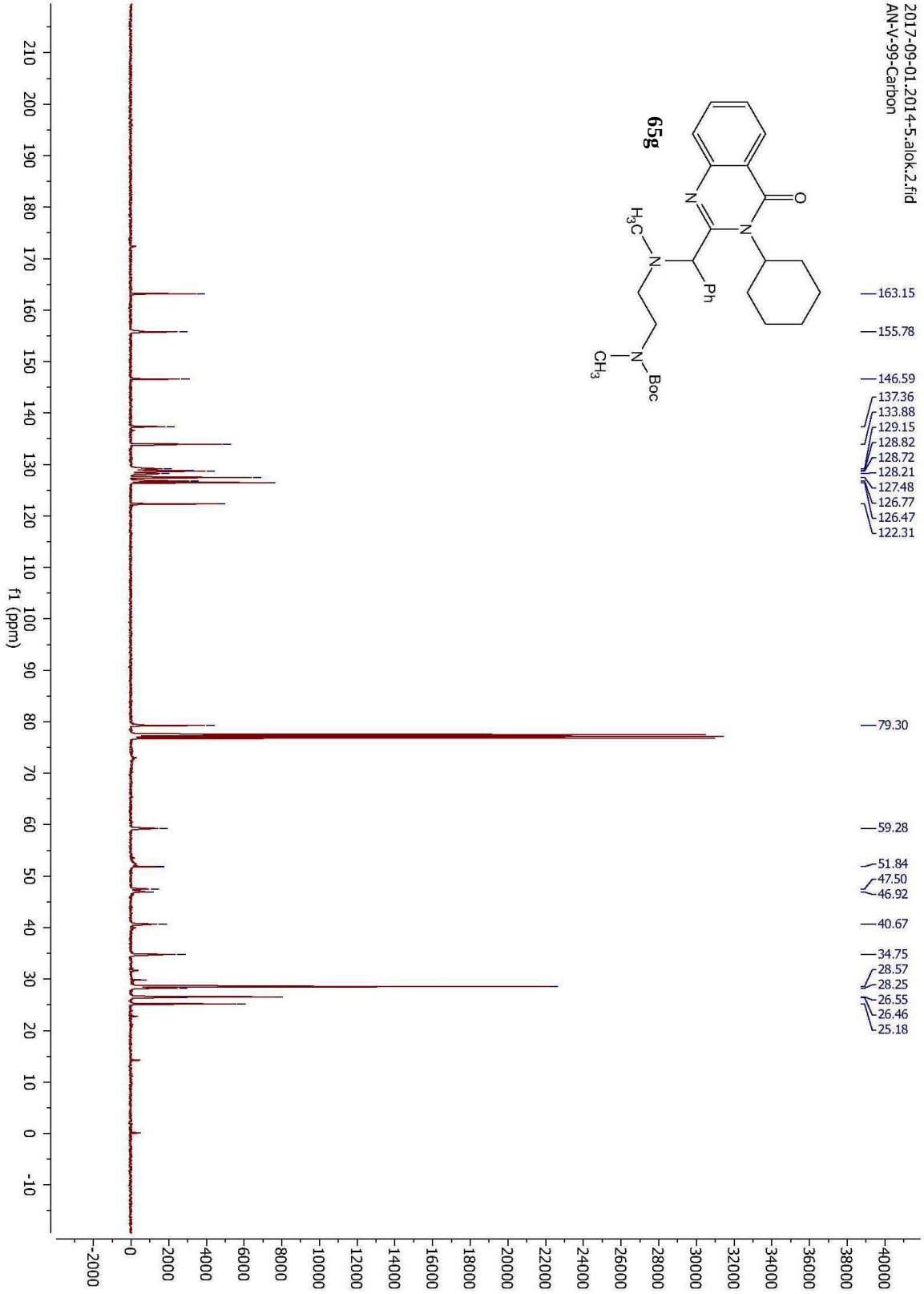
2017-09-01.2014-5.alok.2.fid
AN-V-99-Carbon
65g
f1 (ppm)
163.15
155.78
146.59
137.36
133.88
129.15
128.82
128.72
128.21
127.48
126.77
126.47
122.31
79.30
59.28
51.84
47.50
46.92
40.67
34.75
28.57
28.25
26.55
26.46
25.18

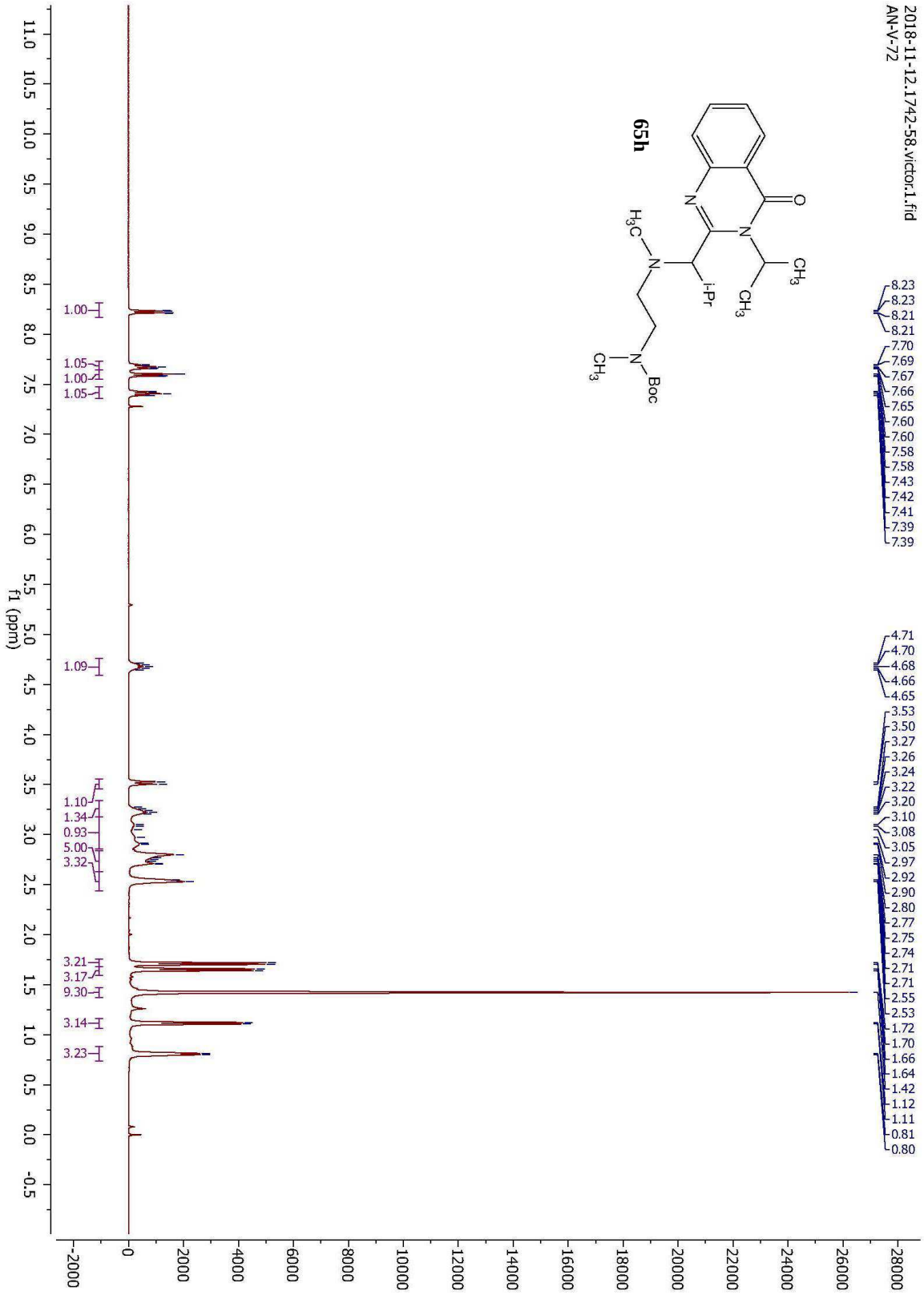
2018-11-12.1742-58.victor.1.fid
AN-V-72
65h
f1 (ppm)

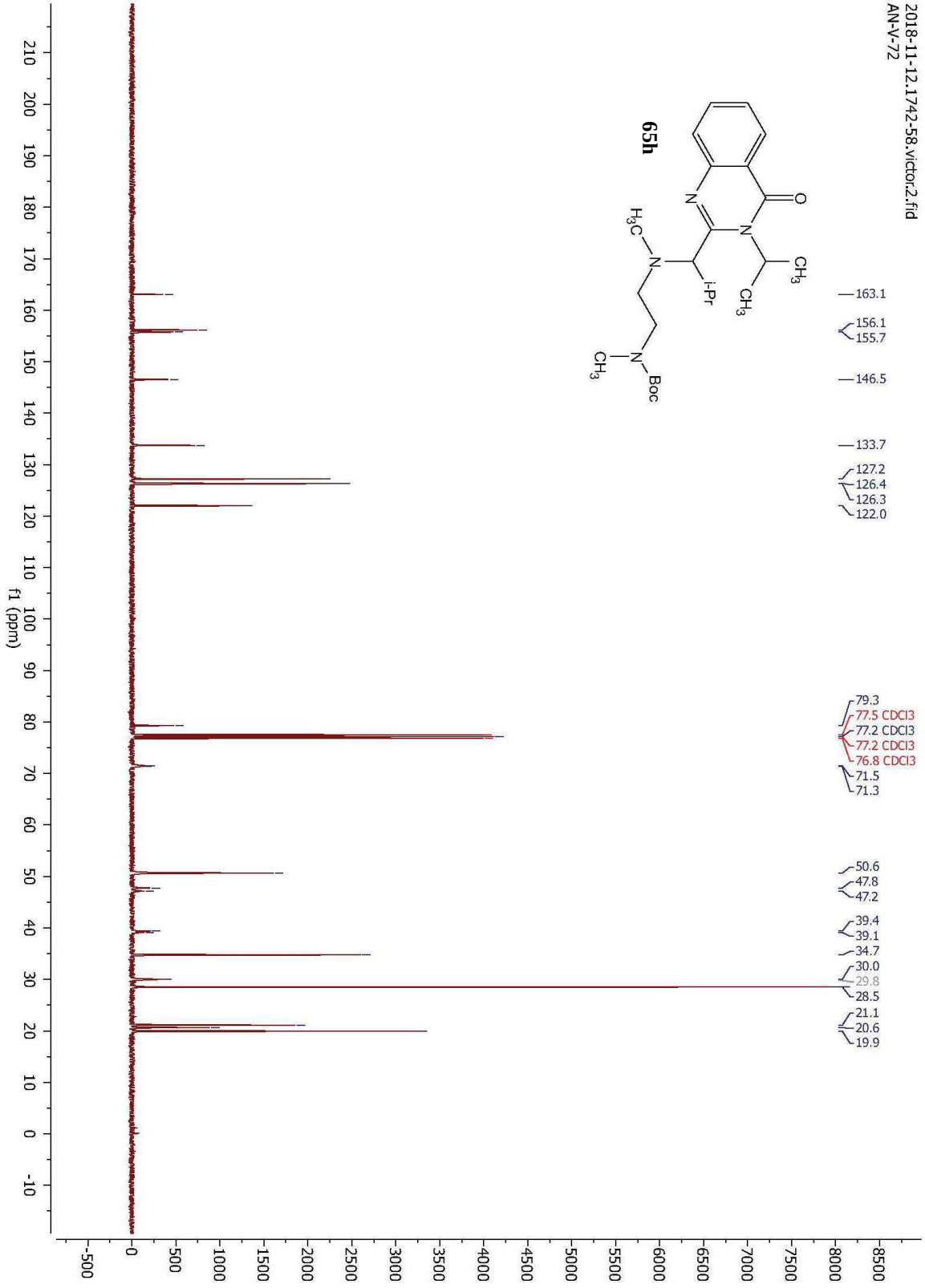
2018-11-12.1742-58.victor2.fid
AN-V-72
65h
f1 (ppm)
163.1
156.1
155.7
146.5
133.7
127.2
126.4
126.3
122.0
79.3
77.5 CDCl3
77.2 CDCl3
77.2 CDCl3
76.8 CDCl3
71.5
71.3
50.6
47.8
47.2
39.4
39.1
34.7
30.0
29.8
28.5
21.1
20.6
19.9

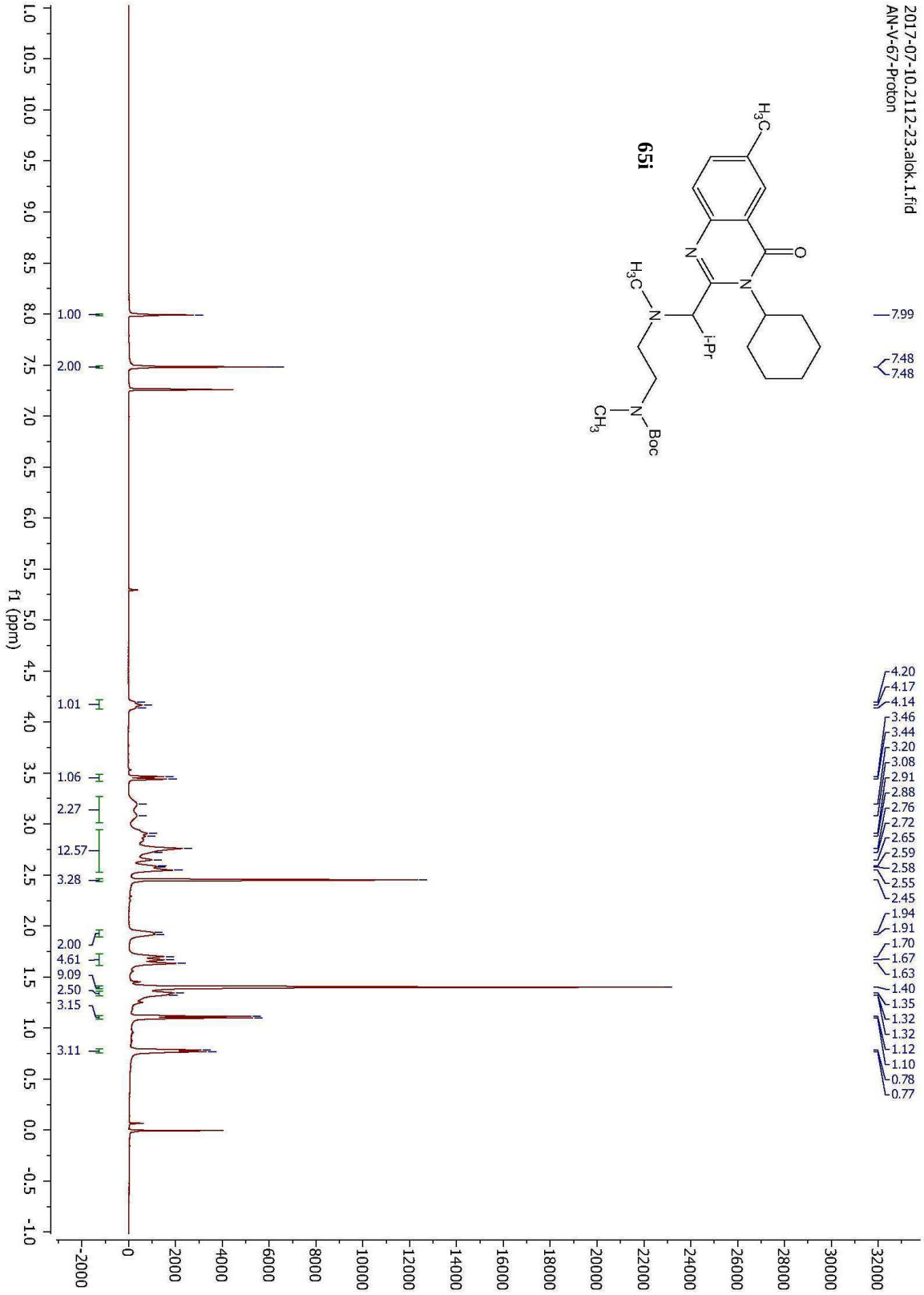
2017-07-10.2112-23.alok.1.fid
AN-V-67-Proton
65i
f1 (ppm)
1.00
2.00
1.01
1.06
2.27
12.57
3.28
2.00
4.61
9.09
2.50
3.15
3.11
7.99
7.48
7.48
4.20
4.17
4.14
3.46
3.44
3.20
3.08
2.91
2.88
2.76
2.72
2.65
2.59
2.58
2.55
2.45
1.94
1.91
1.70
1.67
1.63
1.40
1.35
1.32
1.32
1.12
1.10
0.78
0.77

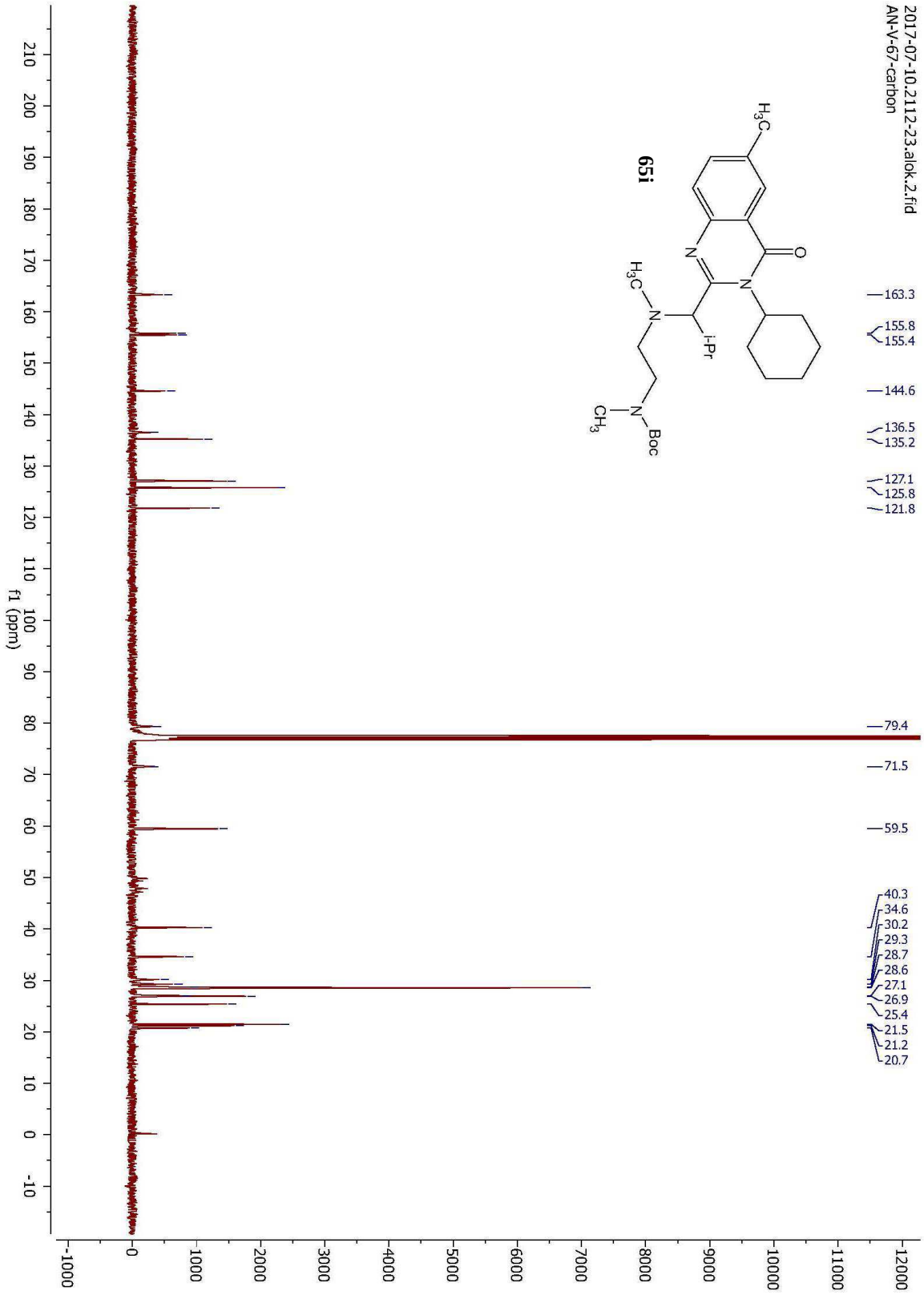
2017-07-10.2112-23.alok.2.fid
AN-V-67-carbon
65i
163.3
155.8
155.4
144.6
136.5
135.2
127.1
125.8
121.8
79.4
71.5
59.5
40.3
34.6
30.2
29.3
28.7
28.6
27.1
26.9
25.4
21.5
21.2
20.7
f1 (ppm)

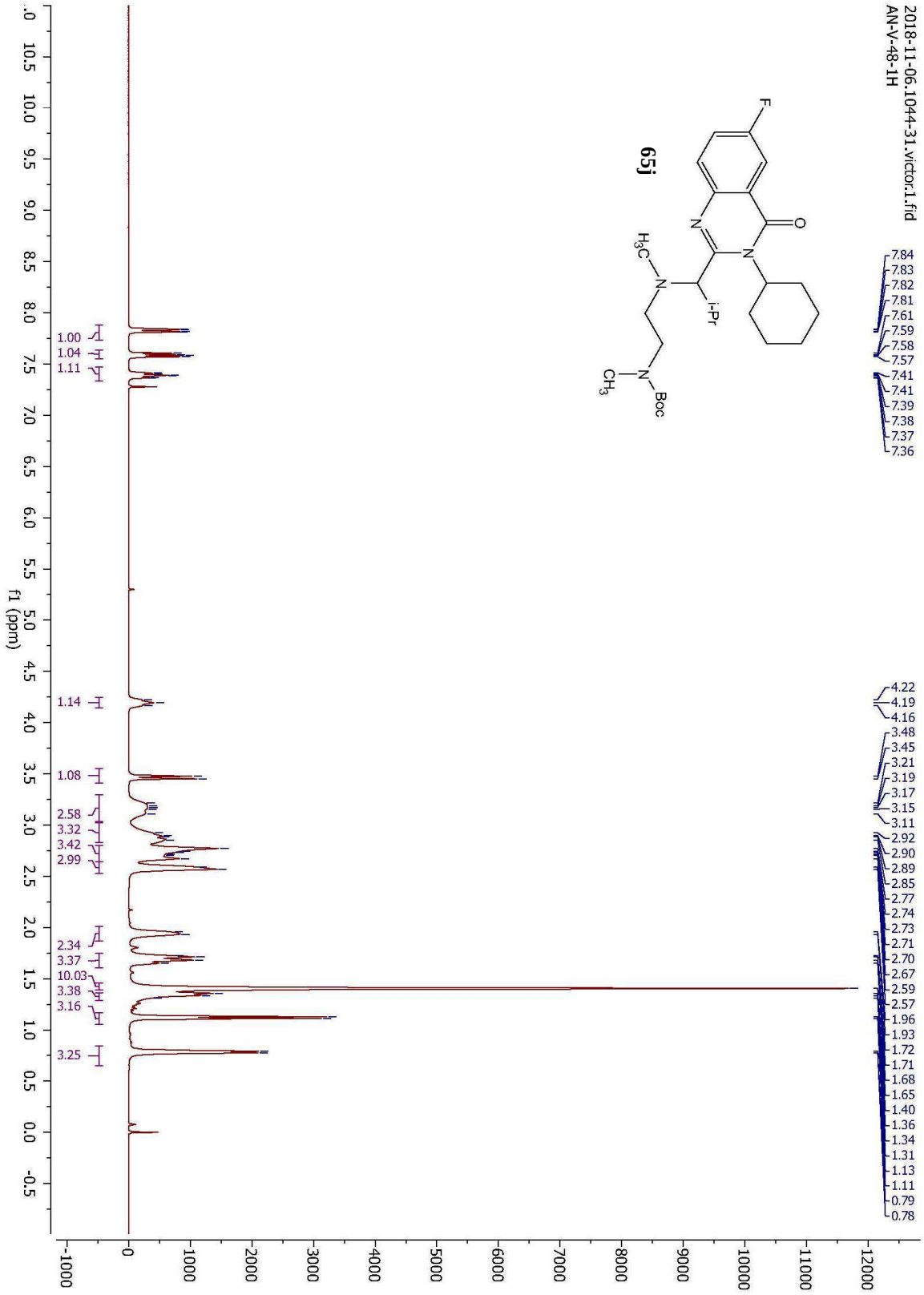
2018-11-06.1044-31.victor.1.fid
AN-V-48-1H
65j
F
O
N
N
N
H3C
i-Pr
CH3
Boc
f1 (ppm)
1.00
1.04
1.11
1.14
1.08
2.58
3.32
3.42
2.99
2.34
3.37
10.03
3.38
3.16
3.25
7.84
7.83
7.82
7.81
7.61
7.59
7.58
7.57
7.41
7.41
7.39
7.38
7.37
7.36
4.22
4.19
4.16
3.48
3.45
3.21
3.19
3.17
3.15
3.11
2.92
2.90
2.89
2.85
2.77
2.74
2.73
2.71
2.70
2.67
2.59
2.57
1.96
1.93
1.72
1.71
1.68
1.65
1.40
1.36
1.34
1.31
1.13
1.11
0.79
0.78

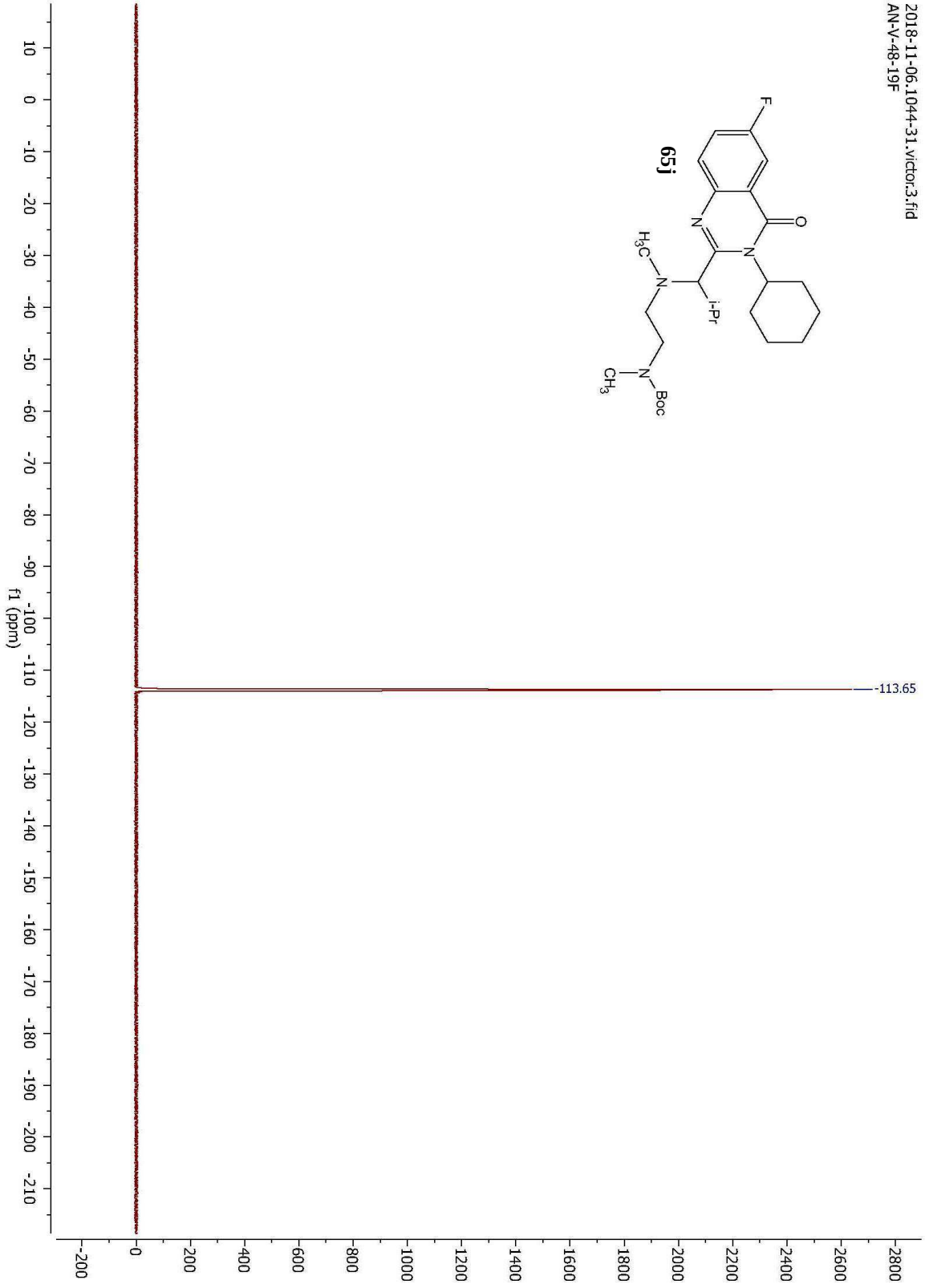
2018-11-06.1044-31.victor3.fid
AN-V-48-19F
65j
F
O
N
N
H3C
N
i-Pr
N
CH3
Boc
-113.65
f1 (ppm)
10
0
-10
-20
-30
-40
-50
-60
-70
-80
-90
-100
-110
-120
-130
-140
-150
-160
-170
-180
-190
-200
-210
-200
0
200
400
600
800
1000
1200
1400
1600
1800
2000
2200
2400
2600
2800

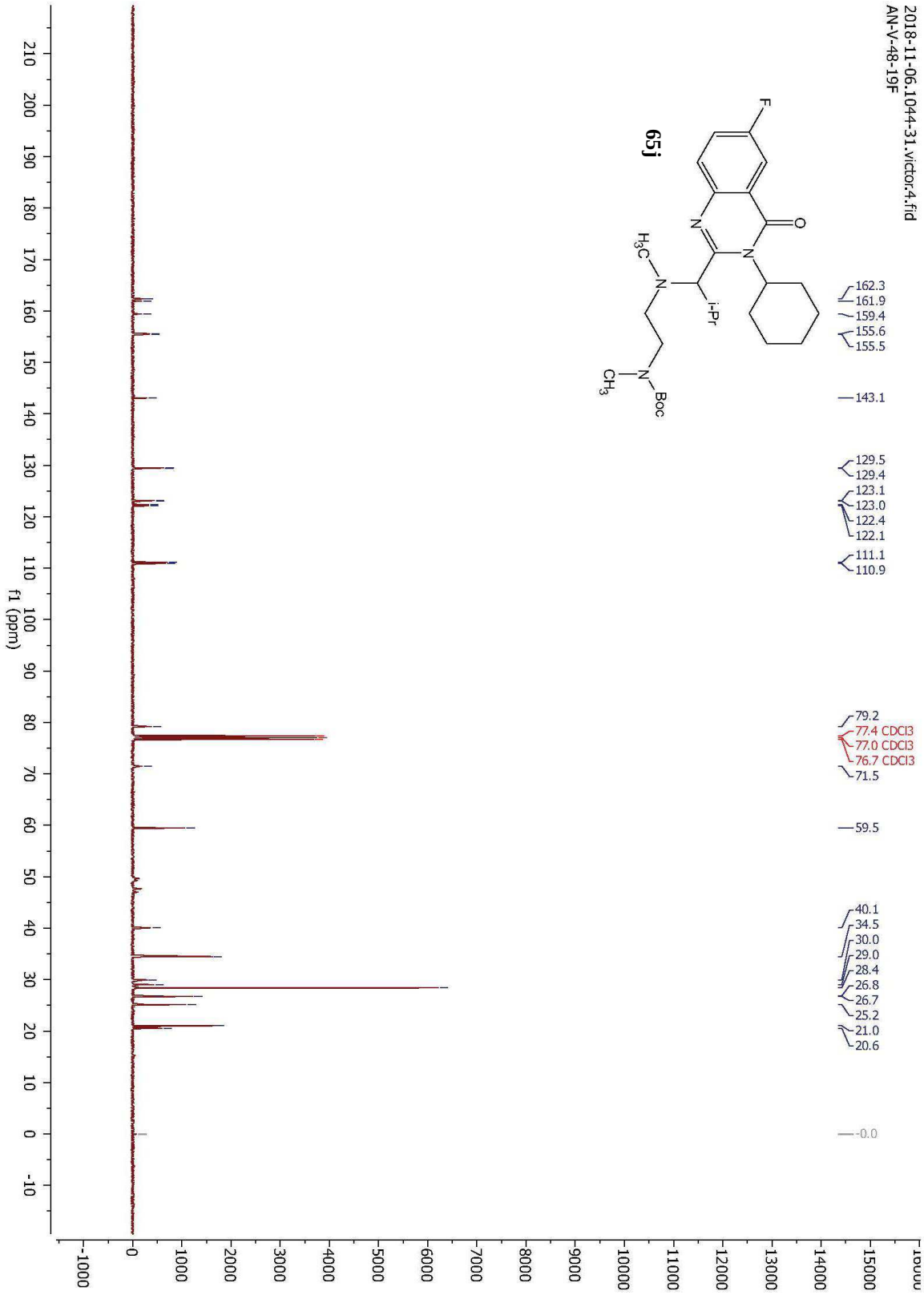
2018-11-06.1044-31.victor.4.fid
AN-V-48-19F
65j
F
O
N
N
N
H3C
i-Pr
CH3
Boc
162.3
161.9
159.4
155.6
155.5
143.1
129.5
129.4
123.1
123.0
122.4
122.1
111.1
110.9
79.2
77.4 CDCl3
77.0 CDCl3
76.7 CDCl3
71.5
59.5
40.1
34.5
30.0
29.0
28.4
26.8
26.7
25.2
21.0
20.6
-0.0
f1 (ppm)

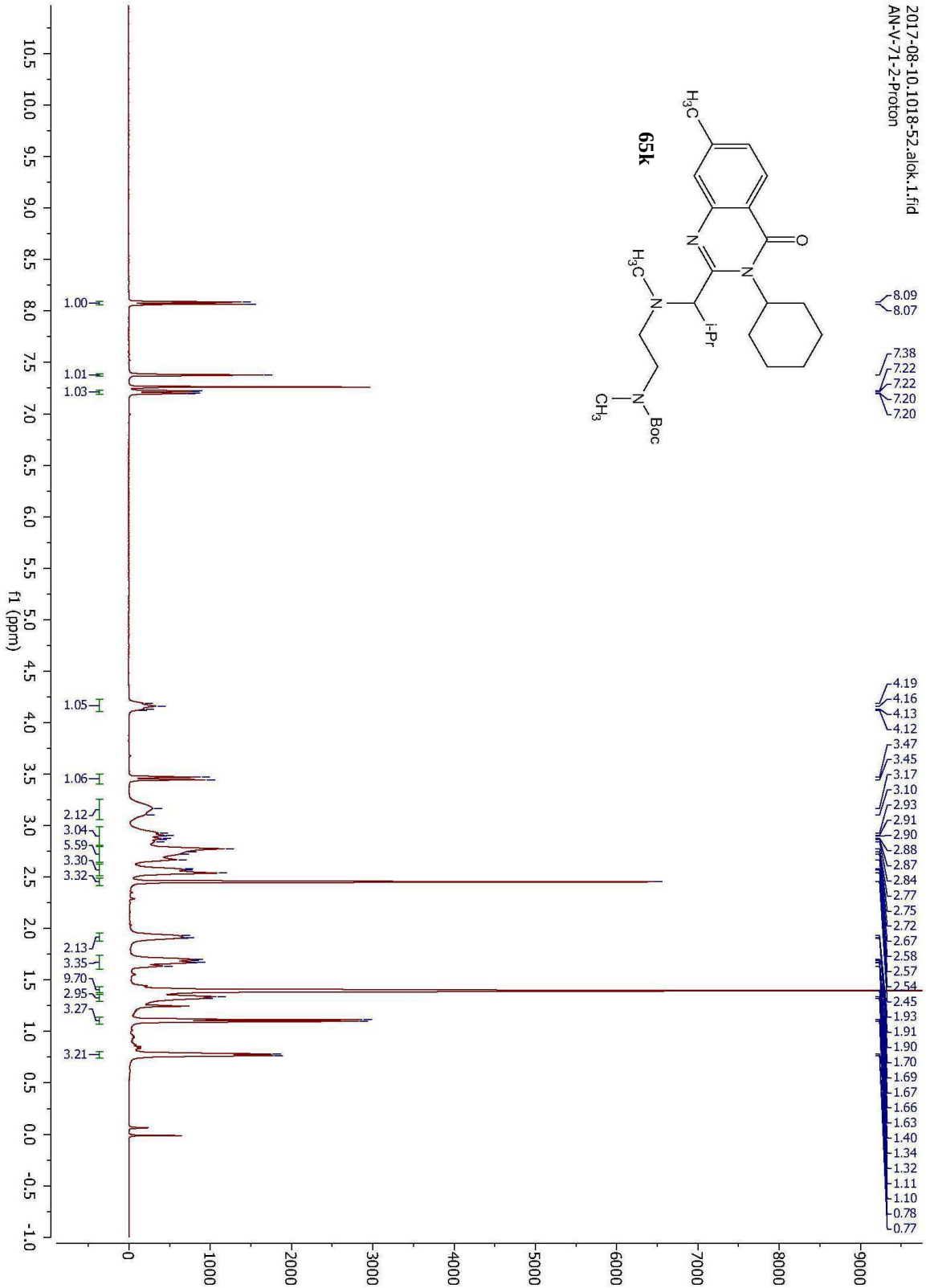
2017-08-10.1018-52.alok.1.fid
AN-V-71-2-Proton
65k
f1 (ppm)

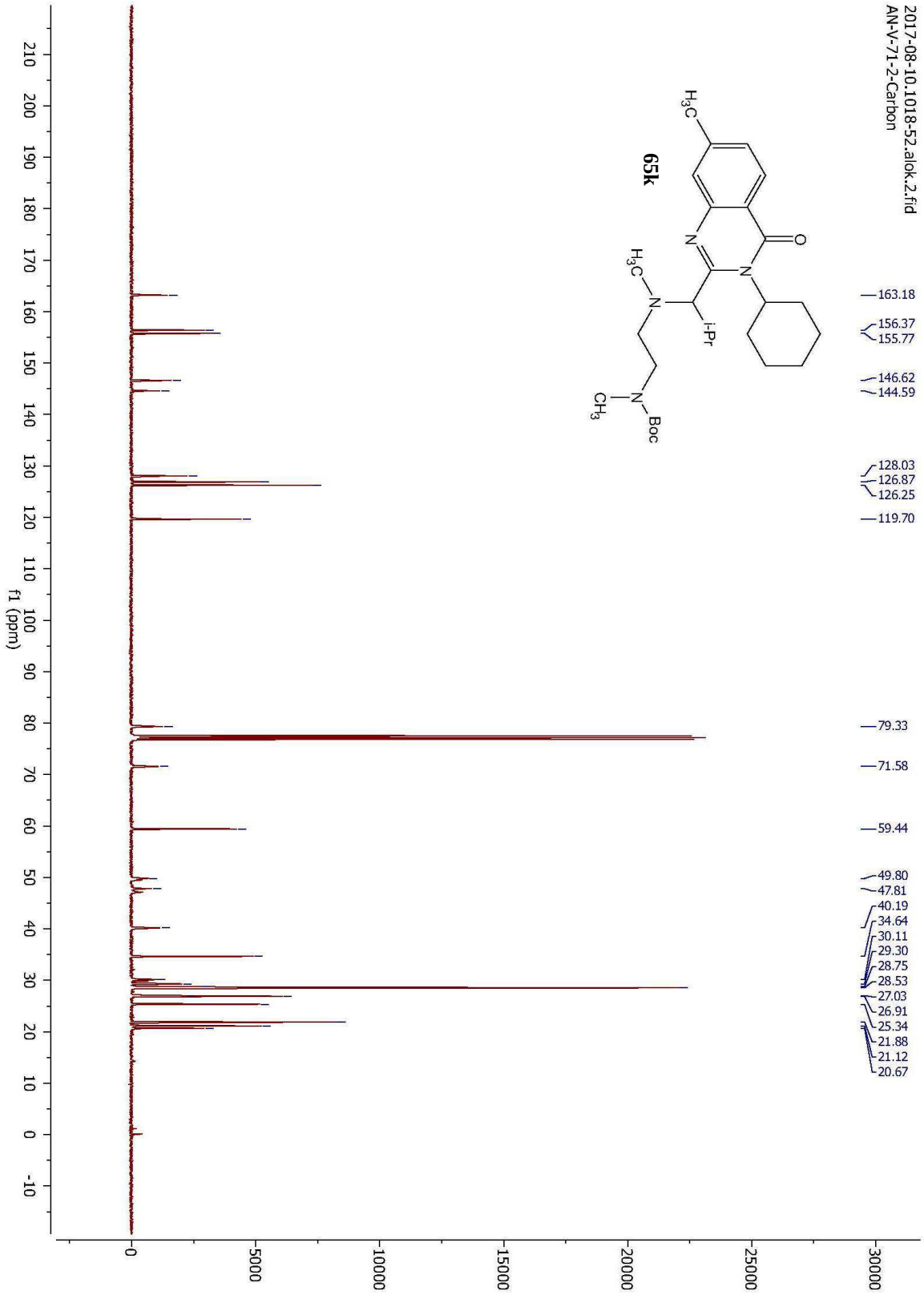
2017-08-10.1018-52.alok.2.fid
AN-V-71-2-Carbon
65k
f1 (ppm)
163.18
156.37
155.77
146.62
144.59
128.03
126.87
126.25
119.70
79.33
71.58
59.44
49.80
47.81
40.19
34.64
30.11
29.30
28.75
28.53
27.03
26.91
25.34
21.88
21.12
20.67

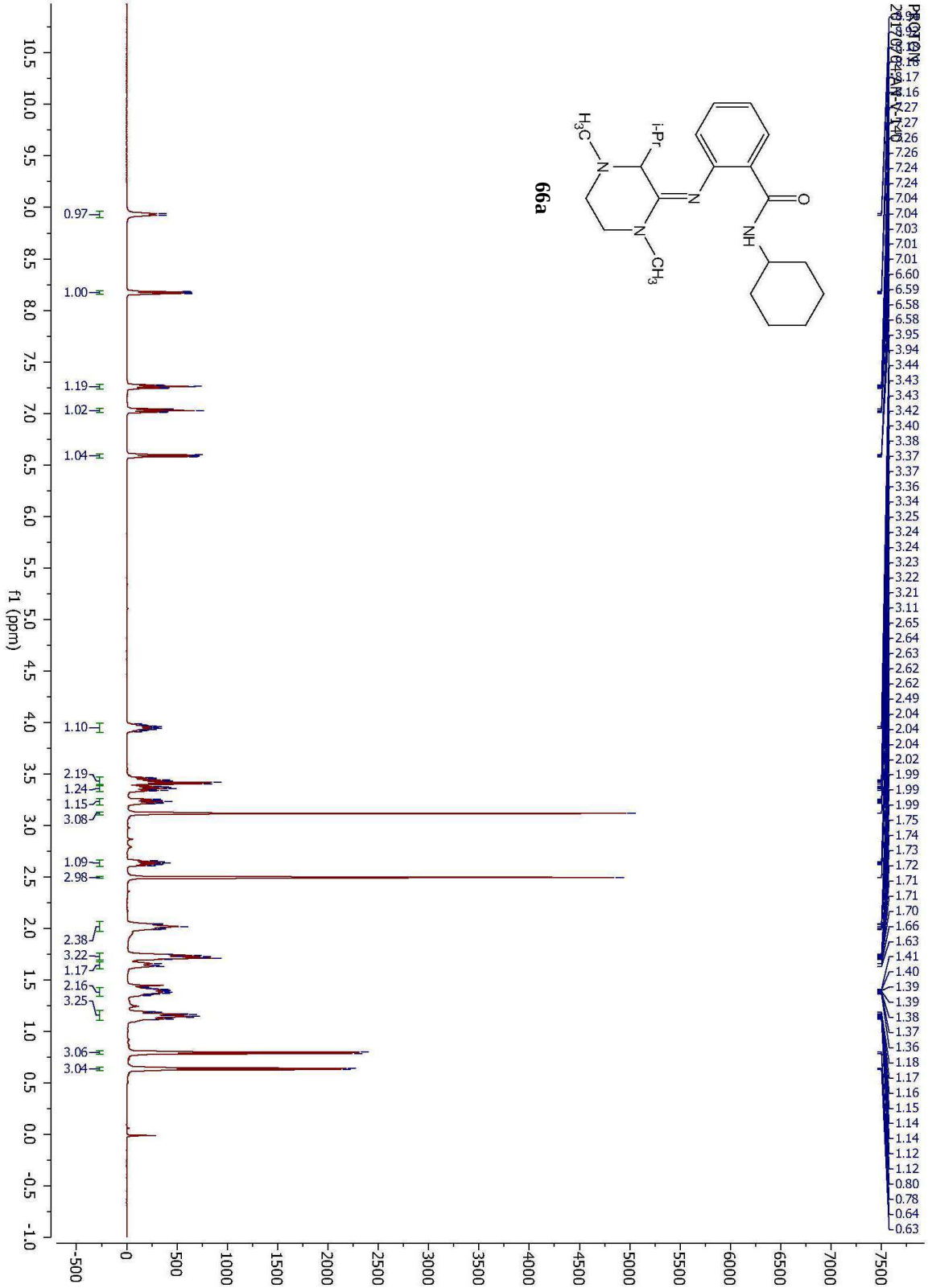
66a
i-Pr
H3C
CH3
NH
O
f1 (ppm)

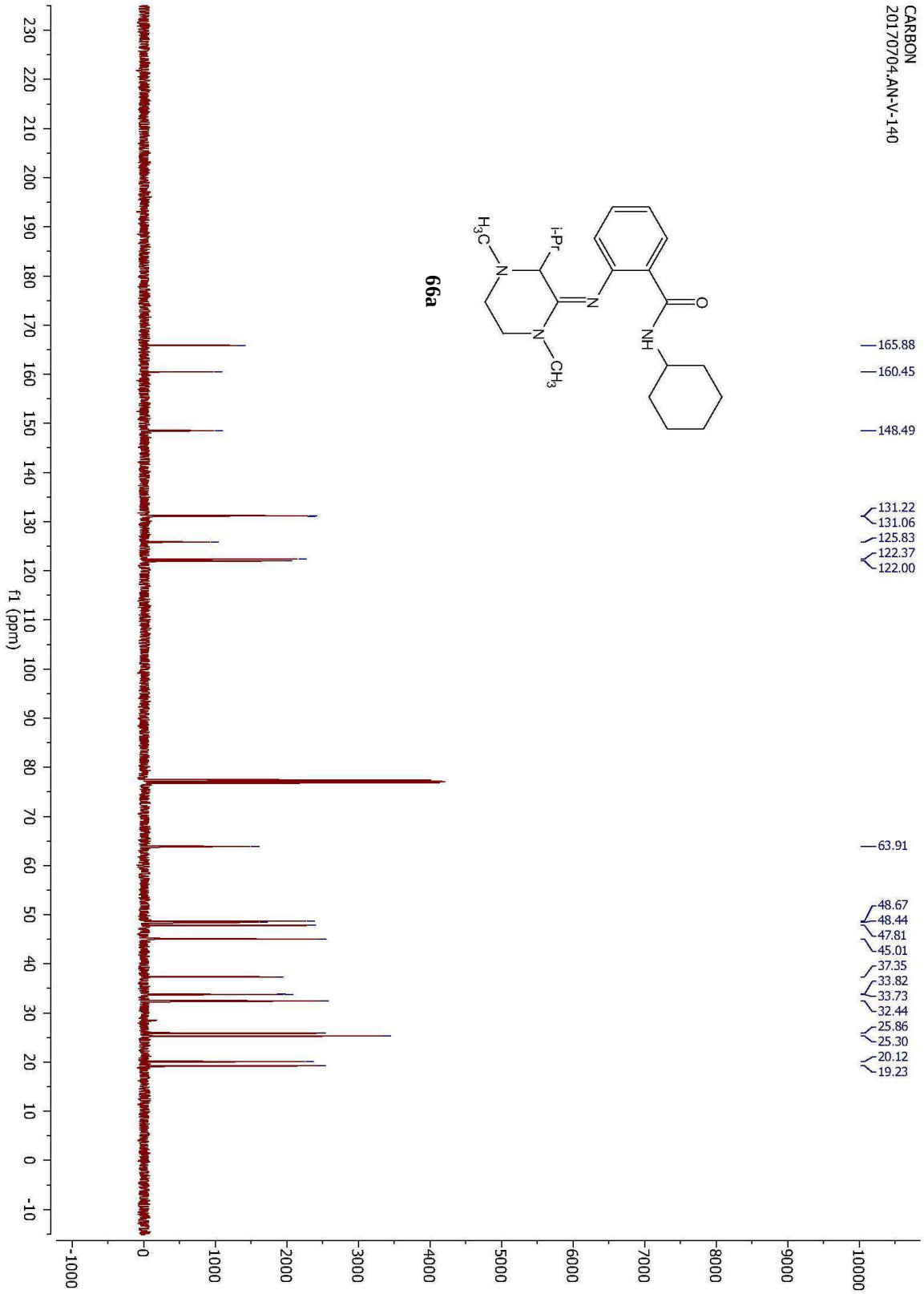
CARBON
20170704.AN-V-140
66a
i-Pr
H3C
N
N
CH3
N
O
NH
165.88
160.45
148.49
131.22
131.06
125.83
122.37
122.00
63.91
48.67
48.44
47.81
45.01
37.35
33.82
33.73
32.44
25.86
25.30
20.12
19.23
f1 (ppm)

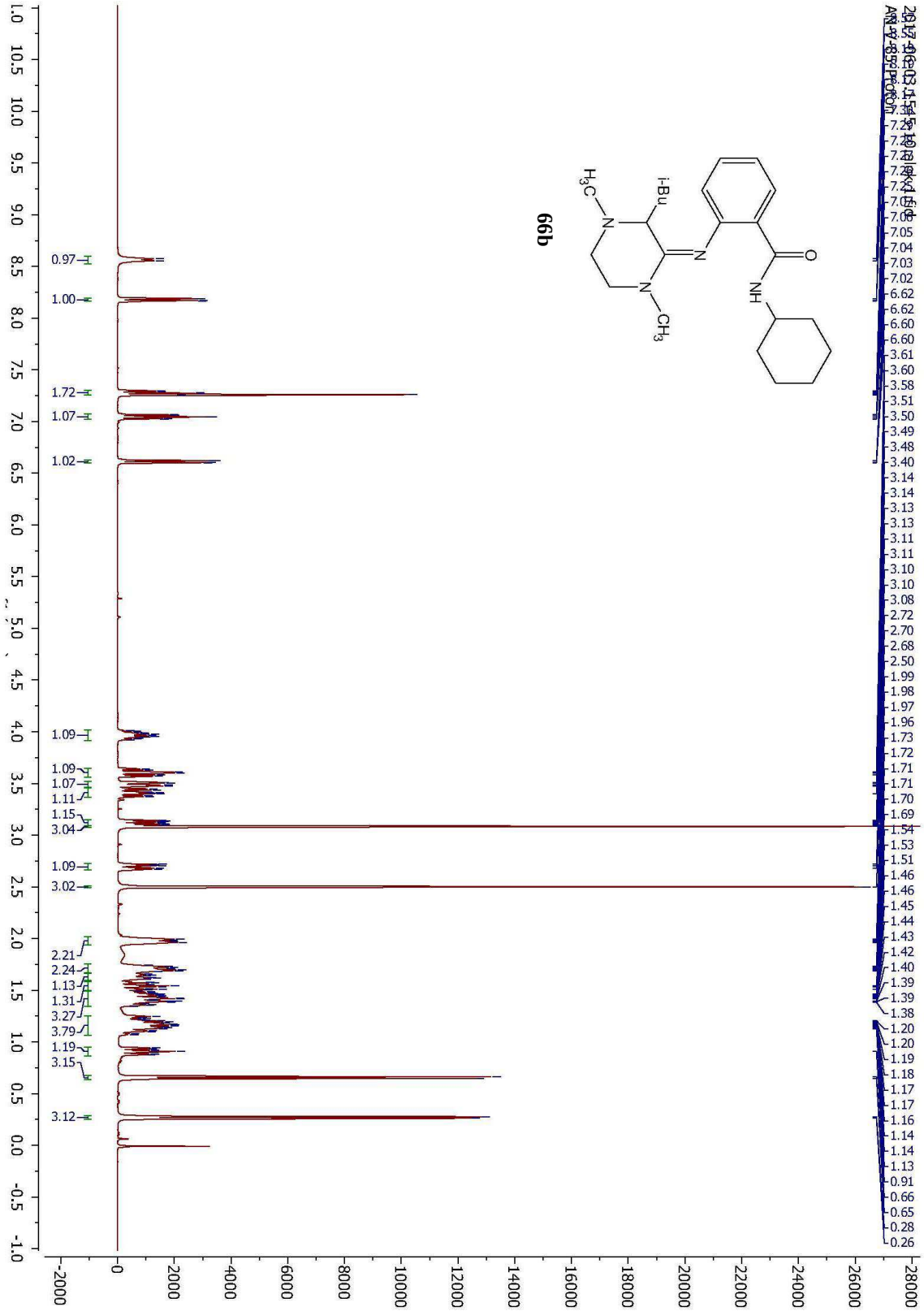
66b
i-Bu
H3C
N
N
CH3
N
O
NH

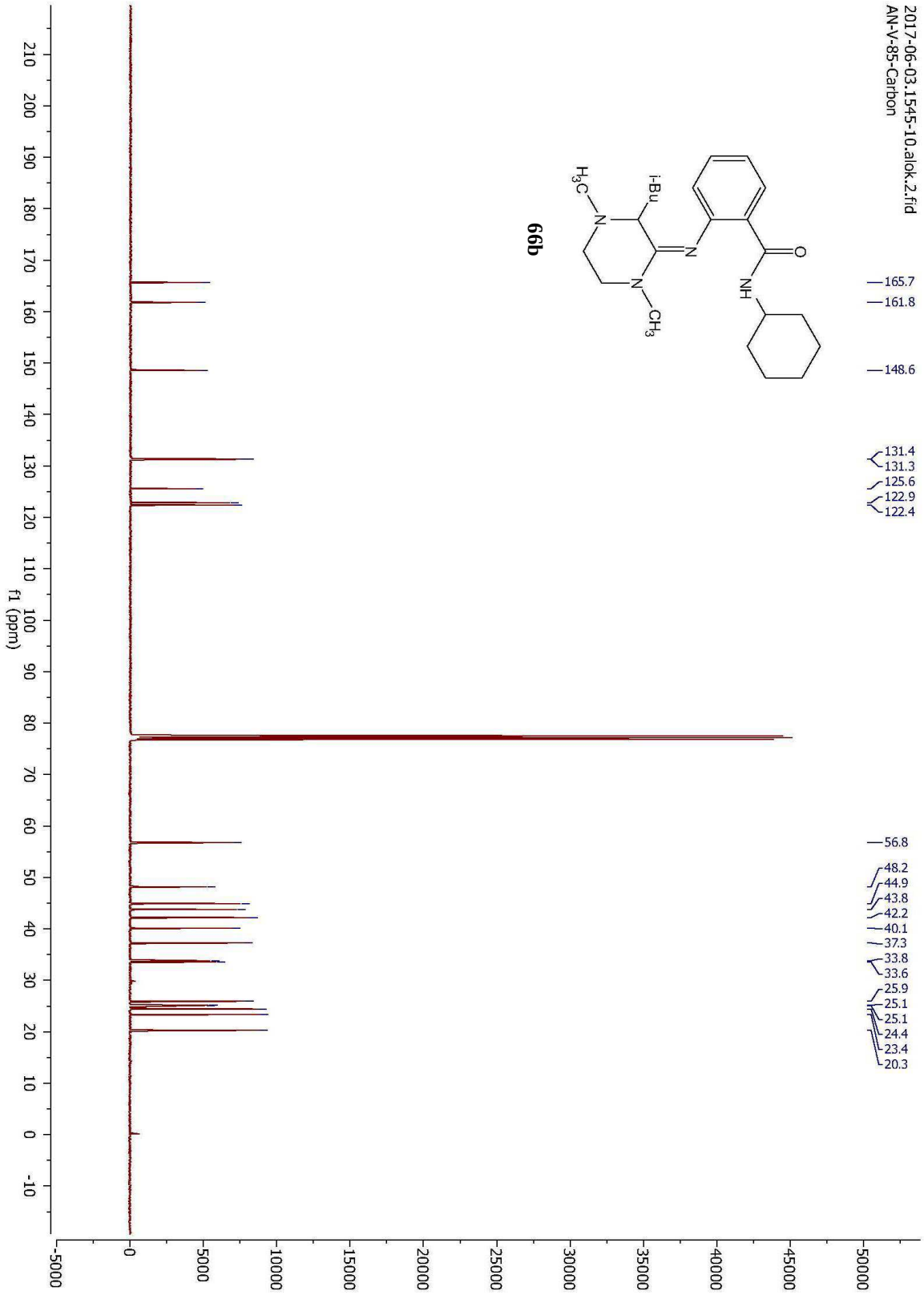
2017-06-03.1545-10.alok.2.fid
AN-V-85-Carbon
66b
i-Bu
H3C
N
N
CH3
N
O
NH
165.7
161.8
148.6
131.4
131.3
125.6
122.9
122.4
56.8
48.2
44.9
43.8
42.2
40.1
37.3
33.8
33.6
25.9
25.1
25.1
24.4
23.4
20.3
f1 (ppm)

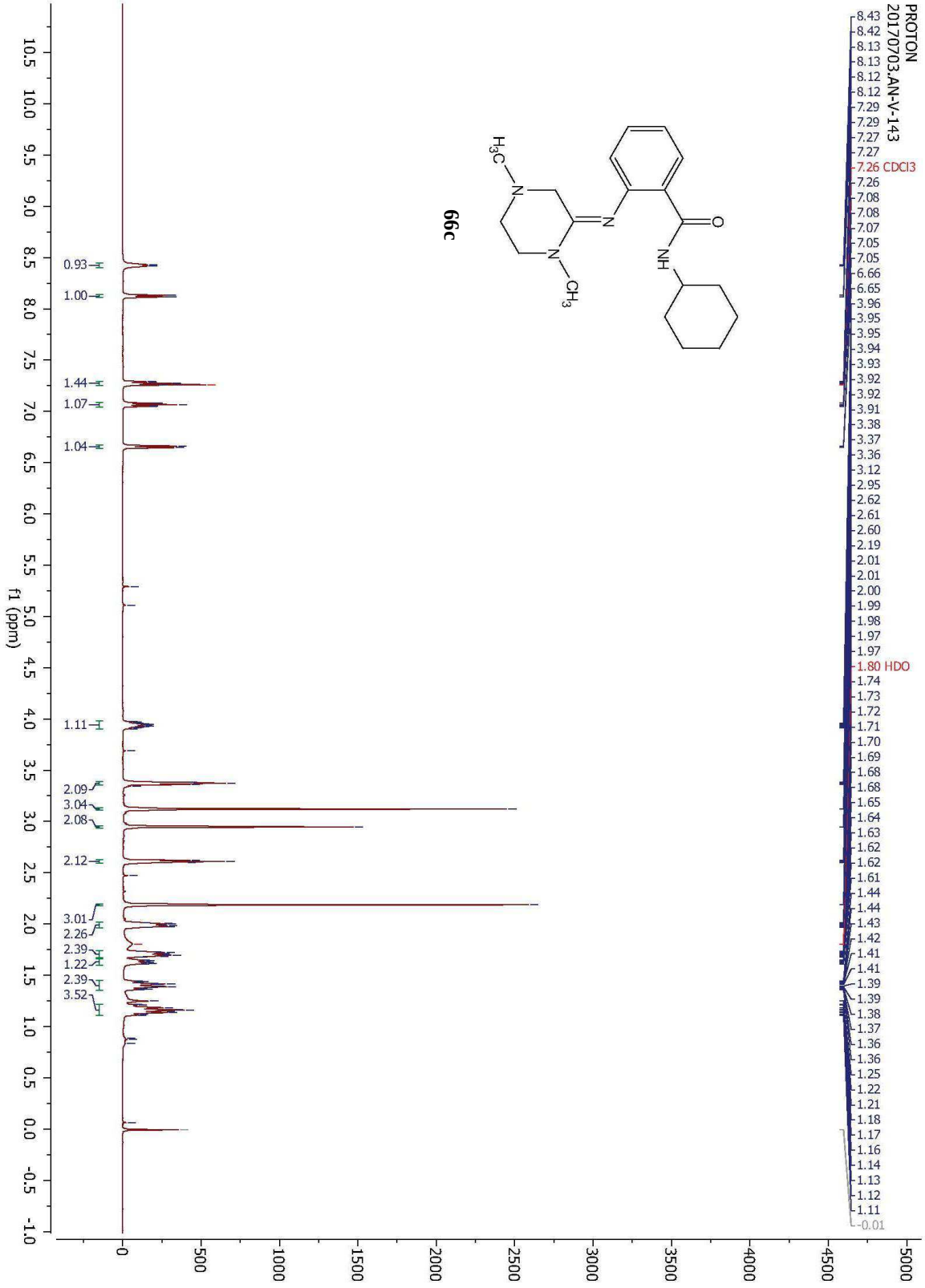
PROTON
20170703.AN-V-143
7.26 CDCl3
1.80 HDO
f1 (ppm)
0.93
1.00
1.44
1.07
1.04
1.11
2.09
3.04
2.08
2.12
3.01
2.26
2.39
1.22
2.39
3.52
99c
H3C
N
N
CH3
O
NH

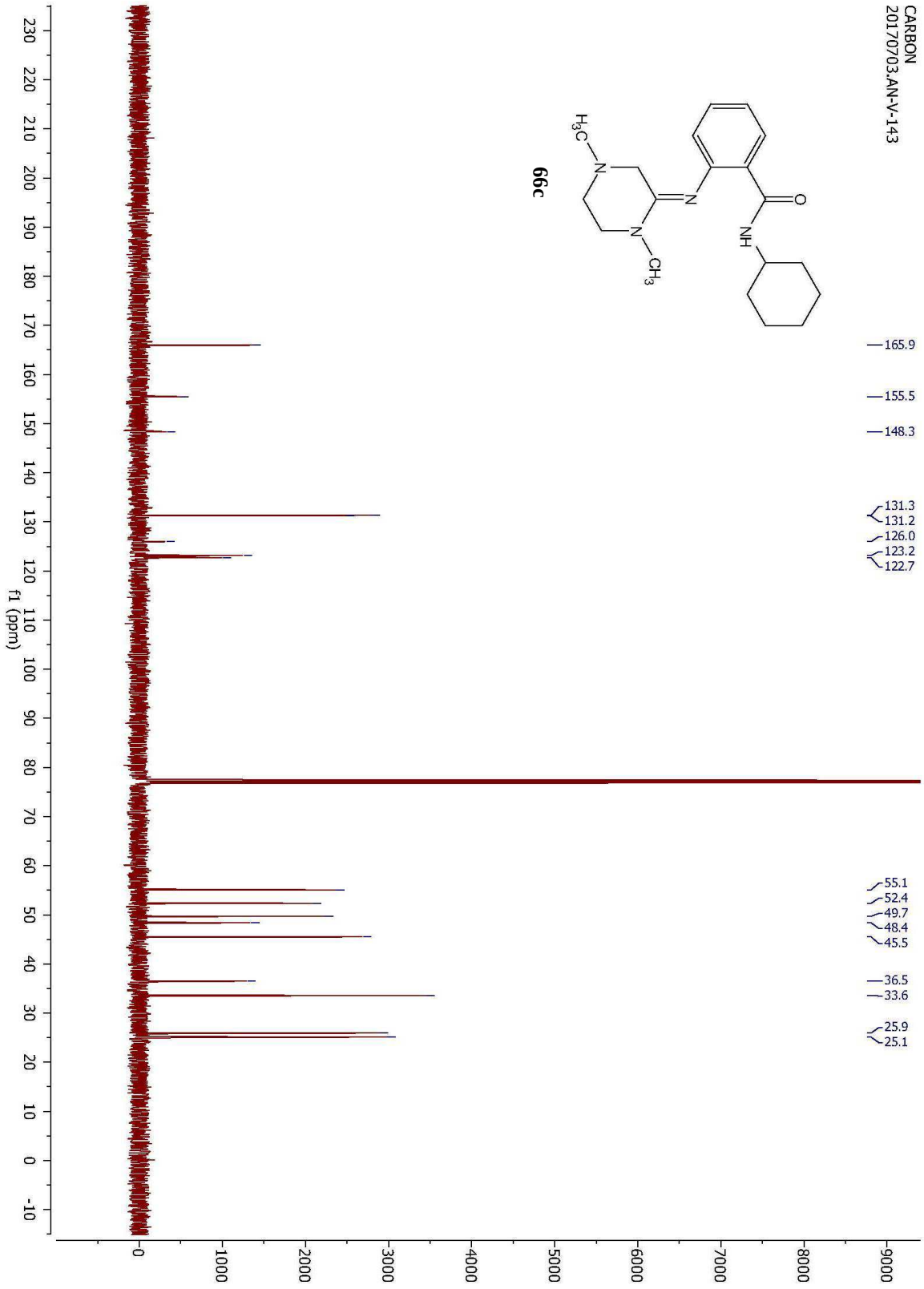
CARBON
20170703.AN-V-143
99c
165.9
155.5
148.3
131.3
131.2
126.0
123.2
122.7
55.1
52.4
49.7
48.4
45.5
36.5
33.6
25.9
25.1
f1 (ppm)

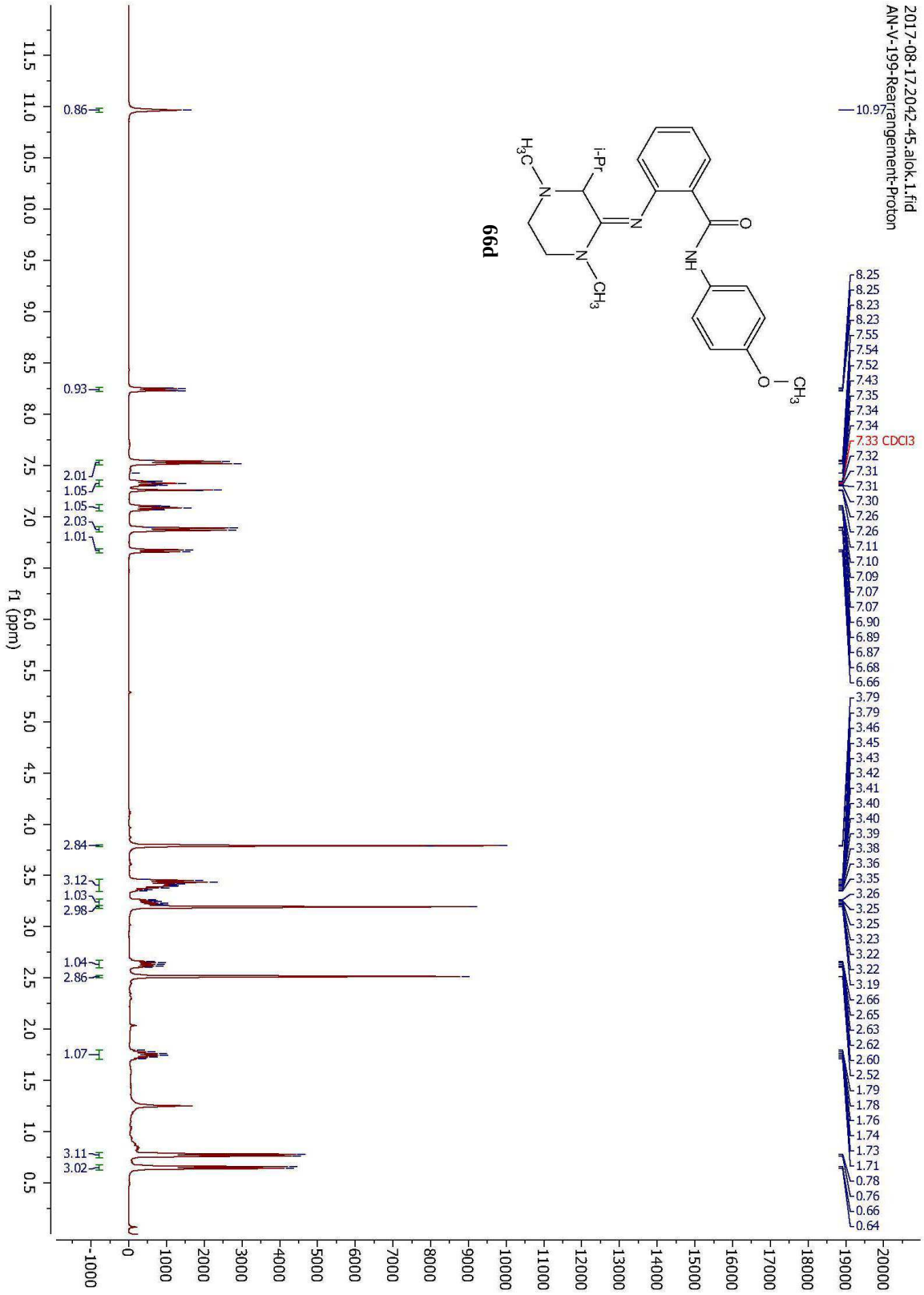
2017-08-17,2042-45.alok.1.fid
AN-V-199-Rearrangement-Proton
P99
f1 (ppm)
0.86
0.93
2.01
1.05
1.05
2.03
1.01
2.84
3.12
1.03
2.98
1.04
2.86
1.07
3.11
3.02
10.97
7.33 CDCl3

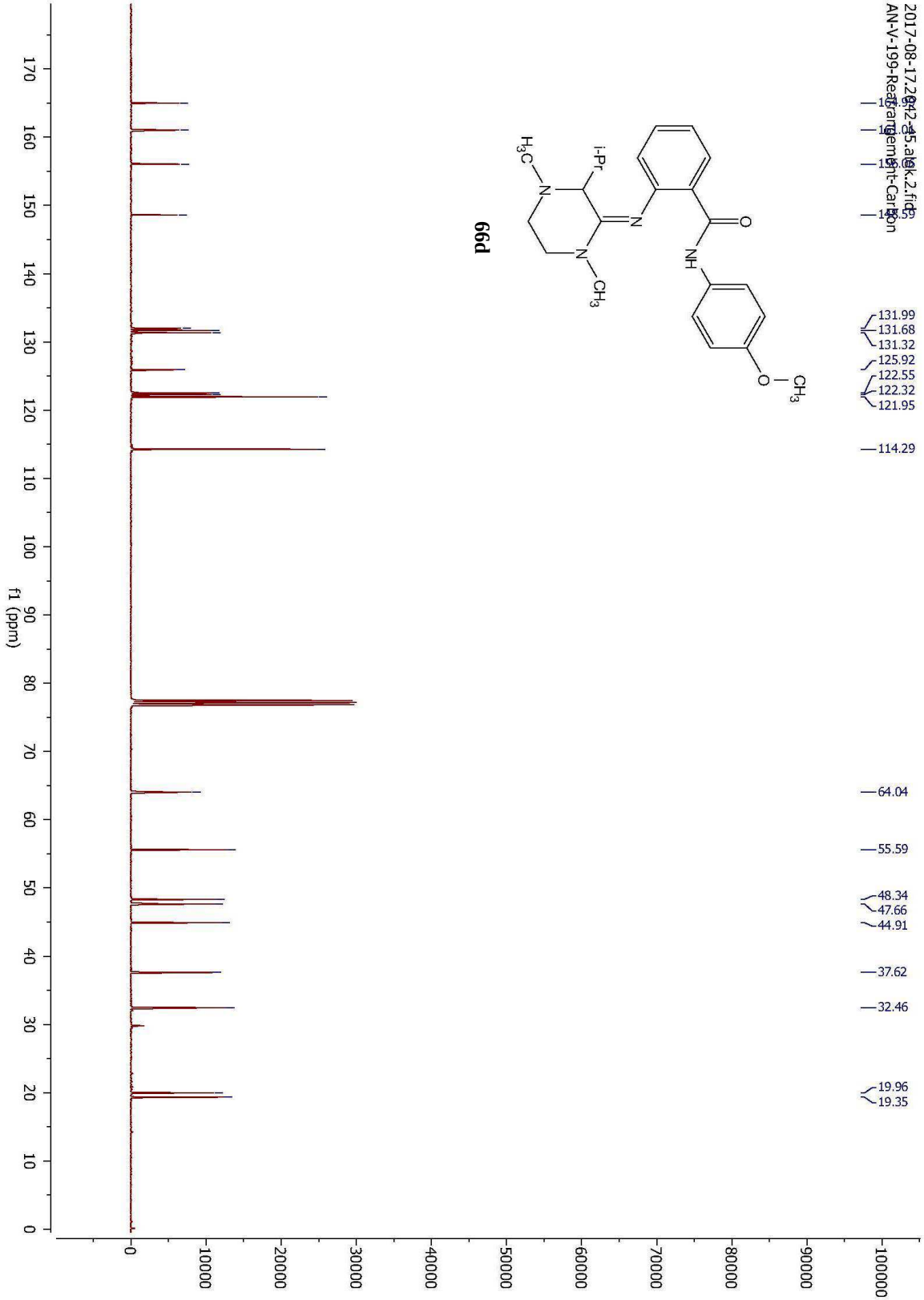
2017-08-17 22:45 ank2.fid
AN-V-199-Rearrangement-Carbon
69d
i-Pr
H3C
CH3
NH
O
CH3
131.99
131.68
131.32
125.92
122.55
122.32
121.95
114.29
64.04
55.59
48.34
47.66
44.91
37.62
32.46
19.96
19.35
f1 (ppm)

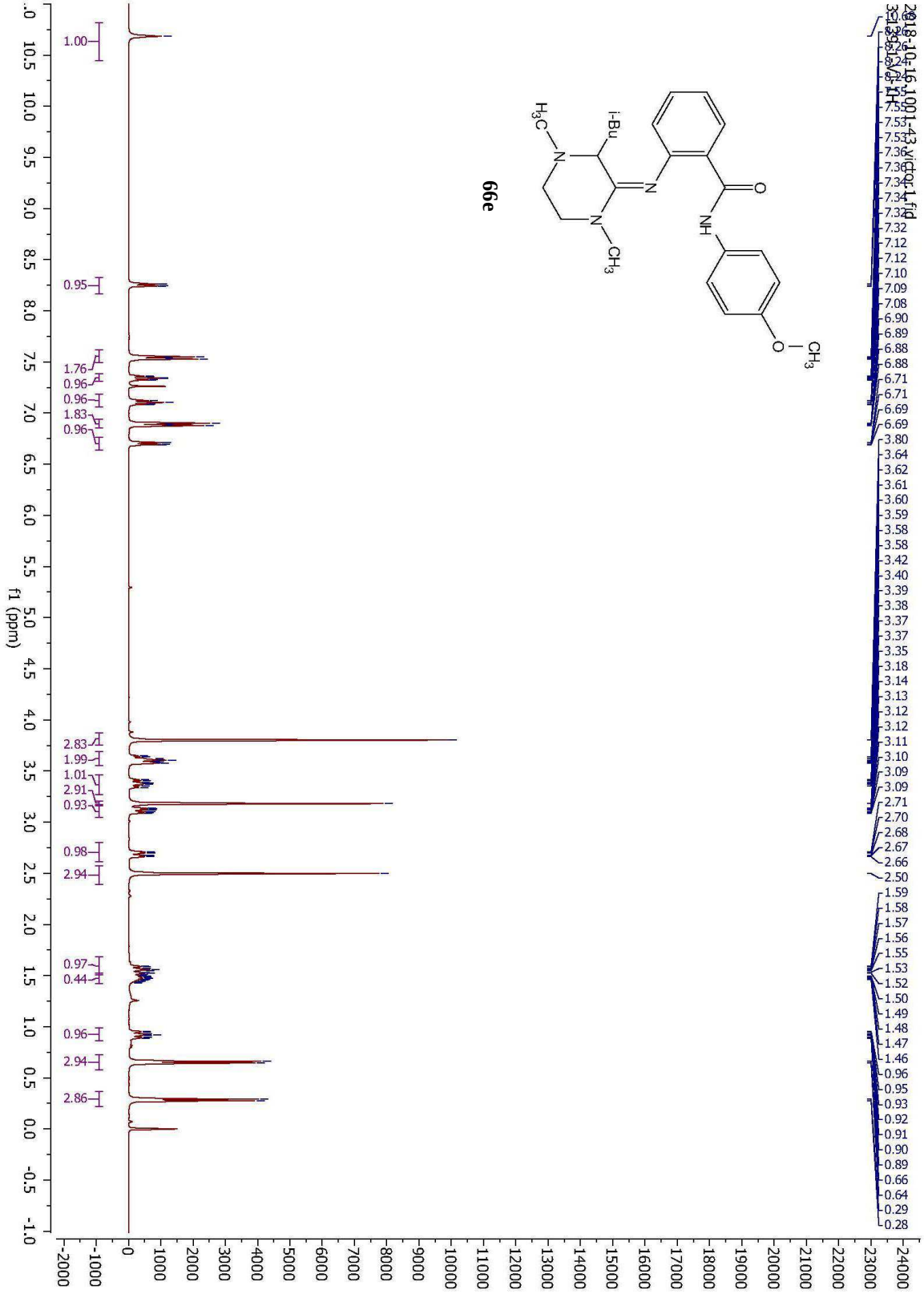
66e
i-Bu
H3C
CH3
NH
O
CH3
f1 (ppm)
1.00
0.95
1.76
0.96
0.96
1.83
0.96
2.83
1.99
1.01
2.91
0.93
0.98
2.94
0.97
0.44
0.96
2.94
2.86

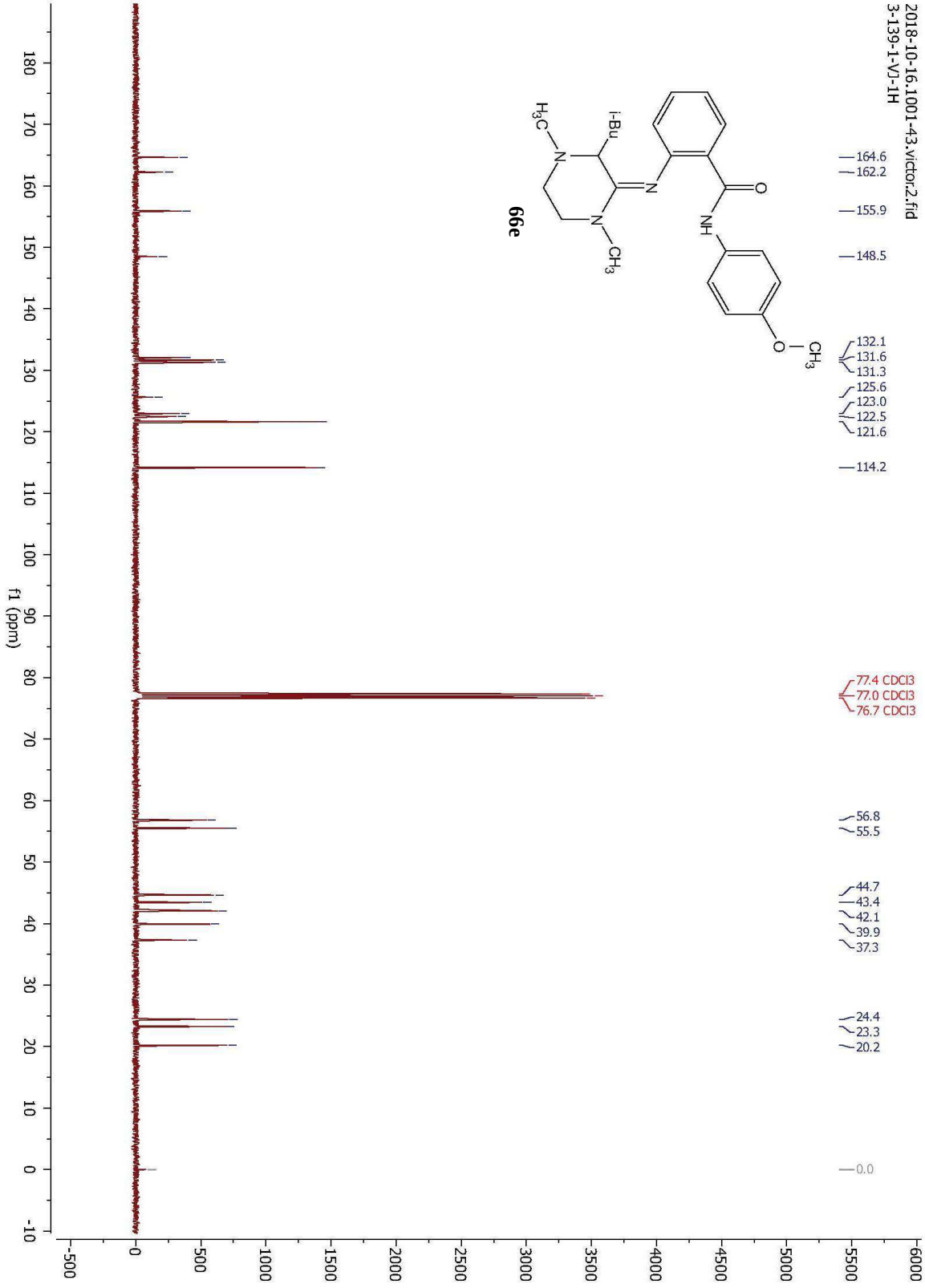
2018-10-16.1001-43.victor2.fid
3-139-1-VJ-1H
99e
i-Bu
H3C
CH3
NH
O
164.6
162.2
155.9
148.5
132.1
131.6
131.3
125.6
123.0
122.5
121.6
114.2
77.4 CDCl3
77.0 CDCl3
76.7 CDCl3
56.8
55.5
44.7
43.4
42.1
39.9
37.3
24.4
23.3
20.2
0.0
f1 (ppm)

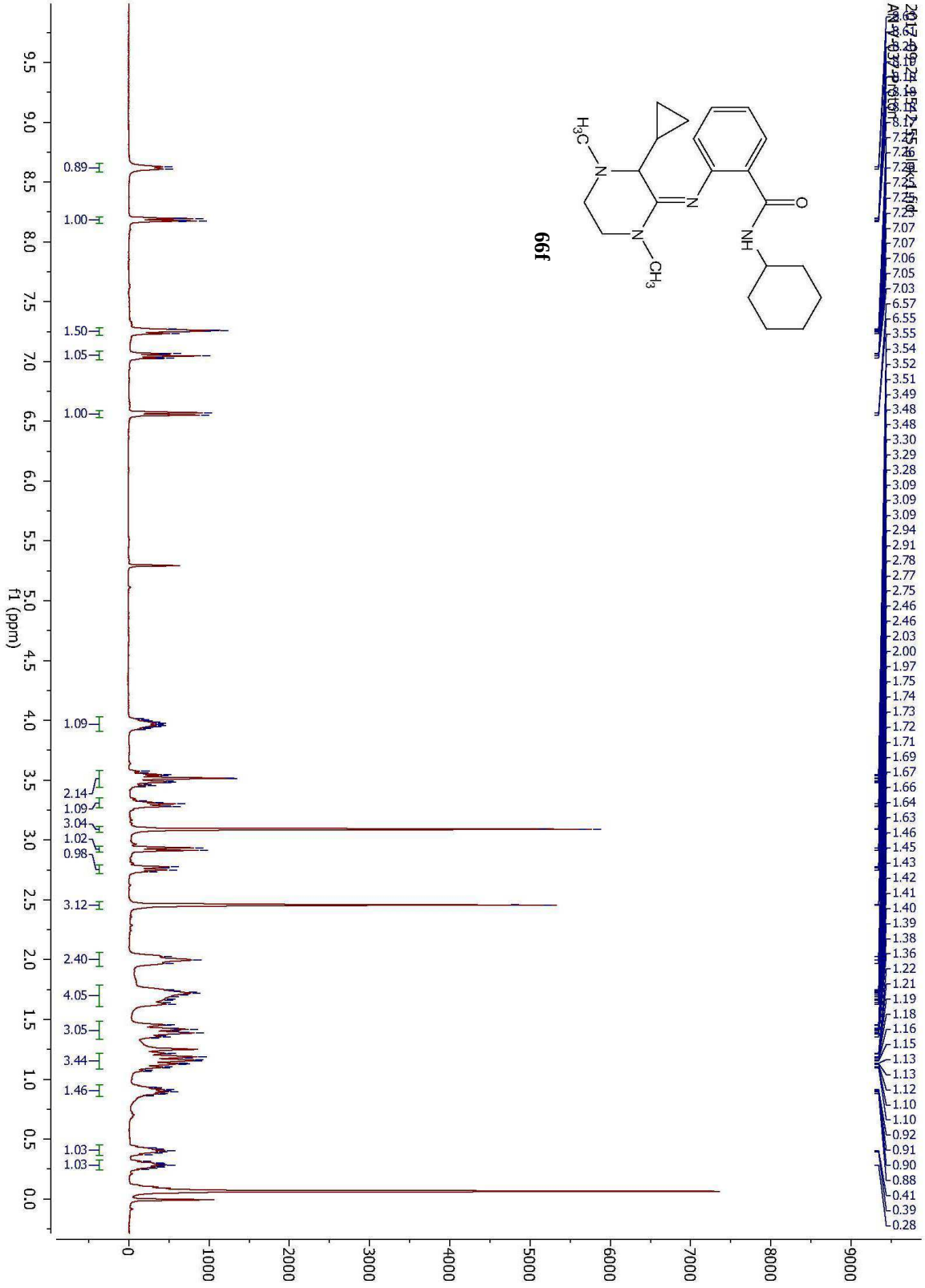
66f
f1 (ppm)
0.89
1.00
1.50
1.05
1.00
1.09
2.14
1.09
3.04
1.02
0.98
3.12
2.40
4.05
3.05
3.44
1.46
1.03
1.03

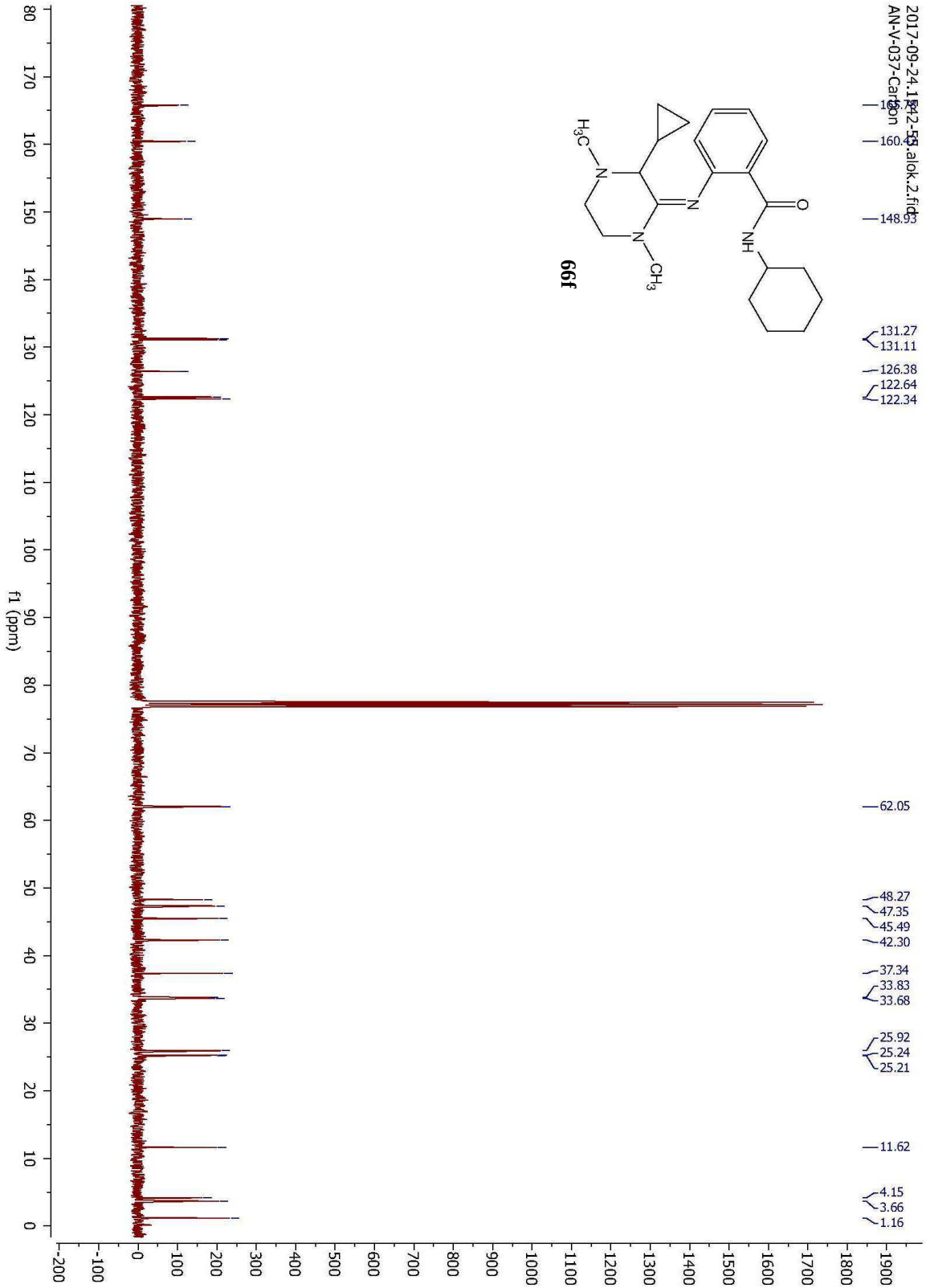
2017-09-24.18442-55.alok.2.fid
AN-V-037-Carbon
66f
160.43
148.93
131.27
131.11
126.38
122.64
122.34
62.05
48.27
47.35
45.49
42.30
37.34
33.83
33.68
25.92
25.24
25.21
11.62
4.15
3.66
1.16
f1 (ppm)

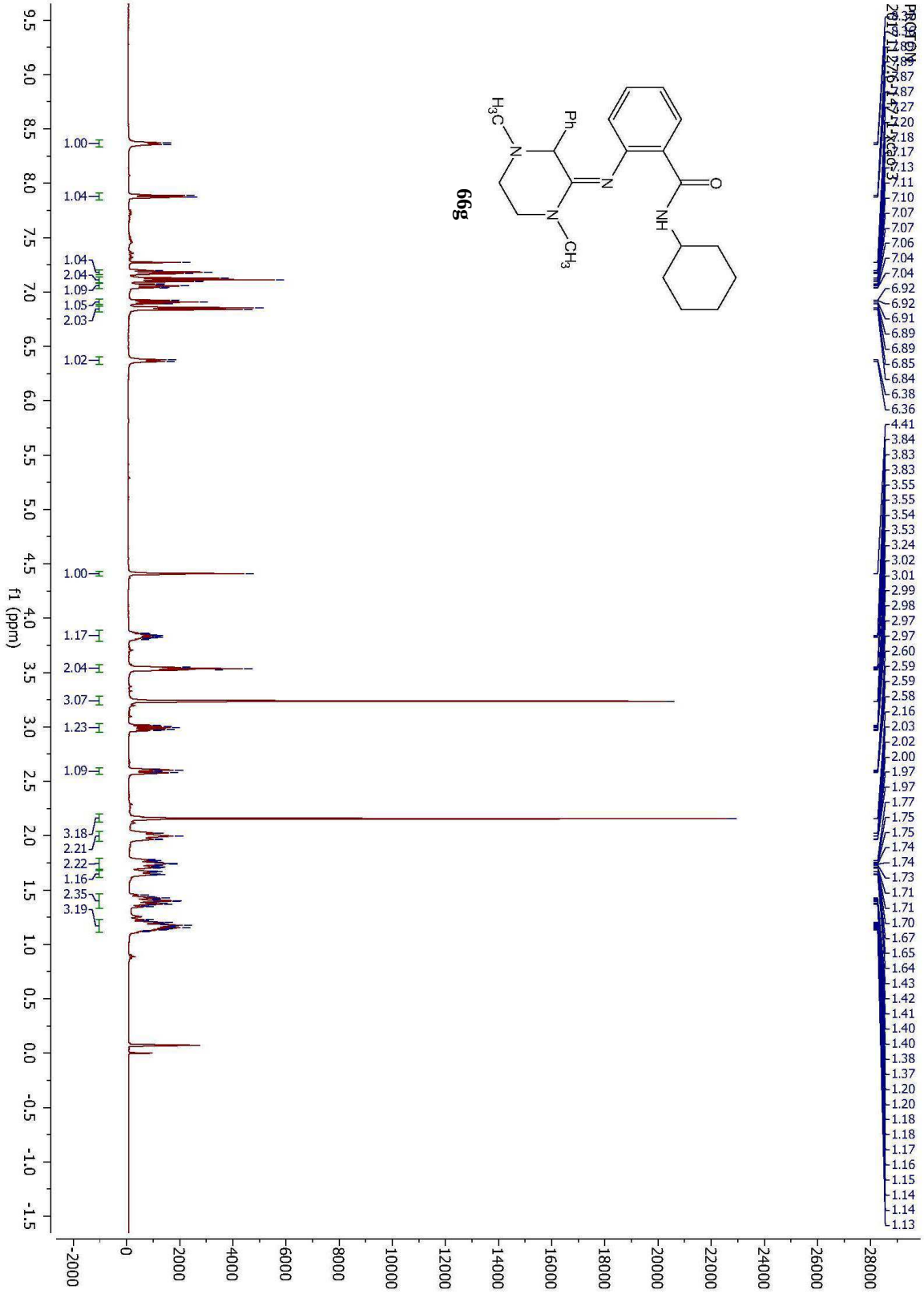
f1 (ppm)
9.5 9.0 8.5 8.0 7.5 7.0 6.5 6.0 5.5 5.0 4.5 4.0 3.5 3.0 2.5 2.0 1.5 1.0 0.5 0.0 -0.5 -1.0 -1.5
1.00
1.04
1.04
2.04
1.09
1.05
2.03
1.02
1.00
1.17
2.04
3.07
1.23
1.09
3.18
2.21
2.22
1.16
2.35
3.19
-2000 0 2000 4000 6000 8000 10000 12000 14000 16000 18000 20000 22000 24000 26000 28000
H3C
N
Ph
N
N
CH3
O
NH
6gg

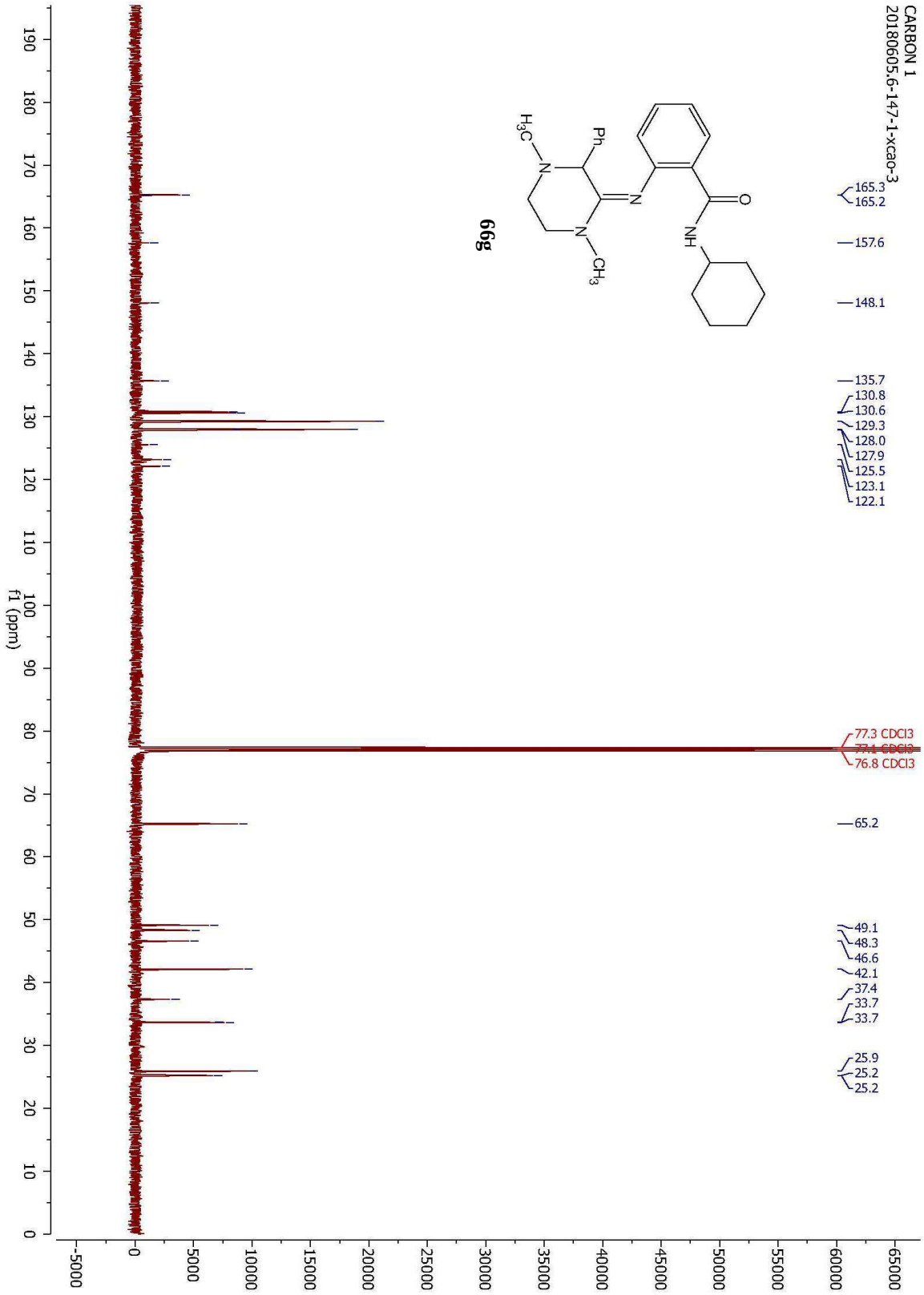
CARBON 1
20180605.6-147-1-xcao-3
ggg
165.3
165.2
157.6
148.1
135.7
130.8
130.6
129.3
128.0
127.9
125.5
123.1
122.1
77.3 CDCl3
77.1 CDCl3
76.8 CDCl3
65.2
49.1
48.3
46.6
42.1
37.4
33.7
33.7
25.9
25.2
25.2
f1 (ppm)

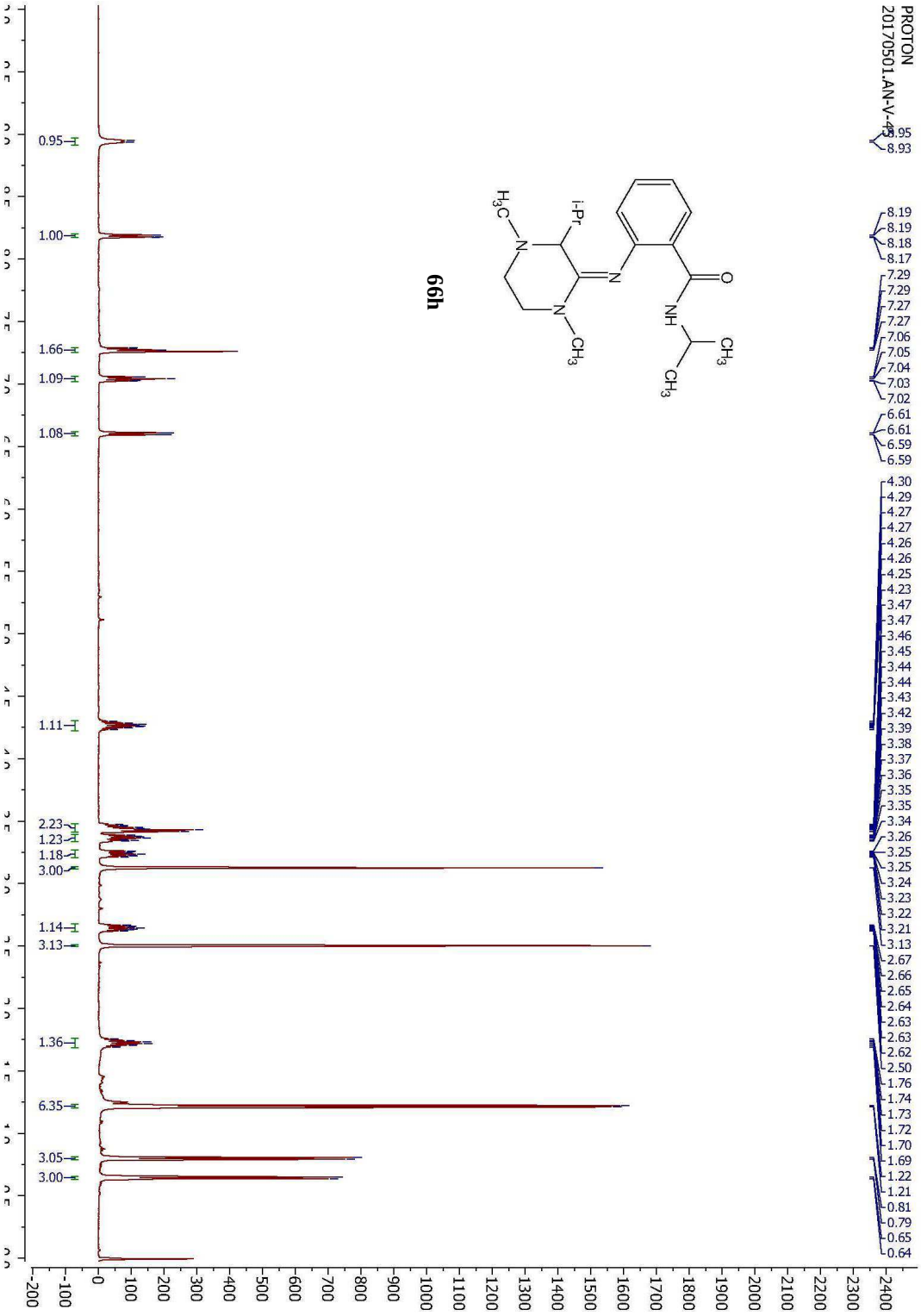
PROTON
20170501.AN-V-48
66h
i-Pr
H3C
CH3
CH3
CH3
NH
O
N
N
0.95
1.00
1.66
1.09
1.08
1.11
2.23
1.23
1.18
3.00
1.14
3.13
1.36
6.35
3.05
3.00

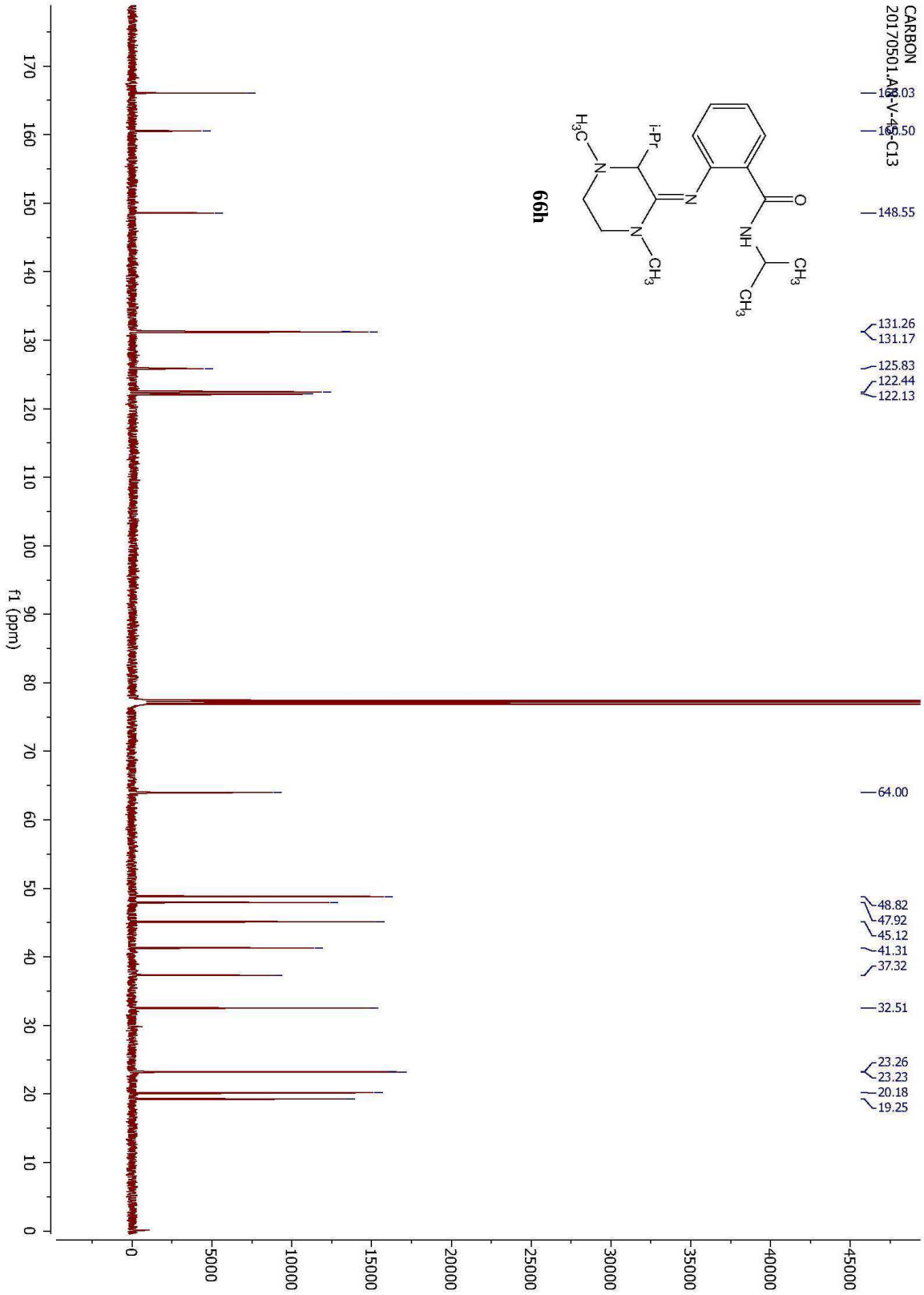
CARBON
20170501.AS-V-45-C13
66h
i-Pr
H_3C
CH_3
CH_3
CH_3
NH
O
N
N
N
163.03
160.50
148.55
131.26
131.17
125.83
122.44
122.13
64.00
48.82
47.92
45.12
41.31
37.32
32.51
23.26
23.23
20.18
19.25
f1 (ppm)
0
10
20
30
40
50
60
70
80
90
100
110
120
130
140
150
160
170
0
5000
10000
15000
20000
25000
30000
35000
40000
45000

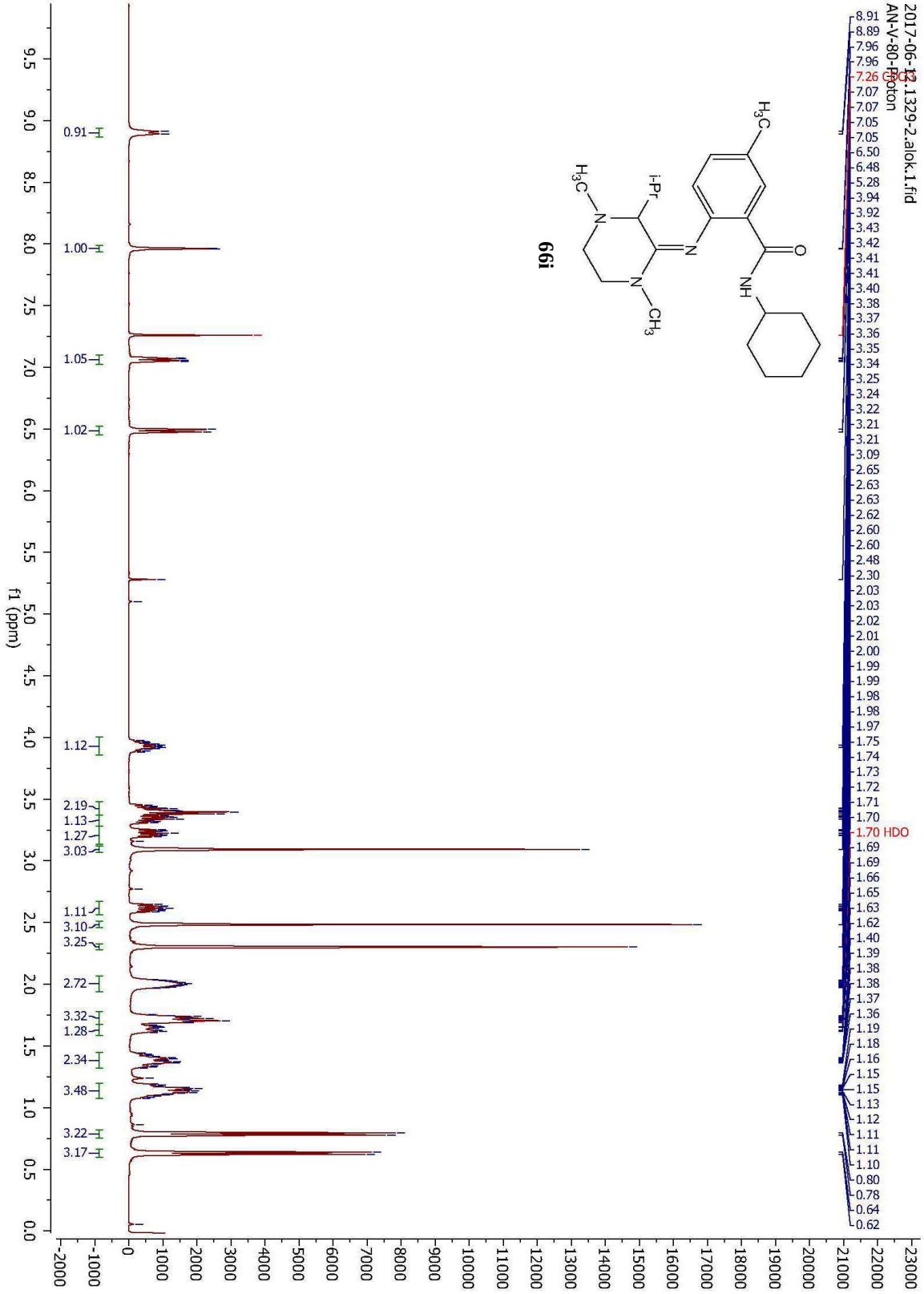
2017-06-12-1329-2.alok.1.fid
AN-V-80-Proton
7.26 CDCl3
1.70 HDO
f1 (ppm)
0.91
1.00
1.05
1.02
1.12
2.19
1.13
1.27
3.03
1.11
3.10
3.25
2.72
3.32
1.28
2.34
3.48
3.22
3.17
i-Pr
H3C
CH3
N
NH
O

66i

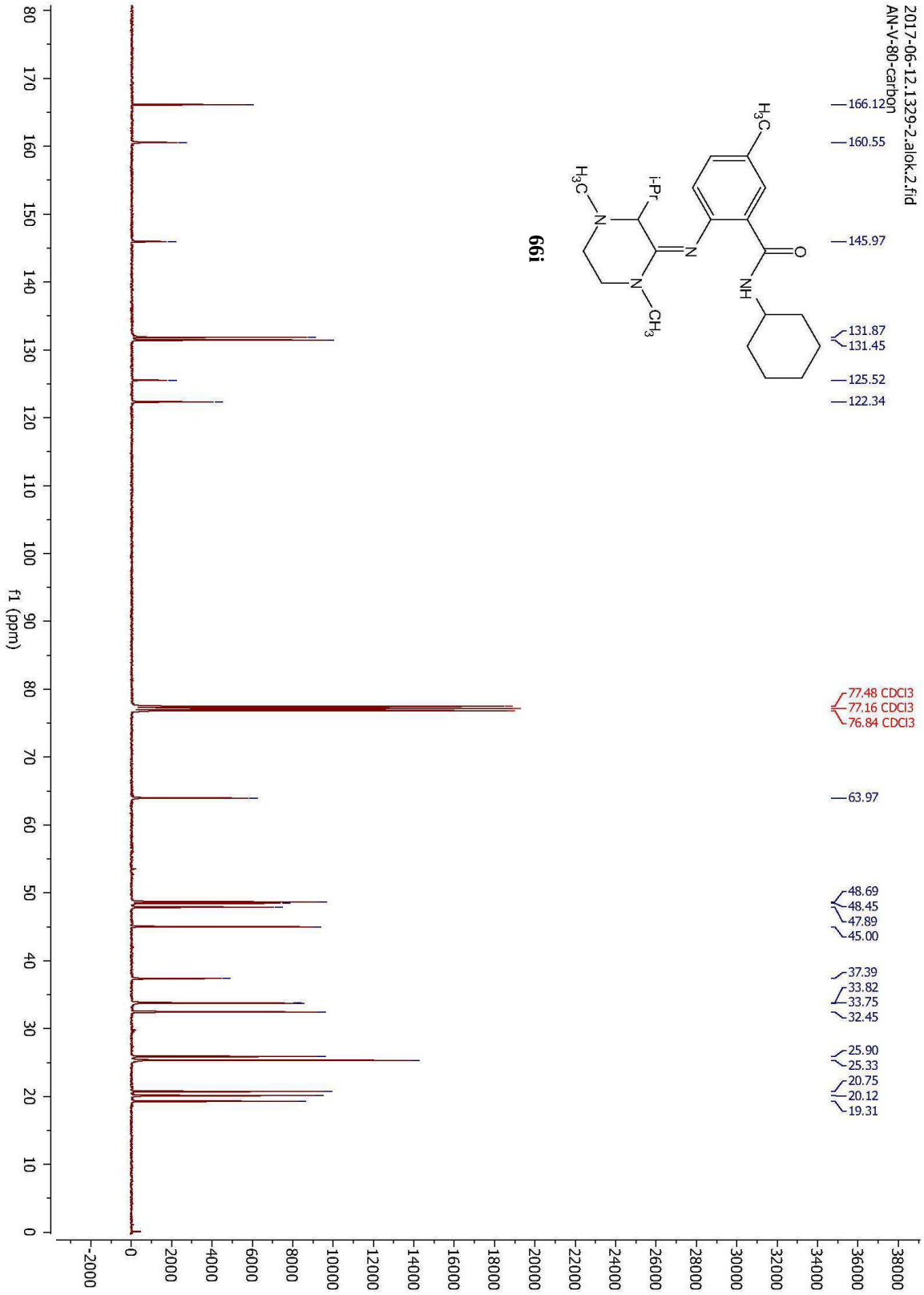
2017-06-12.1329-2.alok.2.fid
AN-V-80-carbon
166.12
160.55
145.97
131.87
131.45
125.52
122.34
77.48 CDCl3
77.16 CDCl3
76.84 CDCl3
63.97
48.69
48.45
47.89
45.00
37.39
33.82
33.75
32.45
25.90
25.33
20.75
20.12
19.31
f1 (ppm)
i-Pr
CH3
NH
O
N
H3C

66i

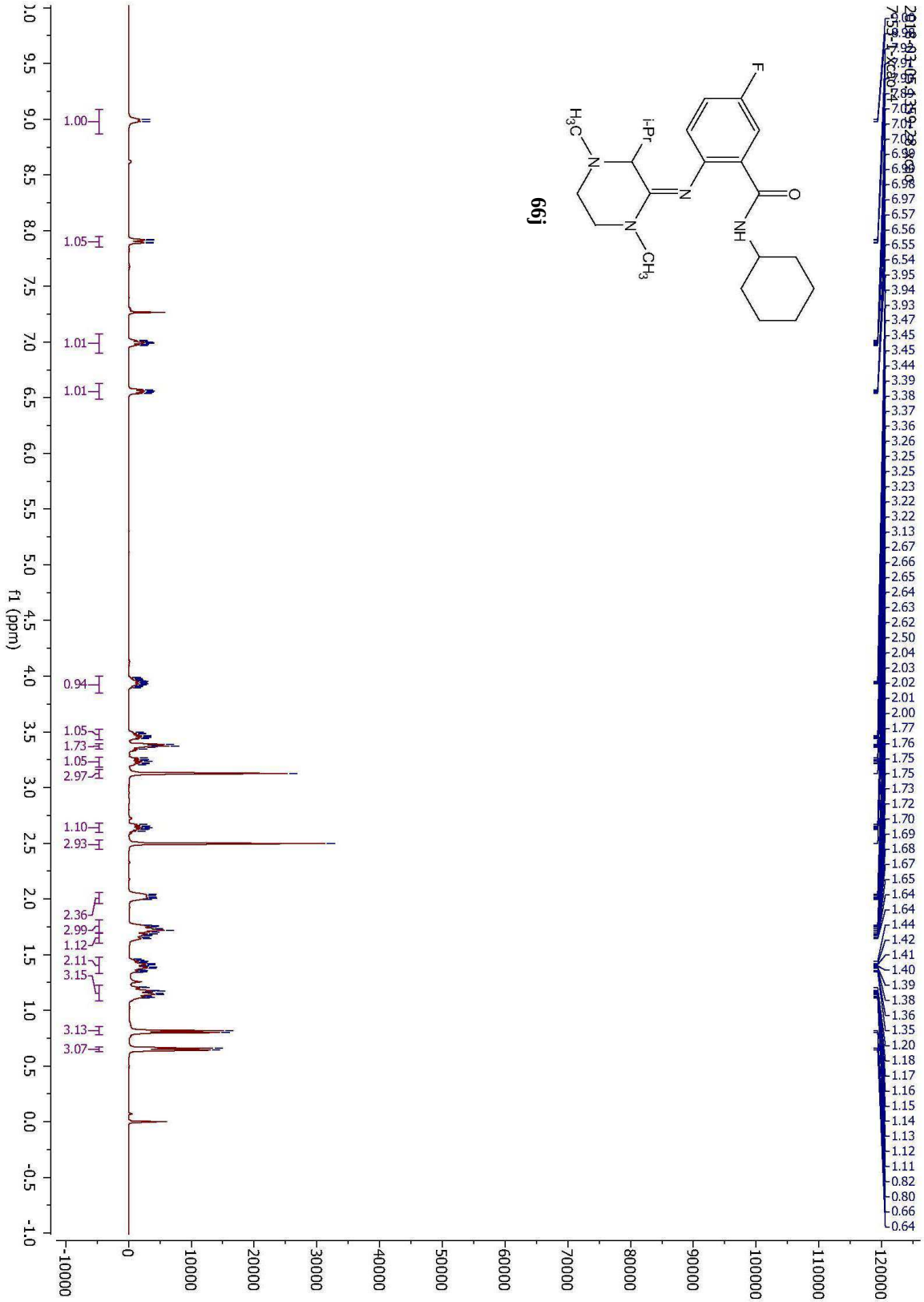
69j
F
O
NH
N
N
CH3
H3C
i-Pr
f1 (ppm)
1.00
1.05
1.01
1.01
0.94
1.05
1.73
1.05
2.97
1.10
2.93
2.36
2.99
1.12
2.11
3.15
3.13
3.07

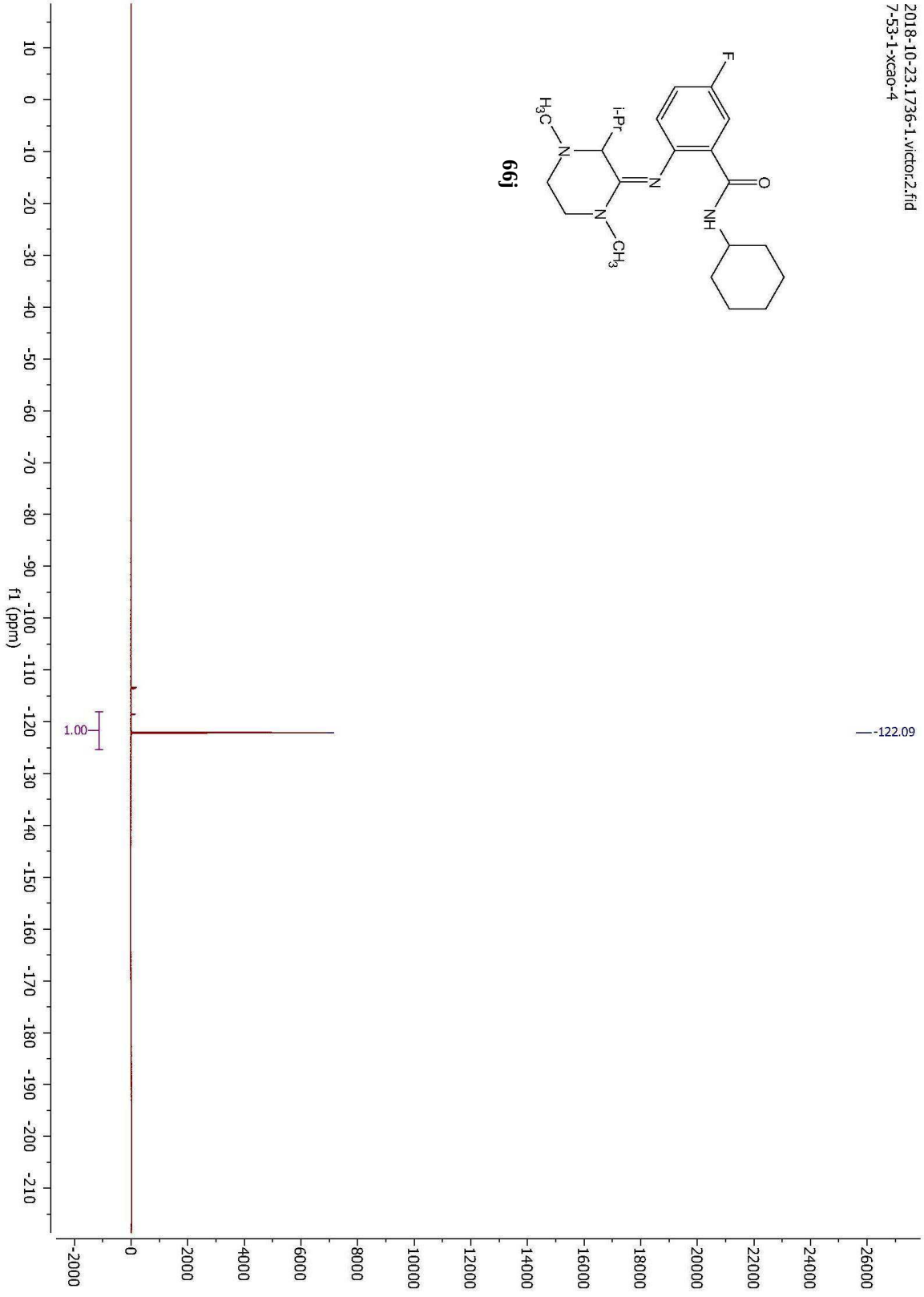
2018-10-23.1736-1.victor.2.fid
7-53-1-xcao-4
66j
F
O
NH
N
i-Pr
H_3C
CH_3
-122.09
1.00
f1 (ppm)

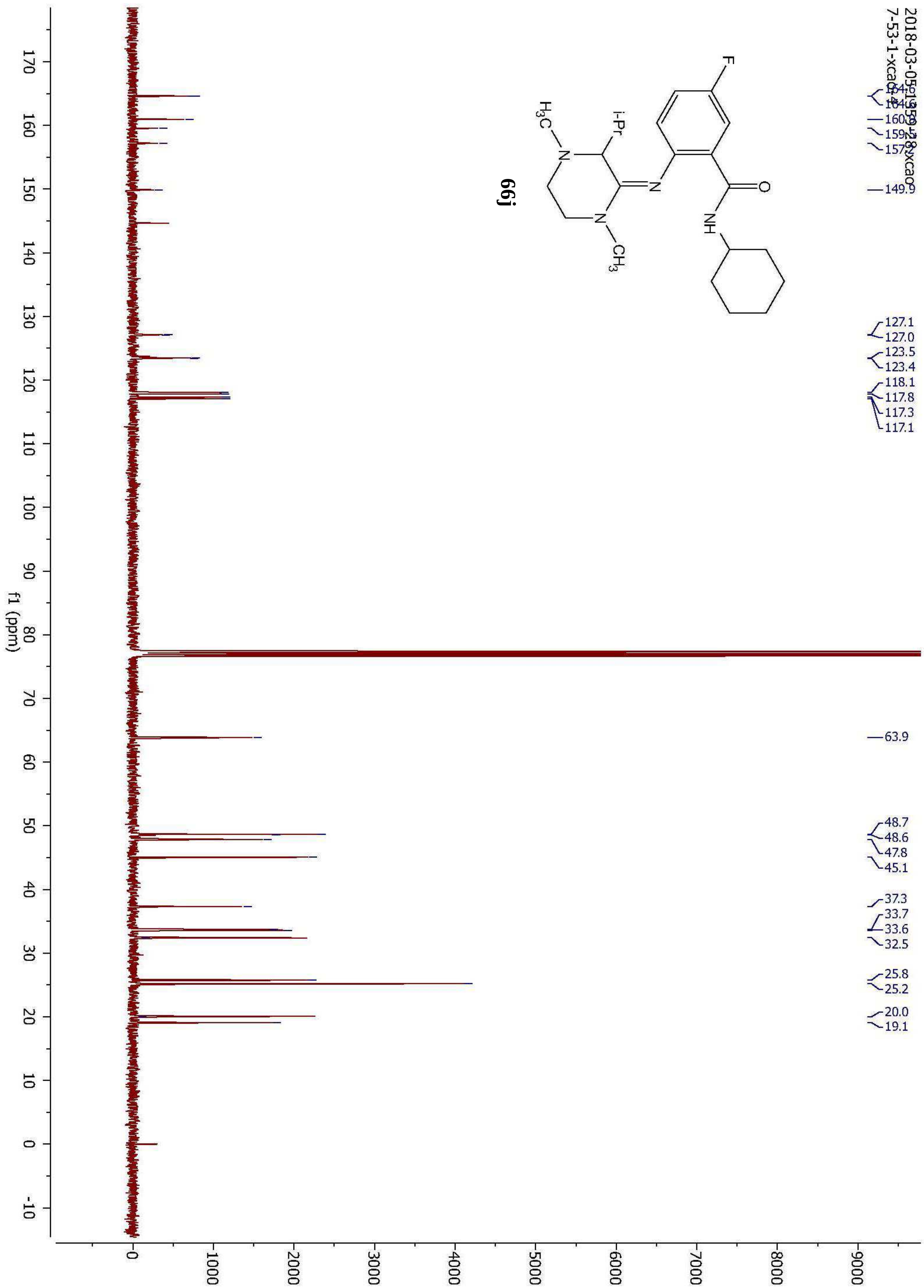

66j
i-Pr
NH
f1 (ppm)
149.9
127.1
127.0
123.5
123.4
118.1
117.8
117.3
117.1
63.9
48.7
48.6
47.8
45.1
37.3
33.7
33.6
32.5
25.8
25.2
20.0
19.1

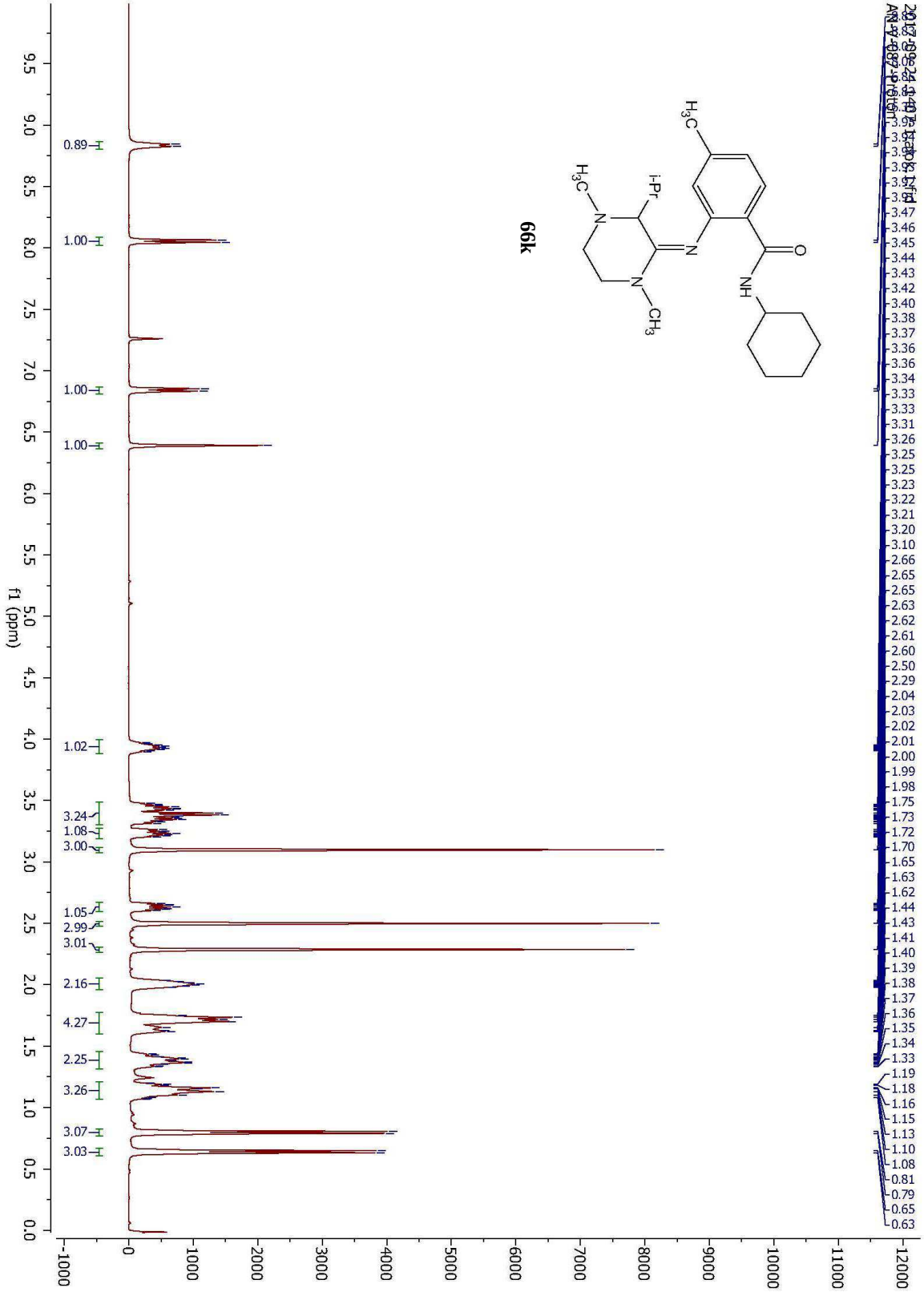
66k
f1 (ppm)
0.89
1.00
1.00
1.00
1.02
3.24
1.08
3.00
1.05
2.99
3.01
2.16
4.27
2.25
3.26
3.07
3.03

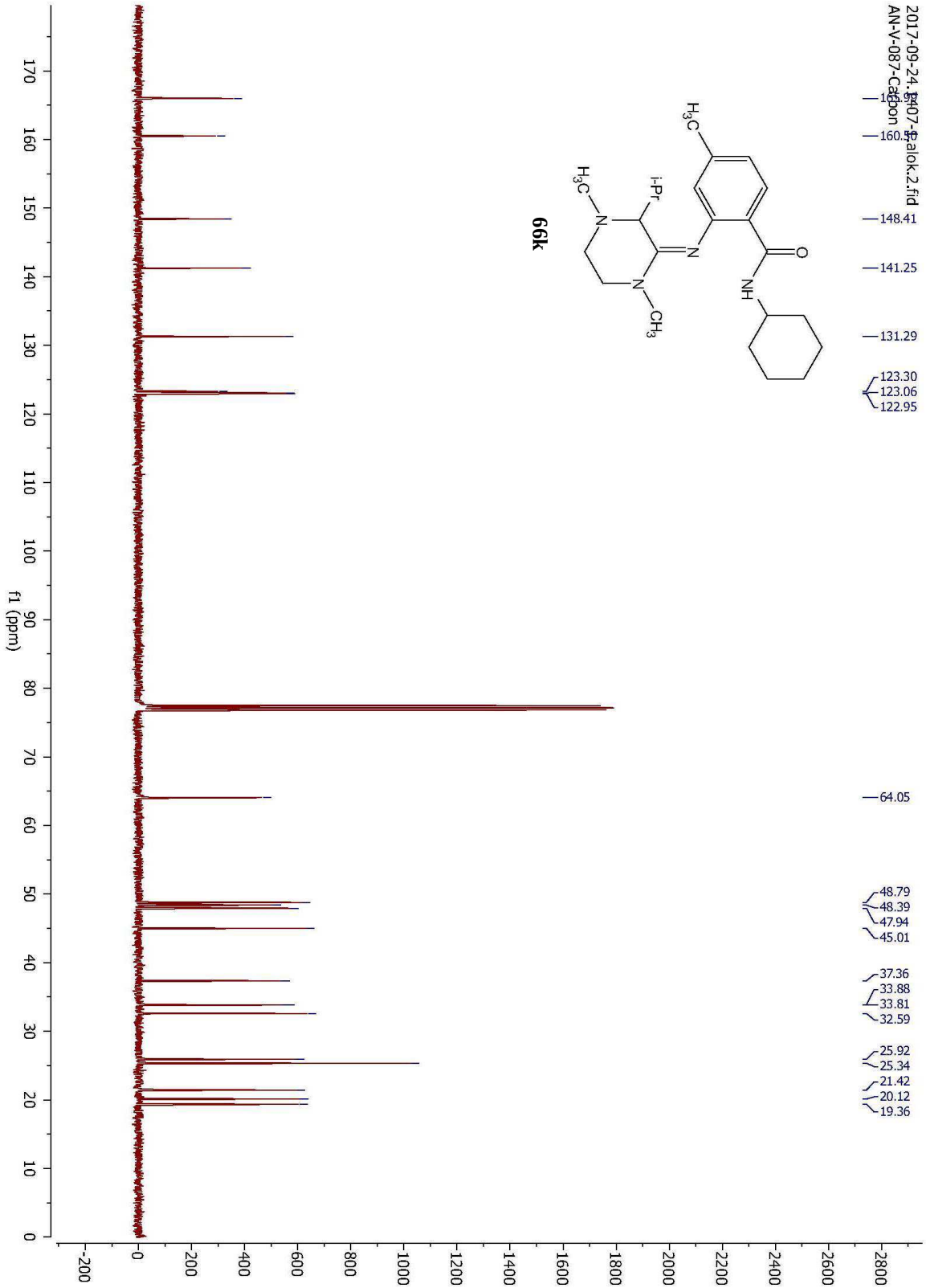
2017-09-24_AN-V-087-Calalok_2.fid
AN-V-087-Calcon
160.58
148.41
141.25
131.29
123.30
123.06
122.95
64.05
48.79
48.39
47.94
45.01
37.36
33.88
33.81
32.59
25.92
25.34
21.42
20.12
19.36
66k
f1 (ppm)

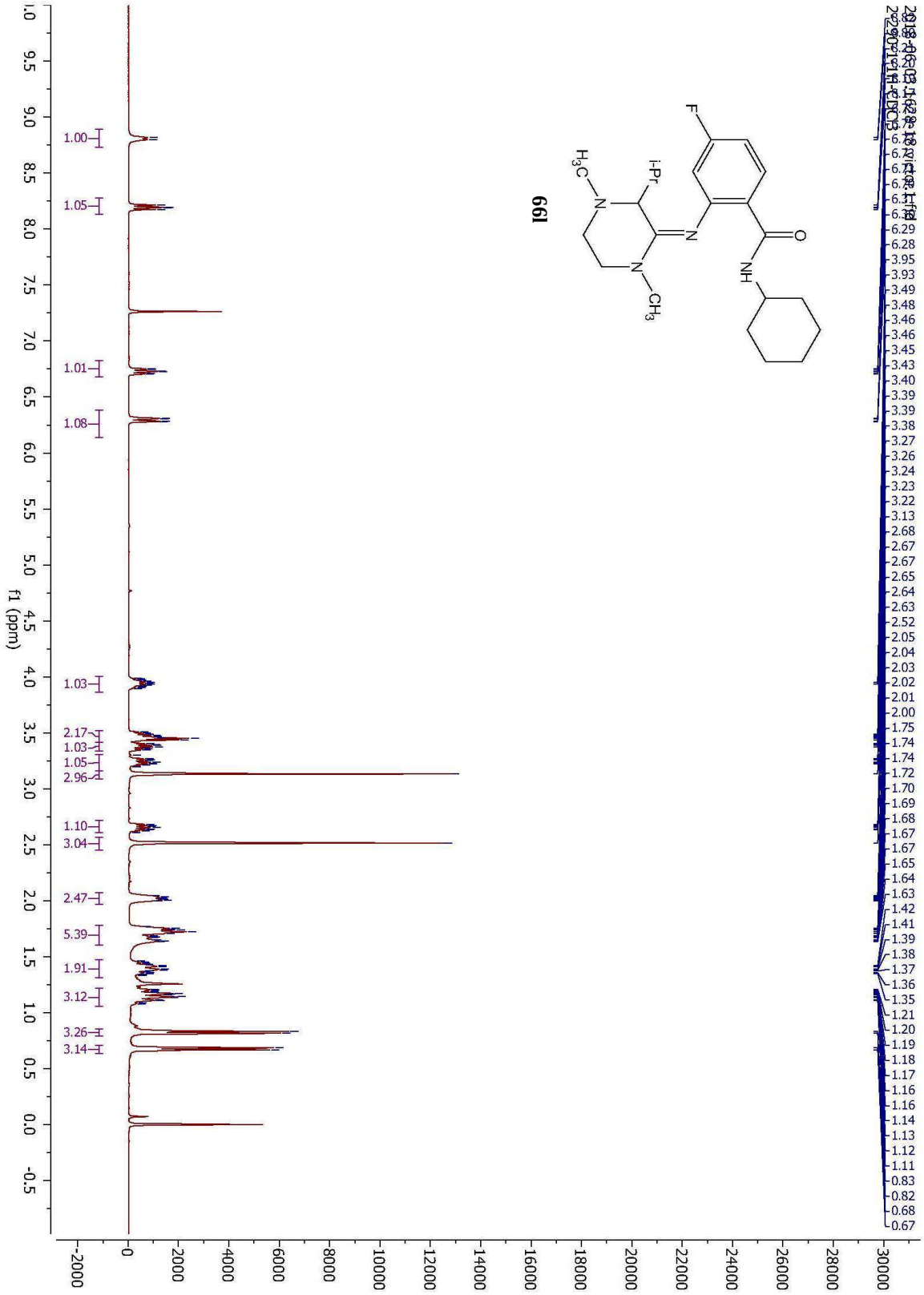
f1 (ppm)
1.00
1.05
1.01
1.08
1.03
2.17
1.03
1.05
2.96
1.10
3.04
2.47
5.39
1.91
3.12
3.26
3.14
F
i-Pr
H3C
N
N
N
CH3
O
NH

19l

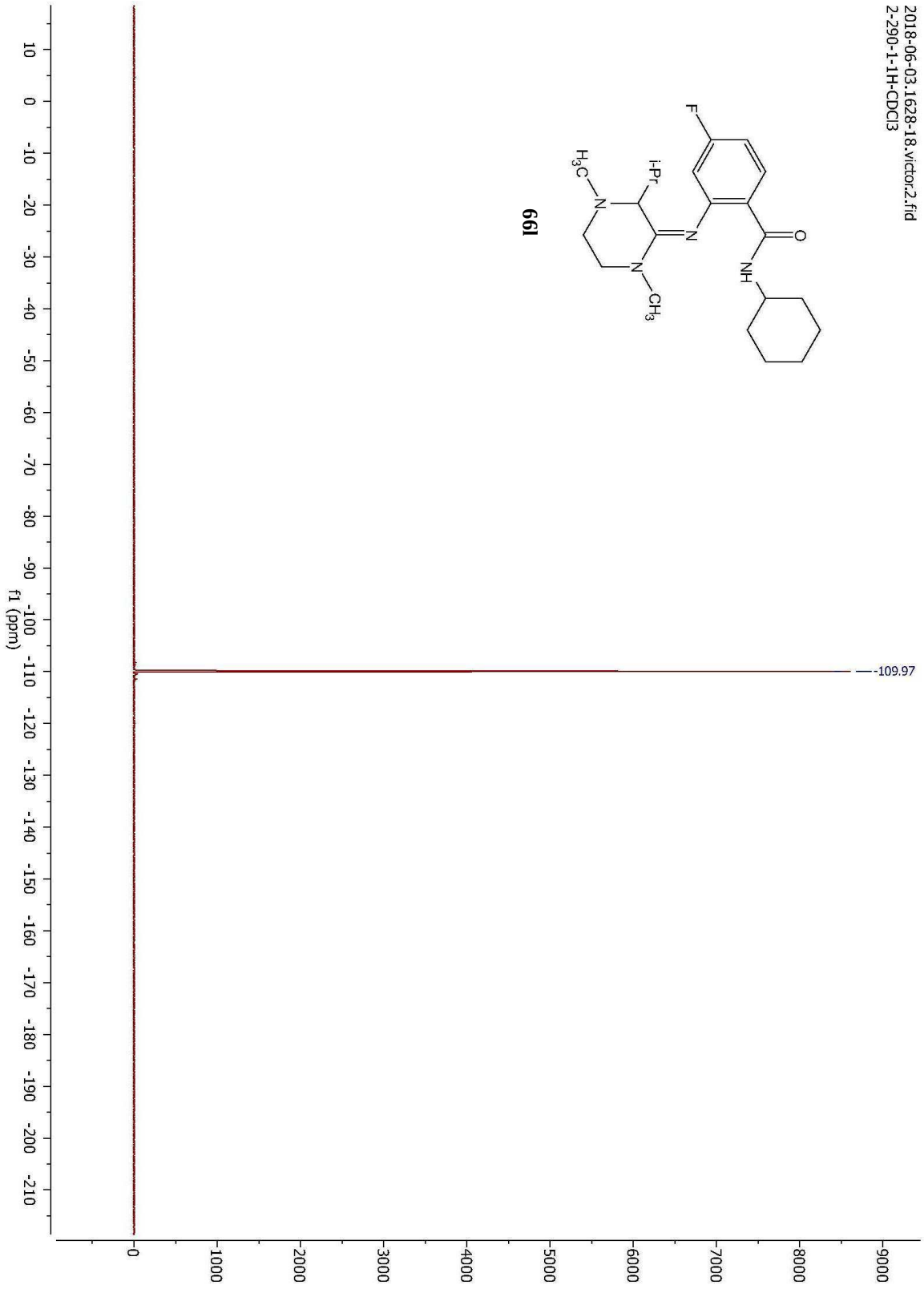
2018-06-03.1628-18.victor2.fid
2-290-1-1H-CDCl3
-109.97
f1 (ppm)
10
0
-10
-20
-30
-40
-50
-60
-70
-80
-90
-100
-110
-120
-130
-140
-150
-160
-170
-180
-190
-200
-210
0
1000
2000
3000
4000
5000
6000
7000
8000
9000

19l

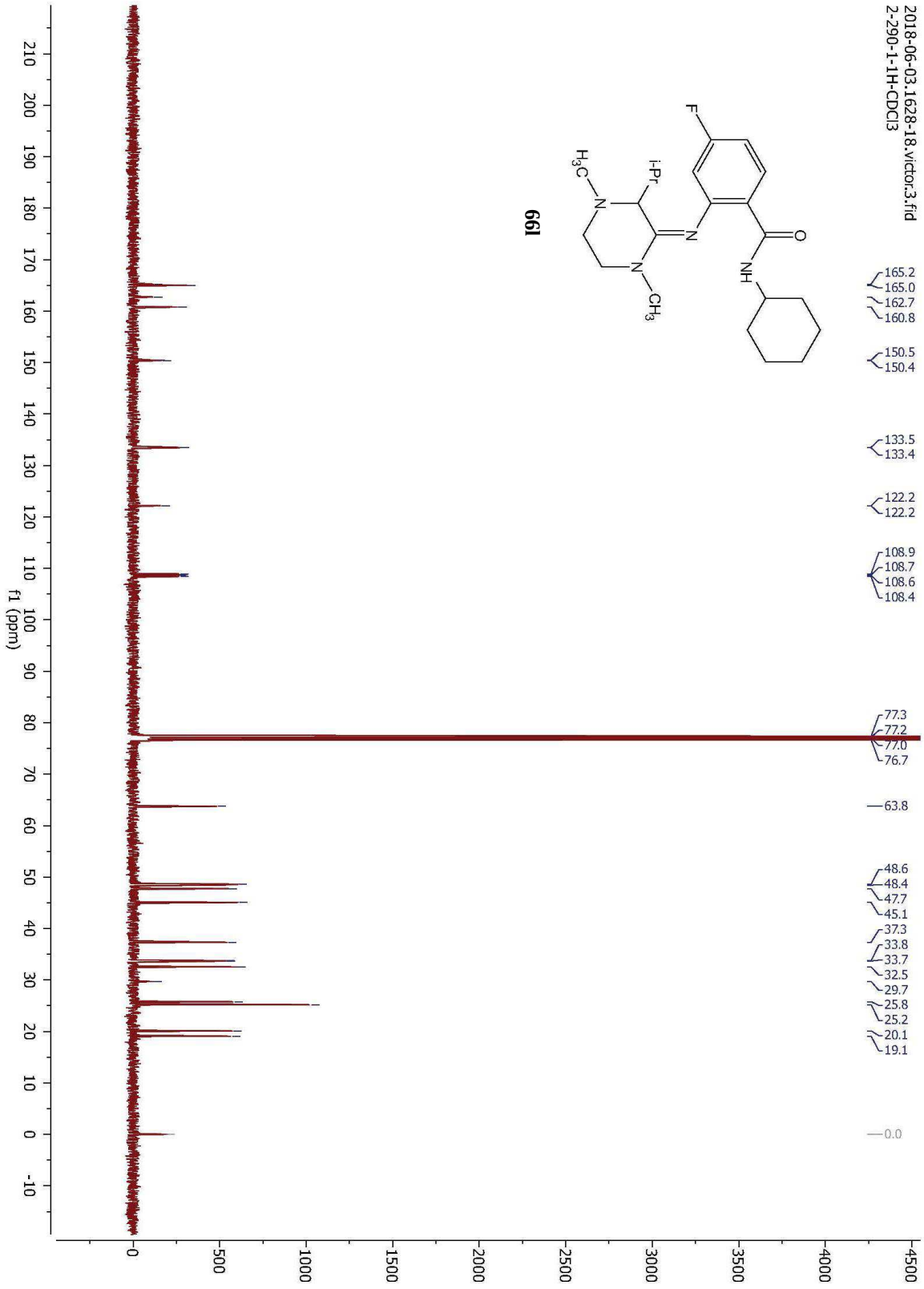
2018-06-03.1628-18.victor3.fid
2-290-1-1H-CDCl3
199
F
i-Pr
H3C
N
N
N
CH3
O
NH
165.2
165.0
162.7
160.8
150.5
150.4
133.5
133.4
122.2
122.2
108.9
108.7
108.6
108.4
77.3
77.2
77.0
76.7
63.8
48.6
48.4
47.7
45.1
37.3
33.8
33.7
32.5
29.7
25.8
25.2
20.1
19.1
0.0
f1 (ppm)

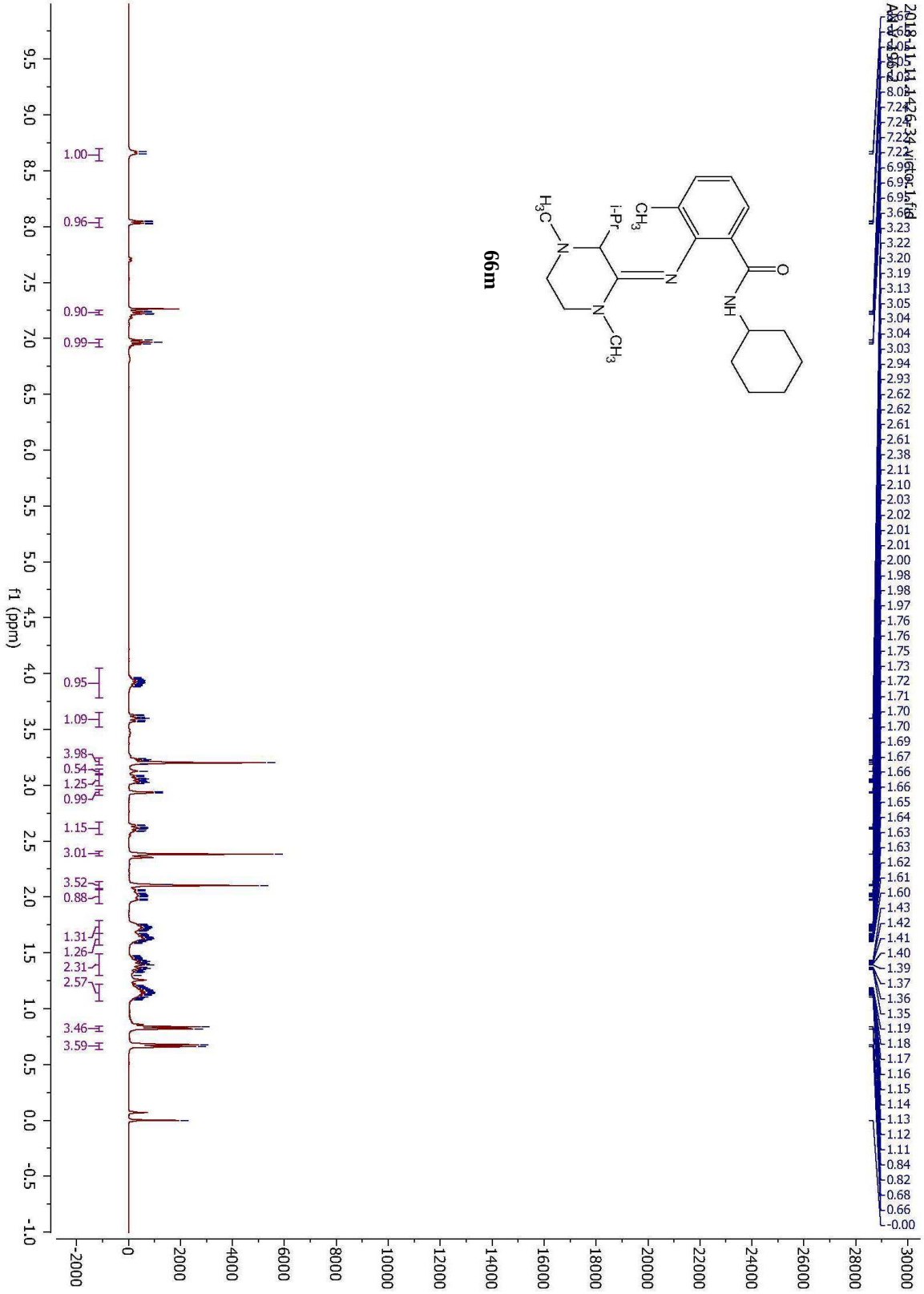
66m
f1 (ppm)
1.00
0.96
0.90
0.99
0.95
1.09
3.98
0.54
1.25
0.99
1.15
3.01
3.52
0.88
1.31
1.26
2.31
2.57
3.46
3.59

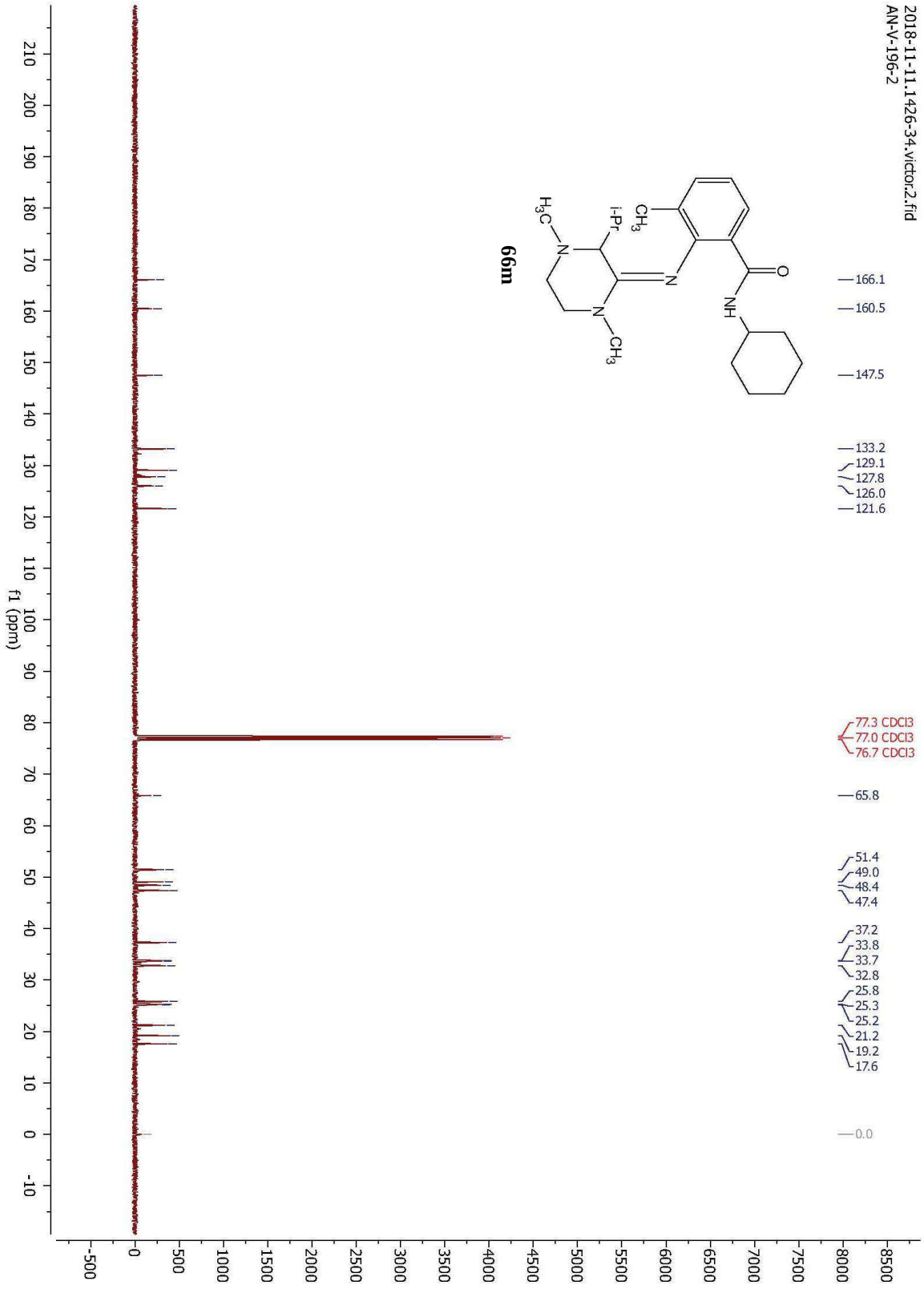
2018-11-11.1426-34.victor.2.fid
AN-V-196-2
66m
166.1
160.5
147.5
133.2
129.1
127.8
126.0
121.6
77.3 CDCl3
77.0 CDCl3
76.7 CDCl3
65.8
51.4
49.0
48.4
47.4
37.2
33.8
33.7
32.8
25.8
25.3
25.2
21.2
19.2
17.6
0.0
f1 (ppm)

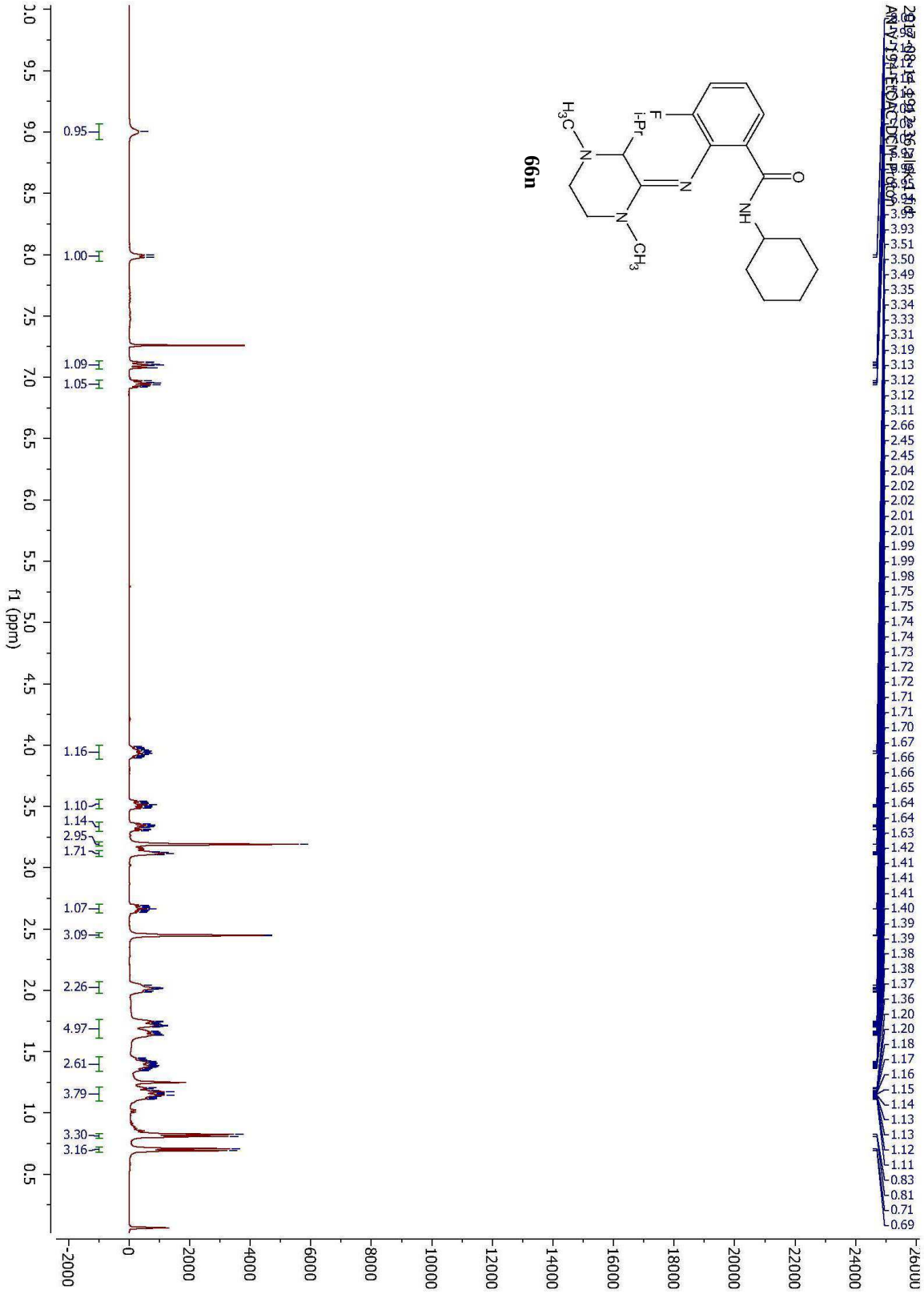
66n
F
i-Pr
H3C
N
N
CH3
N
O
NH
f1 (ppm)
0.95
1.00
1.09
1.05
1.16
1.10
1.14
2.95
1.71
1.07
3.09
2.26
4.97
2.61
3.79
3.30
3.16

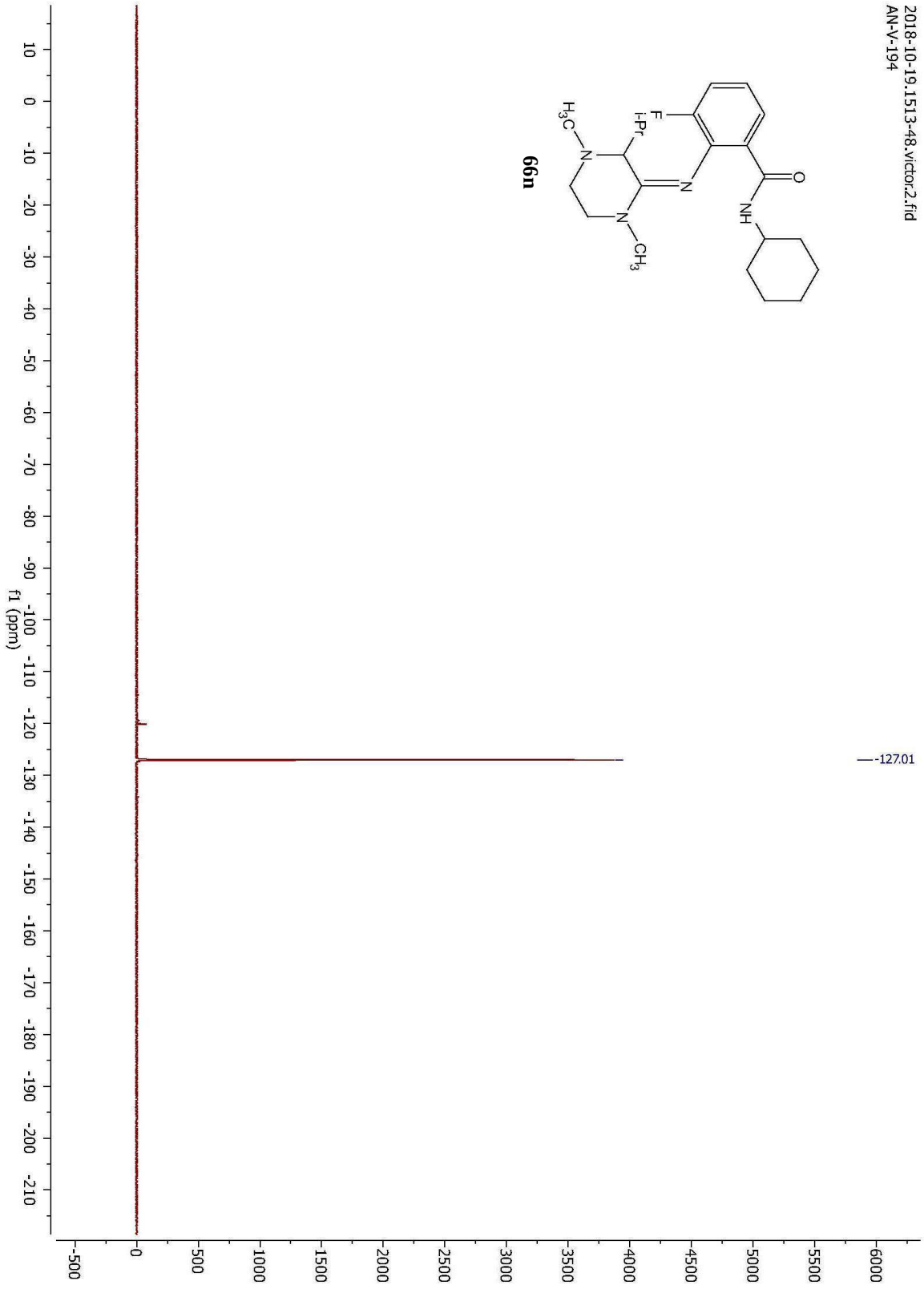
2018-10-19.1513-48.victor2.fid
AN-V-194
66n
-127.01
f1 (ppm)

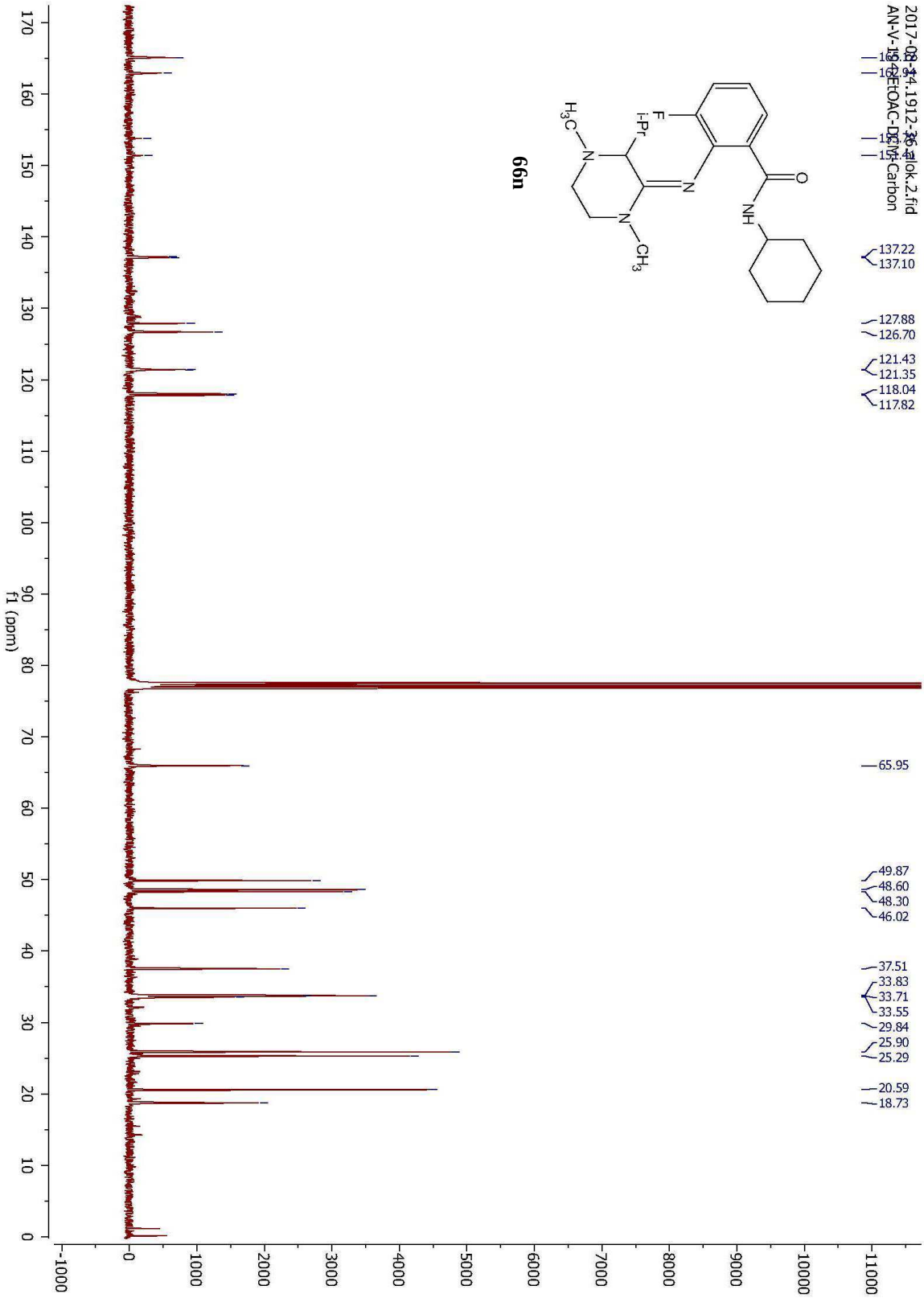
66n
2017-08-14.1912-36.alok.2.fid
AN-V-19-DEtOAC-DCM-Carbon
137.22
137.10
127.88
126.70
121.43
121.35
118.04
117.82
65.95
49.87
48.60
48.30
46.02
37.51
33.83
33.71
33.55
29.84
25.90
25.29
20.59
18.73
f1 (ppm)

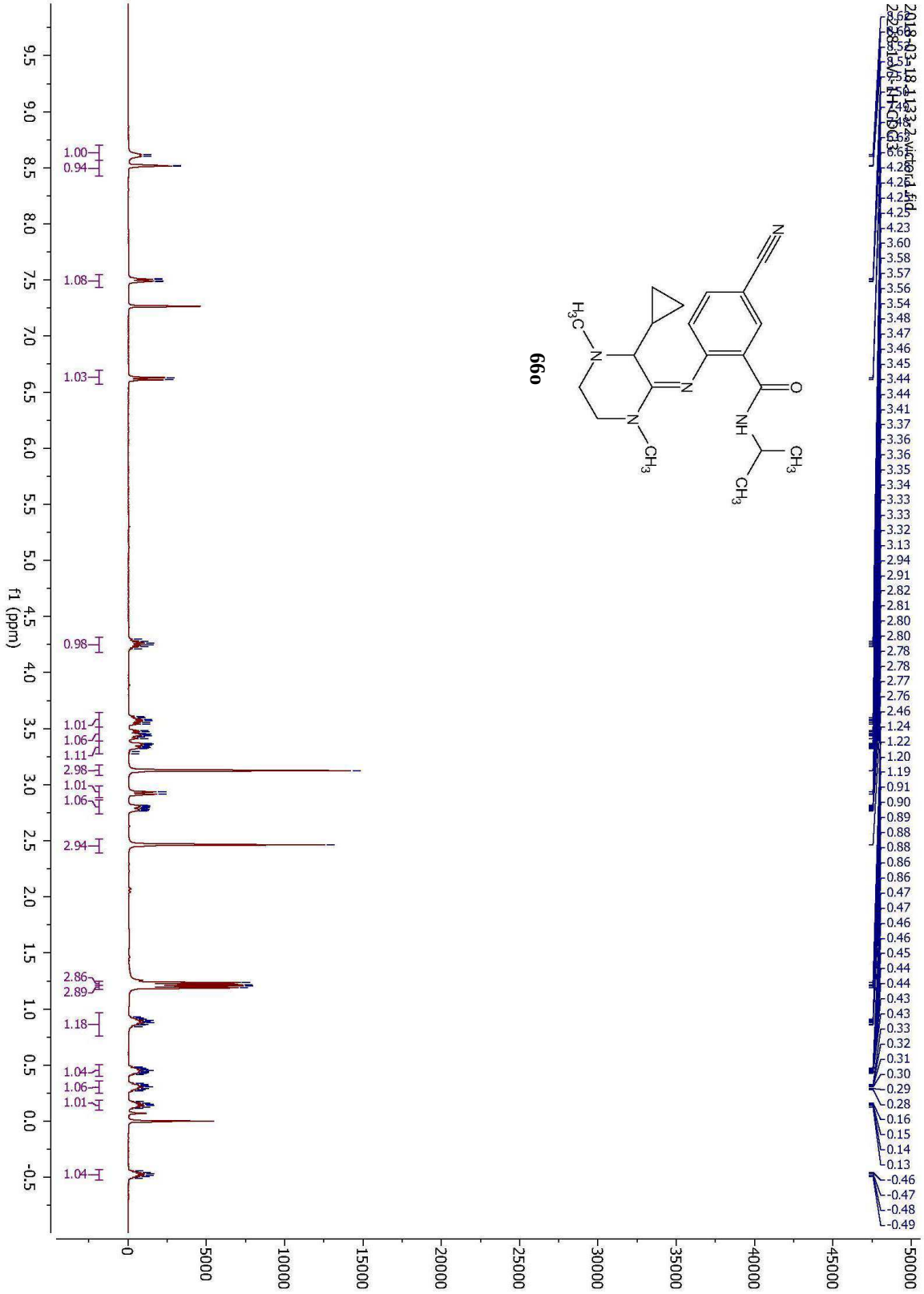
66o
f1 (ppm)
1.00
0.94
1.08
1.03
0.98
1.01
1.06
1.11
2.98
1.01
1.06
2.94
2.86
2.89
1.18
1.04
1.06
1.01
1.04

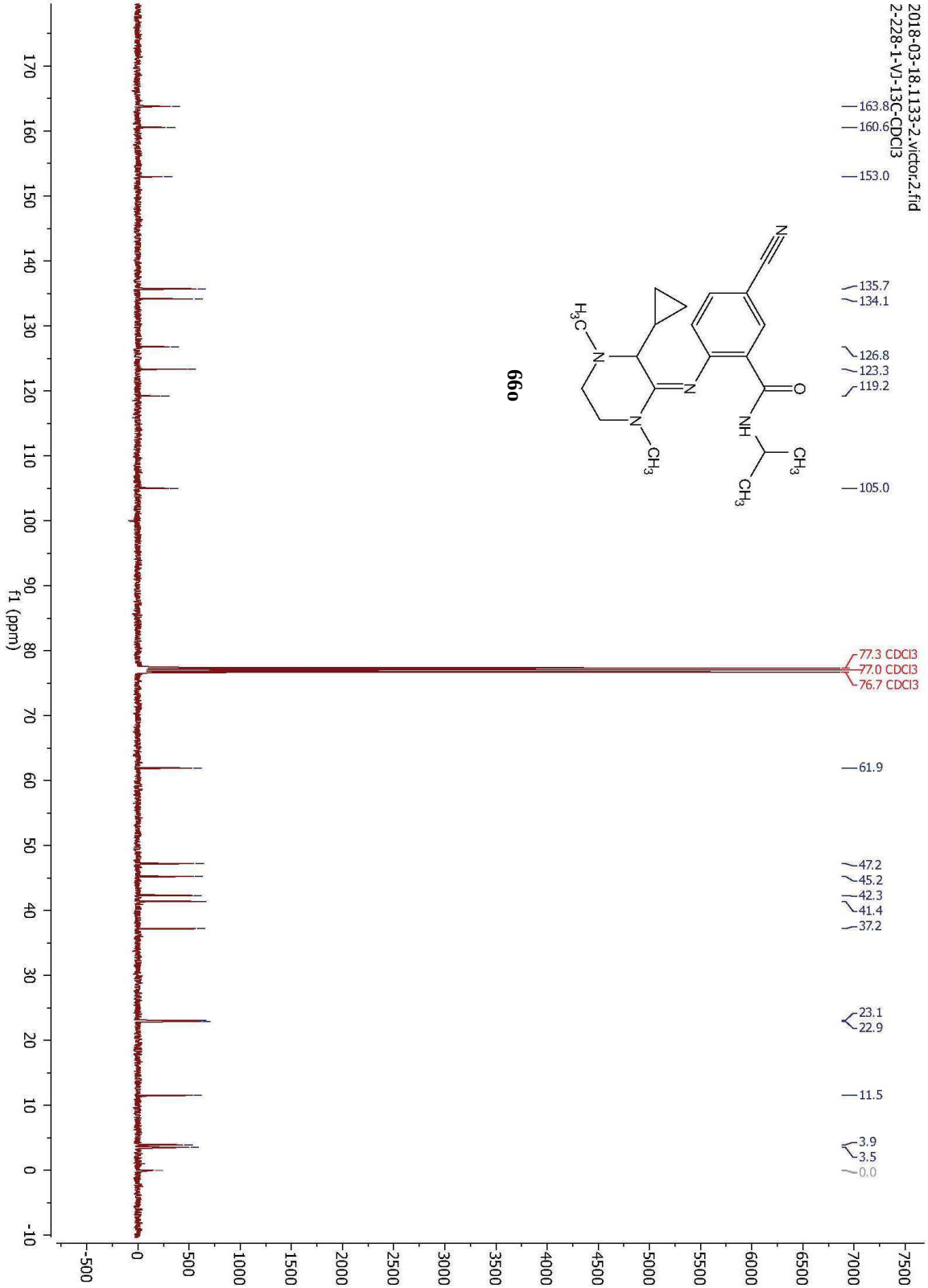
2018-03-18.1133-2.victor2.fid
2-228-1-VJ-13C-CDCl3
163.8
160.6
153.0
135.7
134.1
126.8
123.3
119.2
105.0
77.3 CDCl3
77.0 CDCl3
76.7 CDCl3
61.9
47.2
45.2
42.3
41.4
37.2
23.1
22.9
11.5
3.9
3.5
0.0
f1 (ppm)
69o

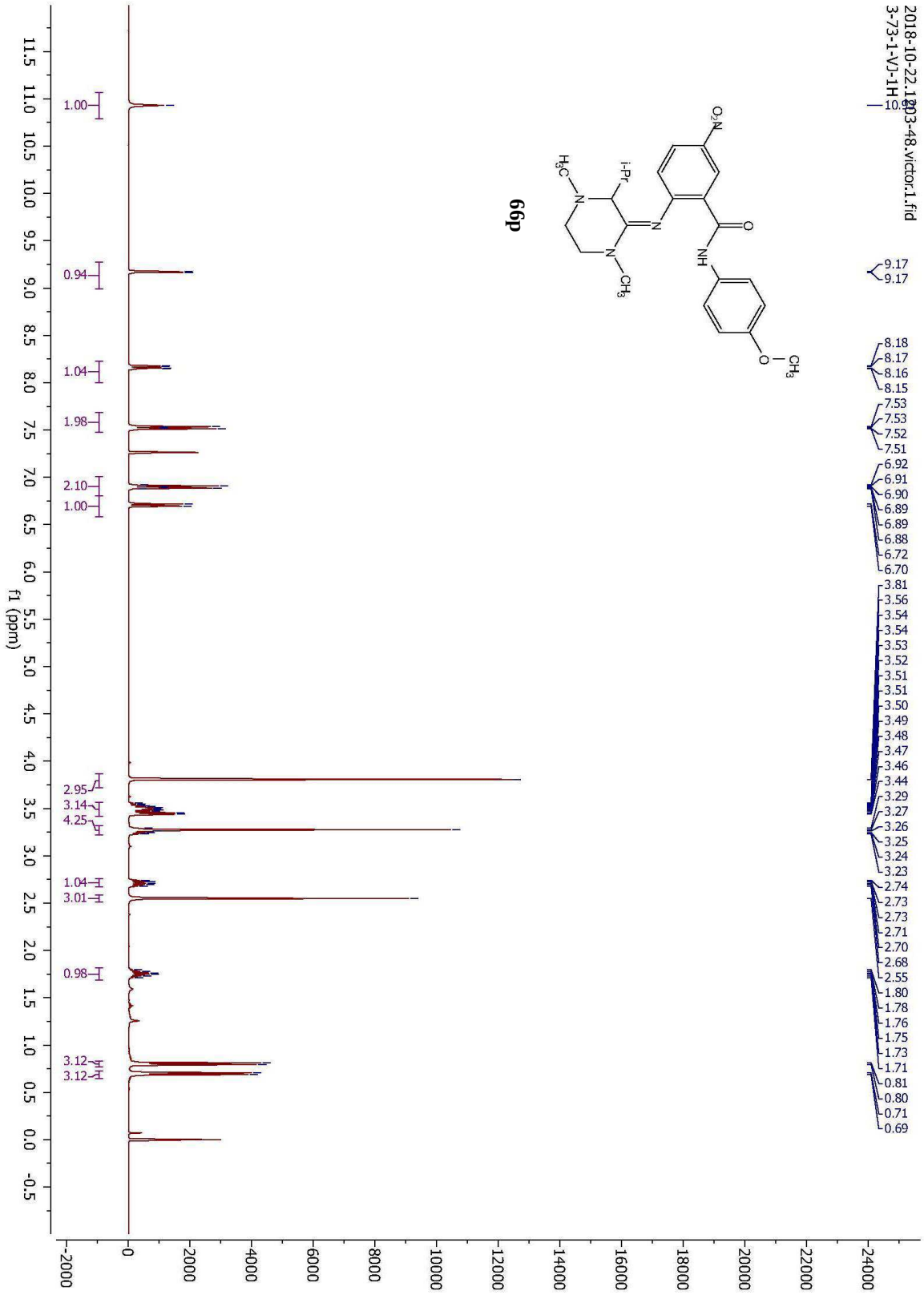
2018-10-22_1203-48.victor.1.fid
3-73-1-VJ-1H
69p
f1 (ppm)

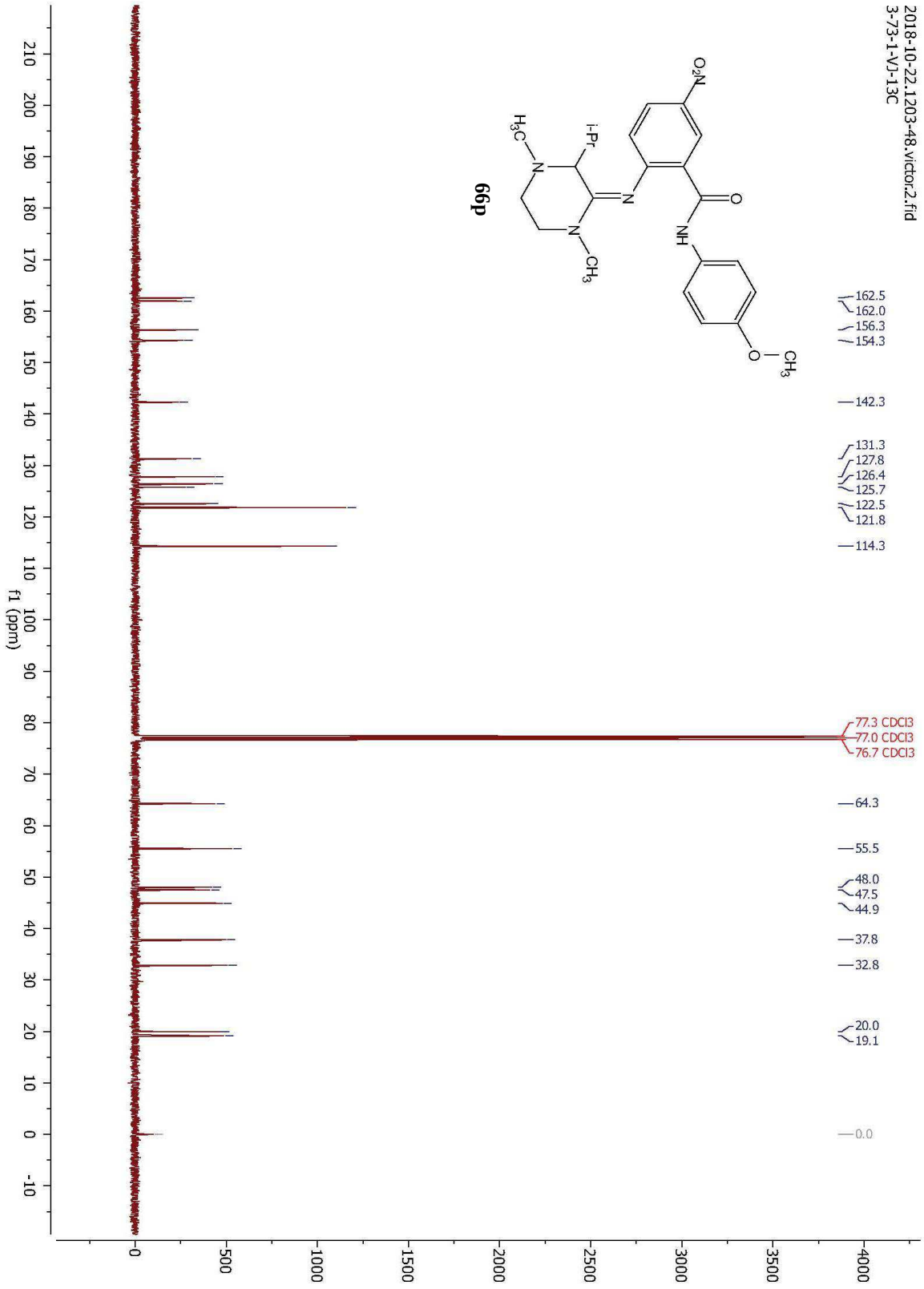
2018-10-22.1203-48.victor2.fid
3-73-1-VJ-13C
69p
O2N
H3C
i-Pr
N
N
CH3
O
NH
O
CH3
162.5
162.0
156.3
154.3
142.3
131.3
127.8
126.4
125.7
122.5
121.8
114.3
77.3 CDCl3
77.0 CDCl3
76.7 CDCl3
64.3
55.5
48.0
47.5
44.9
37.8
32.8
20.0
19.1
0.0
f1 (ppm)

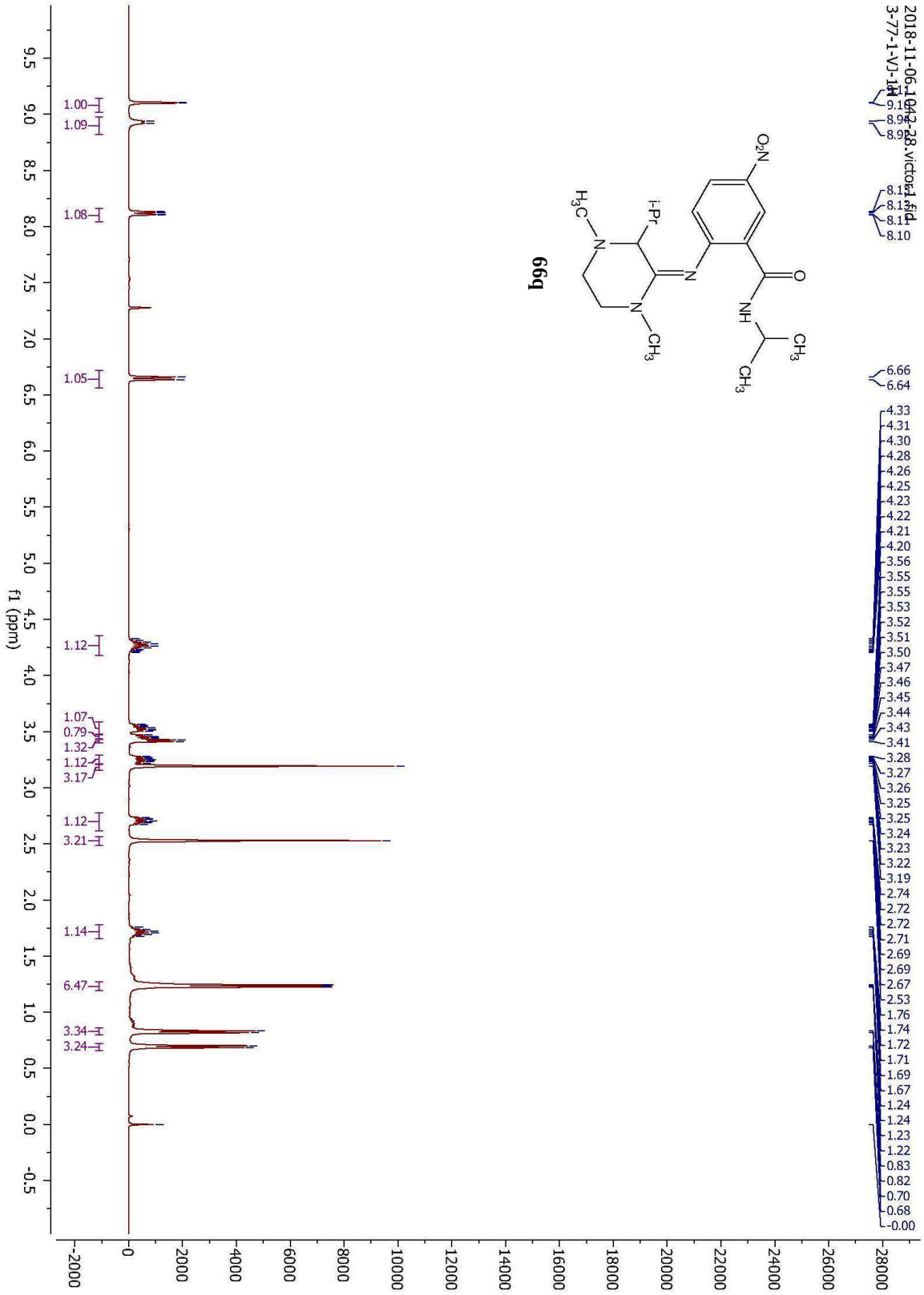
2018-11-06_1042-28_victoria_fid
3-77-1-VJ-1H
9.16
8.94
8.92
8.13
8.12
8.11
8.10
6.66
6.64
4.33
4.31
4.30
4.28
4.26
4.25
4.23
4.22
4.21
4.20
3.56
3.55
3.55
3.53
3.52
3.51
3.50
3.47
3.46
3.45
3.44
3.43
3.41
3.28
3.27
3.26
3.25
3.25
3.24
3.23
3.22
3.19
2.74
2.72
2.72
2.71
2.69
2.69
2.67
2.53
1.76
1.74
1.72
1.71
1.69
1.67
1.24
1.24
1.23
1.22
0.83
0.82
0.70
0.68
-0.00
1.00
1.09
1.08
1.05
1.12
1.07
0.79
1.32
1.12
3.17
1.12
3.21
1.14
6.47
3.34
3.24
f1 (ppm)
9.5
9.0
8.5
8.0
7.5
7.0
6.5
6.0
5.5
5.0
4.5
4.0
3.5
3.0
2.5
2.0
1.5
1.0
0.5
0.0
-0.5
-2000
0
2000
4000
6000
8000
10000
12000
14000
16000
18000
20000
22000
24000
26000
28000

6gg

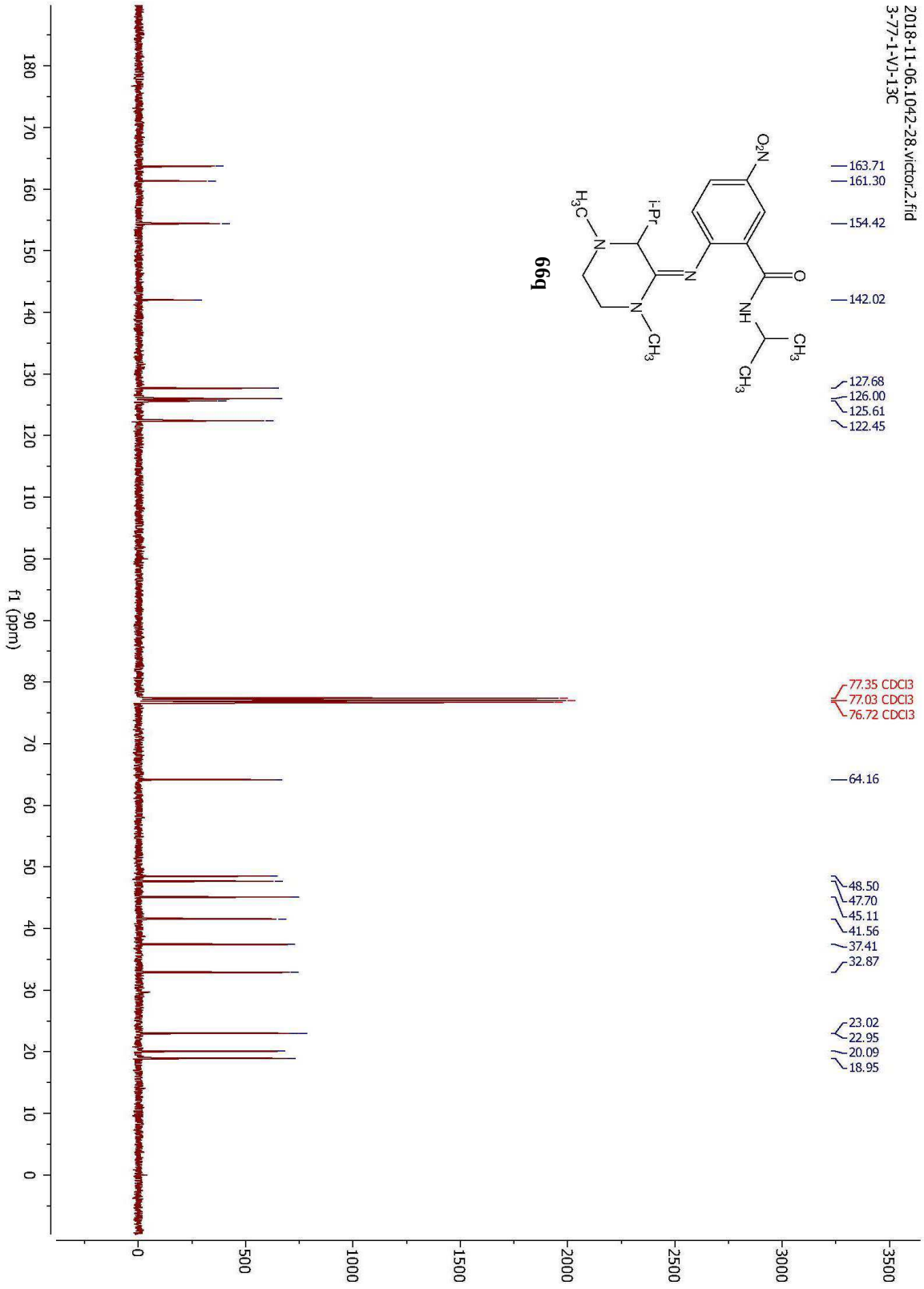
2018-11-06.1042-28.victor2.fid
3-77-1-VJ-13C
69g
163.71
161.30
154.42
142.02
127.68
126.00
125.61
122.45
77.35 CDCl3
77.03 CDCl3
76.72 CDCl3
64.16
48.50
47.70
45.11
41.56
37.41
32.87
23.02
22.95
20.09
18.95
f1 (ppm)

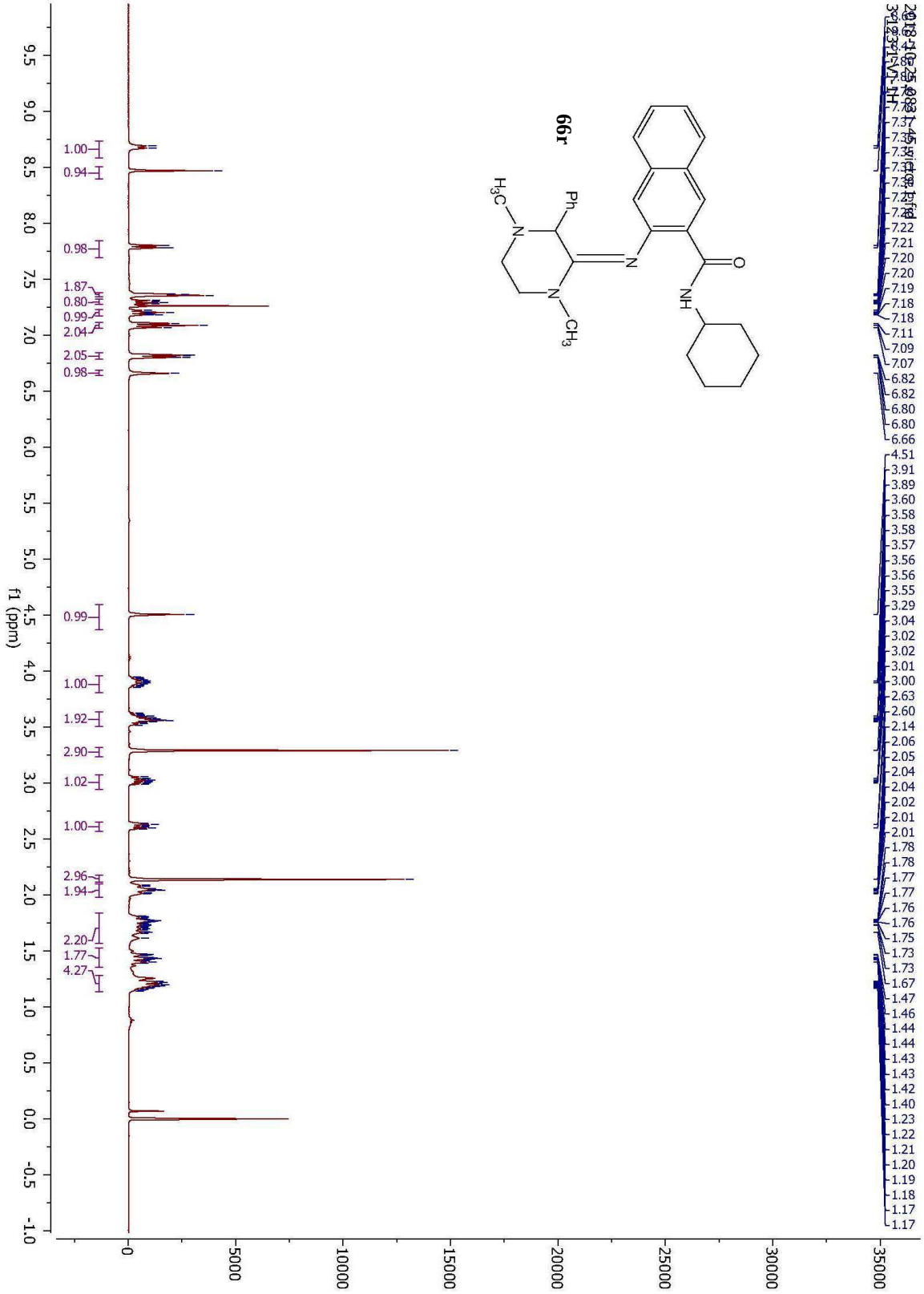
66r
f1 (ppm)

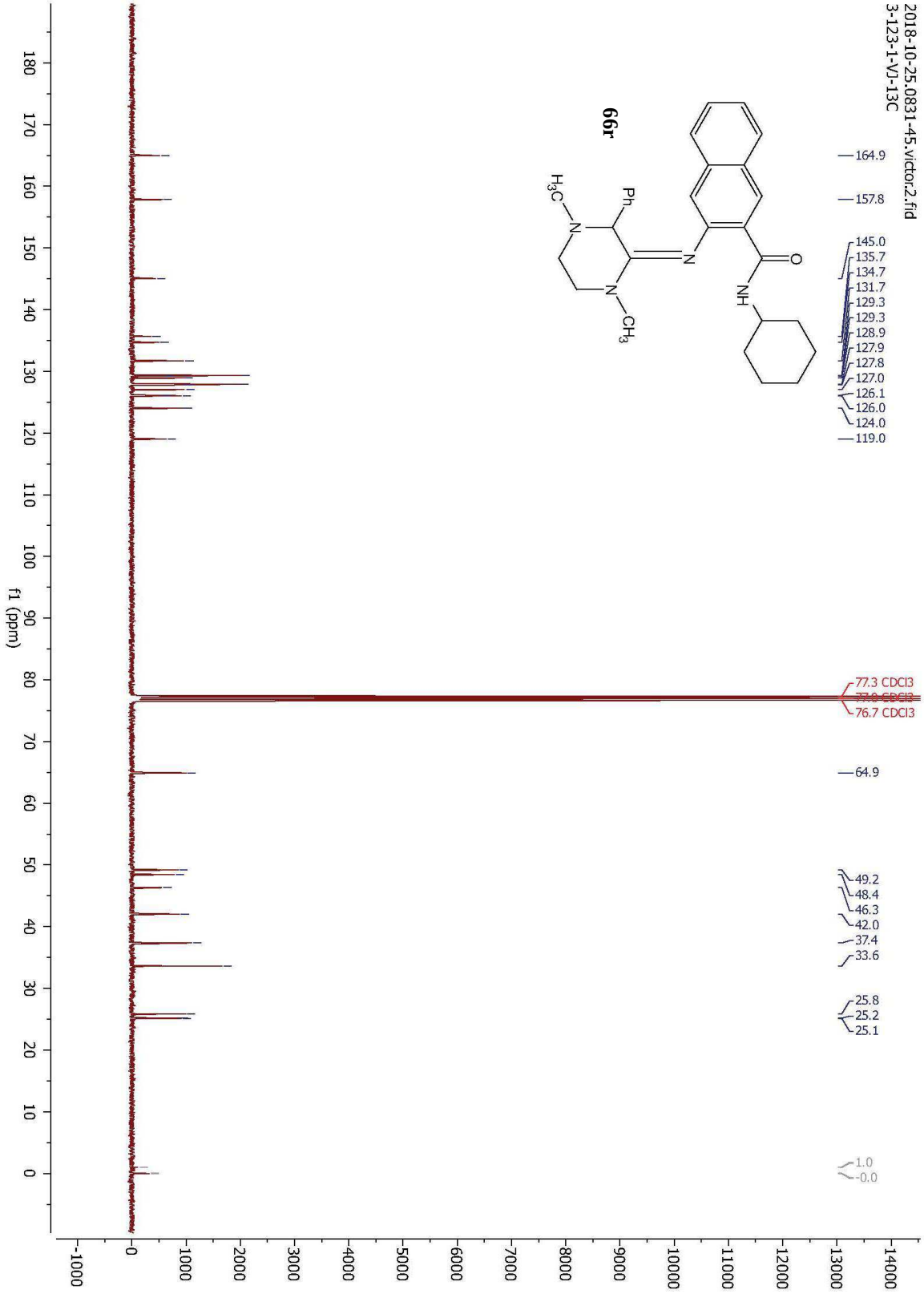
2018-10-25.0831-45.victor.2.fid
3-123-1-VJ-13C
66r
164.9
157.8
145.0
135.7
134.7
131.7
129.3
129.3
128.9
127.9
127.8
127.0
126.1
126.0
124.0
119.0
77.3 CDCl3
76.7 CDCl3
64.9
49.2
48.4
46.3
42.0
37.4
33.6
25.8
25.2
25.1
1.0
-0.0
f1 (ppm)

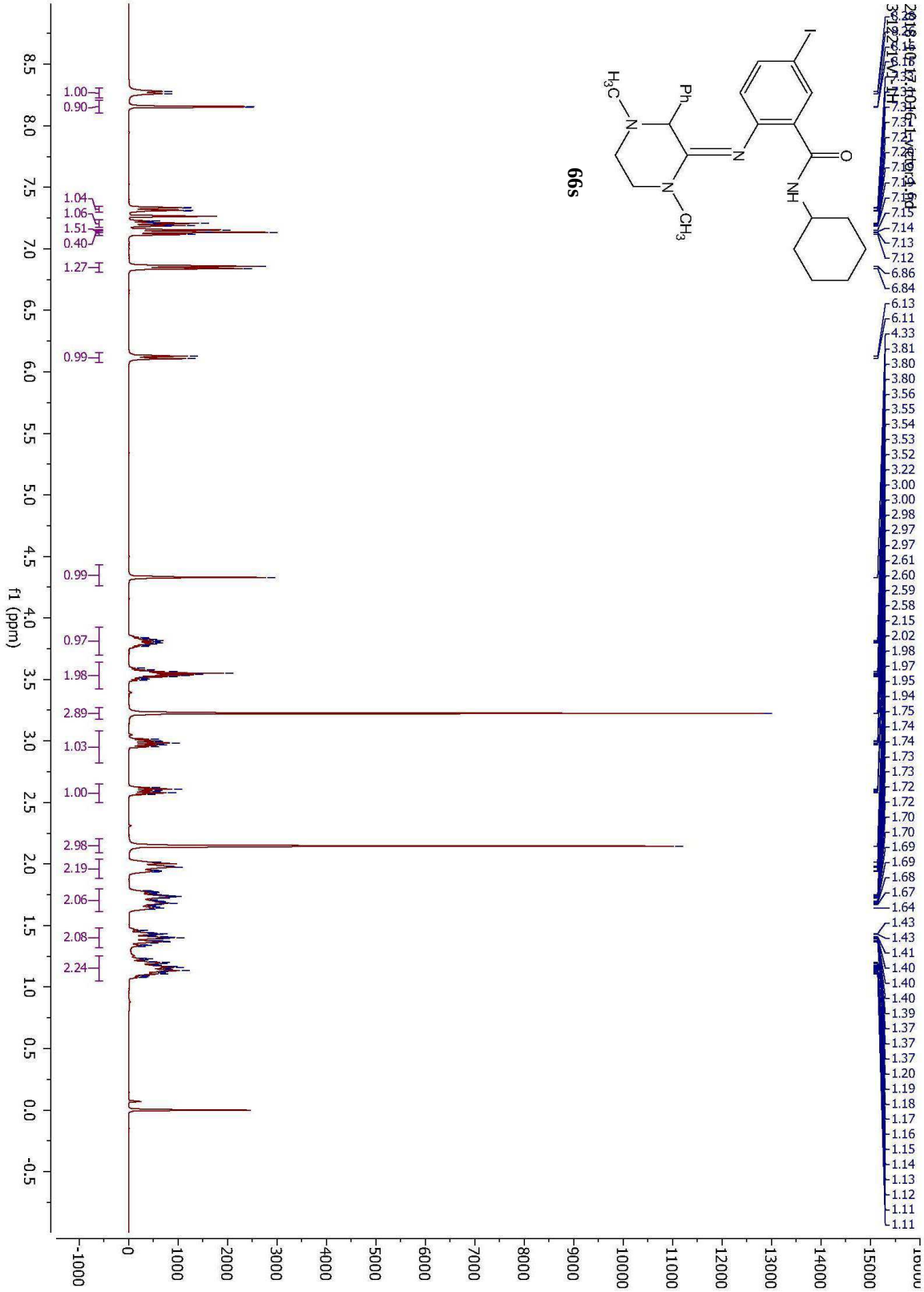
66s
f1 (ppm)

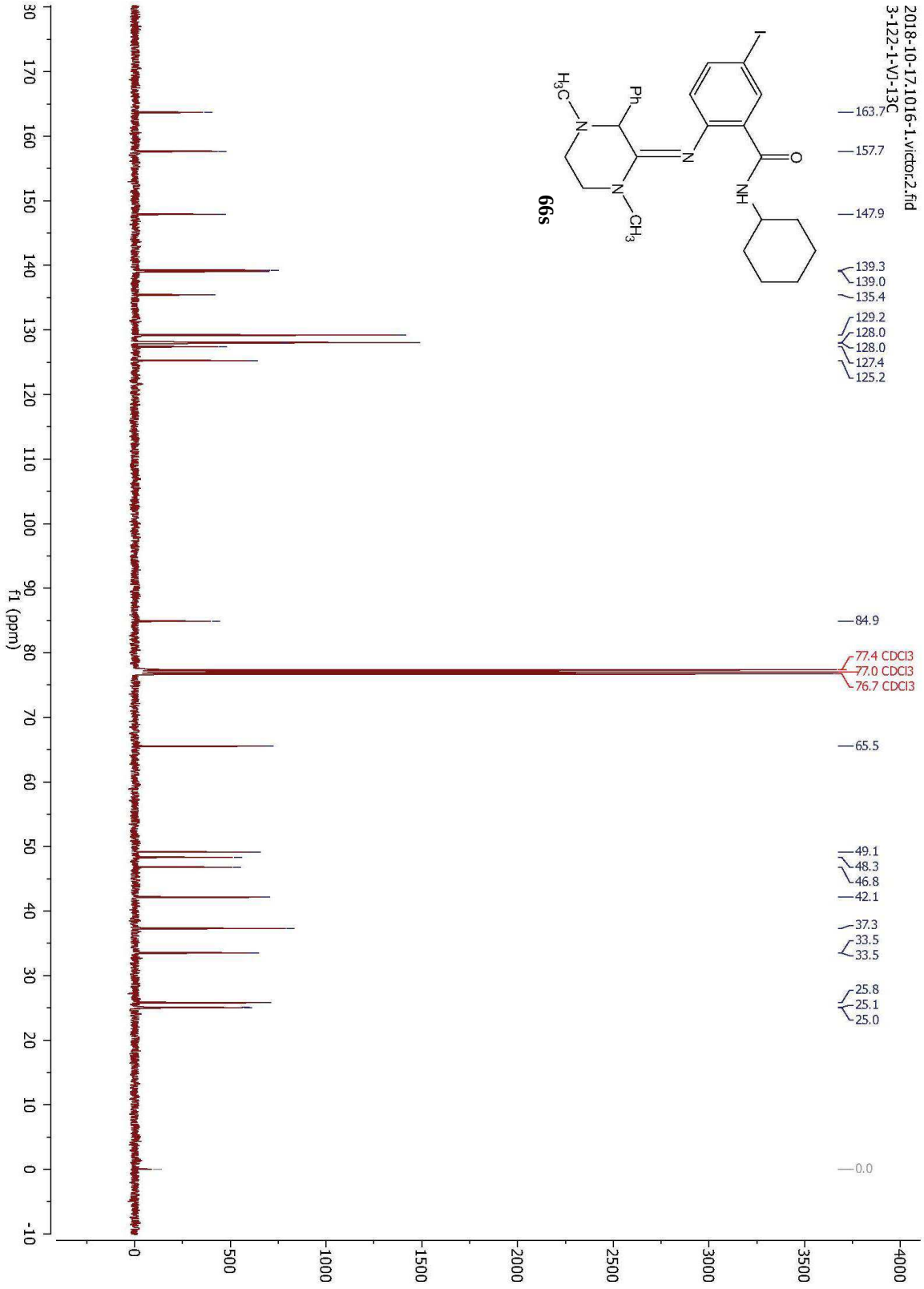
2018-10-17.1016-1.victor2.fid
3-122-1-VJ-13C
66s
163.7
157.7
147.9
139.3
139.0
135.4
129.2
128.0
128.0
127.4
125.2
84.9
77.4 CDCl3
77.0 CDCl3
76.7 CDCl3
65.5
49.1
48.3
46.8
42.1
37.3
33.5
33.5
25.8
25.1
25.0
0.0
f1 (ppm)

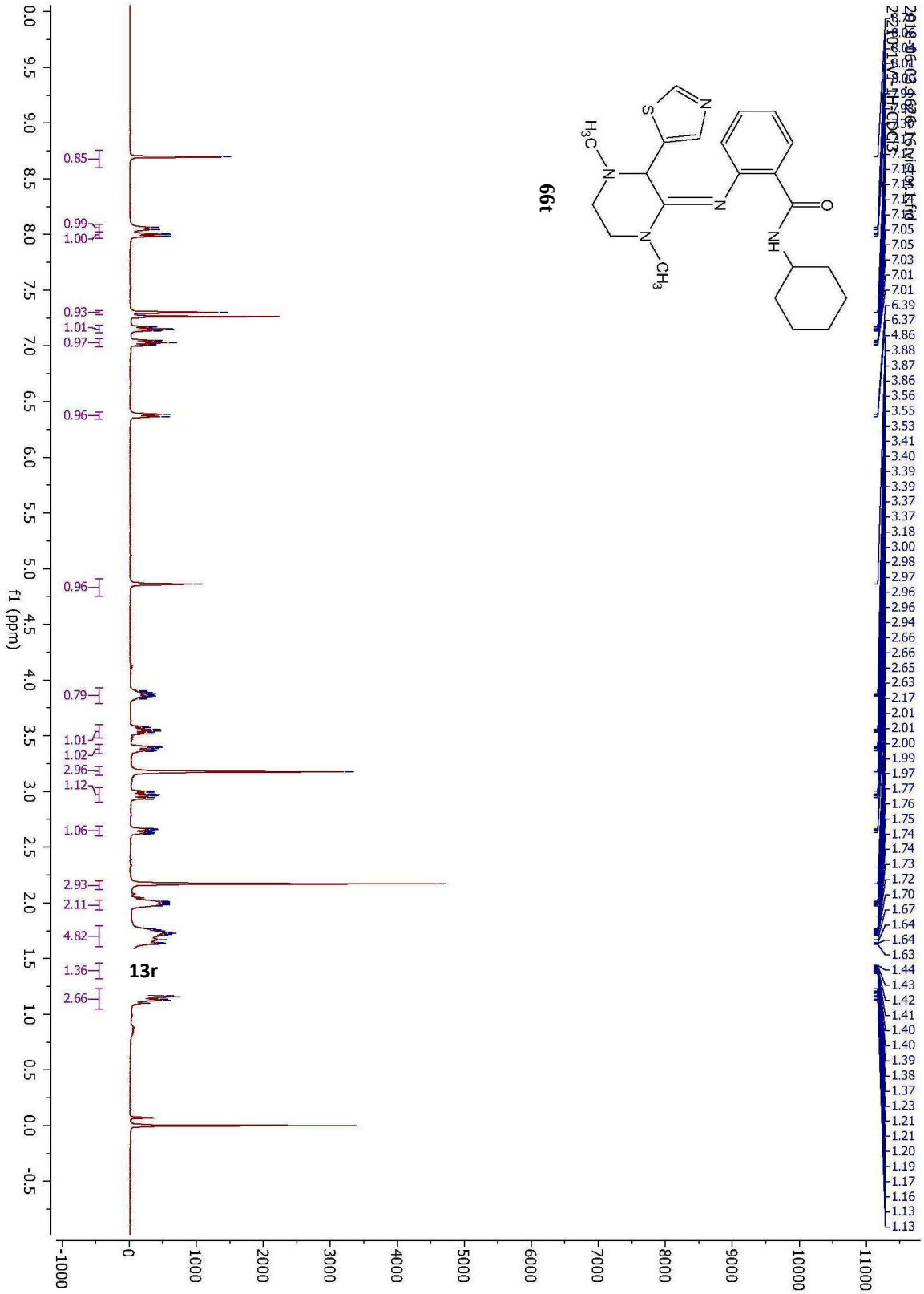
13r
199
f1 (ppm)

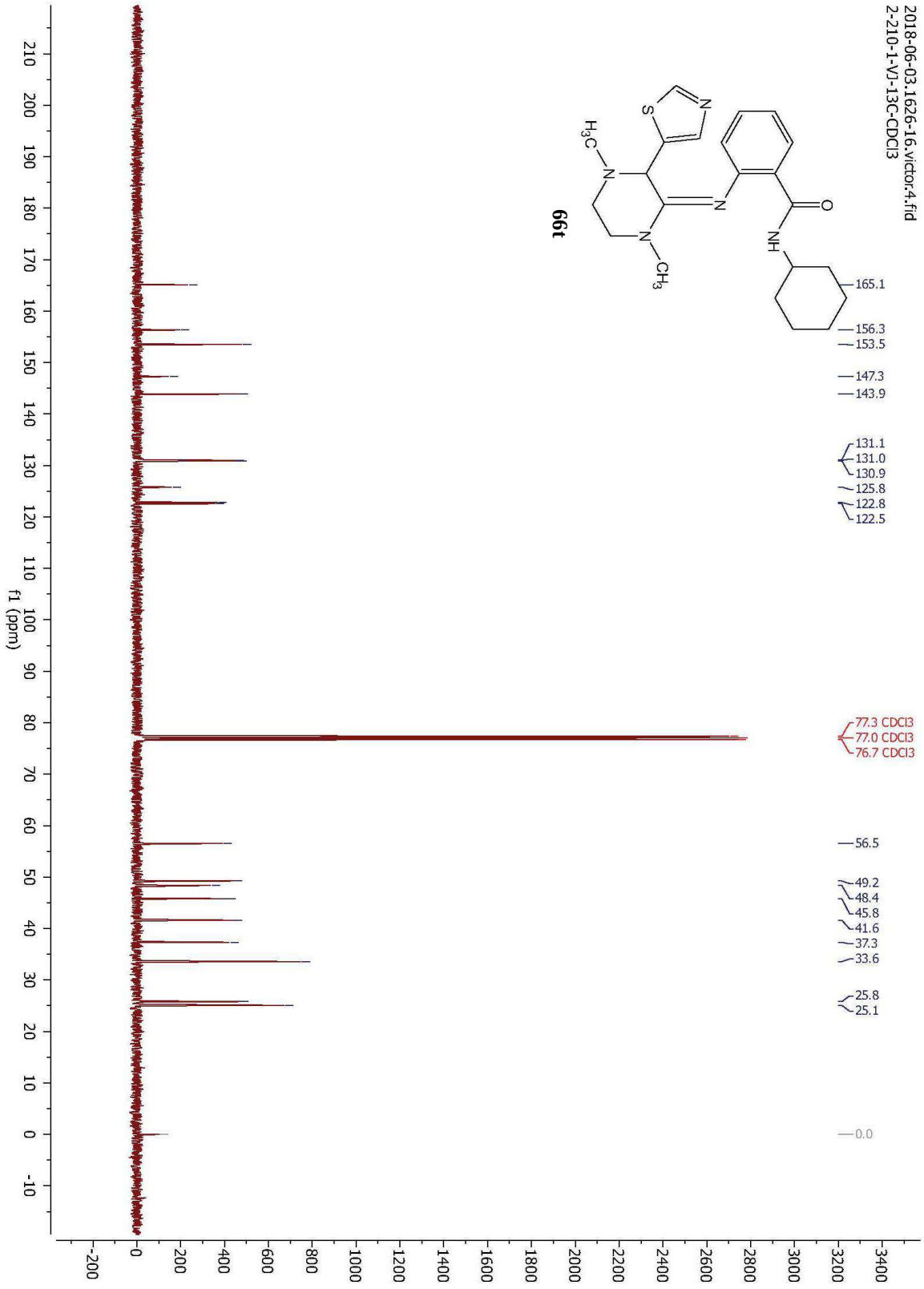
2018-06-03.1626-16.victor.4.fid
2-210-1-VJ-13C-CDCl3
66t
165.1
156.3
153.5
147.3
143.9
131.1
131.0
130.9
125.8
122.8
122.5
77.3 CDCl3
77.0 CDCl3
76.7 CDCl3
56.5
49.2
48.4
45.8
41.6
37.3
33.6
25.8
25.1
0.0
f1 (ppm)

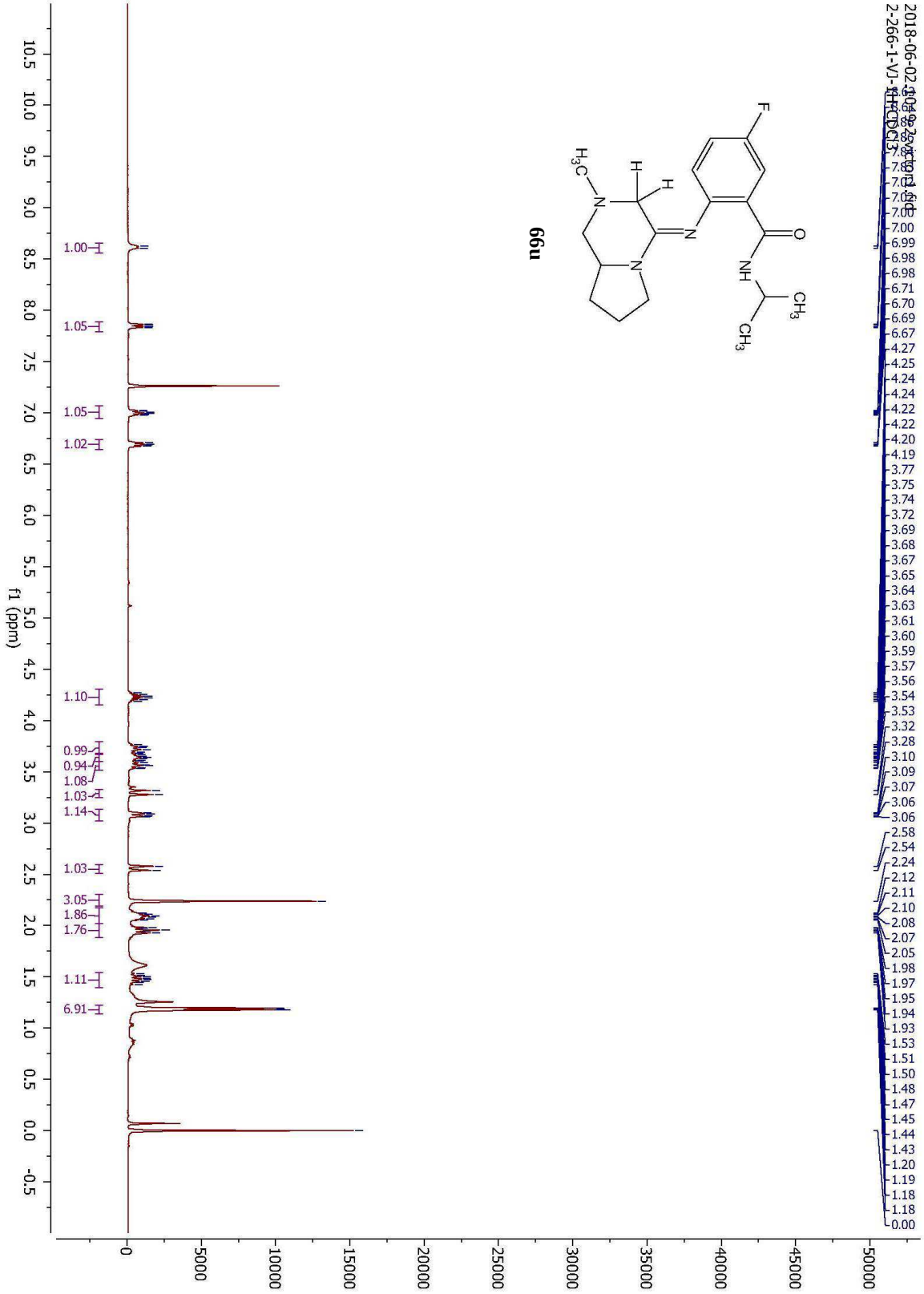
6gn
f1 (ppm)
1.00
1.05
1.05
1.02
1.10
0.99
0.94
1.08
1.03
1.14
1.03
3.05
1.86
1.76
1.11
6.91

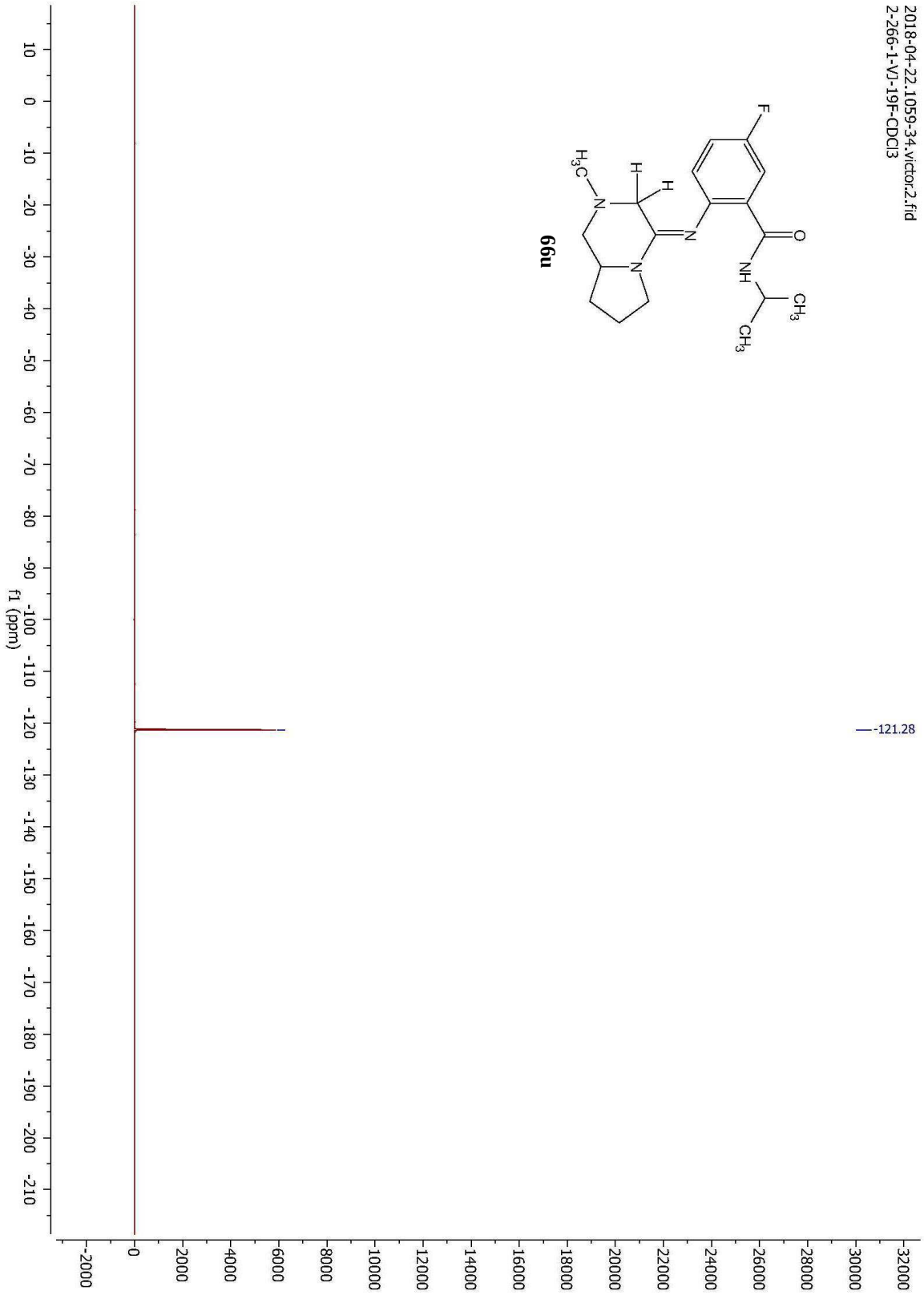

9gu

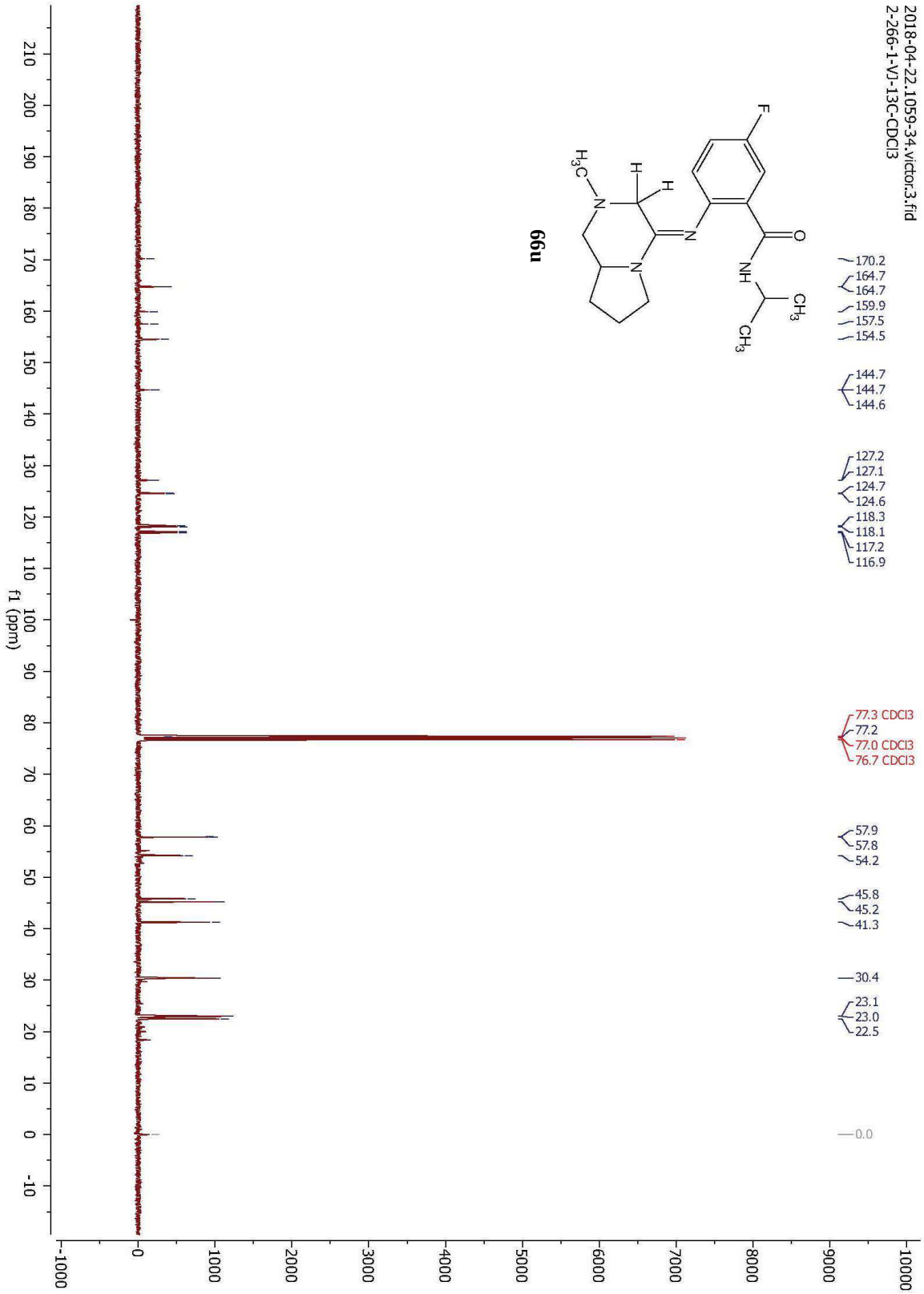
2018-04-22.1059-34.victor.3.fid
2-266-1-VJ-13C-CDCl3
n99
170.2
164.7
164.7
159.9
157.5
154.5
144.7
144.7
144.6
127.2
127.1
124.7
124.6
118.3
118.1
117.2
116.9
77.3 CDCl3
77.2
77.0 CDCl3
76.7 CDCl3
57.9
57.8
54.2
45.8
45.2
41.3
30.4
23.1
23.0
22.5
0.0
f1 (ppm)

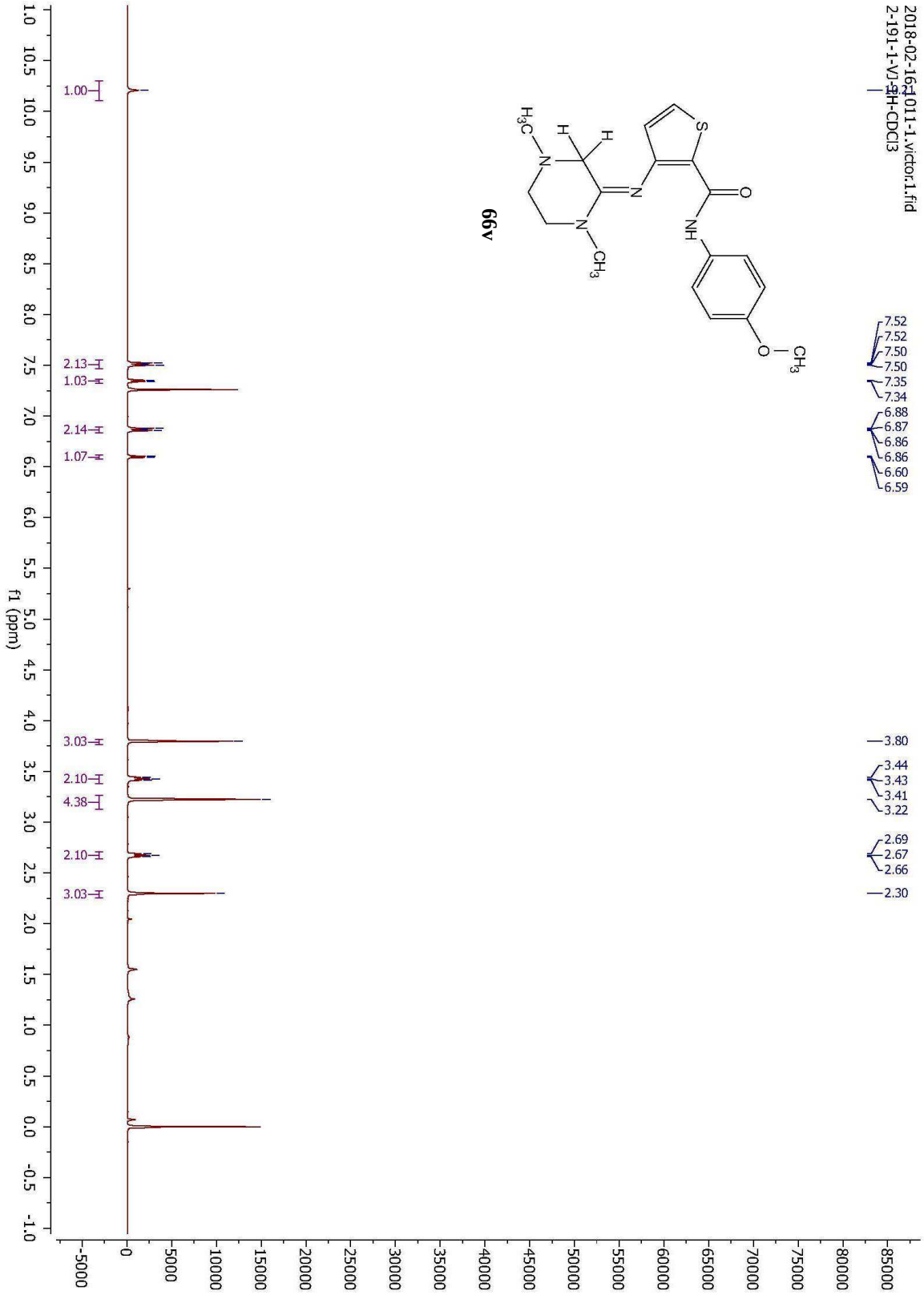
2018-02-16-1011-1.victor.1.fid
2-191-1-VJ-1H-CDCl3
66a
7.52
7.52
7.50
7.50
7.35
7.34
6.88
6.87
6.86
6.86
6.60
6.59
3.80
3.44
3.43
3.41
3.22
2.69
2.67
2.66
2.30
1.00
2.13
1.03
2.14
1.07
3.03
2.10
4.38
2.10
3.03
f1 (ppm)

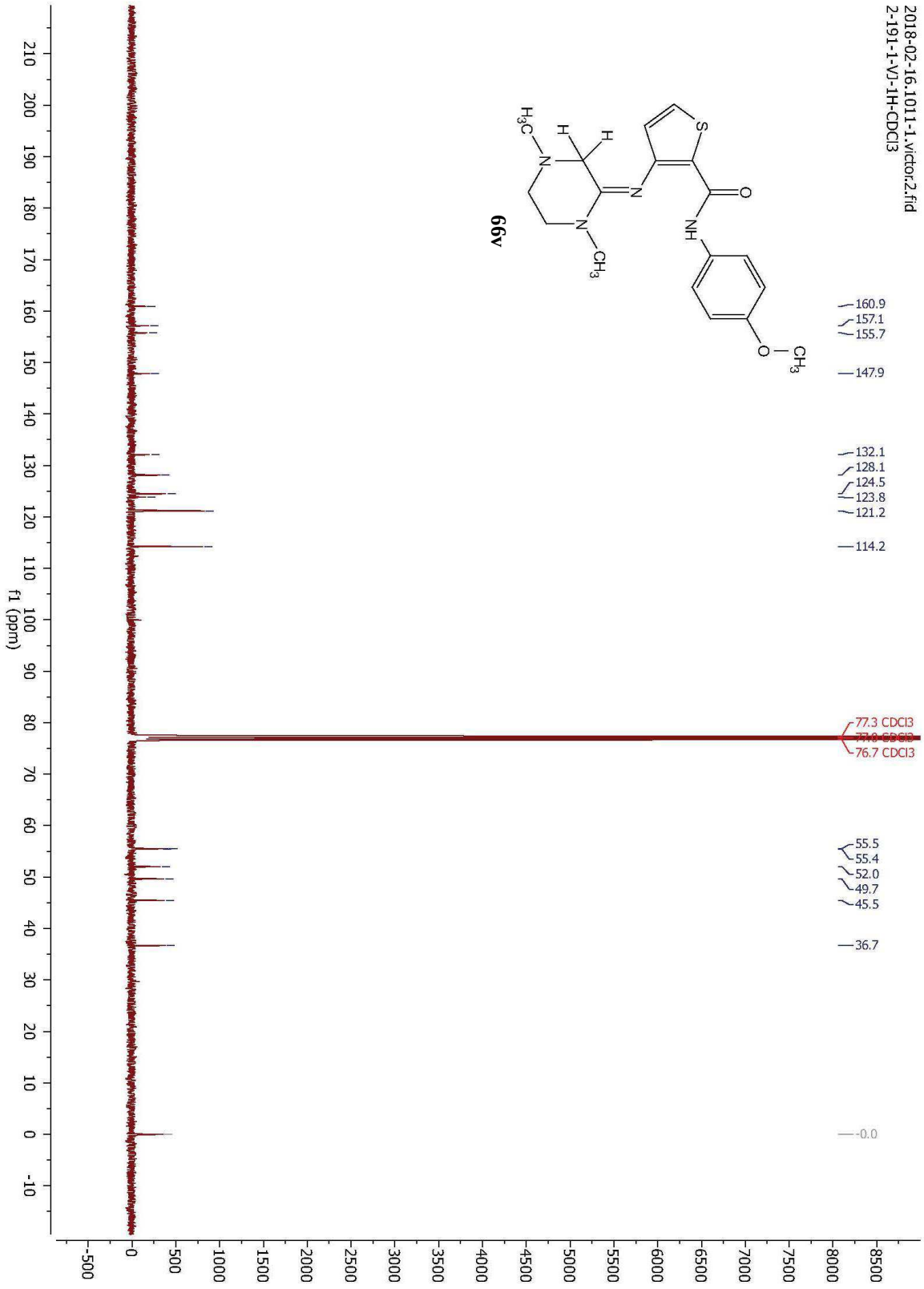
2018-02-16.1011-1.victor2.fid
2-191-1-VJ-1H-CDCl3
66v
160.9
157.1
155.7
147.9
132.1
128.1
124.5
123.8
121.2
114.2
77.3 CDCl3
77.0 CDCl3
76.7 CDCl3
55.5
55.4
52.0
49.7
45.5
36.7
-0.0
f1 (ppm)

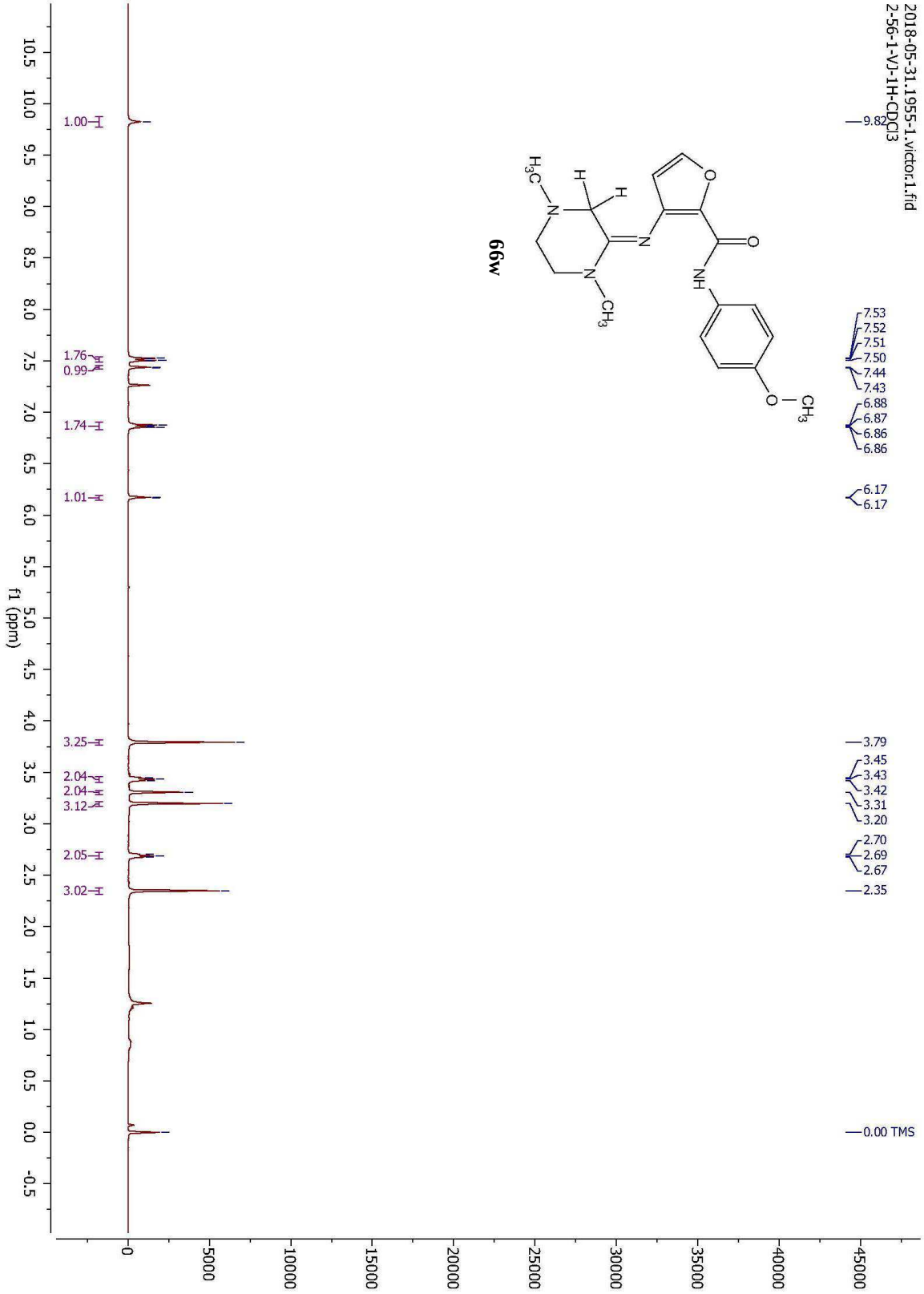
2018-05-31.1955-1.victor.1.fid
2-56-1-VJ-1H-CDCl3
66w
9.82
7.53
7.52
7.51
7.50
7.44
7.43
6.88
6.87
6.86
6.86
6.17
6.17
3.79
3.45
3.43
3.42
3.31
3.20
2.70
2.69
2.67
2.35
0.00 TMS
1.00
1.76
0.99
1.74
1.01
3.25
2.04
2.04
3.12
2.05
3.02
f1 (ppm)

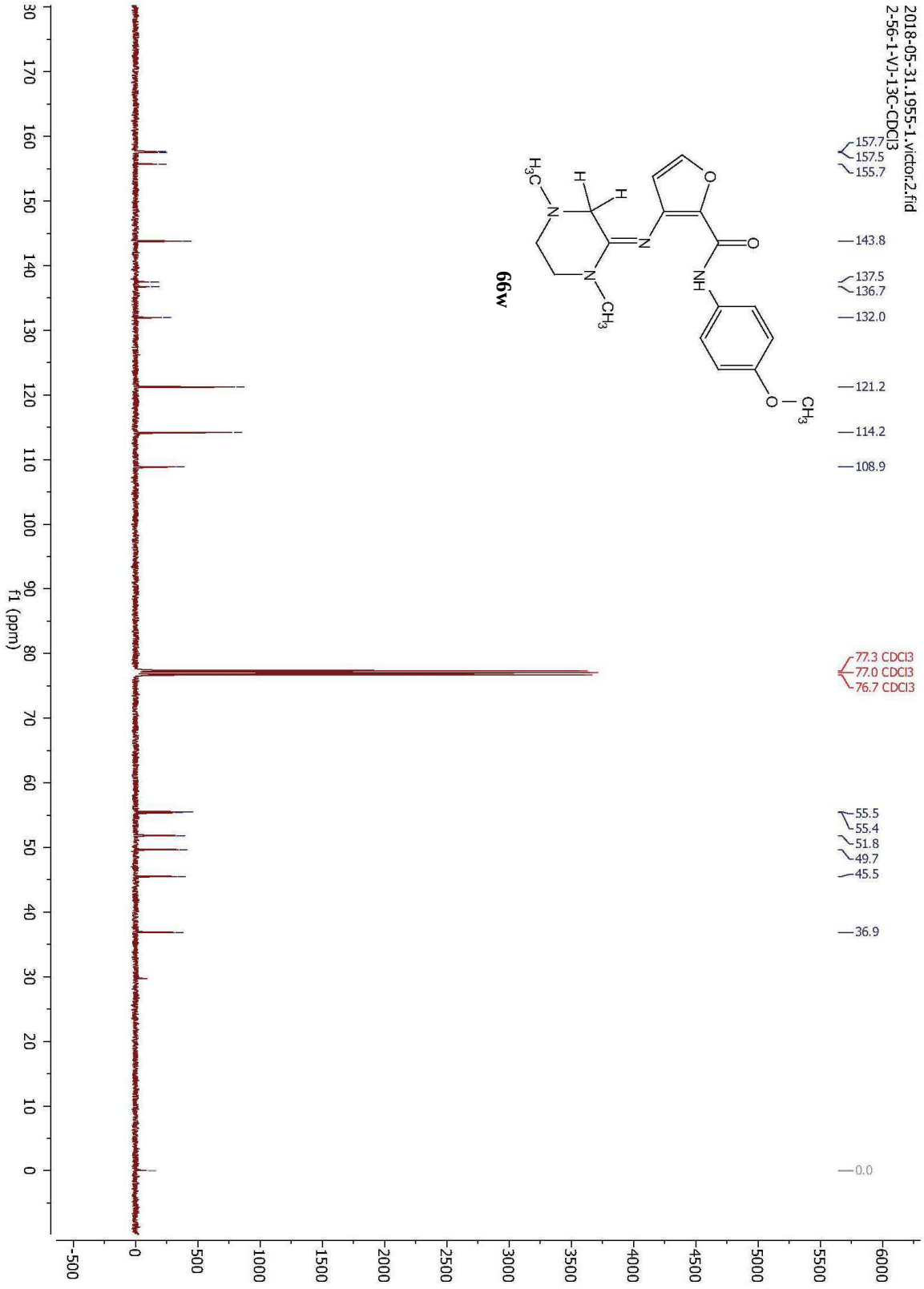
2018-05-31.1955-1.victor2.fid
2-56-1-VJ-13C-CDCl3
157.7
157.5
155.7
143.8
137.5
136.7
132.0
121.2
114.2
108.9
77.3 CDCl3
77.0 CDCl3
76.7 CDCl3
55.5
55.4
51.8
49.7
45.5
36.9
0.0
f1 (ppm)
66w

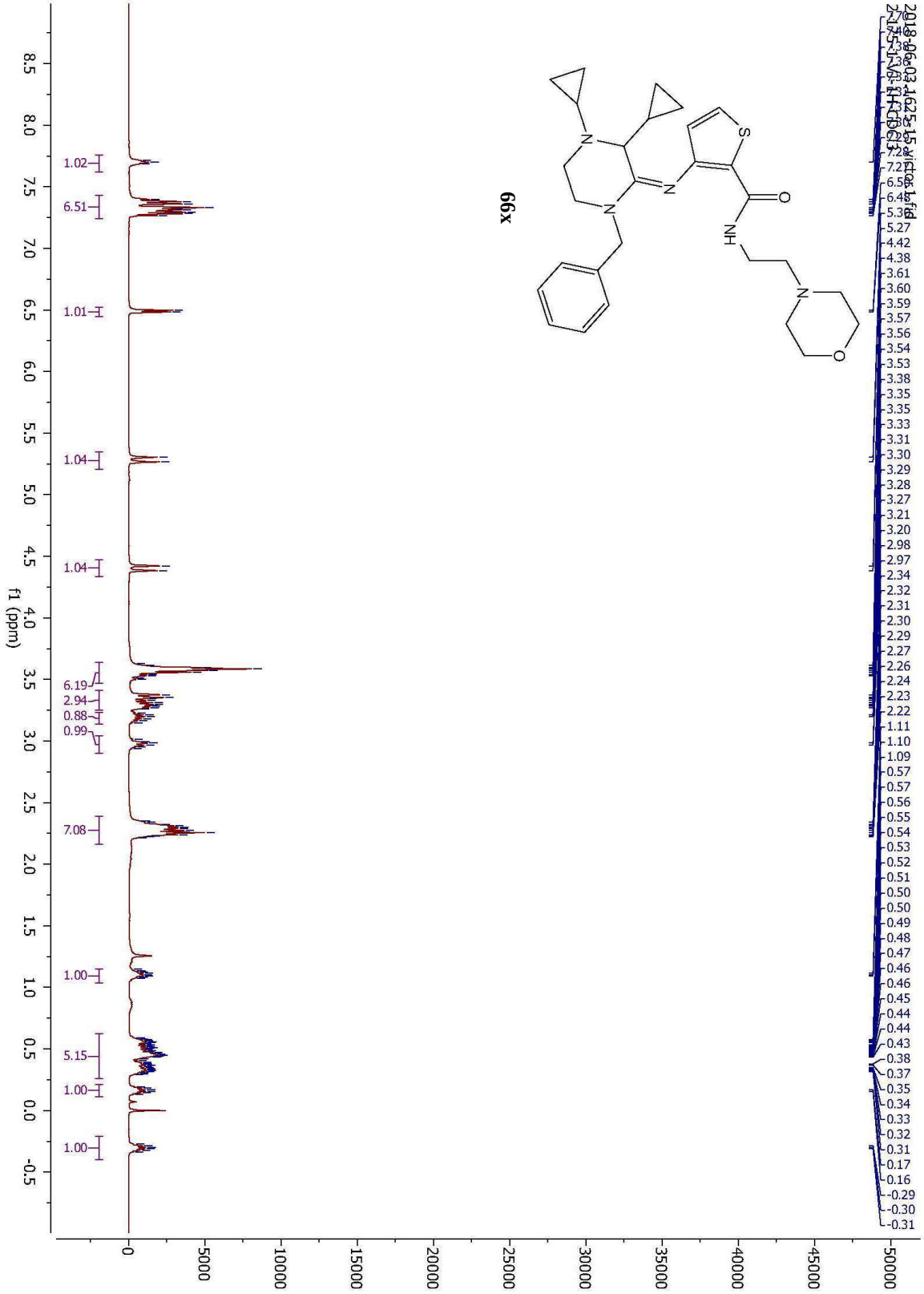
66x
f1 (ppm)
1.02
6.51
1.01
1.04
1.04
6.19
2.94
0.88
0.99
7.08
1.00
5.15
1.00
1.00

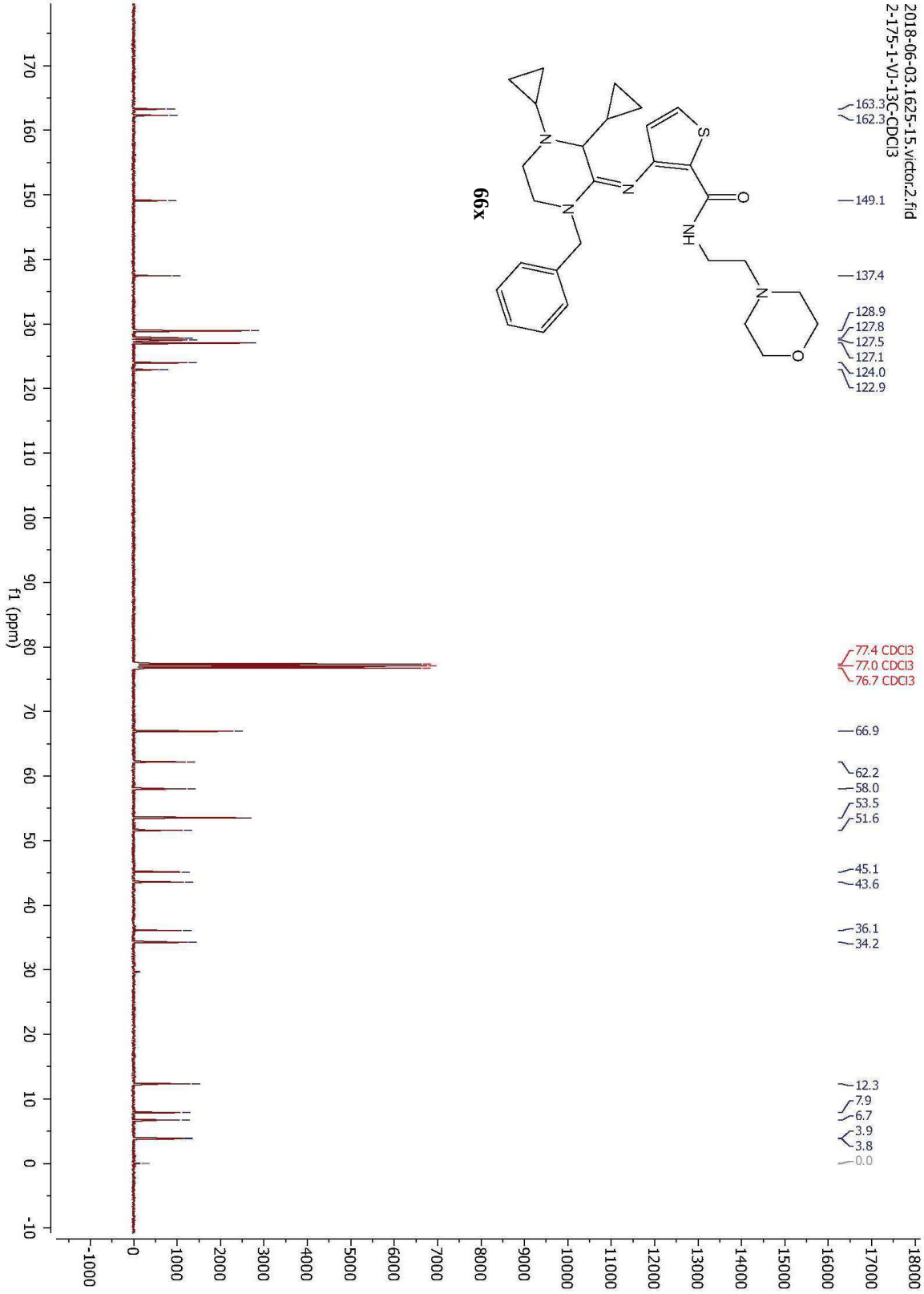
2018-06-03.1625-15.victor.2.fid
2-175-1-VJ-13C-CDCl3
x99
163.3
162.3
149.1
137.4
128.9
127.8
127.5
127.1
124.0
122.9
77.4 CDCl3
77.0 CDCl3
76.7 CDCl3
66.9
62.2
58.0
53.5
51.6
45.1
43.6
36.1
34.2
12.3
7.9
6.7
3.9
3.8
0.0
f1 (ppm)

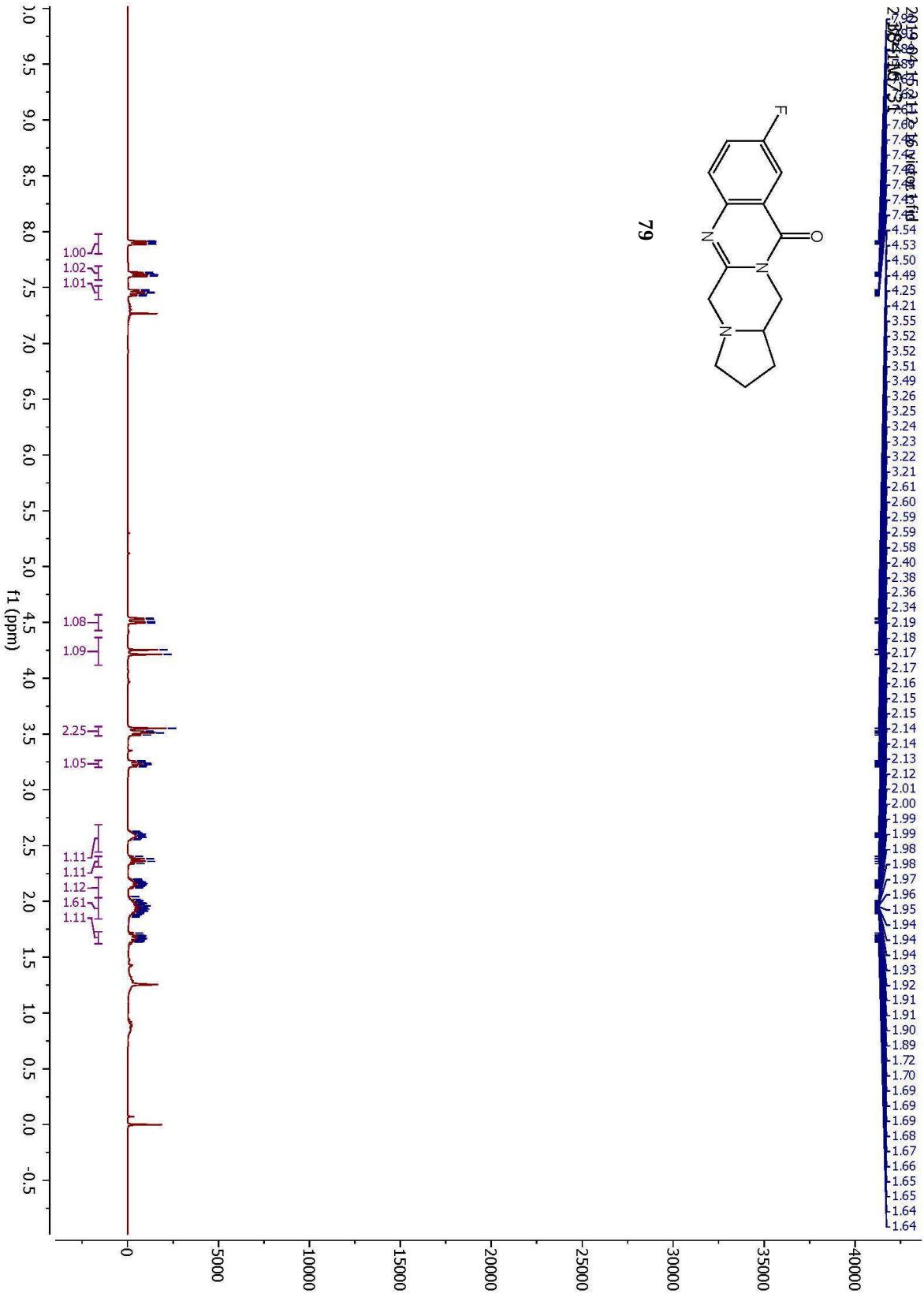
79
F
N
N
N
O
f1 (ppm)
1.00
1.02
1.01
1.08
1.09
2.25
1.05
1.11
1.11
1.12
1.61
1.11

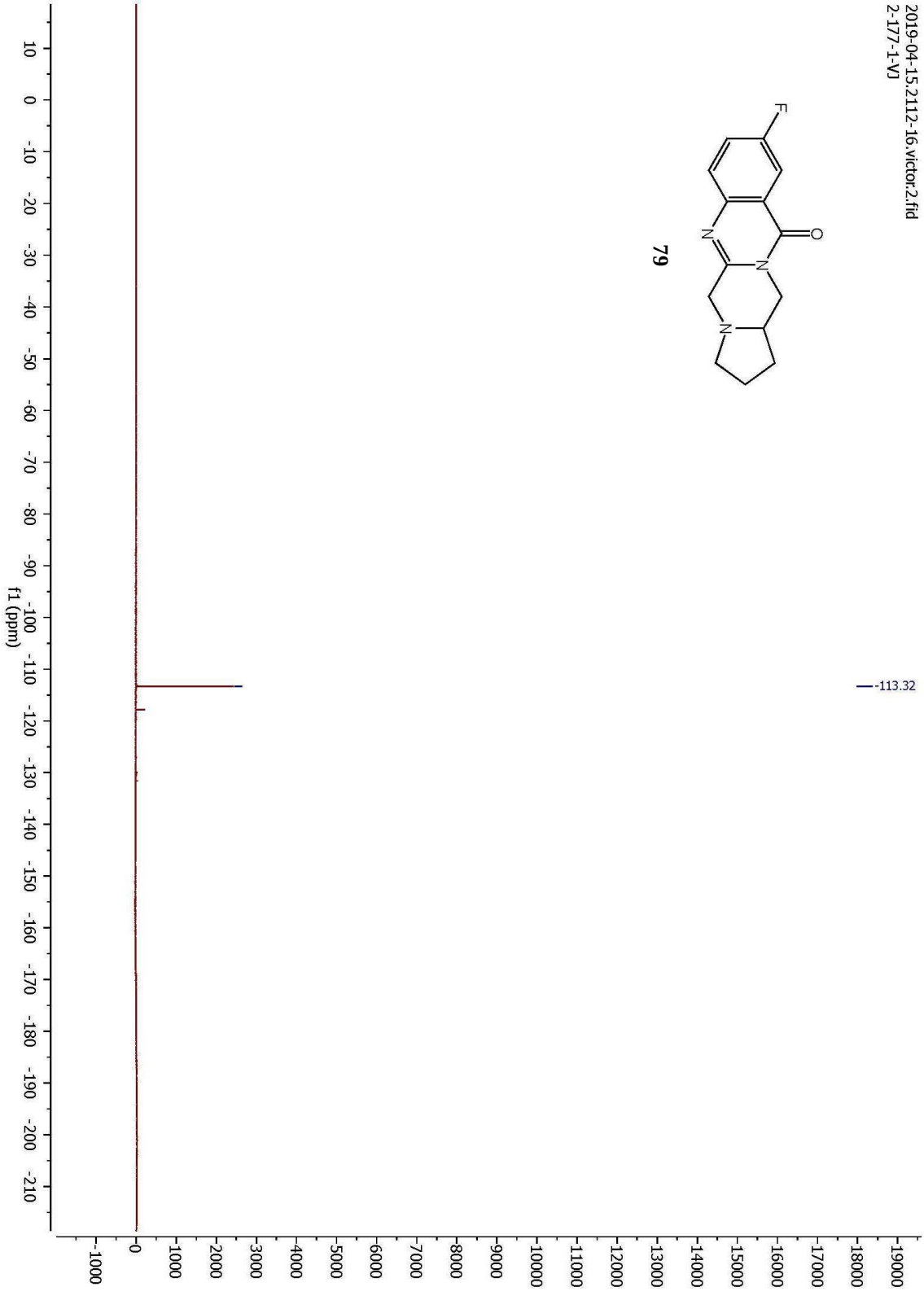
2019-04-15.2112-16.victor.2.fid
2-177-1-VJ
F
O
N
N
N
79
-113.32
f1 (ppm)
10
0
-10
-20
-30
-40
-50
-60
-70
-80
-90
-100
-110
-120
-130
-140
-150
-160
-170
-180
-190
-200
-210
19000
18000
17000
16000
15000
14000
13000
12000
11000
10000
9000
8000
7000
6000
5000
4000
3000
2000
1000
0
-1000

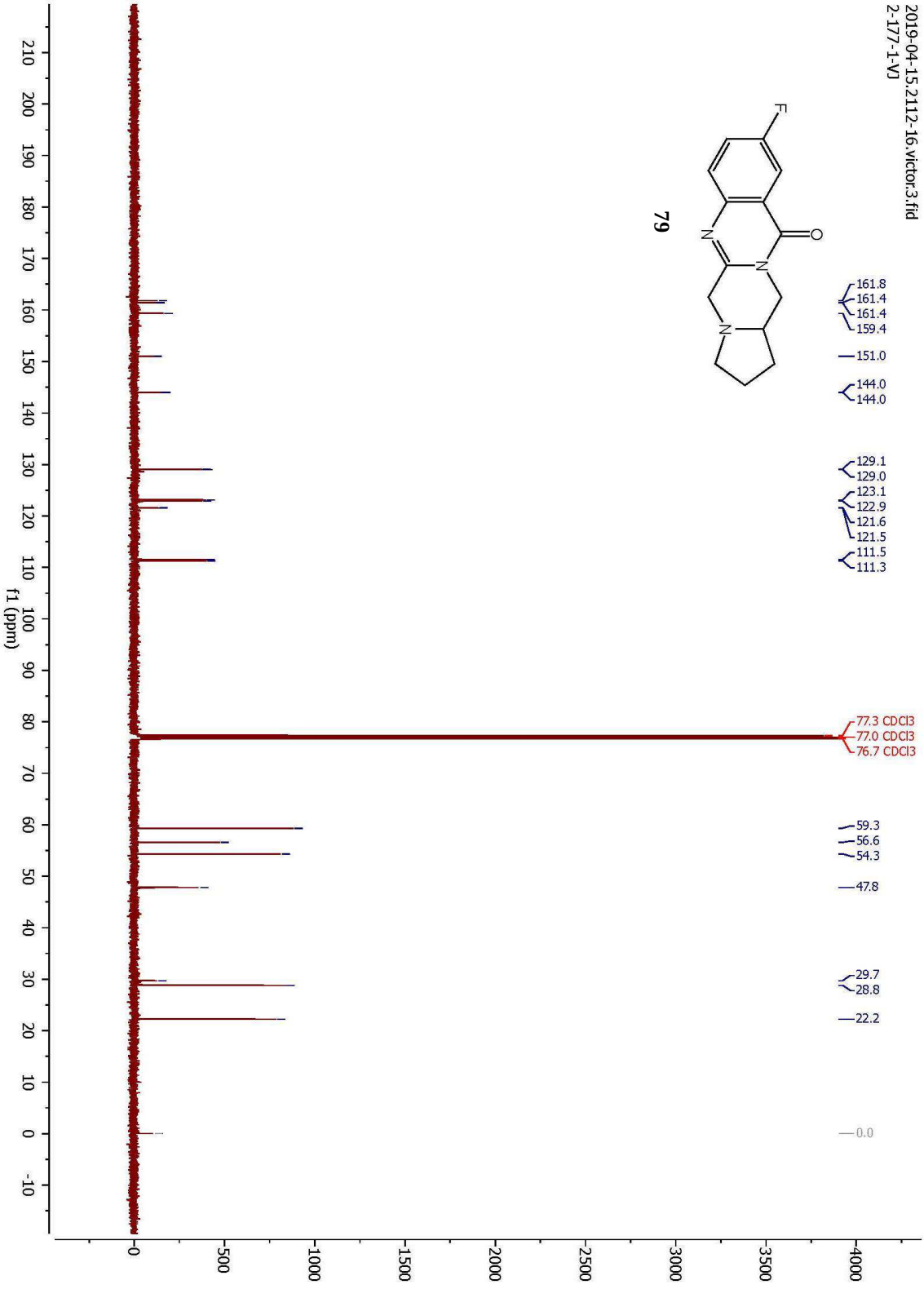
2019-04-15.2112-16.victor.3.fid
2-177-1-VJ
79
F
O
N
N
N
161.8
161.4
161.4
159.4
151.0
144.0
144.0
129.1
129.0
123.1
122.9
121.6
121.5
111.5
111.3
77.3 CDCl3
77.0 CDCl3
76.7 CDCl3
59.3
56.6
54.3
47.8
29.7
28.8
22.2
0.0
f1 (ppm)

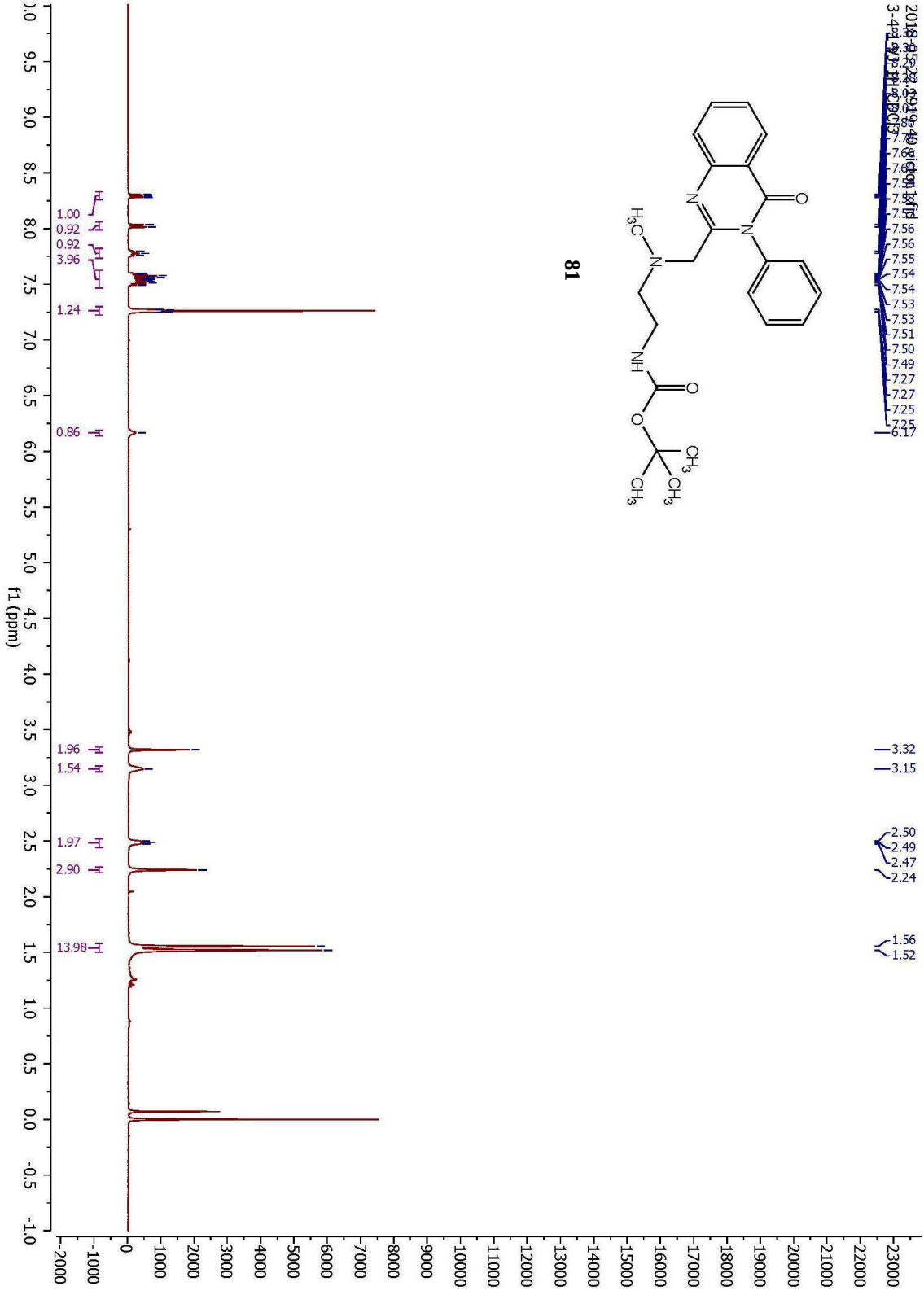
81
f1 (ppm)
1.00
0.92
0.92
3.96
1.24
0.86
1.96
1.54
1.97
2.90
13.98
3.32
3.15
2.50
2.49
2.47
2.24
1.56
1.52

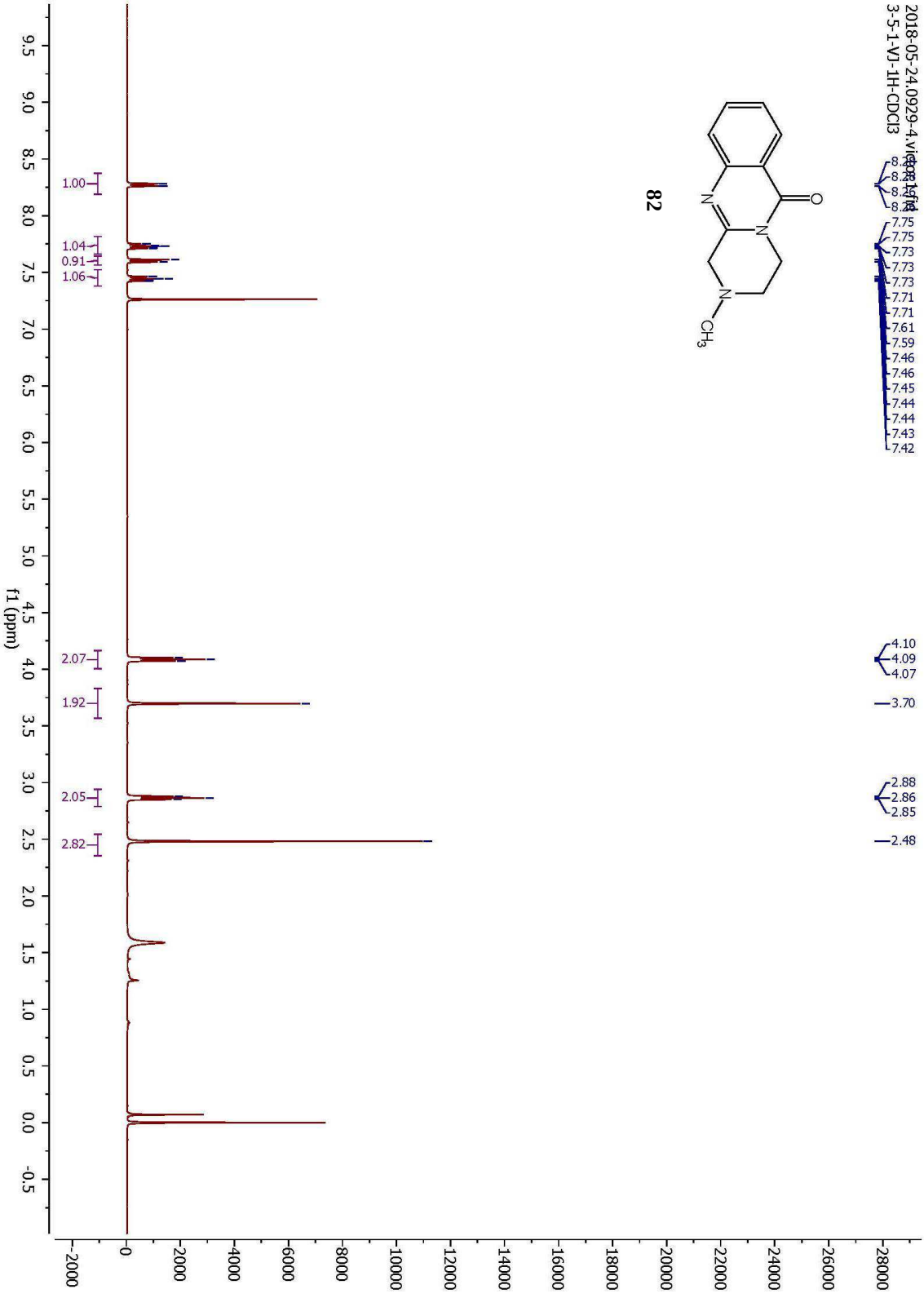
2018-05-24.0929-4.vjoe.1.fid
3-5-1-VJ-1H-CDCl3
82
f1 (ppm)
1.00
1.04
0.91
1.06
2.07
1.92
2.05
2.82
8.44
8.44
8.23
8.23
7.75
7.75
7.73
7.73
7.73
7.71
7.71
7.61
7.59
7.46
7.46
7.45
7.44
7.44
7.43
7.42
4.10
4.09
4.07
3.70
2.88
2.86
2.85
2.48

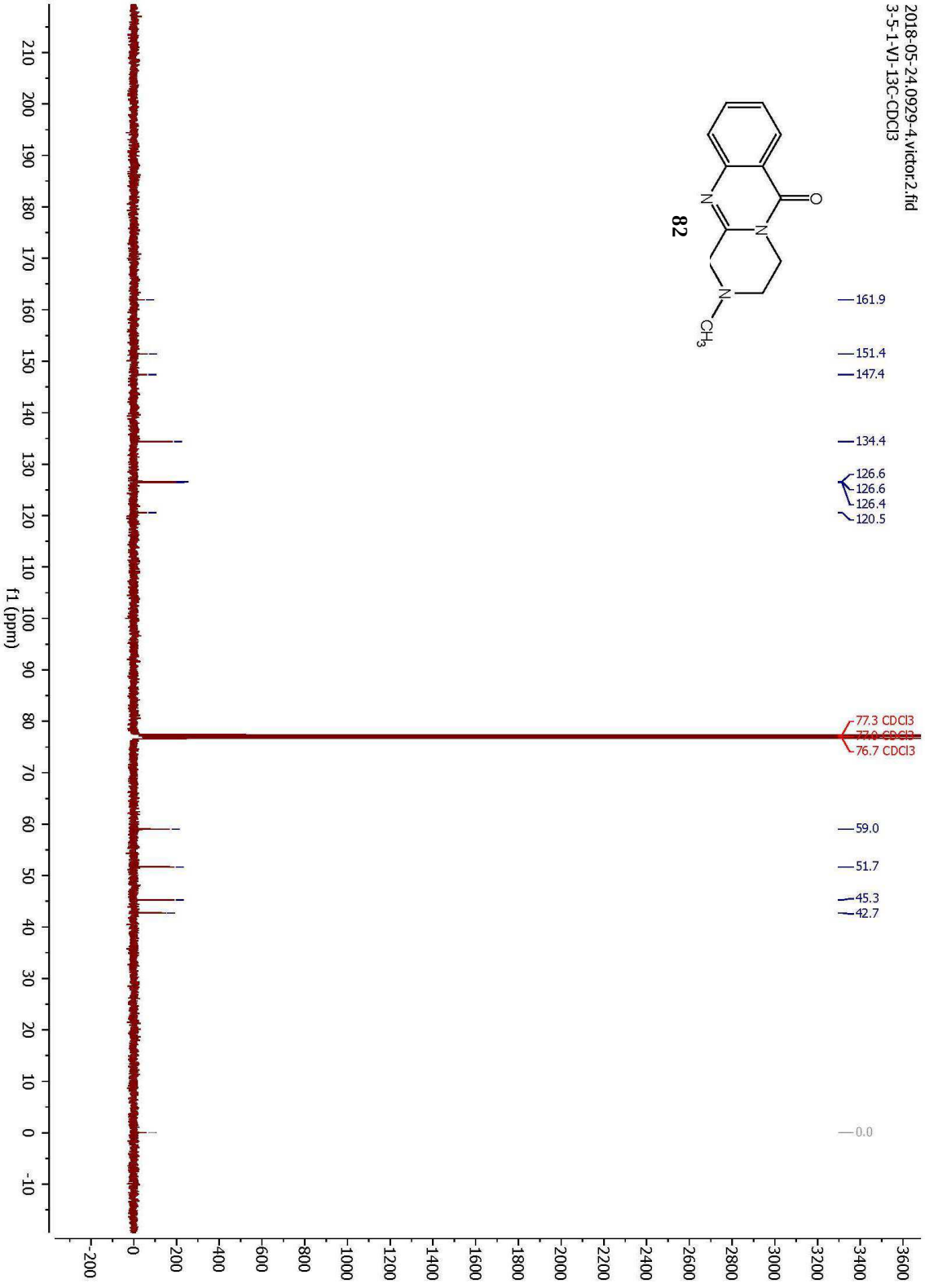
2018-05-24.0929-4.victor2.fid
3-5-1-VJ-13C-CDCl3
82
161.9
151.4
147.4
134.4
126.6
126.6
126.4
120.5
77.3 CDCl3
77.0 CDCl3
76.7 CDCl3
59.0
51.7
45.3
42.7
0.0
f1 (ppm)

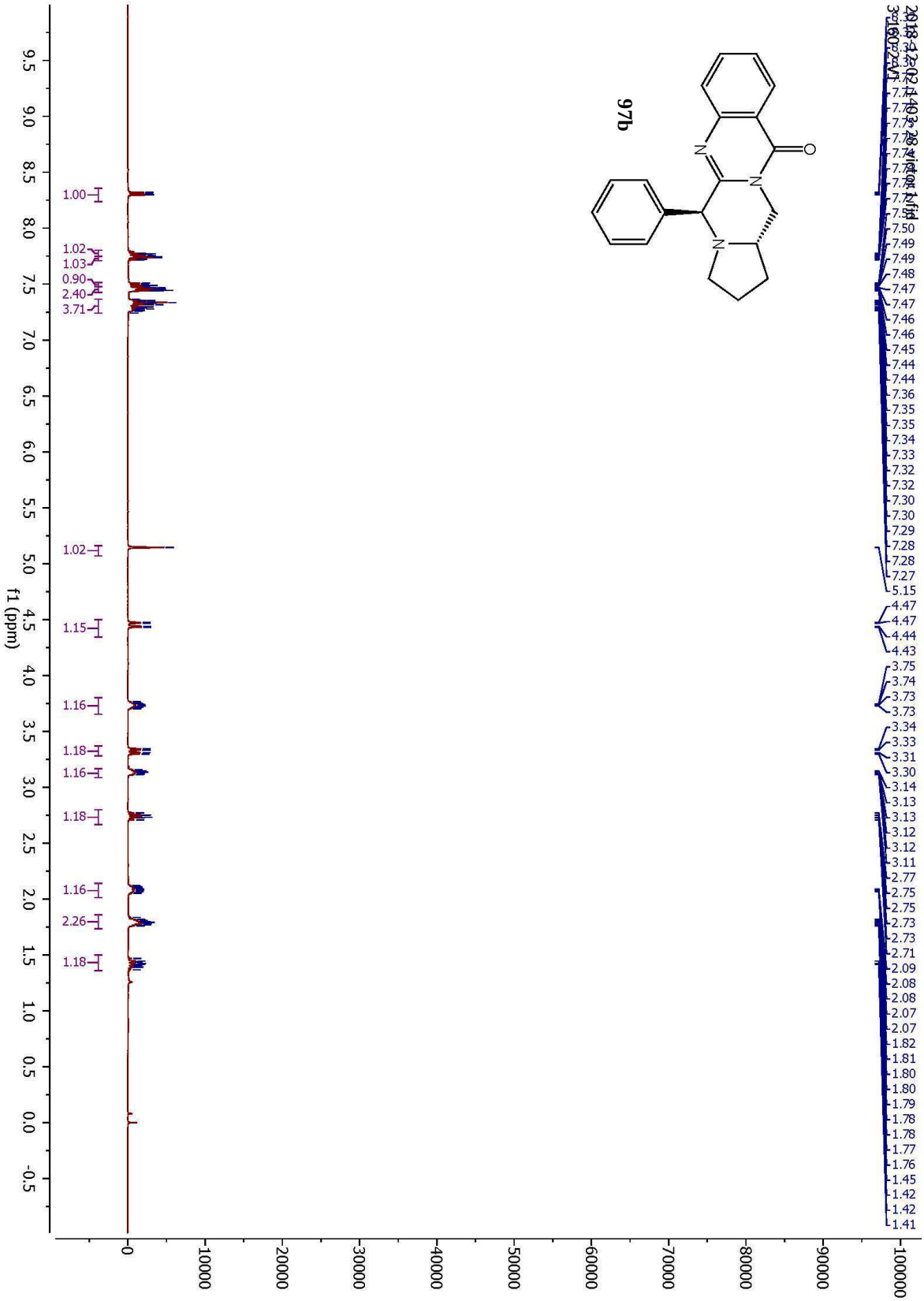
97b
f1 (ppm)
1.00
1.02
1.03
0.90
2.40
3.71
1.02
1.15
1.16
1.18
1.16
1.18
1.16
2.26
1.18

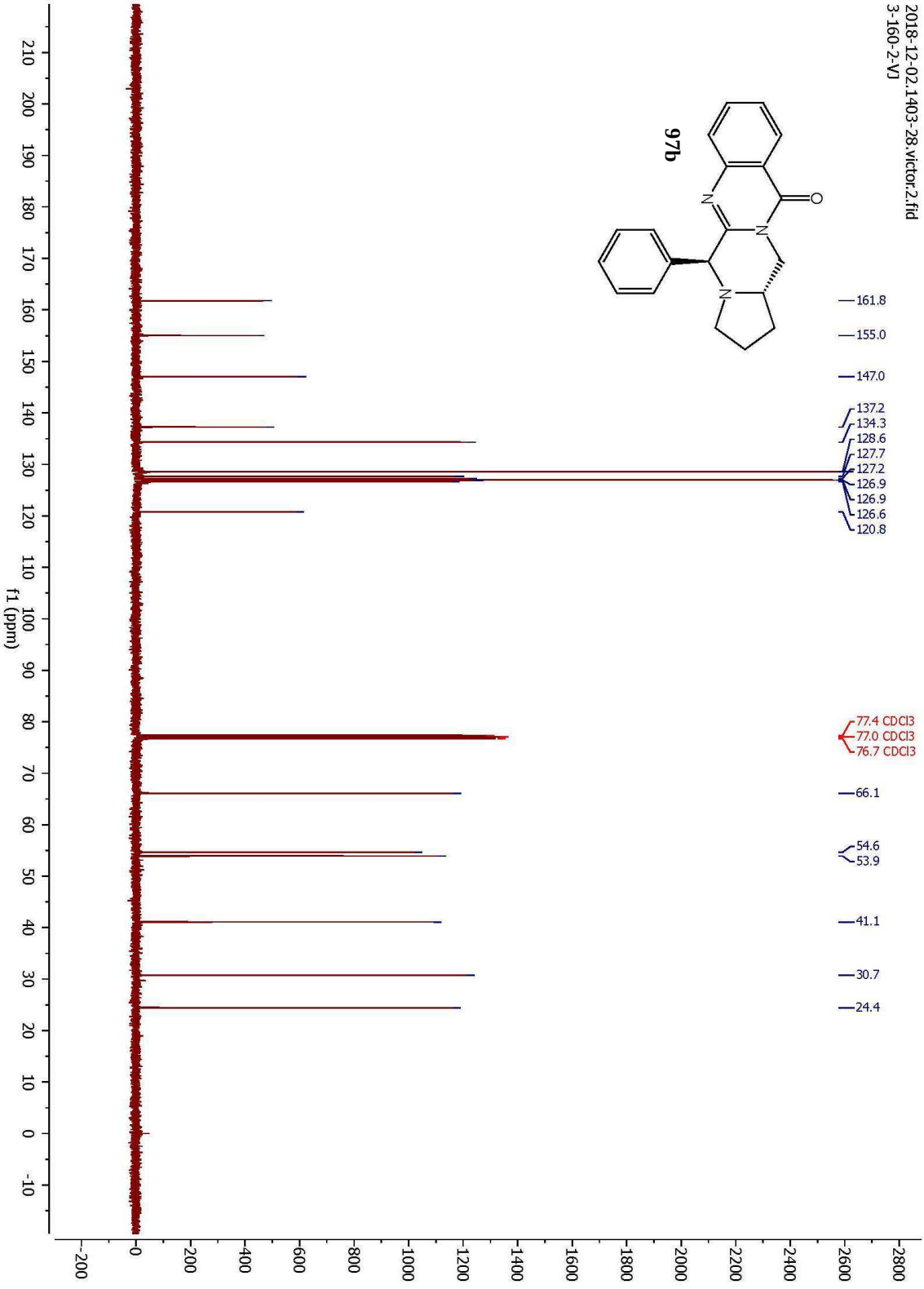
2018-12-02.1403-28.victor.2.fid
3-160-2-VJ
97b
161.8
155.0
147.0
137.2
134.3
128.6
127.7
127.2
126.9
126.9
126.6
120.8
77.4 CDCl3
77.0 CDCl3
76.7 CDCl3
66.1
54.6
53.9
41.1
30.7
24.4
f1 (ppm)

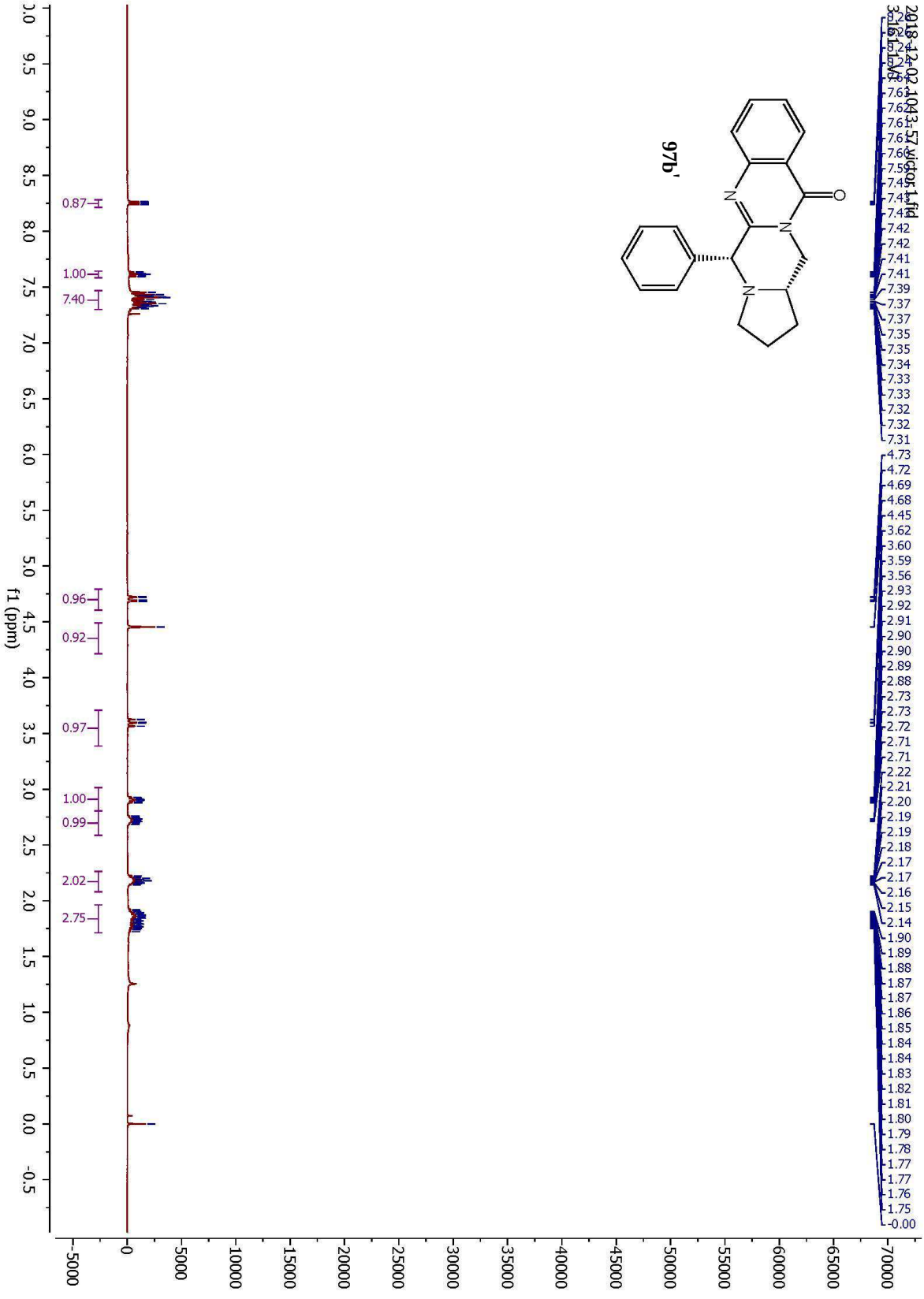
97b'
f1 (ppm)
0.87
1.00
7.40
0.96
0.92
0.97
1.00
0.99
2.02
2.75

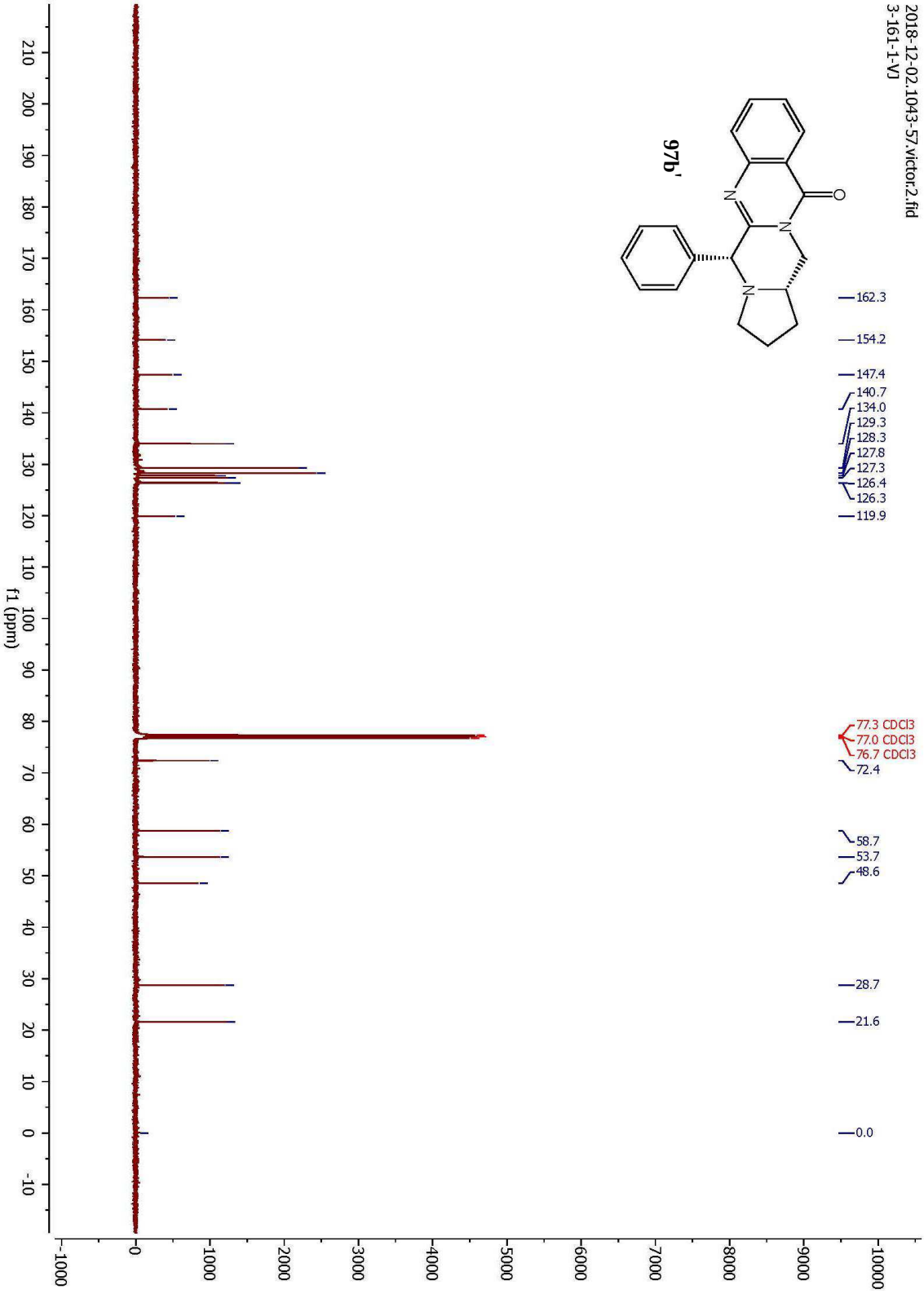
2018-12-02.1043-57.victor.2.fid
3-161-1-VJ
97b'
162.3
154.2
147.4
140.7
134.0
129.3
128.3
127.8
127.3
126.4
126.3
119.9
77.3 CDCl3
77.0 CDCl3
76.7 CDCl3
72.4
58.7
53.7
48.6
28.7
21.6
0.0
f1 (ppm)

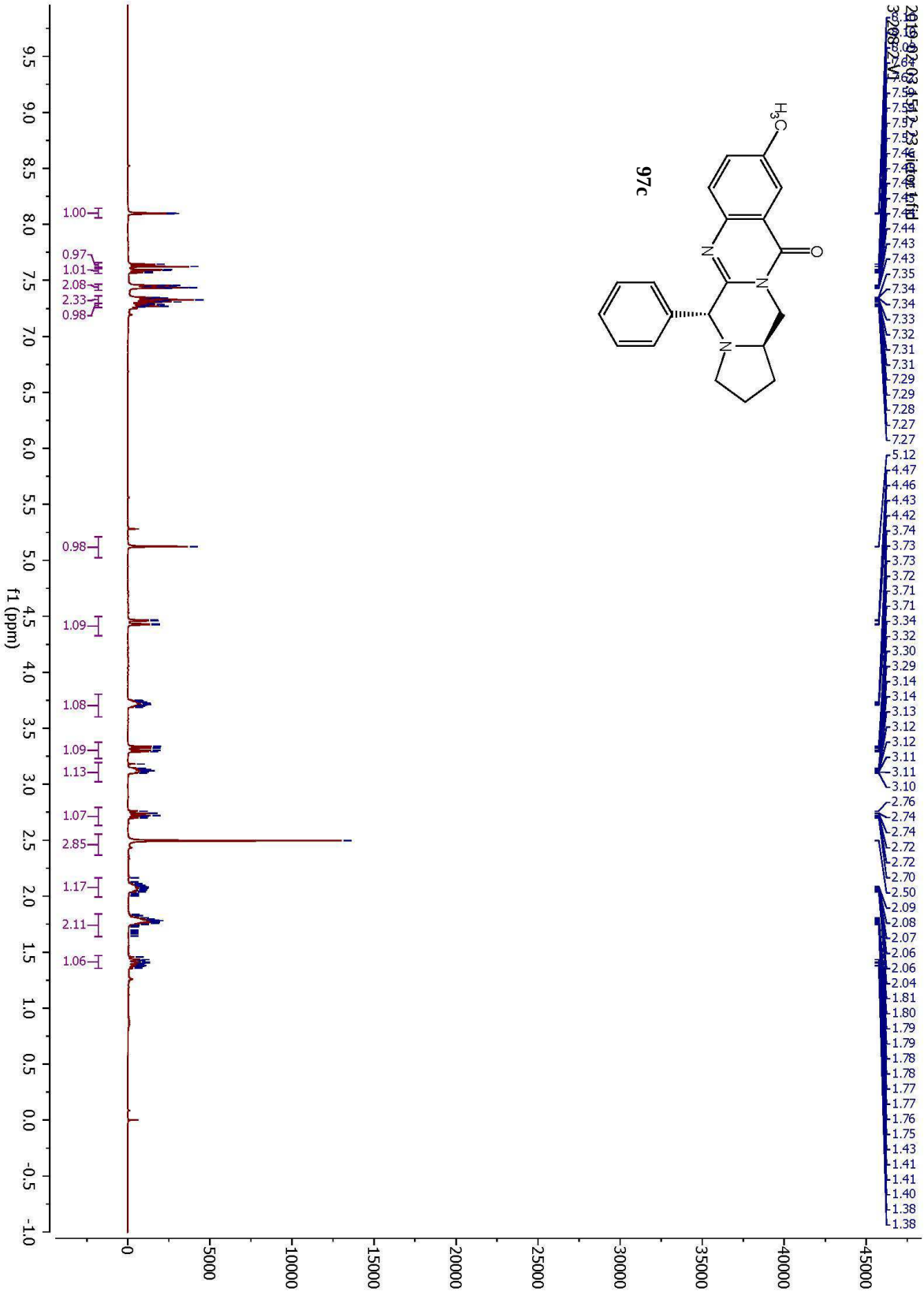
97c
H3C
O
N
N
N
f1 (ppm)
1.00
0.97
1.01
2.08
2.33
0.98
0.98
1.09
1.08
1.09
1.13
1.07
2.85
1.17
2.11
1.06

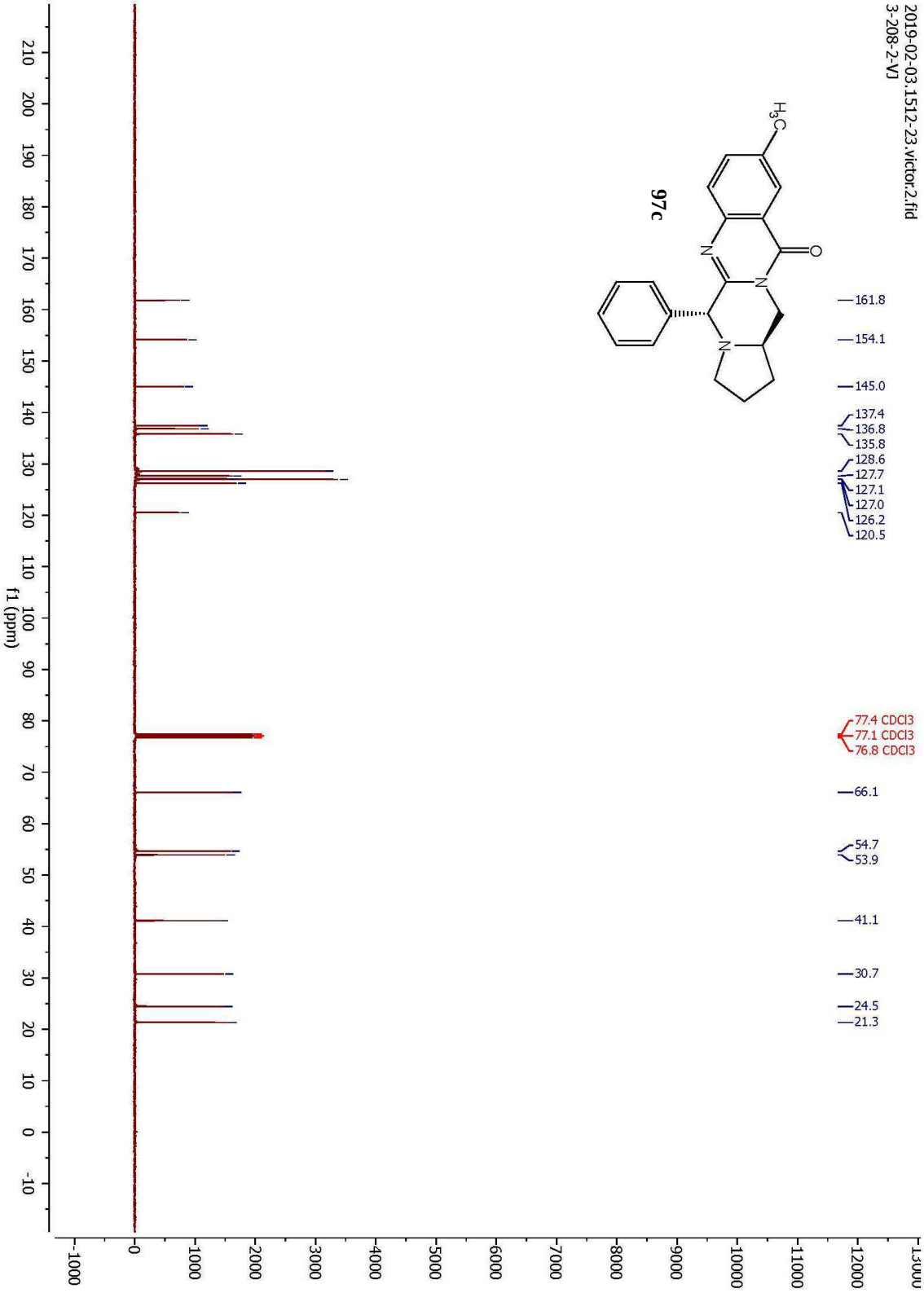
2019-02-03.1512-23.victor.2.fid
3-208-2-VJ
97c
H3C
O
N
N
N
161.8
154.1
145.0
137.4
136.8
135.8
128.6
127.7
127.1
127.0
126.2
120.5
77.4 CDCl3
77.1 CDCl3
76.8 CDCl3
66.1
54.7
53.9
41.1
30.7
24.5
21.3
f1 (ppm)

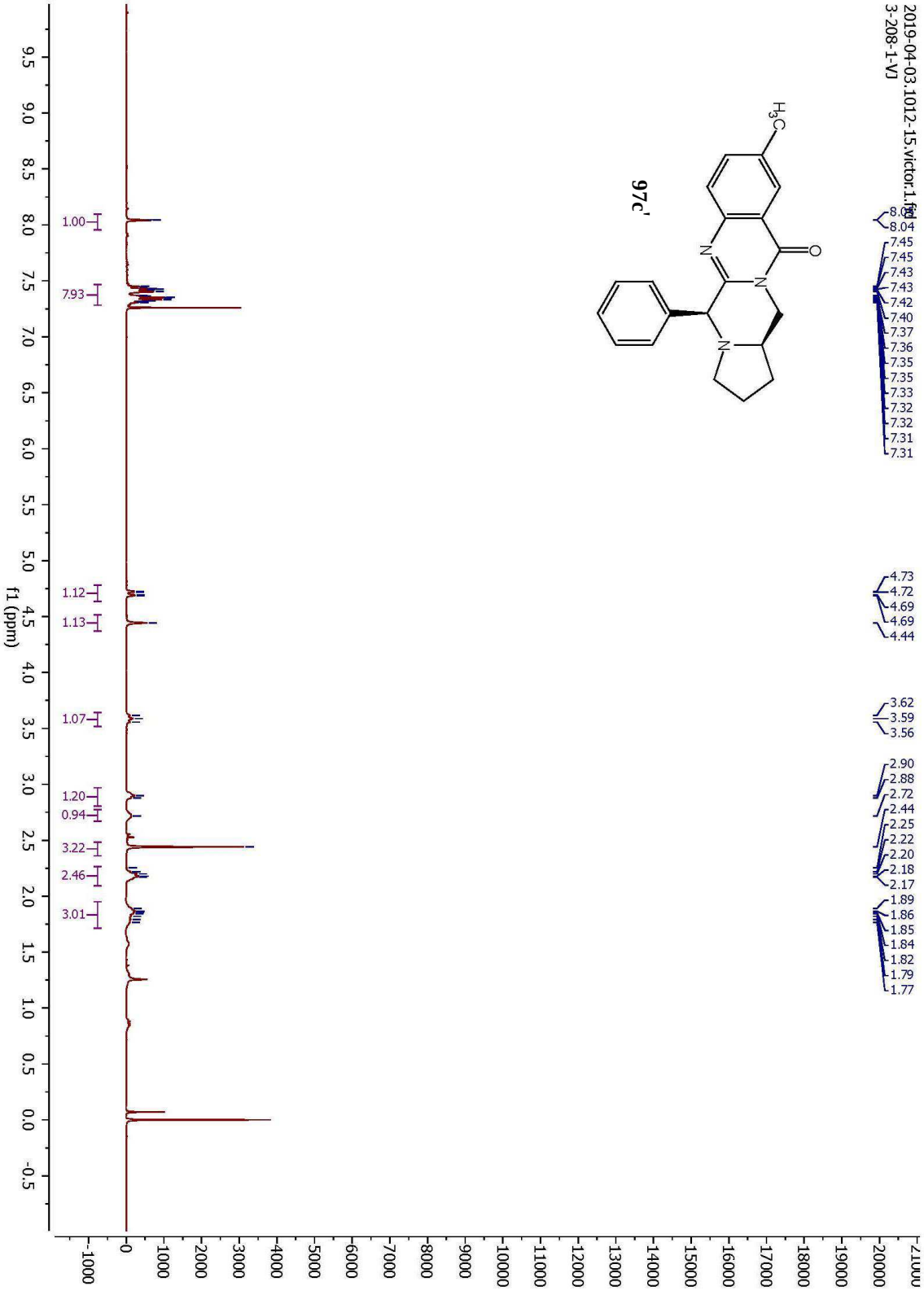
2019-04-03.1012-15.victor.1.fid
3-208-1-VJ
97c'
H3C
O
N
N
N
8.05
8.04
7.45
7.45
7.43
7.43
7.42
7.40
7.37
7.36
7.35
7.35
7.33
7.32
7.32
7.31
7.31
4.73
4.72
4.69
4.69
4.44
3.62
3.59
3.56
2.90
2.88
2.72
2.44
2.25
2.22
2.20
2.18
2.17
1.89
1.86
1.85
1.84
1.82
1.79
1.77
1.00
7.93
1.12
1.13
1.07
1.20
0.94
3.22
2.46
3.01
f1 (ppm)

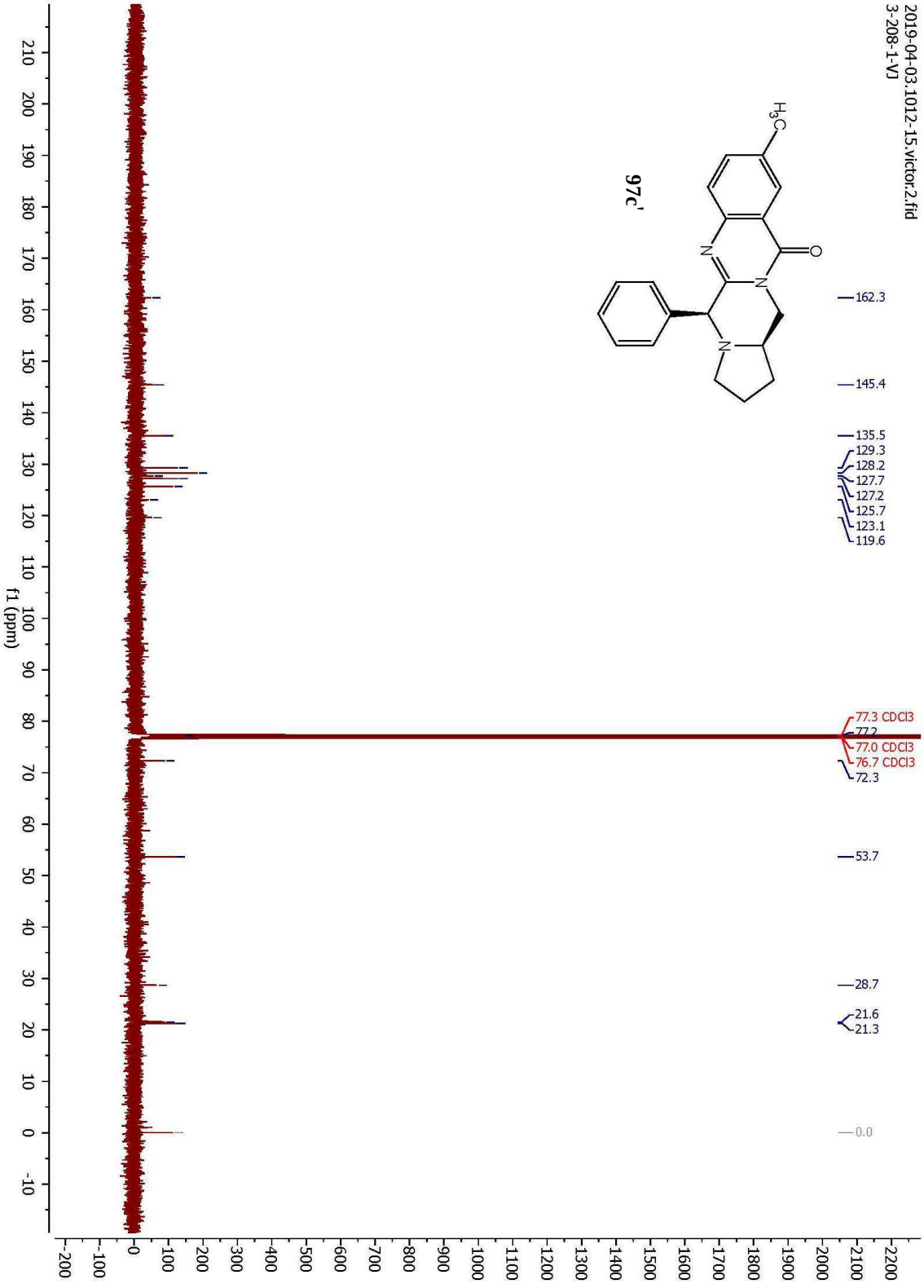
2019-04-03.1012-15.victor.2.fid
3-208-1-VJ
97c'
H3C
O
N
N
N
162.3
145.4
135.5
129.3
128.2
127.7
127.2
125.7
123.1
119.6
77.3 CDCl3
77.2
77.0 CDCl3
76.7 CDCl3
72.3
53.7
28.7
21.6
21.3
0.0
f1 (ppm)

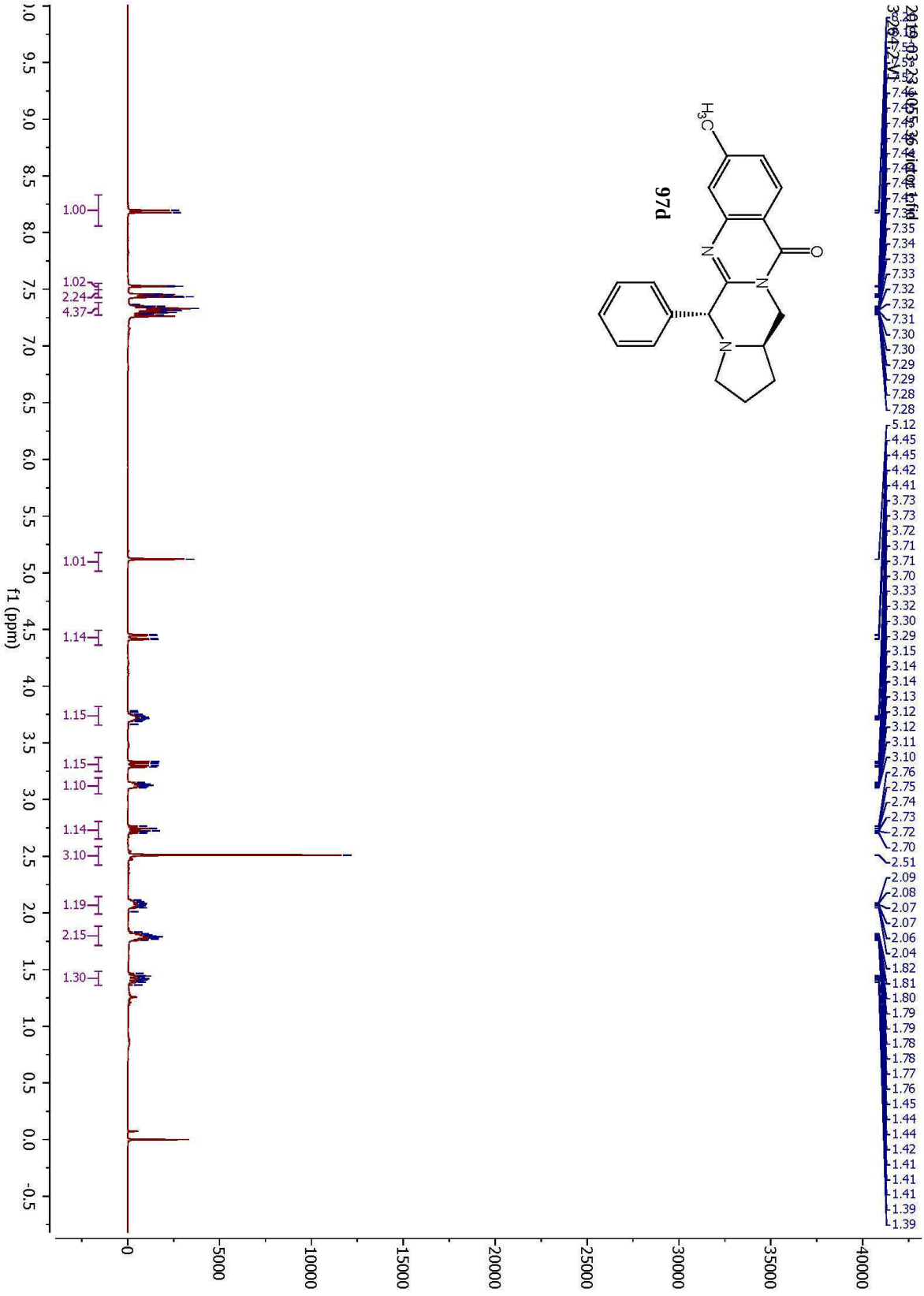
97d
f1 (ppm)
1.00
1.02
2.24
4.37
1.01
1.14
1.15
1.15
1.10
1.14
3.10
1.19
2.15
1.30

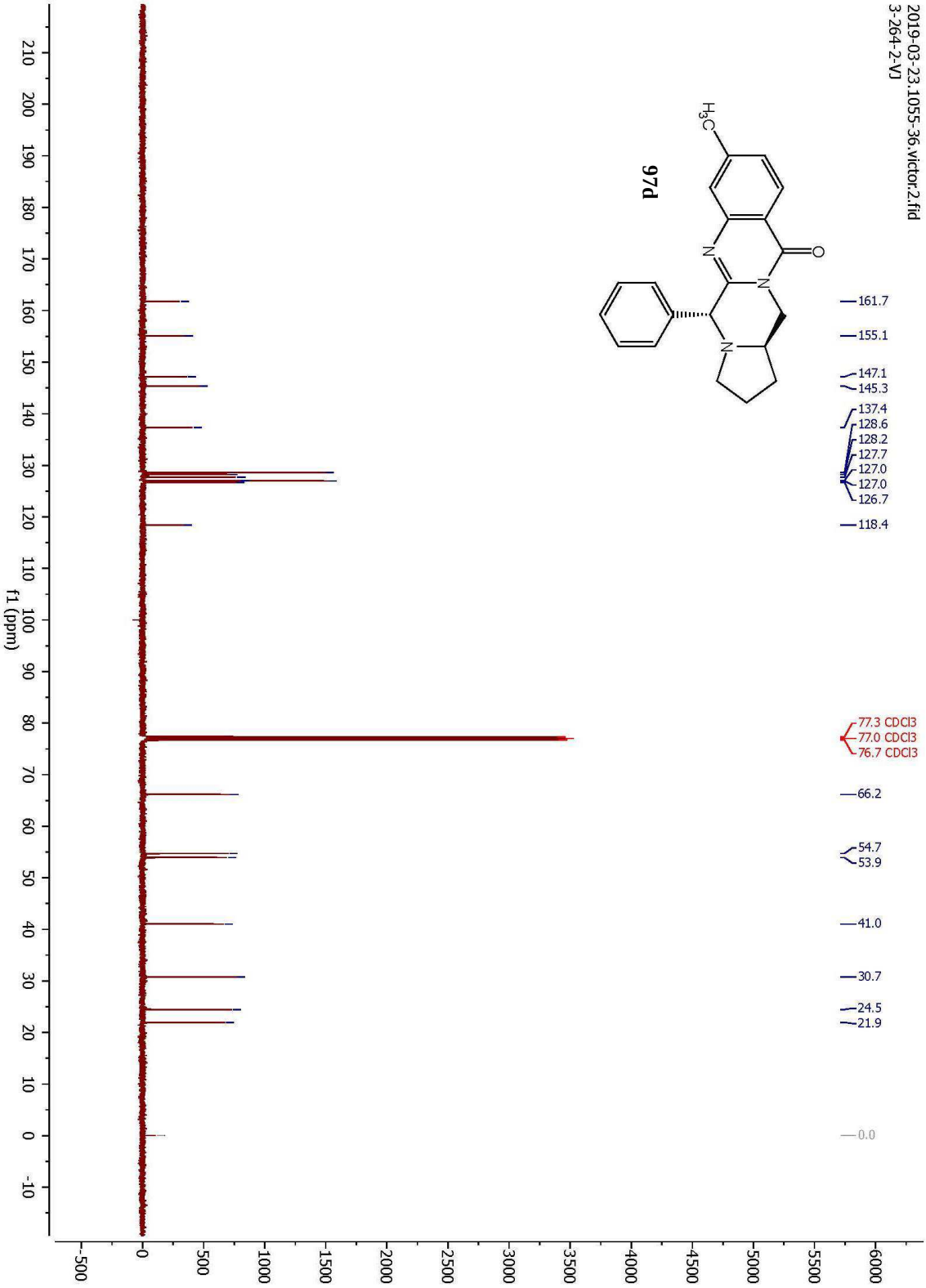
2019-03-23.1055-36.victor.2.fid
3-264-2-VJ
97d
H3C
O
N
N
N
161.7
155.1
147.1
145.3
137.4
128.6
128.2
127.7
127.0
127.0
126.7
118.4
77.3 CDCl3
77.0 CDCl3
76.7 CDCl3
66.2
54.7
53.9
41.0
30.7
24.5
21.9
0.0
f1 (ppm)

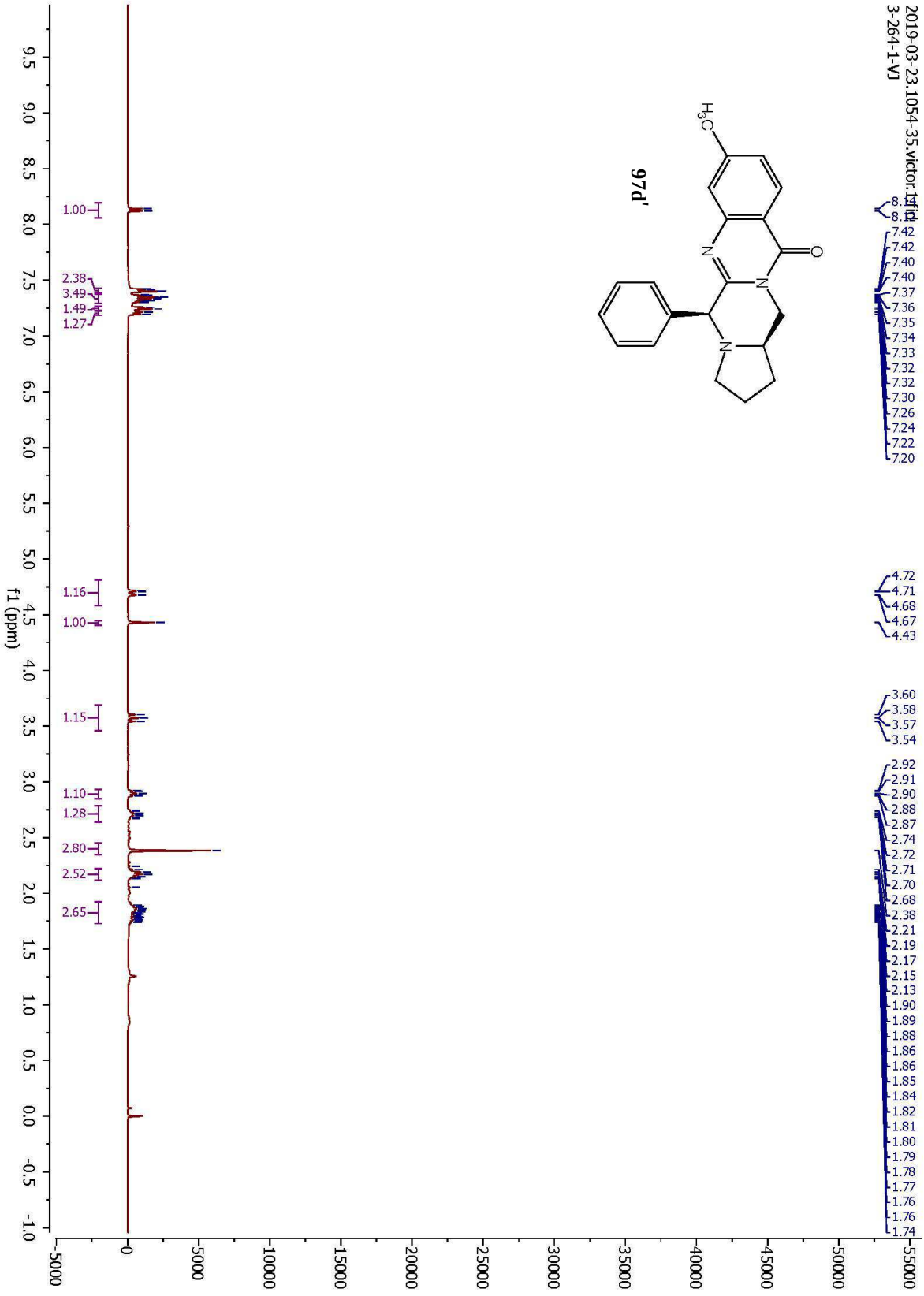
2019-03-23.1054-35.victor.1r
3-264-1-VJ
97d'
H3C
N
N
N
O
f1 (ppm)
1.00
2.38
3.49
1.49
1.27
1.16
1.00
1.15
1.10
1.28
2.80
2.52
2.65
8.
8.
7.42
7.42
7.40
7.40
7.37
7.36
7.35
7.34
7.33
7.32
7.32
7.30
7.26
7.24
7.22
7.20
4.72
4.71
4.68
4.67
4.43
3.60
3.58
3.57
3.54
2.92
2.91
2.90
2.88
2.87
2.74
2.72
2.71
2.70
2.68
2.38
2.21
2.19
2.17
2.15
2.13
1.90
1.89
1.88
1.86
1.86
1.85
1.84
1.82
1.81
1.80
1.79
1.78
1.77
1.76
1.76
1.74

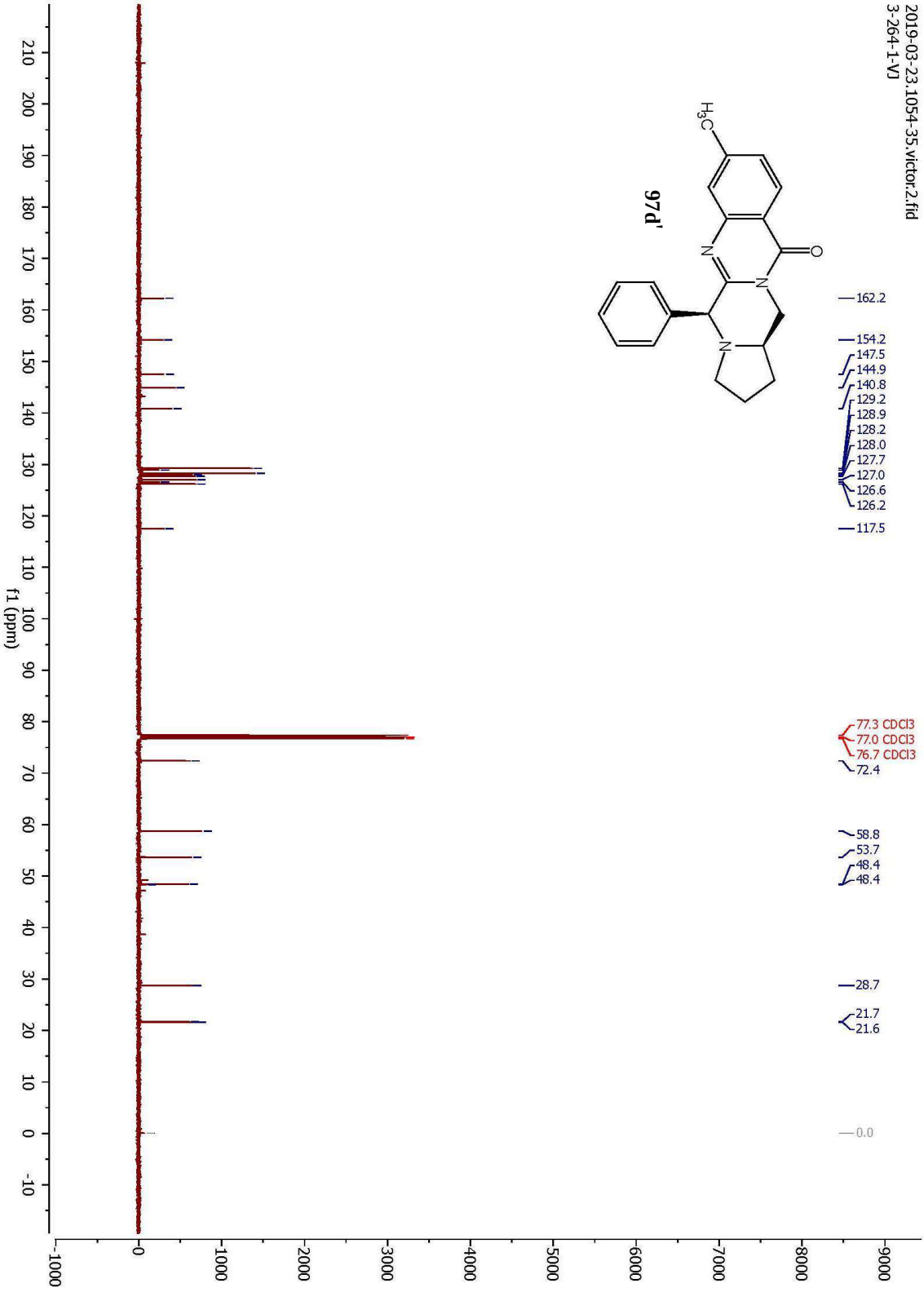
2019-03-23.1054-35.victor.2.fid
3-264-1-VJ
97d'
H3C
O
N
N
N
162.2
154.2
147.5
144.9
140.8
129.2
128.9
128.2
128.0
127.7
127.0
126.6
126.2
117.5
77.3 CDCl3
77.0 CDCl3
76.7 CDCl3
72.4
58.8
53.7
48.4
48.4
28.7
21.7
21.6
0.0
f1 (ppm)

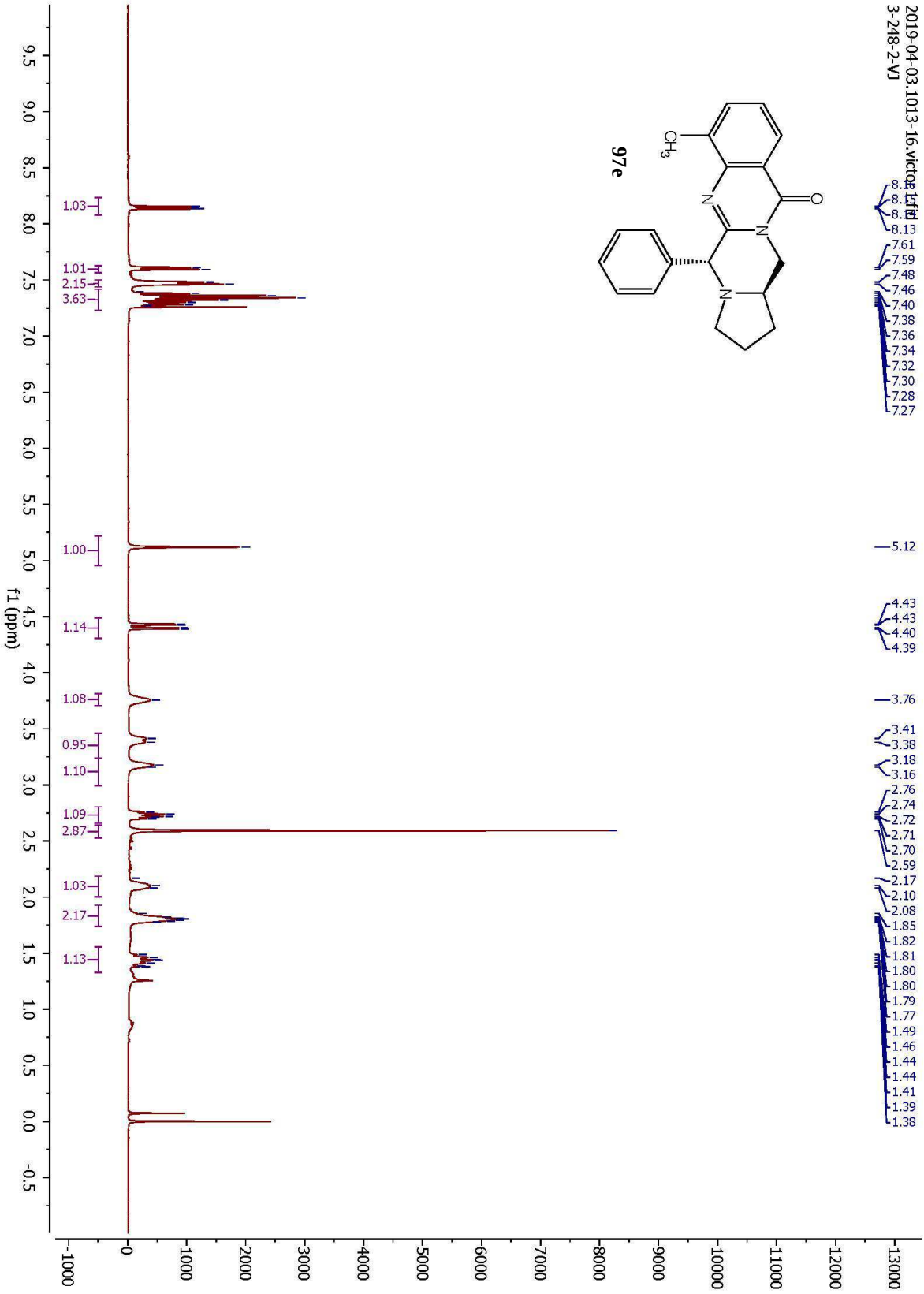
2019-04-03.1013-16.victor.1r.fid
3-248-2-VJ
97e
CH3
N
N
N
O
f1 (ppm)
1.03
1.01
2.15
3.63
1.00
1.14
1.08
0.95
1.10
1.09
2.87
1.03
2.17
1.13
8.13
7.61
7.59
7.48
7.46
7.40
7.38
7.36
7.34
7.32
7.30
7.28
7.27
5.12
4.43
4.43
4.40
4.39
3.76
3.41
3.38
3.18
3.16
2.76
2.74
2.72
2.71
2.70
2.59
2.17
2.10
2.08
1.85
1.82
1.81
1.80
1.80
1.79
1.77
1.49
1.46
1.44
1.44
1.41
1.39
1.38

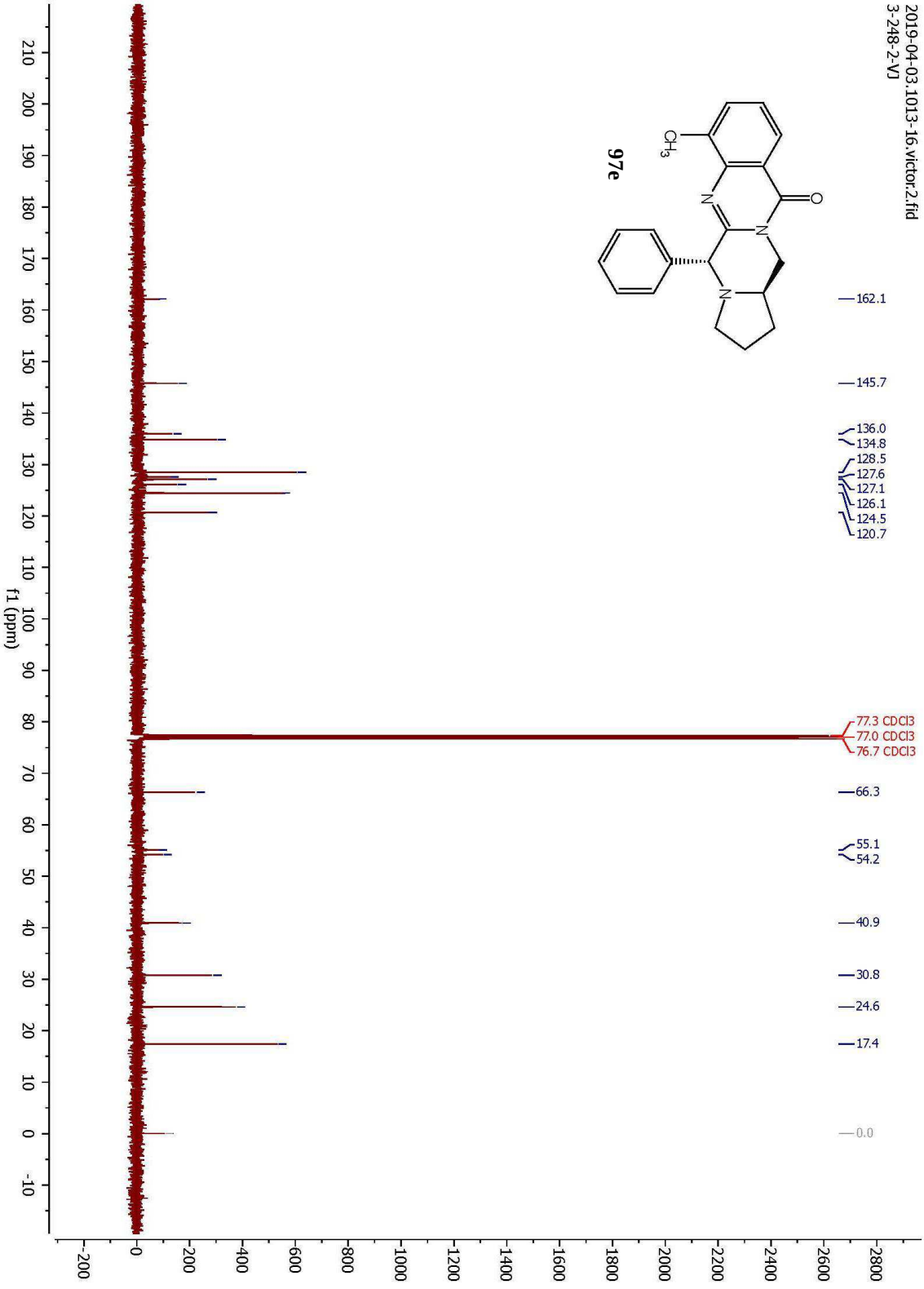
2019-04-03.1013-16.victor.2.fid
3-248-2-VJ
97e
CH3
N
N
N
O
162.1
145.7
136.0
134.8
128.5
127.6
127.1
126.1
124.5
120.7
77.3 CDCl3
77.0 CDCl3
76.7 CDCl3
66.3
55.1
54.2
40.9
30.8
24.6
17.4
0.0
f1 (ppm)

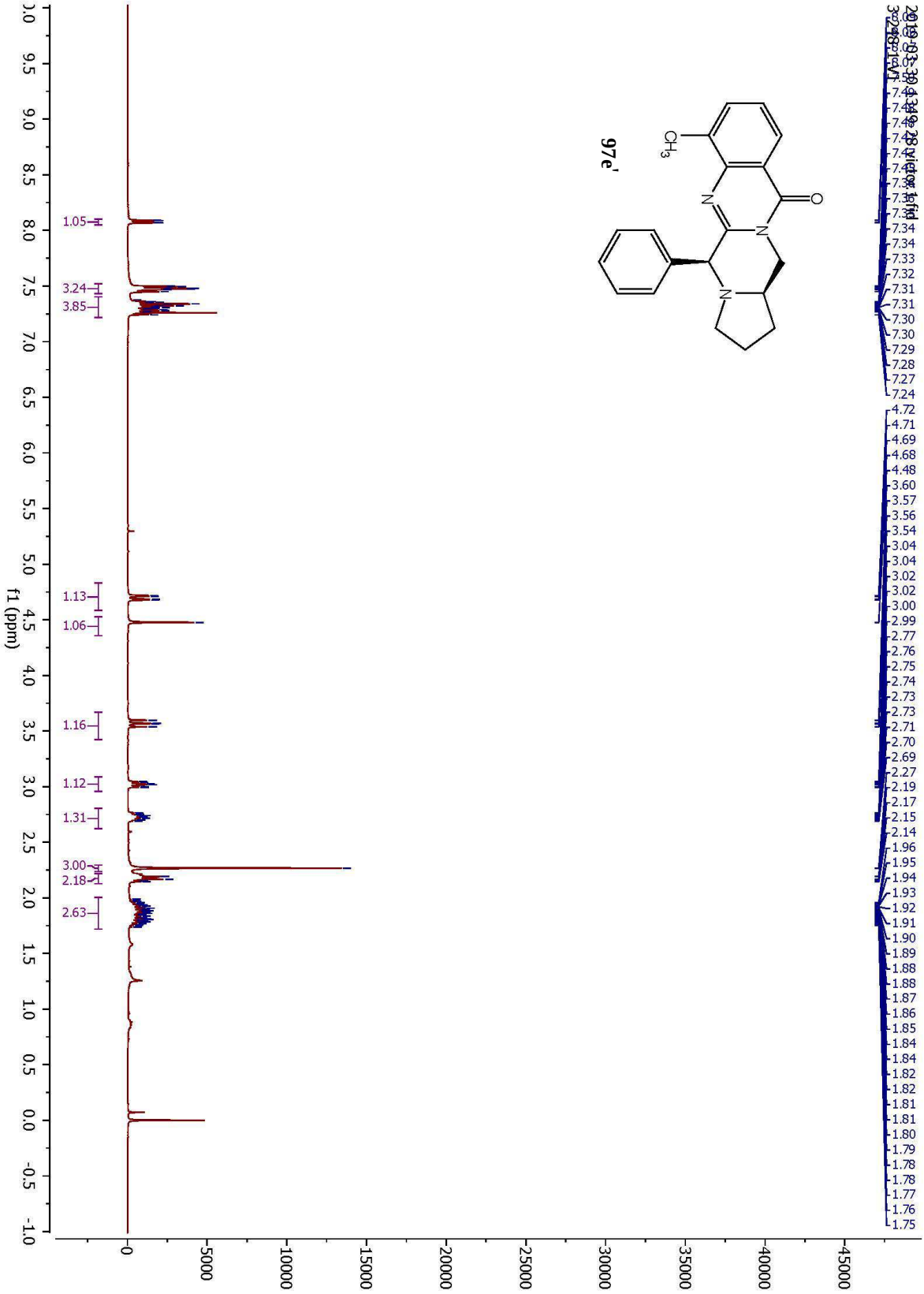
97e'
CH3
N
N
N
O
f1 (ppm)
1.05
3.24
3.85
1.13
1.06
1.16
1.12
1.31
3.00
2.18
2.63

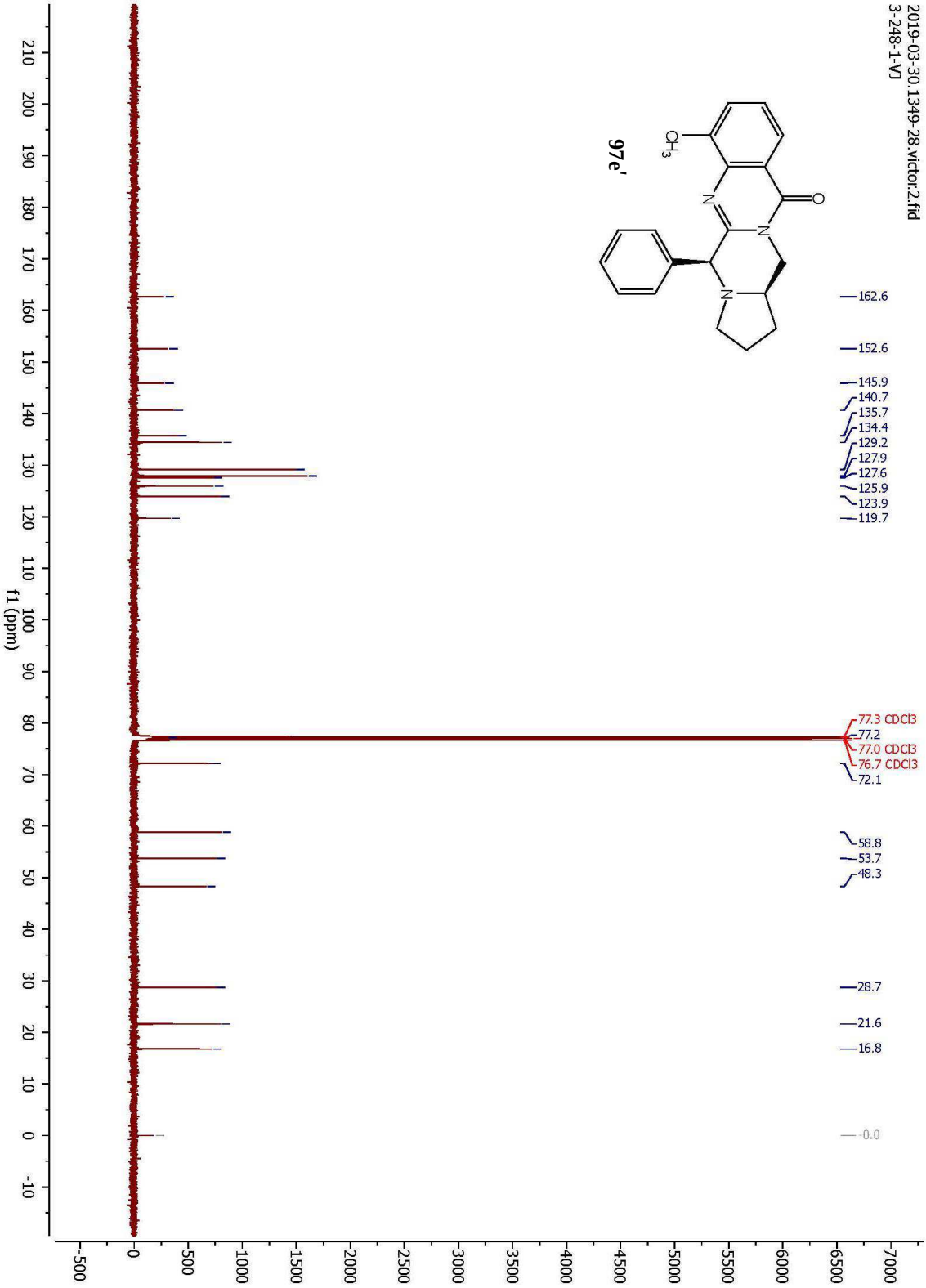
2019-03-30.1349-28.victor.2.fid
3-248-1-VJ
97e'
CH3
O
N
N
N
162.6
152.6
145.9
140.7
135.7
134.4
129.2
127.9
127.6
125.9
123.9
119.7
77.3 CDCl3
77.2
77.0 CDCl3
76.7 CDCl3
72.1
58.8
53.7
48.3
28.7
21.6
16.8
0.0
f1 (ppm)

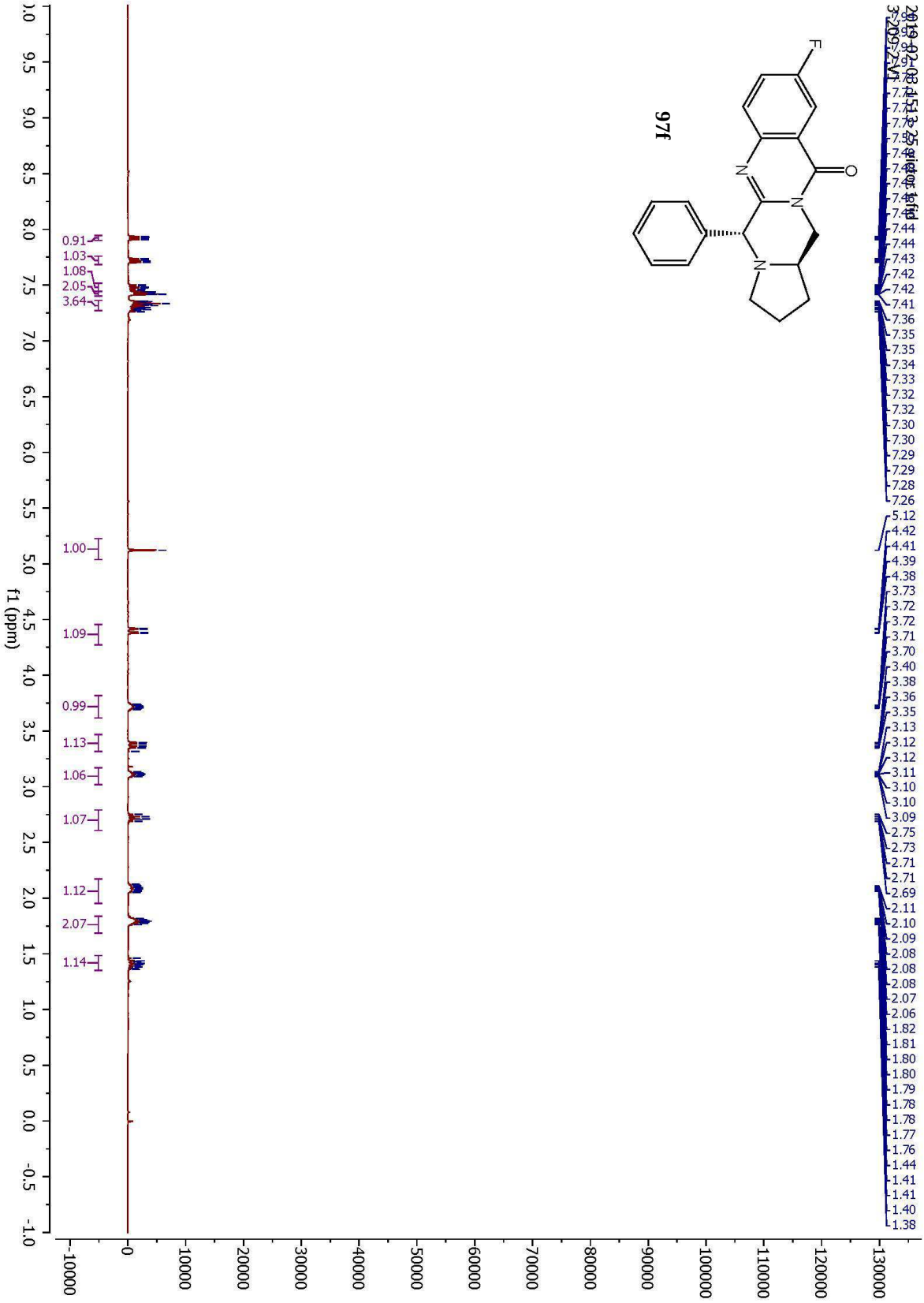
97f
F
O
N
N
N
f1 (ppm)
0.91
1.03
1.08
2.05
3.64
1.00
1.09
0.99
1.13
1.06
1.07
1.12
2.07
1.14

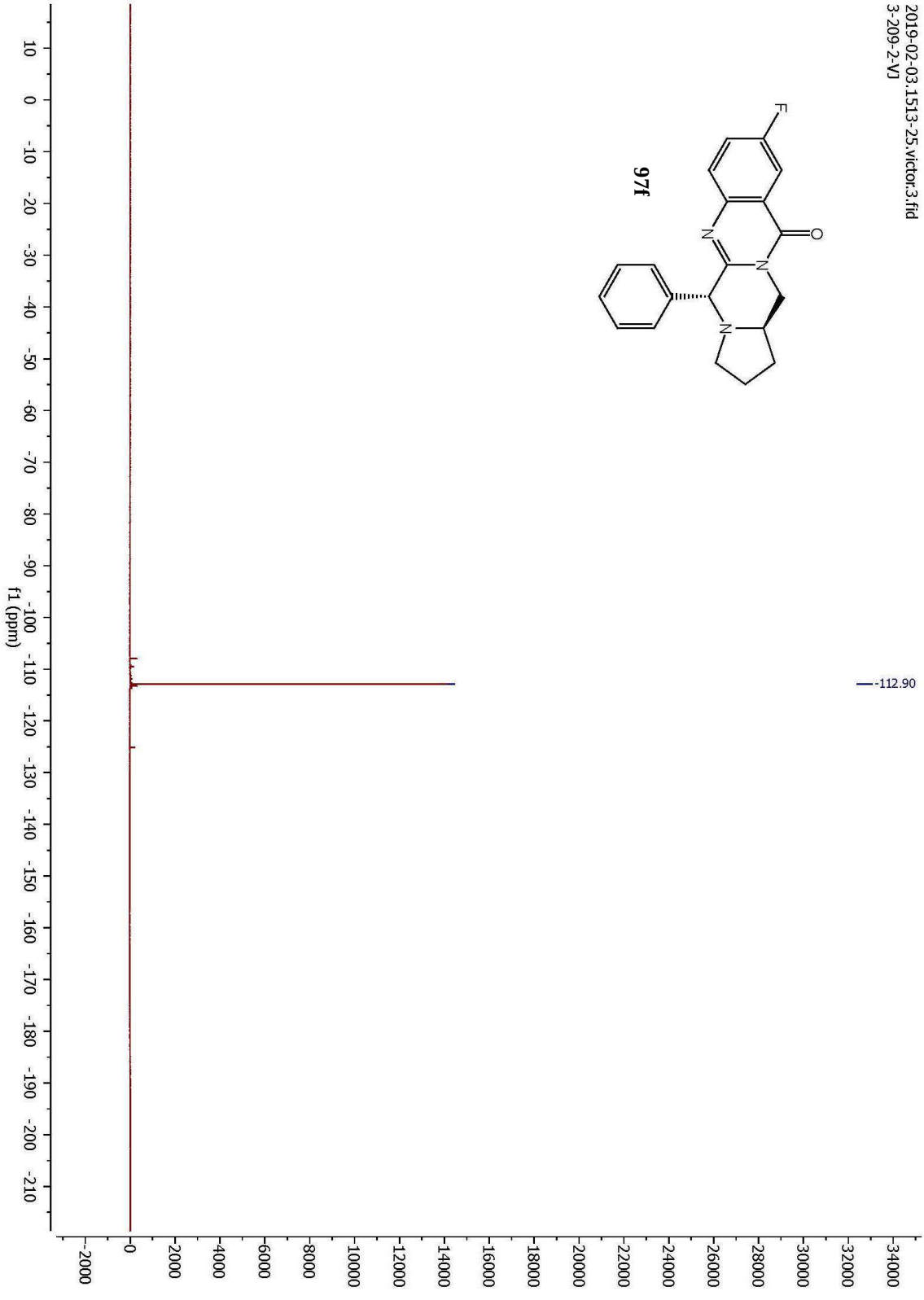
2019-02-03.1513-25.victor.3.fid
3-209-2-VJ
97f
F
O
N
N
N
-112.90
f1 (ppm)

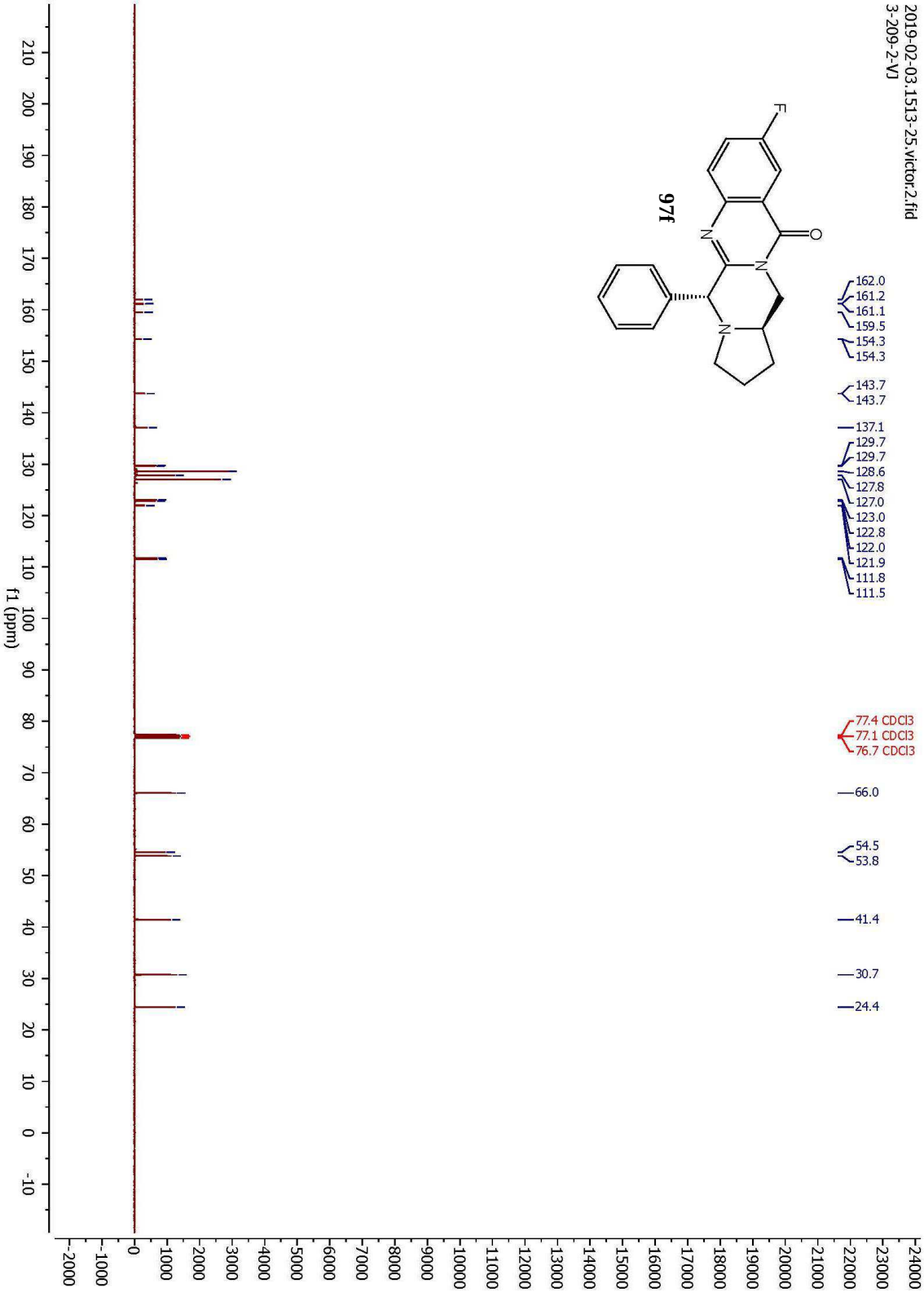
2019-02-03.1513-25.victor.2.fid
3-209-2-VJ
97f
F
O
N
N
N
162.0
161.2
161.1
159.5
154.3
154.3
143.7
143.7
137.1
129.7
129.7
128.6
127.8
127.0
123.0
122.8
122.0
121.9
111.8
111.5
77.4 CDCl3
77.1 CDCl3
76.7 CDCl3
66.0
54.5
53.8
41.4
30.7
24.4
f1 (ppm)

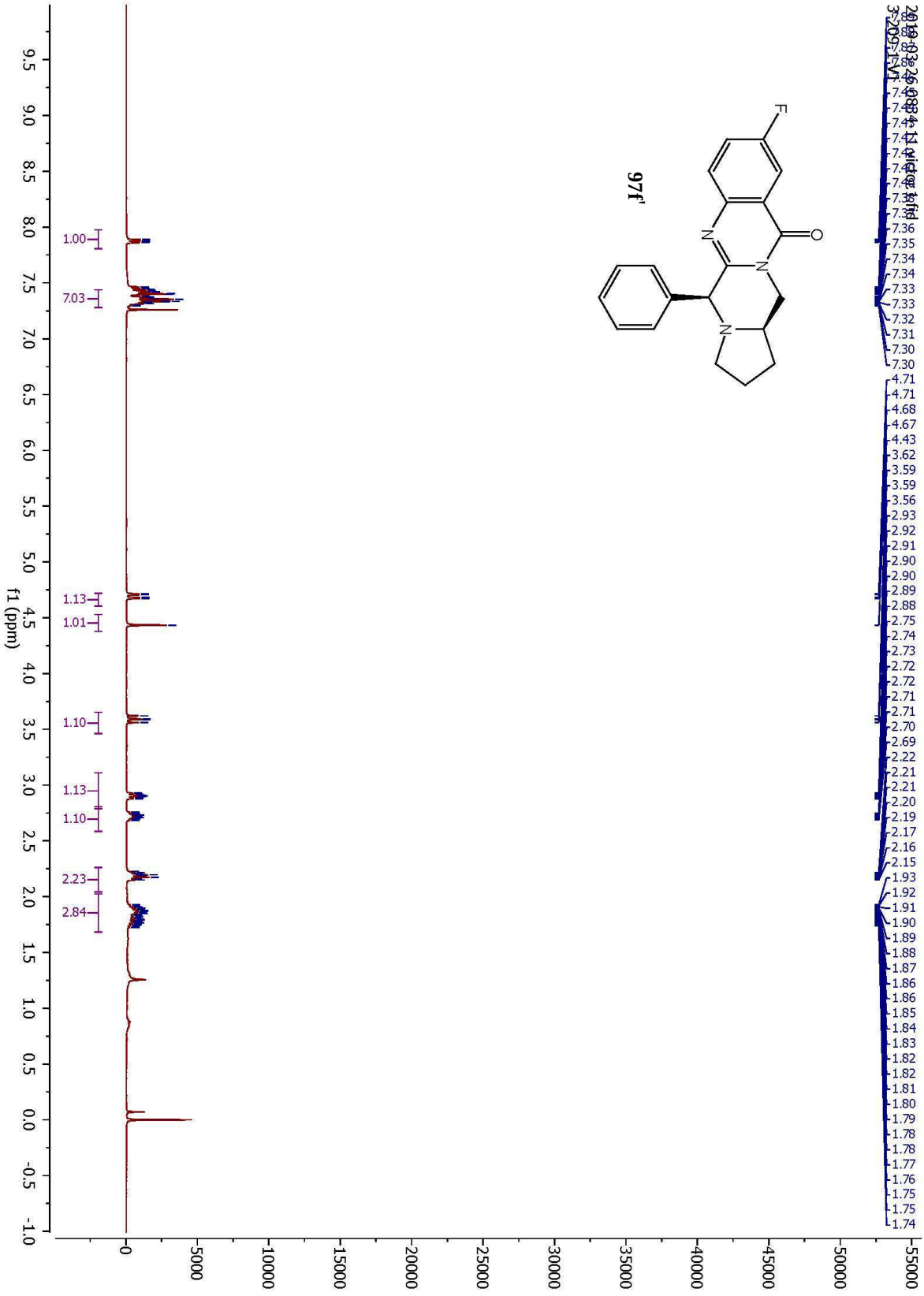
97f'
F
O
N
N
N
f1 (ppm)
1.00
7.03
1.13
1.01
1.10
1.13
1.10
2.23
2.84


2019-03-26.0834-11.victor.2.fid
3-209-1-VJ
97f'
F
O
N
N
N
-113.44
f1 (ppm)

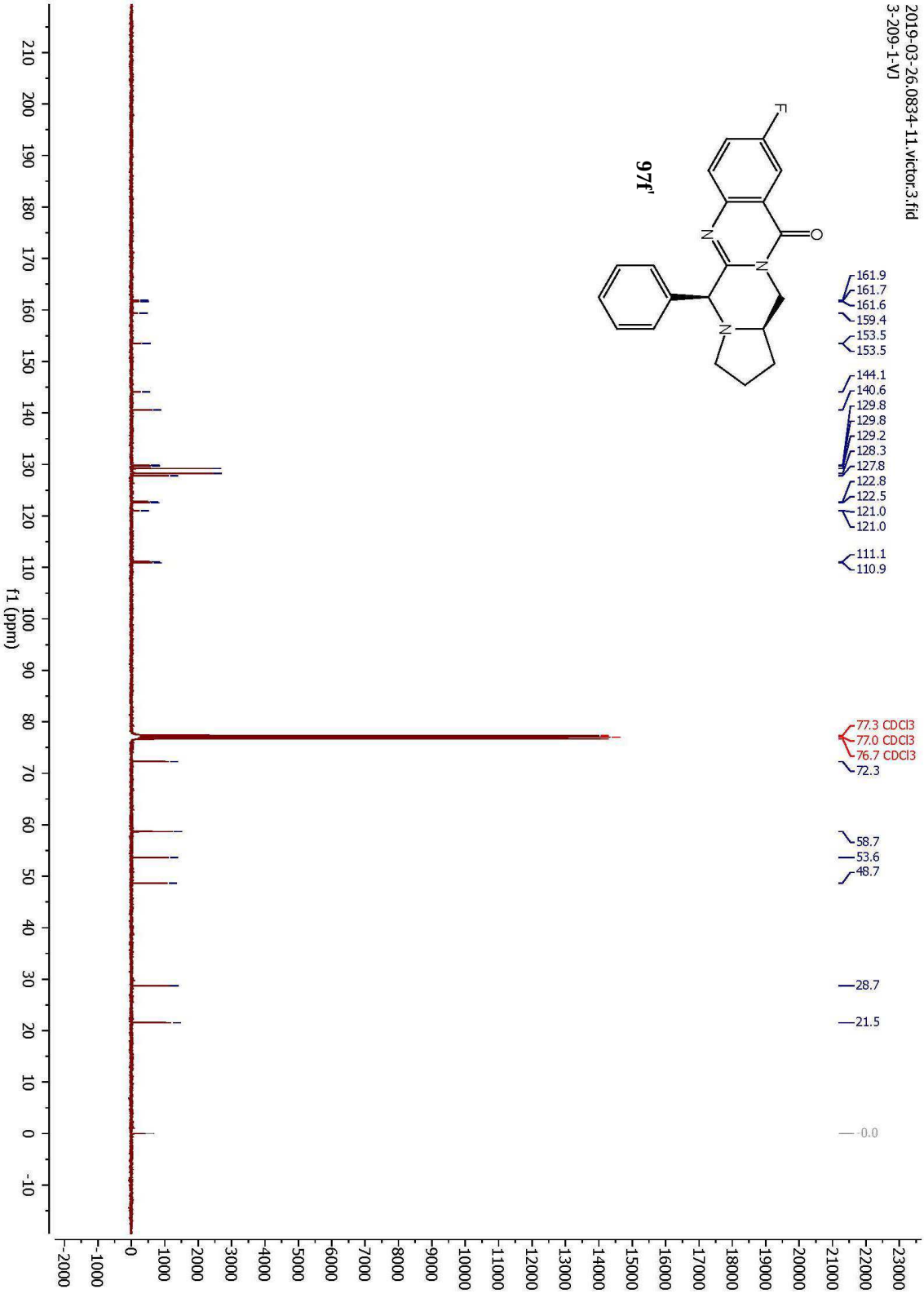
2019-03-26.0834-11.victor.3.fid
3-209-1-VJ
97f
F
O
N
N
N
161.9
161.7
161.6
159.4
153.5
153.5
144.1
140.6
129.8
129.8
129.2
128.3
127.8
122.8
122.5
121.0
121.0
111.1
110.9
77.3 CDCl3
77.0 CDCl3
76.7 CDCl3
72.3
58.7
53.6
48.7
28.7
21.5
0.0
f1 (ppm)

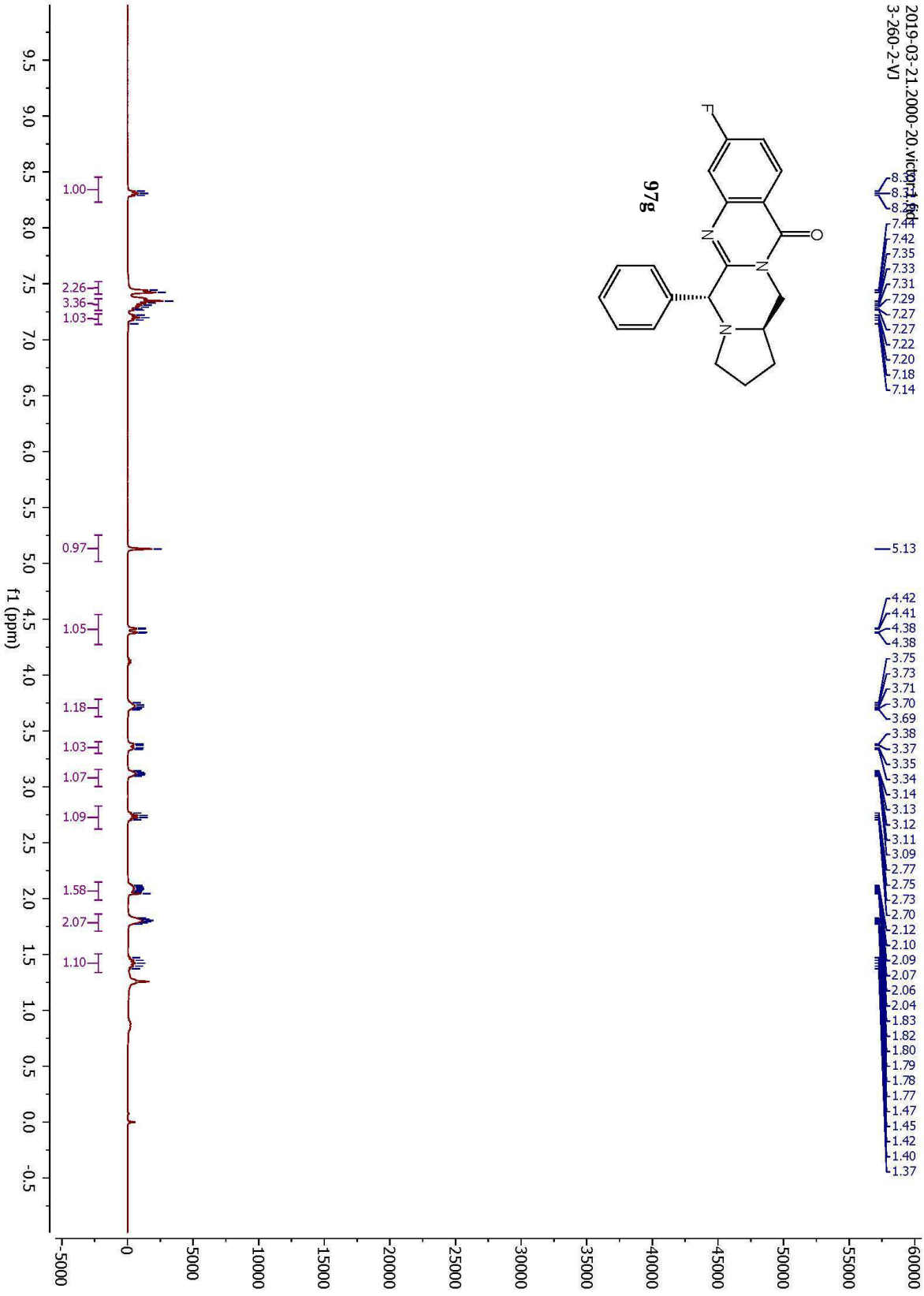
97g
F
N
N
N
O
2019-03-21.2000-20.victor14.fid
3-260-2-VJ
f1 (ppm)

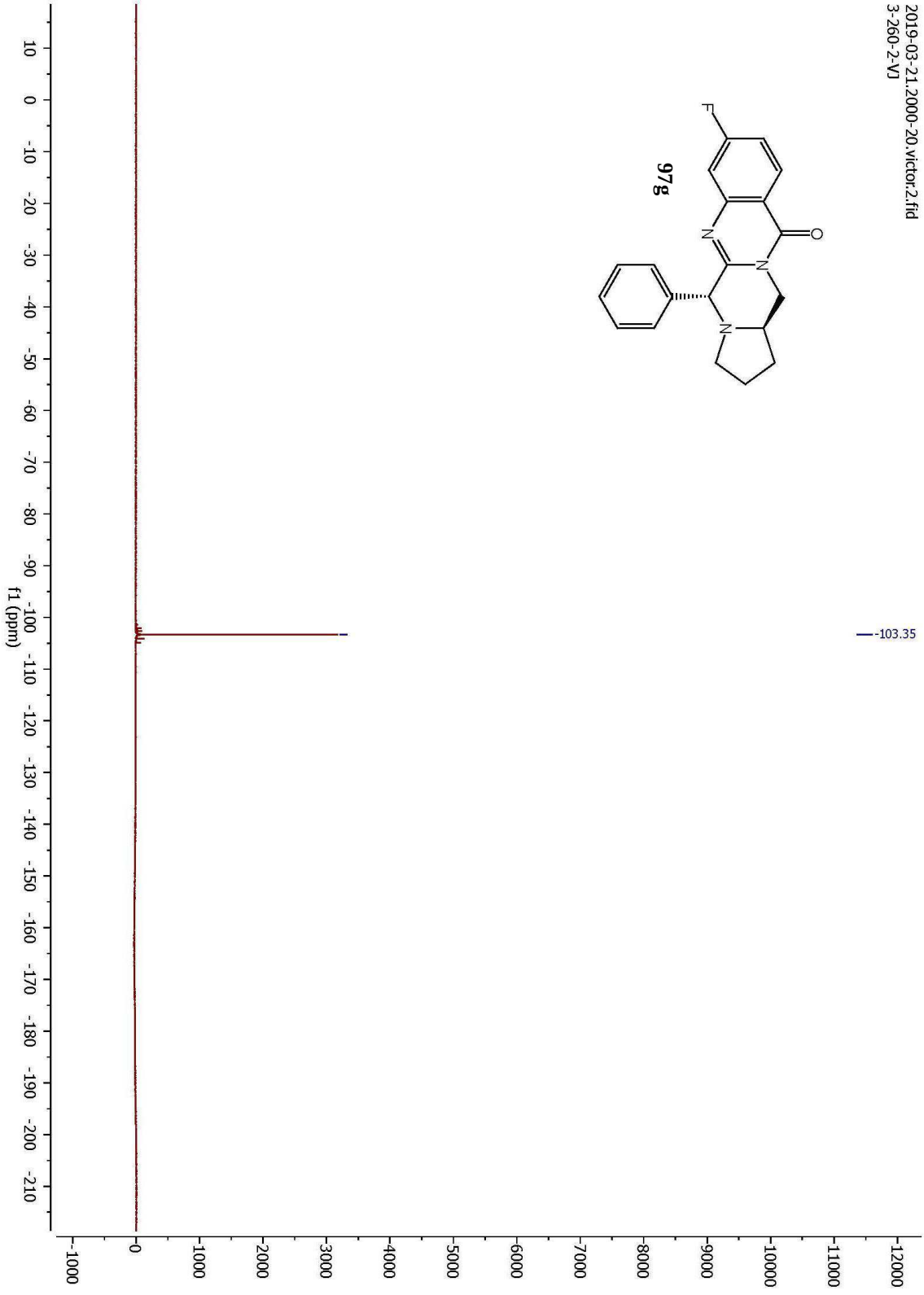
2019-03-21.2000-20.victor.2.fid
3-260-2-VJ
97g
F
N
N
N
O
-103.35
f1 (ppm)
10
0
-10
-20
-30
-40
-50
-60
-70
-80
-90
-100
-110
-120
-130
-140
-150
-160
-170
-180
-190
-200
-210
-1000
0
1000
2000
3000
4000
5000
6000
7000
8000
9000
10000
11000
12000

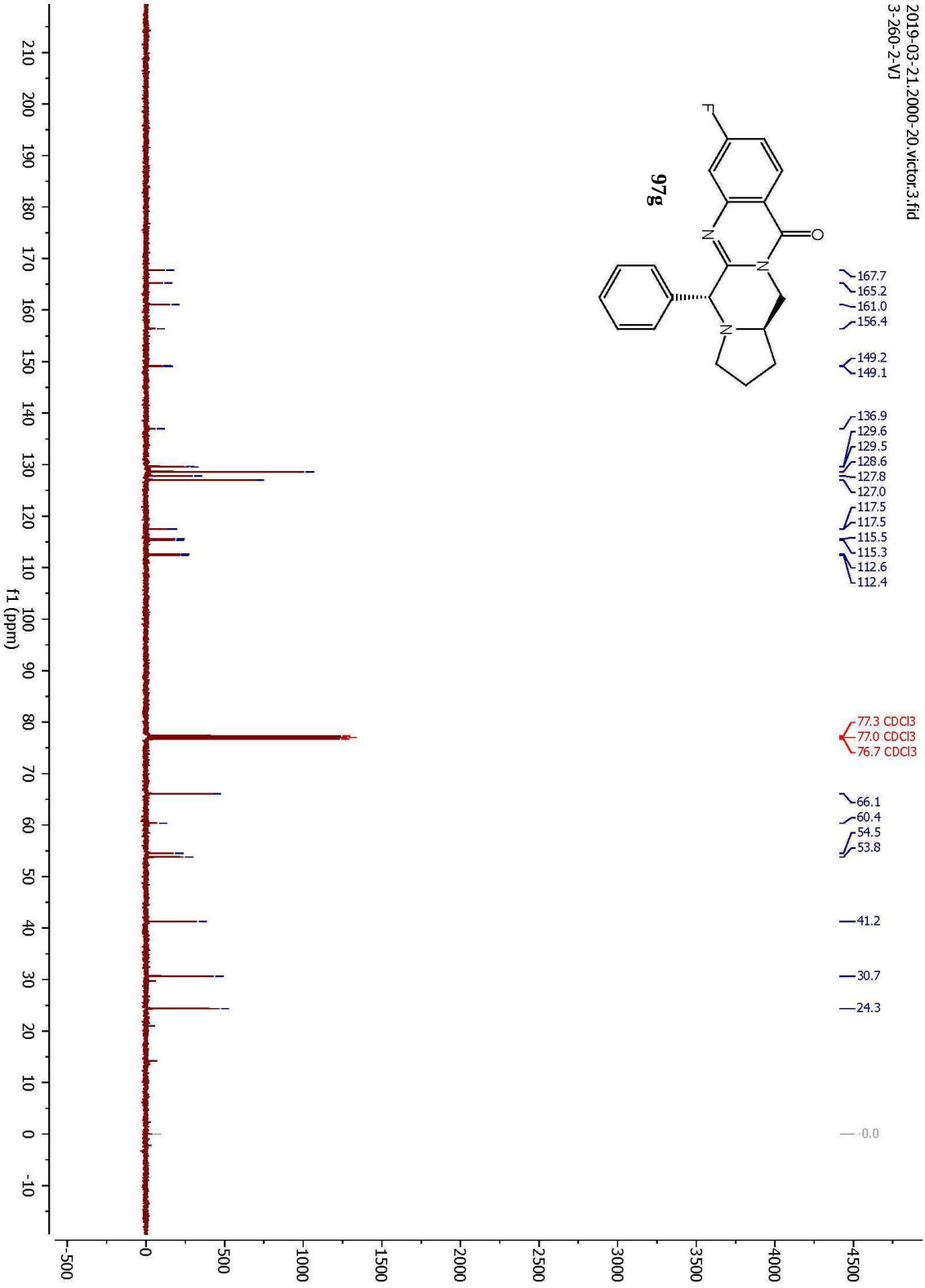
2019-03-21.2000-20.victor.3.fid
3-260-2-VJ
97s
F
N
N
N
O
167.7
165.2
161.0
156.4
149.2
149.1
136.9
129.6
129.5
128.6
127.8
127.0
117.5
117.5
115.5
115.3
112.6
112.4
77.3 CDCl3
77.0 CDCl3
76.7 CDCl3
66.1
60.4
54.5
53.8
41.2
30.7
24.3
0.0
f1 (ppm)

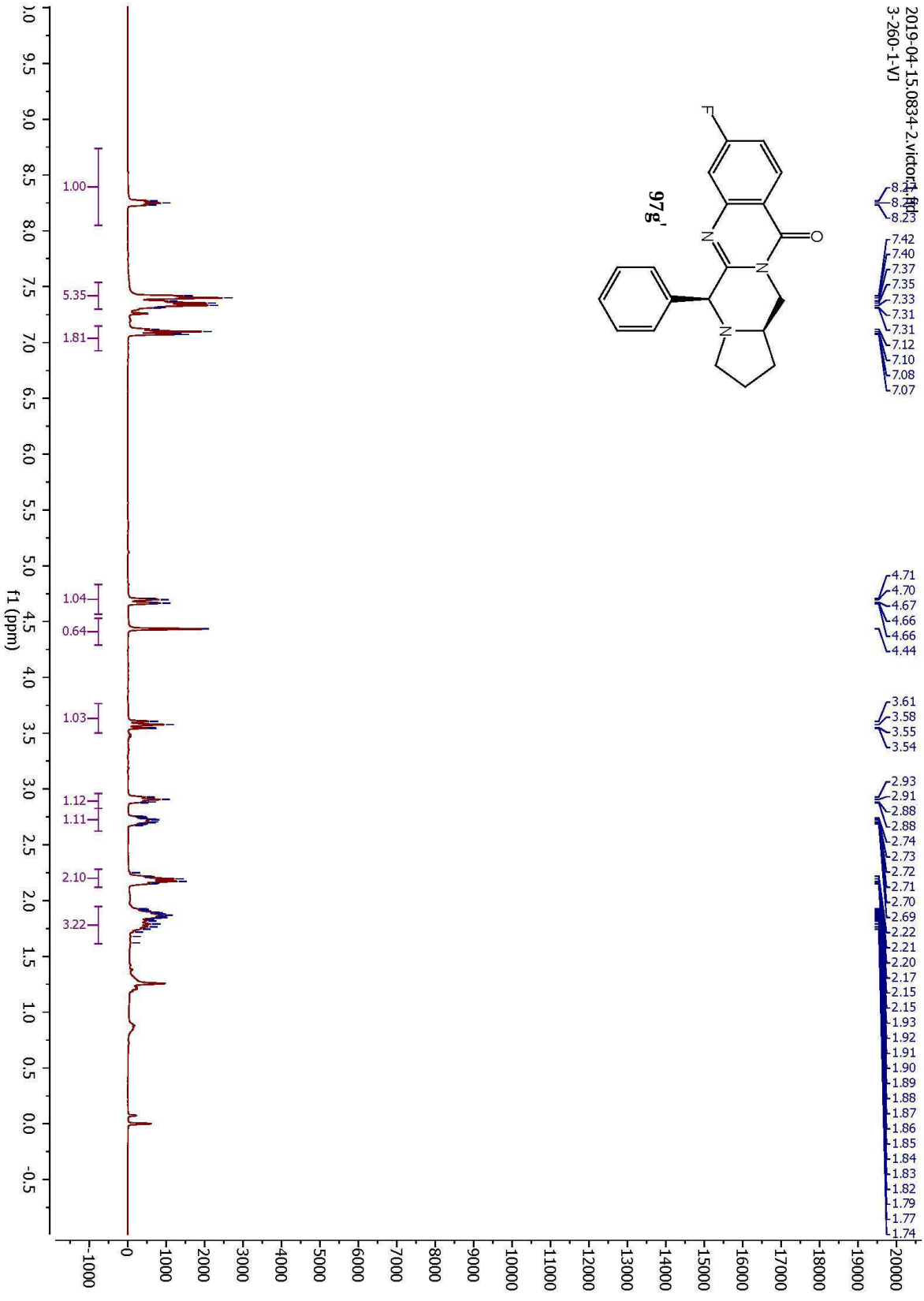
2019-04-15.0834-2.victor.1.fid
3-260-1-VJ
97g'
F
O
N
N
N
8.24
8.23
7.42
7.40
7.37
7.35
7.33
7.31
7.31
7.12
7.10
7.08
7.07
4.71
4.70
4.67
4.66
4.66
4.44
3.61
3.58
3.55
3.54
2.93
2.91
2.88
2.88
2.74
2.73
2.72
2.71
2.70
2.69
2.22
2.21
2.20
2.17
2.15
2.15
1.93
1.92
1.91
1.90
1.89
1.88
1.87
1.86
1.85
1.84
1.83
1.82
1.79
1.77
1.74
1.00
5.35
1.81
1.04
0.64
1.03
1.12
1.11
2.10
3.22
f1 (ppm)

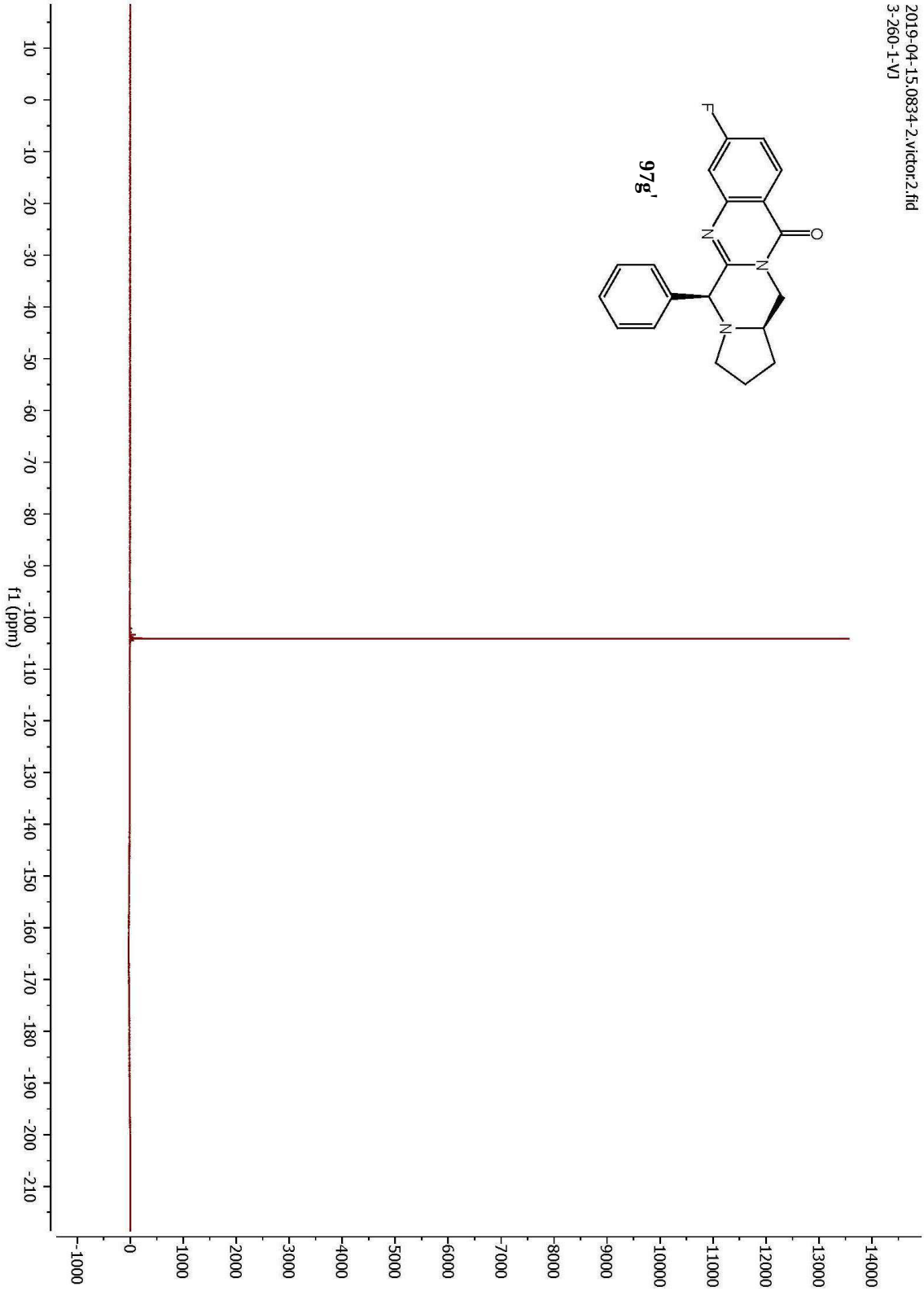
2019-04-15.0834-2.victor.2.fid
3-260-1-VJ
97g'
F
O
N
N
N
f1 (ppm)
10
0
-10
-20
-30
-40
-50
-60
-70
-80
-90
-100
-110
-120
-130
-140
-150
-160
-170
-180
-190
-200
-210
-1000
0
1000
2000
3000
4000
5000
6000
7000
8000
9000
10000
11000
12000
13000
14000

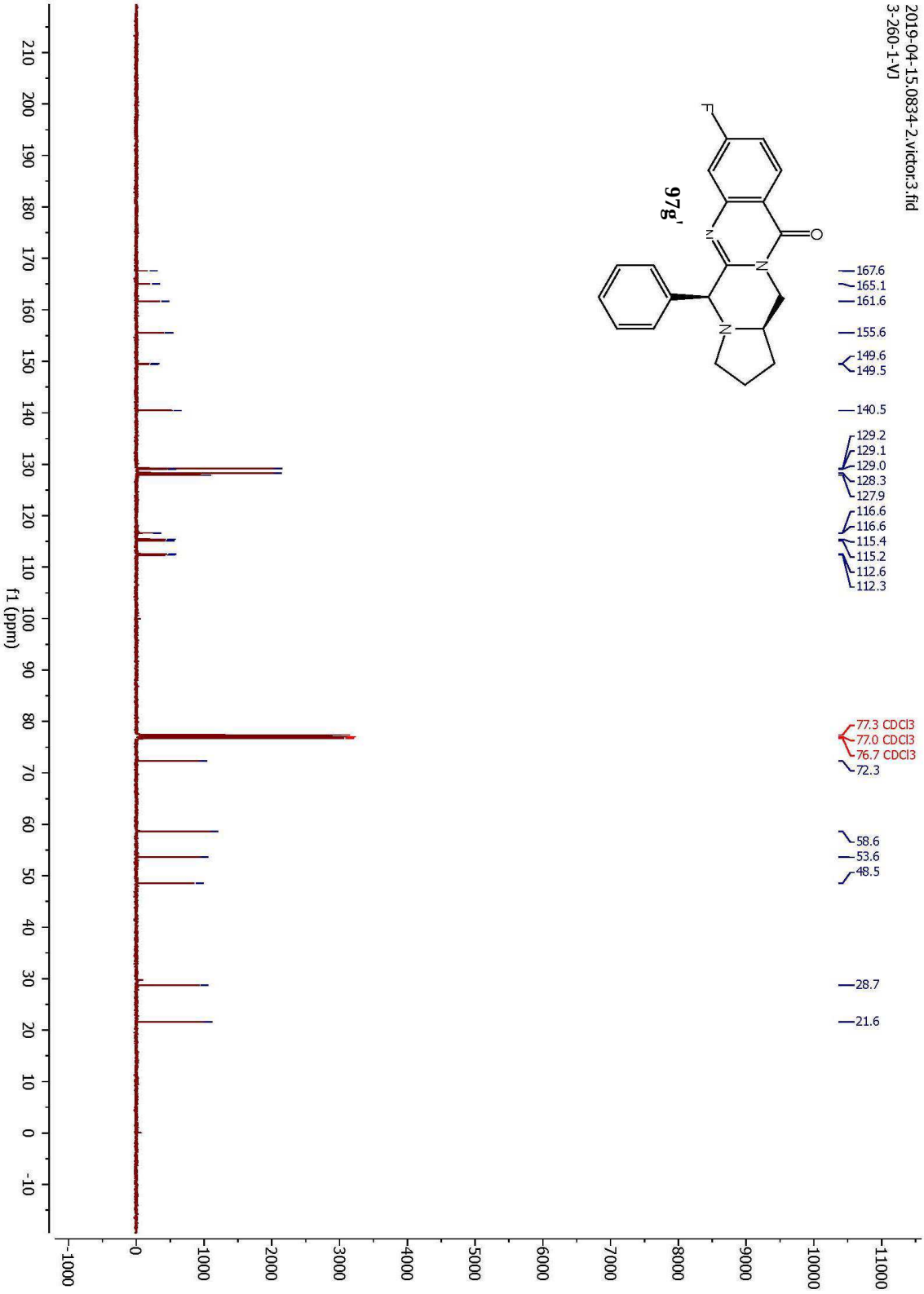
2019-04-15.0834-2.victor.3.fid
3-260-1-VJ
97g'
F
O
N
N
N
167.6
165.1
161.6
155.6
149.6
149.5
140.5
129.2
129.1
129.0
128.3
127.9
116.6
116.6
115.4
115.2
112.6
112.3
77.3 CDCl3
77.0 CDCl3
76.7 CDCl3
72.3
58.6
53.6
48.5
28.7
21.6
f1 (ppm)

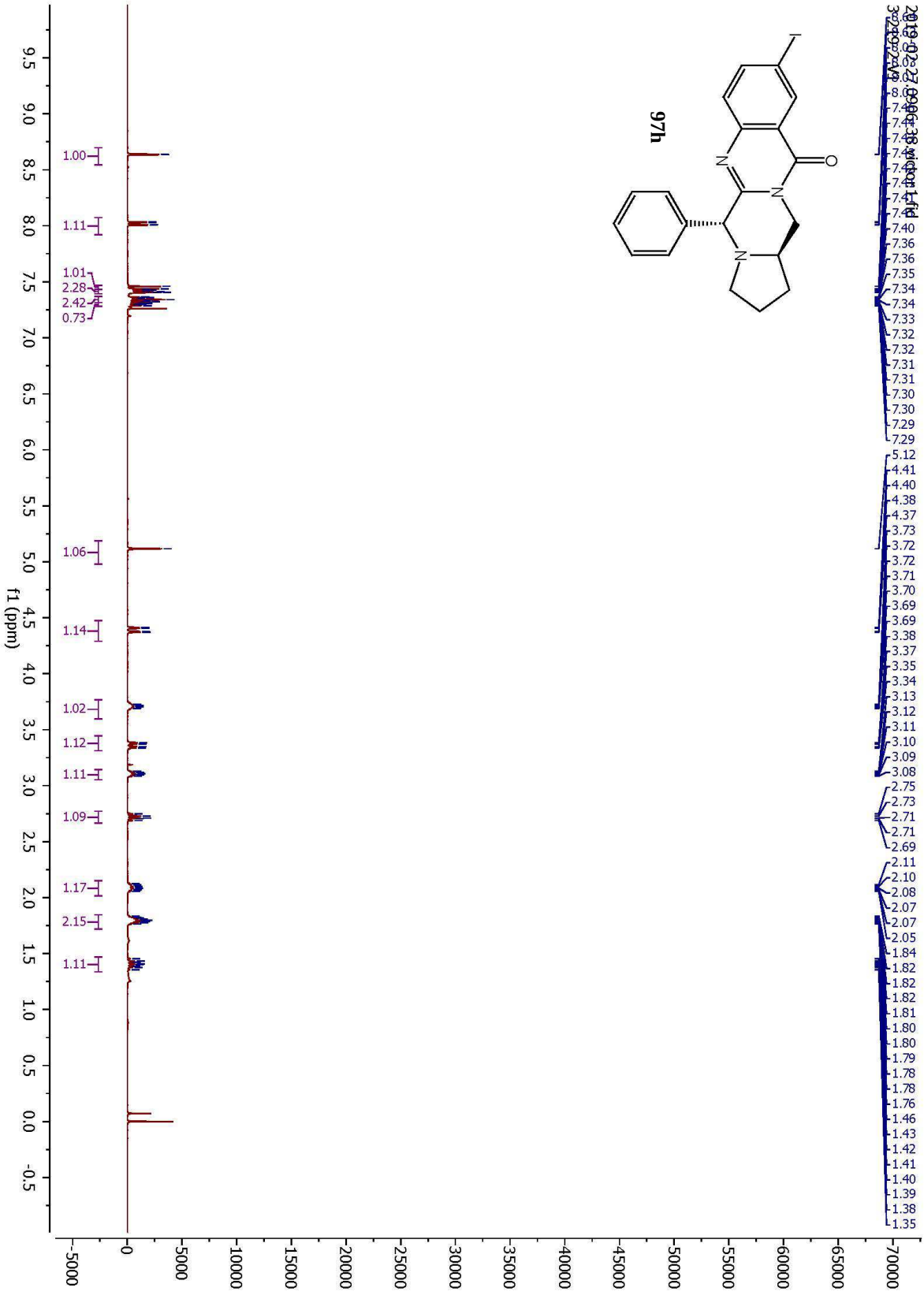
97h
f1 (ppm)
1.00
1.11
1.01
2.28
2.42
0.73
1.06
1.14
1.02
1.12
1.11
1.09
1.17
2.15
1.11

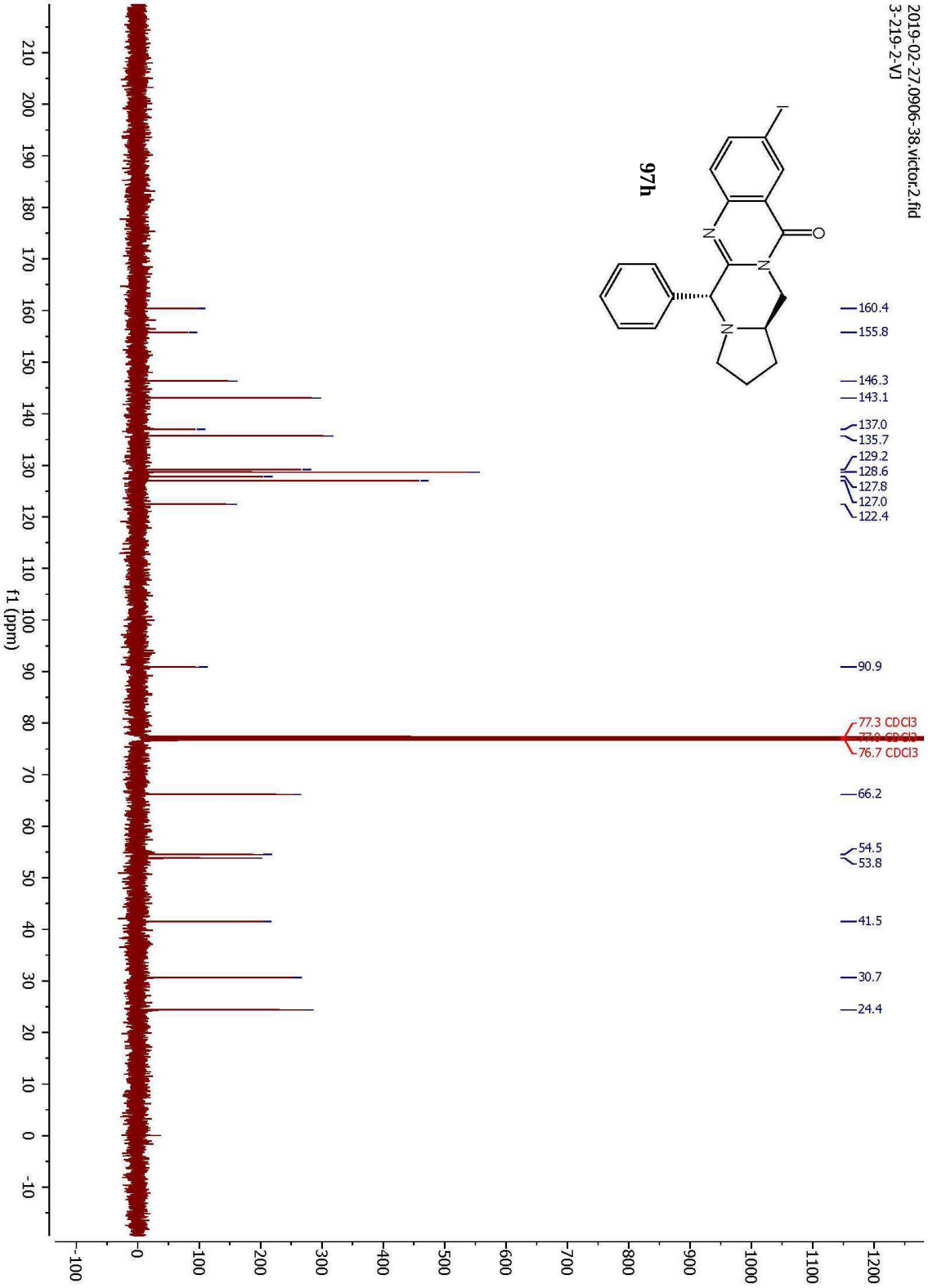
2019-02-27.0906-38.victor.2.fid
3-219-2-VJ
97h
160.4
155.8
146.3
143.1
137.0
135.7
129.2
128.6
127.8
127.0
122.4
90.9
77.3 CDCl3
77.0 CDCl3
76.7 CDCl3
66.2
54.5
53.8
41.5
30.7
24.4
f1 (ppm)

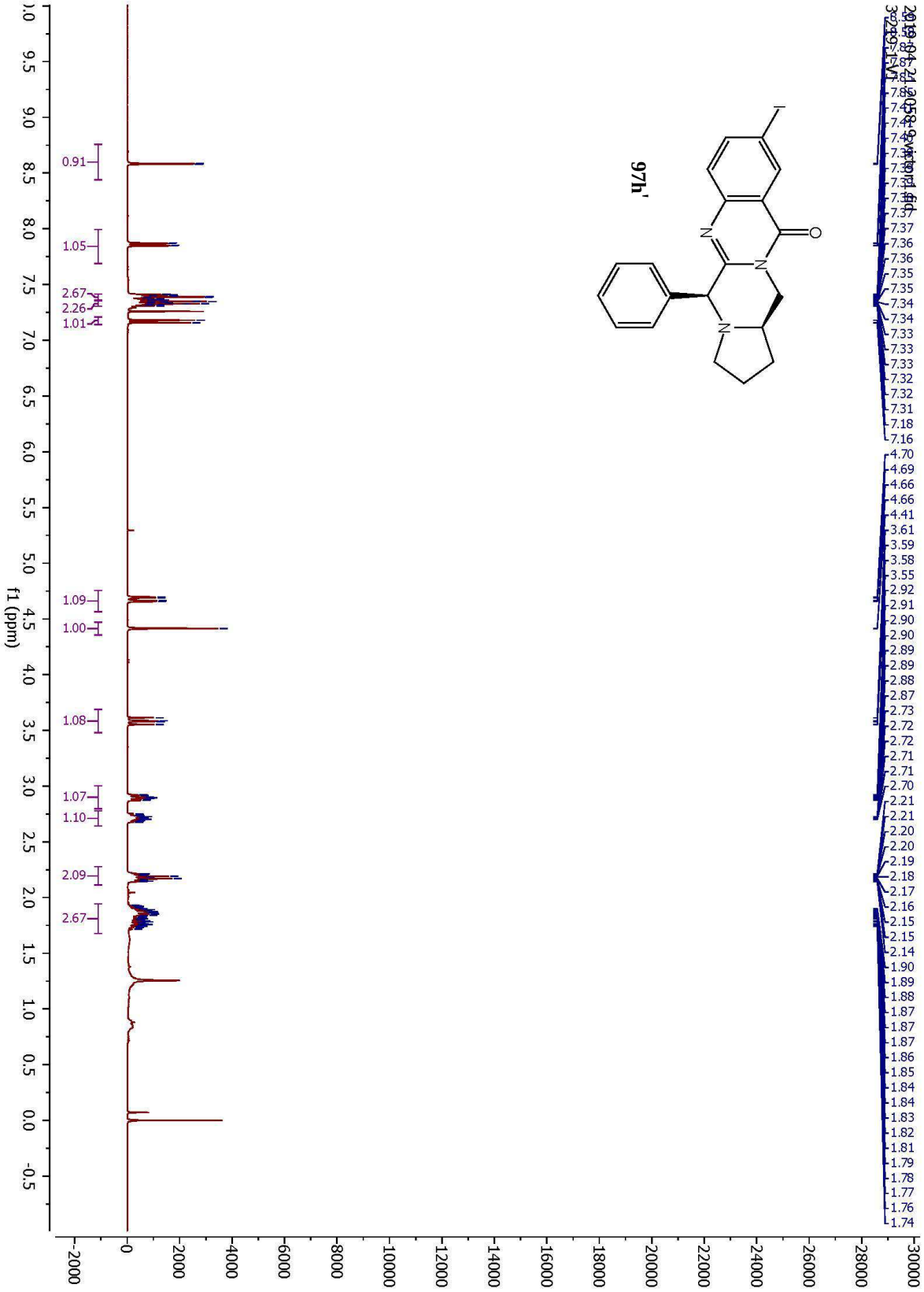
97h'
f1 (ppm)
0.91
1.05
2.67
2.26
1.01
1.09
1.00
1.08
1.07
1.10
2.09
2.67

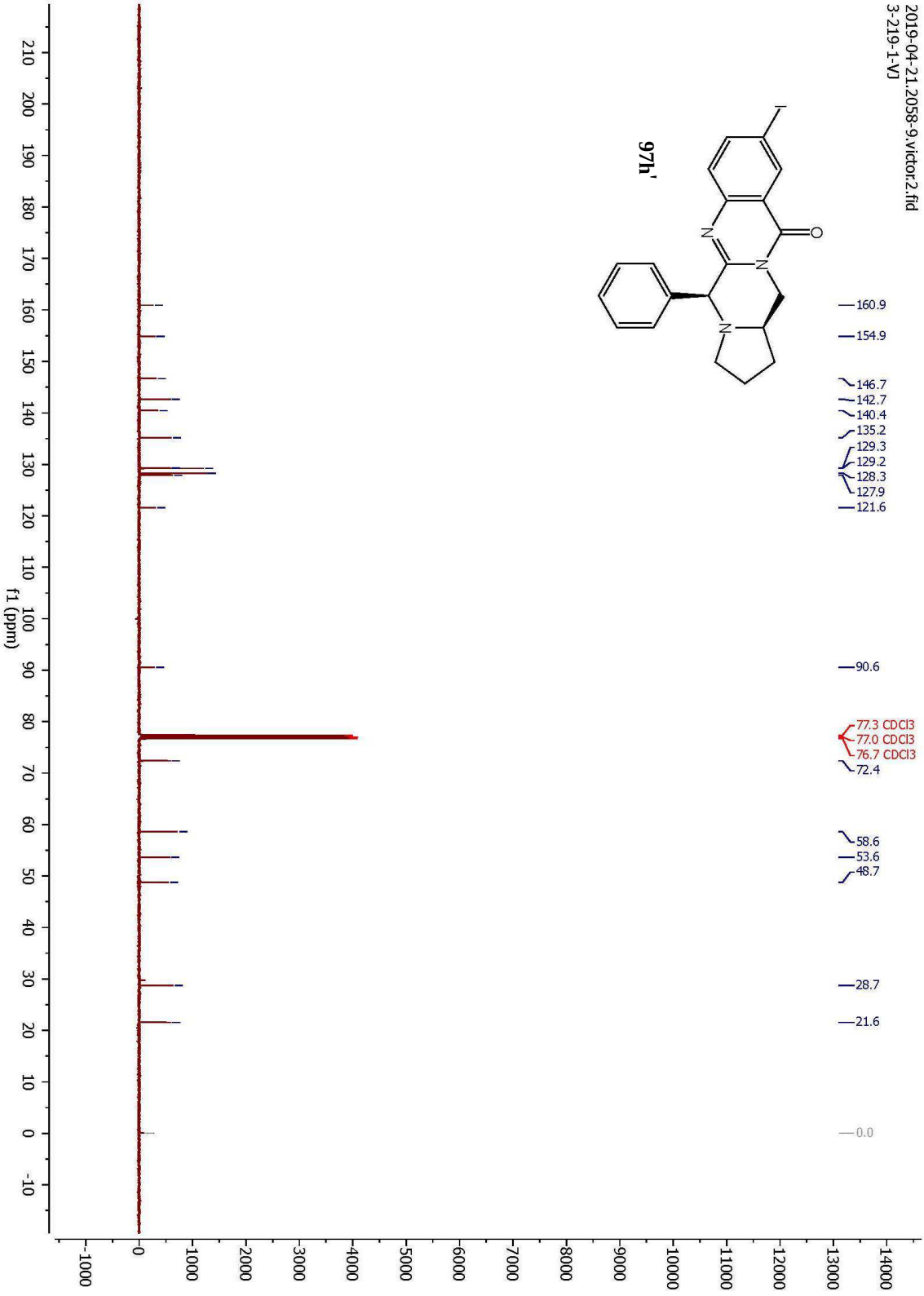
2019-04-21.2058-9.victor.2.fid
3-219-1-VJ
97h'
160.9
154.9
146.7
142.7
140.4
135.2
129.3
129.2
128.3
127.9
121.6
90.6
77.3 CDCl3
77.0 CDCl3
76.7 CDCl3
72.4
58.6
53.6
48.7
28.7
21.6
0.0
f1 (ppm)

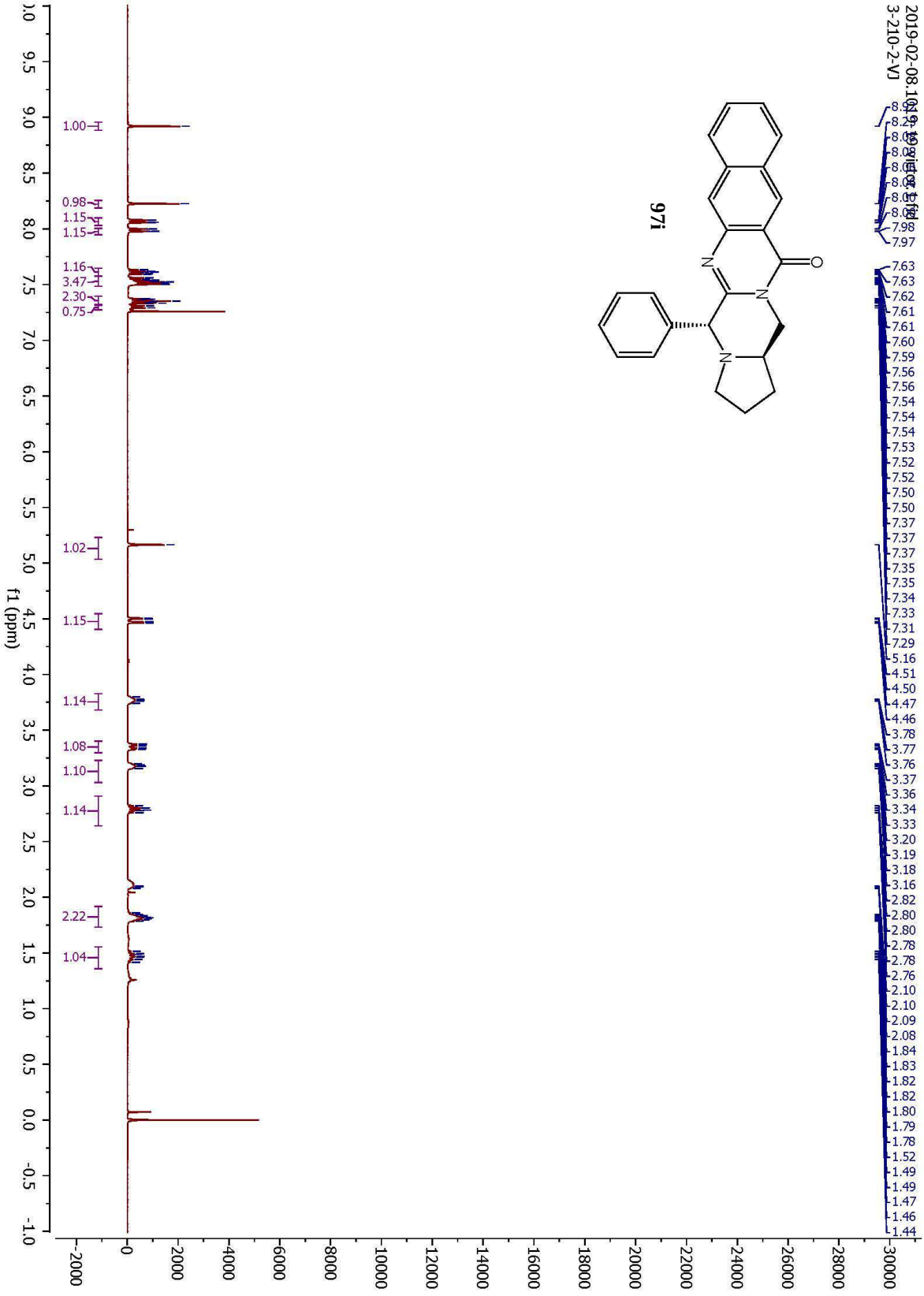
97i
f1 (ppm)
1.00
0.98
1.15
1.15
1.16
3.47
2.30
0.75
1.02
1.15
1.14
1.08
1.10
1.14
2.22
1.04

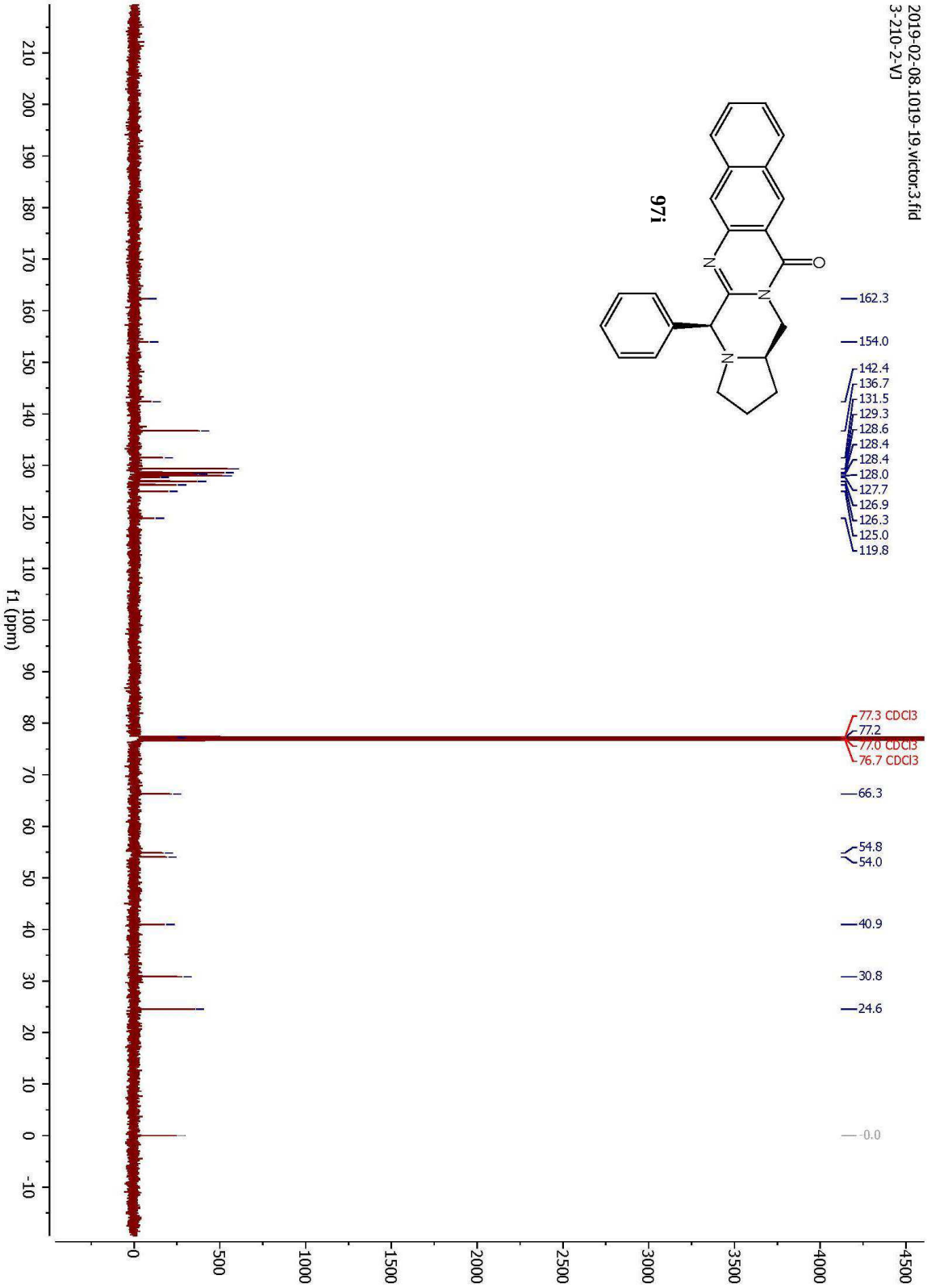
2019-02-08,1019-19,victor,3.fid
3-210-2-VJ
97i
162.3
154.0
142.4
136.7
131.5
129.3
128.6
128.4
128.4
128.0
127.7
126.9
126.3
125.0
119.8
77.3 CDCl3
77.2
77.0 CDCl3
76.7 CDCl3
66.3
54.8
54.0
40.9
30.8
24.6
0.0
f1 (ppm)

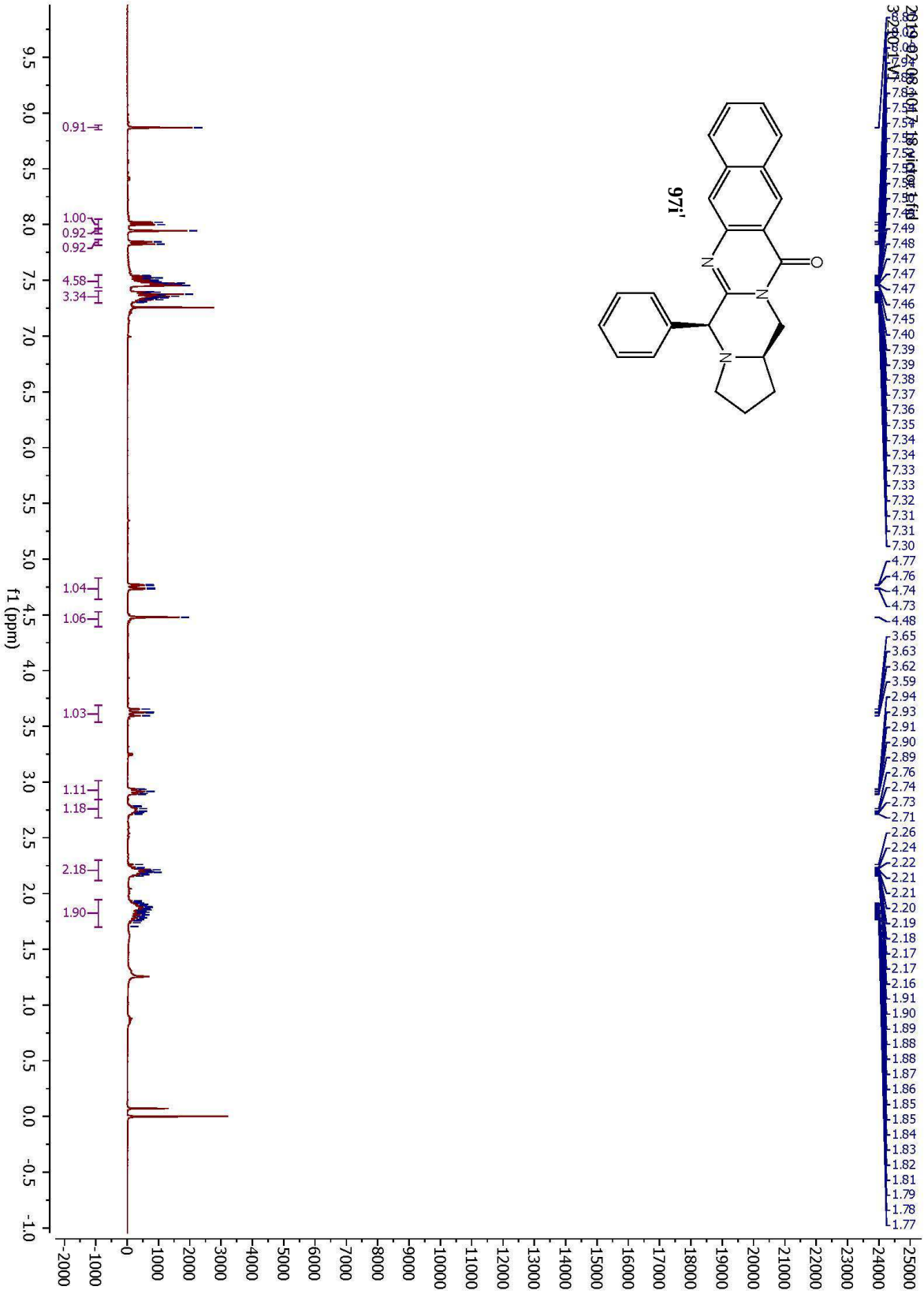
97i'
f1 (ppm)
0.91
1.00
0.92
0.92
4.58
3.34
1.04
1.06
1.03
1.11
1.18
2.18
1.90

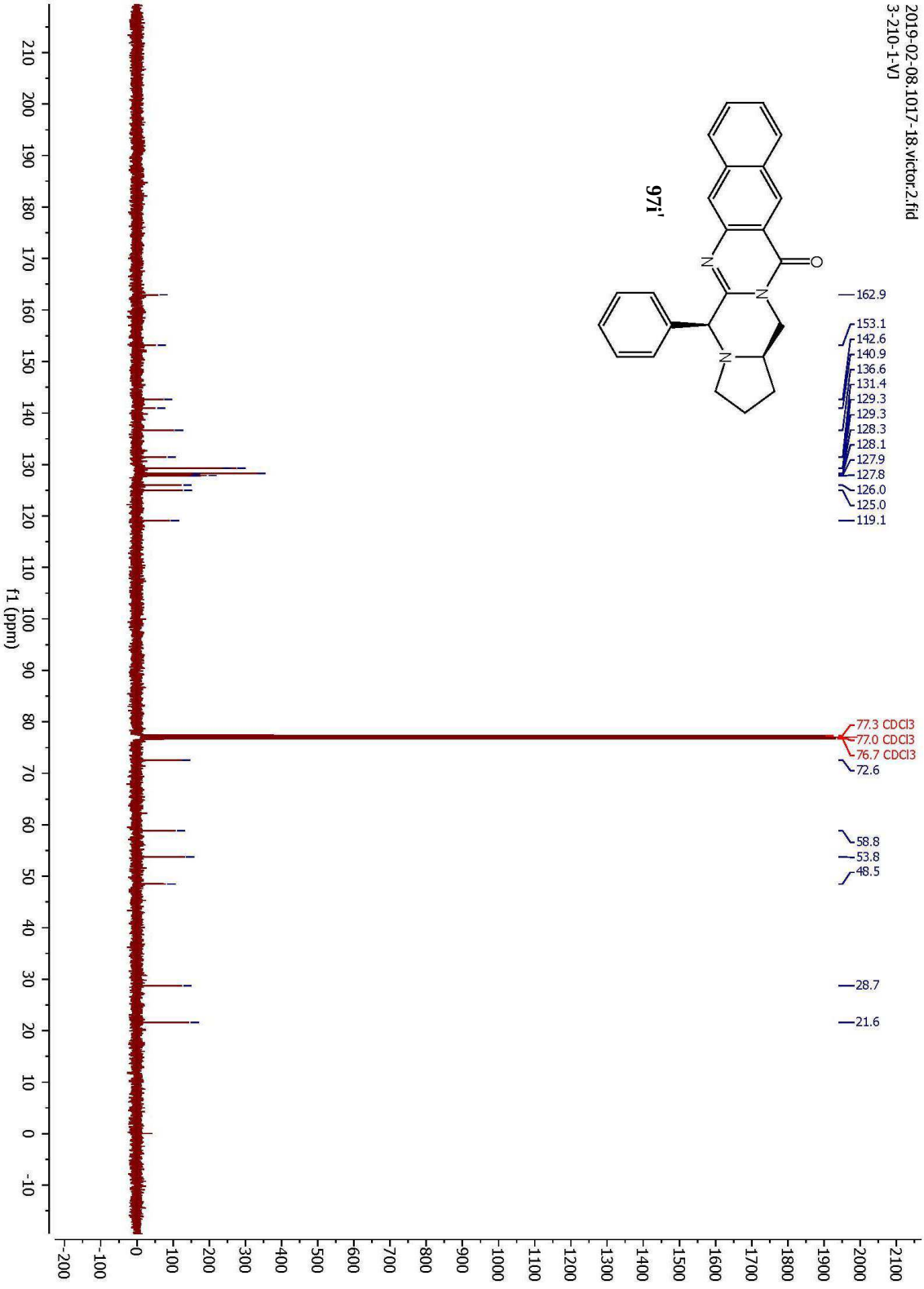
2019-02-08.1017-18.victor.2.fid
3-210-1-VJ
97i'
162.9
153.1
142.6
140.9
136.6
131.4
129.3
129.3
128.3
128.1
127.9
127.8
126.0
125.0
119.1
77.3 CDCl3
77.0 CDCl3
76.7 CDCl3
72.6
58.8
53.8
48.5
28.7
21.6
f1 (ppm)

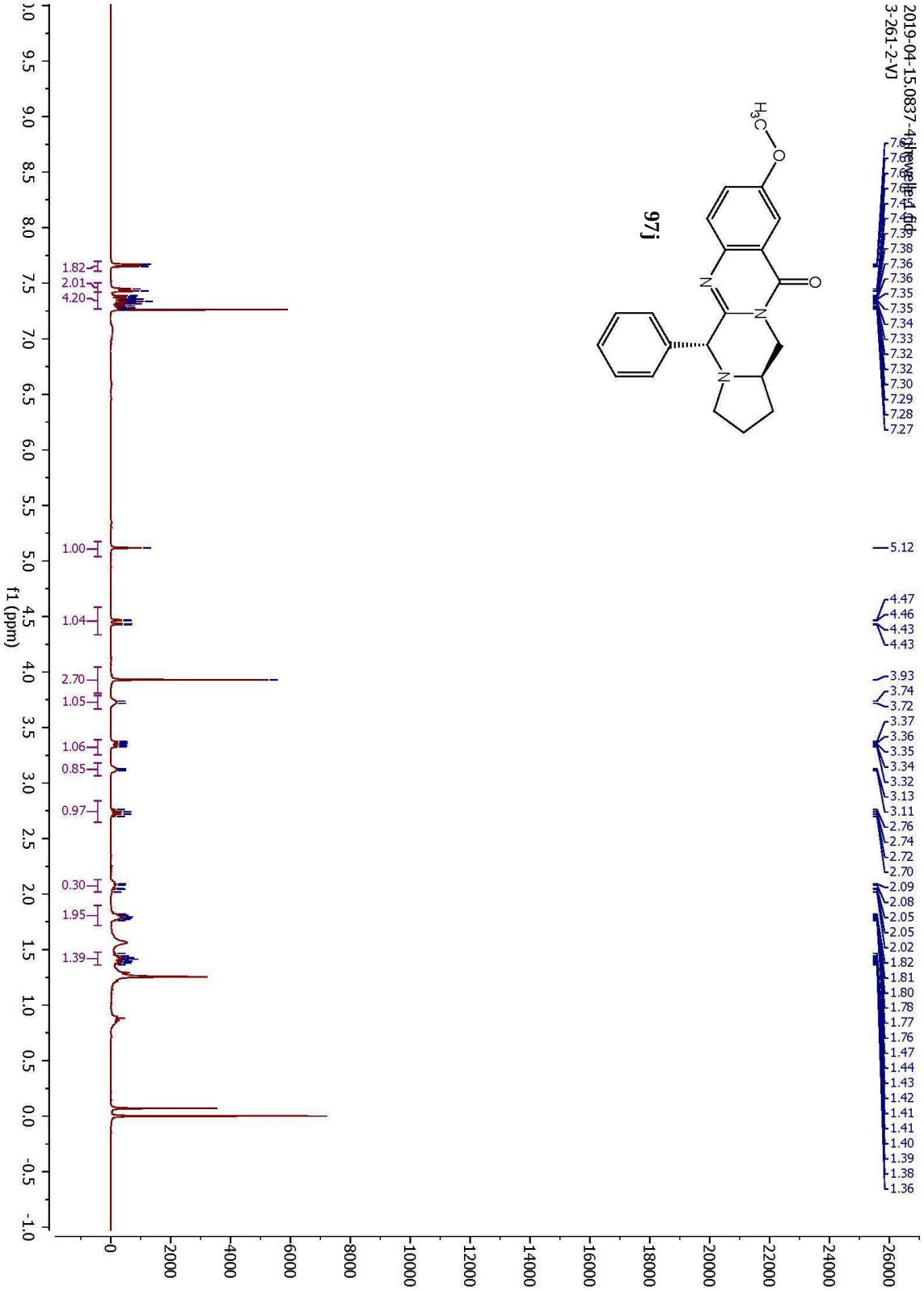
2019-04-15.0837-4-neuelle-1 fob
3-261-2-VJ
97j
f1 (ppm)

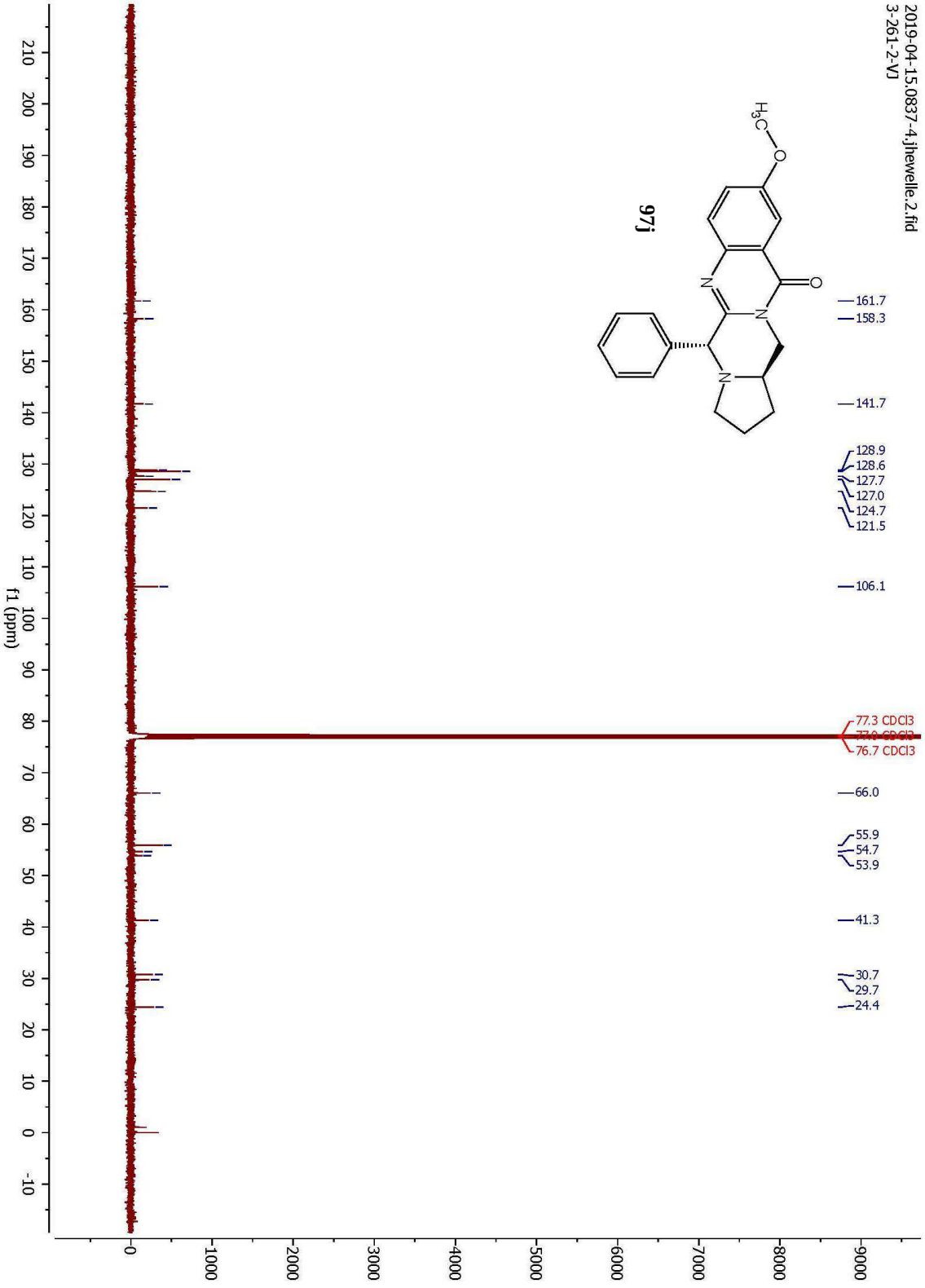
2019-04-15.0837-4.jhewelle.2.fid
3-261-2-VJ
97j
161.7
158.3
141.7
128.9
128.6
127.7
127.0
124.7
121.5
106.1
77.3 CDCl3
77.0 CDCl3
76.7 CDCl3
66.0
55.9
54.7
53.9
41.3
30.7
29.7
24.4
f1 (ppm)

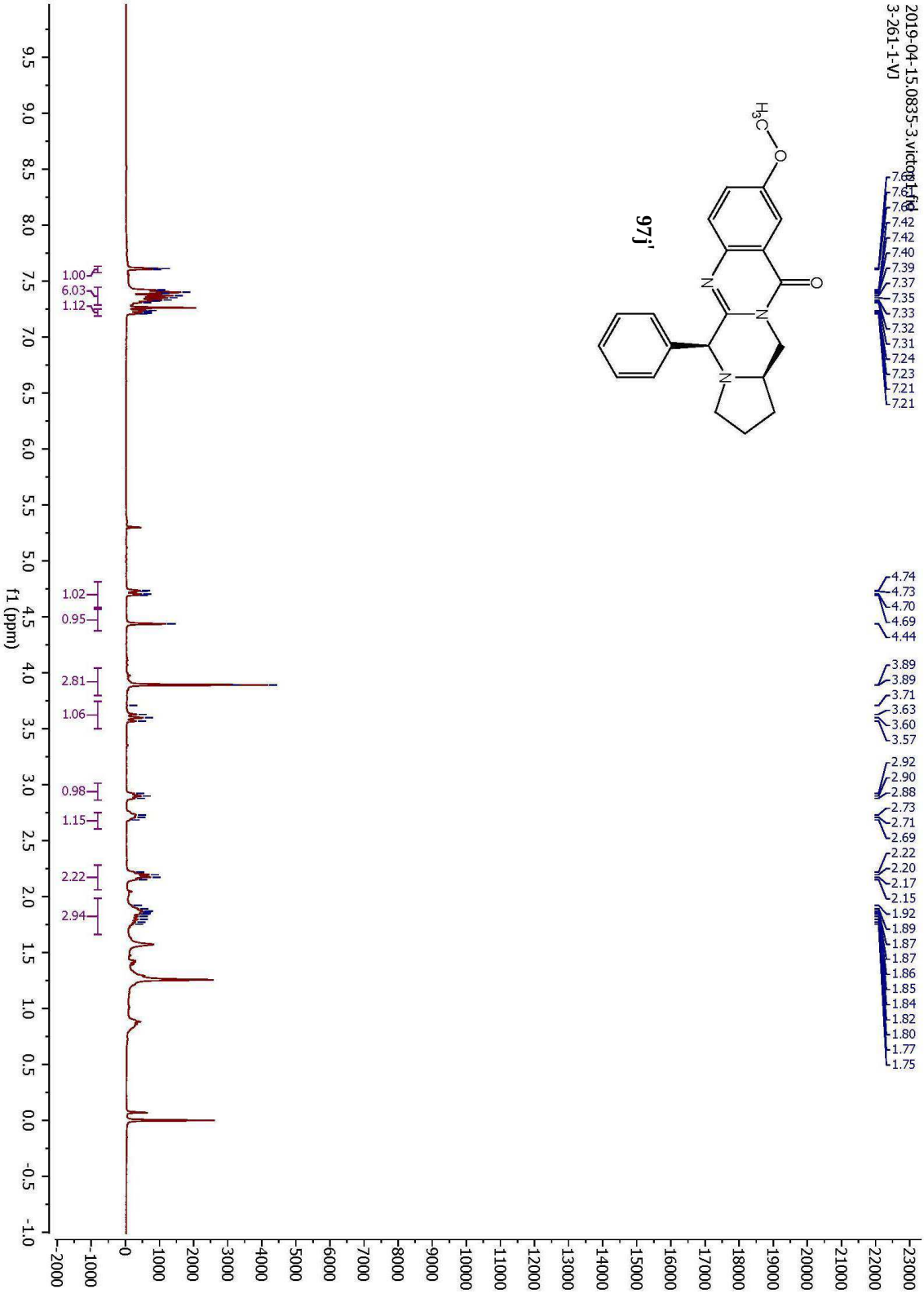
2019-04-15.0835-3.victor-1-fid
3-261-1-VJ
97j'
H3C
O
N
N
N
O
7.78
7.62
7.42
7.42
7.40
7.39
7.37
7.35
7.33
7.32
7.31
7.24
7.23
7.21
7.21
4.74
4.73
4.70
4.69
4.44
3.89
3.89
3.71
3.63
3.60
3.57
2.92
2.90
2.88
2.73
2.71
2.69
2.22
2.20
2.17
2.15
1.92
1.89
1.87
1.87
1.86
1.85
1.84
1.82
1.80
1.77
1.75
1.00
6.03
1.12
1.02
0.95
2.81
1.06
0.98
1.15
2.22
2.94
f1 (ppm)

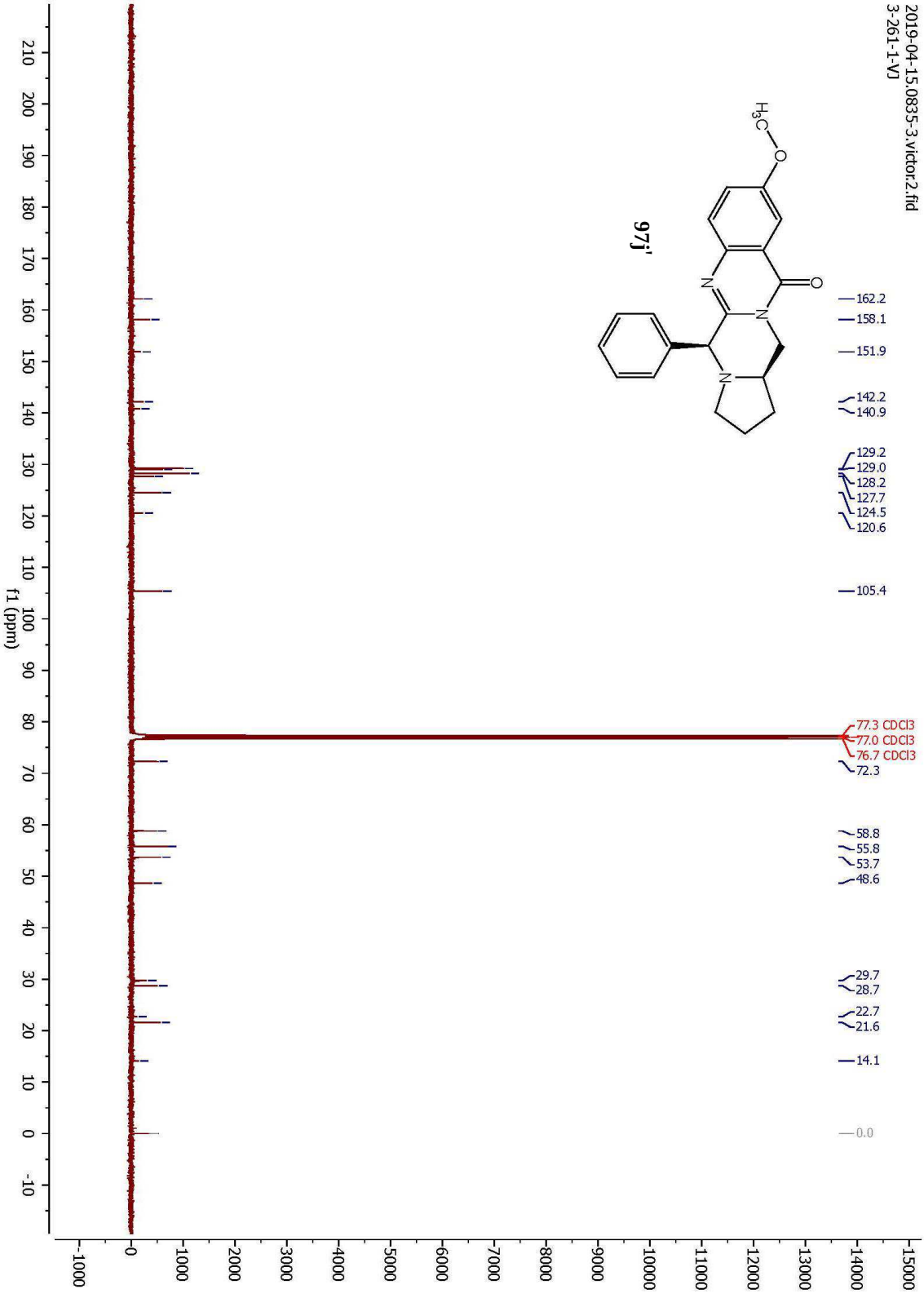
2019-04-15.0835-3.victor.2.fid
3-261-1-VJ
97j'
H3C
O
N
N
N
O
162.2
158.1
151.9
142.2
140.9
129.2
129.0
128.2
127.7
124.5
120.6
105.4
77.3 CDCl3
77.0 CDCl3
76.7 CDCl3
72.3
58.8
55.8
53.7
48.6
29.7
28.7
22.7
21.6
14.1
0.0
f1 (ppm)

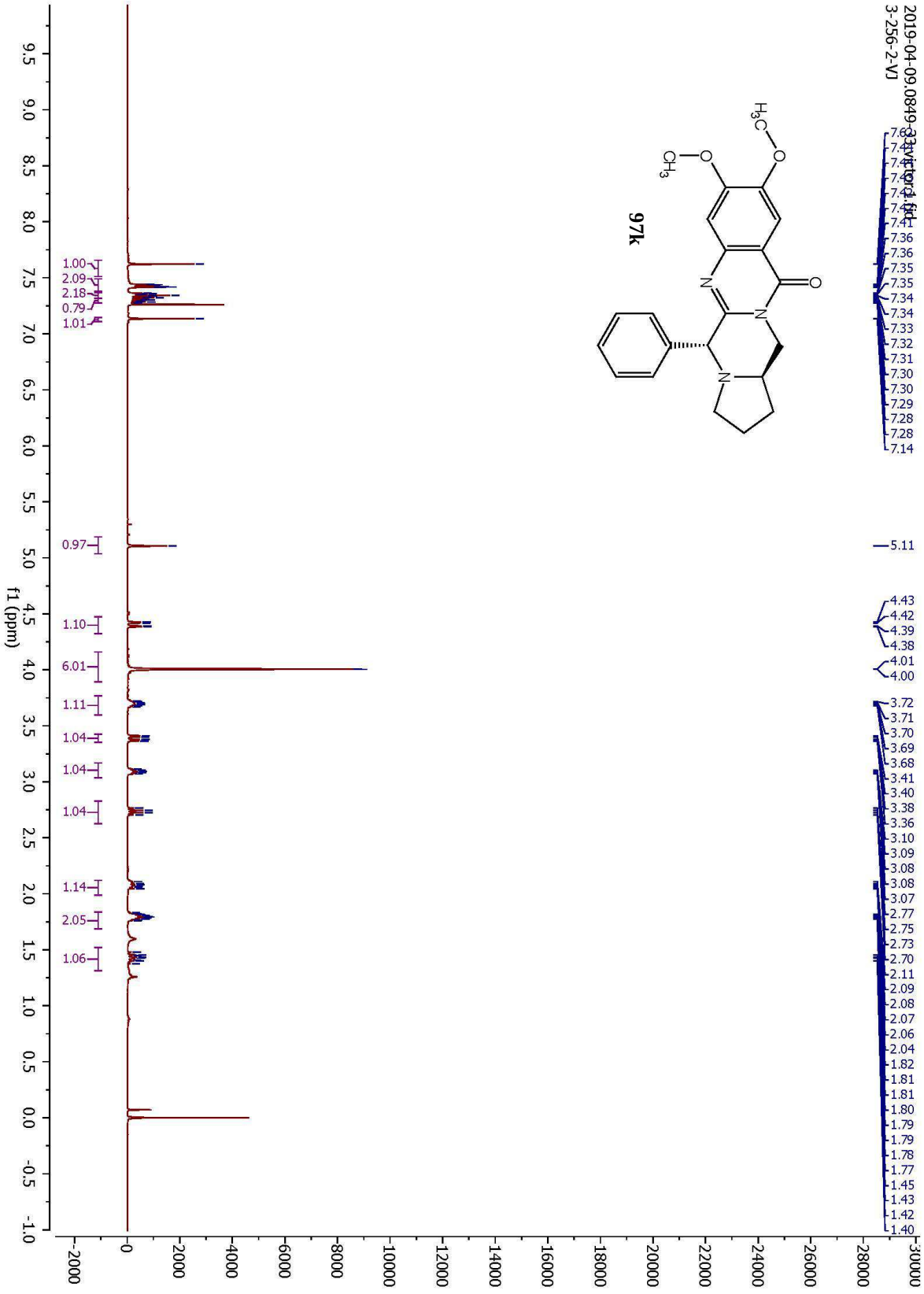
97k
2019-04-09 08:49:33 victor 1 1H
3-256-2-VJ
f1 (ppm)

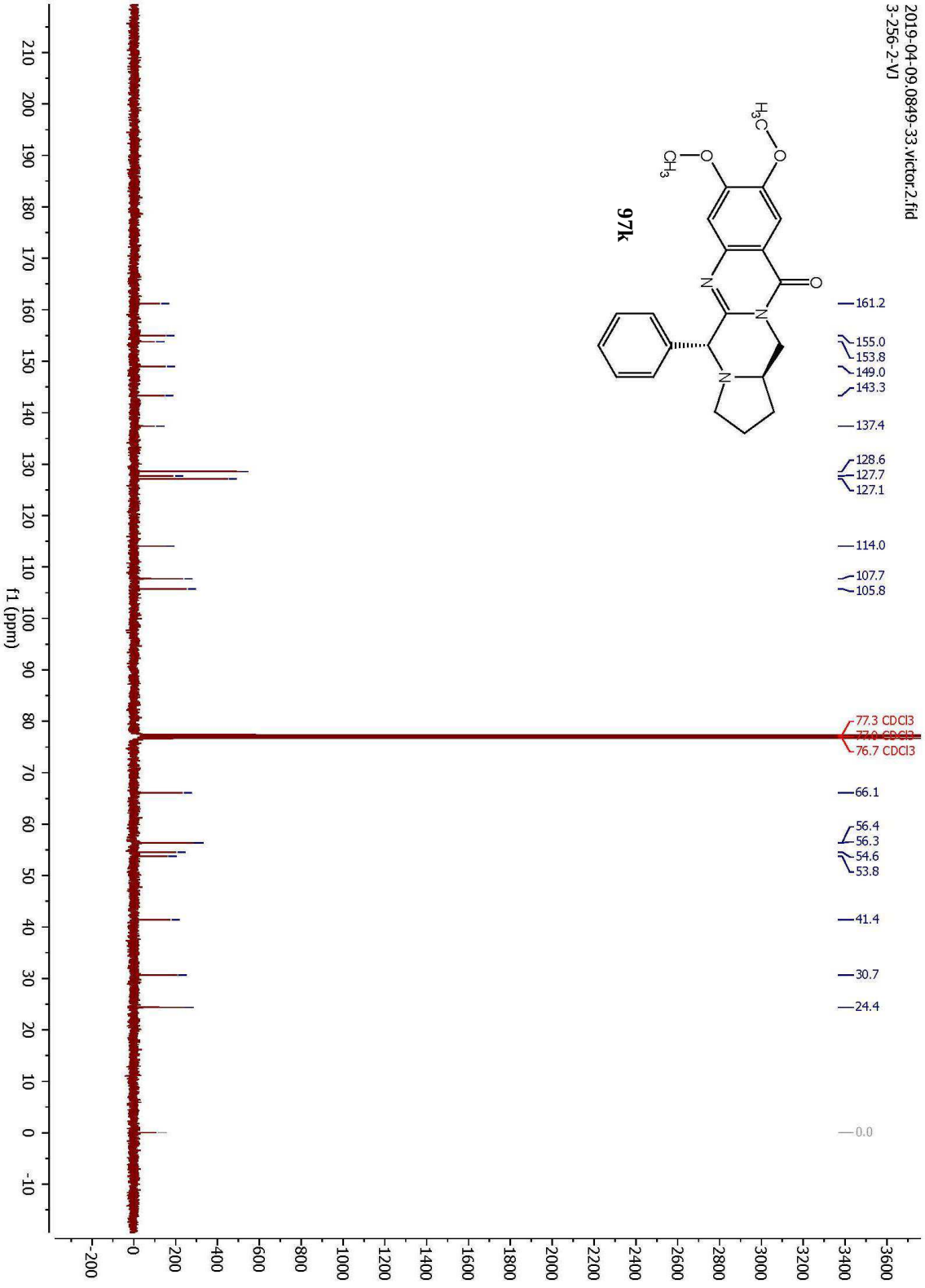
2019-04-09,0849-33.victor.2.fid
3-256-2-VJ
97k
161.2
155.0
153.8
149.0
143.3
137.4
128.6
127.7
127.1
114.0
107.7
105.8
77.3 CDCl3
77.0 CDCl3
76.7 CDCl3
66.1
56.4
56.3
54.6
53.8
41.4
30.7
24.4
0.0
f1 (ppm)

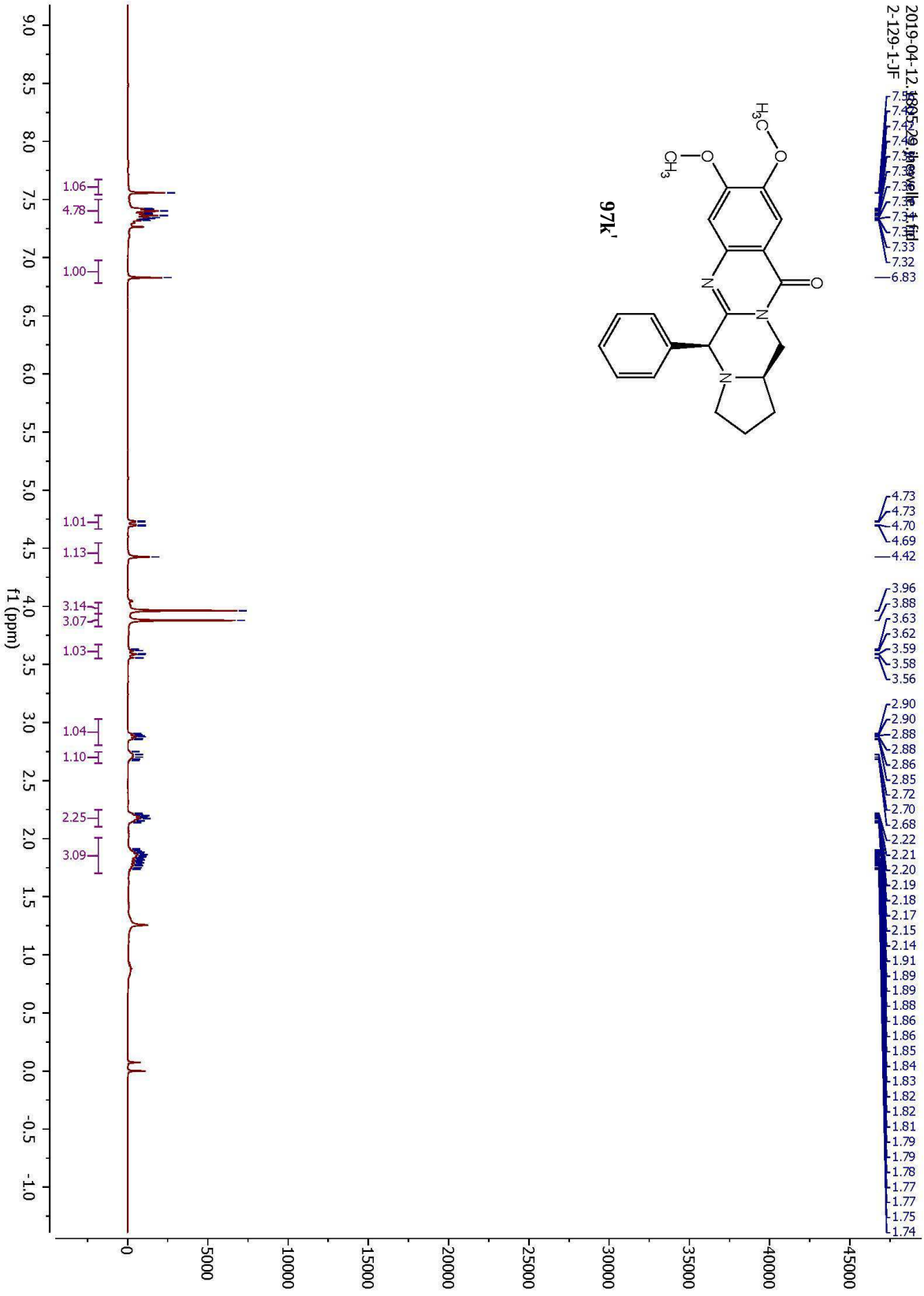
97k'
2019-04-12-1805-29.jdf
2-129-1-JF
f1 (ppm)

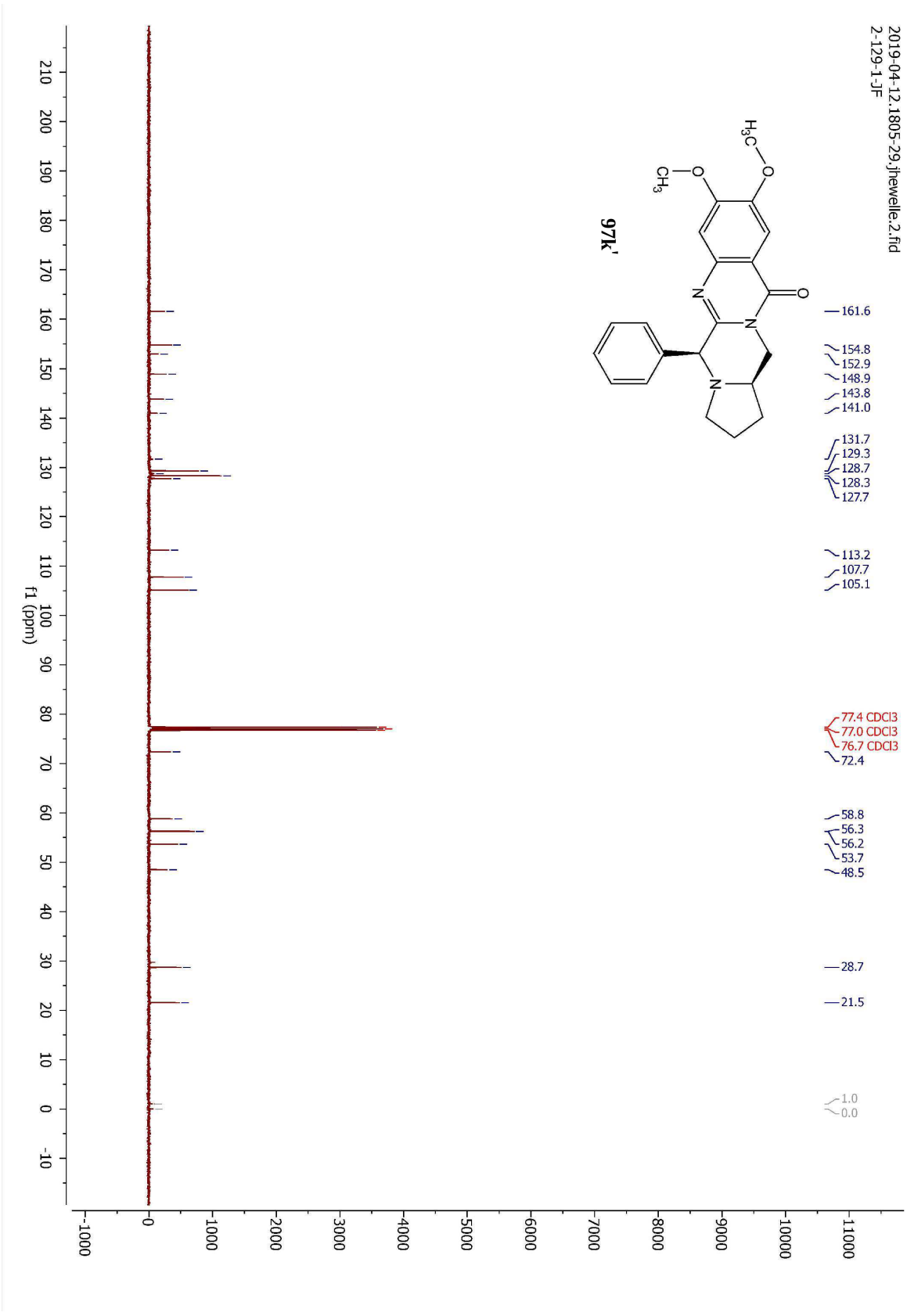
2019-04-12.1805-29.jhewelle.2.fid
2-129-1-JF
97k'
161.6
154.8
152.9
148.9
143.8
141.0
131.7
129.3
128.7
128.3
127.7
113.2
107.7
105.1
77.4 CDCl3
77.0 CDCl3
76.7 CDCl3
72.4
58.8
56.3
56.2
53.7
48.5
28.7
21.5
1.0
0.0
f1 (ppm)

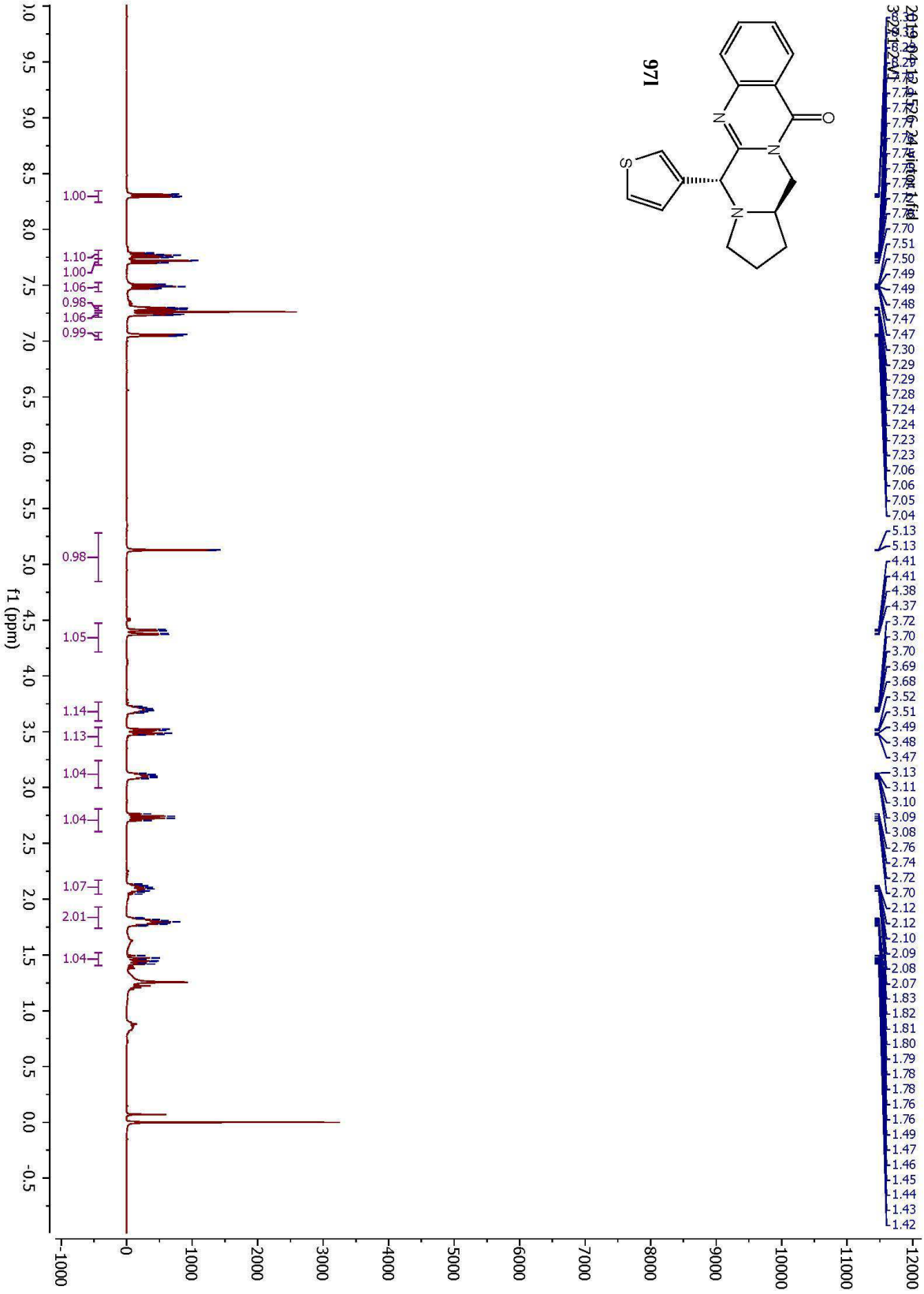
971
f1 (ppm)

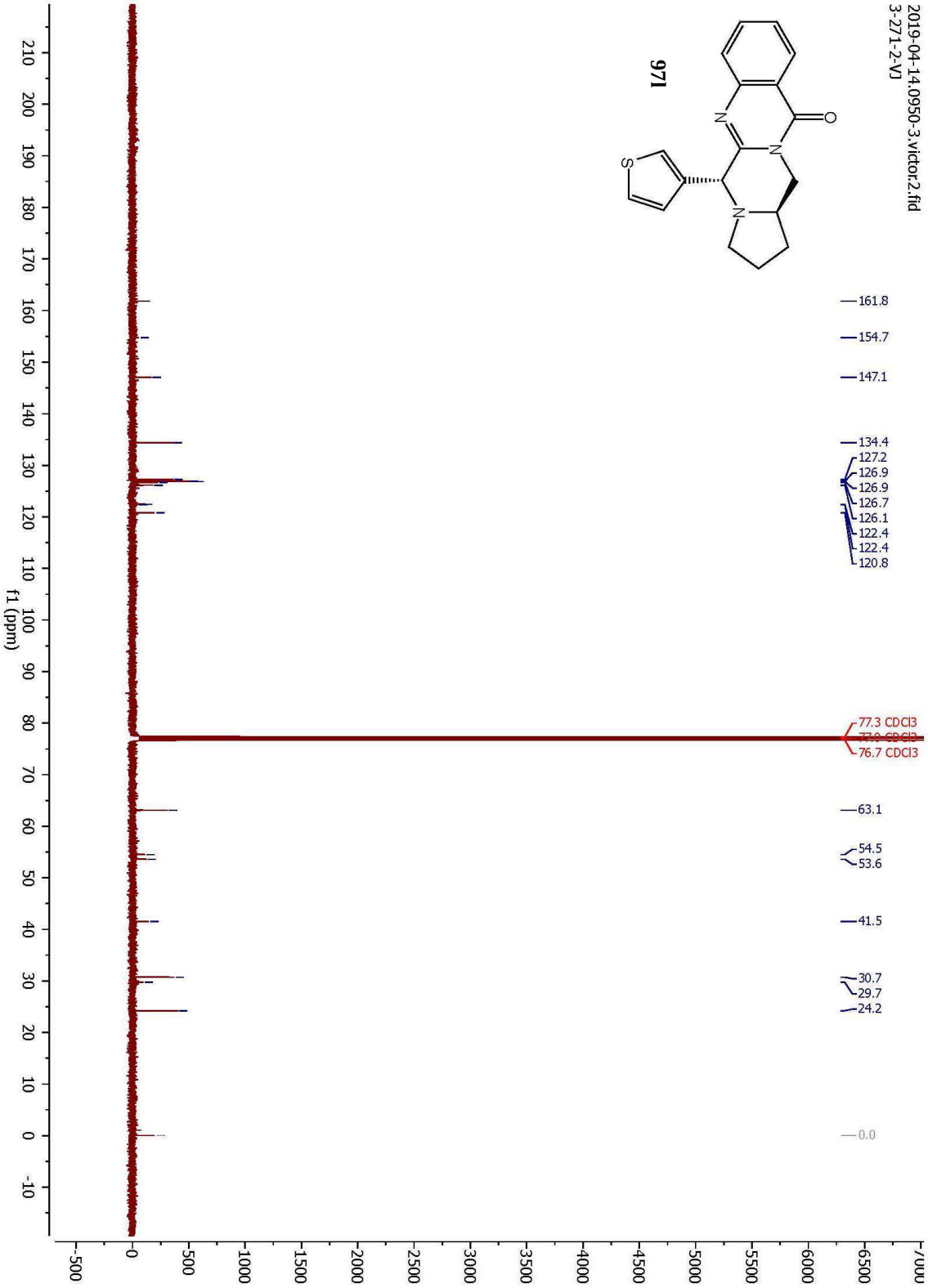
2019-04-14.0950-3.victor2.fid
3-271-2-VJ
97I
161.8
154.7
147.1
134.4
127.2
126.9
126.9
126.7
126.1
122.4
122.4
120.8
77.3 CDCl3
77.0 CDCl3
76.7 CDCl3
63.1
54.5
53.6
41.5
30.7
29.7
24.2
0.0
f1 (ppm)

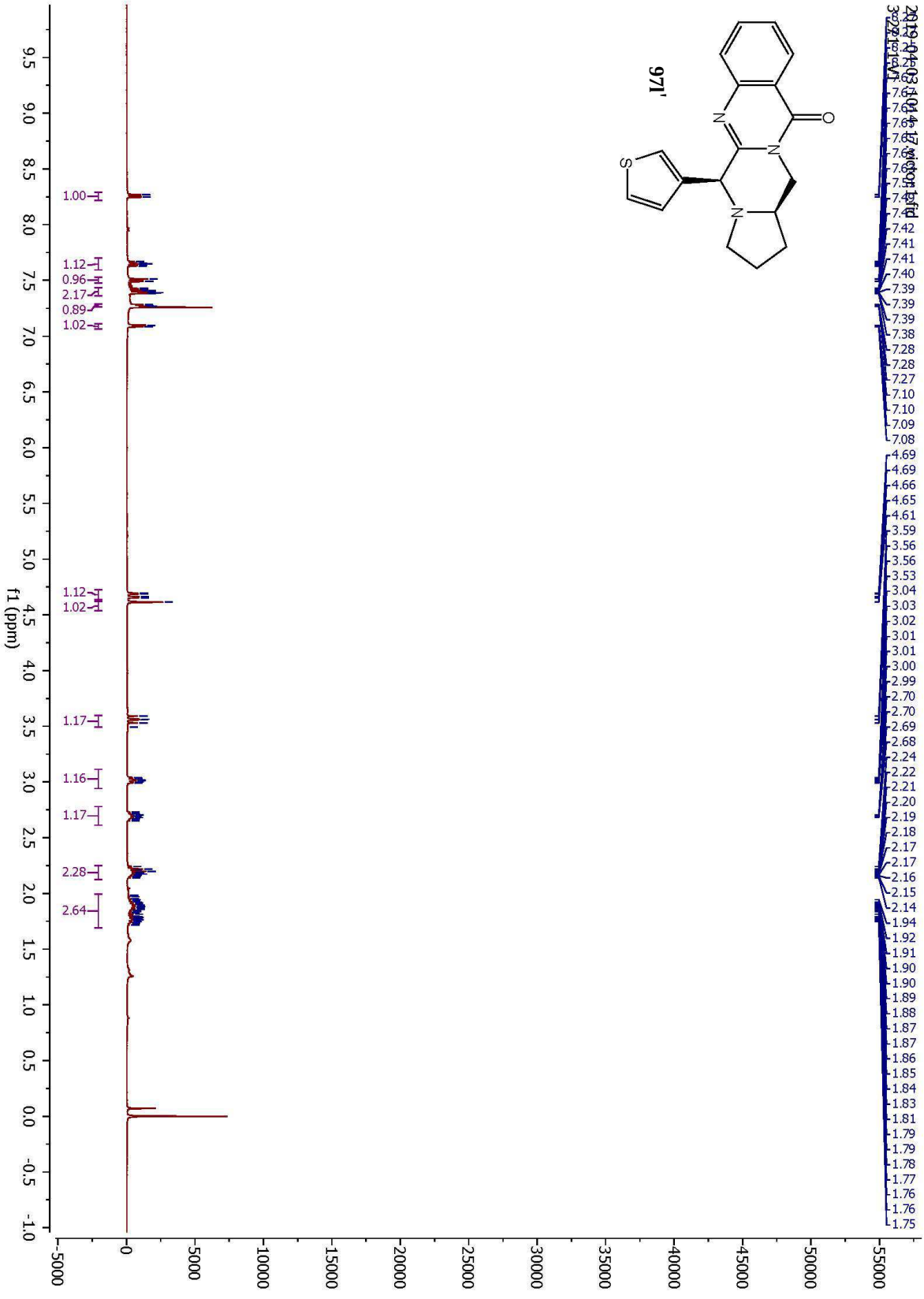
971'
f1 (ppm)
1.00
1.12
0.96
2.17
0.89
1.02
1.12
1.02
1.17
1.16
1.17
2.28
2.64

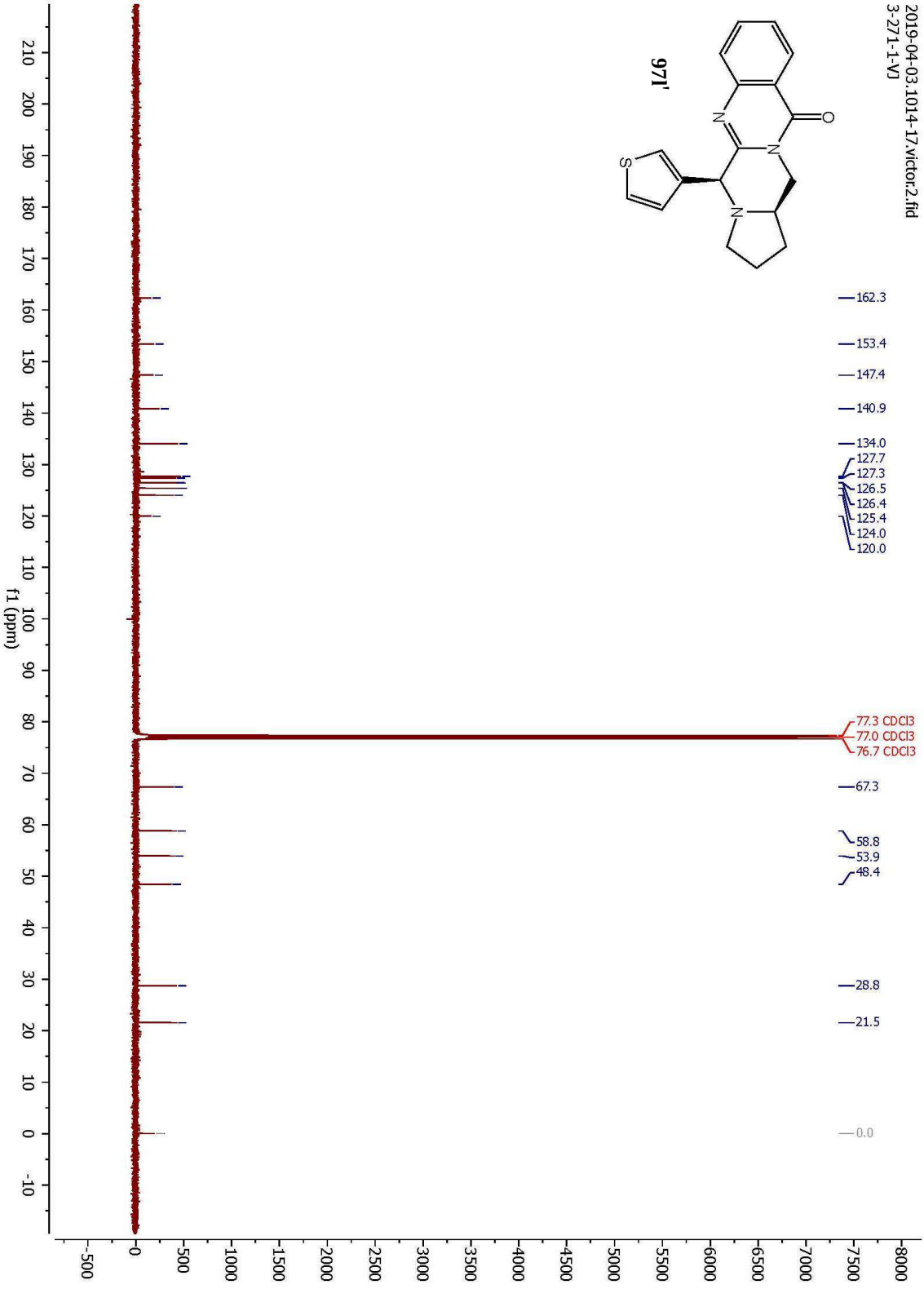
2019-04-03.1014-17.victor.2.fid
3-271-1-VJ
97l'
162.3
153.4
147.4
140.9
134.0
127.7
127.3
126.5
126.4
125.4
124.0
120.0
77.3 CDCl3
77.0 CDCl3
76.7 CDCl3
67.3
58.8
53.9
48.4
28.8
21.5
0.0
f1 (ppm)

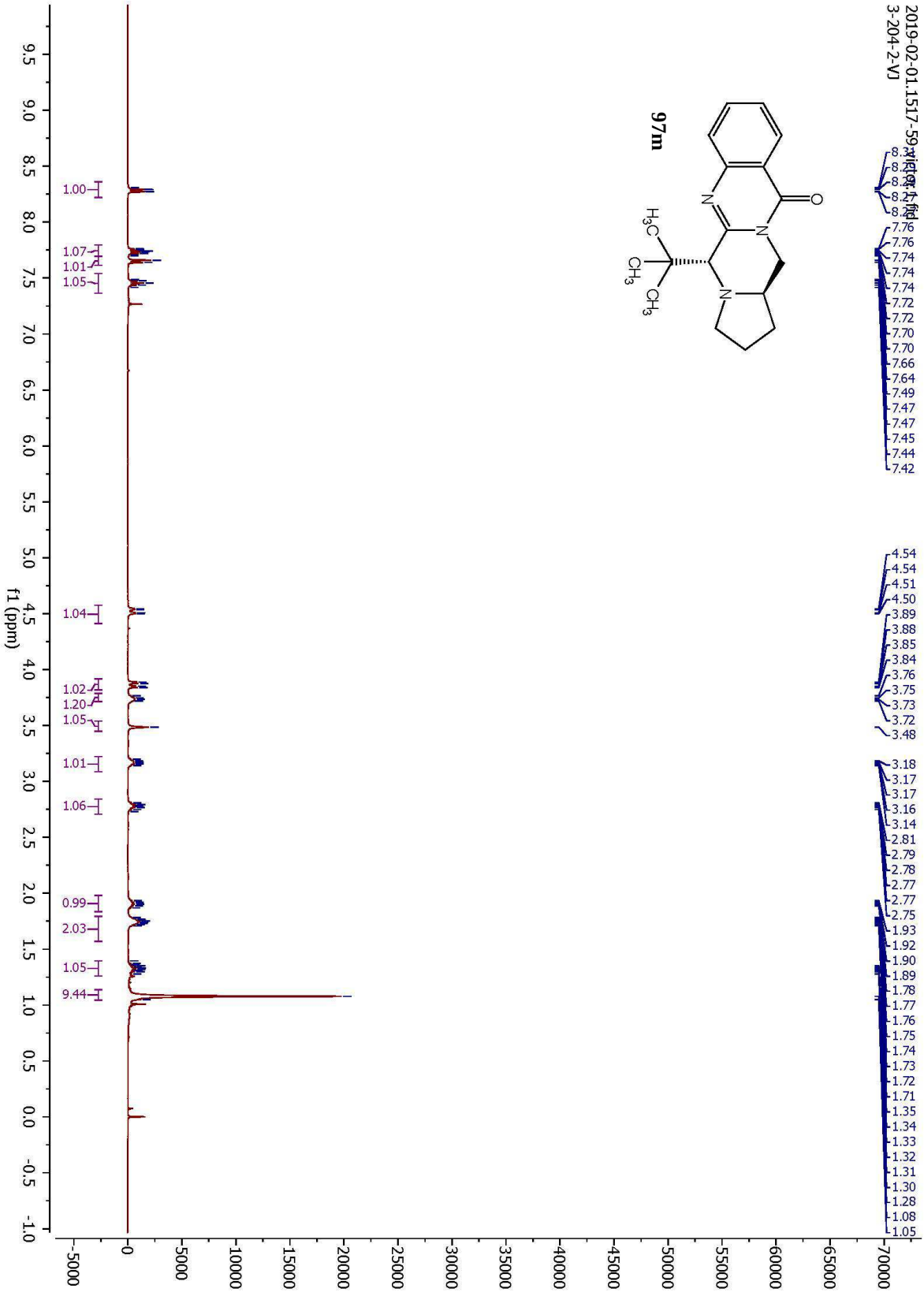
97m
2019-02-01.1517-59-victor-1-fid
3-204-2-VJ
f1 (ppm)

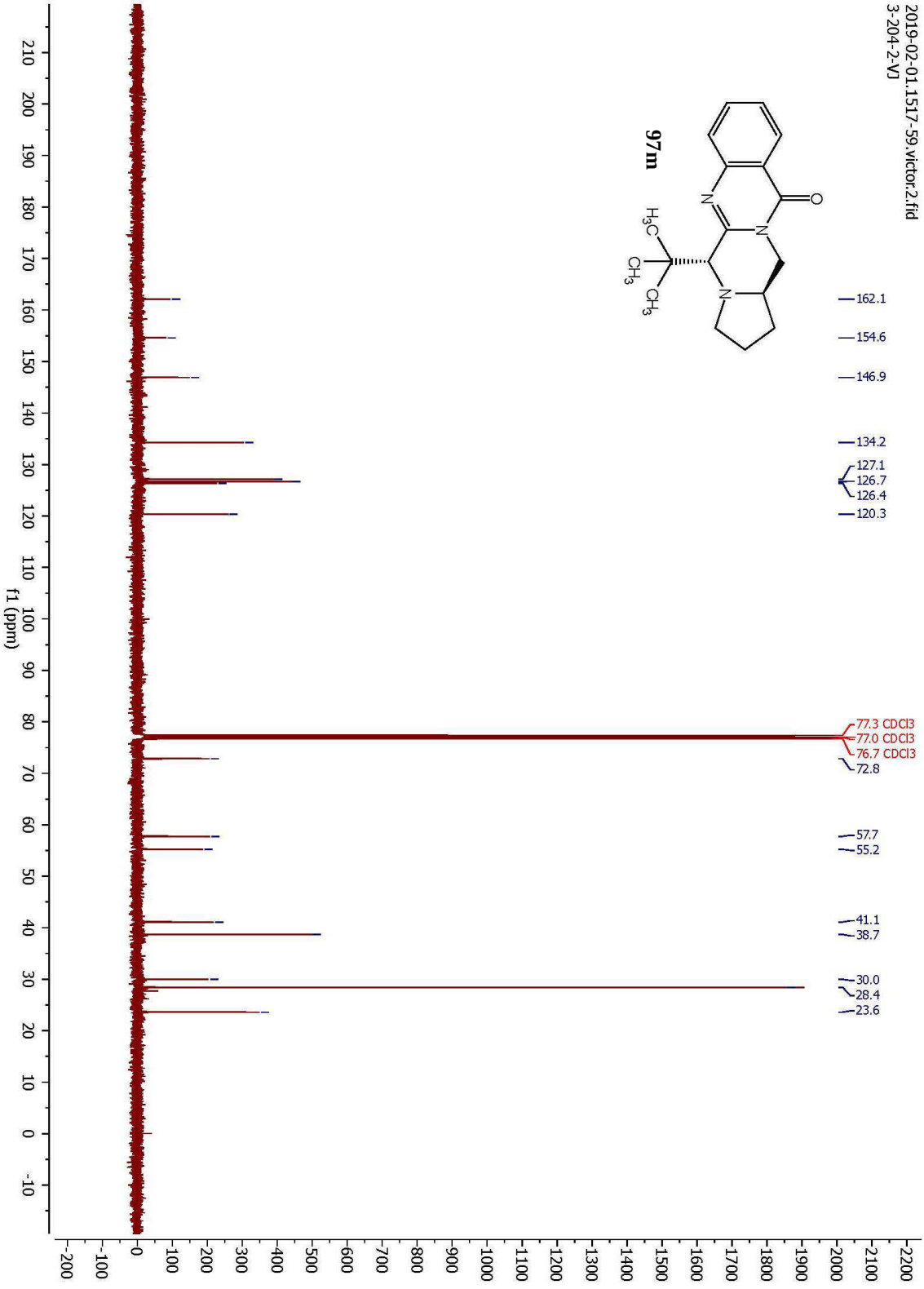
2019-02-01.1517-59.victor.2.fid
3-204-2-VJ
97m
H3C
CH3
CH3
N
N
N
O
162.1
154.6
146.9
134.2
127.1
126.7
126.4
120.3
77.3 CDCl3
77.0 CDCl3
76.7 CDCl3
72.8
57.7
55.2
41.1
38.7
30.0
28.4
23.6
f1 (ppm)

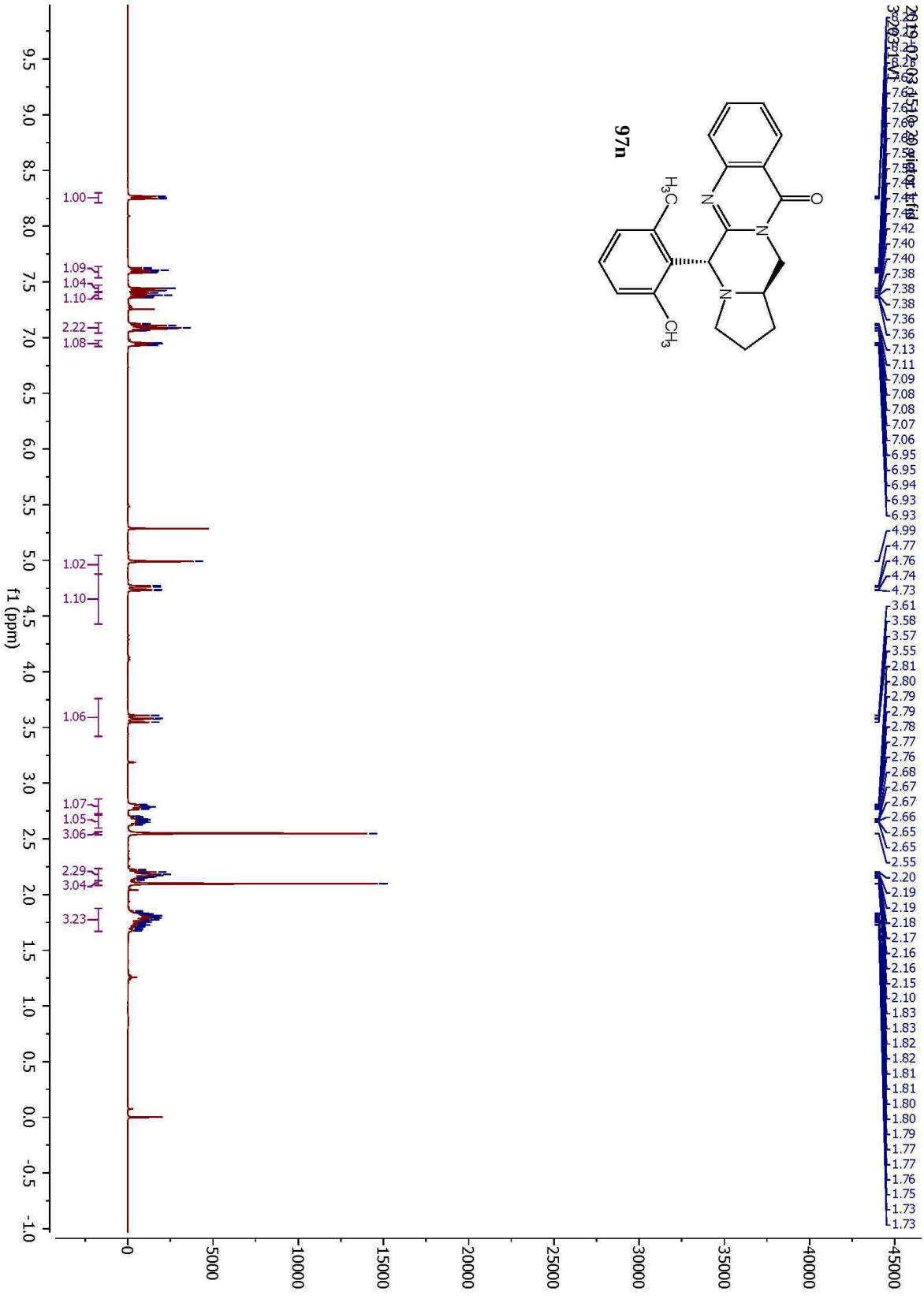
97n
f1 (ppm)
1.00
1.09
1.04
1.10
2.22
1.08
1.02
1.10
1.06
1.07
1.05
3.06
2.29
3.04
3.23

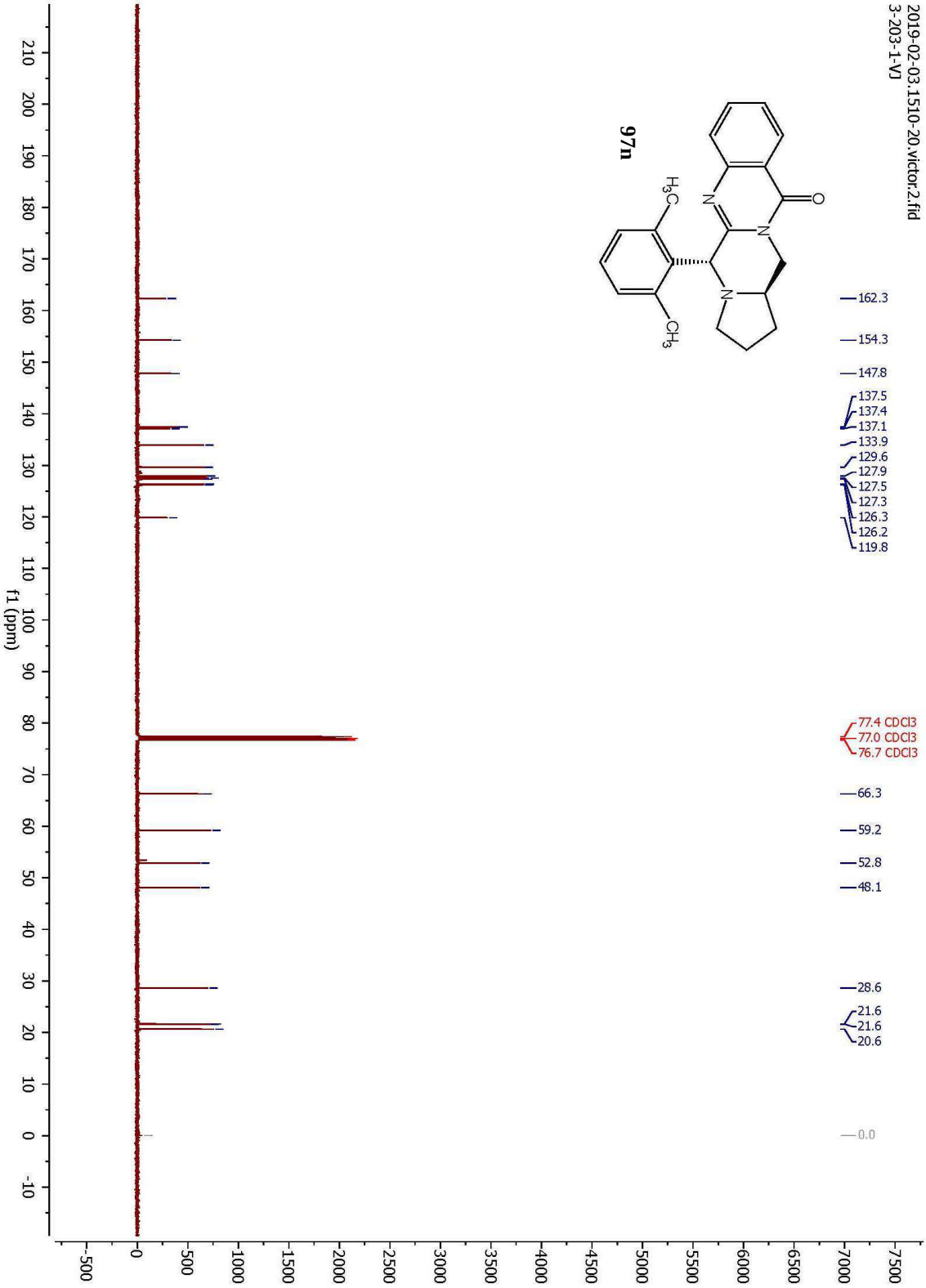
2019-02-03.1510-20.victor.2.fid
3-203-1-VJ
97n
H3C
CH3
O
N
N
N
162.3
154.3
147.8
137.5
137.4
137.1
133.9
129.6
127.9
127.5
127.3
126.3
126.2
119.8
77.4 CDCl3
77.0 CDCl3
76.7 CDCl3
66.3
59.2
52.8
48.1
28.6
21.6
21.6
20.6
0.0
f1 (ppm)

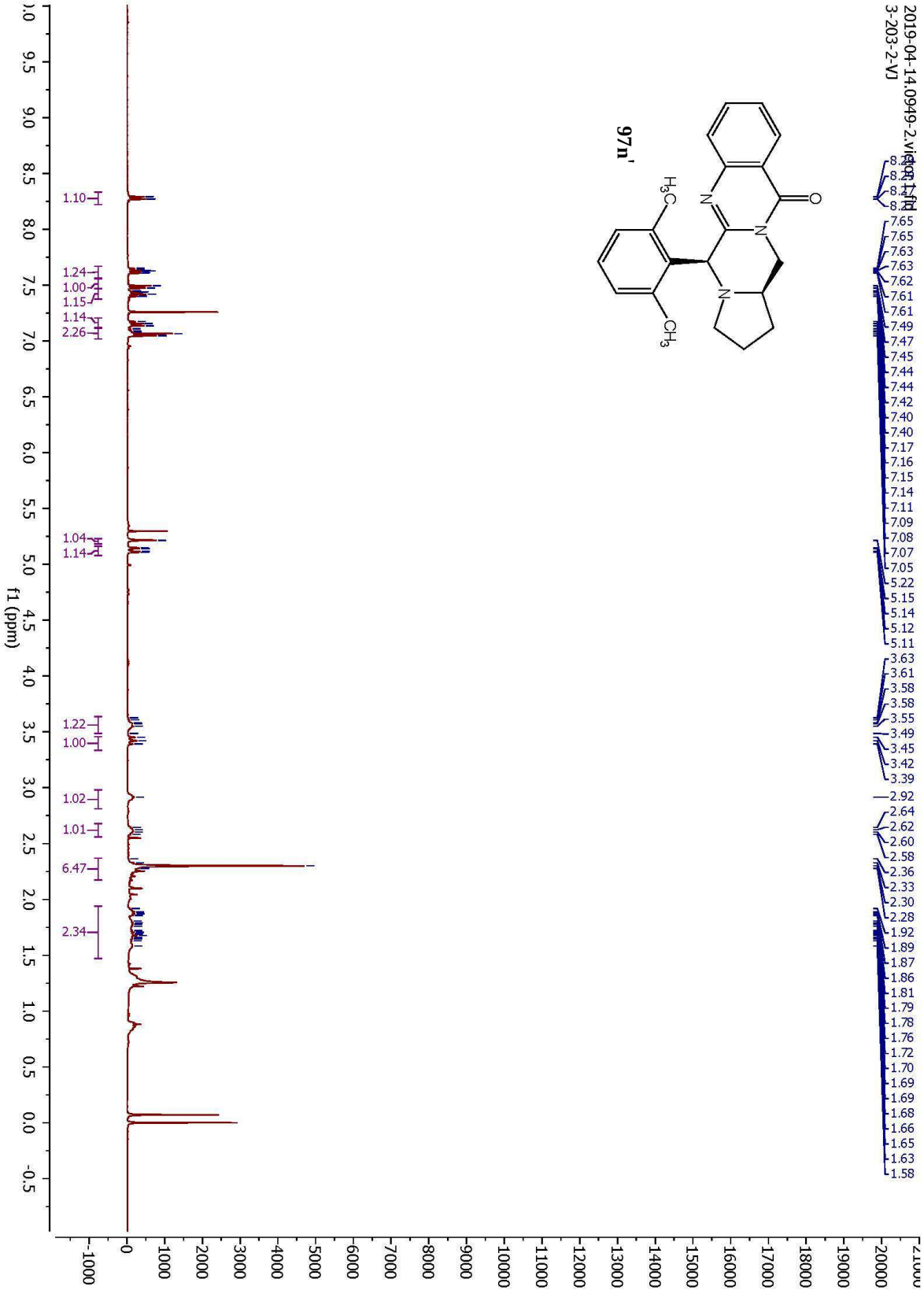
97n'
2019-04-14.0949-2.vjdata.1.fid
3-203-2-VJ
f1 (ppm)

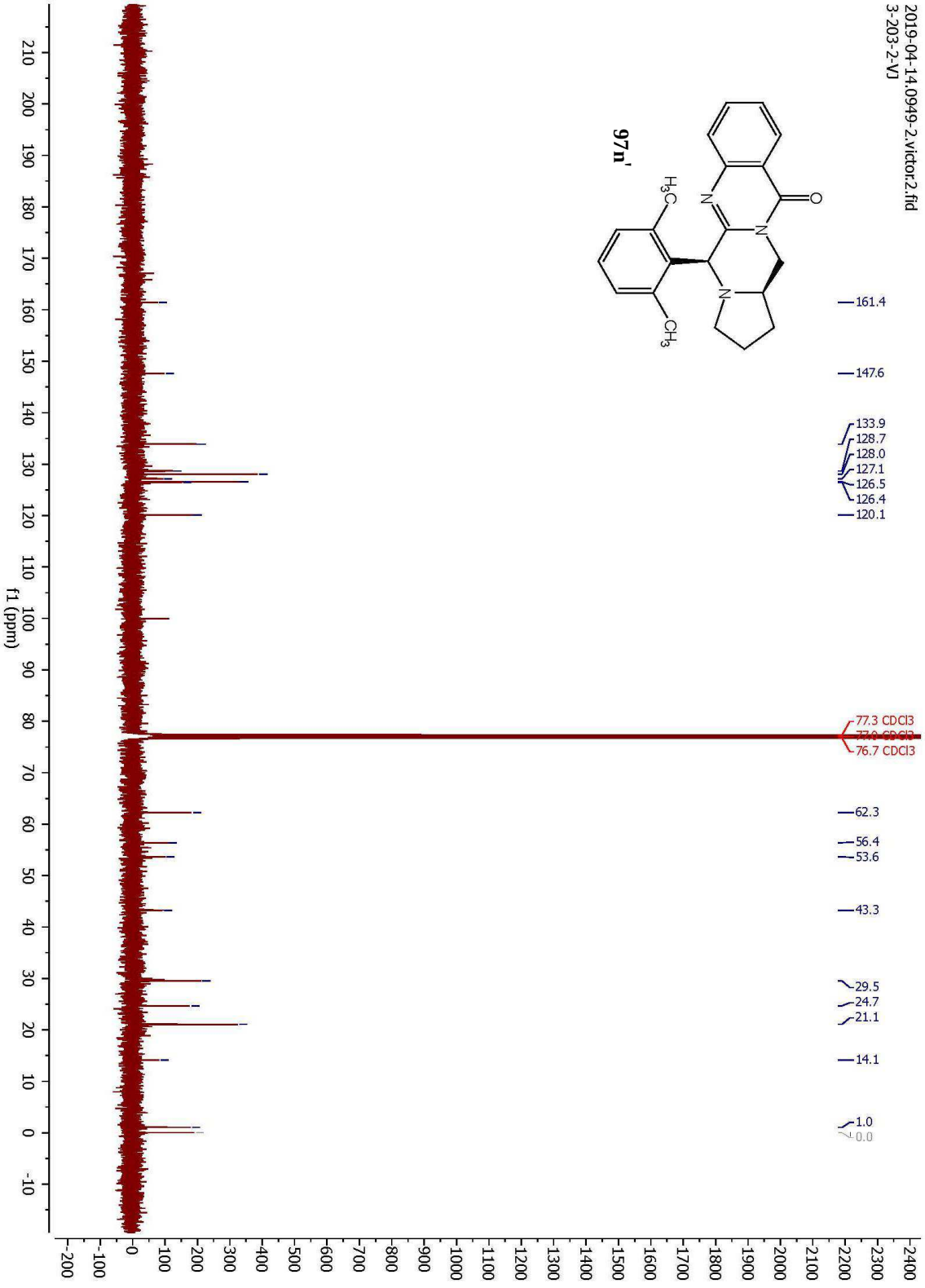
2019-04-14.0949-2.victor.2.fid
3-203-2-VJ
97n'
H3C
CH3
N
N
N
O
161.4
147.6
133.9
128.7
128.0
127.1
126.5
126.4
120.1
77.3 CDCl3
76.7 CDCl3
62.3
56.4
53.6
43.3
29.5
24.7
21.1
14.1
1.0
0.0
f1 (ppm)

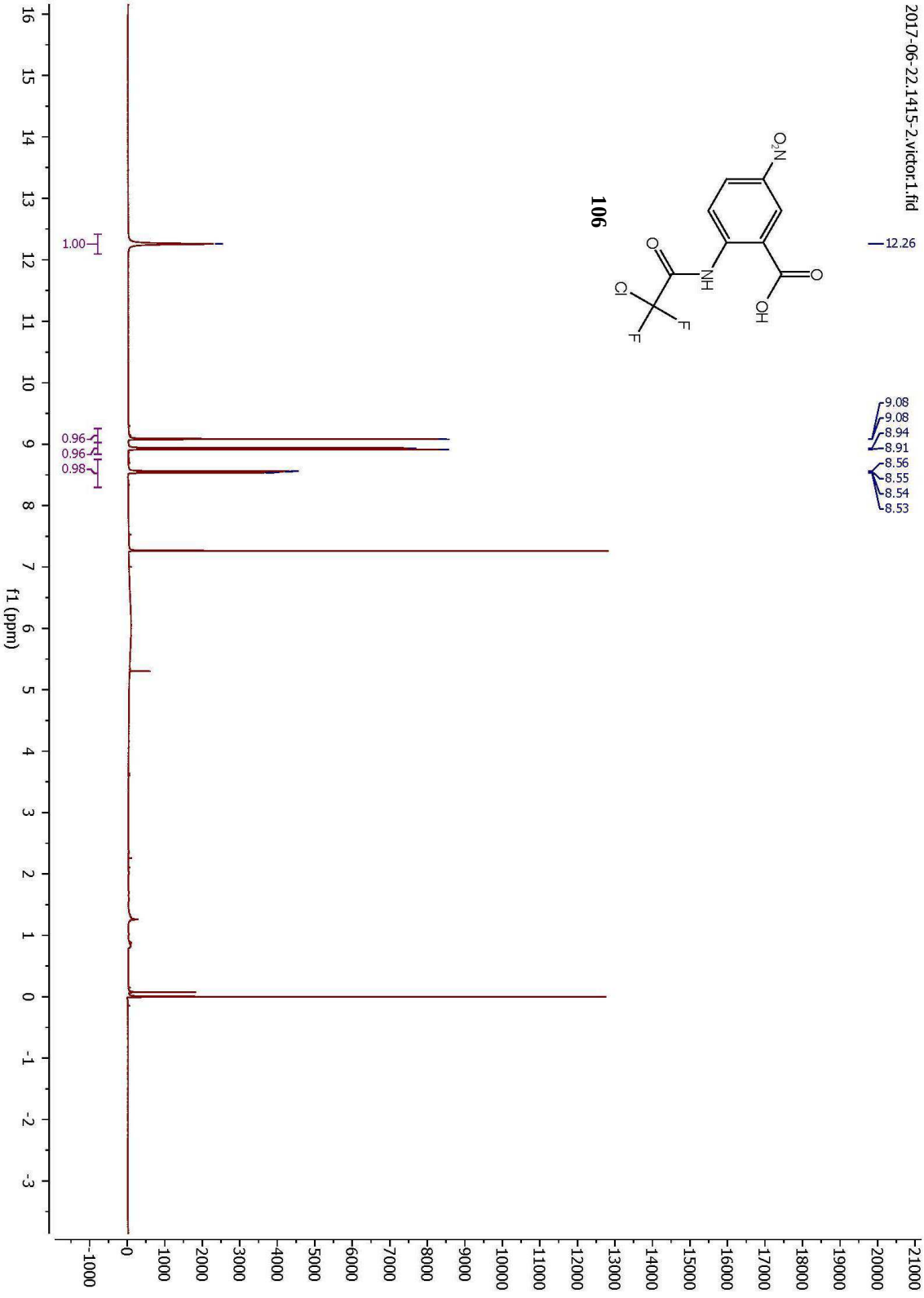
2017-06-22.1415-2.victor.1.fid
106
12.26
9.08
9.08
8.94
8.91
8.56
8.55
8.54
8.53
1.00
0.96
0.96
0.98
f1 (ppm)

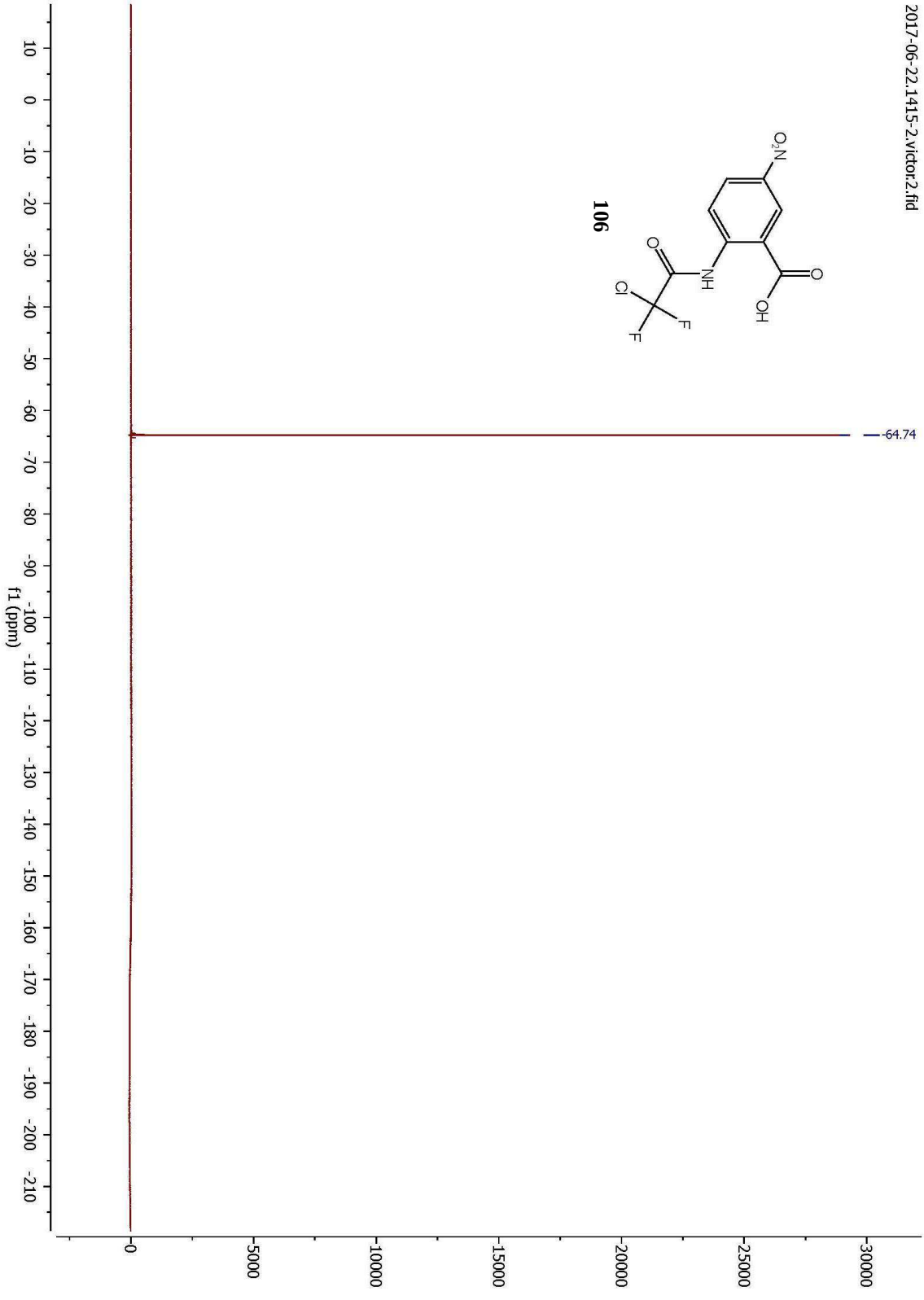
2017-06-22.1415-2.victor.2.fid
106
O2N
NH
O
OH
O
Cl
F
F
-64.74
f1 (ppm)
10
0
-10
-20
-30
-40
-50
-60
-70
-80
-90
-100
-110
-120
-130
-140
-150
-160
-170
-180
-190
-200
-210
0
5000
10000
15000
20000
25000
30000

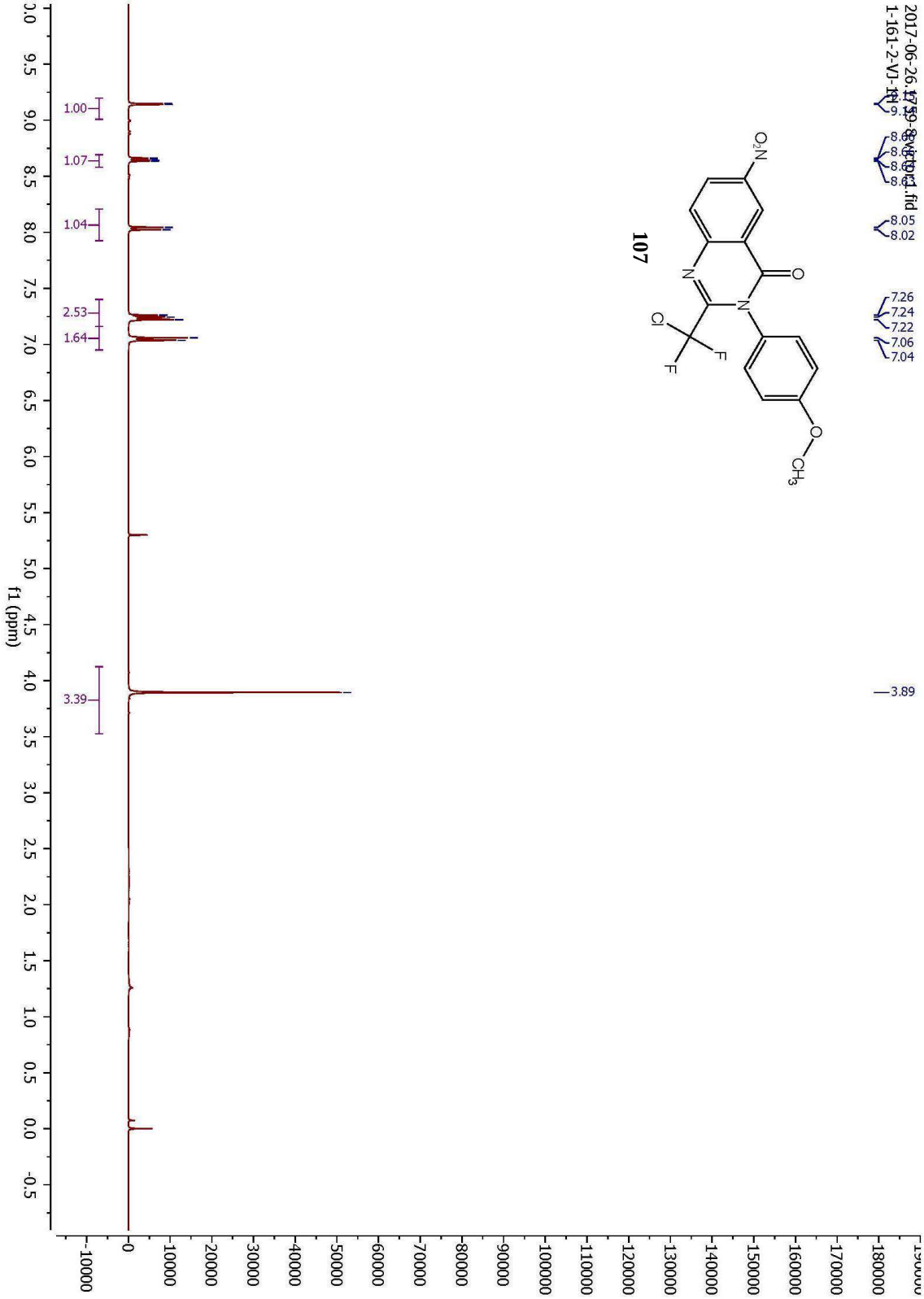
2017-06-26 17:59:8 wwtpd1.fid
1-161-2-VJ-1H-1
9.11
8.69
8.67
8.66
8.64
8.05
8.02
7.26
7.24
7.22
7.06
7.04
3.89
107
O2N
O
N
N
Cl
F
F
O
CH3
1.00
1.07
1.04
2.53
1.64
3.39
f1 (ppm)

2017-06-26.1759-8.victor.2.fid
1-161-2-VJ-19F

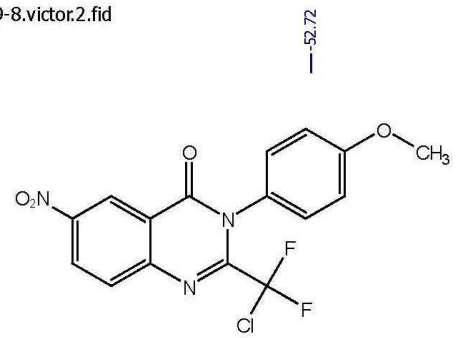

107

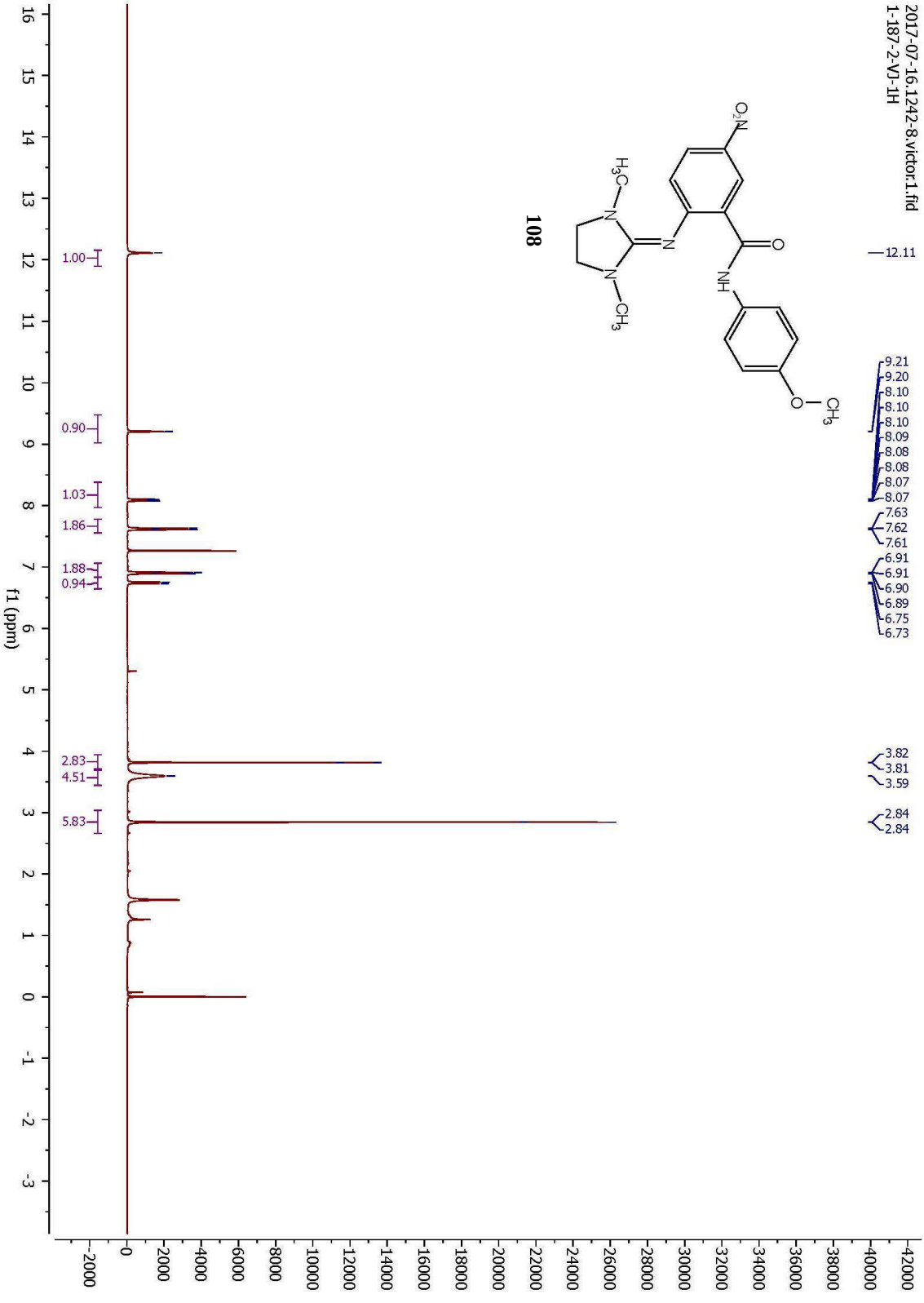
2017-07-16.1242-8.victor.1.fid
1-187-2-VJ-1H
108
12.11
9.21
9.20
8.10
8.10
8.10
8.09
8.08
8.08
8.07
8.07
7.63
7.62
7.61
6.91
6.91
6.90
6.89
6.75
6.73
3.82
3.81
3.59
2.84
2.84
1.00
0.90
1.03
1.86
1.88
0.94
2.83
4.51
5.83
f1 (ppm)

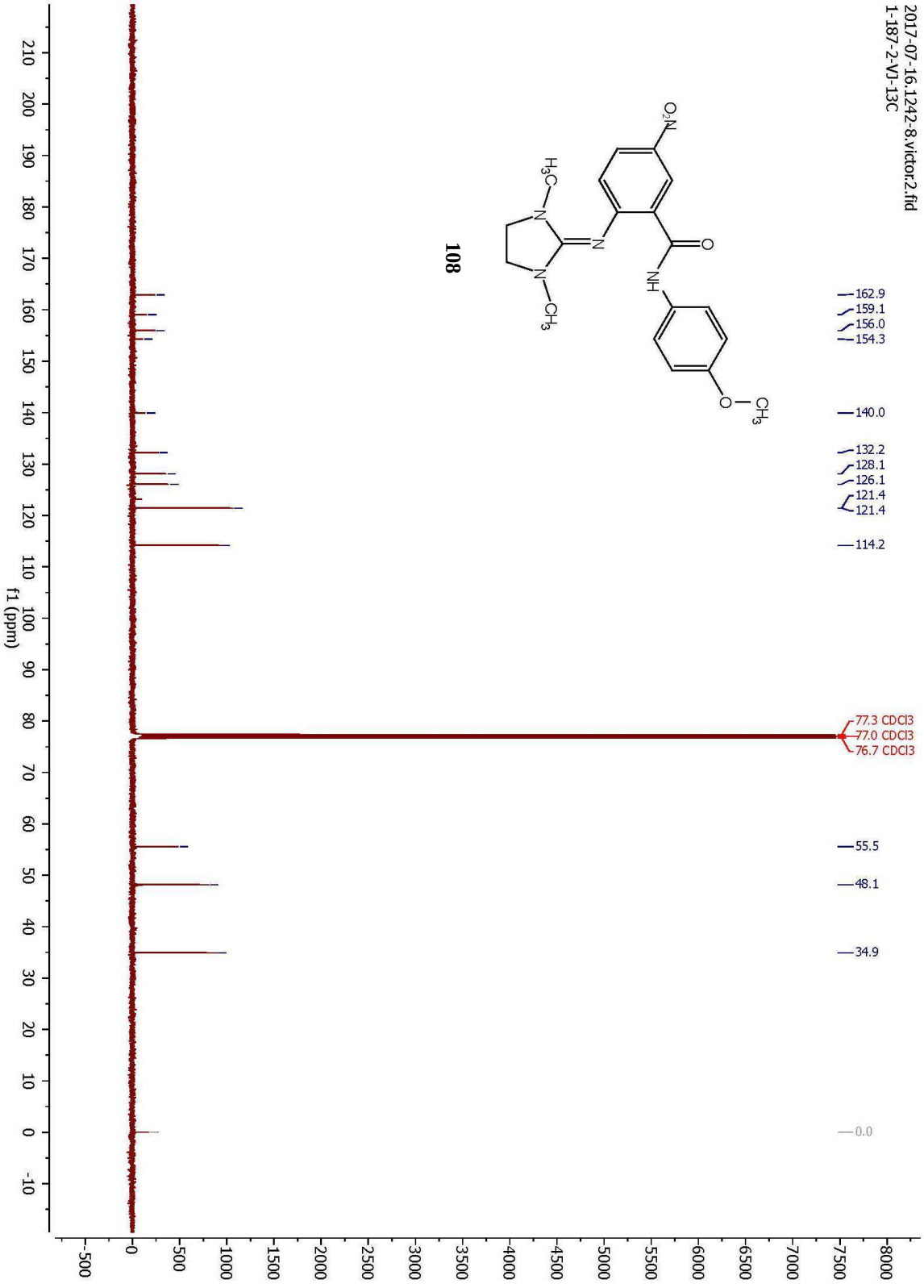
2017-07-16.1242-8.victor.2.fid
1-187-2-V1-13C
108
162.9
159.1
156.0
154.3
140.0
132.2
128.1
126.1
121.4
121.4
114.2
77.3 CDCl3
77.0 CDCl3
76.7 CDCl3
55.5
48.1
34.9
0.0
f1 (ppm)

Appendix B: Crystallographic Structural Report for Selected Compounds

1. Crystallographic Structural Report for 66s

1.1 Data Collection

A colorless crystal with approximate dimensions 0.14 x 0.10 x 0.06 mm^3 was selected under oil under ambient conditions and attached to the tip of a MiTeGen MicroMount©. The crystal was mounted in a stream of cold nitrogen at 100(1) K and centered in the X-ray beam by using a video camera.

The crystal evaluation and data collection were performed on a Bruker Quazar SMART APEXII diffractometer with Mo K_α (λ = 0.71073 Å) radiation and the diffractometer to crystal distance of 4.96 cm [9].

The initial cell constants were obtained from three series of ω scans at different starting angles. Each series consisted of 12 frames collected at intervals of 0.5º in a 6º range about ω with the exposure time of 10 seconds per frame. The reflections were successfully indexed by an automated indexing routine built in the APEX3 program suite. The final cell constants were calculated from a set of 9800 strong reflections from the actual data collection.

The data were collected by using the full sphere data collection routine to survey the reciprocal space to the extent of a full sphere to a resolution of 0.65 Å. A total of 33980 data were harvested by collecting 3 sets of frames with 0.5º scans in ω and φ with exposure times of 40 sec per frame. These highly redundant datasets were corrected for Lorentz and polarization effects. The absorption correction was based on fitting a function to the empirical transmission surface as sampled by multiple equivalent measurements.[10]

1.2 Structure Solution and Refinement

The systematic absences in the diffraction data were uniquely consistent for the space group $P2_1/c$ that yielded chemically reasonable and computationally stable results of refinement[11-16].

A successful solution by the direct methods provided most non-hydrogen atoms from the *E*-map. The remaining non-hydrogen atoms were located in an alternating series of least-squares cycles and difference Fourier maps. All non-hydrogen atoms were refined with anisotropic displacement coefficients. All hydrogen atoms except H4 (bound to N4) were included in the structure factor calculation at idealized positions and were allowed to ride on the neighboring atoms with relative isotropic displacement coefficients.

The crystal structure is that of a racemate. The shown enantiomer (*S*) was chosen arbitrarily.

The final least-squares refinement of 286 parameters against 8585 data resulted in residuals *R* (based on F^2 for $I \geq 2\sigma$) and *wR* (based on F^2 for all data) of 0.0191 and 0.0506, respectively. The final difference Fourier map was featureless.

1.3 Summary

Crystal Data for $C_{25}H_{31}IN_4O$ (*M* =530.44 g/mol): monoclinic, space group $P2_1/c$ (no. 14), *a* = 11.677(4) Å, *b* = 12.610(4) Å, *c* = 16.020(5) Å, β = 99.578(13)°, *V* = 2325.9(13) $Å^3$, *Z* = 4, *T* = 99.99 K, μ(MoKα) = 1.401 mm^{-1}, *Dcalc* = 1.515 g/cm^3, 33980 reflections measured (3.538° ≤

$2\Theta \leq 66.282°$), 8585 unique (R_{int} = 0.0177, R_{sigma} = 0.0156) which were used in all calculations. The final R_1 was 0.0191 ($I > 2\sigma(I)$) and wR_2 was 0.0506 (all data).

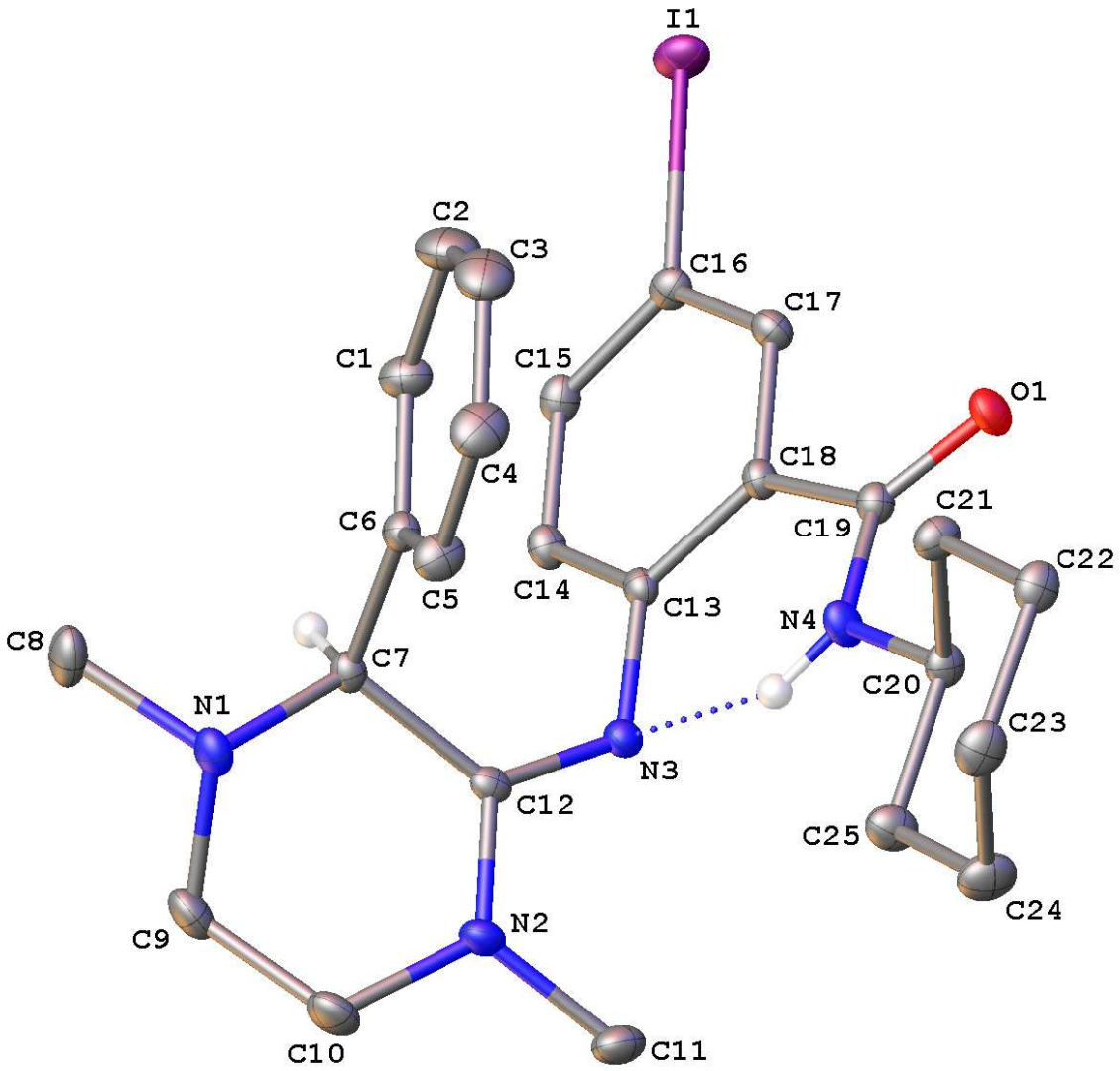

Figure 1. A molecular drawing of Golden01 shown with 50% probability ellipsoids. All H atoms are omitted, except for the amine atom H4 connected to atom N4 (the dotted line represents a hydrogen bonding interaction), and atom H7 attached to the chiral atom C7.

Table 1 Crystal data and structure refinement for golden01.

Identification code	golden01
Empirical formula	$C_{25}H_{31}IN_4O$
Formula weight	530.44
Temperature/K	99.99
Crystal system	monoclinic
Space group	$P2_1/c$
a/Å	11.677(4)
b/Å	12.610(4)
c/Å	16.020(5)
α/°	90
β/°	99.578(13)
γ/°	90
Volume/Å^3	2325.9(13)
Z	4
ρ_{calc}g/cm^3	1.515
μ/mm^{-1}	1.401
F(000)	1080.0
Crystal size/mm^3	0.138 × 0.102 × 0.06
Radiation	MoKα (λ = 0.71073)
2Θ range for data collection/°	3.538 to 66.282
Index ranges	$-17 \le h \le 17$, $-19 \le k \le 19$, $-24 \le l \le 23$
Reflections collected	33980
Independent reflections	8585 [R_{int} = 0.0177, R_{sigma} = 0.0156]
Data/restraints/parameters	8585/0/286
Goodness-of-fit on F^2	1.031
Final R indexes [I>=2σ (I)]	R_1 = 0.0191, wR_2 = 0.0494
Final R indexes [all data]	R_1 = 0.0219, wR_2 = 0.0506
Largest diff. peak/hole / e Å^{-3}	0.56/-0.44

Table 2 Fractional Atomic Coordinates (×10^4) and Equivalent Isotropic Displacement Parameters (Å^2×10^3) for golden01. U_{eq} is defined as 1/3 of of the trace of the orthogonalised U_{IJ} tensor.

Atom	*x*	*y*	*z*	U(eq)
I1	8640.3(2)	-1143.1(2)	3078.8(2)	20.02(2)
O1	8471.8(7)	2478.3(6)	1209.8(4)	16.19(13)
N1	6476.5(8)	4411.5(7)	4874.0(5)	14.73(14)
N2	8371.9(8)	5303.5(6)	4296.4(5)	14.62(14)
N3	8895.1(7)	3789.5(6)	3691.6(5)	11.97(14)
N4	8163.7(8)	3938.6(6)	1968.0(5)	13.45(14)
C1	6178.8(9)	2201.2(8)	3496.6(7)	17.21(17)
C2	5394.7(10)	1830.1(9)	2808.6(8)	24.5(2)
C3	4751.8(10)	2537.2(10)	2257.4(7)	24.9(2)
C4	4897.9(10)	3621.0(9)	2392.0(7)	22.6(2)
C5	5687.2(9)	3993.2(8)	3073.2(6)	17.51(18)
C6	6335.2(8)	3284.3(7)	3634.6(6)	12.20(15)
C7	7148.6(8)	3710.1(7)	4403.6(6)	11.35(15)
C8	5750.0(11)	3775.0(9)	5345.1(7)	21.4(2)

C9	7235.2(10)	5113.0(8)	5434.7(6)	19.39(19)
C10	7802.2(10)	5873.8(8)	4905.4(7)	19.77(19)
C11	9331.1(10)	5854.7(8)	4007.5(7)	18.58(18)
C12	8194.4(8)	4260.6(7)	4124.9(5)	10.82(14)
C13	8854.9(8)	2698.7(7)	3537.5(5)	10.76(14)
C14	9104.7(8)	1986.0(7)	4221.0(6)	12.93(15)
C15	9074.8(8)	898.5(8)	4098.7(6)	13.88(16)
C16	8816.0(8)	496.9(7)	3280.3(6)	13.30(15)
C17	8647.9(9)	1179.7(7)	2594.4(6)	12.82(15)
C18	8672.5(8)	2279.6(7)	2706.9(5)	10.70(14)
C19	8434.5(8)	2910.2(7)	1897.3(6)	11.96(15)
C20	7933.6(8)	4662.0(7)	1249.4(6)	13.15(15)
C21	6792.1(9)	4398.3(8)	672.2(6)	15.44(17)
C22	6530.4(9)	5200.5(8)	-51.1(6)	15.99(17)
C23	6487.0(10)	6328.0(8)	289.6(7)	18.94(18)
C24	7619.0(10)	6602.4(8)	871.6(7)	20.87(19)
C25	7911.9(10)	5793.5(8)	1587.2(6)	17.70(18)

Table 3 Anisotropic Displacement Parameters ($Å^2×10^3$) for golden01. The Anisotropic displacement factor exponent takes the form: $-2\pi^2[h^2a^{*2}U_{11}+2hka^*b^*U_{12}+\ldots]$.

Atom	U_{11}	U_{22}	U_{33}	U_{23}	U_{13}	U_{12}
I1	20.89(4)	10.47(3)	29.34(4)	0.14(2)	6.07(3)	1.91(2)
O1	22.1(4)	16.5(3)	10.0(3)	-1.2(2)	3.0(3)	1.4(3)
N1	16.9(4)	14.3(3)	13.9(3)	-0.5(3)	5.5(3)	4.2(3)
N2	19.3(4)	10.1(3)	14.3(3)	-2.1(3)	2.5(3)	-1.1(3)
N3	13.7(4)	11.7(3)	10.4(3)	-0.8(2)	1.9(3)	-0.4(2)
N4	18.3(4)	13.0(3)	8.9(3)	1.4(2)	2.0(3)	3.5(3)
C1	15.6(4)	14.4(4)	20.8(4)	-0.8(3)	0.7(4)	-0.3(3)
C2	22.0(5)	20.5(5)	29.1(5)	-6.6(4)	-1.0(4)	-4.8(4)
C3	20.1(5)	32.2(6)	20.2(5)	-3.8(4)	-2.7(4)	-6.1(4)
C4	19.1(5)	28.3(5)	18.0(4)	4.0(4)	-4.0(4)	-1.7(4)
C5	16.6(4)	18.0(4)	16.5(4)	3.9(3)	-1.4(3)	0.2(3)
C6	11.3(4)	13.6(4)	12.0(3)	0.2(3)	2.8(3)	0.6(3)
C7	12.7(4)	11.0(3)	10.7(3)	0.5(3)	2.8(3)	2.3(3)
C8	23.6(5)	21.7(5)	22.2(5)	2.9(4)	13.1(4)	5.4(4)
C9	26.0(5)	18.8(4)	13.5(4)	-4.4(3)	4.0(4)	3.8(4)
C10	27.0(5)	12.4(4)	20.2(4)	-4.9(3)	4.6(4)	2.4(4)
C11	21.9(5)	14.2(4)	18.9(4)	-0.1(3)	1.3(4)	-5.5(3)
C12	13.1(4)	10.2(3)	8.2(3)	0.3(3)	-1.0(3)	0.9(3)
C13	9.8(4)	12.4(3)	10.2(3)	-0.7(3)	2.2(3)	0.3(3)
C14	12.7(4)	15.7(4)	10.1(3)	0.8(3)	1.2(3)	2.4(3)
C15	12.8(4)	15.2(4)	13.7(4)	3.5(3)	2.5(3)	3.5(3)
C16	13.1(4)	10.8(3)	16.4(4)	1.2(3)	3.6(3)	2.5(3)
C17	13.8(4)	12.2(4)	12.4(4)	-1.4(3)	2.0(3)	1.6(3)
C18	10.9(4)	12.2(3)	9.1(3)	0.3(3)	1.7(3)	1.4(3)
C19	11.5(4)	13.2(4)	11.2(3)	0.9(3)	1.8(3)	0.8(3)
C20	14.7(4)	13.6(4)	11.2(3)	3.0(3)	1.9(3)	1.8(3)
C21	15.7(4)	15.1(4)	14.7(4)	3.8(3)	0.2(3)	-0.2(3)
C22	15.2(4)	18.3(4)	13.9(4)	4.9(3)	1.0(3)	2.1(3)
C23	19.1(5)	16.9(4)	20.8(4)	7.1(3)	3.1(4)	4.4(3)

C24	25.3(5)	13.7(4)	22.7(5)	4.9(3)	1.1(4)	-0.7(4)
C25	22.9(5)	13.7(4)	15.5(4)	1.7(3)	0.4(4)	0.9(3)

Table 4 Bond Lengths for golden01.

Atom	Atom	Length/Å	Atom	Atom	Length/Å
I1	C16	2.0979(11)	C5	C6	1.3979(14)
O1	C19	1.2360(11)	C6	C7	1.5228(13)
N1	C7	1.4707(12)	C7	C12	1.5343(14)
N1	C8	1.4651(14)	C9	C10	1.5048(16)
N1	C9	1.4524(14)	C13	C14	1.4090(13)
N2	C10	1.4586(13)	C13	C18	1.4146(13)
N2	C11	1.4575(14)	C14	C15	1.3848(14)
N2	C12	1.3523(12)	C15	C16	1.3910(14)
N3	C12	1.3012(12)	C16	C17	1.3839(13)
N3	C13	1.3969(12)	C17	C18	1.3983(13)
N4	C19	1.3440(12)	C18	C19	1.5071(13)
N4	C20	1.4583(12)	C20	C21	1.5271(14)
C1	C2	1.3914(15)	C20	C25	1.5277(14)
C1	C6	1.3907(14)	C21	C22	1.5302(14)
C2	C3	1.3849(18)	C22	C23	1.5268(15)
C3	C4	1.3896(17)	C23	C24	1.5252(16)
C4	C5	1.3876(15)	C24	C25	1.5300(14)

Table 5 Bond Angles for golden01.

Atom	Atom	Atom	Angle/˚	Atom	Atom	Atom	Angle/˚
C8	N1	C7	109.79(8)	N3	C13	C14	119.62(8)
C9	N1	C7	111.13(8)	N3	C13	C18	121.97(8)
C9	N1	C8	111.16(8)	C14	C13	C18	118.17(8)
C11	N2	C10	115.93(8)	C15	C14	C13	121.64(9)
C12	N2	C10	122.94(9)	C14	C15	C16	119.35(8)
C12	N2	C11	119.94(8)	C15	C16	I1	120.28(7)
C12	N3	C13	122.56(8)	C17	C16	I1	119.59(7)
C19	N4	C20	123.51(8)	C17	C16	C15	120.11(9)
C6	C1	C2	120.52(10)	C16	C17	C18	121.18(9)
C3	C2	C1	120.26(11)	C13	C18	C19	126.14(8)
C2	C3	C4	119.65(10)	C17	C18	C13	119.23(8)
C5	C4	C3	120.19(10)	C17	C18	C19	114.56(8)
C4	C5	C6	120.48(10)	O1	C19	N4	122.95(8)
C1	C6	C5	118.88(9)	O1	C19	C18	120.37(8)
C1	C6	C7	121.51(8)	N4	C19	C18	116.67(8)
C5	C6	C7	119.54(8)	N4	C20	C21	111.68(8)
N1	C7	C6	108.20(8)	N4	C20	C25	108.44(8)
N1	C7	C12	113.30(8)	C21	C20	C25	110.71(8)
C6	C7	C12	110.10(7)	C20	C21	C22	111.02(8)
N1	C9	C10	108.67(8)	C23	C22	C21	111.05(8)
N2	C10	C9	110.79(8)	C24	C23	C22	110.66(9)

N2	C12	C7	118.91(8)	C23	C24	C25	111.70(9)
N3	C12	N2	117.62(9)	C20	C25	C24	111.84(9)
N3	C12	C7	123.38(8)				

Table 6 Hydrogen Bonds for golden01.

D	H	A	d(D-H)/Å	d(H-A)/Å	d(D-A)/Å	D-H-A/°
N4	H4	N3	0.841(16)	2.067(16)	2.7576(14)	139.0(15)

Table 7 Hydrogen Atom Coordinates (Å×10^4) and Isotropic Displacement Parameters (Å^2×10^3) for golden01.

Atom	*x*	*y*	*z*	U(eq)
H4	8274(14)	4215(13)	2453(10)	24(4)
H1	6610.86	1710.86	3874.94	21
H2	5300.03	1088.71	2716.71	29
H3	4213.76	2282.74	1789.69	30
H4A	4456.14	4108.63	2016.66	27
H5	5787.9	4735.11	3158.53	21
H7	7439.5	3098.14	4776.44	14
H8A	5259.44	3299.19	4954.46	32
H8B	5257.68	4245.18	5620.18	32
H8C	6246.79	3354.73	5775.94	32
H9A	7835.37	4693.8	5802.33	23
H9B	6779.69	5509.81	5800.38	23
H10A	7208.15	6357.85	4600.12	24
H10B	8382.32	6307.72	5278.13	24
H11A	9180.67	6619.66	3992.14	28
H11B	9403.99	5607.03	3438.84	28
H11C	10053.6	5708.13	4397.17	28
H14	9298.55	2258.24	4779.56	16
H15	9229.44	431.3	4569.21	17
H17	8513.47	896.1	2037.3	15
H20	8580.74	4601.64	914.31	16
H21A	6151.69	4402.66	1006.83	19
H21B	6840.37	3677.88	434.79	19
H22A	7138.71	5155.26	-412.68	19
H22B	5775.65	5025.68	-404.69	19
H23A	6355.56	6834.55	-188.99	23
H23B	5830.92	6392.39	606.18	23
H24A	7550.78	7315.35	1117.39	25
H24B	8258.68	6624.4	536.56	25
H25A	8680.38	5965.41	1922.24	21
H25B	7327.56	5841.87	1968.05	21

2. Crystallographic Structural Report for 97h'

2.1 Data Collection

A yellow crystal with approximate dimensions 0.229 × 0.163 × 0.137 mm^3 was selected under oil under ambient conditions and attached to the tip of a MiTeGen MicroMount©. The crystal was mounted in a stream of cold nitrogen at 100(1) K and centered in the X-ray beam by using a video camera.

The crystal evaluation and data collection were performed on a Bruker Quazar SMART APEXII diffractometer with Mo K_α (λ = 0.71073 Å) radiation and the diffractometer to crystal distance of 4.96 cm [1].

The initial cell constants were obtained from three series of ω scans at different starting angles. Each series consisted of 12 frames collected at intervals of 0.5º in a 6º range about ω with the exposure time of 1 second per frame. The reflections were successfully indexed by an automated indexing routine built in the APEX3 program suite. The final cell constants were calculated from a set of 9856 strong reflections from the actual data collection.

The data were collected by using the full sphere data collection routine to survey the reciprocal space to the extent of a full sphere to a resolution of 0.70 Å. A total of 51493 data were harvested by collecting 6 sets of frames with 0.6º scans in ω and φ with exposure times of 1 sec per frame. These highly redundant datasets were corrected for Lorentz and polarization effects. The absorption correction was based on fitting a function to the empirical transmission surface as sampled by multiple equivalent measurements. [2]

2.2 Structure Solution and Refinement

The systematic absences in the diffraction data were uniquely consistent for the space group $P2_12_12_1$ that yielded chemically reasonable and computationally stable results of refinement [3-8].

A successful solution by the direct methods provided most non-hydrogen atoms from the *E*-map. The remaining non-hydrogen atoms were located in an alternating series of least-squares cycles and difference Fourier maps. All non-hydrogen atoms were refined with anisotropic displacement coefficients. All hydrogen atoms were included in the structure factor calculation at

idealized positions and were allowed to ride on the neighboring atoms with relative isotropic displacement coefficients.

The absolute structure was unequivocally established by anomalous dispersion effects: C9 – *R*; C13 – *S*.

The final least-squares refinement of 226 parameters against 5429 data resulted in residuals *R* (based on F^2 for $I \geq 2\sigma$) and *wR* (based on F^2 for all data) of 0.0193 and 0.0448, respectively. The final difference Fourier map was featureless.

2.3 Summary

Crystal Data for $C_{20}H_{18}IN_3O$ (M =443.27 g/mol): orthorhombic, space group $P2_12_12_1$ (no. 19), a = 9.699(3) Å, b = 9.972(3) Å, c = 18.286(5) Å, V = 1768.5(9) $Å^3$, Z = 4, T = 100.01 K, μ(MoKα) = 1.824 mm^{-1}, *Dcalc* = 1.665 g/cm^3, 51493 reflections measured (4.456° ≤ 2Θ ≤ 61.186°), 5429 unique (R_{int} = 0.0485, R_{sigma} = 0.0251) which were used in all calculations. The final R_1 was 0.0193 (I > 2σ(I)) and wR_2 was 0.0448 (all data).

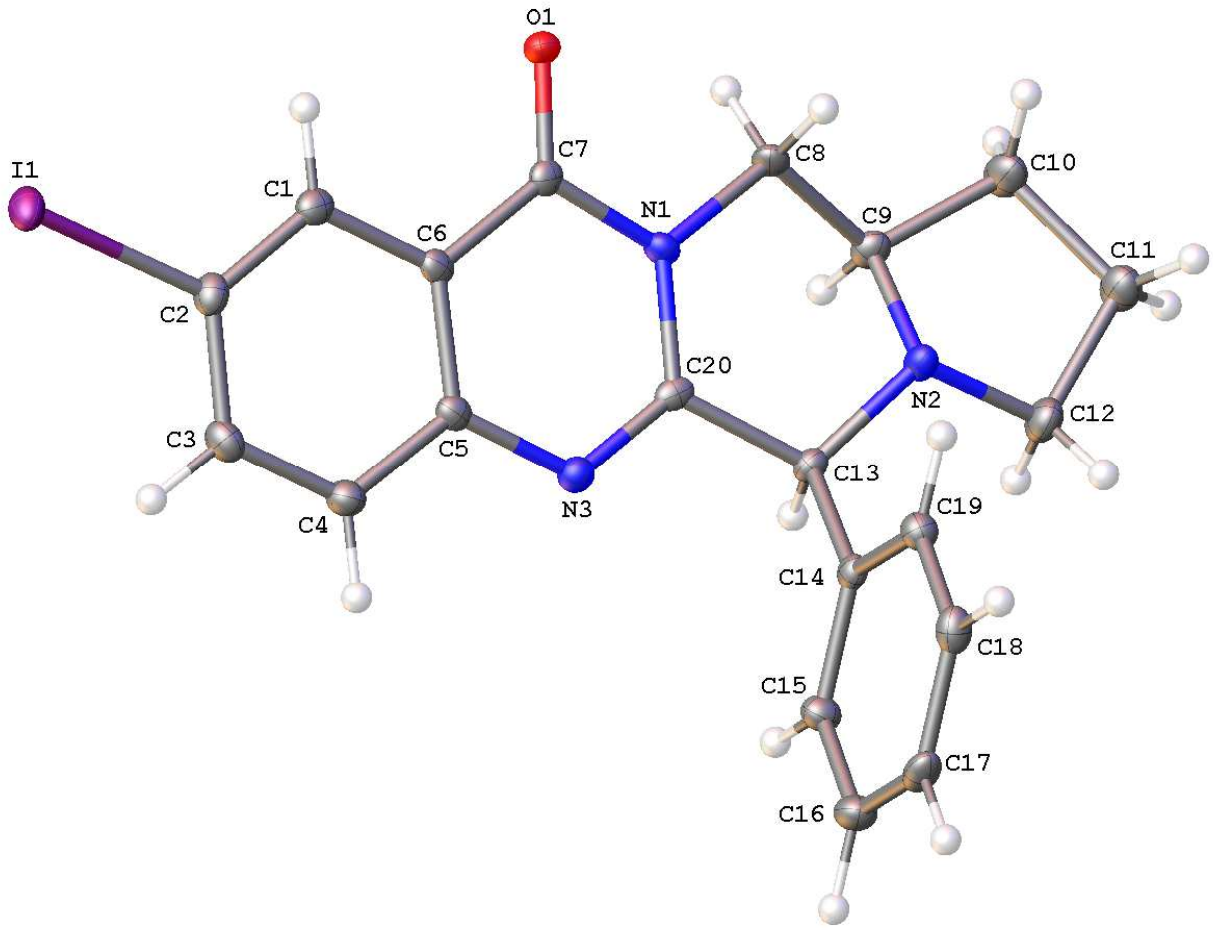

Figure 1. A molecular drawing of Golden02 shown with 50% probability ellipsoids.

Table 1 Crystal data and structure refinement for Golden02.

Identification code	Golden02
Empirical formula	$C_{20}H_{18}IN_3O$
Formula weight	443.27
Temperature/K	100.01
Crystal system	orthorhombic
Space group	$P2_12_12_1$
a/Å	9.699(3)
b/Å	9.972(3)
c/Å	18.286(5)
α/°	90
β/°	90
γ/°	90
Volume/Å^3	1768.5(9)
Z	4
ρ_{calc}g/cm^3	1.665

μ/mm^{-1}	1.824
F(000)	880.0
Crystal size/mm^3	0.229 × 0.163 × 0.137
Radiation	MoKα (λ = 0.71073)
2Θ range for data collection/°	4.456 to 61.186
Index ranges	-13 ≤ h ≤ 13, -14 ≤ k ≤ 14, -26 ≤ l ≤ 26
Reflections collected	51493
Independent reflections	5429 [R_{int} = 0.0485, R_{sigma} = 0.0251]
Data/restraints/parameters	5429/0/226
Goodness-of-fit on F^2	1.034
Final R indexes [I>=2σ (I)]	R_1 = 0.0193, wR_2 = 0.0445
Final R indexes [all data]	R_1 = 0.0201, wR_2 = 0.0448
Largest diff. peak/hole / e Å^{-3}	0.48/-0.30
Flack parameter	-0.014(8)

Table 2 Fractional Atomic Coordinates (×10^4) and Equivalent Isotropic Displacement Parameters (Å^2×10^3) for Golden02. U_{eq} is defined as 1/3 of of the trace of the orthogonalised U_{IJ} tensor.

Atom	*x*	*y*	*z*	U(eq)
I1	1852.2(2)	3091.3(2)	6451.8(2)	17.74(4)
O1	93.5(16)	4787.3(17)	3639.0(10)	15.9(3)
N1	1090.1(18)	3396.7(19)	2804.2(11)	11.5(4)
N2	1836.4(18)	3083.5(19)	1361.8(10)	12.7(3)
N3	2630.7(19)	1661(2)	3138.8(11)	13.3(4)
C1	1425(2)	3406(2)	4820.2(14)	14.1(5)
C2	2077(2)	2632(2)	5339.3(13)	14.7(4)
C3	2883(2)	1517(2)	5140.5(14)	15.7(5)
C4	3054(2)	1213(2)	4412.0(13)	14.8(4)
C5	2404(2)	1980(3)	3867.6(13)	12.6(4)
C6	1574.2(19)	3061(3)	4077.1(12)	12.1(4)
C7	857(2)	3828(2)	3518.9(14)	12.2(4)
C8	313(2)	4116(2)	2229.1(13)	14.5(4)
C9	385(2)	3362(2)	1520.1(13)	14.7(4)
C10	-100(3)	4149(3)	848.3(14)	21.1(5)
C11	888(3)	3720(3)	231.8(14)	21.0(5)
C12	1863(3)	2701(3)	587.7(13)	19.4(5)
C13	2362(2)	2054(3)	1850.6(12)	11.8(4)
C14	3910(2)	1886(3)	1774.4(12)	11.4(4)
C15	4476(2)	612(2)	1770.1(13)	15.5(4)
C16	5893(2)	434(3)	1717.3(14)	19.0(5)
C17	6756(2)	1543(3)	1671.1(13)	17.7(5)
C18	6194(2)	2826(3)	1678.5(14)	16.6(5)
C19	4776(2)	2996(3)	1725.9(13)	14.5(4)
C20	2020(2)	2378(2)	2646.4(12)	11.4(4)

Table 3 Anisotropic Displacement Parameters (Å^2×10^3) for Golden02. The Anisotropic displacement factor

exponent takes the form: $-2\pi^2[h^2a^{*2}U_{11}+2hka^*b^*U_{12}+\ldots]$.

Atom	U_{11}	U_{22}	U_{33}	U_{23}	U_{13}	U_{12}
I1	25.88(7)	15.23(7)	12.10(7)	-0.81(6)	0.83(6)	-1.26(6)
O1	16.4(7)	15.5(8)	15.7(9)	1.7(7)	3.7(6)	4.8(6)
N1	9.0(7)	12.0(10)	13.6(9)	1.1(7)	-0.4(6)	1.8(6)
N2	11.3(7)	16.8(8)	10.1(8)	0.3(7)	-0.8(7)	2.2(8)
N3	12.5(8)	14.2(11)	13.1(9)	0.1(7)	-0.2(7)	1.7(7)
C1	13.7(9)	12.9(11)	15.8(11)	0.6(9)	3.3(8)	-0.8(7)
C2	16.0(11)	15.7(11)	12.3(10)	-0.8(9)	0.4(8)	-2.8(8)
C3	16.7(11)	15.0(11)	15.5(11)	1.5(9)	-3.5(8)	-0.3(8)
C4	14.1(9)	14.7(10)	15.7(10)	0.0(8)	-0.7(9)	2.6(9)
C5	10.2(8)	11.8(10)	15.8(10)	1.1(10)	0.1(7)	-1.1(8)
C6	10.0(8)	12.0(10)	14.4(10)	2.8(9)	1.2(7)	-0.5(8)
C7	9.6(8)	12.9(10)	14.1(10)	1.7(9)	1.9(8)	-1.2(7)
C8	11.5(9)	17.5(11)	14.4(11)	1.7(9)	0.3(8)	5.3(8)
C9	10.4(8)	19.3(11)	14.5(11)	0.0(9)	-1.3(8)	2.1(7)
C10	18.1(11)	29.9(15)	15.3(12)	1.3(11)	-3.3(9)	8.1(10)
C11	18.5(11)	28.8(14)	15.6(12)	1.8(10)	-2.0(9)	5.3(10)
C12	21.1(10)	25.6(12)	11.7(10)	-0.6(9)	0.5(10)	4.2(10)
C13	10.0(8)	13.2(12)	12.0(10)	-0.9(9)	1.2(7)	-0.1(8)
C14	11.2(8)	13.9(10)	9.3(9)	0.5(10)	0.6(7)	0.6(9)
C15	15.5(10)	14.2(11)	16.9(11)	0.6(9)	1.1(9)	1.8(9)
C16	19.4(11)	18.4(12)	19.2(12)	0.8(10)	1.6(9)	7.4(9)
C17	11.4(9)	27.3(12)	14.4(10)	1.1(9)	1.2(8)	3.8(9)
C18	15.3(10)	20.3(13)	14.1(11)	2.5(9)	0.1(8)	-3.4(8)
C19	14.2(9)	14.9(11)	14.3(10)	0.7(10)	0.6(7)	-0.3(9)
C20	8.4(9)	10.7(9)	15.1(10)	-1.7(8)	1.3(8)	-1.0(7)

Table 4 Bond Lengths for Golden02.

Atom	Atom	Length/Å	Atom	Atom	Length/Å
I1	C2	2.097(2)	C5	C6	1.399(3)
O1	C7	1.230(3)	C6	C7	1.453(3)
N1	C7	1.394(3)	C8	C9	1.501(3)
N1	C8	1.480(3)	C9	C10	1.532(3)
N1	C20	1.389(3)	C10	C11	1.540(4)
N2	C9	1.463(3)	C11	C12	1.533(4)
N2	C12	1.466(3)	C13	C14	1.517(3)
N2	C13	1.454(3)	C13	C20	1.527(3)
N3	C5	1.388(3)	C14	C15	1.384(3)
N3	C20	1.293(3)	C14	C19	1.393(3)
C1	C2	1.377(3)	C15	C16	1.389(3)
C1	C6	1.409(3)	C16	C17	1.390(4)
C2	C3	1.407(3)	C17	C18	1.390(4)
C3	C4	1.376(3)	C18	C19	1.389(3)
C4	C5	1.405(3)			

Table 5 Bond Angles for Golden02.

Atom	Atom	Atom	Angle/˚
C7	N1	C8	115.73(17)
C20	N1	C7	121.70(19)
C20	N1	C8	122.55(19)
C9	N2	C12	104.90(18)
C13	N2	C9	110.45(17)
C13	N2	C12	113.80(18)
C20	N3	C5	118.0(2)
C2	C1	C6	118.7(2)
C1	C2	I1	119.91(18)
C1	C2	C3	121.3(2)
C3	C2	I1	118.76(18)
C4	C3	C2	119.4(2)
C3	C4	C5	120.8(2)
N3	C5	C4	119.0(2)
N3	C5	C6	122.0(2)
C6	C5	C4	118.9(2)
C1	C6	C7	120.0(2)
C5	C6	C1	120.8(2)
C5	C6	C7	119.3(2)
O1	C7	N1	120.3(2)
O1	C7	C6	124.9(2)
N1	C7	C6	114.75(19)

Atom	Atom	Atom	Angle/˚
N1	C8	C9	110.30(18)
N2	C9	C8	108.13(17)
N2	C9	C10	103.54(19)
C8	C9	C10	114.9(2)
C9	C10	C11	104.7(2)
C12	C11	C10	104.9(2)
N2	C12	C11	103.1(2)
N2	C13	C14	111.6(2)
N2	C13	C20	111.11(19)
C14	C13	C20	109.00(18)
C15	C14	C13	119.6(2)
C15	C14	C19	119.4(2)
C19	C14	C13	121.0(2)
C14	C15	C16	120.7(2)
C15	C16	C17	119.9(2)
C16	C17	C18	119.7(2)
C19	C18	C17	120.1(2)
C18	C19	C14	120.3(2)
N1	C20	C13	119.60(19)
N3	C20	N1	123.9(2)
N3	C20	C13	116.5(2)

Table 6 Torsion Angles for Golden02.

A	B	C	D	Angle/˚	A	B	C	D	Angle/˚
I1	C2	C3	C4	-179.18(18)	C8	N1	C20	C13	5.4(3)
N1	C8	C9	N2	-52.0(2)	C8	C9	C10	C11	142.3(2)
N1	C8	C9	C10	-167.04(19)	C9	N2	C12	C11	42.6(2)
N2	C9	C10	C11	24.6(3)	C9	N2	C13	C14	-171.8(2)
N2	C13	C14	C15	-138.1(2)	C9	N2	C13	C20	-49.9(2)
N2	C13	C14	C19	43.4(3)	C9	C10	C11	C12	0.8(3)
N2	C13	C20	N1	11.6(3)	C10	C11	C12	N2	-25.8(3)
N2	C13	C20	N3	-168.61(19)	C12	N2	C9	C8	-164.58(19)
N3	C5	C6	C1	-176.4(2)	C12	N2	C9	C10	-42.2(2)
N3	C5	C6	C7	3.8(3)	C12	N2	C13	C14	70.6(3)
C1	C2	C3	C4	1.8(3)	C12	N2	C13	C20	-167.55(19)
C1	C6	C7	O1	-0.4(3)	C13	N2	C9	C8	72.4(2)
C1	C6	C7	N1	179.69(19)	C13	N2	C9	C10	-165.24(19)
C2	C1	C6	C5	-2.1(3)	C13	N2	C12	C11	163.42(19)
C2	C1	C6	C7	177.7(2)	C13	C14	C15	C16	-178.6(2)
C2	C3	C4	C5	-1.8(4)	C13	C14	C19	C18	178.1(2)
C3	C4	C5	N3	178.4(2)	C14	C13	C20	N1	135.0(2)
C3	C4	C5	C6	-0.1(3)	C14	C13	C20	N3	-45.2(3)
C4	C5	C6	C1	2.1(3)	C14	C15	C16	C17	0.2(4)
C4	C5	C6	C7	-177.7(2)	C15	C14	C19	C18	-0.4(3)
C5	N3	C20	N1	-3.9(3)	C15	C16	C17	C18	0.1(4)

C5	N3	C20	C13	176.4(2)	C16	C17	C18	C19	-0.5(4)
C5	C6	C7	O1	179.3(2)	C17	C18	C19	C14	0.7(4)
C5	C6	C7	N1	-0.5(3)	C19	C14	C15	C16	-0.1(4)
C6	C1	C2	I1	-178.90(16)	C20	N1	C7	O1	175.45(19)
C6	C1	C2	C3	0.1(3)	C20	N1	C7	C6	-4.7(3)
C7	N1	C8	C9	-166.47(18)	C20	N1	C8	C9	15.1(3)
C7	N1	C20	N3	7.3(3)	C20	N3	C5	C4	179.8(2)
C7	N1	C20	C13	-172.93(19)	C20	N3	C5	C6	-1.7(3)
C8	N1	C7	O1	-3.0(3)	C20	C13	C14	C15	98.8(3)
C8	N1	C7	C6	176.85(18)	C20	C13	C14	C19	-79.7(3)
C8	N1	C20	N3	-174.3(2)					

Table 7 Hydrogen Atom Coordinates (Å×10^4) and Isotropic Displacement Parameters (Å^2×10^3) for Golden02.

Atom	*x*	*y*	*z*	U(eq)
H1	884.64	4157.78	4960.4	17
H3	3304.49	977.76	5505.89	19
H4	3618.21	475.69	4275.68	18
H8A	704.46	5025.1	2162.97	17
H8B	-662.13	4213.47	2380.5	17
H9	-139.79	2502.14	1560.67	18
H10A	-39.22	5126.37	936.5	25
H10B	-1064.82	3917.3	723.93	25
H11A	372.63	3305.19	-177.06	25
H11B	1408.83	4500.69	43.1	25
H12A	1523.78	1772.88	518.61	23
H12B	2805.28	2773.5	383.7	23
H13	1911.54	1183.24	1721.19	14
H15	3889.2	-148.38	1803.5	19
H16	6271.13	-444.58	1712.89	23
H17	7725.13	1425.39	1634.51	21
H18	6781.49	3586.54	1651.15	20
H19	4395	3874.06	1725.23	17

3. **Crystallographic Structural Report for *ent*-97h'**

3.1 Data Collection

A colorless crystal with approximate dimensions 0.12 × 0.11 × 0.04 mm^3 was selected under oil under ambient conditions and attached to the tip of a MiTeGen MicroMount©. The crystal was mounted in a stream of cold nitrogen at 100(1) K and centered in the X-ray beam by using a video camera.

The crystal evaluation and data collection were performed on a Bruker Quazar SMART APEXII diffractometer with Mo K_α (λ = 0.71073 Å) radiation and the diffractometer to crystal distance of 4.96 cm [1].

The initial cell constants were obtained from three series of ω scans at different starting angles. Each series consisted of 12 frames collected at intervals of 0.5º in a 6º range about ω with the exposure time of 10 second per frame. The reflections were successfully indexed by an automated indexing routine built in the APEX3 program suite. The final cell constants were calculated from a set of 9867 strong reflections from the actual data collection.

The data were collected by using the full sphere data collection routine to survey the reciprocal space to the extent of a full sphere to a resolution of 0.70 Å. A total of 29534 data were harvested by collecting 4 sets of frames with 0.5º scans in ω and φ with exposure times of 30 sec per frame. These highly redundant datasets were corrected for Lorentz and polarization effects. The absorption correction was based on fitting a function to the empirical transmission surface as sampled by multiple equivalent measurements. [2]

3.2 Structure Solution and Refinement

The systematic absences in the diffraction data were uniquely consistent for the space group $P2_12_12_1$ that yielded chemically reasonable and computationally stable results of refinement [3-8].

A successful solution by the direct methods provided most non-hydrogen atoms from the *E*-map. The remaining non-hydrogen atoms were located in an alternating series of least-squares cycles and difference Fourier maps. All non-hydrogen atoms were refined with anisotropic

displacement coefficients. All hydrogen atoms were included in the structure factor calculation at idealized positions and were allowed to ride on the neighboring atoms with relative isotropic displacement coefficients.

The absolute structure was unequivocally established by anomalous dispersion effects: C9 – *S*; C13 – *R*.

The final least-squares refinement of 226 parameters against 4280 data resulted in residuals *R* (based on F^2 for $I \geq 2\sigma$) and *wR* (based on F^2 for all data) of 0.0132 and 0.0346, respectively. The final difference Fourier map was featureless.

3.3 Summary

Crystal Data for $C_{20}H_{18}IN_3O$ (M =443.27 g/mol): orthorhombic, space group $P2_12_12_1$ (no. 19), a = 9.703(3) Å, b = 9.969(3) Å, c = 18.297(5) Å, V = 1769.8(9) Å^3, Z = 4, T = 100.0 K, μ(MoKα) = 1.822 mm^{-1}, *Dcalc* = 1.664 g/cm^3, 29534 reflections measured (4.452° ≤ 2Θ ≤ 55.994°), 4280 unique (R_{int} = 0.0268, R_{sigma} = 0.0148) which were used in all calculations. The final R_1 was 0.0132 (I > 2σ(I)) and wR_2 was 0.0346 (all data).

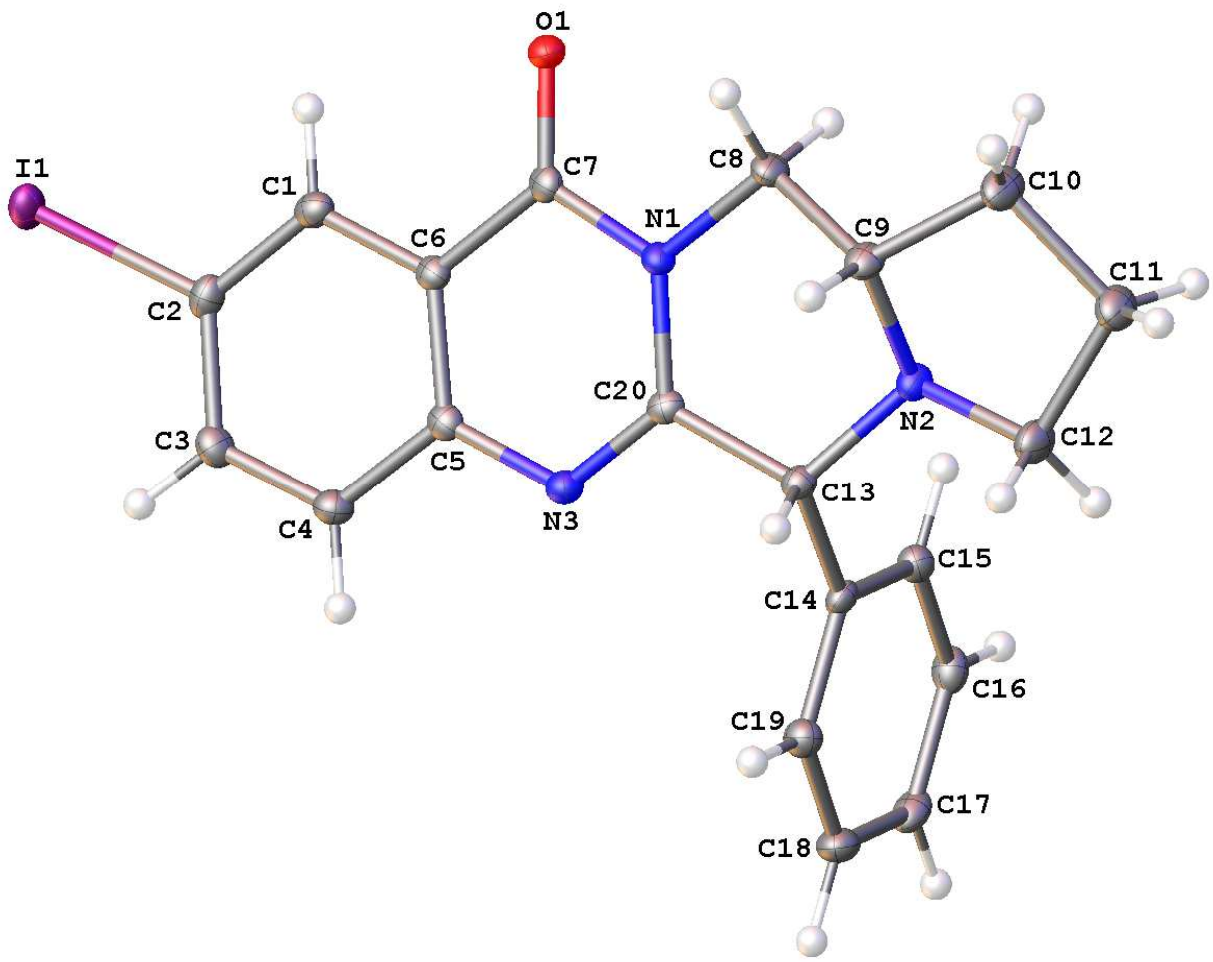

Figure 1. A molecular drawing of Golden02 shown with 50% probability ellipsoids.

Table 1 Crystal data and structure refinement for golden03.

Identification code	golden03
Empirical formula	$C_{20}H_{18}IN_3O$
Formula weight	443.27
Temperature/K	100.0
Crystal system	orthorhombic
Space group	$P2_12_12_1$
a/Å	9.703(3)
b/Å	9.969(3)
c/Å	18.297(5)
α/°	90
β/°	90
γ/°	90
Volume/Å^3	1769.8(9)

Z	4
ρ_{calc}g/cm^3	1.664
μ/mm^{-1}	1.822
F(000)	880.0
Crystal size/mm^3	0.12 × 0.11 × 0.04
Radiation	MoKα (λ = 0.71073)
2Θ range for data collection/°	4.452 to 55.994
Index ranges	-12 ≤ h ≤ 12, -13 ≤ k ≤ 13, -24 ≤ l ≤ 23
Reflections collected	29534
Independent reflections	4280 [R_{int} = 0.0268, R_{sigma} = 0.0148]
Data/restraints/parameters	4280/0/226
Goodness-of-fit on F^2	1.087
Final R indexes [I>=2σ (I)]	R_1 = 0.0132, wR_2 = 0.0345
Final R indexes [all data]	R_1 = 0.0134, wR_2 = 0.0346
Largest diff. peak/hole / e Å^{-3}	0.35/-0.18
Flack parameter	-0.031(5)

Table 2 Fractional Atomic Coordinates (×10^4) and Equivalent Isotropic Displacement Parameters (Å^2×10^3) for golden03. U_{eq} is defined as 1/3 of of the trace of the orthogonalised U_{IJ} tensor.

Atom	*x*	*y*	*z*	U(eq)
I1	8146.9(2)	6908.0(2)	3548.5(2)	17.52(4)
O1	9906.1(15)	5210.7(15)	6360.7(9)	15.8(3)
N1	8910.3(17)	6605.5(17)	7197.3(10)	11.6(3)
N2	8160.5(17)	6917.9(17)	8638.1(9)	13.1(3)
N3	7369.1(17)	8336.8(17)	6860.8(10)	13.0(3)
C1	8574(2)	6595(2)	5177.9(12)	14.3(4)
C2	7926(2)	7368(2)	4660.3(12)	14.8(4)
C3	7116(2)	8479(2)	4860.1(12)	15.3(4)
C4	6943(2)	8789.6(19)	5587.9(11)	14.5(4)
C5	7596.2(18)	8020(2)	6133.2(11)	12.2(3)
C6	8425.7(17)	6938(2)	5920.5(11)	12.0(3)
C7	9142.1(19)	6171.9(18)	6480.0(12)	12.5(3)
C8	9686(2)	5883(2)	7769.9(11)	14.7(4)
C9	9613.7(19)	6641(2)	8481.1(12)	14.6(4)
C10	10100(2)	5852(3)	9150.4(12)	21.0(5)
C11	9110(2)	6278(3)	9768.9(13)	20.9(5)
C12	8134(3)	7298(2)	9412.8(12)	19.2(4)
C13	7639(2)	7947(2)	8149.0(11)	12.0(4)
C14	6088.5(18)	8113(2)	8226.1(10)	11.9(3)
C15	5224(2)	7004(2)	8273.5(12)	14.2(4)
C16	3806(2)	7174(2)	8321.2(12)	16.2(4)
C17	3248(2)	8460(2)	8329.3(11)	17.8(4)
C18	4105(2)	9567(2)	8282.9(13)	18.7(4)
C19	5521(2)	9391(2)	8229.8(12)	15.4(4)

C20	7982(2)	7620.6(19)	7354.2(11)	11.3(4)

Table 3 Anisotropic Displacement Parameters ($Å^2×10^3$) for golden03. The Anisotropic displacement factor exponent takes the form: $-2π^2[h^2a^{*2}U_{11}+2hka*b*U_{12}+…]$.

Atom	U_{11}	U_{22}	U_{33}	U_{23}	U_{13}	U_{12}
I1	25.29(7)	15.55(6)	11.73(6)	-0.87(5)	0.74(5)	-1.13(5)
O1	16.2(7)	15.8(7)	15.3(8)	1.9(6)	3.5(6)	4.8(5)
N1	9.6(7)	13.0(8)	12.1(8)	1.3(6)	-0.1(6)	1.6(6)
N2	10.7(6)	17.3(7)	11.2(8)	-0.1(7)	-0.9(6)	1.2(7)
N3	11.9(7)	13.3(9)	13.8(8)	-0.1(6)	0.5(6)	1.3(6)
C1	13.1(9)	12.7(9)	17.1(10)	-0.5(8)	3.0(7)	-0.6(7)
C2	15.7(10)	16.6(9)	12.0(9)	-1.4(7)	1.3(7)	-3.7(7)
C3	15.0(10)	16.2(9)	14.8(10)	1.7(7)	-3.1(7)	-0.5(7)
C4	13.4(9)	14.0(9)	16.1(9)	0.0(7)	-0.6(8)	2.0(8)
C5	9.6(8)	12.3(9)	14.6(9)	1.2(9)	0.3(7)	-2.1(8)
C6	9.5(8)	12.5(8)	14.0(9)	1.2(8)	1.1(6)	-0.7(7)
C7	10.7(8)	12.8(8)	13.9(9)	2.0(8)	2.1(8)	-1.8(6)
C8	12.8(9)	16.8(10)	14.5(9)	1.7(8)	-1.3(7)	4.8(7)
C9	9.4(8)	19.7(10)	14.6(9)	-0.4(8)	-0.8(7)	2.0(7)
C10	17.9(10)	31.2(13)	13.8(10)	0.7(9)	-2.8(8)	7.8(9)
C11	18.6(10)	28.7(12)	15.6(11)	2.7(9)	-1.3(8)	5.4(9)
C12	20.3(9)	25.3(10)	11.9(9)	-1.0(8)	-0.7(9)	4.3(9)
C13	10.3(8)	13.5(10)	12.1(9)	-0.4(8)	0.2(6)	0.5(7)
C14	11.0(8)	15.8(9)	8.9(8)	-0.9(9)	1.3(6)	1.1(8)
C15	14.8(9)	14.0(9)	13.9(9)	0.4(8)	0.4(7)	0.4(8)
C16	13.9(9)	20.7(11)	14.1(10)	2.1(8)	-0.3(7)	-3.9(8)
C17	10.6(8)	28.7(11)	14.0(9)	1.3(8)	1.0(7)	3.7(8)
C18	18.4(10)	18.8(10)	18.9(10)	0.6(8)	2.8(8)	6.8(8)
C19	15.3(9)	14.8(9)	16.0(9)	0.6(8)	1.1(8)	0.1(8)
C20	8.4(9)	11.5(8)	13.9(9)	-1.0(7)	0.6(7)	-1.7(7)

Table 4 Bond Lengths for golden03.

Atom	Atom	Length/Å	Atom	Atom	Length/Å
I1	C2	2.096(2)	C5	C6	1.401(3)
O1	C7	1.231(2)	C6	C7	1.454(3)
N1	C7	1.400(3)	C8	C9	1.506(3)
N1	C8	1.477(3)	C9	C10	1.530(3)
N1	C20	1.385(2)	C10	C11	1.544(3)
N2	C9	1.465(2)	C11	C12	1.535(3)
N2	C12	1.468(3)	C13	C14	1.521(2)
N2	C13	1.452(3)	C13	C20	1.527(3)
N3	C5	1.386(3)	C14	C15	1.391(3)
N3	C20	1.296(3)	C14	C19	1.388(3)
C1	C2	1.373(3)	C15	C16	1.389(3)
C1	C6	1.409(3)	C16	C17	1.392(3)
C2	C3	1.407(3)	C17	C18	1.384(3)
C3	C4	1.377(3)	C18	C19	1.388(3)

C4	C5	1.409(3)

Table 5 Bond Angles for golden03.

Atom	Atom	Atom	Angle/˚	Atom	Atom	Atom	Angle/˚
C7	N1	C8	115.62(16)	N1	C8	C9	110.13(16)
C20	N1	C7	121.64(17)	N2	C9	C8	107.97(16)
C20	N1	C8	122.72(17)	N2	C9	C10	103.68(17)
C9	N2	C12	104.76(16)	C8	C9	C10	114.77(17)
C13	N2	C9	110.33(16)	C9	C10	C11	104.68(18)
C13	N2	C12	113.99(16)	C12	C11	C10	104.78(18)
C20	N3	C5	118.10(18)	N2	C12	C11	103.17(17)
C2	C1	C6	118.84(19)	N2	C13	C14	111.37(18)
C1	C2	I1	120.00(16)	N2	C13	C20	111.14(17)
C1	C2	C3	121.2(2)	C14	C13	C20	109.09(16)
C3	C2	I1	118.77(16)	C15	C14	C13	121.1(2)
C4	C3	C2	119.7(2)	C19	C14	C13	119.5(2)
C3	C4	C5	120.50(19)	C19	C14	C15	119.35(18)
N3	C5	C4	119.01(19)	C16	C15	C14	120.3(2)
N3	C5	C6	122.24(18)	C15	C16	C17	119.9(2)
C6	C5	C4	118.73(18)	C18	C17	C16	120.0(2)
C1	C6	C7	120.17(18)	C17	C18	C19	119.9(2)
C5	C6	C1	120.91(18)	C18	C19	C14	120.6(2)
C5	C6	C7	118.92(18)	N1	C20	C13	119.65(17)
O1	C7	N1	120.23(19)	N3	C20	N1	123.83(18)
O1	C7	C6	124.9(2)	N3	C20	C13	116.52(18)
N1	C7	C6	114.89(17)				

Table 6 Torsion Angles for golden03.

A	B	C	D	Angle/˚	A	B	C	D	Angle/˚
I1	C2	C3	C4	179.18(16)	C8	N1	C20	C13	-5.2(3)
N1	C8	C9	N2	52.1(2)	C8	C9	C10	C11	-142.20(19)
N1	C8	C9	C10	167.12(17)	C9	N2	C12	C11	-42.6(2)
N2	C9	C10	C11	-24.7(2)	C9	N2	C13	C14	171.91(17)
N2	C13	C14	C15	-43.5(3)	C9	N2	C13	C20	50.0(2)
N2	C13	C14	C19	138.19(19)	C9	C10	C11	C12	-0.7(2)
N2	C13	C20	N1	-11.8(2)	C10	C11	C12	N2	25.7(2)
N2	C13	C20	N3	168.39(17)	C12	N2	C9	C8	164.46(17)
N3	C5	C6	C1	176.32(19)	C12	N2	C9	C10	42.3(2)
N3	C5	C6	C7	-3.9(3)	C12	N2	C13	C14	-70.6(2)
C1	C2	C3	C4	-1.3(3)	C12	N2	C13	C20	167.58(17)
C1	C6	C7	O1	0.4(3)	C13	N2	C9	C8	-72.5(2)
C1	C6	C7	N1	-179.77(17)	C13	N2	C9	C10	165.38(17)
C2	C1	C6	C5	2.2(3)	C13	N2	C12	C11	-163.26(17)
C2	C1	C6	C7	-177.58(18)	C13	C14	C15	C16	-178.01(19)

C2	C3	C4	C5	1.5(3)	C13	C14	C19	C18	178.5(2)
C3	C4	C5	N3	-178.21(19)	C14	C13	C20	N1	-135.0(2)
C3	C4	C5	C6	0.1(3)	C14	C13	C20	N3	45.2(3)
C4	C5	C6	C1	-2.0(3)	C14	C15	C16	C17	-0.7(3)
C4	C5	C6	C7	177.78(17)	C15	C14	C19	C18	0.2(3)
C5	N3	C20	N1	3.7(3)	C15	C16	C17	C18	0.6(3)
C5	N3	C20	C13	-176.50(17)	C16	C17	C18	C19	-0.1(3)
C5	C6	C7	O1	-179.37(18)	C17	C18	C19	C14	-0.3(3)
C5	C6	C7	N1	0.5(3)	C19	C14	C15	C16	0.3(3)
C6	C1	C2	I1	179.01(14)	C20	N1	C7	O1	-175.33(18)
C6	C1	C2	C3	-0.5(3)	C20	N1	C7	C6	4.8(3)
C7	N1	C8	C9	166.54(16)	C20	N1	C8	C9	-15.3(2)
C7	N1	C20	N3	-7.4(3)	C20	N3	C5	C4	-179.79(18)
C7	N1	C20	C13	172.86(17)	C20	N3	C5	C6	1.9(3)
C8	N1	C7	O1	2.9(3)	C20	C13	C14	C15	79.5(2)
C8	N1	C7	C6	-176.98(16)	C20	C13	C14	C19	-98.8(2)
C8	N1	C20	N3	174.55(19)					

Table 7 Hydrogen Atom Coordinates (Å×10^4) and Isotropic Displacement Parameters (Å^2×10^3) for golden03.

Atom	*x*	*y*	*z*	U(eq)
H1	9111.74	5841.46	5037.61	17
H3	6690.46	9014.02	4494.35	18
H4	6378.87	9527.82	5723.21	17
H8A	10660.01	5784.38	7618.35	18
H8B	9292.49	4974.4	7835.7	18
H9	10138.56	7501.05	8440.83	17
H10A	11063.92	6082.61	9274.62	25
H10B	10038.75	4873.94	9060.78	25
H11A	8590.42	5496.33	9957.09	25
H11B	9625.08	6693.05	10177.64	25
H12A	7192.03	7224.44	9616.52	23
H12B	8472.03	8226.76	9482.59	23
H13	8089.23	8817.6	8278.38	14
H15	5604.46	6125.71	8273.35	17
H16	3217.63	6413.4	8348.18	19
H17	2279.5	8578.73	8366.65	21
H18	3725.16	10444.97	8287.45	22
H19	6106.37	10152.37	8195.76	18

References

1. Bruker-AXS (2018). *APEX3*. Version 2018.1-0. Madison, Wisconsin, USA.
2. Krause, L., Herbst-Irmer, R., Sheldrick, G. M. & Stalke, D. (2015). *J. Appl. Cryst.* 48. 3-10.
3. Sheldrick, G. M. (2013b). *XPREP*. Version 2013/1. Georg-August-Universität Göttingen, Göttingen, Germany.
4. Sheldrick, G. M. (2013a). The *SHELX* homepage, http://shelx.uni-ac.gwdg.de/SHELX/.
5. Sheldrick, G. M. (2015a). *Acta Cryst. A*, 71, 3-8.
6. Sheldrick, G. M. (2015b). *Acta Cryst. C*, 71, 3-8.
7. Dolomanov, O. V., Bourhis, L. J., Gildea, R. J., Howard, J. A. K. & Puschmann, H. (2009). *J. Appl. Crystallogr*. 42, 339-341.
8. Guzei, I. A. (2007-2013). Programs *Gn*. University of Wisconsin-Madison, Madison, Wisconsin, USA.